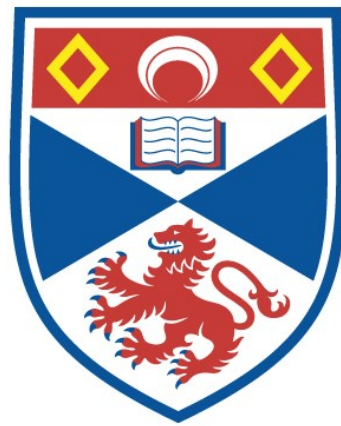


THE SEISMIC INVESTIGATION OF LOCH LOMOND
READVANCE GLACIER LIMITS : EVIDENCE FROM
SCOTTISH LOCHS

Philippa A. Lowe

A Thesis Submitted for the Degree of PhD
at the
University of St Andrews



1993

Full metadata for this item is available in
St Andrews Research Repository
at:
<http://research-repository.st-andrews.ac.uk/>

Please use this identifier to cite or link to this item:
<http://hdl.handle.net/10023/15272>

This item is protected by original copyright

BLUE
LIBRARY!

**THE SEISMIC INVESTIGATION OF
LOCH LOMOND READVANCE GLACIER LIMITS:
EVIDENCE FROM SCOTTISH LOCHS.**

Thesis submitted for the degree of
Doctor of Philosophy
University of St. Andrews

by

Philippa A. Lowe B.Sc. (Hons.) R.H.B.N.C. University of London,
Department of Geography and Geology,
The University of St. Andrews

August 1992



ProQuest Number: 10171083

All rights reserved

INFORMATION TO ALL USERS

The quality of this reproduction is dependent upon the quality of the copy submitted.

In the unlikely event that the author did not send a complete manuscript and there are missing pages, these will be noted. Also, if material had to be removed, a note will indicate the deletion.



ProQuest 10171083

Published by ProQuest LLC (2017). Copyright of the Dissertation is held by the Author.

All rights reserved.

This work is protected against unauthorized copying under Title 17, United States Code
Microform Edition © ProQuest LLC.

ProQuest LLC.
789 East Eisenhower Parkway
P.O. Box 1346
Ann Arbor, MI 48106 – 1346

TH B290

I, Philippa Anne Lowe hereby certify that this thesis has been composed by myself, that it is a record of my own work, and that it has not been accepted in partial or complete fulfilment of any other degree or professional qualification.

Signed

Date 27th August 1992

I was admitted to the Faculty of Science of the University of St. Andrews under Ordinance General No 12 on 1st October 1988 and as a candidate for the degree of Ph.D on 29th September 1989.

Signed

Date 27th August 1992

I hereby certify that the candidate has fulfilled the conditions of the Resolution and Regulations appropriate to the degree of Ph.D.

Signed

Date 27th August 1992

In submitting this thesis to the University of St. Andrews I understand that I am giving permission for it to be made available for use in accordance with the regulations of the University Library for the time being in force, subject to any copyright vested in the work not being affected thereby. I also understand that the title and abstract will be published, and that a copy of the work may be made and supplied to any *bona fide* library or research worker.

ABSTRACT

THE SEISMIC INVESTIGATION OF LOCH LOMOND READVANCE GLACIER LIMITS: EVIDENCE FROM SCOTTISH LOCHS.

Philippa A. Lowe B.Sc.

University of London

This study presents a comparative examination of three lochs, located in the S.E. Grampian Highlands, using seismic reflection survey techniques. Lochs Callater, Muick and Lee, lying inside, across and outside probable Loch Lomond Readvance glacier limits respectively, were surveyed using echosounder (200kHz), Pinger (3.5kHz) seismic subbottom profiling, and sidescan sonar equipment. Calibration of seismic records was achieved through analysis of core and surface sediment samples. Geomorphological maps of the subaerial topography were drawn.

Construction of bathymetric charts of the lochs reveals significant subaqueous topographic variation. The Loch Muick trough contains numerous mounds and hollows, and is crossed by a series of broken ridges, extending up the basin sides. Pinger profiling indicates that these subaqueous landforms are composed of glacial diamict (Sequence 2, Facies 2.1) overlain by draped sediments (Sequence 1). Additional ridges, buried beneath glacial outwash (Facies 2.2), are recognised 1.4km beyond the subaerial margin. It is suggested that the ridges are sublacustrine moraines. Analysis of core material suggests formation of these features during the Loch Lomond Readvance.

Two sequences are recognised in Loch Callater; lacustrine sediment, and glacial diamict. Analyses of core sediment suggest respective Holocene and Loch Lomond Stadial ages of the sequences. Pollen analysis indicates that ice may have remained in Glen Callater into the Ninth Millennium. Within Loch Lee, below Sequence 1 (Holocene lacustrine sediment), the Loch Lomond Stadial is represented by glacial outwash (Sequence 2, Facies 2.1) and nearshore avalanche detritus (Facies 2.2). Sequence 3 is composed of outwash (Facies 3.2) and glacial diamict (Facies 3.1), of proposed Devensian age.

The seismic signatures of the loch sediments are assimilated as a model. It is important that the limits of glaciation in the lacustrine environment be examined as extensively as those in the subaerial environment, to provide an accurate database against which models of climatic change can be tested.

*For my Parents,
Anne and Raymond Lowe*

CONTENTS

List of Figures	
List of Plates	
List of Tables	
List of Appendices	
Acknowledgements	

Chapter One Introduction

1.1	Introduction	1
1.2	Aims and Hypothesis	2
1.3	Thesis Structure	4
1.4	The Loch Lomond Stadial	6
1.5	Field sites: Introduction	13

Chapter Two Bathymetric Surveys

2.1	Introduction	30
2.2	Echosounding	30
2.3	Methodology: Aims	34
2.4	Loch Lee	35
2.5	Loch Callater	40
2.6	Loch Muick	46
2.7	Conclusions	56

Chapter Three Continuous Subbottom Seismic Reflection Profiling

3.1	Introduction	78
3.2	Subbottom Profiling	78
3.3	Seismic Profile Interpretation: Methodology and Classification	83
3.4	Methodology: Aims	94
3.5	Loch Lee	94
3.6	Loch Callater	104
3.7	Loch Muick	107
3.8	Conclusions	114

Chapter Four Sidescan Sonar Surveys

4.1	Introduction	160
4.2	Sidescan Sonar	160
4.3	Methodology: Aims	165
4.4	Loch Lee	166
4.5	Loch Callater	169
4.6	Loch Muick	172
4.7	Conclusions and Discussion	176

Chapter Five Surface Sediment Analyses

5.1	Introduction	192
5.2	Surface Sediment Analysis	192
5.3	Loch Lee	196
5.4	Loch Callater	200
5.5	Loch Muick	202
5.6	Discussion	204
5.7	Conclusions	211

Chapter Six Coring Programme and Core Analysis

6.1	Introduction	245
6.2	Methodology: Aims	245
6.3	Analytical Techniques: Down Core Samples	249
6.4	Loch Callater	251
6.5	Loch Muick	257
6.6	Discussion	264
6.7	Conclusions	281

Chapter Seven

7.1	Introduction	299
7.2	Loch Muick	300
7.3	Loch Callater	342
7.4	Loch Lee	360
7.5	Modelling the Loch Lomond Stadial in the lacustrine environment	379

Chapter Eight Conclulsion

8.1	Introduction	385
8.2	Glacier termini and the subaqueous environment	385
8.3	The case studies	386
8.4	The implications of the model	392

Appendices	394
-------------------	-----

Bibliography	419
---------------------	-----

LIST OF FIGURES

1.1	Location map. South east Grampian Highlands research field sites.	21
1.2	Former glaciers in the south east Grampians. Composite map of research undertaken by Sissons and Grant (1972) and Sissons (1972). After Sissons and Sutherland (1976).	22
1.3	Area covered by the Loch Lomond Readvance glaciation in Scotland. Crosses mark pollen sites indicating that glaciers did not reach that position. From Sissons (1983).	23
1.4	Glen Lee, Angus: Geomorphological map.	24
1.5	Glen Callater, Aberdeenshire: Geomorphological map.	25
1.6	Glen Muick, Aberdeenshire: Geomorphological map.	26
2.1	Loch Lee: Echosounder Traverse Lines.	58
2.2	Loch Lee, Dalhousie Estates, Angus, Bathymetric Chart, contoured at 1m intervals below 272m datum.	59
2.3	Loch Lee: Geomorphological Zones.	60
2.4	Loch Lee: Echogram, Zone 3 northeastern shallows, conical mound.	61
2.5	Loch Lee: Echogram, Zone 3 northeastern shallows, flat topped mound.	61
2.6	Hypsographic (depth-area) curves for Lochs Lee, Callater and Muick.	62
2.7	Bathymetric Chart of Loch Callater, Johnston and Collet, (1905).	63
2.8	Loch Callater: Echosounder Traverse Lines.	64
2.9	Loch Callater, Invercauld Estate, Aberdeenshire, Bathymetric Chart, contoured at 1m intervals.	65
2.10	Loch Callater: Echogram, aquatic weed growth appearing as the poorly defined, 'feathery', part of the profile. Southeastern shallows.	66
2.11	Loch Callater: Echogram, asymmetric profile and deepest trough. Diffuse surface profile due to low amplitude reflections from low density bottom sediments.	66
2.12	Bathymetric Chart of Loch Muick, Johnston and Collet (1905).	67
2.13	Loch Muick: Echosounder Traverse Lines.	68
2.14	Loch Muick, Balmoral Estate, Aberdeenshire, Bathymetric Chart, contoured at 10m intervals.	69
2.15	Loch Muick, Balmoral Estate, Aberdeenshire, Bathymetric Chart, contoured at 1m intervals.	70
2.16	Loch Muick: Geomorphological Zones.	71

2.17	Loch Muick: Echogram, boundary ridge between Zones A and B. Sub-surface profile due to second reflection of outgoing pulse in area of relatively shallow water with a highly reflective bottom.	72
2.18	Loch Muick: Echogram, mound and hollow Zone B. Sub-surface profile due to the second reflection of the outgoing pulse in area of relatively shallow water with a highly reflective bottom.	72
2.19	Loch Muick: Echogram, Zone B asymmetric profile.	73
2.20	Loch Muick: Echogram, subaqueous topography Zones Band C including lower slopes of boundary ridge.	73
2.21	Loch Muick: Echogram, profile across ridge dividing Zones C and D.	74
2.22	Loch Muick: Echogram, profile across Zone D, U-shaped trough.	74
2.23	Loch Muick: Form roughness derived from the formula given by Håkanson (1974).	75
3.1	The relationship between the frequency of the outgoing seismic wave and the depth of penetration for seismic pulses of varying frequency (McQuillin and Ardu, 1977).	117
3.2	Seismic sequence reflection terminations. Explanatory diagram of terms used in the text . After Bally (1987).	118
3.3	Seismic facies geometries and modifications. After Mitchum et al., (1977a).	119
3.4	Loch Lee: Pinger seismic subbottom reflection profile traverse lines.	120
3.5	Loch Lee: Pinger profiles. Cross traverses 11 and 8.	121
3.6	Loch Lee: Pinger profiles. Cross traverses 7 and 13.	122
3.7	Loch Lee: Pinger profile. Longitudinal traverse 12.	123
3.8	Loch Lee: Facies 1.1 Examples of reflection geometries.	124
3.9	Loch Lee: Isopach map showing the distribution of Facies 1.1.	125
3.10	Loch Lee: Facies 1.2 Examples of reflection geometries.	126
3.11	Loch Lee: Isopach map showing the distribution of Facies 1.2.	127
3.12	Loch Lee: Facies 1.3 Examples of reflection geometries.	128
3.13	Loch Lee: Isopach map showing the distribution of Facies 1.3.	129
3.14	Loch Lee: Facies 2.1 Examples of reflection geometries.	130
3.15	Loch Lee: Isopach map showing the distribution of Facies 2.1.	131
3.16	Loch Lee: Facies 2.2 Examples of reflection geometry Traverses 9, 8, 11.	132
3.17	Loch Lee: Facies 2.2 Example of reflection geometry Traverse 7	133
3.18	Loch Lee: Isopach map showing the distribution of Facies 2.2.	134
3.19	Loch Lee: Facies 3.1 Examples of reflection geometry.	135

3.20	Loch Callater: Pinger seismic subbottom reflection profile traverse lines.	136
3.21	Loch Callater: Pinger seismic subbottom profile Traverse 1.	137
3.22	Loch Callater: Facies 1.1 and 2.1 Examples of reflection geometry.	138
3.23	Loch Muick: Pinger seismic subbottom reflection profile traverse lines.	139
3.24	Loch Muick: Pinger profiles. Traverses 1 and 114-111, southwestern end.	140
3.25	Loch Muick: Pinger profiles. Traverses 9 and 96-93, southwestern end.	141
3.26	Loch Muick: Pinger profiles. Traverses 79-83 and 132-136, central section.	142
3.27	Loch Muick: Pinger profile. Traverse 142-137 northeastern end.	143
3.28	Loch Muick: Pinger profile. Traverse 115-131, longitudinal profile from southwest to northeast.	144
3.29	Loch Muick: Facies 1.1. Examples of reflection geometry, Traverses 83-78, 115-131 and 142-137.	145
3.30	Loch Muick: Isopach map showing the distribution of Facies 1.1.	146
3.31	Loch Muick: Facies 1.2 Examples of reflection geometries. Traverses 1, 9 and 132-136.	147
3.32	Loch Muick: Facies 1.2 Examples of reflection geometries. Traverses 57-62, 142-137, 132-136 and 9.	148
3.33	Loch Muick: Isopach map showing the distribution of Facies 1.2.	149
3.34	Loch Muick: Example of Facies 2.1 reflection geometry. Traverse 36-45.	150
3.35	Loch Muick: Example of Facies 2.1, Traverse 4, and Facies 2.2, Traverse 57-63 .	151
3.36	Loch Muick: Isopach map showing the distribution of Facies 2.2.	152
4.1	Loch Lee Sidescan sonar traverse lines.	179
4.2	Loch Callater Sidescan sonar traverse lines.	180
4.3	Loch Muick Sidescan sonar traverse lines.	181
5.1	Loch Lee: Surface sediment sample locations.	215
5.2	Loch Callater: Surface sediment sample locations.	216
5.3	Loch Muick: Surface sediment sample locations.	217
5.4	Loch Lee: Distribution map of the percentage of total organic matter (loss on ignition) in the surface sediment.	218
5.5	Ternary diagram for delimiting sediment texture (Folk ,1974).	219

5.6	Loch Lee: Distribution map of sediment textures derived from the ternary diagram of Folk (1974).	220
5.7	Loch Lee: Cumulative percentage frequency curves of surface sediment size.	221
5.8	Loch Lee: Frequency graphs of surface sediment diameter.	222
5.9	Loch Lee: Distribution map of mean grain size of surface sediment obtained using the Inman (1952) parameter ($M\phi$).	223
5.10	Loch Lee: Distribution map of Standard Deviation of surface sediment using the Inman (1952) parameter ($\sigma\phi$).	224
5.11	Loch Lee: Distribution map of Second ϕ Skewness Measure of surface sediment using the Inman (1952) parameter ($\alpha\phi$).	225
5.12	Loch Lee: QDa-Md plot showing the environmental trend envelopes of Buller and McManus (1972, 1973).	226
5.13	Loch Callater: Distribution map of the percentage of total organic matter (loss on ignition) in the surface sediment.	227
5.14	Loch Callater: Distribution map of sediment textures derived from the ternary diagram of Folk (1974).	228
5.15	Loch Callater: Cumulative percentage frequency curves of surface sediment size.	229
5.16	Loch Callater: Frequency graphs of surface sediment diameter.	230
5.17	Loch Callater: Distribution map of mean grain size of surface sediment using the Folk and Ward (1957) parameter (M_z).	231
5.18	Loch Callater: Distribution map of Standard Deviation of surface sediment using the Folk and Ward (1957) parameter (σ_I).	232
5.19	Loch Callater: Distribution map of Skewness of surface sediment using the Folk and Ward (1957) parameter (SK_I).	233
5.20	Loch Callater: Distribution map of Kurtosis of surface sediment using the Folk and Ward (1957) parameter (K_G).	234
5.21	Loch Callater: QDa-Md plot showing the environmental trend envelopes of Buller and McManus (1972, 1973).	235
5.22	Loch Muick: Distribution map of the percentage of total organic matter (loss on ignition) in the surface sediment .	236
5.23	Loch Muick: Surface sediment textural facies distribution map derived from the ternary diagram of Folk, (1974).	237
5.24	Loch Muick: Cumulative percentage frequency curves of surface sediment size.	238
5.25	Loch Muick: Frequency graphs of surface sediment diameter.	239

5.26	Loch Muick: Distribution map of mean grain size of surface sediment obtained using the Inman (1952) parameter ($M\phi$).	240
5.27	Loch Muick: Distribution map of Standard Deviation of surface sediment using the Inman (1952) parameter ($\sigma\phi$).	241
5.28	Loch Muick: Distribution map of Second ϕ Skewness Measure of surface sediment using the Inman (1952) parameter ($\alpha\phi$).	242
5.29	Loch Muick: QDa-Md plot showing the environmental trend envelopes of Buller and McManus (1972, 1973).	243
6.1	The Russian peat borer. After West (1968).	284
6.2	Loch Callater: Location of coring sites.	285
6.3	Loch Callater: Core 1. Down-core variation in particle size and total organic matter.	286
6.4	Loch Callater: Core 1. QDa-Md plot showing the environmental trend envelopes of Buller and McManus (1972, 1973).	287
6.5	Loch Callater: Core 1. Down-core chemical composition and Fe/Mn ratio.	288
6.6	Down-core qualitative mineral composition, Lochs Callater (Core 1) and Muick.	289
6.7	Loch Callater: Core 1. Pollen diagram. From Whittington, 1991.	290
6.8	Loch Callater: Core 2. Pollen diagram. From Whittington, 1991.	291
6.9	Loch Muick: Location of core site.	292
6.10	Loch Muick: Down-core variation in particle size, total organic matter and water content.	293
6.11	Loch Muick: QDa-Md plot showing the environmental trend envelopes of Buller and McManus (1972, 1973).	294
6.12	Loch Muick: Down-core chemical composition and Fe/Mn ratio.	295
7.1	A model for the seismic identification of glaciated and extra glacial water bodies during the Loch Lomond Stadial	384

PLATE LIST

- 1.1 Glen Lee: View south west across Loch Lee up the valley of the Burn of Inchgrundle. Note the low-lying alluvial plain at the western end of the loch, the steep valley sides adjacent to the loch showing bare rock surfaces and a cover of angular boulders, the lobate form of the boulder deposit in the centre of the picture and the till surface extending up the Inchgrundle valley. 27
- 1.2 Glen Lee: End moraine ridges 2-3m high surrounding Carloch. View northeast from within the glacier limit down Glen Lee. 27
- 1.3 Glen Callater: Hummocky till on the lower valley slopes surrounding the shores of Loch Callater. Note the gradational boundary into the undifferentiated till surface above the hummocky till. View southeast close to the outlet. 28
- 1.4 Glen Callater: Boulder-strewn hummocky till damming the outlet of Loch Callater. Note the evidence of estate management (burnt heather patches) in the background. View west from the survey boat. 28
- 1.5 Glen Muick: Loch Muick, December 1988. View to the south west. Corrie Chash can be identified in the centre of the Plate and hummocky till in the centre of this tributary valley. At the extreme left the mouth of the Black Burn valley joins Glen Muick and hummocky drift may be distinguished midslope. The main direction of ice flow was from the right fork in the valley, behind the plantation at Glas-Allt-Shiel. 29
- 1.6 Glen Muick: Down valley limit of hummocky till on the northern slopes above Loch Muick. The stream on the left of the Plate feeds the loch from the Dubh Loch. View south west from the survey boat. 29
- 2.1 Lowrance X-15M Recording Echosounder in operation. 76
- 2.2 Alluvial plain of the Allt an Loch and strath lochan, southeastern end, Loch Callater. 77
- 3.1 Giffit graphic recorder in use on Loch Callater. Note the number of reflection multiples resulting from operation in shallow water. 153
- 3.2 Waves on Loch Lee, 17 October 1989. View towards the northeast, outlet end. 153

- 3.3 Loch Lee: Pinger seismograph, Traverse 8, overdrawn with seismostratigraphic interpretation showing multiple layers of Facies 1.3, undulating surface of Facies 3.1 and Facies 1.1, 1.2, 2.1, 2.2, 3.1 and 4.1. Red lines = Sequence boundary Black lines = Facies boundary. 153
- 3.4 Loch Lee: Examples of some seismic facies. 3.4A Facies 1.1, Traverse 10, subparallel lenticular reflectors forming a fill in the underlying topography. 3.4B Facies 1.2, Traverse 13, parallel reflection geometry. 3.4C Facies 1.2, Traverse 14, point hyperbolae truncate parallel wavy reflectors. 3.4D Facies 2.1, Traverse 7, subparallel wavy and hummocky reflectors and concentrations of point hyperbolae. 3.4E Traverse 11, Facies 2.2 chaotic total geometry with scattered point hyperbolae. Note double thickness of Facies 1.2. Red lines = Sequence boundary Black lines = Facies boundary. 155
- 3.5 Pinger array for use on Loch Callater. Float-mounted transducer (left) secured to pole, Giffit graphic recorder on dinghy. External hydrophone not visible. 156
- 3.6 Loch Muick: Pinger seismograph, Traverse 132-136, indicating coring position (see Chapter 6) and overdrawn with seismostratigraphic interpretation. Red lines = Sequence boundary Black lines = Facies boundary. 157
- 3.7 Loch Muick: Pinger seismograph, Traverse 36-45, section between 36-38. Showing the undulating, hummocky surface of Facies 2.1 with internal compressional reflectors and infilling Facies 2.2 overlain by a drape of Facies 1.2. Red lines = Sequence boundary Black lines = Facies boundary. 158
- 3.8 Loch Muick: Pinger seismograph, Traverse 77-83, section 79-80. Examples of seismic Facies 1.1 (reflection free internal geometry), Facies 1.2 (poorly defined subparallel reflectors) and Facies 2.1 (containing numerous point hyperbolae). Red lines = Sequence boundary Black lines = Facies boundary. 159
- 4.1 Split trace graphic output from the Klein Hydroscan (Model 401) operating on Loch Lee. Note the central trackline of the survey vessel (white), the first return of the sonic pulse (adjacent paired dark lines) and following reflections from the loch floor. In all sonographs presented, the vessel track is at the bottom of the Plate. The scan is upslope towards the loch shore. 182

- 4.2 Loch Lee: Sonograph, Zone 1. Dark reflectors representing patches of aquatic weed growth distributed over the surrounding low backscatter (fine grained) loch floor. 182
- 4.3 Loch Lee: Sonograph. Shore-parallel terraces in Zone 2 showing boulders lying on the most shore-proximal terrace flats. The linear distribution of the low backscatter level below the lowest shore-parallel terrace can be clearly recognised. 183
- 4.4 Loch Lee: Sonograph, Zone 2. Extremely steep slope angles close to the mouth of the Burn of Duchrey. In the midslope area a mound composed of boulders with a distinct acoustic shadow zone can be recognised. 183
- 4.5 Loch Lee: Sonograph, Zone 2. Lobate distribution of the low level backscatter reflector on the northern slopes of Loch Lee. 184
- 4.6 Loch Lee: Sonograph, Zone 2. Linear topographic low extending from the base of the shore-parallel terraces and terminating at a boulder. 184
- 4.7 Loch Lee: Sonograph, Zone 3. Shore-parallel terraces with a maximum extent of 75m into the loch at the head of promontories. Areas of medium backscatter levels with boulders adjoin the promontories and low backscatter levels cover the remainder of the loch floor. 185
- 4.8 Loch Lee: Sonograph, Zone 3. Highly reflective mound rising above the intermediate backscatter intensity of the surrounding loch floor. 186
- 4.9 Loch Callater: Sonograph, northeastern side. Shore-parallel terraces, boulder spreads and relatively featureless loch floor with areas of medium and low backscatter levels. 186
- 4.10 Loch Callater: Sonograph, southwestern side. First type of sonograph signatures; steep nearshore slope below which a featureless loch floor composed of low to medium backscatter level reflectors forms the remainder of the floor. 187
- 4.11 Loch Callater: Sonograph, southwestern side. Second type of sonograph signatures; gradational boundary between upper and lower slopes combined with a scattered distribution of boulders. Note the small islet (marked). 187

- 4.12 Loch Muick: Sonograph, northwestern slopes. The southerly mouth of the Allt an Dubh-loch showing nearshore low backscatter levels with a discontinuous covering of small boulders and cobbles, break in slope and lower angle slopes covered by uniform fine grained sediment. Adjacent shore-parallel terraces can be recognised to the northwest, below which a minor change in slope angle has been identified where darkening occurs on the sonograph. 188
- 4.13 Loch Muick: Sonograph, northwestern slopes. Shore-parallel terrace with boulders lying on the terrace flat and a boulder spread on an area of low reflection backscatter close to the mouth of Lindsay's Burn. 188
- 4.14 Loch Muick: Sonograph, northwestern slopes. Concentration of boulder spreads blanketing the nearshore slopes between Lindsay's Burn and the Allt an Dearg. This sonograph was recorded at a low sensitivity to highlight the topographic variation on the boulder-clad slopes. The darker line which occurs approximately half way down the slope is noise resulting from multiple reflections received by the transducer. 189
- 4.15 Loch Muick: Sonograph, northwestern slopes. Loch slopes close to the mouth of the Allt an Dearg showing high-low backscatter banding representing sediment size variation. The dark areas probably represent fine gravel and the lighter areas fine sand or silt. 189
- 4.16 Loch Muick: Sonograph, southwestern slopes. Boulder spreads on the nearshore slopes showing distinct lobate downslope termination. 190
- 4.17 Loch Muick: Sonograph, southwestern slopes. Cobble shoreline, shore -parallel terrace and extensive boulder spreads. White areas on the lower part of the slopes are interpreted as representing finer grained sediments not covered by boulders. The darker line running parallel to the shore is a second reflection received by the transducer. 190
- 4.18 Loch Muick: Sonograph, southwestern slopes. The mouth of the Black Burn. Note the short gradational change from boulder spreads to areas of finer grained sediment (low backscatter) at the southwestern and southeastern edges of the Plate. The darker line running parallel to the shore is a second reflection received by the transducer. 190
- 4.19 Loch Muick: Sonograph, southwestern slopes. The northeastern shore, a shallow water area (see first bottom return) with groups of boulders or rocky outcrops surrounded by areas of low to medium backscatter levels. 191

- 5.1 Van Veen grab in open position prior to sampling. Note the teeth at the opening. 244
- 5.2 Van Veen grab in closed position with collected sample visible through viewing hatch. 244
- 6.1 Mackereth corer prior to deployment. The internal piston is contained within the 6m long outer casing, which is attached to the anchor drum (at the left of the photograph). The corer was towed on the inflatable dinghy to the coring site behind R.V. Mya (middleground). 296
- 6.2 Close-up of the tonal and textural transition zone in Core 1 from Loch Callater. The blue-grey silt on the left (core section bottom) is Munsell colour 5 GY 5/1 and the brown sandy silt on the right (core section top) 5 Y 3/1. 296
- 6.3 Loch Muick: 500cm core X-radiograph negatives. Unit 1, high density sediment extends between 500cm-475cm with an unconformable boundary with Unit 2. Unit 2 extends from 475cm-187cm and comprises fine grained, stratified, medium density sediments broken by small fractures (wavy black lines). Clastic concentrations at 263cm-290cm, 228cm-337cm, 187cm, 197cm and 462cm. The basal 15cm of this unit is composed of laminae of fine grained material. The boundary between Unit 2 and Unit 3 is gradational over 5.5cm. Unit 3 extends from 187cm-0cm and is composed of fine laminae and strata with occasional, stratified, concentrations of clasts. The core section missing between 46.5cm-55cm was covered by a metal band impenetrable to X-rays. Lower density spots between 40cm-60cm result from holes drilled in the core barrel. 297-8

LIST OF TABLES

3.1	Propogation velocities of selected rock types.	81
3.2	Seismic stratigraphy boundary determination. After Mitchum et al., (1977).	87
3.3	Reflection configurations. After Mitchum et al., (1977).	90
3.4	Reflection configuration modifying terms. After Mitchum et al., (1977).	90
5.1	Loch Lee: Pearson's Product Moment Correlation Coefficient for surface sediment variables.	205
5.2	Loch Callater: Pearson's Product Moment Correlation Coefficient for surface sediment variables.	208
5.3	Loch Muick: Pearson's Product Moment Correlation Coefficient for surface sediment variables.	210
6.1	Loch Callater: Pearson's Product Moment Correlation Coefficient for core sediment variables.	268
6.2	Loch Muick: Pearson's Product Moment Correlation Coefficient for core sediment variables.	274

LIST OF APPENDICES

A	Operation of the SediGraph 5100.	394
B	Example of a SediGraph data sheet.	396
C	Sedimentary statistics. 1. Folk and Ward (1957) 2. Inman (1957) 3. QDa-Md Buller and McManus (1972).	397
D	Organic matter, sand, silt and clay percentages of Loch Lee surface sediments with sampling depths and textural classification after Folk (1974) for samples lacking gravel.	398
E	Phi-based sedimentary statistics (after Inman, 1952) of Loch Lee surface sediment.	399
F	Metric (mm) sedimentary statistics (after Krumbein, 1936) of Loch Lee surface sediment.	400
G	Loch Callater sand, silt, clay and organic matter percentages of surface sediment with sampling depths and textural classification after Folk (1974).	401
H	Phi-based sedimentary statistics (after Folk and Ward, 1957) of Loch Callater surface sediment.	402
I	Metric (mm) sedimentary statistics (after Krumbein, 1936) of Loch Callater surface sediments.	403
J	Loch Muick sand, silt and organic matter of surface sediment with sampling depths. Textural classification follows Folk (1974) for samples lacking gravel.	404
K	Phi-based sedimentary statistics (after Inman (1952) of Loch Muick surface sediment.	405
L	Metric (mm) sedimentary statistics (after Krumbein, 1936) of Loch Muick surface sediments.	406
M	Comparison between values for Skewness obtained from surface sediment data from Loch Callater using the sedimentary statistics given by Folk and Ward (1957) and Inman (1952).	407
N	Sample preparation and analysis by Coulter Counter.	408
O	Total extractable element preparation and analysis.	409
P	Sample preparation and analysis by X-Ray Diffraction.	410
Q	Sand, silt, clay and organic matter percentages of Loch Callater core sediment with sample depth and textural classification after Folk (1974) for samples lacking gravel.	411

R	Metric (mm) statistics (after Krumbein, 1936) of Loch Callater core sediment.	412
S	Elemental composition of Loch Callater core sediment and Fe/Mn ratio.	413
T	Sand, silt, clay, organic matter and water content percentages of Loch Muick core sediment with sample depth and textural classification after Folk (1974) for samples lacking gravel.	415
U	Metric (mm) statistics (after Krumbein, 1936) of Loch Muick core sediment.	416
V	Elemental composition of Loch Muick sediment and Fe/Mn ratio.	417

ACKNOWLEDGEMENTS

This thesis could not have been completed without the considerable help and support of many people and organisations:-

First, my long-suffering and patient supervisors at the University of St. Andrews, Dr. John McManus and Dr. Robert Duck, for their support in the field, frequently during 'extreme' weather conditions, and for their help and encouragement during the colossal task of writing up, particularly the long distance supervision received since February. The support of my third supervisor, Professor David Sugden, at the University of Edinburgh, is also gratefully acknowledged.

For assistance in the field, Allan Ramsay and Ian Lorimer (boatmen), Jack Jarvis, Jill Tate, Justin Dix, Lindsay Shen, Katrina Bennett, Christopher Lowe, Anne Lowe and Raymond Lowe.

For access to the three lochs, Invercauld Estate, Dalhousie Estate and Balmoral Estate.

For laboratory and cartographic assistance I am grateful for the help and trouble shooting abilities of Colin Cameron, Bert Bremner, Graeme Sandeman and Janet Mykura.

The Natural Environment Research Council for providing funding, and to Jim and Christian Robb, and Murray & Donald for providing part-time work when the money ran out.

My Parents and Grandparents who gave up their holidays for fieldwork and provided 'Grannisnax'.

Florence McAndie for being Florence (at all times).

The St. Andrews Cottage Hospital, for providing X-ray facilities.

The libraries of the Departments of Geography and Geology at the University of Cambridge, and their librarians, for providing help and facilities during the last few months.

The Institute of Earth Studies, University of Wales, Aberystwyth, for support during the final stages.

Finally, I acknowledge the tremendous help, encouragement, and support of my husband, Dr. John Bryson. An urban geographer, who previously knew relatively little about matters glacio-lacustrine in the Grampians, he has shown an active interest in my research and guided me through the difficult times of writing up. A heartfelt 'Thank you'.

*Cambridge,
July 1992*

CHAPTER 1

INTRODUCTION

1.1 INTRODUCTION

The value of Quaternary research has never been greater than in the present decade. The escalating demand for models of the causes and impacts of climatic change has increased the importance of research into the last significant climatic event in Britain. This period, which is known variously as the Loch Lomond-, Lateglacial- or Younger Dryas Stadial occurred between approximately 11,000 to 10,000 years ago (11ka-10kaBP). During this time in Britain there was a re-expansion and recrudescence of glaciers in the mountainous areas of Scotland, Wales, and northern England.

The development and verification of models of climatic change has been derived from pre-determined evidence, thereby inverting Lyell's Uniformitarian concept to 'The past is the key to the present' and, by extension, the future. Crucial in quantifying the predictive capabilities of models of ice sheet growth has been the ability to validate model data against former ice limits determined by field research.

In Scotland 'There is a wealth of field evidence with which to test any model' (Payne and Sugden, 1990, p.625), especially from the Loch Lomond Readvance glaciation (see section 1.4.2, Figure 1.3, below). This field evidence primarily results from the pioneering research undertaken by Sissons and his co-workers (e.g. Sissons 1972a,b, 1973a, b, 1974, 1975, 1977a, b, c, 1978, 1979a, b, c, 1980a, b; Sissons and Grant, 1972; Sissons et al., 1973; Sissons and Sutherland, 1976). The extent of the former major West Highland glacier complex, smaller ice caps, valley and corrie glaciers, pro- and periglacial features in Scotland during the Loch Lomond Readvance has been established through geomorphological mapping and other analytical techniques including palynology, combined with radiocarbon assay. Thus Sissons concluded:-

'The reality of the last readvance, the Loch Lomond Readvance, is firmly established. There is however, much scope for future research in clarification and

further definition of glacial limits through new techniques and new applications of existing techniques' (Sissons, 1972a, p.168).

With few exceptions the investigation of Loch Lomond Readvance ice limits has hitherto been restricted to terrestrial mapping. These exceptions include seismic reflection subbottom profiling studies of west coast sea lochs (Boulton et al., 1982, Lochs Nevis, Ailort, Sound of Arisaig, sounds between Sleat, Eigg and Muck and the mainland; Dix, 1992 pers. comm., Loch Ainort, Skye). There has been no systematic analysis of the nature and extent of former Loch Lomond Readvance glacier margins now submerged in the subaqueous environment of Scotland's numerous inland waterbodies.

1.2 AIMS AND HYPOTHESIS

The aims of this thesis are to establish a unique, pioneering, database of information on the extent and geomorphological expression of presumed former Loch Lomond Readvance glaciers in Scottish lake basins. This is achieved through the application of seismic reflection techniques, normally applied to marine survey, to investigate a suite of Scottish lochs which are believed to have experienced widely differing conditions during the Loch Lomond Stadial. Establishing the underwater seismostratigraphic characteristics of deposits in areas, where the positions of glacier limits (regardless of absolute age) are well defined on land, should enable the locations of ice margins to be identified in areas where terrestrial evidence is poor or equivocal. The hypothesis to be tested is:-

'It is possible to identify the presence of former Loch Lomond Readvance glaciers in lakes, infer the related processes and define the limits of glaciation through the geophysical analysis and seismostratigraphic interpretation of lake sediments.'

1.2.1 Research field sites selection

In order to test the above hypothesis it is necessary to identify a suitable site. The ideal site would comprise three lochs occurring within a restricted area which experienced varied degrees of glaciation during the Loch Lomond Stadial.

In the south east Grampian Highlands (Figure 1.1) glaciers of presumed Loch Lomond Readvance age were restricted in size and extent (Sissons and Grant, 1972; Sissons, 1972a; Figure 1.2, see also section 1.4.3 below). The age of these former glaciers has been the subject of considerable controversy (see section 1.4.3 below). The absolute age of the glacier limits, however, is not central to the aims of this thesis. In the absence of either relative or radiometric dates prior to this research, the interpretations of Sissons and Grant (1972) and Sissons, (1972a), based upon their detailed maps, are accepted for the purposes of this thesis. Thus, within a relatively small area (Figure 1.1) widely differing glaciated environments existed broadly contemporaneously.

The area now occupied by the Loch Callater water body was entirely covered by the Glen Callater valley glacier. Loch Lee remained unaffected by the direct input of glacier ice and Loch Muick lay astride two separate glacier margins, those of the main Glen Muick valley glacier and a smaller ice cap outlet glacier (Figure 1.2). The latter is hereafter referred to as the 'Black Burn' glacier (Sissons and Grant, 1972; Sissons, 1972a). The well defined terrestrial limits, spatial proximity, range of former glacial environments and comparative ease of access to these three lochs provided an ideal field area in which to test the applicability of seismic reflection profiling techniques as a diagnostic tool in the identification of the impact and extent of glaciation in the lacustrine environment.

1.3 THESIS STRUCTURE

This thesis is structured in order to illustrate the continuum of research techniques applied in each of the lochs. The five methodological chapters (Chapters 2, 3, 4, 5 and 6) concentrate individually on a single technique, presenting a discussion and interpretation of the data where appropriate. Due to the varied nature of the techniques used, an integrated literature review is inappropriate. Thus each methodological chapter, where relevant, is prefaced by an explanatory introduction and review of the literature. This sequence of methodologies and data, interpreted in the context of each individual loch, culminates in Chapters 7 and 8 which present a discussion of the data obtained, conclusions, and directions for further research.

The remainder of Chapter 1 comprises an introduction to the Loch Lomond Stadial, a brief overview of the causes of the Loch Lomond Stadial and the Loch Lomond Readvance glaciation in Scotland. A detailed review of the published research which has been undertaken in the selected field area, the south east Grampians, and its significance in the definition and chronology of the former limits of glaciation is provided. An introductory analysis of the field sites and new geomorphological maps, completed for the purposes of this thesis, are presented.

Chapter 2 is the first of the series of methodological chapters and presents data from echosounder surveys undertaken in Lochs Lee, Callater and Muick. Following an historical overview and introduction to the principles of echosounding, detailed bathymetric charts, contoured at 1m intervals, derived from original echosounder data, are given. In the case of Loch Lee, this is the first bathymetric chart for which records could be traced. Lochs Callater and Muick were included in the '*Bathymetrical Survey of the Scottish Freshwater Lochs*' (Murray and Pullar, 1910). The new charts form the base maps upon which all subsequent surveys and investigations in the lochs were undertaken. The underwater geomorphology of each loch is described, zones of morphological variation identified and, in the case of Loch Muick, quantified. Where appropriate, comparisons are made between the previously published charts and those constructed during this research programme.

Chapter 3 provides an account of the methodology and data from continuous subbottom seismic reflection profiling using 3.5kHz Pinger equipment. This technique is the second in the continuum of seismic geophysical techniques and represents an extension of the echosounding process. A lower frequency sound pulse is used to penetrate the loch floor sediment and is reflected from discontinuities in the underlying substrate. The graphic output enables an examination of the subbottom stratigraphy and interpretation of the composition of underwater landforms to be made. Following an overview of the development of the technique and of seismic stratigraphic interpretation, descriptions of the seismic sequences and facies identified are given. Parastratigraphic interpretations of these data are made.

Chapter 4 further extends the use of seismic reflection techniques through the application of sidescan sonar. Investigations using sidescan sonar advance the understanding of present and former subaqueous processes in two ways. First through the ability to identify relatively small subaqueous landforms, below the resolution of those appearing on the 1m contoured bathymetric charts, and secondly by providing greater detail of sedimentological variation across the loch floors than can be obtained by sediment sampling programmes. However, substantiation of interpretations, through the physical examination of the loch floor surface sediments (Chapter 5), is essential. Pending the analysis of all the data obtained in this research programme, a non-genetic (descriptive), interpretation of the sonographs from each loch is given.

Chapter 5 presents statistical analyses of particle size data from surface sediment samples obtained from the floors of Lochs Lee, Callater and Muick during a grab sampling programme. It is designed to permit validation, or otherwise, of the interpretations made from the sidescan sonar data given in Chapter 4. Analyses of the total organic matter content and the environment of deposition (by QDa-Md analysis) of the samples are also included and compared with data reported from other lochs.

Chapter 6 is the final methodological chapter, in which data from a coring programme and analyses of core material are presented. The aim of using this technique is principally to aid correlation of the seismic subbottom reflection profile data and

parastratigraphic interpretations. Through this link correlation can be made between data obtained from all the other techniques. Total organic matter, particle size, water content, total extractable elemental composition, mineral composition and X-ray analyses were carried out on cores obtained from Lochs Callater and Muick. All attempts at coring the bed of Loch Lee failed. Distinct units are recognised within each core and genetic interpretations of the environment of deposition of each unit, based solely on data derived from core analyses, are given.

Chapter 7 provides an holistic analysis of data obtained from Lochs Muick, Callater and Lee, based upon the sequence and facies framework identified in Chapter 3. Data from each loch are examined, and the former and modern processes operating within the water body inferred, to enable a reconstruction of the former lacustrine environment to be made. The significance of these interpretations within the context of the available subaerial evidence is discussed. An examination of the seismostratigraphic variation between the lochs is made. This chapter culminates in a model developed from the distinctive seismostratigraphic signatures obtained from the sediments in Lochs Muick, Callater and Lee.

Chapter 8 concludes this thesis by examining the contribution it has made to the identification of former glacier limits and processes in the lacustrine environment. It highlights the main findings of this thesis and suggests avenues for further research.

1.4 THE LOCH LOMOND STADIAL

1.4.1 Evidence, possible causes and extent

The Loch Lomond Stadial climatic cooling event occurred between approximately 11-10kaBP (Gray and Lowe, 1977; Ruddiman and McIntyre, 1981). However, the accuracy of radiometric 'dates' derived from radiocarbon assay (both beta-decay and AMS) during the Lateglacial period has recently been questioned (Amman and Lotter, 1989;

Lowe, 1991). Constant age plateaux have been identified which are interpreted as resulting from temporal variations in atmospheric ^{14}C concentration. These findings have important implications regarding the reliability of previously reported radiocarbon 'dates' including those referred to in this section and section 1.4.2 below.

During the Loch Lomond Stadial the northern Atlantic Ocean experienced a significant cooling. The North Atlantic polar front advanced south and east, from an interglacial position aligned with the west coast of Iceland and eastern Canada at 11kaBP, to the northern coast of Portugal, 5° poleward of the full glacial position (Ruddiman and McIntyre, 1981). The retreat of the polar front and return to interglacial conditions at 10kaBP was equally rapid. Dansgaard et al. (1989) suggest that the termination of the Loch Lomond Stadial 'Must have been extremely fast, on the order of a couple of decades.'

The cause of the sudden, brief return to glacial conditions is the subject of considerable debate. Explanatory suggestions include the abrupt disintegration of a hypothetical Arctic ice shelf (Mercer, 1969; Grosswald, 1980; Denton and Hughes, 1981), a decrease in salinity (Ruddiman and McIntyre, 1981), the temporary shut-down of the North Atlantic deep water circulation system (Broecker et al., 1985, 1988; Broecker and Denton, 1989) and cooling caused by the diversion and mixing of meltwater drainage into the North Atlantic (Johnson and McClure, 1976).

The effects of climatic cooling have been reported extensively from Europe (e.g. Lowe et al., 1980; Watts, 1980), Greenland (Dansgaard et al., 1982) and it has been suggested that correlations with climatic events on the continent of America and the Antarctic (see reviews in Rind et al., 1986; Peteet et al., 1990) indicate a possible world-wide event.

1.4.2 Glaciers of the Loch Lomond Readvance in Scotland

The existence of a distinct phase of valley glaciation post-dating major ice sheet glaciation was recognised in Scotland following the acceptance of the Glacial Theory (Chambers, 1855; Maclaren, 1855). However, the term 'Loch Lomond Readvance', used to describe the expansion and recrudescence of glaciers that occurred during the Loch

Lomond Stadial, was not introduced until 1933, by Simpson, in reference to former glaciers identified in the Loch Lomond basin and along the Highland border west of the River Tay. Research by Charlesworth (1955), Synge (1956) and Sissons (1967a) identified further post-Devensian readvance stages that have subsequently been rejected following further investigation of the evidence (see Sissons, 1972b). The Loch Lomond Readvance has thus remained as one of only two widely accepted readvance stages, the other being the Wester Ross Readvance (Robinson and Ballantyne, 1979).

The extent of the Loch Lomond Readvance glaciation was mapped during the 1970s by J.B. Sissons and his co-workers (for references see section 1.1 above) using geomorphological features, particularly the limits of 'hummocky moraine' to define the glacier margins. Refinements to the basic map continue to be made. These include a previously unidentified corrie glacier in the Northwest Highlands (Lawson, 1986), small glaciers in the Southern Uplands (Cornish, 1981) and a major icefield and additional glaciers on the Isle of Skye (Walker et al., 1988; Ballantyne, 1989). In Figure 1.3 a compilation of the data available to 1983 on maximum glacier extent is presented.

Radiometric dating techniques, particularly radiocarbon dating, have been used in numerous recent studies in an attempt to define the temporal limits of the Loch Lomond Readvance glaciation. However, problems have arisen regarding both the dating technique (see section 1.4.1 above), and the identification of temporal and spatial non-contemporaneity in maximum glacial extent. The following information should be viewed in the light of these findings. Maximal glacier extents in the West Highland glacier complex include those dated to 10,500-10,000BP (Creran glacier, Peacock et al., 1989), 10,350BP (Loch Lomond glacier, Browne and Graham, 1981), 10,560BP (Loch Lomond glacier, Rose et al., 1988) and 11,800BP (Menteith glacier, Sissons 1967b). Selected radiocarbon dates from sites outside the glaciated area indicate that in the central Grampians, at Loch Etteridge, 8km from the West Highland glacier complex, the Loch Lomond Stadial cooling began around 10,764BP and ceased at approximately 9,405BP (Sissons and Walker, 1974) and at Varragill, Skye, the Loch Lomond Stadial closed between 10,370BP and 9,500BP (Walker et al., 1988).

1.4.3 The Loch Lomond Readvance in the south east Grampian Highlands.

The existence of former valley glaciers in the south east Grampians was first reported by Collet and Johnston (1906), contributory surveyors to the massive *'Bathymetrical Survey of the Scottish Freshwater Lochs'* (1910) co-ordinated by Sir John Murray and Mr. Laurence Pullar. Collet and Johnston published hypotheses on the formation of three lochs including Lochs Callater and Muick. Loch Callater is recognised as 'A true barrier basin, dammed up by a frontal moraine' (p110) and Loch Muick a compound rock/barrier basin:- 'The barrier is the latest moraine thrown down by the glacier that once crept along the glen' (p108).

Subsequent surveys of the area were carried out by Barrow et al. (1912), of the Geological Survey of Scotland, who made a breakthrough in the interpretation of geomorphology. Two phases of glaciation were recognised. They attributed the morainic forms of valley and corrie glaciers to the period of 'Local valley glaciers' (p115) and landforms outside these margins as belonging to the 'Period of maximum glaciation' (p115). In Glen Muick:-

'Local valley moraines occur in great quantity. They are numerous about the head of Loch Muick, and in sounding the lake a submerged moraine was met with opposite the Glas Allt Lodge' (p121).

It is believed that the latter statement refers to unpublished data from the 'Bathymetrical Survey' since no reference is made to further boat-based surveys. Evidence of former glacial conditions in Glen Muick is also found in the 'Glaciated [striated] surfaces' (p117) and the suggestion that the loch occupies a glacially overdeepened trough. Loch Lee is also interpreted as occupying a partly filled, overdeepened rock basin. The existence of a former glacier terminus in Glen Callater may be inferred from the Report:-

'The lower portion of Glen Callater is relatively free from this deposit; but the drift increases in thickness in the glen above the loch' (p.120).

After this flurry of investigations in the early Twentieth Century the glacial history of the south east Grampian area remained unchallenged and unresearched until the 1970s.

In 1972 two papers presenting maps and interpretations of the subaerial geomorphology of part of the south east Grampians were published by Sissons (Sissons and Grant, 1972; Sissons, 1972a; see Figure 1.2). In Glen Muick the former glacier was identified by numerous landforms; hummocky drift limits, fresh morainic topography, undifferentiated drift limits, a morainic ridge, a lateral boulder moraine, and truncated solifluction deposits. The Glen Muick glacier terminus is marked where 'The hummocky moraine terminates in Loch Muick' (Sissons et al., 1973, p.75) and that of the Black Burn glacier where:-

'The distribution of mounds points to the former existence of a glacier tongue that flowed down the valley to terminate in the loch' (Sissons, 1972a, p.176).

Evidence for the former existence of the Glen Callater valley glacier includes the landforms given above, excepting the morainic ridge and truncated solifluction deposits, plus additional fluted moraines and terraced outwash. In Glen Lee the most proximal former glacier to Loch Lee was that occupying the basin now filled by the Carlochay Lochan. The glacier is marked by:-

'An excellent gently-curving terminal moraine a few metres high and 700m long that abuts against the steep bounding slopes at each end and within which traces of later end moraines are discernible' (Sissons, 1972a, p.174).

North west of Loch Lee, at the head of Glen Lee, the down-valley limit of another former glacier is marked by the abrupt termination of morainic mounds which are replaced by a low outwash terrace.

The former glaciers were dated to the Loch Lomond Readvance on the basis of the available geomorphological evidence. No relative or radiometric dating methods were employed. The geomorphological evidence comprised:-

1) Moraines. 'This readvance is characterized by fresh hummocky moraines and is the only known readvance in Scotland frequently associated with clear lateral and terminal moraines...fluted moraines have so far been identified...only in locations known or believed to have been covered by Zone III ice' (Sissons and Grant, 1972 p90).

2) Periglacial features, especially large solifluction lobes are 'Nowhere found within the readvance limit but they do occur just outside it' (p90).

This evidence was interpreted to imply, first, the contemporaneity of the glaciers, secondly, post-glacial reduction in periglacial activity and thus, thirdly, as the last major climatic cooling event occurred during Zone III (the Loch Lomond Stadial), the lobes formed or were reactivated during this period, finally implying that the glaciers existed during the Loch Lomond Stadial.

During the 1970s and into the next decade there was an intense, occasionally heated, debate between Sissons, D.E Sugden and their fellow researchers as to the extent and nature of the Loch Lomond Readvance glaciation. This debate centred upon Sugden's work in the Cairngorms (e.g. Sugden, 1970, 1972, 1973, 1977, 1980; Sugden and Clapperton, 1975; Clapperton et al., 1975) and Sissons' in the south east Grampians and Cairngorms (e.g Sissons 1972a, b, 1973b, 1975, 1979b; Sissons and Grant, 1972; Sissons et al., 1973). Three hypotheses regarding the extent of the Loch Lomond Readvance in the Cairngorms, sharply contrasting with those of Sissons, were proposed by Sugden (1970) and Sugden and Clapperton (1975):-

- 1) It is represented by eight corrie glaciers.
- 2) The Devensian ice sheet covered the area.
- 3) The stadial was represented by a relatively minor fluctuation during the decay of the Devensian ice sheet.

Subsequent pollen analysis at Loch Etteridge in the central Grampians (Sissons and Walker, 1974) indicated that the Devensian ice sheet had retreated from much of Scotland by 13kaBP. Thus Sugden's latter two hypotheses were eliminated (Sissons, 1973b). Clapperton et al., (1975) meanwhile disproved Sissons' proposal that:-

'Fresh hummocky morainic terrain is characteristic of the Loch Lomond Readvance and is not known to occur outside its limits' (Sissons, 1972a, p.178).

Pollen analysis in the vicinity of Loch Builg, Cairngorms, proved the existence of pollen characteristic of Zone III vegetation, radiocarbon dated to 11,770BP, within an area of hummocky moraine (Clapperton et al., 1975). Exceptions to Sissons' relative dating technique, utilising the distribution of periglacial landforms solely outside the Loch Lomond Readvance glacier limits, were reported by Sugden (1972) from Corrie an Lochain in the north Cairngorms. However, these data did not prevent Sissons from maintaining his view that 'It will require very strong evidence to disprove the argument' (Sissons, 1972b, p.41).

The debate continued with Sugden's subsequent hypothesis that some of the corrie moraines could have formed during the Little Ice Age (17th-19th Centuries) (Sugden, 1977). Investigations by Rapson (1985) into the age of corrie moraines in the Cairngorms revealed that sedimentation in the corries has been continuous from 6-9kaBP. Interpretations of the geomorphology made by Clapperton (1986) and Sugden and Clapperton (1975) maintain that, even in the light of the minimum dates for the corrie moraines, the:-

'Hummocky deposits of morainic and fluvio-glacial debris located in upper Glen Muick, the Dubh Loch trough, and in Glen Callater' (Clapperton, 1986, pp392-3) could have formed through the 'Catastrophic stagnation of ice fields and glaciers' (Clapperton, 1986) during the rapid deglaciation at the close of the Devensian glaciation. Re-mapping of part of the Cairngorms (Bennett and Glasser, 1991) has not contributed to the Loch Lomond Stadial versus the Late Devensian stagnation debate, but further reiterated the fundamental underlying problem:-

'We believe it [the Glen Geusachan glacier] *probably dates from the Loch Lomond Stadial interval, but have no direct chronological evidence to support this opinion*' (Bennett and Glasser, 1991 p117, my emphasis).

In view of the above evidence, for the purposes of this thesis and in common with Bennett and Glasser, the interpretation made by Sissons is favoured. This is primarily

because, in the field area selected, in the vicinity of Lochs Lee, Callater and Muick, the only available published geomorphological maps and interpretations are those of Sissons and Grant (1972) and Sissons (1972a). It must be stressed, however, that the age of the glacier margins investigated is peripheral to the aims of this thesis, as outlined above.

1.5 FIELD SITES: INTRODUCTION

1.5.1 South east Grampian Highlands

Lochs Lee, Callater and Muick lie within the highland belt of the south eastern Grampian mountains, in Tayside (Lee) and Grampian (Callater and Muick) Regions. The mountains surrounding the lochs are composed of Dalradian metamorphic (schists and gneisses) and Caledonian igneous (granite and diorite) rocks, rising to the highest, granite peak of Lochnagar (1154m) above Loch Muick. Annual rainfall is relatively high for this eastern area, in the range 1000-1500mm (Coppock, 1976). During the period January to September the mean daily rainfall is 3-4mm, whereas between October and December it is slightly higher at 4-5mm (White and Smith, 1982). The annual temperature ranges from 0°C to -2°C in the period January to March to between 10°C and 12°C in July to September (White and Smith, 1982). Soils are frequently poorly drained organic soils, peat or completely undeveloped bare rock surfaces (Coppock, 1976). These soils support *Calluna* and *Eriophorum* dominated plant assemblages, with locally frequent areas of *Betula*. Agricultural activity is restricted to hill sheep farming (particularly in Glen Lee), the main economic value of the area being in sporting estates which provide stalking and grouse shooting. This area of the south east Grampians, especially the Balmoral Estate, is popular with walkers and climbers. The medium distance footpath, Jock's Road, runs along the shores of Loch Callater for part of its route (see Figure 1.1).

For the purposes of this thesis, geomorphological maps of the area immediately adjacent to the three lochs including the zone in which the most proximate glacier terminus or termini had previously been mapped (see section 1.4.3 above) were prepared. These maps (see sections 1.5.2.2.1-2, 1.5.3.2.1-2 and 1.5.4.2.1-2 below) provide a more detailed survey of the geomorphology than that given by Sissons and Grant (1972) and Sissons (1972a). This information thus permits independent examination of the available evidence. The maps were constructed on a 1:25000 O.S. base map by analysis of aerial photographs and by detailed field work.

1.5.2 Loch Lee

1.5.2.1 Setting

Loch Lee [NO 425 795] lies at an altitude of 272m OD in Glen Lee, at the head of Glen Esk, in the River North Esk drainage basin. It has a maximum length of 1.95km, breadth of 0.45km, surface area of 0.9km² and catchment area of 57.1km² (Lowe et al., 1991b). The water level of the loch was raised by 1m in 1962, by the construction of a small concrete dam, to increase the available domestic supply for the Brechin area. Loch Lee is surrounded by feldspathic and other gneisses and undifferentiated schists, locally permeated by granitic material (Barrow et al., 1904). It lies within the Dalhousie Estate, Angus.

1.5.2.2 Geomorphological map

1.5.2.2.1 Description

Geomorphological mapping undertaken during October 1990 (Figure 1.4) indicates that the majority of the steep slopes around the loch are either covered by thin soils with a relatively high angular boulder component or by bare rock surfaces (Plate 1.1). Precipitous rock surfaces occur intermittently above 400m. At the entrance of the Inchgrundle valley

angular boulders exhibit a lobate form, terminating at a break of slope within an undifferentiated till surface. The lobe substantially overlies the till surface (see Plate 1.1). The course of the principal influent to the loch, the Water of Lee, is flanked by an alluvial plain approximately 250m wide which extends for 2.75km from the head of the loch.

The lower slopes of the glen above Loch Lee are similar in nature to those surrounding the loch until the valley bears northward. At this point a hummocky till surface straddles the Water of Lee and an undifferentiated till surface is identified adjacent to the small tributary which enters the Water of Lee from the east. Terraced sand and gravel is recognised in the upper part of Glen Lee, both within and outwith the hummocky till surface in the extreme north of the area mapped. This hummocky till surface exhibits distinct upslope limits, particularly on the northern side of the glen.

The small lochan, Carloch, which occupies a steep, cliffed hollow approximately 150m above the floor of the glen is enclosed by till ridges. These features (Plate 1.2), which form four, broken, broadly concentric arcs 2-3m high, are continuous for a maximum of approximately 100m and enclose small ponds.

1.5.2.2.2 Interpretation and discussion

The geomorphological evidence is interpreted as indicating that, during the last glacial period in Glen Lee, a small corrie glacier existed on the upper slopes to the south west of Loch Lee. The outermost morainic ridge is believed to mark the maximum extent of the glacier as there is continuity of landforms across the slopes beneath the corrie. Former glacier activity is also apparent in the upper part of Glen Lee. A distinct terminal position is marked at the head of the glen, where the hummocky till surface terminates down-valley against what is interpreted as an outwash terrace, and against the valley sides by an upper limit to the morainic features. A glacier limit may exist further down-valley close to the confluence of the Water of Lee where a till surface and hummocky till are identified. The latter features can be explained in two ways, first, they represent a former maximum limit of the glacier identified up-valley, and secondly, they date from the last Devensian ice sheet.

Verification of either of these hypotheses must await either radiometric or relative dating.

The undifferentiated till surface at the mouth of the Inchgrundle valley is interpreted as dating from the Devensian glaciation due to the stratigraphic relationship of the overlying lobate boulder forms and the formless nature of the till surface. The remainder of the area, outside the limits proposed above, including Loch Lee, is interpreted as existing in the extra-glacial environment during the period of glacial activity.

Evidence from geomorphological mapping by Sissons (1972a) was interpreted to suggest that, during the Loch Lomond Stadial, Loch Lee remained unaffected by direct glacial ice input. The most proximal ice margin was approximately 1.5km from the loch shores and a valley glacier existed approximately 3km further up the glen, to the northwest. The findings in this thesis do not represent a substantial departure from the former glacier limits proposed for Glen Lee by Sissons (1972a), except in the possible former maximum extent of the Glen Lee glacier. Geomorphological evidence therefore implies that the Loch Lee basin was not directly influenced by glaciation during the last glacial phase, which is believed to have been the Loch Lomond Readvance.

1.5.3 Loch Callater

1.5.3.1 Setting

Loch Callater [NO185 840] is a natural, moraine dammed lake lying at an altitude of approximately 500m OD, close to the head of Glen Callater. The loch, which forms part of the Invercauld Estate, Aberdeenshire, drains into the Dee drainage basin and has a maximum length of 1.4km, breadth of 0.32km, surface area of 0.33km² and catchment area of 19km² (Lowe et al., 1991b). The water body and adjacent valley floor has been designated a National Nature Reserve due to the diversity of bird and plant life utilising the area. Loch Callater straddles a geological boundary between the Lochnagar Complex (granite, microgranite and granodiorite) to the north east and Gleann Beag Schist with felsite and epidiorite/amphibolite/hornblende schist units to the south west (Upton et al., 1989). The outlet of the loch runs across strata of Gleann Beag Limestone and Glean Beag Phyllite. The southerly inlet stream crosses Cairn of Claise Transition Psammite and

Graphitic Schist, Creag Leacach Quartzite and Glen Callater banded group semipelite with psammite and quartzite.

1.5.3.2 Geomorphological map

1.5.3.2.1 Description

Field research for the geomorphological map (Figure 1.5) was undertaken during September 1990 and indicates that two landform assemblages exist in Glen Callater. The first comprises hummocky and undifferentiated till surfaces within which terraced sand and gravel and an alluvial plain occur. Distinct upper till limits exist at the western and eastern extremes of the area mapped, forming lateral and terminal moraines. The lateral moraines can be traced from approximately 625m in the east to 460m in the west over a distance of approximately 4km. In the remainder of the area the margins are more diffuse. The hummocky till is concentrated on the lower slopes, surrounding the shores of Loch Callater (Plate 1.3) and damming the western end of the loch (Plate 1.4).

The second landform assemblage is composed of steep cliffed areas, particularly at the eastern end of the valley, with exposed or thinly till covered bedrock lying adjacent. A concentration of angular boulders occurs beneath the most westerly precipitous surface. Lower angle slopes do not exhibit medium or large scale landforms but are covered by thin soils with scattered boulders lying on the surface.

1.5.3.2.2 Interpretation and discussion

The glacial landforms identified in Glen Callater are interpreted as indicating the existence of a former valley glacier which terminated down valley at approximately 460m. It is suggested that the terraced sand and gravel deposits represent fluvio-glacial outwash deposited during the retreat of the Glen Callater glacier. The broad alluvial plain at the head of the loch is believed to be the result of the infilling of Loch Callater by deposition of sediment from the principal influent stream, the Allt an Loch. It is proposed that the upper slopes of Glen Callater, which are covered by distinctly different landforms from the lower slopes, were not covered by glacial ice when the Glen Callater glacier occupied the valley.

Thus the geomorphological evidence suggests that the site of Loch Callater was occupied by the Glen Callater glacier during the last period of glacial activity in the area.

The interpretation of this new, detailed geomorphological map does not differ from that made by Sissons and Grant, (1972).

1.5.4 Loch Muick

1.5.4.1 Setting

Loch Muick [NO 290 830] lies on the Balmoral Estate, Aberdeenshire, at an altitude of 400m. The loch, which has a catchment area of 34km² has a maximum length of 3.67km, breadth of 0.80km and surface area of 2km², drains into the Dee drainage basin (Lowe et al., 1991b) and is a National Nature Reserve. The water body occupies a steep sided glacially eroded trough cut into the Lochnagar Granite Complex (W. Ashcroft, pers. comm. 1991). The trough has a characteristically curved shape, apparently controlled by the geological structures within the Lochnagar Granitic Ring Complex (Oldershaw, 1974).

1.5.4.2 Geomorphological map

1.5.4.2.1 Description

Geomorphological mapping was carried out in Glen Muick during September 1990. The upper part of the glen around the shores of the Dubh loch is covered by undifferentiated till and hummocky till which extends down the valley towards Loch Muick. A small area of alluvium and a terraced deposit of sand and gravel occur at the extreme western end of the area covered. On the northern upper slopes, adjacent to the small lochan (Loch Buidhe), a morainic ridge and hummocky till surface are recognised. Formless till covers the steeper slopes between the Dubh Loch and Loch Muick and at the southern end of Loch Muick. The upper limit of till and lower limit of the boulder scattered slope can be identified at the head of Corrie Chash, which exhibits fine examples of hummocky till midslope below the till limit (Plate 1.5). At the southern end of the loch there is an alluvial plain. On the northwestern shore of Loch Muick a hummocky and undifferentiated till limit descends from 500m, close to the Glas Allt, to the

loch shore approximately 500m further down valley (Plate 1.6). Steep, boulder scattered slopes with poorly developed soils extend along this shore to the outlet. A small area of undifferentiated till exists close to the mouths of two minor streams.

The southern slopes adjacent to Loch Muick do not exhibit a sharp down valley limit to the extent of undifferentiated till. However, a thinning in the till depth, identified in the steep downslope gullies, occurs opposite the hummocky till limit on the northern shore. The tributary valley of the Black Burn, which enters approximately half way along the length of the loch, is covered by hummocky till on the lower and midslopes, which extends up the valley sides to a distinct lateral limit. On the eastern slopes of the Black Burn valley, till ridges are identified from a height of 500m descending to the shore of the loch. Northwest from this position the lochside slopes are identical in character with those on the opposite shore, with thin deposits of till at the base of the slope. The centre of the valley around the outlet is covered by a thick accumulation of peat.

1.5.4.2.2 Interpretation and discussion

The subaerial geomorphology in Glen Muick is interpreted as indicating the former existence of two valley glaciers. The larger extended down the glen in an easterly direction and terminated in the basin now occupied by Loch Muick. This glacier terminus is more easily defined on the northern slopes, extending over one third of the length of the loch. The second glacier debouched into the loch basin from the tributary valley of the Black Burn. Lateral limits extending to the loch shoreline indicate that the Black Burn glacier was probably never confluent with the main Glen Muick glacier if the maximum extent of both glaciers was reached contemporaneously.

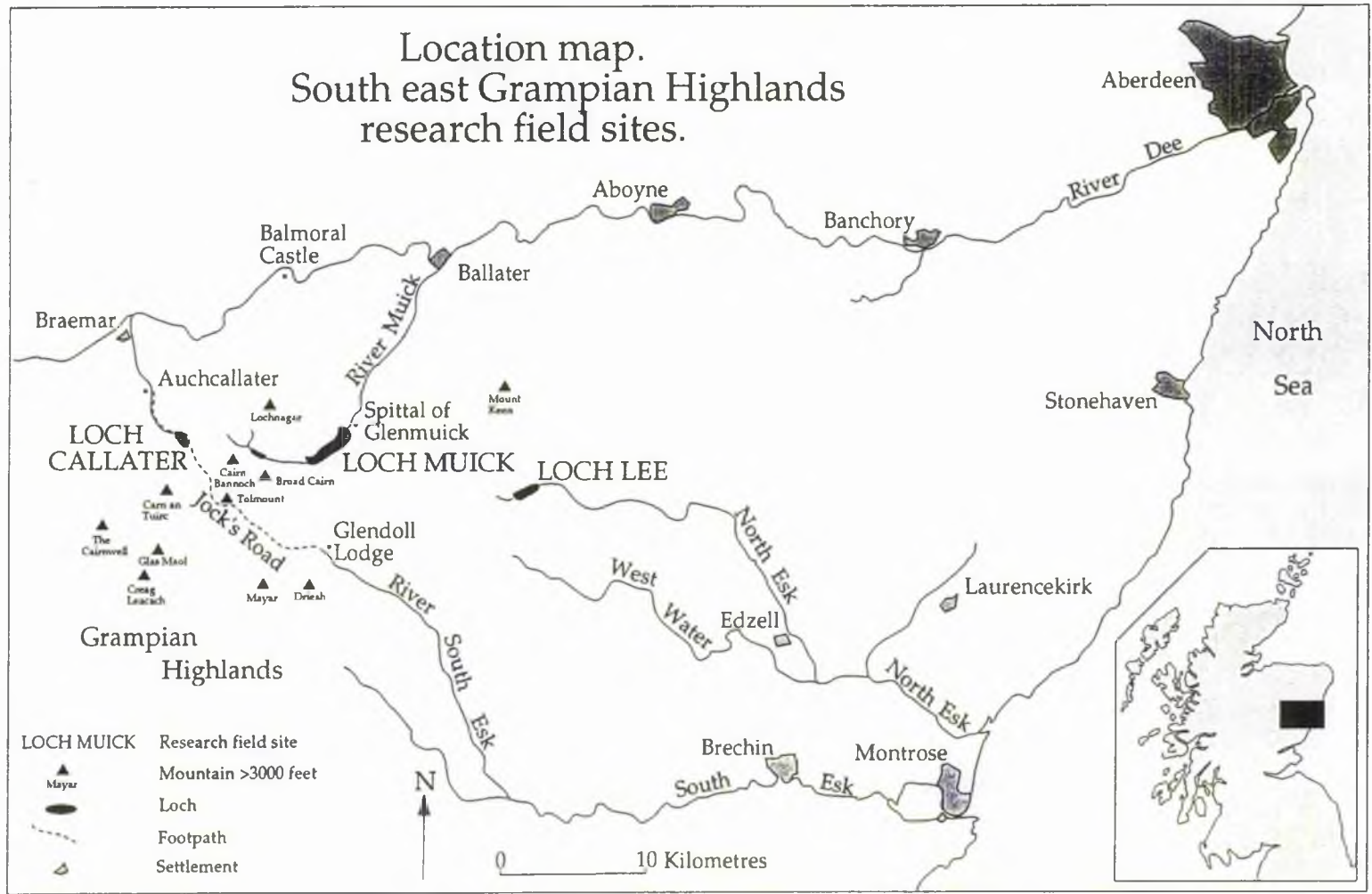
Two hypotheses are proposed to explain the existence of the thin till cover identified at the base of the slopes beyond the glacier limits proposed above:-

- i) The till was deposited during an earlier glacial phase.
- ii) The till was deposited by the glaciers identified above and subsequent erosion and mass movement processes on the steep trough slopes have redistributed the sediment.

The first hypothesis is believed to be more plausible given the geomorphological evidence from the Black Burn. If the Black Burn and Glen Muick glaciers reached their maximum limits contemporaneously and the Loch Muick basin was water-filled to approximately the current level, the Glen Muick glacier could not have extended beyond the Black Burn without destroying the lateral ridges which are present at that point. It should be emphasised that fluctuations in the loch water level are controlled by a broad peat covered ridge of sand and gravel at the northern end of the loch and there is no shoreline or sedimentary evidence of higher water levels. It is recognised that acceptance of this hypothesis requires several assumptions, which, given only the available subaerial evidence, cannot be verified or disproved. However, if either hypothesis be supported, the terrestrial geomorphology indicates that at least one ice margin crossed the Loch Muick basin and furthermore suggests that an investigation of the subaqueous environment is necessary to the understanding of the glacial history of this area.

The geomorphological map presented here, although similar in appearance to that of Sissons and Grant (1972) and Sissons (1972a), indicates that the interpretation of the landforms in Glen Muick can be considerably more equivocal than previously proposed. All three surveys reveal that at least one glacier partially covered the Loch Muick basin.

Figure 1.1



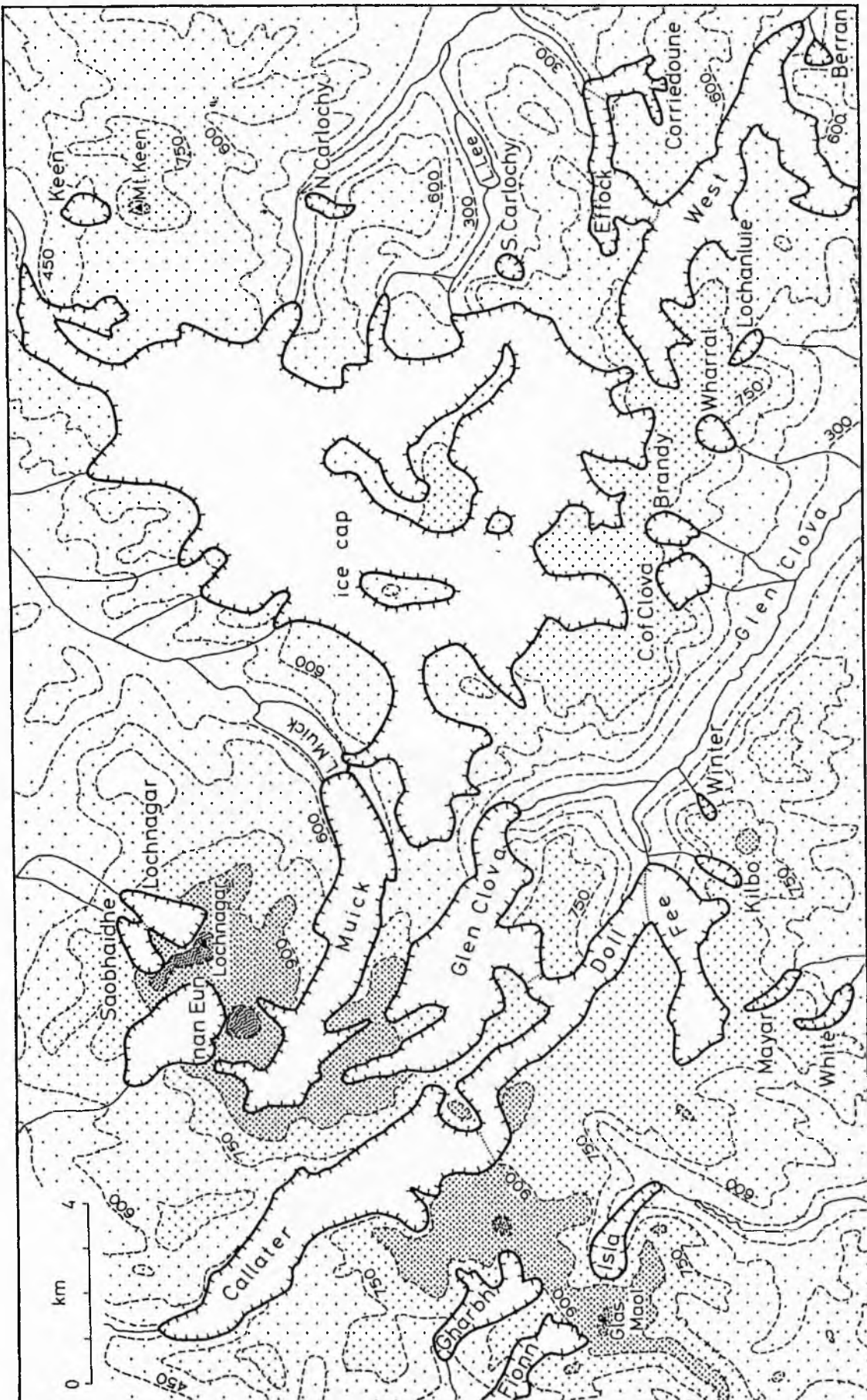


Figure 1.2 Former glaciers in the south east Grampians. Composite map of research undertaken by Sissons and Grant (1972) and Sissons (1972). After Sissons and Sutherland (1976).

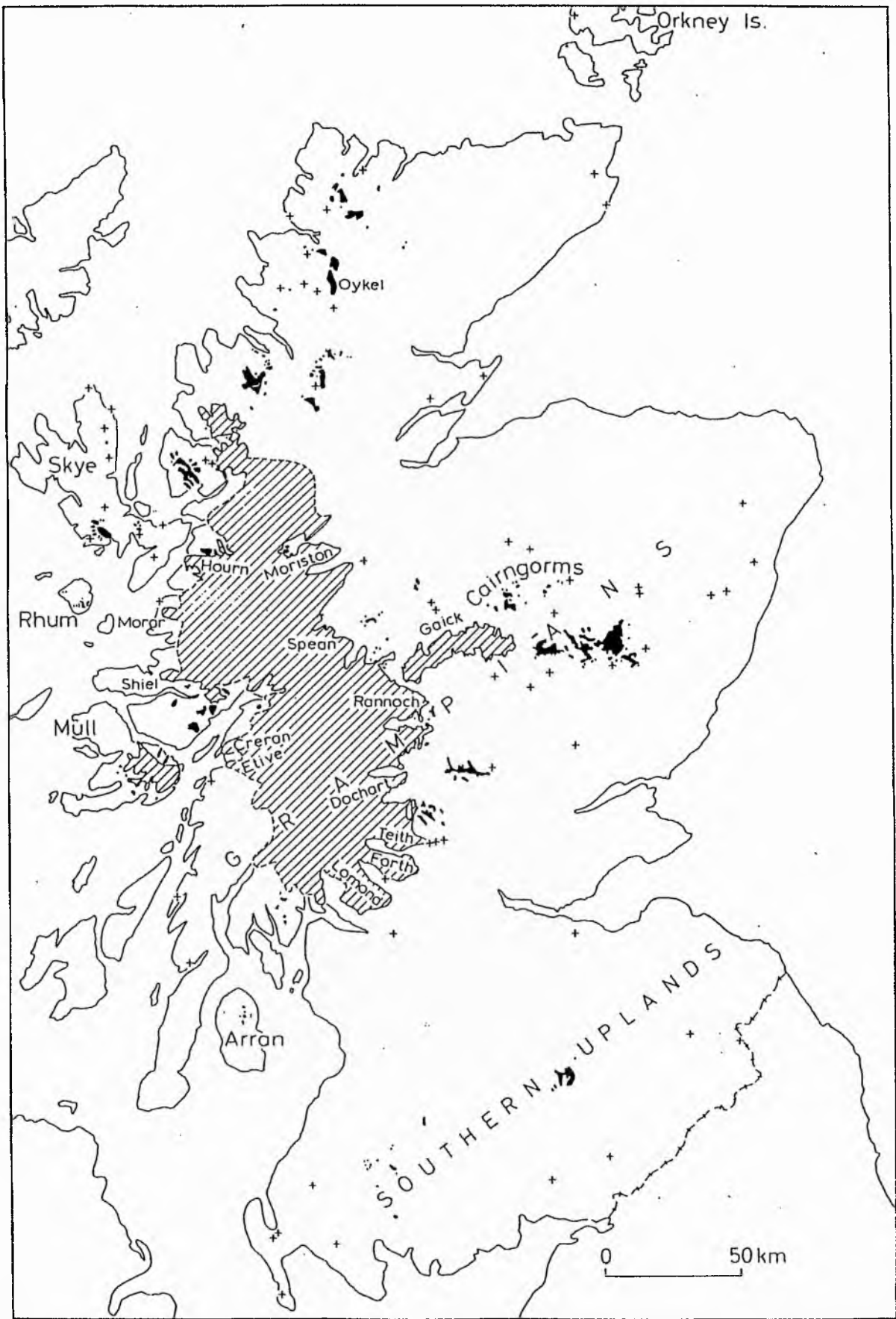


Figure 1.3 Area covered by the Loch Lomond Readvance glaciation in Scotland.

Crosses mark pollen sites indicating that glaciers did not reach that position.

From Sissons (1983).

GLEN LEE, ANGUS. Geomorphological map.

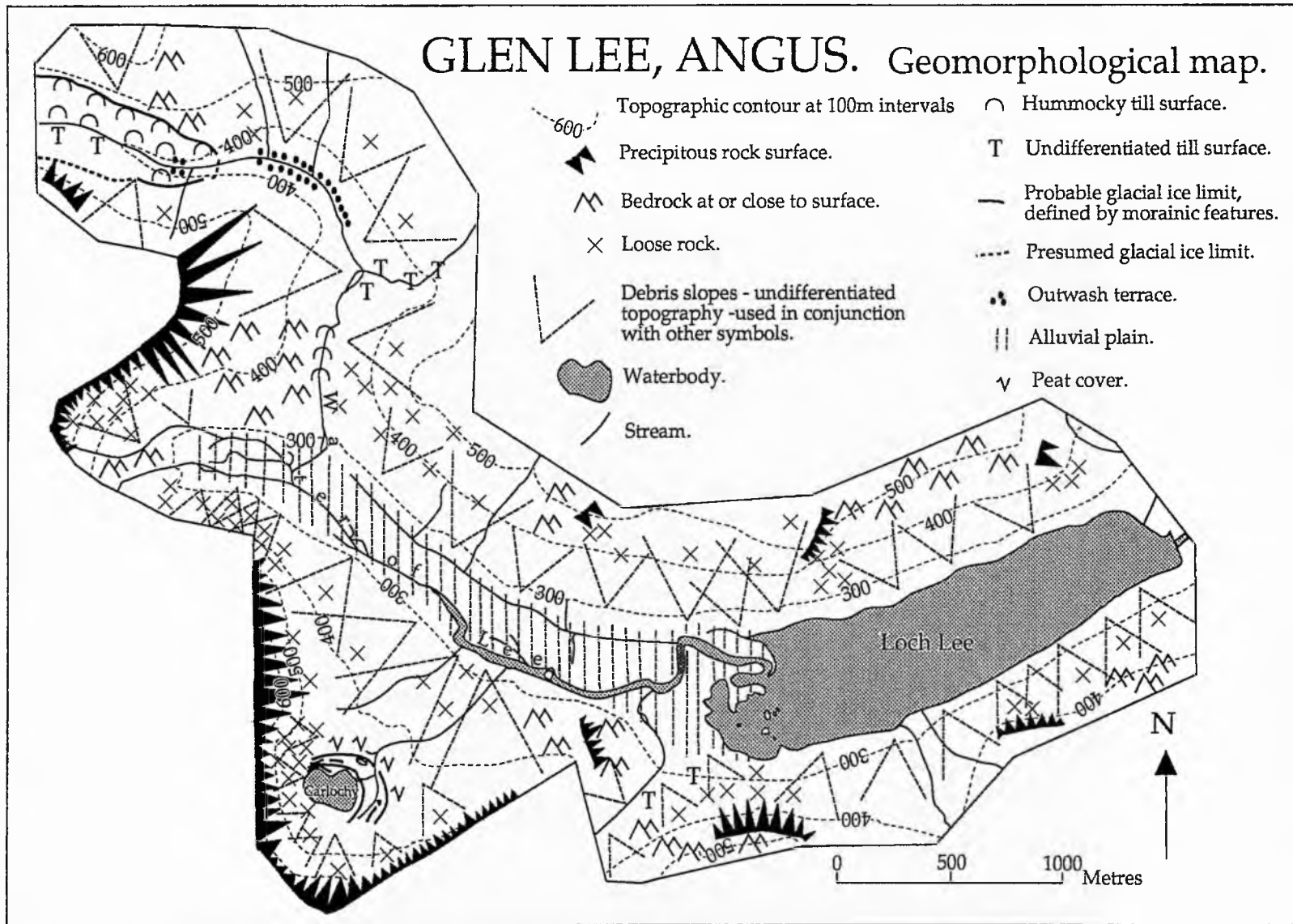


Figure 1.4
24

GLEN CALLATER, ABERDEENSHIRE

Geomorphological map.

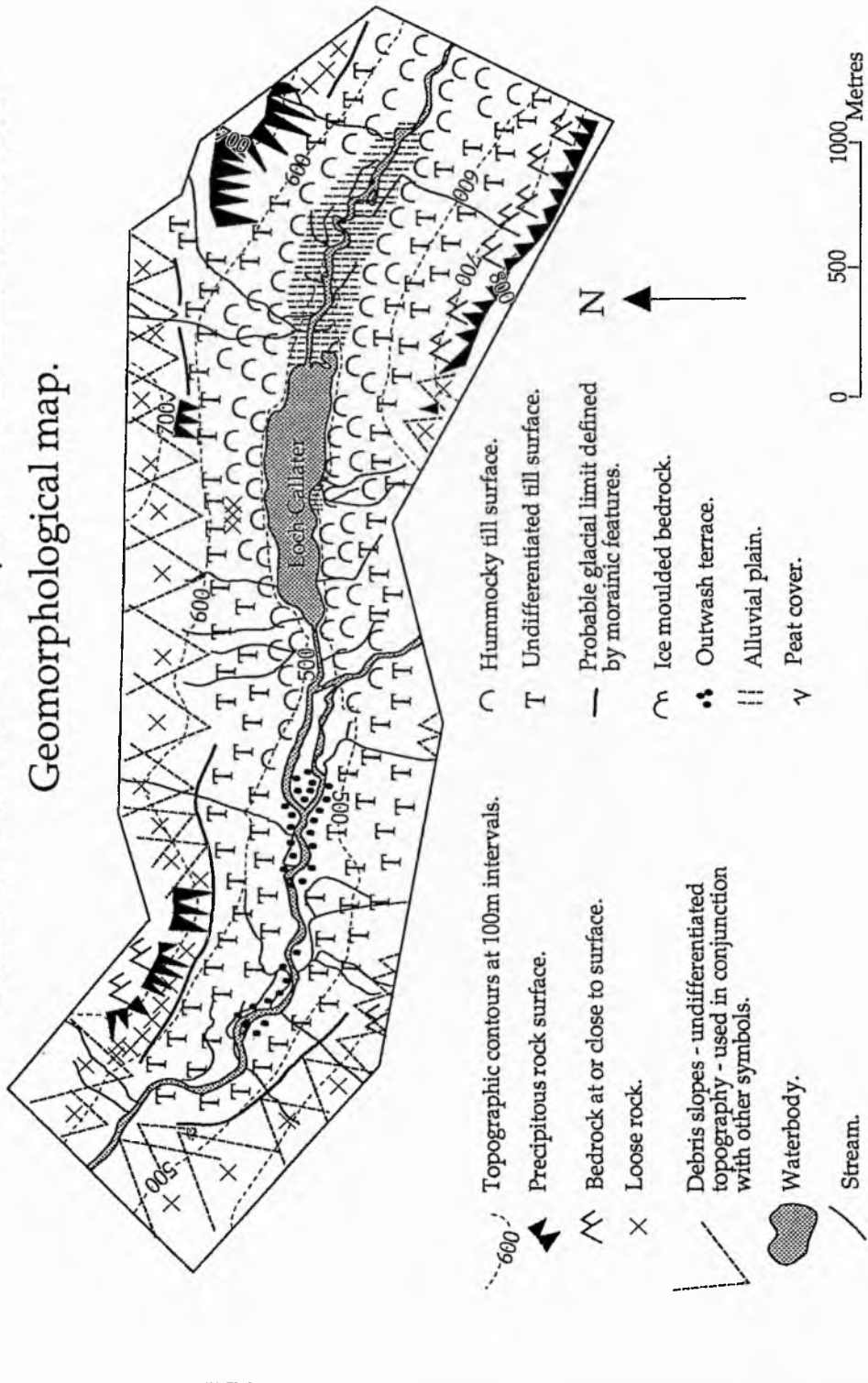


Figure 1.5
25

GLEN MUICK, ABERDEENSHIRE

Geomorphological map.

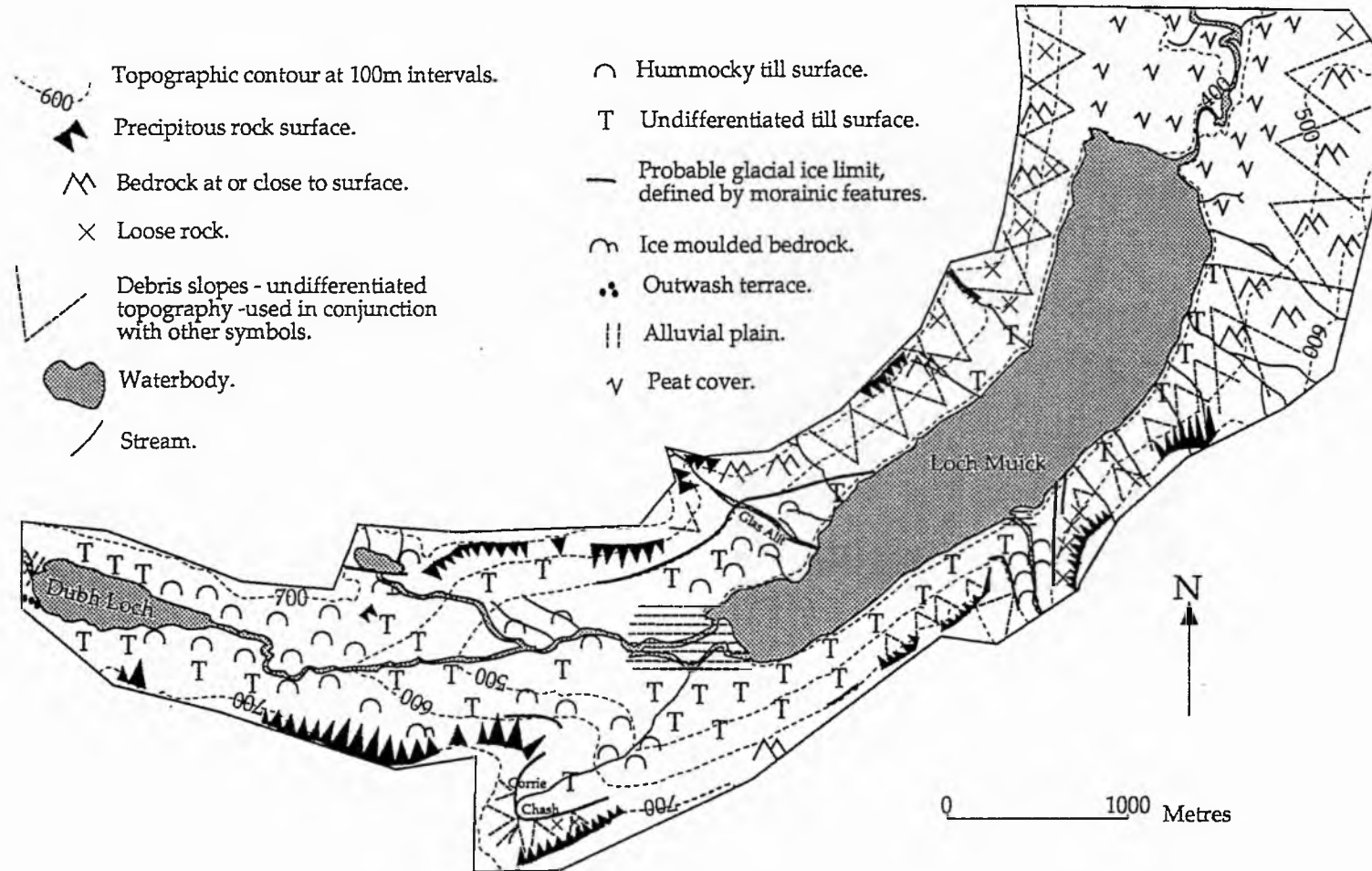


Figure 1.6
26



Plate 1.1 Glen Lee: View south west across Loch Lee up the valley of the Burn of Inchgrundle. Note the low-lying alluvial plain at the western end of the loch, the steep valley sides adjacent to the loch showing bare rock surfaces and a cover of angular boulders, the lobate form of the boulder deposit in the centre of the picture and the till surface extending up the Inchgrundle valley.



Plate 1.2 Glen Lee: End moraine ridges 2-3m high surrounding Carlochy. View northeast from within the glacier limit down Glen Lee.



Plate 1.3 Glen Callater: Hummocky till on the lower valley slopes surrounding the shores of Loch Callater. Note the gradational boundary into the undifferentiated till surface above the hummocky till. View southeast close to the outlet.



Plate 1.4 Glen Callater: Boulder-strewn hummocky till damming the outlet of Loch Callater. Note the evidence of estate management (burnt heather patches) in the background. View west from the survey boat.



Plate 1.5 Glen Muick: Loch Muick, December 1988. View to the south west. Corrie Chash can be identified in the centre of the Plate and hummocky till in the centre of this tributary valley. At the extreme left the mouth of the Black Burn valley joins Glen Muick and hummocky drift may be distinguished midslope. The main direction of ice flow was from the right fork in the valley, behind the plantation at Glas-Allt-Shiel.



Plate 1.6 Glen Muick: Down valley limit of hummocky till on the northern slopes above Loch Muick. The stream on the left of the Plate feeds the loch from the Dubh Loch. View south west from the survey boat.

CHAPTER 2

BATHYMETRIC SURVEYS

'Apart from inaccessibility due to remoteness from roads and high elevation, involving considerable loss of time before reaching these lakes, weather conditions at the site of the lakes may inhibit the work of sounding after they have been reached....the result is a serious addition to the time which should normally suffice for the work' (Seymour, 1939, p. 298).

2.1 INTRODUCTION

This Chapter provides a detailed description of the bathymetry of Lochs Lee, Callater and Muick. It reviews the development, applications and principles of echosounding. An account of the survey methods used in the lochs is given and a new bathymetric chart of each is presented. Zones of geomorphological variation within each water body have been identified and are described in detail. In the case of Loch Muick, in which the subaqueous geomorphology exhibits extreme diversity, a quantitative measure, Håkanson's form roughness (Rf) (1974) is applied. Comparisons are made between bathymetric charts derived from surveys undertaken of Lochs Callater and Muick in 1905 (Murray and Pullar, 1910) and the new charts presented here.

2.2 ECHOSOUNDING

2.2.1 Historical overview

Bathymetric surveying has been documented since the time of Herodotus (5th Century B.C.) when lead and line were used to sound safe channels through the shoals at the mouth of the Nile. Adaptations were made to the lead line during the Fifteenth Century whereby an apple or similar buoyant object was attached to a crescent shaped lead. When lowered to the sea floor the impact caused the apple to be released. The time

taken for the apple to surface was noted from which the depth of water was calculated. Marin Mersenne (1588-1648) reported that this technique overcame the possible oblique descent of the sounding line and consequent over-estimation of depth. So-called line-less sounding persisted in marine surveying until the early Twentieth Century advent of echosounding technology (see Deacon, 1971).

In inland waters, where the effects of currents and wave motion are less important, bathymetric surveys were conducted utilising the lead line technique. The *'Bathymetrical Survey of the Scottish Freshwater Lochs'* (Murray and Pullar, 1910) used a variant of the basic lead line, the 'F.P. Pullar Sounding Machine'. This comprised a series of pulleys, including a measuring device, from which a weight was suspended on a galvanised steel wire. The 'survey' resulted in the publication of 562 bathymetric charts in six volumes. Subsequent re-surveys of some of the lochs (e.g. Al-Ansari and McManus, 1980; Asaad and McManus, 1986; Duck, 1986) with recording echosounders has not revealed major differences between the two surveys. The Murray and Pullar project inspired a similar, small scale survey programme in Ireland (Seymour, 1939).

The foundations for acoustic profiling had been laid as early as 1827 by Colladon and Sturm in their experiments to determine the speed of sound in water. Fox Talbot (1833) suggested the possible 'Method of ascertaining the greatest depth of the ocean' by exploding a shell on the sea floor to propagate sound which could be heard at the surface. Further development of acoustic techniques for sea floor sounding was restricted by the lack of sensitive hydrophones and amplifying apparatus. In 1912 Fessenden built a machine to measure the time taken for sound waves to be reflected from the sea bed (see D'Olier, 1979), but it was not until the late 1920s that the first practical fathometer (echosounder), which operated with high frequency sound waves, was produced (Wood et al, 1935). An early use of a recording echosounder was in the study of the bathymetry of Lake Windermere (Mortimer and Worthington, 1940) and the principal Cumbrian lakes (Ramsbottom, 1976). More advanced echosounders have been used to survey some of the larger Scottish lochs (e.g. Kirby, 1971; Al-Jabbari et al., 1983; Al-Bayati and McManus 1984; Duck and McManus, 1985b).

Current developments in swathe bathymetry systems (Grant and Schreiber, 1990) combine some aspects of sidescan sonar (see Chapter 4) with echosounding. These systems produce data which can be displayed as either a graduated colour contour map or cross sectional profile.

2.2.2 Principles of echosounding

All seismic survey techniques utilise the principle that a stress applied to a substrate causes a proportional fluctuation in length or volume per unit. The amount of expansion on application of stress is quantified by elastic moduli: Young's Modulus (k) and the Shear Modulus (n). In the case of subaqueous seismic survey techniques, stress initiated at a point in the water moves through the water column as a longitudinal/compressional or P-wave. The movement of water particles occurs in the same direction as that of the initial pulse. Shear waves (i.e. normal to the pulse direction) are not transmitted through water. The speed at which the compressional waves travel, or propagation velocity (V) can be calculated using the equation:

$$V = \sqrt{\frac{k + \frac{4}{3}n}{\rho}}$$

where ρ = density of substrate

Reflection of compressional waves occurs when the wave encounters a variation in acoustic impedance (propagation velocity * density), such as the interface between water and sediment on the floor of a loch. The amount of energy reflected is proportional to the contrast in propagation velocity. This reflection coefficient is given by:

$$C_R = \frac{A_R}{A_I} = \frac{\rho_2 v_2 - \rho_1 v_1}{\rho_2 v_2 + \rho_1 v_1}$$

where

C_R = Reflection coefficient

A_I = amplitude of incident wave

A_R = amplitude of reflected wave

ρ_1, ρ_2 = densities of substrates of differing propagation velocity

v_1, v_2 = velocities of the substrates

The point at which reflection of the acoustic pulse occurs within the water and sediment column depends upon the frequency of the emitted sound. High frequency sound such as that in the range used by echosounders (12-200kHz) is rapidly absorbed and attenuated in sediments, therefore it is usually reflected from the upper sediment surface permitting precise measurement of water depths. However, in certain conditions, echosounders may penetrate low density bottom sediments such as liquid muds. Mortimer and Worthington (1940, pp. 212-213) cite an early example of this phenomenon:-

'The double echo seen on the records could be explained on the assumption that only some of the sound waves transmitted by the machine were reflected from the interface between mud and water, and that others penetrated the waterlogged deposits and were reflected by the harder glacial clay, or solid rock underneath.'

The time taken by the emitted pulse of sound to be reflected from the bed sediment to the water surface is known as the two way travel time. Given that the propagation velocity of fresh water is known to be 1483 ms^{-1} (Kaye and Laby, 1966), the actual depth can be calculated thus:

$$\text{Depth} = \frac{1}{2} vt$$

where

t = two way travel time

v = propagation velocity of water.

Echosounding apparatus comprises a transmitter which also usually doubles as the receiving transducer. Piezoelectric transducers convert electrical energy to a pulse of high frequency sound. On reflection the acoustic pulse is picked up by the receiving transducer, or a single transducer that automatically switches to receiver mode. The weaker return

signal is amplified to activate recording and display units. Echosounders can be calibrated according to the amount of dissolved solids present in the water. Thus the time taken for the acoustic pulse to be received after reflection is automatically converted to the actual water depth below the transducer. The data are displayed digitally, as a video display, or graphically, by the build-up of points drawn by a stylus on a moving drum carrying electro-sensitive or pressure sensitive paper. Water depth can then be read from this echogram and a correction factor applied to account for the submersion of the transducer.

2.3 METHODOLOGY: AIMS

A recording echosounder (Lowrance X-15M, operating frequency 192 kHz) was used in this study to undertake bathymetric surveys of Lochs Lee, Callater and Muick. The use of a high frequency sound pulse ensures the identification of the sediment-water interface even in areas of low density gelatinous mud (see section 2.2.2 above), which typifies the sediment of many loch floors (Duck, 1986). Thus a continuous depth profile, in metres, of the loch basin is produced along a given survey line. The aim of these surveys was to provide data for the production of a bathymetric chart of each loch basin. Although charts published by Murray and Pullar (1910) exist for Lochs Callater and Muick, evidence for a previous bathymetric survey of Loch Lee could not be traced in either Estate or Water Authority records (Invercauld Estate Office and Tayside Regional Council pers. comm. 1990). Thus the new charts, using modern echosounding equipment, provide four principal sources of information:-

- i) Maps of the underwater topography of each loch, permitting comparisons to be made between the basins.
- ii) Charts on which to base further seismic and sedimentological investigations; subbottom profiling (Chapter 3), sidescan sonar, (Chapter 4), surface sediment (Chapter 5) and coring (Chapter 6).
- iii) Indications of the volume and rate of sedimentation that has occurred in Lochs Callater and Muick between the 1905 and present surveys.

2.4 LOCH LEE

2.4.1 Bathymetric survey and chart compilation

The echosounder survey of Loch Lee was carried out in November 1989 using a hull-mounted transducer from the motor-propelled R.V. Mya (Plate 2.1) which has a draught of 1m. This vessel was used on Loch Lee for all the surveys undertaken in this research. Boat positions throughout the survey were precisely established using Motorola Mini Ranger MkIII radio position fixing apparatus. This comprises two radio beacons and an onboard receiver. The beacons were placed on tripods at accurately identified positions on the Ordnance Survey 1:10000 scale map. The sites of the beacons were chosen so that the angle of intersection of the radio waves emitted was close to 90° to minimise potential uncertainty of position which results from low angle intersection. To ensure complete radio wave coverage of the loch it proved necessary to re-position the beacons during the survey. The onboard aerial receives the signals from both beacons and the distance in metres from each is continuously displayed on a control console. Polar co-ordinates could then be computed from these distances.

Echosounding traverses were run along and across the loch at a boat speed as near constant as possible of 1.5ms⁻¹. A total of 39 traverses were completed over 21.91km of the 1.95 km long, 0.45km wide loch (Figure 2.1). Event marks were made on the echograms at the start and finish of each traverse, and at intermediate points of morphological interest. A total of 449 precisely defined sites of known depth were recorded. Intervening depths were interpolated from the continuous echograms where necessary.

The depth of submersion of the echosounder transducer was measured by bar check. At the completion of the survey a metal bar approximately 1.5m long was lowered beneath the echosounder transducer on a graduated rope whilst the boat was held stationary. The echosounder was activated resulting in a reflection from the bar appearing on the echogram. The length of rope paid out was noted and the difference between the actual depth of the bar measured by the rope and that recorded on the echogram was calculated.

Depth data were extracted from the echograms by means of a Tectronix 4956 digitiser. A correction factor of +1.0m, derived from the bar check was added to each measurement. To plot the data a grid of concentric circles emanating from the positions of each of the radio beacons was drawn on a 1:10000 scale base map. The position of each known depth point was then plotted using polar co-ordinates. Points for which radio position fixing was not available and where topographical variation occurred were plotted using the transformation technique (Håkanson, 1981). The bathymetric chart was constructed by manual drawing from the depth data on an overlay. Throughout this manual drawing stage continual reference was made to the original echograms to ensure accuracy. A contour interval of 1m was selected to highlight the small scale topographic variations apparent on the echograms and to facilitate comparison with the charts previously constructed during this research programme from Lochs Muick and Callater. Over those parts of the loch floor where slope angles were steepest or where topographic variation was great it proved impossible to complete the bathymetric chart at a 1m contour interval by manual drawing methods. Therefore it was decided to complete the data reduction and present the chart using a computer graphics package.

The incomplete chart was divided into six pieces which were individually scanned into the Adobe Illustrator '88 software package for the Apple Macintosh P.C. These pieces appeared as 'templates' on screen and were over-drawn using the 'freehand draw' tool of the package, operated by the mouse. This facility, used in combination with the 'magnify' tool (which allows temporary enlargement of parts of the artwork), enabled the insertion of contours in the areas of steepest slopes where manual drawing had been impossible. All the pieces were joined in the program and the completed bathymetric chart (Figure 2.2), contoured at 1m intervals, was printed on a Varityper VT600 laser printer.

2.4.2 Bathymetric chart description

Loch Lee occupies a single basin with a maximum determined depth of 30.8m. For descriptive purposes it can be subdivided on the basis of geomorphological variation into three zones (Figure 2.3):-

Zone 1 Southwestern Shallows

Zone 2 Central Trough

Zone 3 Northeastern Shallows

For ease of description a verbal classification of loch floor slope angle ranges has been used in the description of all three lochs:-

Sub-horizontal	0-1°
Very low angle	2-3°
Low angle	4-6°
Moderate	7-11°
Inclined	12-15°
Steep	16-20°
Very steep	21-25°
Extremely steep	>26°

2.4.2.1 Zone 1 Southwestern Shallows

The southwestern end of Loch Lee comprises an area of 20.4ha with a maximum depth of 3m. The 1962 reservoir impoundment (see section 1.5.2.1) resulted in a 1m rise in water level and an increase in area of this zone of at least 15.3ha. This 'new loch' is characterised by dense aquatic and semi-aquatic plant growth, some of which has colonised the six small islands in the extreme southwestern corner of the loch. Consequently boat access in the shallowest parts of this area was not possible and the 1m contour was drawn through visual inspection from the boat, shores, and aerial photos.

The loch floor is sub horizontal in this zone, the steepest slope angle is attained in the centre of the loch close to the inlet of the Water of Lee. The boundary with Zone 2 is gradational on the northern and southern slopes, but clearly defined in the central loch area.

2.4.2.2 Zone 2 Central Trough

The Central Trough Zone covers an area of 50.1ha. It forms a steep sided, elongate basin. The maximum depth determined, 30.7m, occurs in the northeastern trough, at the base of the northwestern slopes. The boundary between Zones 1 and 2 is marked by a sharp break in slope from sub-horizontal to inclined at a water depth of 2m in the centre of the loch. Low angle slopes occur between water depths of 13 and 25m. Below 25m the loch floor is sub-horizontal, sloping down towards the southwestern trough.

The southern slopes of Zone 2 are irregular in form. Four hollows with a maximum depth of 5m below the surrounding loch floor can be identified at the extreme southwestern end of the zone. They are situated at a depth of 13-18m at a break in slope from steep to low angle loch sides. Two mounds with maximum heights of 2m and 5m respectively above the adjacent loch floor can be identified within Zone 2. The southwestern mound, situated at a water depth of 24m is of irregular form. The maximum slope angle (inclined) is orientated towards the southwestern trough, with a moderate angle tail extending upslope in a southwesterly direction.

Between the Burn of Duchrey and the adjacent, unnamed stream, precipitous slope angles occur locally. However, moderate upper slopes to a depth of 10-14m and very low angle to low angle lower slopes are more typical of the southern slopes of Zone 2.

The northern slopes have a more regular form than the southern slopes and fall within the moderate slope angle range. The highest angle (steep) slope is attained close to the boathouse. Two minor mounds with a maximum amplitude of 3m above the surrounding floor are located on moderate slopes at the northeastern end of the zone.

The boundary with Zone 3 is gradational at the loch shores, but is marked by a break in slope from moderate to low angle in the centre of the loch.

2.4.2.3 Zone 3 Northeastern Shallows.

Zone 3 is characterised by a number of small mounds situated on a gently sloping floor. This zone has a maximum depth of 10m at the boundary with Zone 2. The northeastern end of Loch Lee has very low angle sides on the northern slope and low angle slopes on the southern side to a break in slope at 6m or 7m depth. Below the break in slope the loch floor is sub-horizontal. It is on this surface that four minor mounds occur. These range in amplitude between 1m and 2m above the adjacent loch floor. Two mounds are located at depths of 6m and 7m on the southeastern side of the loch. The more westerly of these two mounds (Figure 2.4) has a pointed summit, identifiable on two intersecting echograms, rising to 5m below the water surface. The other mound is flat-topped over an area of approximately 400m² in a water depth of 4m (Figure 2.5). Minor hollows, with amplitudes of approximately 1m, are distributed throughout the sub-horizontal loch floor.

2.4.2.4 Hypsographic curve

A hypsographic (depth-area) curve was drawn for Loch Lee (Figure 2.6a). The curve is of a convex nature which indicates that the lake has gently sloping sides and a small area of deep water (Håkanson, 1977). Loch Lee has an extensive area of shallow water - 50% of the surface area overlies water with a maximum depth ≤ 6 m. Steeper slopes are associated with water depths of 16-25m which have a surface area of only 12% of the total area. Deep water (>25 m) covers 13% of the loch floor, highlighting the essentially flat bottomed form of the deepest part of the basin.

2.5 LOCH CALLATER

2.5.1 1905 BATHYMETRIC SURVEY

2.5.1.1 Introduction

Loch Callater was surveyed on 11 July, 1905 by T.N. Johnston and L.W. Collet, as part of the '*Bathymetrical Survey of the Scottish Freshwater Lochs*' (Murray and Pullar, 1910). Evidence from this chart suggests that nine traverses were run across the loch and 52 depth soundings were taken (Figure 2.7).

2.5.1.2 1905 Bathymetric chart description

According to the surveyors, Collet and Johnston (1906), Loch Callater (Figure 2.7) is:-

'A small, narrow, loch....at an elevation of 1625 feet. Its length is 0.84 mile and the maximum depth recorded is 29 feet.' (p.110)

It 'Trends in a north-west and south-east direction, and is nearly a mile in length....the superficial area being about 73 acres, and the drainage area nearly 8 square miles.' (Murray and Pullar, 1910, p. 146)

However, on the bathymetric chart and in Murray and Pullar (1910), Loch Callater is quoted as having a maximum depth of 30 feet (9.1m) 'Observed near the middle of the loch, but towards the south-western shore' (Murray and Pullar, 1910, p. 146). At the extreme southeast end a small island and marshy area, close to the mouth of the Allt an Loch, are recorded. Marsh is also indicated near the stream influent from the southwestern slopes. The loch sides are steepest close to this stream and against the opposite bank. Murray and Pullar (1910) note that:-

'The floor of the loch shows one or two slight irregularities, but on the whole the basin is simple in conformation.' (p. 146)

2.5.2 Bathymetric survey and chart compilation

The resurvey of Loch Callater was carried out in September 1989. Due to problems regarding access and the shallowness of the loch, it was necessary to use an inflatable dinghy for this and all other surveys, which imposed some restrictions. The echosounder was operated with a rod-mounted transducer at the stern of the boat. Position fixing, however, could not be carried out safely using the 240 volt A.C. powered Motorola Mini Ranger in the space available onboard. Therefore boat positions were fixed by dead reckoning along traverse lines between accurately defined end points. These were measured at 50m intervals by two field assistants each on opposite shores of the loch. Traverses run between the two markers on a progressive basis from northwest to southeast along the loch provided the basis for the survey. Traverses along the length of the loch could not be constrained in such a manner. However, accurate determination of the position of end points was possible. The survey could not be completed at the southeastern end of the loch due to the occurrence of sandy shoals and dense aquatic weed growth. A total of 12.6km of traverses were run along and across the 1.40km long loch (Figure 2.8).

The data were processed as in section 2.4.1, above. Depth points were corrected by the addition of +0.70m (the depth of transducer submersion) and plotted using the transformation technique (Håkanson, 1981) from traverse end points marked on a 1:10000 Ordnance Survey map. The long traverses were tied in where necessary to the across-loch traverses. No discrepancies in the data were encountered. The bathymetric chart (Figure 2.9) was drawn manually on an overlay. The final version was reproduced in the same manner as for Loch Lee using the Adobe Illustrator '88 package for the Apple Macintosh P.C.

2.5.3 Bathymetric chart description

The new bathymetric chart of Loch Callater presented here (Figure 2.9) is based on a significantly higher level of information than that of Murray and Pullar (1910). A total of 40 continuous cross traverses and four longitudinal traverses were carried out during the

1989 survey, whereas only 52 depth points over nine traverses were used to construct the 1905 bathymetric chart (Figure 2.7).

The loch is naturally divided into two basins, the northwestern and northeastern basins, which provides a suitable framework for descriptive purposes.

2.5.3.1 Northwestern Basin

This small basin with an area of 5.0ha underlies 14% of the surface area of Loch Callater. The basin slopes are low to very low angle and uniform to a depth of 3m. Below a depth of 3m inclined slope angles occur on the southern slope to a depth of 9m. A further break in slope occurs at this depth beneath which very low angle slopes descend to the lowest point of the trough at 9.7m. Three minor, unnamed streams enter the loch within the northeastern basin.

The boundary between the northeastern and northwestern basins is marked by a ridge rising to 5m below the water surface in the centre of the loch. This feature is less well defined on the flanks of the loch in water shallower than 5m (Figure 2.9).

2.5.3.2 Northeastern Basin

Occupying an area of 25.3ha, the northeastern basin forms the remainder of the loch. The transverse profile of Loch Callater within the basin becomes sharply asymmetric and the maximum determined depth (11.1m), occurs at the base of the southwestern slopes.

The northeastern slopes are typically of low angle and are irregular in form. A hollow, 2m deep, is located on the northeastern slope on the upper part of the boundary ridge. The ridge curves in an up-glen direction at a depth of 2-3m for a distance of 25m before recurving down valley in the centre of the loch. Several minor spurs are identified on the northeastern slopes, one spur close to the deepest trough. Further eastwards a spur divides an 8m deep basin in half, and an adjacent spur, 60m long and orientated down valley, occurs at a depth of 5m. A hollow and a mound (amplitude 2m) occur in the central tract of the northeastern slope.

The loch slopes curve towards the southwest, 200m from the head of the loch. The remainder of the loch, southeastwards from this point is very shallow with a maximum depth of 2m in the centre. Aquatic weed growth is very dense in this area and may be identified on echograms (e.g. Figure 2.10) as the poorly defined, 'feathery', section of the profile. At the head of the loch formation of a spit by sand deposition is taking place at the mouth of the inflowing Allt an Loch. A very shallow, lagoonal area (strath lochan, Murray and Pullar, 1910), with an estimated maximum depth of less than 0.5m, is located on the floodplain of the Allt an Loch.

The southwestern slopes of Loch Callater are more uniform, with higher slope angles at the western end of the basin. The exception to this occurs offshore from point 'A' (Figure 2.9) at the southern end of the loch. Here a narrow, symmetrical ridge 25m wide, extends 113m into the loch and can be traced to a depth of 4.5m below water level. This ridge appears to be a continuation of the smaller feature on the northeastern slopes. It is flanked by two hollows, lying 1m and 2m below the adjacent loch floor, on the southeastern side.

Westwards from the ridge a small islet of boulders and cobbles, rising no more than 0.5m above the water surface, occurs in shallow water, close to the loch shore. The slopes in this area are low angle, extending down to a trough at a depth of 8.5m. Close to the more westerly, forked stream, the slope characteristics change. Two breaks in slope, from low angle to extremely steep, occur close to the mouth of this unnamed stream. West of the stream the upper break in slope is replaced by inclined loch sides that extend, with minimal variation in gradient, to the deepest determined part of the loch at a depth of 11.1m (Figure 2.11). The deepest point in Loch Callater occurs close to the southwestern shore within part of a rounded basin. Westwards from the deepest basin the asymmetric profile of the loch becomes less pronounced, gradational change occurring to an almost symmetrical profile at the boundary between the northeastern and northwestern basins. At the base of the southeastern slopes, and on the very low angle central floor, numerous minor hollows and mounds occur.

2.5.3.3 Hypsographic curve

The hypsographic curve (Figure 2.6b) drawn from the echosounder depth data, shows that Loch Callater has gently sloping sides and a small area of maximum depth (Håkanson, 1977) (depths >10m are considered to be deep in the context of Loch Callater). 60% of the surface water area of the loch overlies water with a maximum depth ≤ 2 m. Slightly steeper slopes occur between depths of 2m and 6m, which occupies approximately 22% of the surface area. Between depths of 6m to 10m, <8% of the surface area occurs, indicating that there are significantly steeper slopes at this depth. Approximately 10% of the surface water area overlies water with a depth of 10m to 11.1m, signifying that the deepest part of Loch Callater is essentially flat bottomed.

2.5.4 Comparison of the bathymetry 1905-1989

Prior to any comparisons between the two surveys, the differences in methodology, chart production and final chart presentation should be reiterated. It is primarily for these reasons that the two bathymetric charts, which appear to be similar at an initial overview, reveal five significant differences on closer inspection.

i) The 1905 chart shows Loch Callater to be a single basin. The 1989 chart reveals the existence of two basins.

ii) The 1905 chart shows a maximum depth of 9.1m at the base of the southeastern slope near to the mouth of a small stream. The 1989 chart has a maximum determined depth of 11.1m located within 50m of the deepest point identified in the 1905 survey. However, different datum levels were used by the survey teams. Due to the long distance from a benchmark, the 1905 survey team based their depth measurements on a spot height of 1625 feet (493m). This survey was undertaken in July when the water level of Loch Callater is likely to have been below its maximum level. The 1989 survey datum of 500m was based upon the Ordnance Survey 1:10000 map, which gives a top water level at 500m O.D. At the time of survey the loch water level was abutting the small (0.5m) cliffs around the shore, at its maximum level. The distance from the nearest benchmark (>5km) rendered levelling of the water surface impracticable in the time available. Thus it is suggested that

the 2.3m difference in maximum depth obtained by the two surveys is only partially due to seasonal variation in the water level of Loch Callater, the significant factor being the differences in datum level.

iii) The 1905 chart shows a single island and marshy area at the inflow of the Allt an Loch. The 1989 survey shows that the island is now joined to the shore by a spit (tombolo), and the marshy area has been enclosed by spit aggradation to form a strath lochan (area 0.4ha) with a narrow channel to the open water.

iv) The 1989 survey shows an area with a sharply asymmetric profile. This is not apparent on the 1905 chart.

v) A wide diversity of geomorphological forms can be identified on the new chart which are below the limit of resolution of the 1905 survey.

The only significant variation attributable to geological change between the 1905 and 1989 surveys is the development of a tombolo and strath lochan at the extreme southeastern end of the loch (Plate 2.2). An area of approximately 0.4ha has built up in the 84 years between the two surveys. This represents an average reduction in water area of 50m² per annum. The volume of accumulated sediment cannot be estimated due to the low level of depth data obtained from this area. The existence of the alluvial plain at the southeastern end of the loch was commented on by Collet and Johnston (1906, p. 110):-

'At the head of the loch is a large alluvial tract, which evidently at one time formed part of the lake....Indeed the loch is destined to disappear in the future.'

A very crude estimate of the time required for complete infilling of Loch Callater to occur at the present average rate of 50m² per annum would be approximately 6000 years. The data available, however, enable only a preliminary estimate of the rate of aggradation to be made. In the future, the rate of decrease of the surface area of Loch Callater can be expected to reduce as the delta and alluvial plain advance towards the deepest part of the loch.

Due to the differences in survey techniques and bathymetric chart production, an estimate of the rate of sedimentation for the remainder of the loch could not be made.

Analysis of the sounding positions and spot depths on the 1905 chart could not identify any one very low or low angle area where the depths measured were in close or near agreement. The 1905 chart exhibits depth soundings in the central loch areas persistently 1-2m shallower than those determined by the 1989 survey. It is suggested that this phenomenon may be due to the technique of even distribution of depth soundings along the survey line during the production of the 1905 chart, and the difference in datum level.

2.6 LOCH MUICK

2.6.1 1905 Bathymetric survey

2.6.1.1 1905 Introduction and methodology

Loch Muick was surveyed on 8 July 1905 by T.N. Johnston and L.W. Collet as part of the wider '*Bathymetrical Survey of the Scottish Freshwater Lochs*' (Murray and Pullar, 1910). The survey of the loch, undertaken using the 'F.P. Pullar Sounding Machine', comprised 87 depth measurements taken along 12 traverses, 11 across the loch, and one along the long axis. The chart (Figure 2.12) was produced by placing the depth soundings at equal distances along the traverse line, 'Thus distributing any errors' (Murray and Pullar, 1910, p. 14).

2.6.1.2 1905 Description of the bathymetry

The bathymetry of Loch Muick (Figure 2.12) has been described by Collet and Johnston (1906), who also suggested the mode of formation of the basin, and by Murray and Pullar (1910). The deepest sounding of 256 feet (78m) was obtained in the centre of the trough, northeast of the mouth of the Black Burn. The basin was described as being:-

'Simple in conformation, the shores sloping on all sides to the deepest part of the loch' (Murray and Pullar, 1910, p. 147),

However, the 'sinuous' 50 feet and 100 feet contours were attributed to fluvial deposition. Fluvial processes associated with the Glas Allt were also identified as:-

'Forming a big delta which is extending into the loch' (Collet and Johnston, 1906, p.108).

In cross section the basin slopes appear to be steep with an indication of submerged ledges on the southeast side. The longitudinal section shows gentle shallowing in the southwest towards the influent Allt an Dubh-loch, whereas at the northeastern end a gently sloping shelf extends for 740m into the loch. This platform falls to a depth of 23m, before an abrupt increase in water depth to 61m. Hypsographic (depth-area) data for Loch Muick led Collet and Johnston (1906, p. 108) to conclude:-

'Indeed the bottom of Loch Muick is a very flat one.'

2.6.2 1989 Bathymetric survey and chart compilation

The resurvey of Loch Muick was carried out in April 1989 using the same methods and equipment as described in section 2.4.1 above. R.V. Mya was used in this, and all other surveys subsequently undertaken on Loch Muick. In total 70 traverses were completed, covering a distance of 54.78km on the 3.67km long, 0.80km wide loch (Figure 2.13). 817 precisely defined sites of known depth were determined, between which intervening depths could be interpolated from the echograms. Owing to the density of data gathered, the original 1:10000 Ordnance Survey map was enlarged to a scale of 1:5750 for plotting purposes. The position of each sounding was plotted as in section 2.4.1. A contour map was constructed from this information, combined with continual reference to the original echograms. Initially a contour interval of 10m was chosen (Figure 2.14). However, it became apparent that a significant proportion of the geomorphological variation recognised on the echograms fell below this resolution. The surrounding subaerial geomorphology, mapped by Sissons and Grant (1972) and Sissons (1972a), is typically of an amplitude of less than 10m. A contour interval of 1m was deemed necessary, therefore, to describe the complex bottom morphology indicated. To enable comparison between this and subsequently constructed charts the same contour interval was used for all three charts.

In order to scan the completed 1m contoured hand drawn chart into the Adobe Illustrator '88 package for the Apple Macintosh P.C. it was subdivided into 30 segments, scanned individually into the program. Each segment then appeared on screen as a 'template' over which the contour lines were drawn. Blocks of six completed segments were joined together in the program, and printed by a Varityper VT600 laser printer. Due to the extreme complexity of the chart, the memory capacity of the computer was not sufficient to allow complete joining of all 30 segments simultaneously. In consequence, five pieces of six joined segments with large areas of overlap were joined by the traditional cut and paste technique. The complete chart was photographically reduced to its final form (Figure 2.15).

2.6.3 Bathymetric chart description

Visual inspection of the new bathymetric chart of Loch Muick (Figure 2.15) has enabled the identification of four distinct zones of geomorphological variation (Figure 2.16).

2.6.3.1 Zone A

Zone A is characterised by gently sloping sides, descending to a maximum depth of 38.4m in a trough at the base of the southeastern slope. The loch profile is asymmetric in this basin, low angle northwestern slopes descending to a break of slope at 20m where a steep slope is attained. The southeastern slopes fall within the steep slope angle range (see section 2.4.2).

At the extreme southwestern end of Loch Muick, close to the southern inlet of the Allt an Dubh-loch, a very low angle spur extends for 86m into the loch to a depth of 5m, where a sharp break to extremely steep slope angles occurs. Below this slope low angles obtain, shelving to the deepest part of the basin. Surrounding the northern inlet of the Allt an Dubh-loch a shelf at a depth of 1m below the water surface extends for 75m into a small embayment in the loch and terminates at a steep slope.

The boundary between Zones A and B is formed by a ridge with a maximum amplitude of 12m above the surrounding topography. The ridge can be identified on the northwest slope to a depth of 45m (upper slopes identifiable on an echogram, Figure 2.17) and ends at an extremely steep slope 200m offshore. A small island lying 30m from the northwestern shore forms the upper part of the dividing ridge. There is an indication of a corresponding subdued ridge on the southeastern slope where a 75m wide spur can be traced from 10m to 23m below surface.

2.6.3.2 Zone B

Zone B lies north of the dividing ridge and comprises an area of mounds and hollows concentrated in the central trough of this section of Loch Muick. This can be seen in the original echograms (e.g. Figure 2.18). The western 200m of this zone shows a concentration of 11 of these features, each with a positive or negative relief of up to 8m above or below the adjacent loch floor. The eastern part of Zone B consists of a 200m wide, low to very low angle floor descending to 67m with a step 7m high. The basin of Loch Muick has an asymmetric profile (e.g. Figure 2.19), with very steep southeastern slopes and an inclined northwestern side. The loch slopes are frequently irregular, expressed as sinuous contours, especially in the middle and lower slopes. Two distinct spurs occur on the northwestern slope. One is a symmetrical ridge, identifiable from a depth of 17m-28m projecting into the area of dense geomorphic variation. The other is located close to the boundary between Zones B and C. It can be recognised on the echogram (Figure 2.20) and can be traced on the bathymetric chart between 31m and 47m.

The eastern 450m of Zone B exhibits a line of seven mounds and hollows on the southeastern side of the basin floor extending as far as the bounding ridge. One mound, 7m high, which lies 80m from the mouth of the Glas Allt, occurs below a break in slope from steep to low angle on the upper slopes .

2.6.3.3 Zone C

Zone C contains a series of up to six ridges distributed primarily along the northern side of the loch, which has a steep slope angle. It is bounded by the extension of a feature reaching the loch side approximately 75m northeast of Lindsay's Burn. This ridge (1, Figure 2.16) consists of two segments with an intervening less well defined area of 150m. It becomes morphologically identifiable at 21-22m depth, extends 300m from the northwestern shore and reaches a depth of 40m below water surface. The form of the ridge is markedly asymmetric, with extremely steep slopes to the southwest. Within the low lying central loch section the lowest point of the feature is at a depth of 65m. The southeastern section of ridge 1 curves in a southeasterly direction down the glen and descends continuously from 15m below surface to 62m. In contrast, the northwestern part rises in two sections with an intervening platform 60m long at a depth of 40m. This southeastern section is symmetrical on the upper and middle slope, becoming more asymmetrical on its southeastern side near to the central gap.

Another ridge (2, Figure 2.16) occurs on the northwestern side of the loch and extends 187m into the loch, reaching a depth of 30.3m before terminating as a sharp drop to 50m. It is symmetrical in form throughout. Below a depth of 50m the bed exhibits no continuation of positive relief. A third ridge (3, Figure 2.16) is identified on the northwestern slope of the basin at 40m extending 200m into the loch. The southern end of this symmetrical structure curves southeastwards and terminates at a rise to 51.7m. A steep slope descending to 73m marks the end of this portion of the ridge (e.g. Figure 2.20). The 150m wide basin floor below ridge 3 slopes at a moderate angle to the southwest where a deep asymmetric hollow reaching a maximum depth of 82.4m lies to the east of a narrowing of the trough. In the southeast of this basin an isolated mound, rising 21m above the surrounding loch floor, reaches to 46m below water surface. Up the southeastern slope, above this mound, an amphitheatre-shaped depression on the loch sides occurs. A small, ill-defined rise may mark the continuation of ridge 3 up the southeast marginal slope.

The fourth ridge (4, Figure 2.16), a wide, irregular feature reaches a maximum width of 104m and amplitude of 12m above the surrounding topography. It terminates in the central trough of Loch Muick as a conical mound 3m above the adjacent loch floor. Although it may be traced on the northeastern slope to a depth of 73m, no evidence exists for its continuation up the opposite slope of the loch. The deepest part of Loch Muick occurs in the central trough between ridges 4 and 5 where an almost flat-bottomed basin, approximately 2.5ha in area, reaches a maximum depth of 83.2m at the base of the western slope.

Ridge 5 consists of a narrow, finger-like feature rising 8m above the surrounding loch floor and may be identified from a depth of 74m below surface on the northern slope to 82m in the centre of the loch. It is symmetrical, approximately 30m wide and may form part of one compound feature linked with ridge 6. The final ridge (6, Figure 2.16) forms the northern boundary of Zone C. It can be traced from 60m below surface on the northern slope of the loch, close to the small, unnamed stream, to 53m on the southern side. The lower part of this ridge appears on the echogram presented in Figure 2.21. On the western slope the ridge width varies widely, from a constriction to 40m at 67m depth, then widening to a maximum of 120m close to the centre of the loch. Ridge amplitude above the adjacent topography also varies to a maximum height of 12m. The lowest part of the ridge, in the centre of the loch, is at 78m depth. This separates the deepest basin to the southwest from the slightly shallower southeasterly basin (maximum depth 81.4m). On the southern slopes the feature is less well defined, with a maximum amplitude of 7m. It can be identified as a ridge to a depth of 64m and may continue as an isolated mound, 1m high, on the middle southern slope.

Within Zone C the loch slopes exhibit minor irregularities in form. Mounds and hollows occur in Zone C, although with one exception, the 21m high mound, on a smaller scale and at a much lower density than in Zone B. A total of five hollows and four mounds not directly associated with the ridges can be identified.

2.6.3.4 Zone D

Zone D, the remainder of Loch Muick, comprises an area of more subdued morphology. To the northeast of the boundary ridge between Zones C and D the basin profile is U-shaped (Figure 2.22). The loch floor rises as a relatively uniform low angle slope from 80m northeast of the Allt an Dearg, to 30m where the slope is very low angle, rising to the effluent River Muick. Water of less than 10m depth extends an average of 100m into the loch at its northern extremity. Within Zone D, at depths of 54m and 58m, three discrete, laterally discontinuous (15-22m by 26-45m wide) hollows occur, with gullies leading down to them.

Towards the northeast of this zone, two areas of relatively shallow water rising above 16m form a broken ridge aligned northeast to east across the loch. The northeastern portion is in the form of a mound 4m high which terminates at a low angle slope dropping to 17.5m. The eastern half of the ridge rises as a low angle slope to an elongated mound which forms the crest of the ridge at 3.8m. Within Zone D minor mound and spurs on the loch sides can be identified. Due to the lower density of survey lines in this area, less confidence is placed in the quantification of the landforms.

2.6.3.5 Hypsographic curve

A hypsographic curve (Figure 2.6c) was drawn from the depth data obtained from Loch Muick. It indicates that the loch has gently sloping sides descending to the maximum depth (Håkanson, 1977). 50% of the surface water area overlies water with a maximum depth of 30m. The remaining 50% of the surface water area overlies an equal distribution of water depths in the range 31m to 83.2m.

2.6.4 Quantification of the geomorphology.

In an attempt to quantify the geomorphological variations on the floor of Loch Muick, an analysis of the Form Roughness (Rf) has been made using the method of Håkanson (1974). Rf is formulated as:

$$Rf = \frac{0.165 * (lc+2) * \sum_{i=0}^n li}{a}$$

where

lc = the contour line interval in m

li = the length of the given contour line in m

a = the lake area in km²

This formula yields a dimensionless measure which provides a basis for the quantitative comparison of topographic diversity within a lake; comparison of form roughness values thus cannot be made between water bodies. The range of geomorphic variation in the Loch Muick basin rendered it suitable for application of the form roughness formula. Analysis of the bathymetric charts of Lochs Lee (section 2.4.2, Figure 2.2) and Callater (section 2.5.3, Figure 2.9) have not revealed enough variation to justify the application of this time-consuming procedure.

To apply the technique to Loch Muick, the 1m contoured chart was divided into squares each of 4500m² area. The area of the squares was selected to minimize the number of squares used in the calculation, whilst maximising the degree of geomorphological variation identified visually. The maximum and minimum water depth in each square was determined, and the difference (ΔD) calculated. Five new contour lines were then drawn in each square. The interval between contour lines was calculated as the positive integer of the ratio $\Delta D/5$. The total length of these contour lines within each square was measured using a Tecktronix 4956 digitiser. From this information the form roughness within each square was determined according to Håkanson (1974). High form roughness values indicate a

relatively high degree of geomorphological variation within the base square, whereas low Rf values are associated with more subdued geomorphology. The data derived are presented as a distribution map (Figure 2.23).

The distribution of form roughness over the floor of Loch Muick correlates with the four visually defined zones of geomorphological variation. The small basin at the southwestern end of the loch has a relatively smooth morphology in which maximum Rf values, in the range 0.500-0.749, occur at the northerly mouth of the Allt an Dubh-loch. The boundary ridge between Zones A and B is identifiable as the most southwesterly occurrence of the 1.00-1.249 Rf range. Zone B, the area dominated by mounds and hollows is characterised by relatively high Rf values (1.250-1.749) in the centre of the loch. The highest Rf value (1.749) occurs in this zone, associated with the small hollow on the southern slope, and the 6m deep hollow near the boundary of the zone. Zone B has the highest average Rf values of all four zones. Zone C has a wider range of Rf values (0.250-1.520). The highest value in this zone is located close to the mouth of the Black Burn (Rf = 1.520). The steep northwestern loch slopes, on which the ridges are developed, and where mounds occur on the eastern slopes, are also characterised by relatively high Rf values. The more subdued ridges (4, 5, 6), central troughs, and remaining southeastern slopes occur within areas of relatively low Rf (0.500-1.249). The boundary between Zones C and D appears to be gradational in terms of computed Rf values (0.500-1.249). This is due to the steep, uneven slopes at the boundary between the zones becoming smoother within Zone D towards the outlet of the loch. Areas of higher Rf occur on the steep slopes of the northwestern shore, on the delta front of the Allt an Dearg, and where the small breaks in slope at 54m and 30m occur. The minor mounds at the extreme northeastern end of the loch, close to the outlet, are not differentiated from the surrounding 'background' topography by this technique.

2.6.5 Comparison of the bathymetry: 1905-1989

The new bathymetric chart (Figure 2.15) differs considerably from that of Murray and Pullar. Most of the changes are considered to be the result of advances in echosounder

technology and the intensity of survey traverses as opposed to actual changes in loch floor level.

i) The outstanding difference between the products of the two surveys is the intricate detail of the information on the new chart. It reveals that the floor and sides of Loch Muick are not 'Of simple conformation' (Murray and Pullar, 1910, p. 147) and that the bottom of the loch is not 'Flat'. This is confirmed by the hypsographic curve (Figure 2.6c) An abundance of geomorphological features including ridges, spurs, mounds, hollows and troughs have been highlighted by the 1989 survey.

ii) The 1905 survey recorded a maximum depth of 78m below an *estimated* datum of 1308 feet (396m) in the centre of Loch Muick, northeast of the Black Burn. However, a maximum depth of 83.2m, 5.2m deeper than that measured by the earlier survey, was recorded in approximately the same area in 1989. The datum of 400.26m O.D. used in the 1989 survey was measured by levelling a closed traverse from a benchmark at the Spittal of Glen Muick to the loch. The cause of the difference in maximum measured depth is believed to be largely due to the use of different datum levels by the two surveys. It appears that the traverses covered during the 1905 survey did not coincide with the deepest part of the Loch Muick trough. Thus an estimate of the rate of sedimentation in the 83 years between surveys cannot realistically be determined. Attempts were made to calculate the amount of sedimentary infill in low angle areas of the central trough, but discrepancies in the depths of up to +5m were encountered between the two charts.

iii) The new chart has identified that the water body of Loch Muick occupies two distinct basins, a) a small basin at the southwestern end and b) the remainder of the loch.

iv) The base maps used for the 1905 survey were the Ordnance Survey 6" (1:10560) series, which show the Allt an Dubh-loch as entering Loch Muick at a single point. The 1974 Ordnance Survey 1:50000 sheet shows the stream to have two mouths. On the 1989 bathymetric chart (Figure 2.15) distinct differences in the nearshore morphology associated with the two mouths of the Allt an Dubh-loch have been noted. Deltaic sedimentation has been interpreted by Collet and Johnston (1906) as being associated with

the southern mouth of the Allt an Dubh-loch (extant at the time of the 1905 survey). Morphological evidence shows no such aggradation near to the more northern inflow. It is suggested therefore that since the last glacial episode, particularly in recent years, inflow and sedimentation through the southern mouth of the Allt an Dubh-loch has been dominant.

v) Finally, both descriptions of the bathymetry based on the 1905 chart refer to the existence of a large subaerial delta at the mouth of the Glas Allt, although this is not identifiable in the subaqueous environment on the bathymetric chart. The new chart indicates that at the point where the stream flows into the loch a gully, flanked by two gently sloping areas, occurs. This is interpreted on morphological grounds as the subaqueous extension of a subaerial feature. In this case data from the 1989 survey have identified a topographical form merely inferred at the time of the earlier survey.

2.7 CONCLUSIONS

The new bathymetric charts of Lochs Lee, Callater and Muick (Figures 2.2, 2.9, 2.14, 2.15) represent a considerable improvement in the level of information previously available. The bathymetric survey of Loch Lee, undertaken during November 1989, is the first recorded survey of the water body, and has revealed that the loch occupies a simple basin with a maximum depth of 30.7m. The hypsographic curve indicates that the loch has compound sloping sides which descend to a small flat bottomed area. Three zones of geomorphological diversity have been visually identified in Loch Lee.

Loch Callater has been shown to occupy two distinct basins and has a maximum determined depth of 11.1m, 2.3m deeper than previously charted. Hypsographic data confirm that the loch has sides which slope at compound angles to an essentially flat bottom.

The bathymetric chart of Loch Muick (Figure 2.15) represents the most detailed chart of a major Scottish freshwater loch yet produced. The water body has been shown to be composed of two basins and to reach a maximum determined depth of 83.2m. The previous (1905) survey had identified a maximum depth of 78m. The hypsographic curve

indicates that the loch has evenly sloping sides to the maximum depth, and is not flat bottomed, as suggested by Collet and Johnston (1906). Geomorphological assemblage zones have been visually identified on the bathymetric chart and the delimiting parameters supported on application of the quantitative Form Roughness (Rf) measure (Håkanson, 1974).

Within the wider field of inland bathymetric surveys, the new charts set a precedent. Bathymetric surveys of Scottish freshwater lochs since the work of Murray and Pullar have usually comprised a minor, but important, part of sedimentological research (e.g. Al-Ansari, 1976; Duck, 1982; Al-Bayati and McManus, 1984). The loch basins studied have been contoured at 10m, 5m, 2m and exceptionally, in the case of Lindores Loch (Duck and McManus, 1985b), which has a maximum depth of 3.66m, at one foot intervals. Thus the detailed geomorphological information provided on the continuous profiles produced by recording echosounders has been overlooked in favour of large scale geomorphological variations. Small scale subaqueous geomorphological features, which can provide information regarding former and currently occurring processes, have hitherto largely been ignored. Therefore the bathymetric surveys presented here provide an important advance in the level of information available on landforms within the lacustrine environment.

Estimates of the rate of sedimentation within the Callater and Muick basins proved impossible to achieve due to the considerable improvements in survey equipment and technique since the 1905 survey. Depth measurements obtained during the 1905 surveys of Lochs Callater and Muick consistently fluctuate between 1m to 5m shallower than those obtained during this research programme. It is believed that this results from the use of different, probably inaccurate, in the case of the 1905 survey, datum levels.

Evidence regarding the processes of formation of the underwater geomorphology identified in Lochs Lee, Callater and Muick are discussed in Chapter 7, in conjunction with sidescan sonar (Chapter 4), surface sediment (Chapter 5), seismic subbottom reflection profiling (Chapter 3) and core (Chapter 6) data.

LOCH LEE

Echosounder Traverse Lines

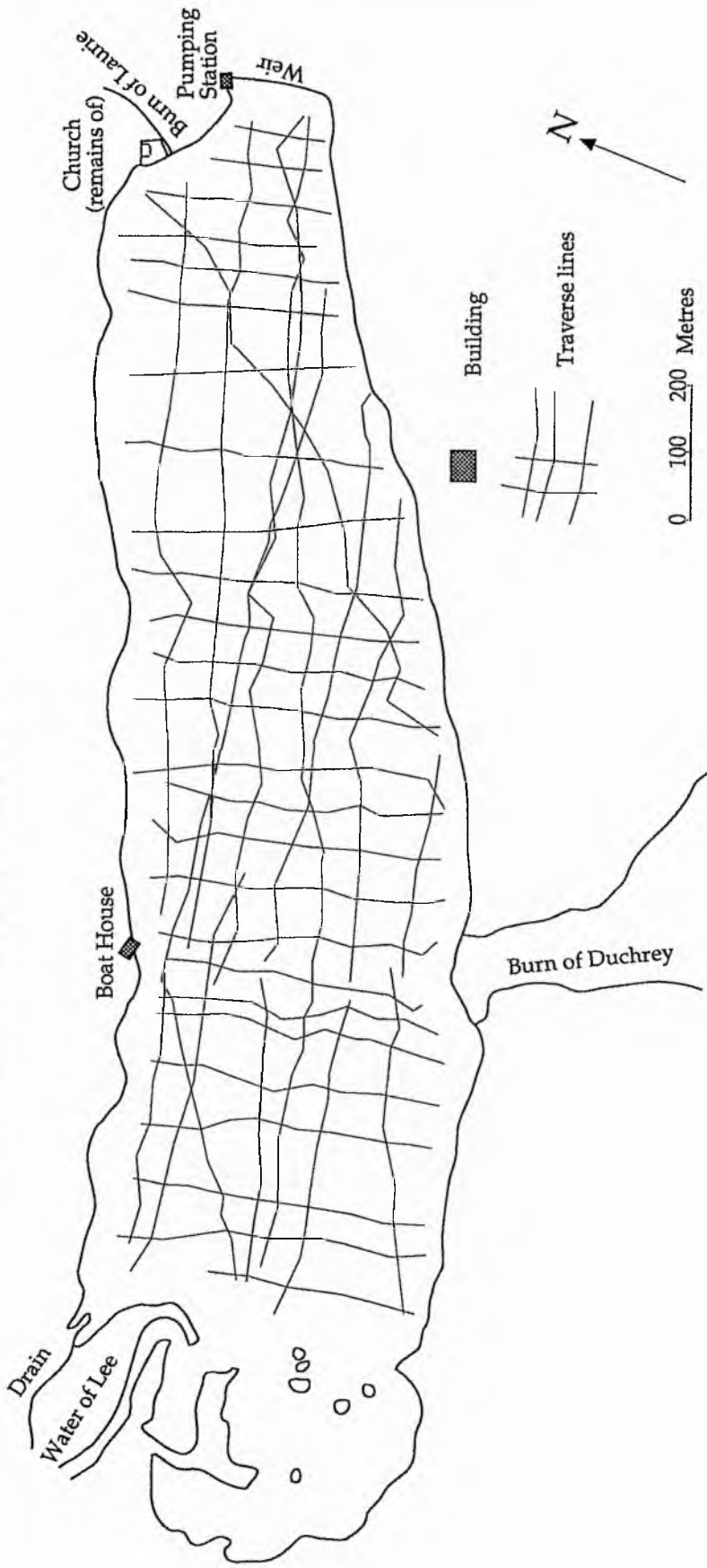


Figure 2.1
58

A Bathymetric Chart of
LOCH LEE
Dalhousie Estate, Angus.

SURVEYED NOVEMBER 1989
P.A.LOWE
R.W.DUCK
J.McMANUS
A.RAMSAY Boatman

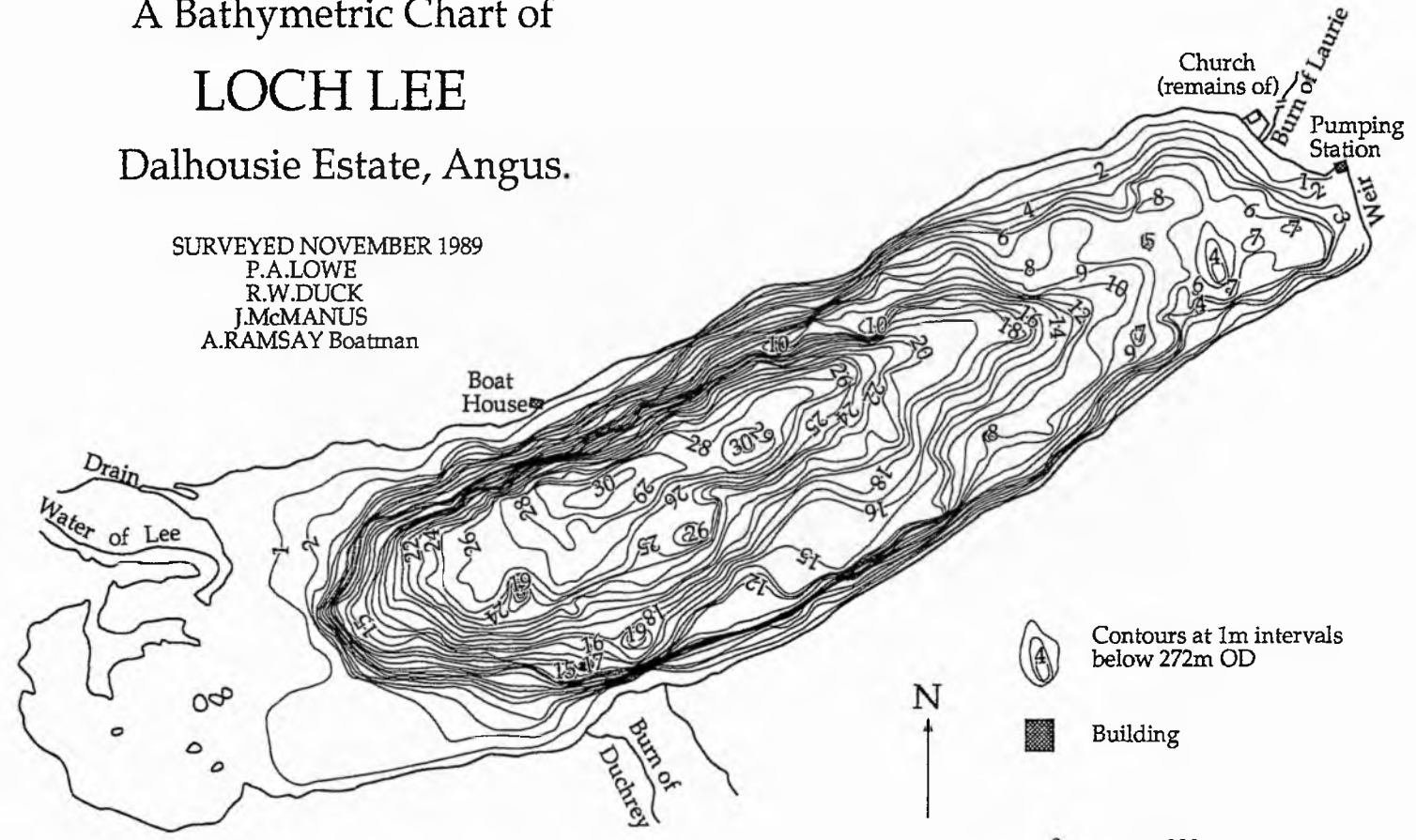
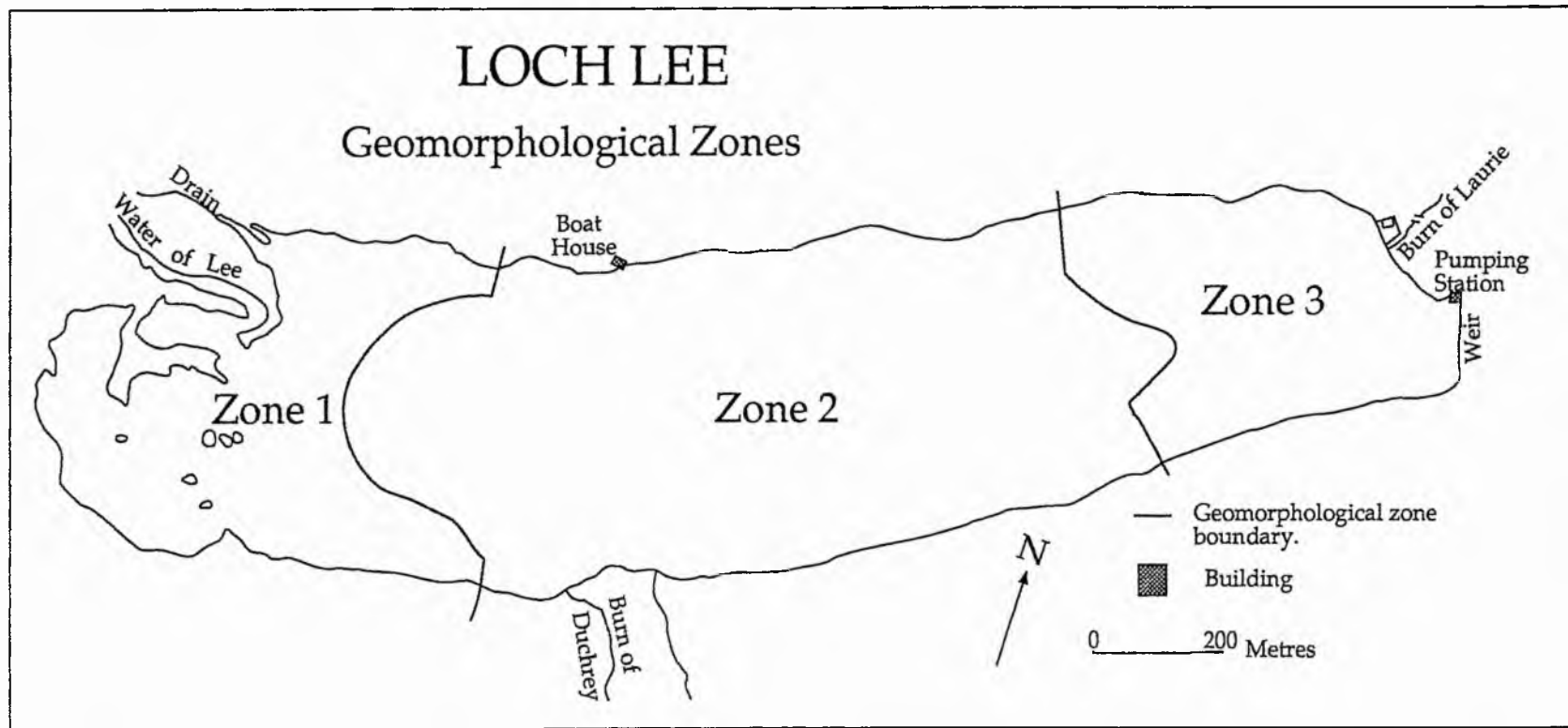


Figure 2.2
59

Figure 2.3
60



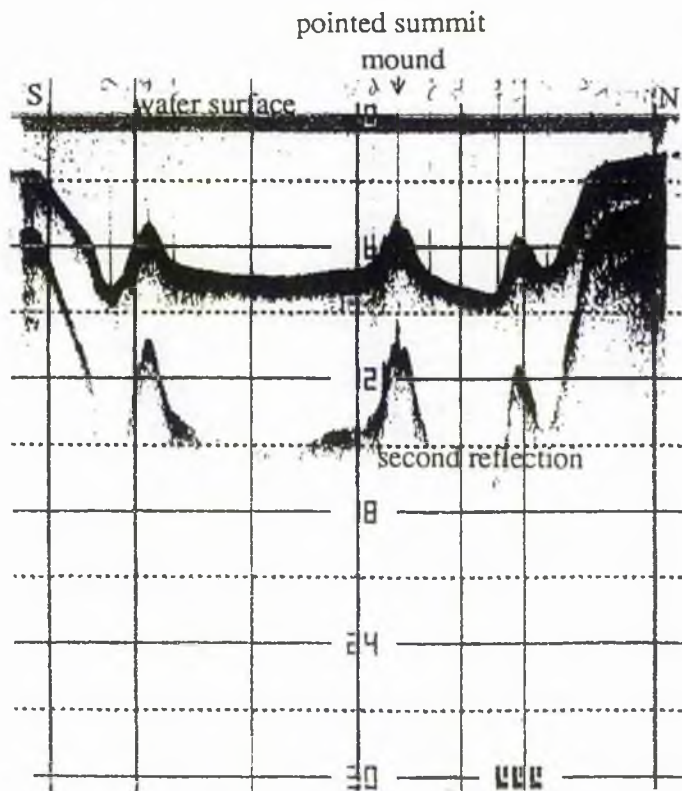


Figure 2.4 Loch Lee: Echogram, Zone 3 northeastern shallows, conical mound.

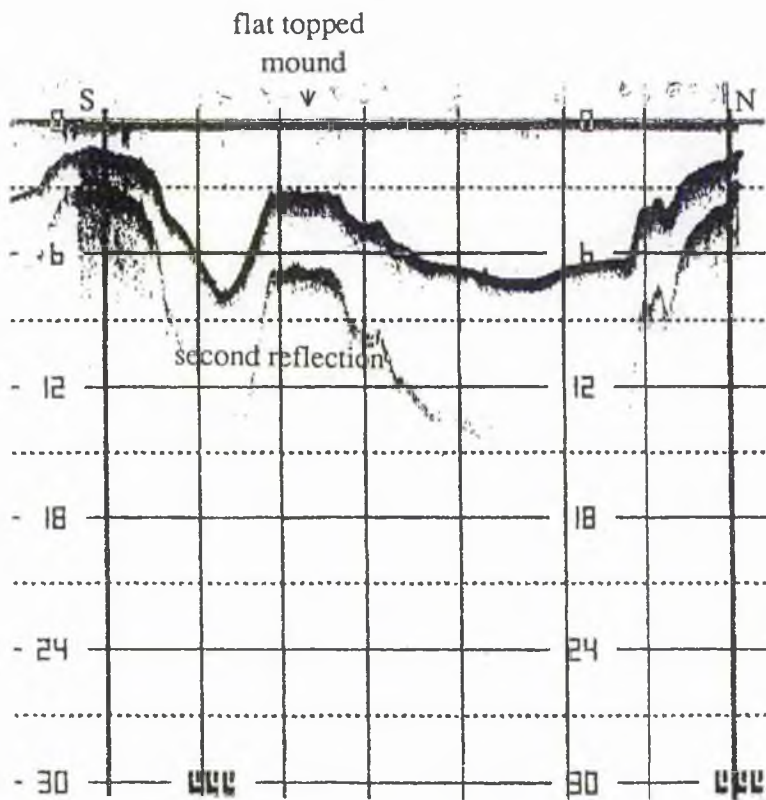


Figure 2.5 Loch Lee: Echogram, Zone 3 northeastern shallows.

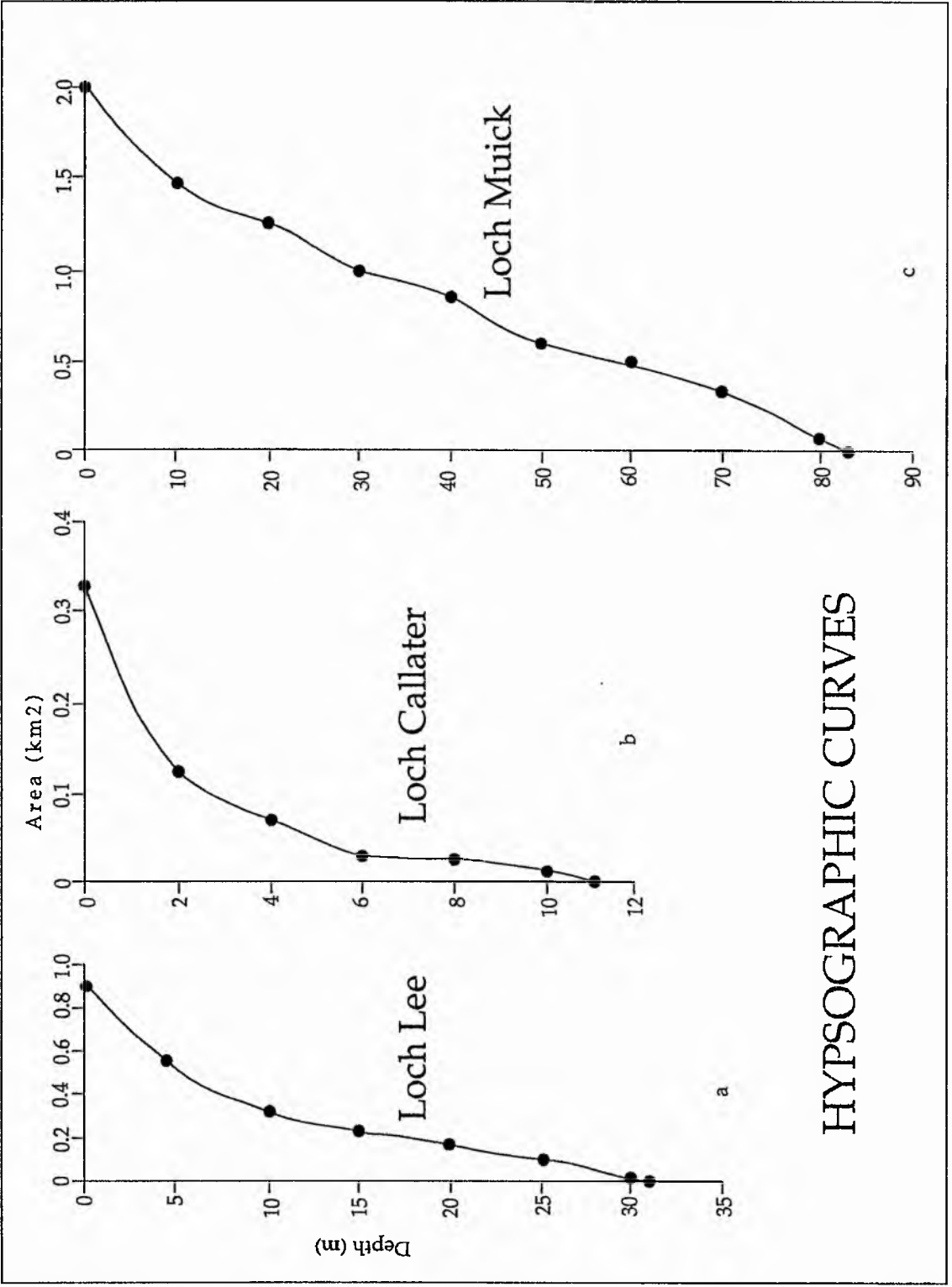


Figure 2.6
62

HYPSOGRAPHIC CURVES

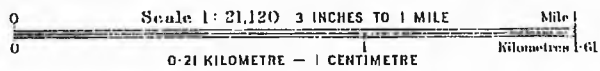
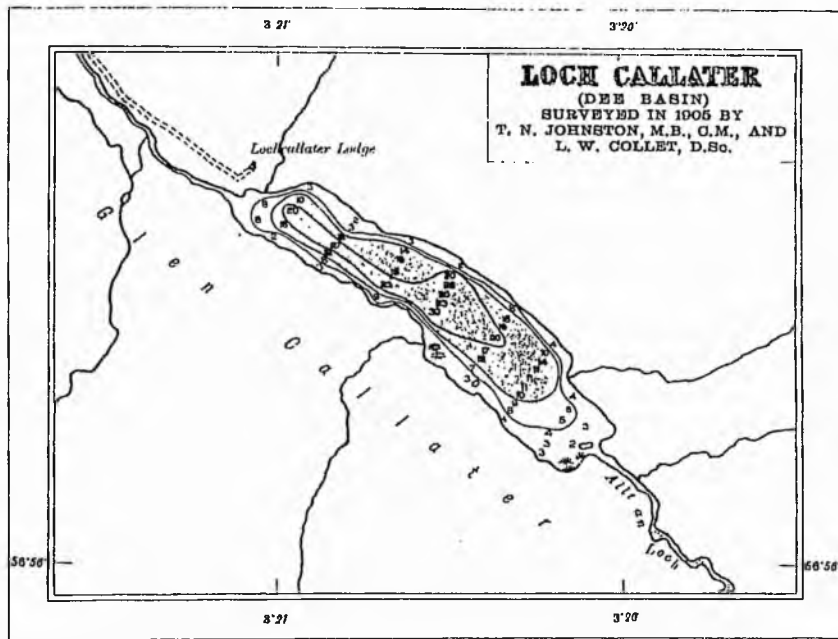


Figure 2.7 Bathymetric Chart of Loch Callater, Johnston and Collet, (1905).

LOCH CALLATER

Echosounder Traverse Lines

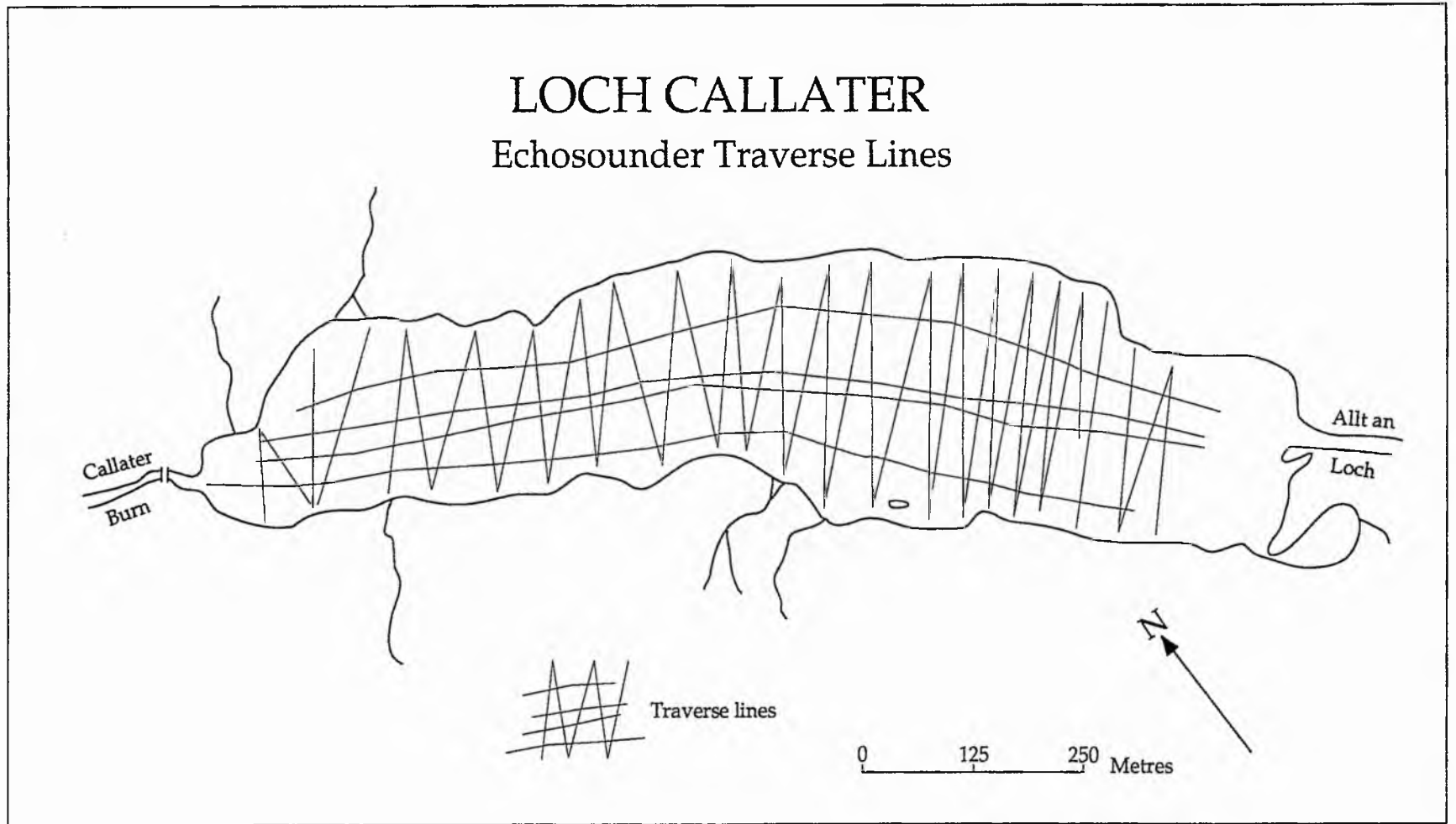
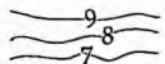
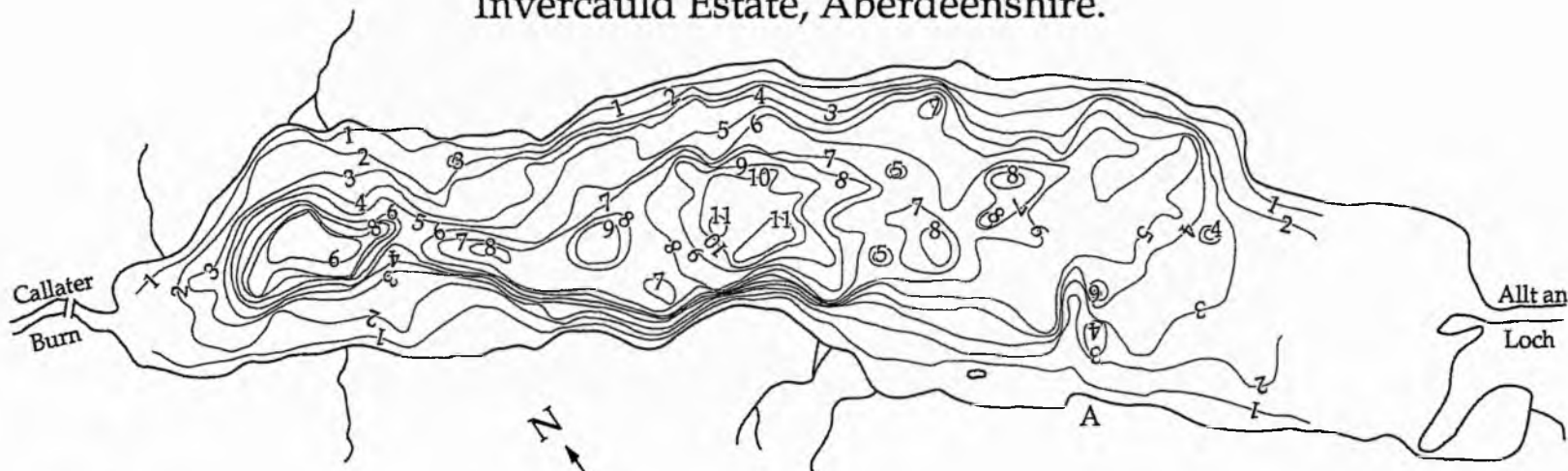


Figure 2.8
64

A Bathymetric Chart of
LOCH CALLATER
Invercauld Estate, Aberdeenshire.



Contour lines at 1m intervals
below 500m OD

0 100 200 Metres

SURVEYED SEPTEMBER 1989
P. A. LOWE
R. W. DUCK
J. McMANUS
A. RAMSAY Boatman

Figure 2.9
65

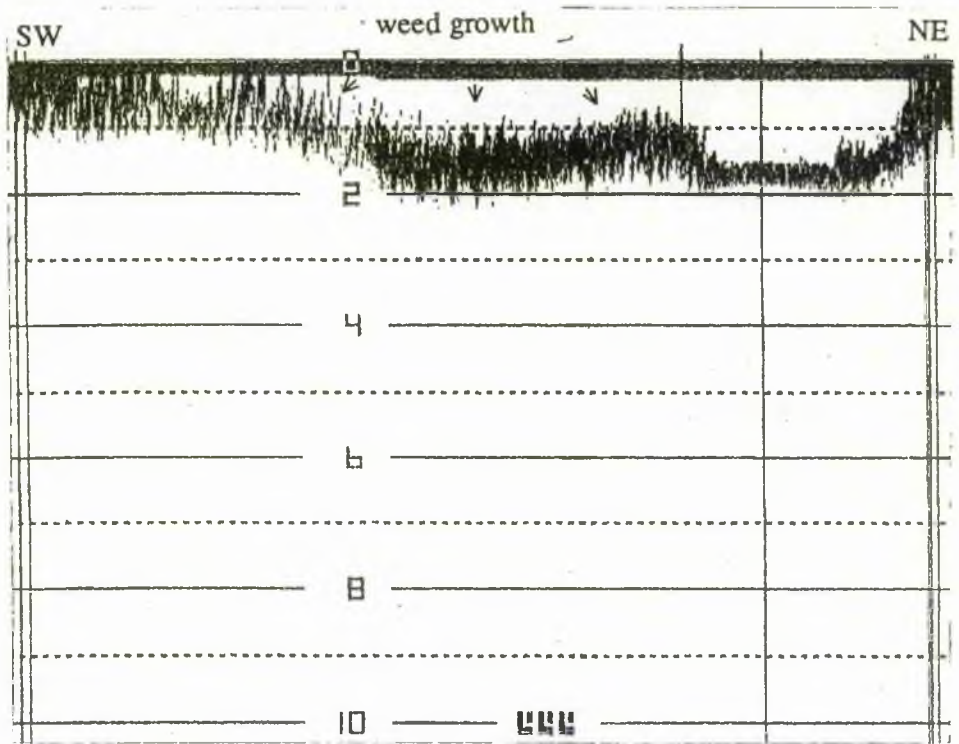


Figure 2.10 Loch Callater: Echogram, aquatic weed growth appearing as the poorly defined, 'feathery', part of the profile. Southeastern shallows.

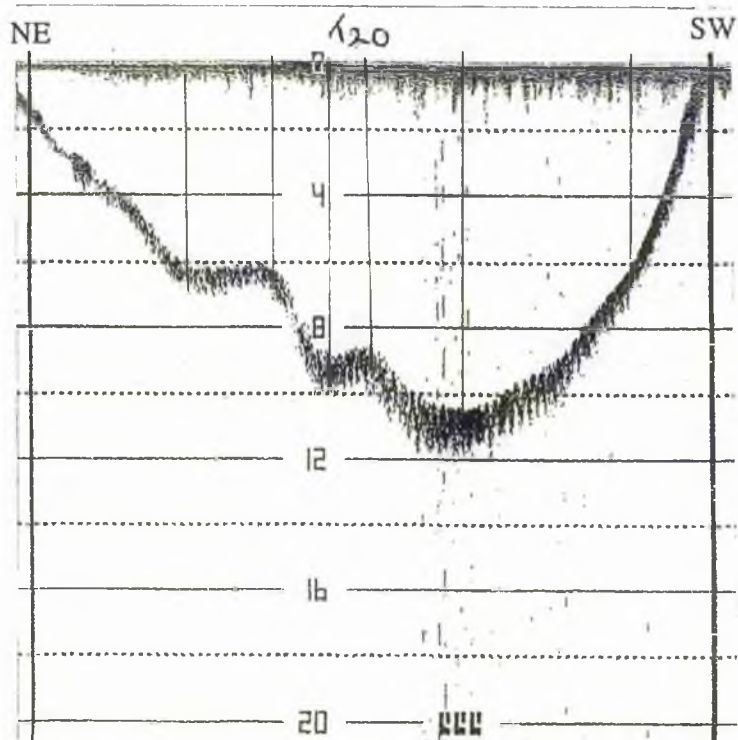


Figure 2.11 Loch Callater: Echogram, asymmetric profile and deepest trough. Diffuse surface profile due to low amplitude reflections from low density bottom sediments.

Loch Muick
After Murray & Pullar. Surveyed Johnston & Collet 1905.

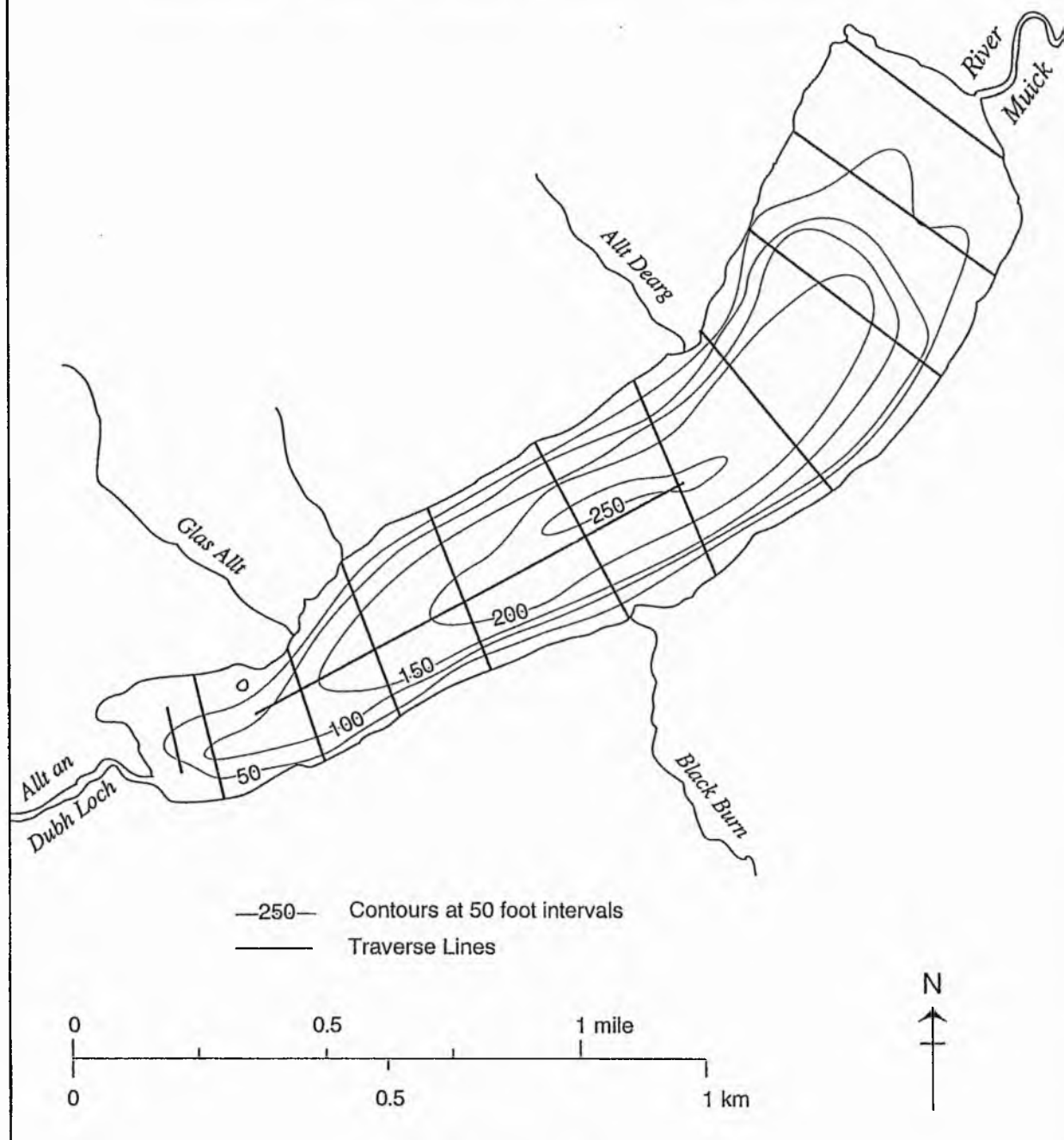


Figure 2.12

LOCH MUICK

Echosounder Traverse Lines

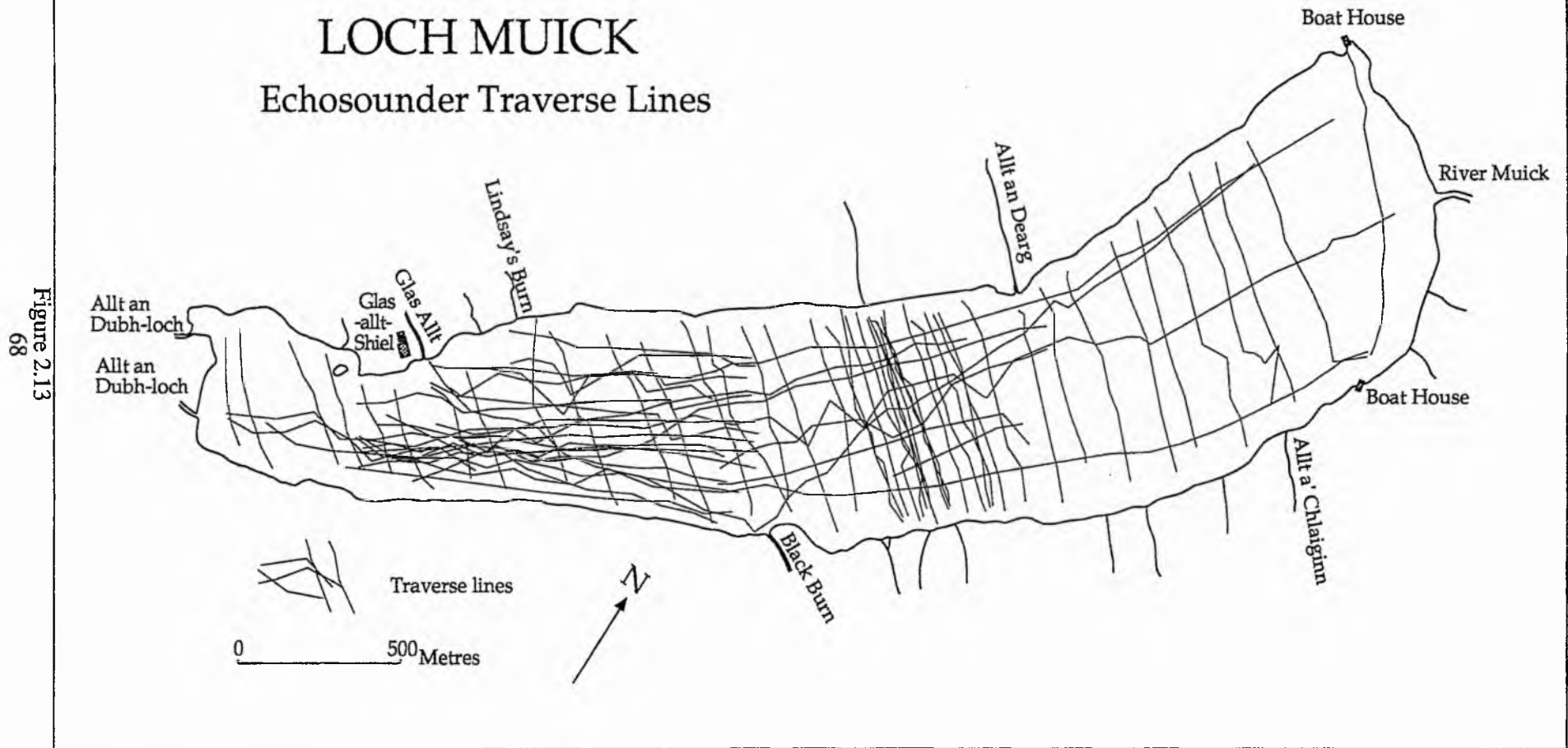
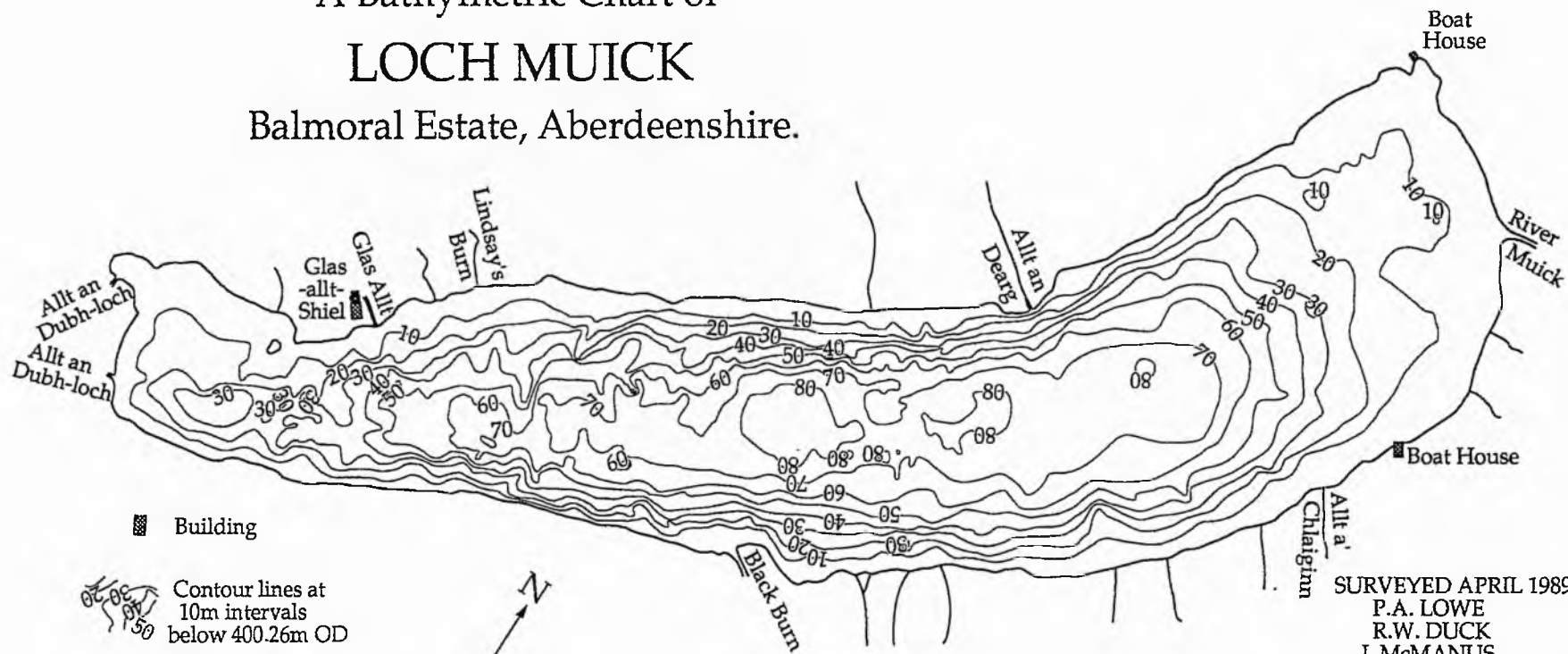


Figure 2.13
68

A Bathymetric Chart of LOCH MUICK

Balmoral Estate, Aberdeenshire.



SURVEYED APRIL 1989
 P.A. LOWE
 R.W. DUCK
 J. McMANUS
 A. RAMSAY, Boatman

Figure 2.14
69

A BATHYMETRIC CHART OF

LOCH MUICK

Balmoral Estate, Aberdeenshire

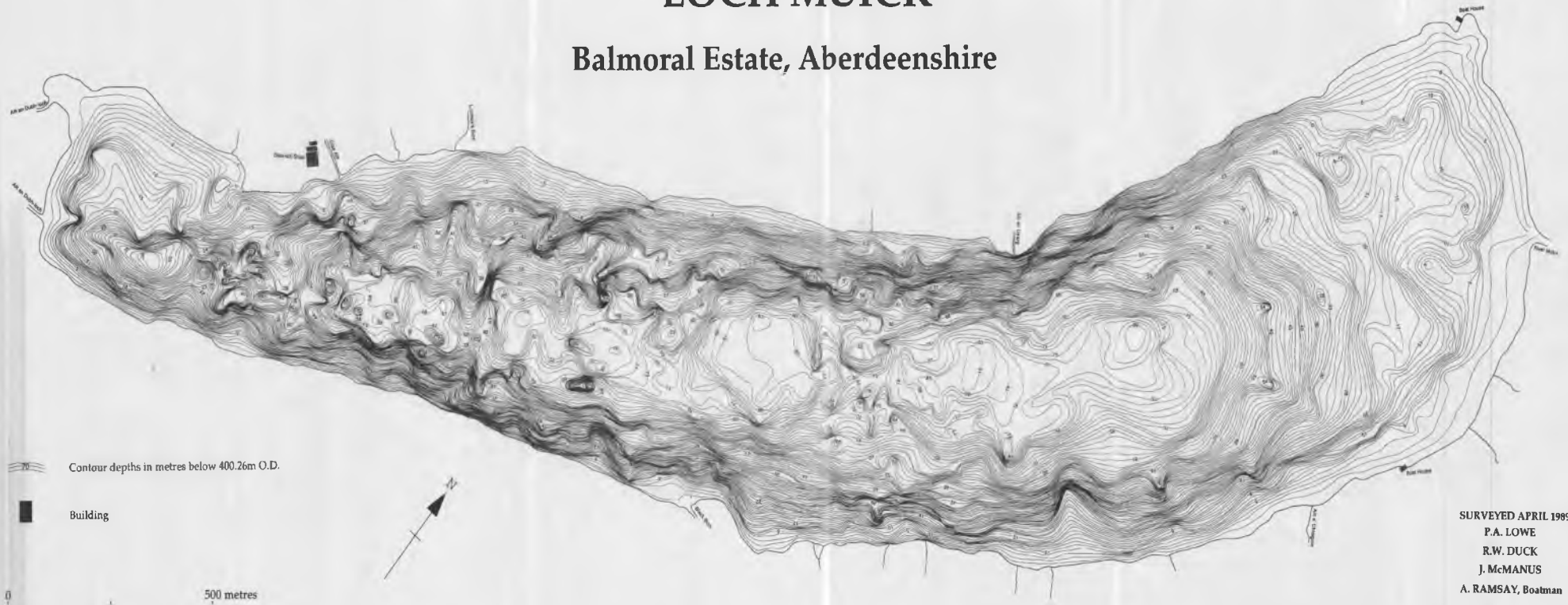
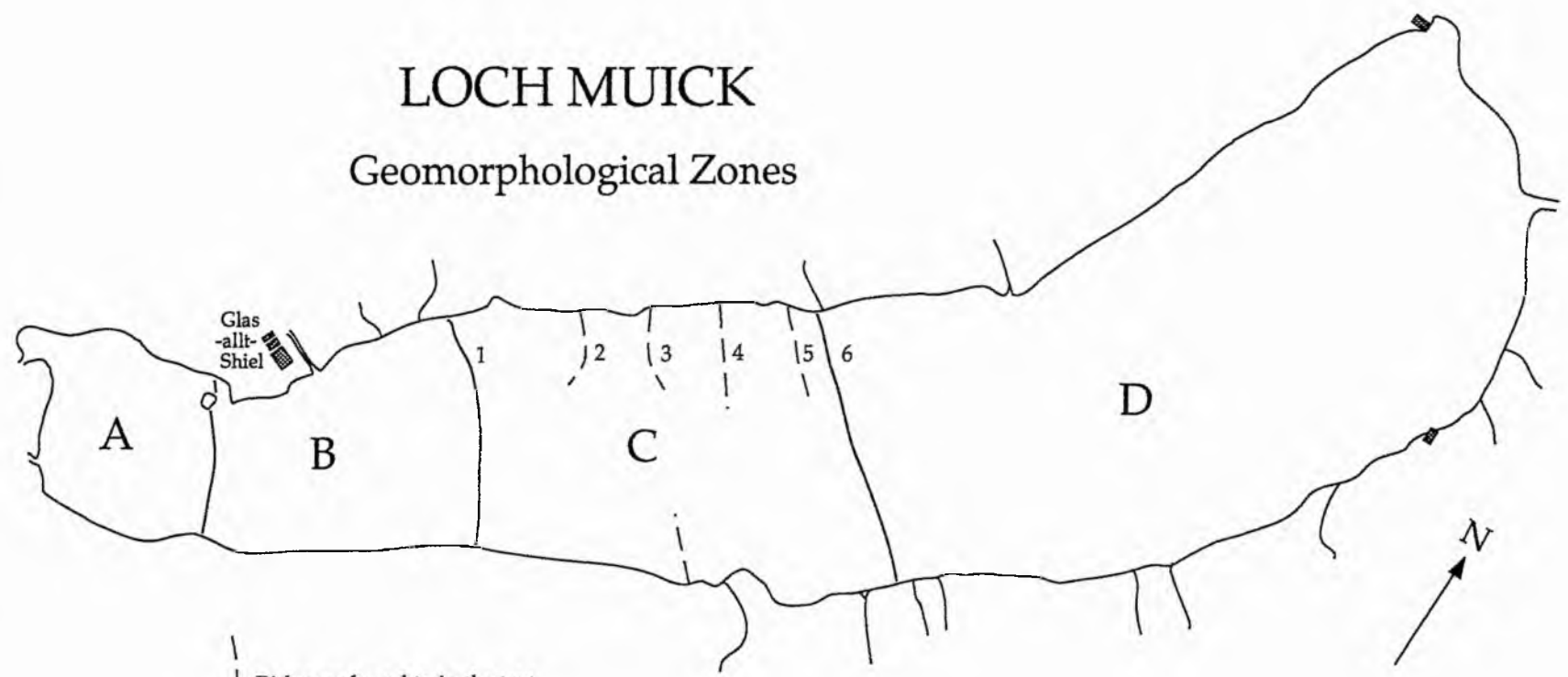


Figure 2.15 Revised bathymetric chart of Loch Muick contoured at 1 m intervals.

LOCH MUICK

Geomorphological Zones



--- Ridges referred to in the text

B Geomorphological Zones

0 500 Metres

Figure 2.16
71

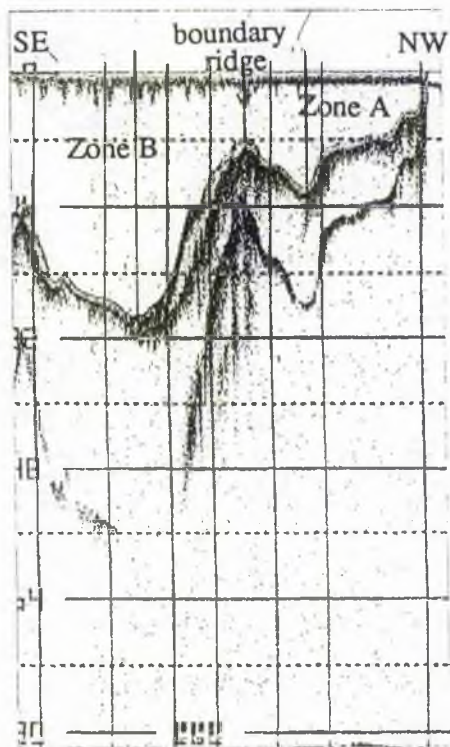


Figure 2.17 Loch Muick: Echogram, boundary ridge between Zones A and B. Subsurface profile due to second reflection of outgoing pulse in area of relatively shallow water with highly reflective bottom.

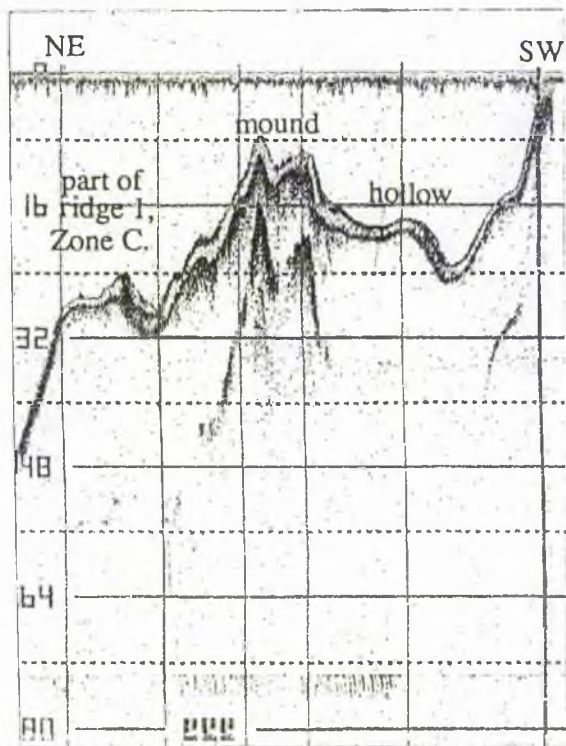


Figure 2.18 Loch Muick: Echogram, mound and hollow Zone B. Sub-surface profile due to second reflection of outgoing pulse in area of relatively shallow water with a highly reflective bottom.

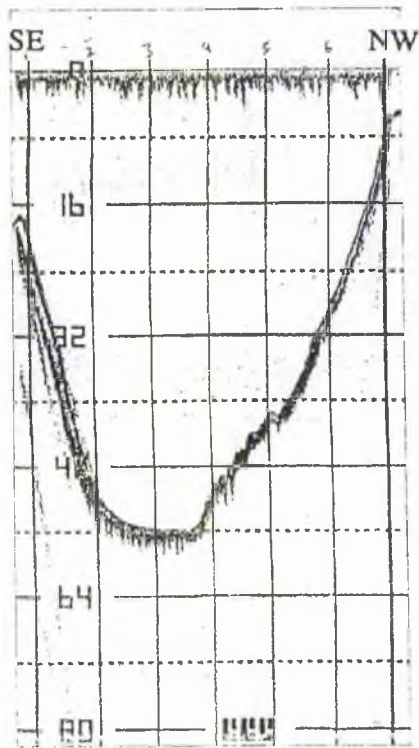


Figure 2.19 Loch Muick: Echogram, Zone B asymmetric profile.

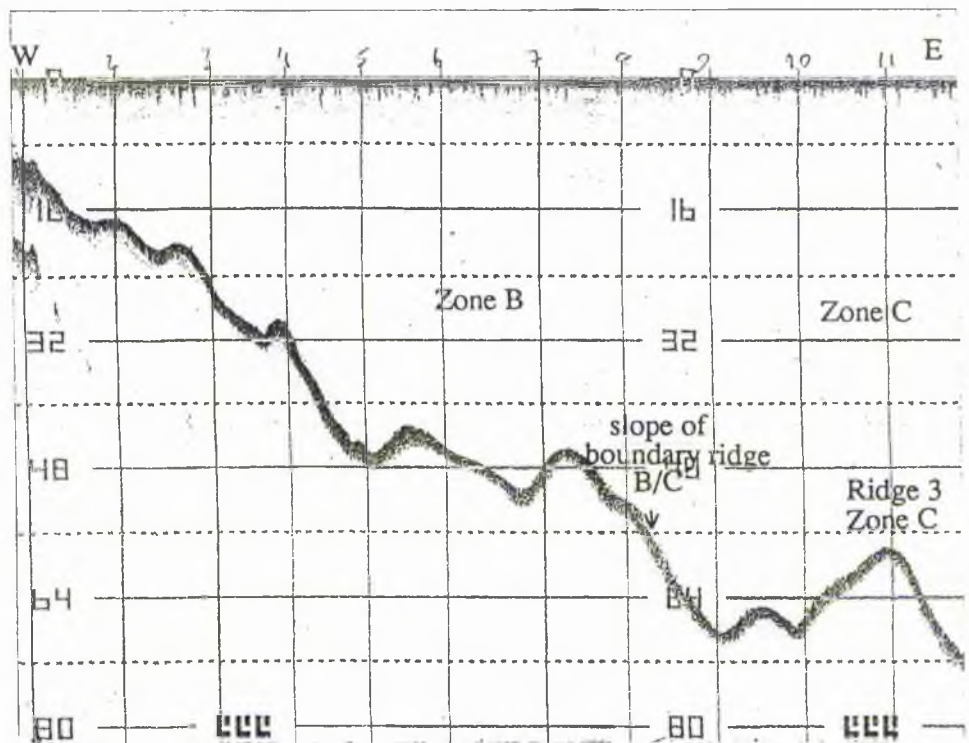


Figure 2.20 Loch Muick: Echogram, subaqueous topography Zones B and C including lower slopes of boundary ridge.

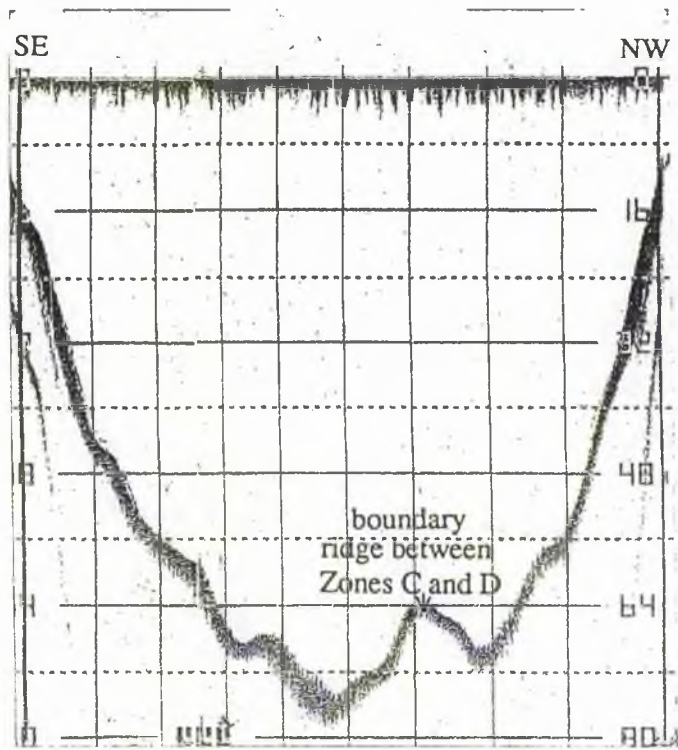


Figure 2.21 Loch Muick: Echogram, profile across ridge dividing Zones C and D.

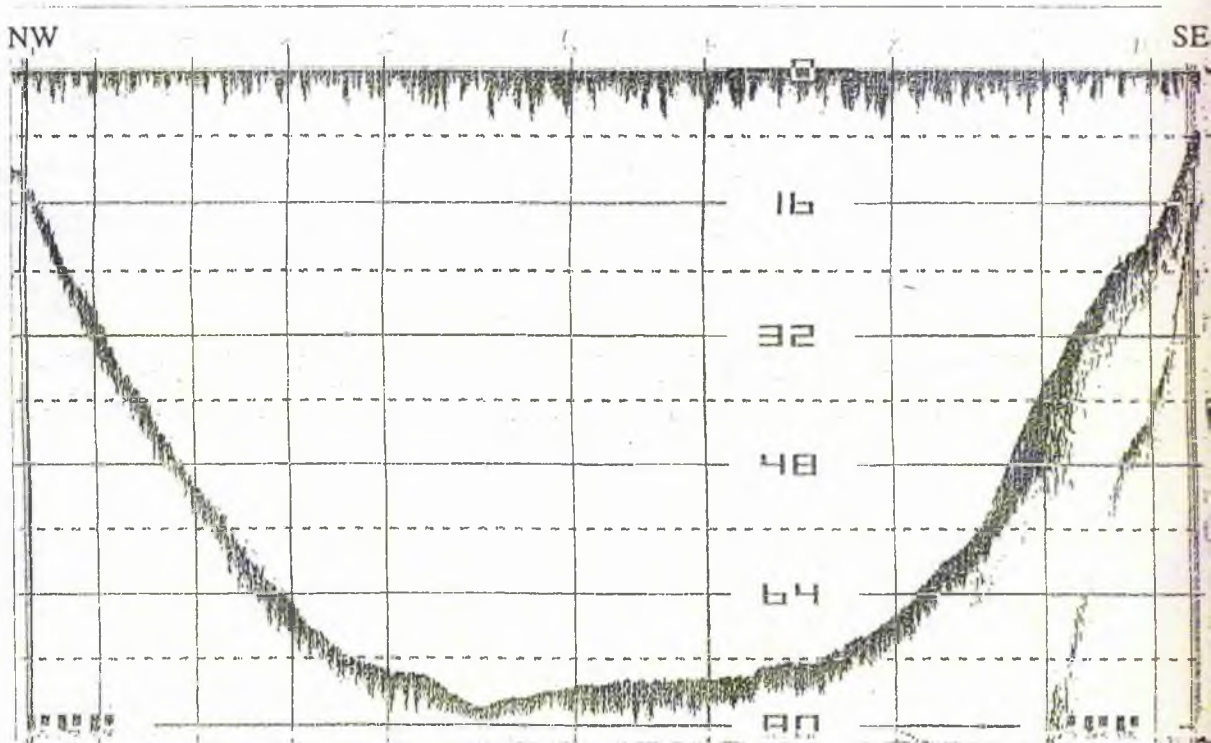
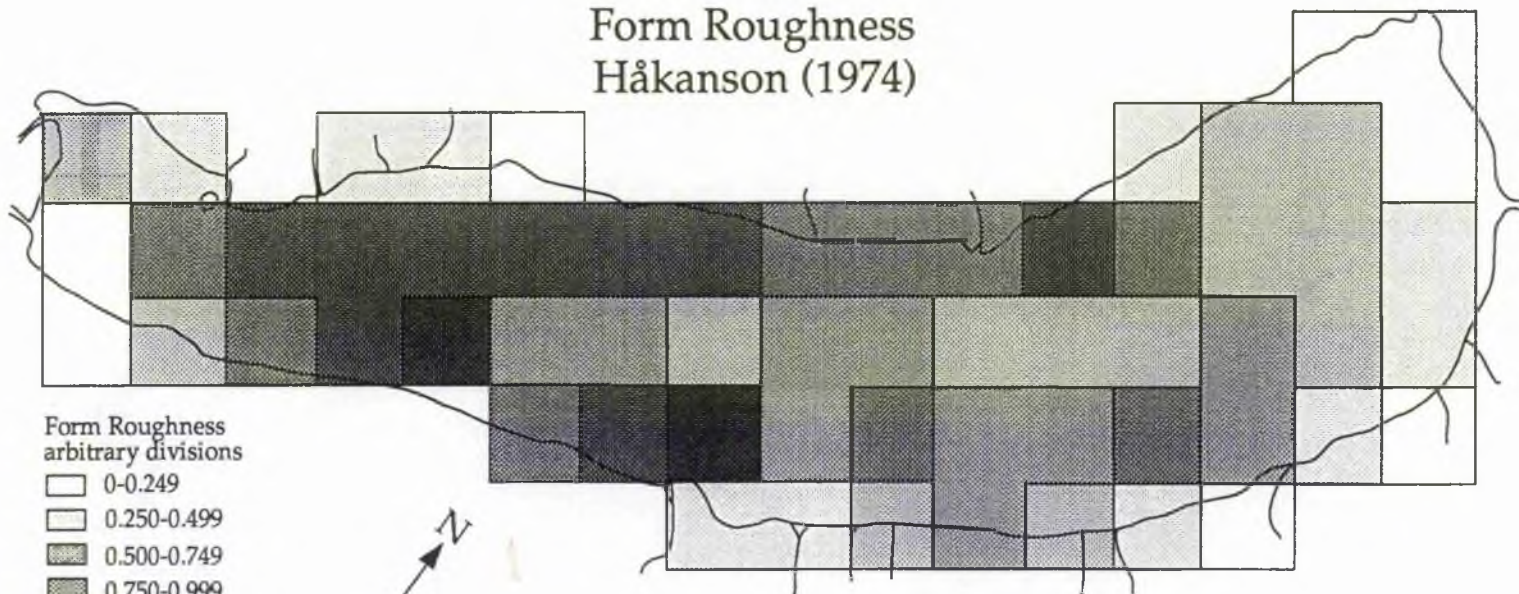


Figure 2.22 Loch Muick: Echogram, profile across Zone D, U-shaped trough.

LOCH MUICK

Form Roughness
Håkanson (1974)



Form Roughness
arbitrary divisions

- 0-0.249
- 0.250-0.499
- ▨ 0.500-0.749
- ▩ 0.750-0.999
- 1.00-1.249
- 1.250-1.499
- 1.500-1.749

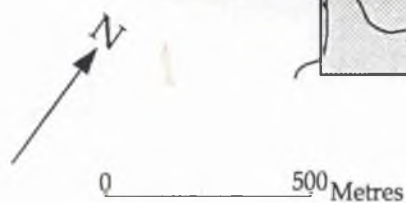


Figure 2.23
75



Plate 2.1 Lowrance X-15M Recording Echosounder in operation.

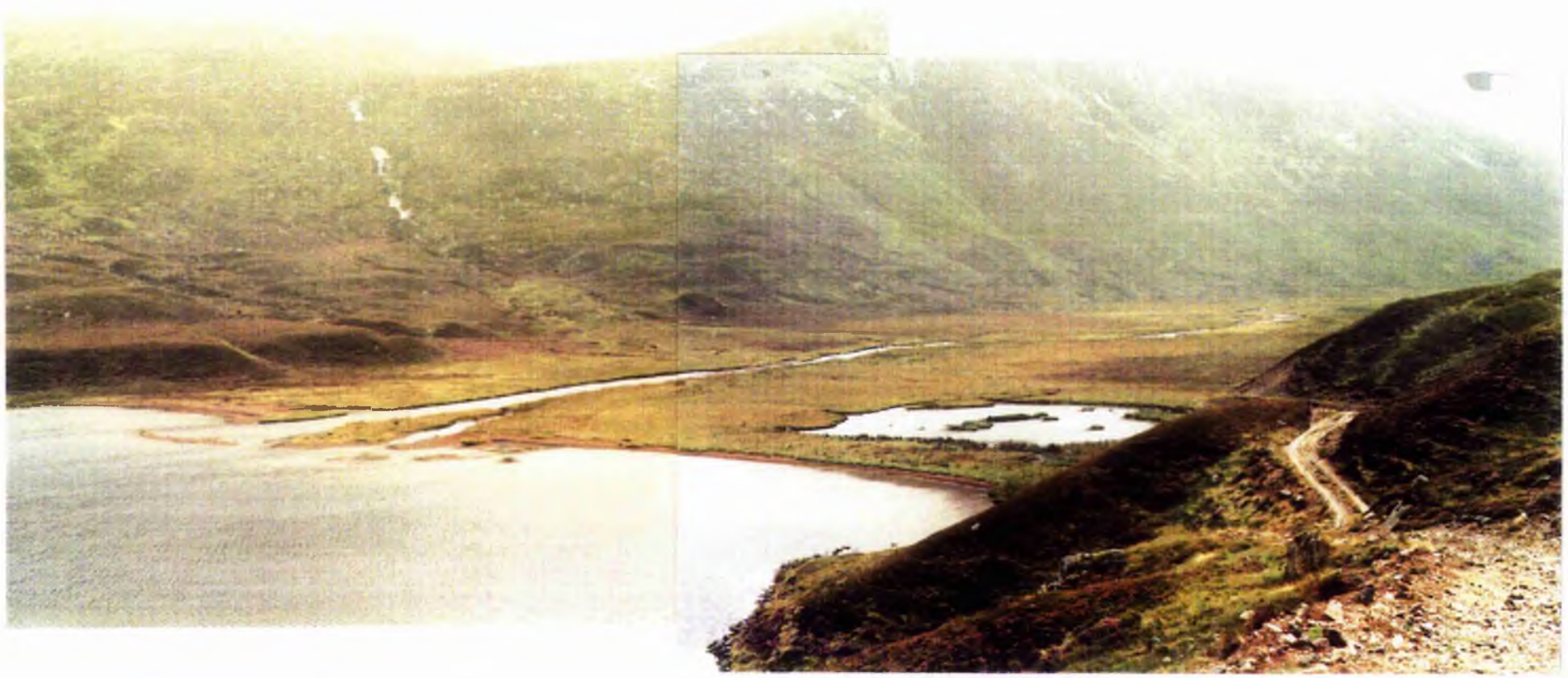


Plate 2.2 Alluvial plain of the Allt an Loch and strath lochan, southeastern end, Loch Callater.

CHAPTER 3

CONTINUOUS SUBBOTTOM SEISMIC REFLECTION PROFILING

'A window through the sedimentary cover is provided by proglacial lakes which allow high resolution seismic surveys to be undertaken, and reveal a stratigraphic record which is otherwise hidden' (Boulton et al., 1982, p. 37).

3.1 INTRODUCTION

In this Chapter are presented seismic subbottom reflection profile data from surveys carried out on Lochs Lee, Callater and Muick using Pinger 3.5kHz profiling equipment. It reviews the development and principles of subbottom reflection profiling techniques. An overview of seismic reflection profile interpretation methods and detailed examination of the methodology of Mitchum, Vail and others is given. Interpretation of the seismic data follows the 'Seismic stratigraphy' procedure of Mitchum and Vail (1977) and Mitchum et al. (1977a, b). Seismograms and the interpreted profiles are presented. Detailed descriptive analyses of the seismic sequences and facies identified within each water body are presented. A seismic parastratigraphy (broadly equivalent to a subaerial lithostratigraphy) providing litho-seismic interpretation is given for each loch.

3.2 SUBBOTTOM PROFILING

3.2.1 Historical overview

Continuous subbottom reflection profiling is a development of echosounding technology. Research using recording echosounders had indicated that some penetration of sediments was occurring, even at relatively high sound frequencies (e.g. Rust, 1935; Stocks, 1935; Mortimer and Worthington, 1940 (see section 2.2.2 above)) and the value of subbottom profiling equipment was therefore beginning to be recognised:-

'The echosounding machine provides a means of measuring the result of subaqueous deposition over long periods of time' (Mortimer and Worthington, 1940).

Experimentation with lower frequency sub-surface profilers was carried out during the 1950s, one of the earliest applications of the technique being the tracing of a widespread ash layer in the eastern Pacific with a 12kHz echosounder (Worzel, 1959). Hersey (1963) carried out pioneering research with subbottom profilers and the technique became widely used due to its essential simplicity, adaptability and ease of interpretation (Leenhardt, 1969). A range of subbottom profilers has been produced including pingers, sparkers, boomers and air-guns allowing profiles to be obtained in all subaqueous environments. Low frequency echosounders, such as the Kelvin Hughes MS26, operating at 26kHz have achieved penetration of up to 6m into the sediments of Loch Benachally, Perthshire, in late spring (Al-Bayati and McManus, 1984).

Further adaptations to the general principle continue to be made; the Atlas Parasound system is a combination of a narrow beam deep sea survey echosounder with a subbottom profiling capability. It utilises two signals at adjacent frequencies to produce a low frequency sound pulse with a very narrow beam virtually free of side lobes. This results in greatly improved vertical resolution of up to 30cm even in deep sea sediments (see below, section 3.2.2).

3.2.2 Principles of continuous subbottom profiling

Continuous subbottom reflection profiling provides a relatively cheap and rapid graphic display of sub-surface acoustic impedance interfaces, analogous to a geological section of the area surveyed (Reynolds, 1990). The technique utilises lower frequency sound (in the range 2kHz to 300Hz, depending on the system) than echosounders resulting in the penetration of the underlying substrate.

A pulse of sound is initiated that moves through the water column as a compressional wave and is reflected at contrasts in acoustic impedance (see section 2.2.2 above). The main pulse splits when it reaches the first interface of contrasting acoustic impedance and part of the pulse is reflected directly to the transducer. The remainder is transmitted through the substrate and continues to be reflected at further impedance

contrasts, resulting in a progressively weakening reflected signal. The amount of penetration achieved is dependent upon the frequency of sound emitted by the profiler. The rate at which the sound is attenuated within the substrate depends on the 'Quality Factor' (Q) which describes the quality of a rock as a sound transmitter (McQuillin and Ardu, 1977) (see below, this section). Q is inversely proportional to the absorption (Z). The relationship between these two parameters is formulated:

$$Z = \frac{27.3}{Q} \text{ dB}$$

where Z = the absorption of sound (dB)

Q = the rock quality factor

Figure 3.1 shows the relationship between the frequency of the sound source and the depth of penetration. Higher frequency systems such as Pinger (3.5 kHz) provide shallow penetration (< 30m) high resolution output. Low frequency systems including boomers operate at frequencies of 14-300Hz, penetrating to 100m, but with reduced resolution. Thus it is especially important to determine the type of information required by a research programme prior to survey commencement.

Resolution of all records is dependent on the outgoing pulse repetition rate, the speed of the vessel, and the depth of the reflecting surface. This is due to the received reflected pulse representing only a small part of the area covered by the acoustic pulse. This area is termed the first Fresnel zone. A high pulse repetition rate and slow vessel speed increase the overlap of Fresnel zones and consequently the resolution of the record. Vertical resolution is also dependent on the pulse repetition rate. If the pulse generated is long, the incoming signals from depth will be masked by the next outward pulse. Therefore, to identify fine stratification in the underlying sediment, a high pulse rate must be used. The maximum vertical resolution that can be obtained is where the distance between the upper

and lower bounding surfaces of a unit is greater than or equal to one eighth of the central frequency of the acoustic pulse (Widess, 1973). This thickness is known as the critical resolution thickness.

Propagation velocities down the profile vary according to several factors that cause contrasts in acoustic impedance; sediment porosity, degree of compaction, grain size, grain orientation, degree of cementation, nature of grain to grain contact and moisture content (Palmer, 1967; Van Overeem, 1978). Typical propagation velocities of selected rock types are given in Table 3.1. This illustrates that dense, more rigid, substrates transmit compressional wave energy most efficiently. Minor changes in porosity significantly change the propagation velocity of a rock.

Table 3.1
Propagation velocities of selected rock types

	Propagation velocities ms ⁻¹
Recent estuarine sands and silts	1530- 1600 (D'Olier, 1979)
Glacial moraine	1600-2700 (McQuillin and Ardus, 1977)
Limestone	3500-6500 (McQuillin and Ardus, 1977)
Granite	4600-7000 (McQuillin and Ardus, 1977)

Occasionally penetration by the acoustic pulse is not achieved resulting in 'acoustic blanking' or turbidity. Research involving the coring of acoustically turbid sediments has revealed that this phenomenon is often caused by high levels of gas produced during the decay of buried organic material (Schubel and Scheimer, 1973; Muller, 1976; Jones et al., 1986). Gas usually occurs as small bubbles within the sediment which causes attenuation of sound waves and prevents further penetration (Van Overeem, 1978). The production of methane hydrates during the decay of organic matter can be the cause of reflection surfaces unrelated to sedimentary bedding planes (Manley and Flood, 1989). Such reflectors may be identified by their parallelism with the surface reflector and tendency to cut across bedding planes.

Seismic records may also contain side reflections produced when reflections are received from a target outside the Fresnel zone. This occurs if the target is orientated directly towards the transducer and appears as a hyperbola as signals are received before, during and after the transducer has passed. Hyperbolae are also produced on a smaller scale within the sediment by reflections from uneven surfaces or individual boulders (point reflectors).

Multiple reflections occur when part of the reflected wave passes the receiving transducer, is reflected by the water surface to the bottom and back to the transducer. This results in a second reflection appearing at twice the depth of the first, and at twice the amplitude. Multiples can have the effect of masking detail at depth on the profile, and in very shallow water may occur up to six times. The amplified detail on these reflections can be of value. Removal of multiple reflections can be achieved by the employment of seismic systems that record data on magnetic tape which can then be replayed and the signal filtered.

Verification of the presence and nature of reflection surfaces indicated on a seismogram is thus important. This may be carried out in several ways. Cores may be taken from the survey area and samples of material analysed by ultrasonic impulse whereby a high frequency sound pulse is passed through a sample to measure the attenuation of sound (Mayer, 1979). The bulk density and gas content of core samples are also measured. Problems associated with this method are the disturbance caused during coring, extraction and sampling, especially in recent, unconsolidated sediments. Wire line logs of seismic velocities can be taken in consolidated sediments, or a seismic survey line can be made to coincide with a previously cored site.

Pinger seismic subbottom reflection profiling apparatus comprises a hull mounted or towed, single channel transducer from which low frequency pulses of sound are emitted. This transducer also receives the incoming pulse. Other systems require the towing of hydrophone arrays for signal reception. The reflected signal is transmitted to a recorder where time variable gain is applied to the weaker subbottom signals. Time variable gain intensifies the signals received from the most distant parts of the Pinger range to enable

accurate comparison between signal intensities across the record. The data are displayed on electrosensitive paper by the passing of an electric current through the paper via a continuously moving electrode band. Varying signal intensity is indicated through a proportional 'darkening' or 'lightening' on the chart record.

3.3 SEISMIC PROFILE INTERPRETATION: METHODOLOGY AND CLASSIFICATION

3.3.1 Historical Overview.

Prior to the pioneering work of Vail, Mitchum and others in Payton (1977), who first applied seismic stratigraphy to seismic reflection profile interpretation, the methods of data analysis and presentation varied considerably between research groups. Due to the lack of a unifying framework for seismic record analysis before that date, earlier accounts of seismic records presented numerous studies containing non-comparable data. Thus the impact of early research utilising seismic profiling techniques was considerably reduced.

Lineback et al. (1971), working on Lake Michigan, recognised the importance of subbottom reflection profiling to provide 'Instant cross sections of acoustic reflections.' Seismic stratigraphy was used to aid the correlation of sediments between core sites, allowing information on thickness, distribution, structure and topography to be determined. Two 'Formations' were identified one of which comprised three major 'Episodes' of sedimentation. Damuth (1975) formed a classification based on the 'Echo character' of sediments. 'Classes' were distinguished by their visual appearance, primarily by the nature of the surface reflector. Subsequent subdivisions were made on the grounds of the nature, presence or absence of internal reflectors and the size and density of point hyperbolae.

Acoustic reflection records were used by Jansen (1976) in an investigation of the late Pleistocene and Holocene history of the northern North Sea. A comprehensive

stratigraphy of the area was described from a detailed study of principal reflection surfaces and internal reflectors. 'Acoustic units' were given the status of 'Deposits' (e.g. Witch Deposits, Hills Deposits) or a genetic term (e.g. tidal sand ridge, channel fill).

A basic procedure for interpreting seismic reflection profiles was presented by McQuillin and Arduş (1977). This involved the identification of 'Important horizons' for measurement and interpretation and included the elimination of multiple- and side-reflections. According to their procedure sections should be corrected to illustrate scale distortion, the dip of reflectors should be calculated, and structural phenomena should be identified. No indication of how an 'Important horizon' might be quantitatively defined was given. In common with all previous accounts, this basic outline failed to provide the unifying framework for a seismic reflection interpretation procedure that was so urgently required for comparative purposes. A volume of papers on seismic stratigraphy, published in the same year (Payton, 1977), established the framework for seismic stratigraphic interpretation, the importance of which was still recognised a decade after its appearance:-

'A major breakthrough revitalized stratigraphy when Vail et al. (1977)...opened up entirely new vistas of global stratigraphy by introducing for the first time a rigorous stratigraphic interpretation of seismic reflection profiles' (Bally, 1987).

In this significant series of papers (e.g. Vail and Mitchum, 1977; Mitchum et al., 1977a, b.; Mitchum and Vail, 1977) the sequence concept of Sloss (1963) was applied to seismic profiles, but reduced in scale by an order of magnitude. The new approach to seismic analysis involved; first, seismic sequence analysis, whereby the record is subdivided into large scale components; secondly, further subdivision by seismic facies analysis, and finally, sea level analysis. In this thesis the final analytical process is replaced by a more general lithostratigraphic analysis relevant to the study of inland waterbodies.

This technique, originally applied to low frequency profiles run for petroleum exploration purposes, has been successfully transposed to high frequency, high resolution seismic profiles (e.g. Rokoengen et al., 1979 (Norwegian shelf); Landmesser et al., 1982

(Great Lakes); Bellaiche et al., 1986 (Rhône fan) ; Canals et al., 1988 (Ebro delta); Aarseth et al., 1989 (Norwegian fjords); Hequette and Hill, 1989 (Beaufort Sea) ; Mullins et al., 1990 (Kalamalka Lake, British Columbia)). Despite using the framework offered by earlier researchers, the terminology 'seismic sequence' and 'seismic facies unit' has not been universally applied. Terms such as 'Layer' (e.g. Finckh et al., 1984; Ben Avraham et al., 1986) and 'Type' (e.g. Johnson, 1980a; Johnson and Davis, 1989; Wingfield, 1990a) have been used where the previously proposed terminology would have sufficed.

3.3.2 Seismic stratigraphic interpretation.

Seismic record interpretation in this study follows the 'seismic stratigraphy' procedure established by Mitchum and Vail, (1977) and Mitchum et al., (1977 a,b). The more recently developed 'sequence stratigraphy' (Van Wagoner et al., 1988) is not used for the interpretation of seismic records in this thesis. Sequence stratigraphy is concerned with the identification of 'Repetitive, genetically related strata bounded by surfaces of erosion or nondeposition, or their correlative conformities' (Van Wagoner et al., 1988) associated directly with cyclical changes in sea level. This cyclicity is usually absent in the deposits in small inland waterbodies.

When applied to high resolution profiles obtained for non-exploitative purposes, seismic stratigraphic analysis has been adapted from its primary aim of sea level analysis to provide a genetic lithostratigraphic interpretation having wider applicability. This is possible as the aim of seismic stratigraphy is not solely to establish cyclicity of sedimentation.

The interpretation of subbottom seismic reflection profile data generates a stratigraphy which enables the identification of principal reflection surfaces and geometries. This does not necessarily represent the actual lithostratigraphy due to the limitations of the resolution of profiling equipment. The term 'Seismic para-stratigraphy' (Krumbein and Sloss, 1963) has been used to describe the stratigraphy derived from seismic profiles.

The method used in this research has two stages; seismic sequence analysis and seismic facies analysis from which a seismic parastratigraphic interpretation is made.

3.3.3 Seismic sequence analysis.

The first stage in record interpretation requires the identification of the basic sequence which is defined as :-

'A stratigraphic unit composed of a relatively conformable succession of genetically related strata and bounded at its top and base by unconformities or their correlative conformities' (Mitchum et al., 1977b, p. 59).

Sequences can range in amplitude (thickness) from millimetres to thousands of metres, however, they are most commonly in the range of 10-100m.

The above procedure creates a framework based solely on an objective criterion, the physical relations of reflection termination patterns - unconformities and conformities. Mitchum et al., (1977b, p. 59) defined an unconformable boundary in a depositional environment as one where there are;

'Observable discordancies in a given stratigraphic section showing evidence of erosion or non-deposition with obvious stratal terminations.'

Unconformities may be traced laterally to areas where discordancy of strata is less visually obvious. Differing reflection terminations at seismic stratigraphic sequence boundaries (see Table 3.2, Figure 3.2) allow inferences to be made about the mechanism of boundary formation.

Table 3.2
Seismic Stratigraphy Boundary Determination

Reflection Terminations					
Conformable	Unconformable				
Concordant	<u>Nondepositional</u>		<u>Truncational</u>		
	Lapout		Truncation		
	Toplap	Baselap		Erosional	Structural
		Onlap	Downlap		

After Mitchum et al., (1977b)

At unconformable sequence boundaries toplap occurs where reflectors terminate up dip by lapout and approach the upper boundary asymptotically. Baselap is further subdivided into:-

a) onlap, where an initially horizontal reflector laps out against an initially inclined surface, or where an initially inclined stratum laps out up dip against a surface of greater initial inclination and

b) downlap, where an initially inclined reflector terminates down dip against an initially horizontal or inclined surface.

Truncational unconformities can result from erosion of the upper boundary of a sequence or by structural disruption through processes including faulting and gravity sliding. Conformable seismic stratigraphic sequence boundaries can be delimited where older strata are separated from younger strata, but where there is no evidence of a hiatus due to erosion or non-deposition.

Sequences have a chronostratigraphic significance; the sediment deposited in a sequence is limited by the age of the upper and lower boundaries where they are conformable. Where a sequence boundary is unconformable the entire sequence cannot necessarily be dated at any one locality. On an individual basis, however, both single reflectors and unconformable boundaries are chronostratigraphic surfaces:-

'Perhaps the most fundamental assumption of the seismic stratigraphic method is that a seismic reflector in most cases, and for all practical purposes, is a time line' (Bally, 1987).

In this project more emphasis has been placed on the second stage of the Mitchum et al. (1977a) seismic interpretation procedure; seismic facies analysis.

3.3.4 Seismic facies analysis

The aim of seismic facies analysis is:-

'To determine objectively all the variation of seismic parameters within an individual seismic sequence' (Vail, 1987, p.1).

Thus seismic facies units have been defined as:-

'Mappable, three dimensional seismic units composed of groups of reflections whose parameters differ from those of adjacent facies units'

(Mitchum et al., 1977a, p.117).

Six parameters are used in the identification of seismic facies units (Vail, 1987; Mitchum et al. 1977).

i) Reflection geometry

This provides data on bedding pattern and configuration from which depositional processes, erosion and palaeotopography may be inferred.

ii) Reflection continuity

This reveals the extent of individual beds and allows further understanding of the process of deposition.

iii) Reflection amplitude

Reflection amplitude is closely related to the velocity and density contrasts of reflection interfaces. Significant velocity and density contrasts result in a high reflection amplitude. Information on the spacing of beds, their lateral continuity and fluid content can also be obtained from this parameter.

iv) Reflection frequency

This is primarily related to the initial pulse of sound emitted from the survey equipment, but it also enables the estimation of bed thickness and fluid content of subsurface sediments to be made.

v) Interval velocity

The interval velocity is related to porosity, fluid content, and lithology permitting further understanding of these factors.

vi) External form and areal association of facies

The topography and distribution of facies units allows interpretations regarding the gross depositional environment, sediment source, and overall geologic setting to be made.

Identification and analysis of each parameter provides increasing information about the facies, facilitating a progressive build up of knowledge, and thus enabling a final detailed lithoseismic interpretation to be deduced from the seismic profile. However, in the initial stages of seismic facies analysis, reflection geometry provides an important basic framework which can then be modified by data from subsequent seismic facies parameters.

Mitchum et al. (1977a) provide the following list of facies reflection geometries (Figure 3.3, Table 3.3) to which modifying terms may be added (Table 3.4).

Table 3.3
Reflection Configurations

STRATAL CONFIGURATION		
Parallel		
Subparallel		
Divergent		
Prograded Clinofolds	Sigmoid	
	Oblique	Tangential oblique
		Parallel oblique
	Shingled	
	Hummocky	
Chaotic		
Reflection Free		

After Mitchum et al. (1977)

Table 3.4
Reflection Configuration Modifying Terms

Even	Wavy
Regular	Irregular
Uniform	Variable
Hummocky	Lenticular
Disrupted	Contorted

After Mitchum et al., (1977)

Parallel and subparallel reflectors are frequently identified in seismic reflection studies (e.g. Howell, 1971; Boulton et al., 1981; Finckh et al., 1984; Canals et al., 1988; Mullins et al., 1990; Wingfield, 1990a). Aarseth et al., (1989) described parallelism of reflectors as 'acoustic lamination' whilst recognising that, as is the case in all seismic facies parameters, the number of reflectors identified is a function of instrument type and resolution, rather than an accurate representation of lithostratigraphy. Parallel reflectors are often present as a drape of high lateral continuity (e.g. Finckh et al., 1984; Mullins et al., 1990), although draped sediments may be found restricted to infills in depressions in the underlying lithology. Draped sediments are interpreted as having been deposited in a low energy environment, such as a lake (Howell, 1971; Mullins et al., 1990) or below wave base and unaffected by current activity in the marine environment (Boulton et al., 1981). Parallelism may also result from sheet deposition in high or low energy environments (Mitchum et al., 1977a).

The divergent reflector configuration is usually associated with a wedge shaped facies topography. Thickening of individual reflectors causes an overall thickening of the unit. Reflectors characteristically terminate non-systematically within the facies. Divergent reflectors indicate lateral variations in depositional rates, or the gentle downwards inclination of the surface of deposition (Mitchum et al., 1977a). The recognition of this reflection geometry appears to be unusual in the literature relating to high resolution profiling.

Prograding clinoform geometry is indicative of the lateral outbuilding of sloping strata (clinoforms) into areas of deeper water. Diversity in the configuration of progradational clinoforms (see Table 3.2) is interpreted to be due to variations in water depth at the point of deposition and the rate of deposition.

Sigmoid clinoforms consist of a series of laterally accreting S-shaped reflectors; topset strata are horizontal or low angled, foresets form low angle, thick, lenses of sediment and bottomsets are very low angled or horizontal strata. This reflection facies is

interpreted as being the result of low sediment supply and requires the rapid subsidence of underlying rocks or a rapid rise in water level (Mitchum et al., 1977a).

Oblique clinoforms differ from sigmoid reflectors in having an overall higher angle of deposition. Two basic types of oblique clinoforms have been identified, but complex clinoforms also exist. All oblique clinoforms are interpreted as being deposited in high energy environments with a constant sediment supply (Ravenne, 1978). Parallel oblique facies exhibit internal reflectors having high angles of downlap against the lower bounding surface (e.g. Canals et al., 1988). Tangential oblique reflectors are characterised by the progressive, tangential decrease in the angle of down dip deposition towards the lower facies boundary (e.g. Mitchum et al., 1977a; Canals et al., 1988). The overall facies form is concave upward and forward.

Shingled clinoforms are very similar in form to the parallel oblique type clinoform. The thinness of the entire facies and very gentle angle of parallel reflectors differentiate this facies geometry. The termination of reflectors by toplap and downlap is also at very low angles (Mitchum et al., 1977a; Canals et al., 1988) and the depositional setting is interpreted as being shallow water into which the units prograde.

Hummocky (Mitchum et al., 1977a) or irregular (Canals et al., 1988) clinoforms are characterised by a complete lack of lateral continuity resulting in a disjointed, hummocky reflection pattern. Sedimentological analysis of such facies by Bouye (1983) has established that they are composed of interfingering, sand dominated, heterogenous deposits. This supports the interpretation of Mitchum et al., (1977a). The depositional environment is interpreted as being inter- or pro- deltaic.

Non progradational forms include the chaotic acoustic reflection geometry. This type is widely reported in literature relating to high resolution seismic profiling (e.g. Hyne et al., 1972; Boulton et al., 1981; Landmesser et al., 1982; Canals et al., 1988; Prior and Bornhold, 1989; Wingfield, 1990a). Chaotic facies lack internal coherency (Boulton et al., 1981), having an 'Amorphous acoustic character' (Wingfield, 1990a) with no horizontal reflectors (Hyne et al., 1972) or small discontinuous reflectors (e.g. Mitchum et al., 1977a;

Canals et al., 1988). Individual point hyperbolae, formed through the scattering of the acoustic energy pulse from large blocks or boulders within a finer grained matrix, are also frequently associated with chaotic facies units (e.g. Gammelsaeter and Haugland, 1970; Boulton et al., 1981; Wingfield, 1990a). The unsorted nature of chaotic facies units is usually given one of two genetic interpretations, the final distinction being made on the grounds of external form and areal association of facies. The first mode of deposition is by reworking through slippage or slumping (e.g. Hyne et al., 1972; Bellaiche et al., 1982; Aarseth et al., 1989) where a distinct mound or series of mounds are identified. Secondly, chaotic facies units have been interpreted as being directly deposited glacial diamicts (e.g. Lineback et al., 1971; Jansen, 1976; Boulton et al., 1981; Landmesser et al., 1982). This genetic distinction is made when a facies unit has an extensive spatial distribution and may have a ridge or hummocky topographical expression. Chaotic reflections can also result from faulting, folding and contortion (e.g. Tinghuan and Bo 1989), but such causes are unusual in high resolution profiles pertaining to Quaternary sequences.

The final facies type is the transparent (Jansen, 1976) or reflection free (Mitchum et al., 1977a) facies unit. This unit has a seismic expression with either no or very few low amplitude internal reflectors due to lack of velocity-density contrasts within the facies. Lithologies that are homogenous, for example poorly compacted muddy sediments of recent origin (Canals et al., 1988; Johnson and Davis, 1989) or rapidly deposited proglacial clays (Johnson, 1980a; Landmesser et al., 1982; Mullins et al., 1990) can produce transparent seismic signals. Highly organic recent sediments can also cause reflection-free seismic profiles due to a high gas content which absorbs acoustic energy and prevents further penetration (e.g. Hutchinson et al., 1979; Ben-Avraham et al., 1986) (see also section 3.2.2 above). Slumping in homogenous sediments may result in transparent facies units through the removal of original bedding surfaces by internal deformation (e.g. Bellaiche et al., 1989). Again, the topography and distribution of the facies unit can be critical in the final interpretation of the origin of the transparent seismic facies unit.

Seismic facies analysis provides valuable detailed information on the nature of the

lithologies within seismic sequences. When data from both seismic sequence analysis and seismic facies analysis are combined, it may be seen that seismic reflection profiling is a very important tool for rapid, extensive surveys of subsurface lithology and lithological relationships.

3.4 METHODOLOGY: AIMS

Seismic subbottom reflection profiling was carried out on Lochs Lee, Callater and Muick using 3.5kHz 'Pinger' equipment. The subbottom surveys aimed:-

- i) To provide an extensive database of subbottom reflection profiles for each loch.
- ii) To enable seismic sequence and facies analyses to be undertaken for each water body, permitting seismic parastratigraphic interpretations, and comparisons to be made between each loch.
- iii) To complement echosounder (Chapter 2), sidescan sonar (Chapter 4), surface sediment (Chapter 5) and core (Chapter 6) data.

The configuration of Pinger components used varied between the water bodies, however, a Giffit graphic recorder was used in all surveys (Plate 3.1). This provided a sepia coloured graphic output by passing an electric current derived from the reflected sound pulse through wet electrosensitive paper.

3.5 LOCH LEE

3.5.1 Pinger survey

Loch Lee was surveyed during September and October 1989. To conduct the survey two rod-mounted Pinger transducers were positioned over the stern of the boat. An external hydrophone was used to receive the reflected signals. This achieved a significant improvement in Pinger record quality over that derived from the internal hydrophone, particularly in the distinction of lower amplitude internal reflectors. Due to high winds at

the time of survey (see Plate 3.2) it proved impossible to use the radio position fixing apparatus (Motorola Mini-Ranger Mk III) available. Mooring for a sufficient length of time to allow the siting of the radio beacons risked damage to both the equipment and survey personnel. Therefore position fixing was achieved on Loch Lee by running traverses between shoreline landmarks identified on the Ordnance Survey 1:10000 map, or where this was impossible, by following compass directions. The total length of survey lines amounted to 10.07 km on the 1.95km long loch (Figure 3.4). A maximum subbottom penetration of 11ms was achieved.

3.5.2 Seismic stratigraphic interpretation

Four seismic sequences comprising seven seismic facies have been recognised in Loch Lee, following the 'Seismic stratigraphy' procedure proposed by Mitchum and Vail, (1977) and Mitchum et al. (1977) (see sections 3.3.2-3.3.3 above). For clarity, the description of seismic facies is presented after that of each seismic sequence. For examples of the descriptive terms used throughout the following sections (3.5.2, 3.6.2, 3.7.2) refer to Figures 3.2 or 3.3.

3.5.2.1 Sequence 1

Sequence 1 occurs at the top of the Loch Lee seismostratigraphic succession. Its upper boundary is conformable and forms the sediment-water interface (Figures 3.5, 3.6, 3.7, Plates 3.3, 3.4A, 3.4B). The reflection amplitude of this boundary exhibits spatial variability within the water body. The lower boundary has a high reflection amplitude and overlies Sequences 2 and 3 unconformably. Reflectors at the lower boundary terminate updip by onlap and downdip by downlap (Figure 3.12, Plate 3.3). Sequence 1 is composed of three seismic facies (1.1, 1.2, 1.3) and varies in thickness from 0.1ms to 6.5ms.

3.5.2.1.1 Facies 1.1

Facies 1.1 has a subparallel even to subparallel wavy reflection geometry (see Figure 3.8). However, occasionally the internal reflectors exhibit the 'chaotic total' geometry (Figure 3.8d northwest). This facies is characterised by reflectors with a low reflection amplitude. On some profiles the reflection amplitude of the upper surface is only marginally above that of the background 'noise'. Individual reflectors can be traced continuously over distances up to 40m. Facies 1.1 is distributed discontinuously within Loch Lee (Figure 3.9, Plate 3.3), but is most widely recognised at the eastern end of the loch. The maximum thickness (1.4ms) occurs at a depth of 21m below a break in slope descending to the deepest trough. Facies 1.1 exhibits varied external forms. It frequently occurs as a lobe on low angle slopes (Figure 3.8a, c). In this configuration the internal reflectors thicken in a downslope direction. At the base of moderate to inclined slopes Facies 1.1 has been recognised with a chaotic total reflection geometry (Figure 3.8d northwest). This facies also fills depressions in the underlying topography. Reflection geometries of the fills vary between subparallel wavy (Figure 3.8b) and subparallel lenticular (Figure 3.8d southeast, Plate 3.4A). Facies 1.1 occurs only at the top of the seismostratigraphic column overlying Facies 1.2 and 1.3, with a distinct, non-gradational boundary (see Figures 3.5 and 3.7, Plate 3.3).

3.5.2.1.2 Facies 1.2

Facies 1.2 has a predominantly parallel reflection geometry (Figure 3.10a, Plate 3.4B) However, this facies exhibits occasional gradational change to parallel wavy (Figure 3.10b, Plate 3.4C), chaotic stratal (Figure 3.10c) and subparallel lenticular (Figure 3.10e) geometries. These reflection geometries rarely extend laterally for more than 40m. At the western end of the loch numerous small point hyperbolae truncate the parallel wavy reflectors (Figure 3.10b, Plate 3.4C) and are identified at the sediment-water interface. The reflection amplitude of the surface and internal reflectors is high. Facies 1.2 is distributed extensively throughout Loch Lee (Figure 3.11). Individual reflectors can be traced over

distances in excess of 100m. The facies has an average thickness of 0.5ms (see Traverse 11, Figure 3.5) and a maximum thickness of 3.5ms at the western end of the loch (see Traverse 13, Figure 3.6). It forms a drape over underlying reflectors, infilling topographic lows, resulting in a subparallel lenticular reflection geometry (e.g. Figure 3.10e). On low angle slopes (e.g. Figure 3.10c) there is evidence for the disruption the stratification. Facies 1.2 has a gradational boundary with Facies 1.3 and overlies Sequences 2 and 3 unconformably (e.g. Figure 3.5, Traverse 8, Plate 3.3).

3.5.2.1.3 Facies 1.3

Facies 1.3 comprises a series of seismic reflectors occurring on moderate to inclined slope angles. It has a gradational boundary updip with the parallel and subparallel reflectors of Facies 1.2. This facies is made up of major and minor internal reflectors. The former have been identified as being continuous over approximately 60m whereas the latter rarely extend beyond 20m (Figure 3.12). With increasing slope angle the major reflectors diverge to form a sigmoidal or oblique parallel geometry (Plate 3.3). A maximum of seven major reflectors have been identified (Figure 3.12, Traverse 10). At the base of the slope the uppermost major reflector merges laterally with Facies 1.2 (e.g. Figure 3.12, Traverse 10). Lower major reflectors which also form the sequence boundary terminate updip by onlap and downdip by downlap. The minor reflectors also exhibit a range of geometries from subparallel wavy updip to chaotic or contorted downdip. Reflection amplitude varies between these two types of reflector. The major reflectors have a higher (medium) amplitude than the minor reflectors, however, both types of reflector decrease in amplitude with depth. The external form of Facies 1.3 is infrequently lobate (Figure 3.12, Traverse 3) and frequently acts as a masking drape over underlying sequences. On Traverse 10 (Figure 3.12) Facies 1.3 can be identified infilling a deep (6ms) hollow in Sequences 2 and 3. This facies has a restricted distribution in Loch Lee, concentrated away from the basin sides at the eastern end of the central trough (Figure 3.13). A maximum thickness of 6ms is attained. Facies 1.3 partially forms the unconformable boundary between the underlying Sequences 2 and 3.

3.5.2.2 Sequence 2

Sequence 2 is characterised by unconformable upper and lower boundaries. The upper boundary has a high reflection amplitude and is marked by truncated internal reflectors (see Figure 3.14). The lower boundary overlying Sequence 3 is recognised by the termination of internal reflectors by onlap updip and downlap downdip (Figure 3.14, Traverse 7). This sequence is composed of two seismic facies (2.1, 2.2) and varies in thickness between 0ms and 4.5ms.

3.5.2.2.1 Facies 2.1

This facies is composed of subparallel wavy and hummocky reflectors (Figure 3.14, Plate 3.4D) with occasional concentrations of point hyperbolae (e.g. Traverse 7, Figure 3.14, Plate 3.4D). At the sequence boundary Facies 2.1 reflectors terminate by toplap updip and downlap downdip. An exception to this occurs where a conformable boundary is recognised with Sequence 3 at locations where the sequence boundary is formed between Facies 2.1 and 3.2. Facies 2.1 reflectors range in lateral continuity between 5m to >40m. This facies has a medium reflection amplitude. However, medium levels of internal backscatter within the facies partially mask the reflectors, hindering identification. The upper surface of Facies 2.1 has a uniform linear nature, but the lower boundary follows the underlying topography of Sequence 3 (e.g. Figure 3.6). The isopach map (Figure 3.15) illustrates the spatial variation of this infill. A maximum depth of 3.5ms is achieved in two hollows on the surface of Sequence 3. Facies 2.1 thins upslope on the underlying topography to thicknesses of less than 0.5ms. The thickness of this facies could not be accurately determined where the thickness of overlying Facies 1.3 attenuated the seismic signal. Facies 2.1 underlies Sequence 1, overlies Sequence 3 and has a gradational boundary with Facies 2.2.

3.5.2.2.2 Facies 2.2

Facies 2.2 is characterised by a chaotic total geometry within which scattered point hyperbolae are distributed (see Figures 3.16; 3.17, Plate 3.4E). Individual reflectors are

discontinuous and can be traced over a maximum distance of approximately 2m. At the margins of this facies reflector continuity increases (e.g. Figure 3.16a) to form a gradational boundary with Facies 2.1. The reflection amplitude of Facies 2.2 is high, but, as in Facies 2.1, the internal backscatter within the facies impedes reflector identification. Facies 2.2 does not exhibit a characteristic external form, broadly reflecting the topography of the underlying Sequence 3 (Figure 3.17). It has a limited distribution within Loch Lee (Figure 3.18, Plate 3.3), principally restricted to the sides of the Loch upon moderate, inclined, and extremely steep slope angles (Figure 3.5b; 3.7). A few outlying areas occur at the eastern end of the basin (Figure 3.5a). It has a maximum thickness of 4.5ms close to the mouth of the small unnamed stream on the southwestern shore. Facies 2.2 underlies Facies 1.2 has a gradational boundary with Facies 2.1 and overlies Sequence 3 (Plate 3.3).

3.5.2.3 Sequence 3

Sequence 3 has been recognised solely by the characteristics of its upper boundary reflectors. The lower boundary of this sequence cannot confidently be identified, due to the attenuation of the high frequency sound waves used by the Pinger system (section 3.2.2). The upper boundary has a characteristic undulating or hummocky surface of medium reflection amplitude (see Figures 3.5; 3.6; 3.7, Plate 3.3). The boundary is largely unconformable with Sequences 1 and 2 due to non deposition, however, where the boundary is formed by Facies 3.2 it appears conformable. Two facies (3.1, 3.2) have been identified in this sequence (Plate 3.4C; 3.4D; Figure 3.19c).

3.5.2.3.1 Facies 3.1

Facies 3.1 is recognised by the complete absence of stratification within the internal reflectors (Figure 3.19a, b) which are composed almost entirely of point hyperbolae. The density of these hyperbolae results in a characteristic 'mottled' effect. Thus reflection continuity is discontinuous, individual hyperbolae spanning a maximum of approximately 5m. Facies 3.1 has a medium to high reflection amplitude and a highly irregular external

5m. Facies 3.1 has a medium to high reflection amplitude and a highly irregular external form (Figure 3.19a). The surface reflector has a 'hummocky' topography (Figure 3.19a) with a maximum amplitude of 3ms between mound and hollow. This facies is distributed throughout Loch Lee and has a maximum thickness >10ms.

3.5.2.3.2 Facies 3.2

Facies 3.2 is identified forming an infill within the topographic lows of Facies 3.1 (Figure 3.5, Traverse 11; 3.6; 3.7). This facies is composed of basal, crudely stratified, point hyperbolae that grade upwards through the facies to subparallel and subparallel wavy reflectors which have a lateral continuity of <20m (Figure 3.19c). Facies 3.2 has a gradational lower boundary with Facies 3.1 and a conformable upper boundary with Facies 2.1. The similarity in seismic response between Facies 3.2 and 3.1 in the basal areas of the former facies render distinction difficult and may have resulted in data omission. However, Facies 3.2 is identified throughout Loch Lee and has a maximum thickness of 2ms.

3.5.2.4 Sequence 4, Facies 4.1

Below Facies 3.1, on Traverses 8 and 7 only (Figure 3.5b; 3.6; Plate 3.3), a high amplitude reflector with a smooth external form is identified, forming Sequence 4. Seismic penetration of this reflector is minimal (<0.5ms) preventing analysis of reflection geometry, continuity and thickness of the facies. Sequence 4 is the base of the seismic succession identified using 3.5kHz Pinger seismic reflection profiling apparatus.

3.5.3 Seismic parastratigraphy

3.5.3.1 Sequence 1

This sequence is interpreted to result from Holocene lacustrine deposition due to the stratified geometry and draped form of the reflectors. The low amplitude internal reflectors of Facies 1.1 are typical of fine-grained, homogenous, Holocene lacustrine sediment (e.g. Hutchinson et al., 1981). The subparallel reflectors are interpreted as resulting from deposition below wind wave base, in quiet conditions. Chaotic reflectors are believed to

sediments, at the top of the seismostratigraphic column, indicates that sedimentation of this sequence is occurring at present. Finckh and Kelts (1976) measured the seismic velocity of Holocene muds and silts in Lake Zurich to be 1500ms^{-1} . Surface sediment samples (Chapter 5) indicate that Sequence 1 is composed of sand, silt, and organic matter similar to that described by Finckh and Kelts. Facies 1.1 therefore has a maximum measured thickness of 2.1m.

Facies 1.2 is principally composed of parallel to subparallel reflectors with a high lateral continuity. This geometry is also typical of lacustrine sedimentation in quiet water. The high amplitude internal reflectors indicate that the sediment has either undergone more post-depositional compaction than Facies 1.1 or has a higher percentage of slightly coarser grained sediment, such as fine sand. The small areas of chaotic stratal reflectors located on the loch sides are believed to result from mass movement processes (section 7.4.1.2.2). Occasional small point hyperbolae identified at the western and central areas of Loch Lee are interpreted as boulders (section 4.4.2.2). These may be derived from anchor weights used by fishermen. Facies 1.2 has an average thickness of 0.75m and a maximum measured thickness of 5.25m.

Facies 1.3 comprises prograding clinoforms (sigmoidal and oblique parallel) which form when strata extend from shallow to deeper water areas (Mitchum et al., 1977a). This facies occupies a topographic low, approximately 9m deep, in Sequences 2 and 3. The identification of the major reflection surfaces within Facies 1.3 suggests episodic sedimentation events (Desloges and Gilbert, 1991). The medium-low amplitude of the reflectors indicates poorly consolidated, fine grained sediments. The sediment supply for this facies is believed to be from the northeastern shallow water areas. During an aborted survey attempt in October 1989 high winds, Gale Force 8 or Strong Gale Force 9 were experienced in Glen Lee. Observed wave heights at this time were in the range 0.5-0.7m (Plate 3.2). Thus it is proposed that Facies 1.3 was formed by the entrainment of fine grained materials by waves in the nearshore environment (Johnson, 1980b). It is suggested that the entrained sediments are redeposited close to, or at the break of slope between Zones 2 and 3 from where downslope redistribution by mass movement into deeper water occurs.

This process accounts for the gradational boundary between Facies 1.2 and 1.3, and for the episodic nature of sedimentation caused by low frequency high magnitude wind events. Facies 1.3 has a maximum measured thickness of 9m.

3.5.3.2 Sequence 2

Sequence 2 has an unconformable upper and lower boundary. It is distinguished by two facies that exhibit varied concentrations of point hyperbolae.

Facies 2.1 comprises subparallel reflectors of medium to high amplitude which terminate by lapout. These reflectors are interpreted as forming by the settling of fine grained materials from suspension in the lacustrine environment. The stratification of the reflectors may be due to compaction of the sediment or temporal variations in grain size. Clusters of point hyperbolae (boulders) within this draped facies are concentrated around the edge of the loch, within approximately 100m of the shore. Due to the location and size of these clasts it is proposed that these boulders result from avalanche or debris flow activity on the slopes surrounding the loch. Thus two environmental processes, subaerial mass movement, and lacustrine sedimentation, were operational contemporaneously in the formation of this facies. Evidence from Sequence 1, which is believed to represent Holocene deposition, shows that this combination of processes is not presently occurring. Sissons et al. (1973) suggested that during the Loch Lomond Readvance, outside glacier limits, enhanced periglacial activity including rockfall and solifluction activity occurred. Geomorphological evidence suggests that the Loch Lee basin was not glaciated during the Loch Lomond Readvance (sections 1.4.2, 1.5.2.2.2). However, the loch must have been affected by seasonal surface ice cover during this period. It is therefore proposed that the bimodal sediment deposition identified from the seismic records resulted from :-

a) Sedimentation of fine grained material during the Loch Lomond Readvance by settling during the winter months and possibly during the summer. This formed the stratification and draped external form of the facies.

b) Sedimentation of boulders during the summer months as boulders deposited on the winter ice by rockfall and avalanche activity fell through the melting ice surface. This resulted in the nearshore clusters of point hyperbolae.

This interpretation is discussed in more detail in section 7.4.5.1.

The conformable basal boundary with Facies 3.2 is interpreted as indicating that deposition at these locations has been uninterrupted, and is marked only by a basal increase in grain size in Facies 2.1. At the boundary with Facies 2.2, Facies 2.1 has a seismic signature comparable with glacial diamict (1740ms^{-1} , Finckh and Kelts, 1976). Thus Facies 2.1 has a maximum measured thickness of 6m which thins upslope to 0.8m.

Facies 2.2 has a gradational boundary with Facies 2.1. It differs from Facies 2.1 in that the internal reflectors are discontinuous and chaotic. It is distributed primarily around the shores of the loch on moderate, inclined, and extremely steep angle slopes, with scattered outliers at the eastern end of the basin. Due to this distribution it is suggested that this facies was formed by mass movement activity on the slopes surrounding Loch Lee. The lateral gradational boundary with Facies 2.1 indicates contemporaneous deposition and thus a probable Loch Lomond Stadial age. In this context mass movements on the adjacent slopes would be dominated by avalanche and debris flows/slides. The deposition of this facies in Zone 3 on very low to low angle slopes is less likely to be the result of direct mass movements. It is suggested that in these central loch positions Facies 2.2 may have been formed by avalanche deposits which were deposited through the lake ice during the summer melt (Weirich, 1985). Evidence in support of this hypothesis is found in the lobate outline of the distribution of Facies 2.2 at the eastern end of the loch (Figure 3.18). Facies 2.2 has a maximum measured thickness of 7.8m against the southwestern shore.

3.5.3.3 Sequence 3

Facies 3.1 has a characteristic hummocky external form. This factor, combined with the high concentration of point hyperbolae typifies glacial diamict (e.g. Boulton et al. 1982; Mullins and Hinchey, 1989) which has a seismic velocity of approximately 1740ms^{-1} . Assuming this velocity, Facies 3.1 has a maximum measured thickness $>17\text{m}$.

Facies 3.2 has a gradational basal boundary with Facies 3.1, indicating broadly contemporaneous deposition of coarse grained material. Stratification of boulders is interpreted as representing the deposition of large clasts by high velocity glacial meltwaters. During glacier retreat sediment grain size and current velocity reduced in Loch Lee, resulting in the sedimentation of stratified fine grained material which has a conformable boundary with Facies 2.1. A maximum thickness of 3.4m is recorded.

3.5.3.4 Sequence 4

This Sequence comprises one facies (4.1) which occurs only at the base of the seismic sequence identified by Pinger profiling. The smooth external form and stratigraphic position leads to the tentative suggestion that this facies represents ice moulded bedrock.

3.6 LOCH CALLATER

3.6.1 Pinger Survey

The seismic subbottom reflection survey of Loch Callater was undertaken in August 1990. Position fixing on the water body was achieved by dead reckoning between known end points along the length of the loch. High voltage (240 volt AC) radio position fixing equipment could not be accommodated on the dinghy because of the limited space available (Plate 3.5) and danger to the surveyors. To overcome the lack of secure positions upon which to fix a rod-mounted transducer on an inflatable dinghy, the Pinger transducer was towed beside the dinghy on the starboard side, secured to a pole fixed to the rowlocks. An external hydrophone was trailed from the port side, fastened to the other end of the pole. Due to the shallowness and narrowness of the loch attempts at transverse profiling failed. Approximately 3km of subbottom profile traverses were obtained (Figure 3.20).

3.6.2 Seismic stratigraphic interpretation

Two seismic sequences comprising two seismic facies have been identified in Loch Callater. The profiles obtained were of relatively poor quality due to equipment failure resulting in indistinct tonal contrasts, and numerous reflection multiples. Photographic reproduction of the records was unsuccessful, therefore diagrammatic representations are given.

3.6.2.1 Sequence 1, Facies 1.1

Sequence 1 comprises the top of the Loch Callater seismostratigraphic succession. It has a medium level seismic reflector amplitude and conformable upper boundary. The upper surface of Sequence 1 forms the sediment-water interface. The lower boundary of this sequence has a high reflection amplitude, but is recognised at only two points on the data available (Figure 3.21). However, from this limited information the lower boundary is believed to be conformable with the underlying Sequence 2. Sequence 1 is composed of one facies (1.1).

Facies 1.1 (Figure 3.22a) has a predominantly parallel to subparallel reflection geometry which locally has a gradational boundary with chaotic stratal reflectors. Individual chaotic stratal reflectors have a lateral continuity of approximately 5m and the area of chaotic strata has a lateral extent of 20m. Subparallel reflectors have been traced continuously over distances of up to 50m. Occasional individual point hyperbolae have been identified in this facies (Figure 3.22a). All reflectors within Facies 1.1 are of medium reflection amplitude. This facies has been recognised in Loch Callater wherever seismic penetration was achieved and forms a drape over the underlying topography, thinning upslope (see Figure 3.21). The maximum thickness of Facies 1.1 could not be ascertained, as seismic penetration did not reach the base of the facies over the majority of the loch floor, however it is known to exceed 4.5ms.

3.6.2.2 Sequence 2, Facies 2.1

Sequence 2 underlies Sequence 1 conformably. The upper boundary has a high reflection amplitude. The lower boundary could not be identified from the data available, due to attenuation of the seismic signal. It is distinguished from the overlying sequence by the nature of the characteristic internal reflectors. Sequence 2 has been identified in this survey as comprising one facies (2.1).

Facies 2.1 is characterised by numerous point hyperbolae distributed within an unstratified matrix (Figure 3.22b). The reflection amplitude of these reflectors is medium to high. The facies has a distinctive, mound-like external form, which reaches a maximum

height of 2ms within Facies 1.1 (Figure 3.21). Facies 2.1, as recognised from the Pinger data, has a limited distribution within Loch Callater. It is believed that this facies has a more extensive lateral distribution in this water body, beyond the range of penetration of the survey equipment.

3.6.3 Seismic parastratigraphy

3.6.3.1 Sequence 1, Facies 1.1

The parallel to subparallel, medium intensity, continuous, draped reflectors of Facies 1.1 are typical of sedimentation in a quiet water lacustrine environment. Evidence of a small number of point hyperbolae within the facies suggests the scattered occurrence of small boulders. It is suggested that these boulders may be due to anthropogenic input. The popular walkers' path 'Jock's Road' runs along the northeastern shore of Loch Callater. During winter the surface of Loch Callater has been observed to freeze to a depth of 10cm. Numerous small (10-30cm) cobbles were seen scattered over the ice, the highest concentrations occurring where Jock's Road descends to the waterline. No evidence of recent rockfall or avalanche activity was observed in association with these cobbles. Thus it is concluded that the cobbles had been thrown onto the ice by passing walkers. During the spring melt the cobbles would be released into the fine grained lacustrine sediment. There was no evidence for the removal of nearshore clasts to deep water by inclusion in the ice and subsequent rafting at ice break up. Where ice melt at the shoreline was occurring, in insulated areas, ice was melting preferentially around the clasts, which had apparently not been moved.

The local occurrence of chaotic reflectors on low to inclined slopes is believed to result from small scale mass movements. Sequence 1 has a maximum thickness in excess of 6.75m assuming a seismic velocity of 1500ms^{-1} (see section 3.5.3.1).

3.6.3.2 Sequence 2, Facies 2.1

This sequence is composed of one facies with a hummocky upper reflection surface and numerous point hyperbolae. This is the form typical of glacial diamict. Sequence 2 has a maximum thickness of >3.5m assuming a seismic velocity of 1740ms^{-1} (see section 3.5.3.3).

3.7 LOCH MUICK

3.7.1 Pinger survey

Numerous seismic subbottom profiling surveys were carried out on Loch Muick during the period April 1989-October 1990, owing to a combination of extreme weather conditions, and equipment failure. Motorola Mini-Ranger MkIII radio position fixing apparatus was used in all surveys. Early surveys were carried out with two rod-mounted Pinger transducers lowered over the stern of the boat. High winds combined with equipment failure resulted in poor quality records necessitating further surveys to be undertaken. These were carried out during weather windows, and involved the use of a towed transducer (Plate 3.5) and a combination of the internal and external hydrophones. The external hydrophone operated successfully in areas of shallow water, providing detailed graphic records. The internal hydrophone operated in all water depths but produced seismic profiles of considerably lower definition. Of the 49km of survey lines covered over this time period 19km were of usable quality (Figure 3.23).

3.7.2 Seismic stratigraphic interpretation

Three seismic sequences comprising five seismic facies have been identified in Loch Muick. As in section 3.5.3 above, the description of seismic facies follows that of each sequence.

3.7.2.1 Sequence 1

Sequence 1 has been identified at the top of the Loch Muick seismostratigraphic succession. The upper boundary forms the division between sediment and water (Figures 3.24, 3.25, 3.26, 3.27, 3.28, Plates 3.6, 3.7, 3.8). The reflection amplitude of the upper boundary varies spatially between high and low amplitude, according to the facies present at the surface. The upper sequence boundary is conformable with the water. The lower sequence boundary overlies Sequence 2 unconformably. The facies within Sequence 1 terminate upslope by onlap (e.g. Figures 3.31; 3.26, Traverse 79-83). However, this unconformable boundary is not apparent in the central area of the trough (Figure 3.28). In these areas the sequence is draped over the underlying reflectors. Downlap against Sequence 2 has been identified on one traverse (Traverse 132-136, Figure 3.26). Sequence 1 is composed of two seismic facies (1.1 and 1.2) and varies in thickness between 0ms and 7ms.

3.7.2.1.1 Facies 1.1

Facies 1.1 has a reflection-free internal geometry (Figure 3.29, Plate 3.8). Its upper surface has a very low reflection amplitude and low reflection continuity. This facies has a maximum lateral continuity of approximately 250m (Figure 3.30). The external form of Facies 1.1 is a drape which thins upslope (Figure 3.29a, b, Plate 3.8), typically infilling topographic irregularities (Figure 3.29a), or occurring at the base of a slope (Figure 3.29b). At one locality (Figure 3.29c) on a low angle slope it has a lobate external form. This facies has a limited distribution in Loch Muick (Figure 3.30), occurring in the central and northeastern areas. Facies 1.1 has a maximum thickness of 1.5ms and forms the top of the seismostratigraphic sequence, overlying Facies 2.2 (Figure 3.28).

3.7.2.1.2 Facies 1.2

Facies 1.2 is characterised by a range of reflector geometries, but is predominantly composed of subparallel reflectors (Figure 3.31b, d; Plate 3.7). Parallel reflectors (Figure

3.31a), subparallel merging into chaotic at the base of the profile (Figure 3.31c), subparallel lenticular (Figure 3.32d), and chaotic (Figure 3.32b) reflectors are distributed locally throughout the Loch Muick basin. The detected continuity of reflectors appears to be at least partially dependent on the type of hydrophone used (see section 3.7.1 above). The external hydrophone resulted in seismic sections that show small scale internal reflectors with lateral continuities in excess of 40m. The traverses completed using the internal Pinger hydrophone have a much lower internal resolution, showing only large scale internal reflectors (e.g. Plates 3.6, 3.7), even in areas where small scale reflectors are known to exist. Thus facies interpretations based upon these deep water traverses (e.g. Figure 3.31b, d, 3.32) are believed to lack internal reflector detail. Where present, in deep water traverses, minor internal reflectors are continuous over distances of less than 20m. Major reflectors in Facies 1.2 extend over distances of over 100m (Figure 3.26, Traverse 132-136, Plate 3.6) terminating by downlap against Sequence 2 (Figure 3.31d). This downlapping configuration is unique to one profile, Traverse 132-136 (Figure 3.26, Plate 3.6). The major reflectors recognised from all other deep water traverses are of a subparallel geometry.

The reflection amplitude of Facies 1.2 in all traverses is high. Facies 1.2 is widely distributed throughout Loch Muick forming a drape (see Figure 3.28). The average thickness of this drape is 1ms on the loch sides and a maximum of 7ms in the central trough. This facies frequently forms trough infills (Figure 3.32d), masking the underlying topography. Facies 1.2 underlies Facies 1.1 and overlies Sequence 2.

3.7.2.2 Sequence 2

Sequence 2 is identified on the basis of its upper boundary and internal characteristics (see section 3.3.3). As in section 3.5.2.3 above, attenuation of the high frequency Pinger signals occurred before reflection from the base of this sequence. The upper boundary of Sequence 2 is unconformable with Sequence 1. The unconformity can be identified on the upper basin slopes where Facies 1.2 terminates by onlap (Plate 3.8)

(see section 3.7.2.1 above). The surface of Sequence 2 has a high reflection amplitude and a characteristic topography. This takes the form of 'hills' up to 12ms high rising above planar reflection surfaces (Figure 3.28). Two seismic facies (2.1 and 2.2) have been identified in this Sequence.

3.7.2.2.1 Facies 2.1

Facies 2.1 is characterised by numerous point hyperbolae with occasional, clustered, parallel to subparallel reflectors inclined in a southwest to northeast direction (Figure 3.34, 3.35a; Plate 3.7). These lateral reflectors are discontinuous and can be traced over a maximum distance of 80m. The reflection amplitude of both point hyperbolae and lateral reflectors is medium to high, the density of the point hyperbolae producing a mottled effect within the facies. The upper surface of Facies 1.2 has a hummocky topography. Mounds rise to 12ms above the surrounding facies to form rounded hummocks (e.g. Figures 3.24 Traverse 114-111; 3.25 Traverse 9, 3.28, 3.34; Plates 3.7, 3.8). However, the composition of the mounds cannot be determined below 10ms depth. This facies also extends upslope to form ridges (e.g. Figure 3.26 Traverse 79-83; Figure 3.25 Traverse 96-93; Plate 3.8). The maximum depth of Facies 2.1 exceeds 10ms, but cannot be more accurately determined. It has been identified throughout Loch Muick (see Figures 3.27 and 3.28). Facies 2.1 underlies Facies 1.2, and is believed to outcrop at the bed/water interface at least at one point (see Figure 3.25, Traverse 96-93). This facies has a partially gradational boundary with Facies 2.2 (see Figure 3.27).

3.7.2.2.2 Facies 2.2

The reflection geometry of Facies 2.2 is subparallel horizontal, with local concentrations of point hyperbolae (Figure 3.35b, 3.35c, Plate 3.7). The same problem of internal hydrophone data resolution outlined above (section 3.7.2.1.2) is thought to apply to this facies, probably resulting in loss of data. The upper boundary of Facies 2.2 has a high reflection amplitude (Plate 3.7). The internal reflectors exhibit a continuity of less than

20m, with a medium amplitude. The lower boundary is of a medium to low reflection amplitude and can be recognised as locally having a gradational boundary with Facies 2.1 (Figure 3.27, 3.35c). Facies 2.2 occurs only as a basin fill in Facies 2.1 (Figures 3.24, Traverse 1; 3.25, Traverse 96-93; 3.26, 132-136; 3.28; Plates 3.6, 3.7) and thus has a limited distribution in Loch Muick. The isopach map (Figure 3.36) shows that the facies is located along the longitudinal axis of the loch, in discrete deposits, with a maximum thickness of more than 7ms.

3.7.2.3 Sequence 3, Facies 3.1

Below Facies 1.2 and 2.1, at the base of the inclined to very steep angle loch sides, a high amplitude reflector, similar to that described in section 3.5.2.4 above, has been identified (e.g. Figure 3.25, Traverse 96-93; 3.26, Traverse 79-83; 3.28; Plate 3.8). No seismic penetration into this inclined reflector with a smooth upper surface has been recognised in any of the traverses.

3.7.3 Seismic parastratigraphy

The following seismic parastratigraphy is proposed for the Loch Muick basin.

3.7.3.1 Sequence 1

Sequence 1 is interpreted as resulting from the sedimentation of fine particles in a quiet water lacustrine environment. It has a maximum measured thickness of 10.5m, assuming a seismic velocity of 1500ms^{-1} (see section 3.5.3.1). The details of each facies are given below.

Facies 1.1 has a draped form with a low amplitude surface reflector and no internal reflectors. This configuration is typical of unconsolidated lacustrine sediments. The low amplitude surface reflector suggests that this facies is the current sedimentary deposition surface. The limited distribution of this facies identified by the Pinger equipment may result from the low reflection amplitude of the surface reflector as opposed to an actual absence of

the facies. The maximum measured thickness of this facies is 2.25m.

The predominantly subparallel draped reflectors of Facies 1.2 are also typical of fine grained lacustrine sedimentation by settling through the water column. The major reflectors identified are believed to represent strata containing coarser material. Evidence for sediments possibly deposited by mass movement can be found in Traverse 132-136 (Figure 3.26). Downlapping major reflectors terminate in the central trough area or extend part way up the opposite slope suggesting a rapid, pulsatory sedimentary input. Minor mass movements are evidenced by the localised occurrence of chaotic reflectors on the loch sides and at the base of slopes. Facies 1.2 thins upslope, has an average thickness of 1.5m and attains a maximum measured thickness of 10.5m in the central trough.

3.7.3.2 Sequence 2

Sequence 2 underlies the lacustrine sediments of Sequence 1 and is characterised by contrasting internal reflector and topographic configurations. It is proposed that this sequence is composed of glacial sediments with different genetic origins. A seismic velocity of 1740ms^{-1} is assumed for this sequence (see section 3.5.3.3).

Facies 2.1 is composed of concentrated point hyperbolae underlying a hummocky topography. This is interpreted as resulting from direct glacial deposition. The clustered parallel to subparallel discontinuous reflectors, aligned southwest to northeast identified within this glacial facies may result from one of the following processes:-

- a) Deposition of a distinct stratum of higher seismic reflectivity
- b) Compaction by glacial overriding.

The first hypothesis is rejected on the grounds that the strata are not defined as aligned point hyperbolae along a plane. This hypothesis does not explain the restricted distribution of the reflectors on the southwestern side of the hummocky topography. The second hypothesis of glacial compaction fits the available data more successfully. Finckh et al., (1984) report changes in sonic velocity of sediments in Lake Zurich which are attributed to 'Glacial loading by overriding ice'. This results in the formation of seismically reflective

surfaces within a given facies. Evidence of further deformation by faulting and folding is less likely to be seismically distinguishable in a coarse grained, hyperbolae-packed glacial facies. The restricted distribution of the stratification to the southwestern, formerly ice-proximal, slopes of glacial diamict in Loch Muick lend support to this mode of formation. Therefore it is proposed that the second hypothesis be accepted.

Facies 2.2 which has a maximum measured thickness in excess of 11m, has a gradational boundary with Facies 2.1 suggesting broadly contemporaneous deposition. This facies contains horizontal reflectors with local concentrations of point hyperbolae. It is believed that the stratification recognised results from sedimentary variation as opposed to compaction by overriding ice. Evidence in support of this hypothesis is found in the apparent dominance of fine grained material in this facies. Had the stratification resulted from glacial compaction, deformation by folding and shearing of the sediments, similar to that reported by Finckh et al., (1984) could be expected to be apparent in the seismic records. Despite the possible problems of resolution outlined in section 3.7.2.1.2 above, there is no evidence of deformation on the seismic profiles. It is suggested therefore, that the stratification is derived from sedimentation by proglacial meltwaters. The predominantly fine grained composition probably indicates deposition of the sediment in an ice-distal environment during glacial retreat. The local concentrations of point hyperbolae are believed to result from iceberg dumping of coarse, boulder-sized debris into the finer grained sediment (Thomas and Connell, 1985). The basin fill external form further confirms the fluvio-glacial-lacustrine origin proposed for this facies. Ice-proximal coarse grained material has not been identified within this facies. This may be due to the similarity of coarse grained outwash material to direct glacial diamict, thus producing a seismic reflection indistinguishable from the densely packed point hyperbolae of glacial diamict in the Loch Muick basin.

3.7.3.3 Sequence 3

Sequence 3 is recognised only at the base of the seismic sequence identified by Pinger 3.5kHz subbottom reflection profiling. It is suggested that this reflector may represent the underlying Lochnagar Granite Complex bedrock.

3.8 CONCLUSIONS

Based on detailed seismic reflection studies of Lochs Lee, Callater and Muick, the following conclusions have been drawn. No absolute dates have been obtained from core samples in any of the water bodies. The relative ages suggested in sections 3.8.1, 3.8.2 and 3.8.3 below are derived from their stratigraphic positions and seismic signatures.

The Pinger seismic reflection profiles provide the first source of information on the nature of the subbottom sediments in all three water bodies. This research has shown that the sedimentary fill of the lochs in this study extends to depths beyond the penetration of 3.5kHz profiling equipment. The maximum thickness penetrated by seismic signals was approximately 20m in Loch Lee, 8m in Loch Callater and 22m in Loch Muick.

3.8.1 Loch Lee

Four seismic sequences comprising seven facies have been identified in Loch Lee. These have been interpreted as:-

- a) Surficial lacustrine sediment of presumed Holocene age, containing evidence of small scale mass movements and wave redistribution.
- b) A lacustrine sequence containing a significant input from avalanche and other periglacial activity of probable Loch Lomond Stadial age.
- c) A glacial diamict and associated outwash containing large numbers of boulder-sized clasts indicating a retreating ice margin. Probably of Devensian age.
- d) Underlying ice smoothed gneiss bedrock.

3.8.2 Loch Callater

Two seismic sequences have been recognised in Loch Callater. These are interpreted as:-

- a) Surficial draped lacustrine sediment, predominantly fine grained but containing a small number of cobble sized clasts deposited in the loch by anthropogenic action. This sequence is believed to have formed during the Holocene.
- b) Glacial diamict with hummocky upper surface containing high concentrations of boulders. This sequence was probably deposited by glacial activity during the Loch Lomond Readvance.

3.8.3 Loch Muick

Three seismic sequences have been recognised in Loch Muick comprising five seismic facies. The sequences are interpreted as:-

- a) Surficial draped lacustrine sediment composed of fine grained material. This sequence probably represents Holocene sedimentation undergoing active accretion and disturbance by mass movement.
- b) A sequence composed of two distinct glaciogenic facies, having a gradational boundary. Facies 2.1 is interpreted as being composed of glaciogenic diamict, containing stratification due to glacial overriding which created compressional reflectors. Facies 2.2 is believed to be derived from ice distal meltwater deposition of fine grained material by sedimentation from suspension through the water column. The concentrations of boulders were probably derived from deposition of sediment by iceberg rafting. It is suggested that Sequence 2 was deposited by glacier activity during the Loch Lomond Readvance.

c) The underlying Lochnagar Granite Complex bedrock.

The implications of these findings (sections 3.8.1, 3.8.2, 3.8.3) are discussed in Chapter 7.

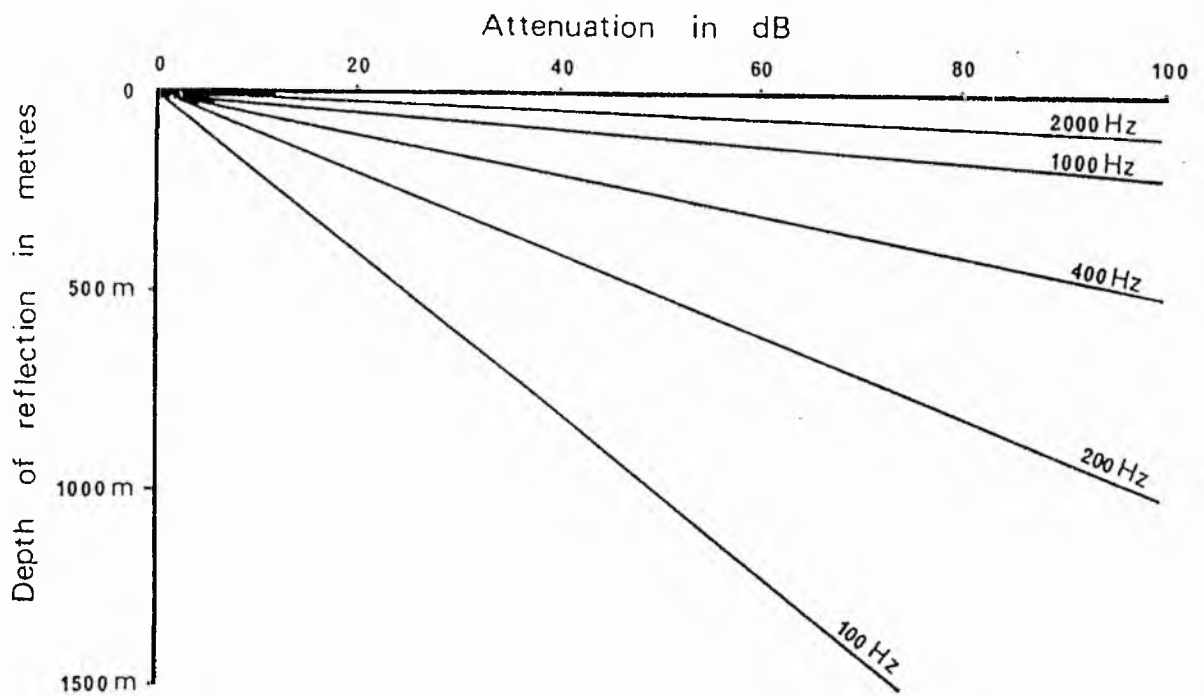


Figure 3.1 The relationship between frequency of the outgoing seismic wave and the depth of penetration for seismic pulses of varying frequency. After McQuillin and Ardu (1977).

Seismic sequence reflection terminations

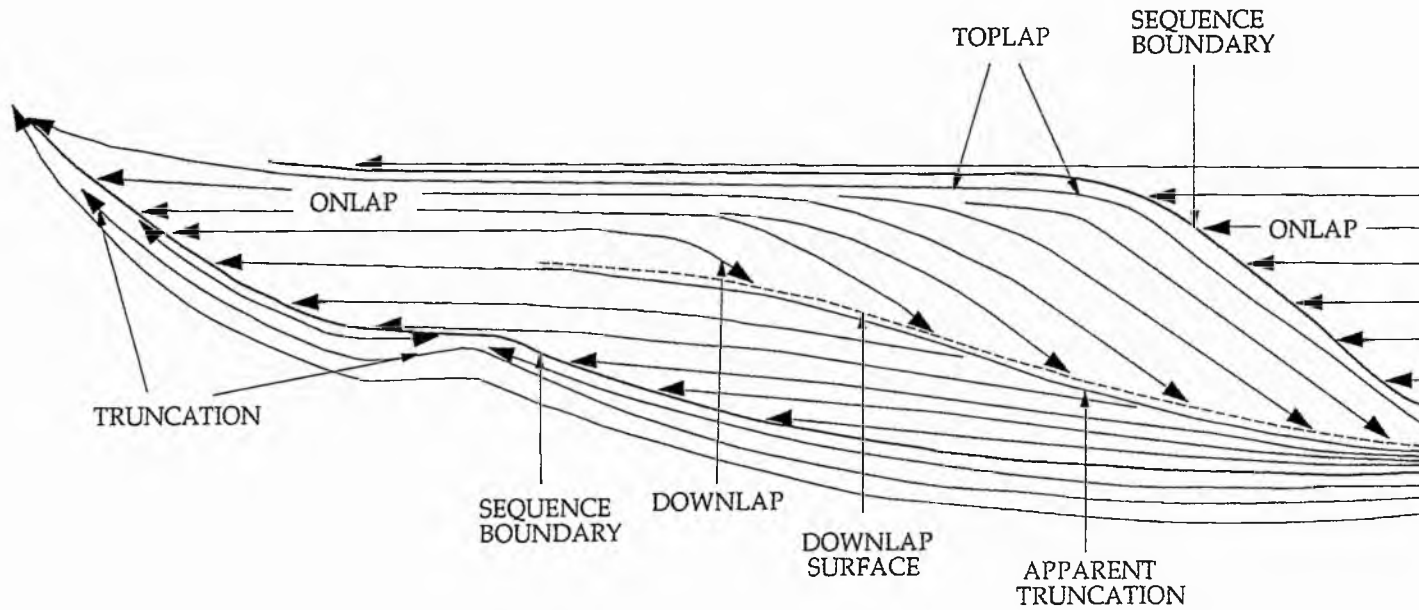
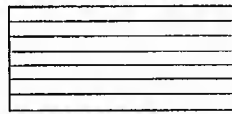


Figure 3.2
118

From Bally (1987)

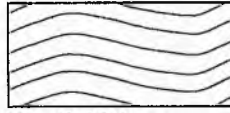
Seismic Facies Geometries and Modifications



Parallel Even



Subparallel

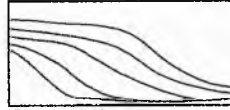


Parallel Wavy

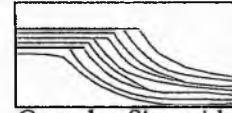


Divergent

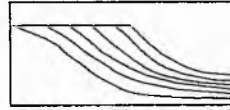
Prograding Clinoforms



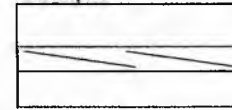
Sigmoid



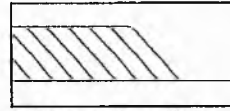
Complex Sigmoid-Oblique



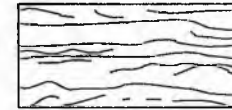
Oblique Tangential



Shingled



Oblique Parallel



Hummocky Clinoforms



Chaotic Stratal

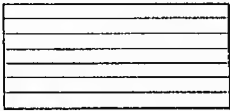


Chaotic Total

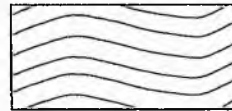


Reflection-Free

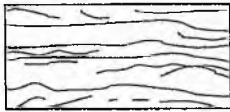
Modifying Terms



Even



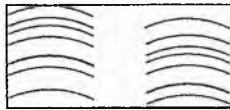
Wavy



Hummocky



Lenticular



Disrupted



Contorted

After Mitchum et al., (1977a)

Figure 3.3
119

LOCH LEE

Pinger traverse lines

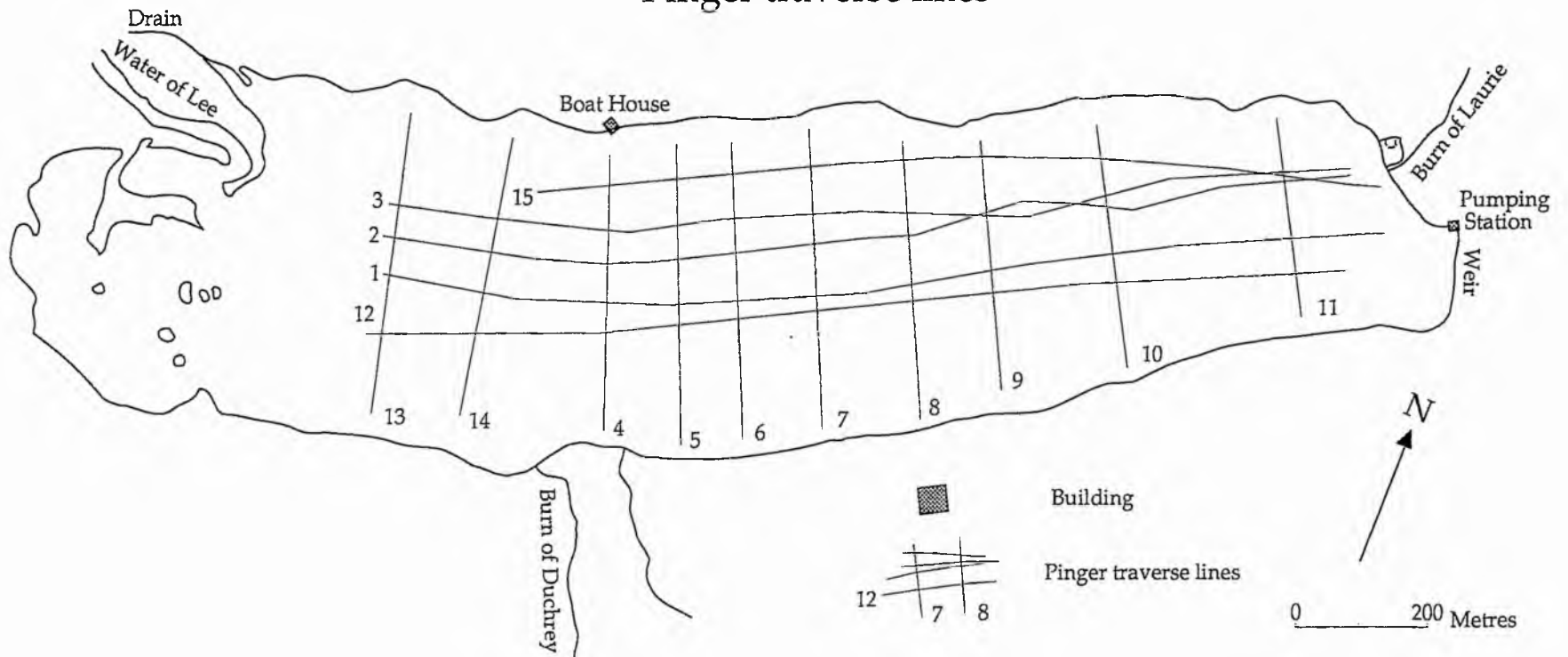


Figure 3.4
120

LOCH LEE

Pinger profiles

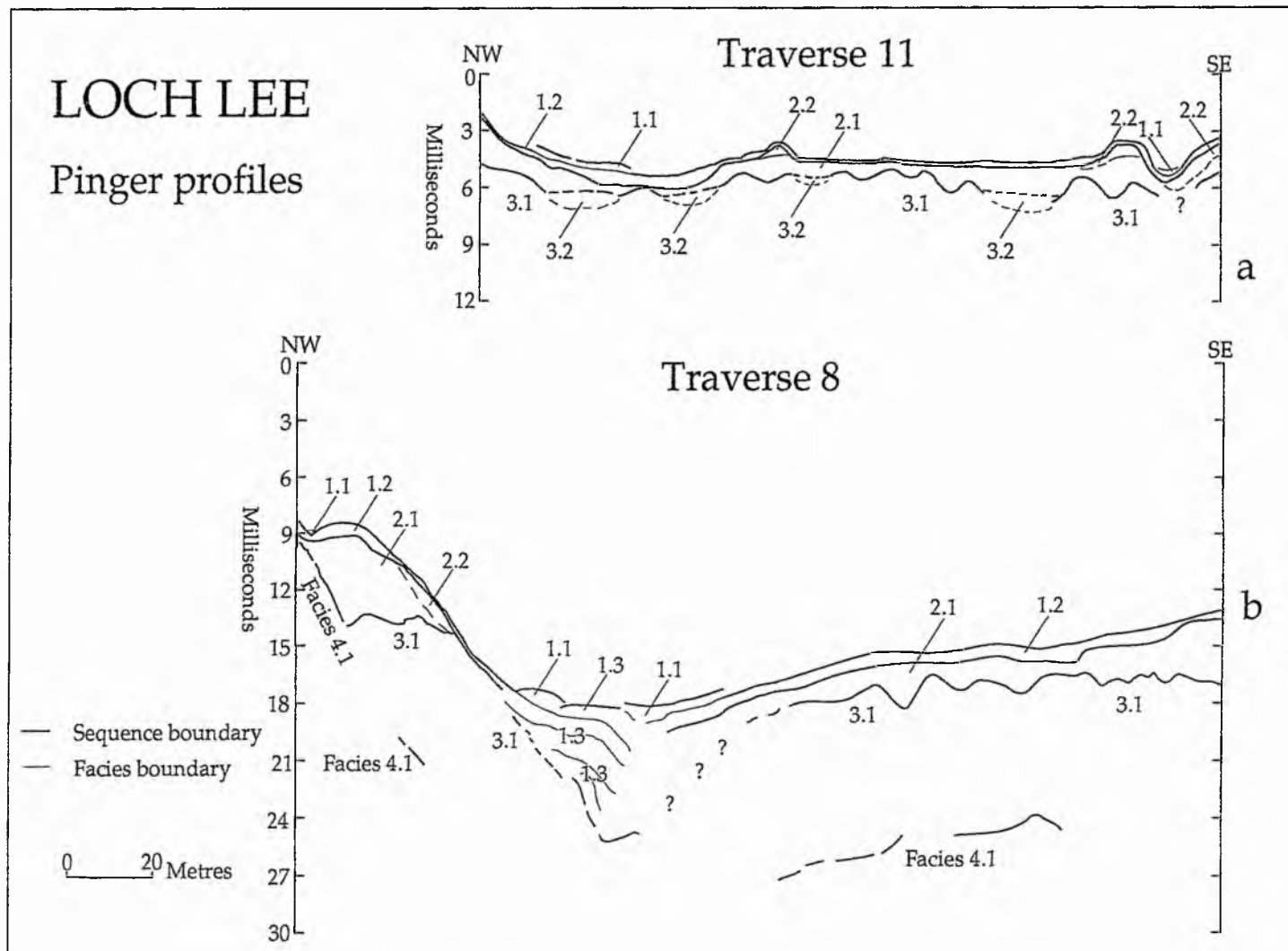
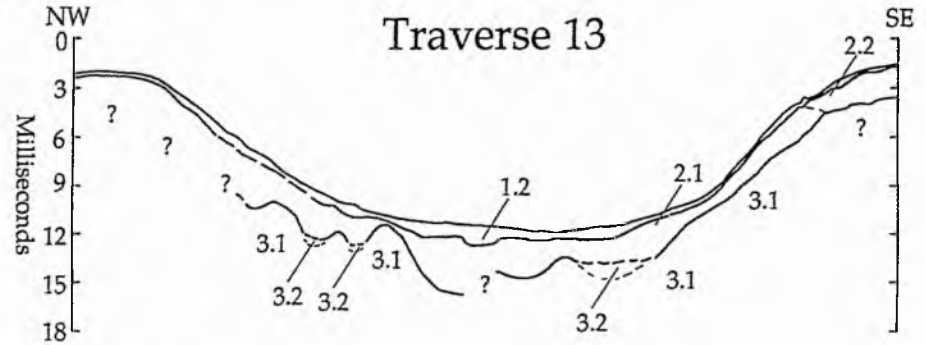
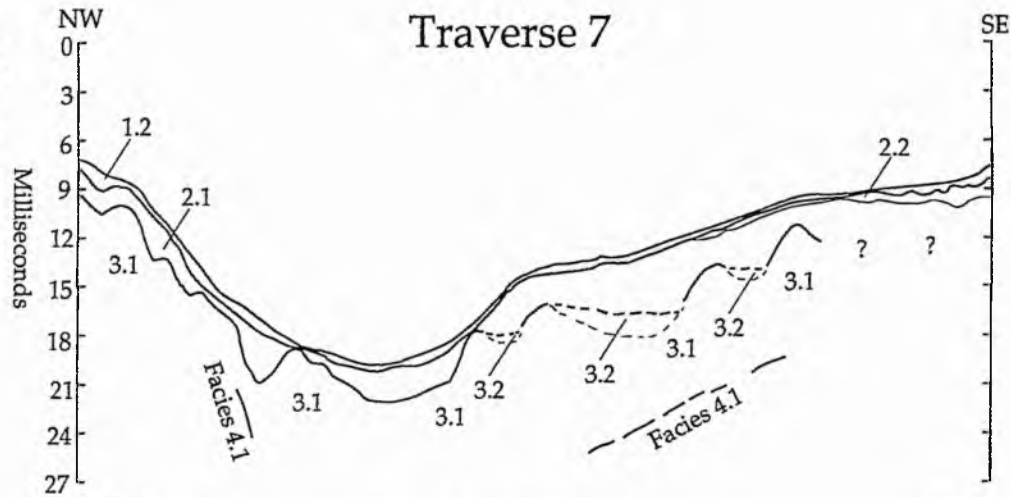


Figure 3.5
121

LOCH LEE

Pinger profiles



— Sequence boundary
 - - - Facies boundary

0 20 Metres

Figure 3.6
122

LOCH LEE

Pinger profile Traverse 12

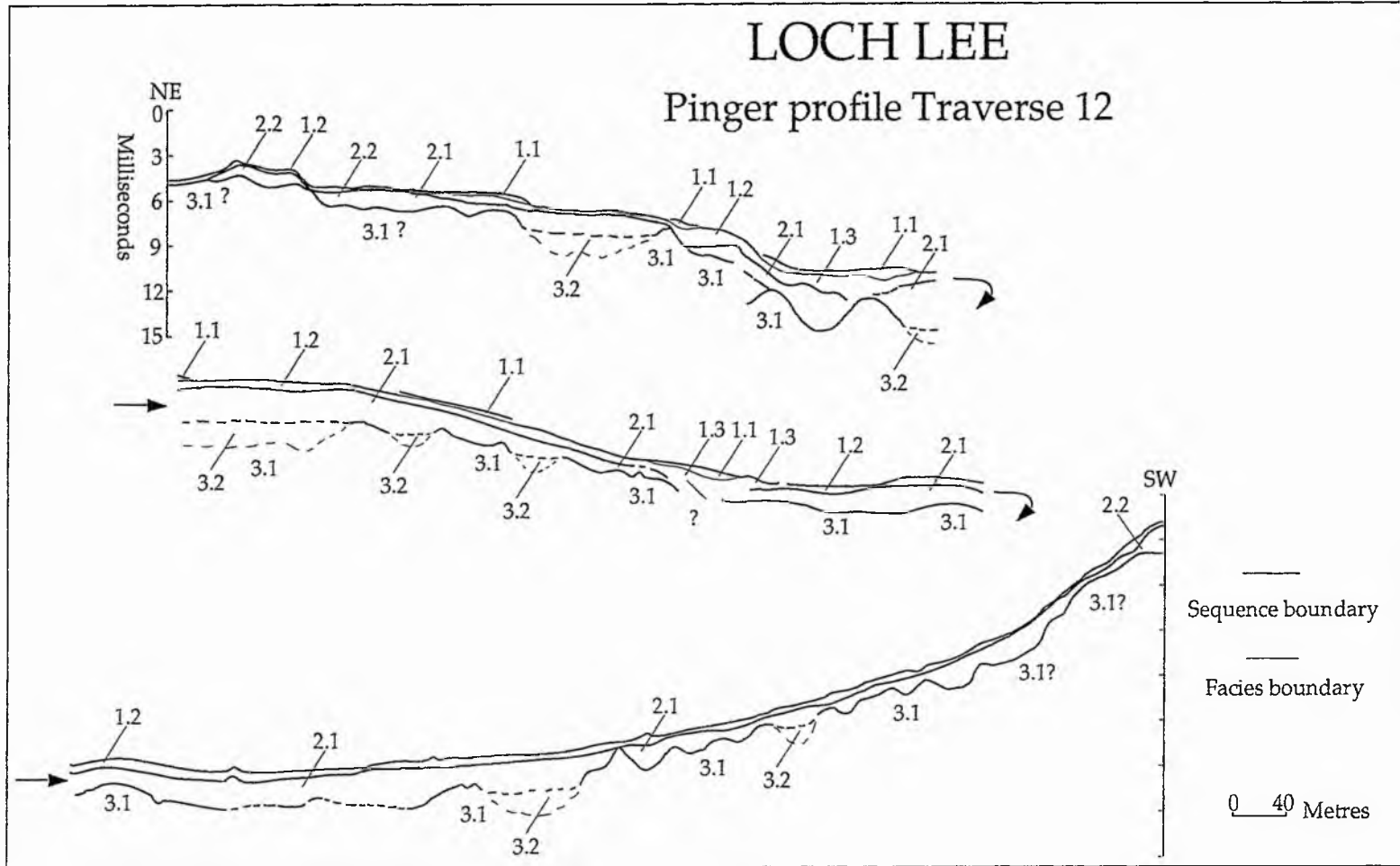


Figure 3.7
123

LOCH LEE

Facies 1.1

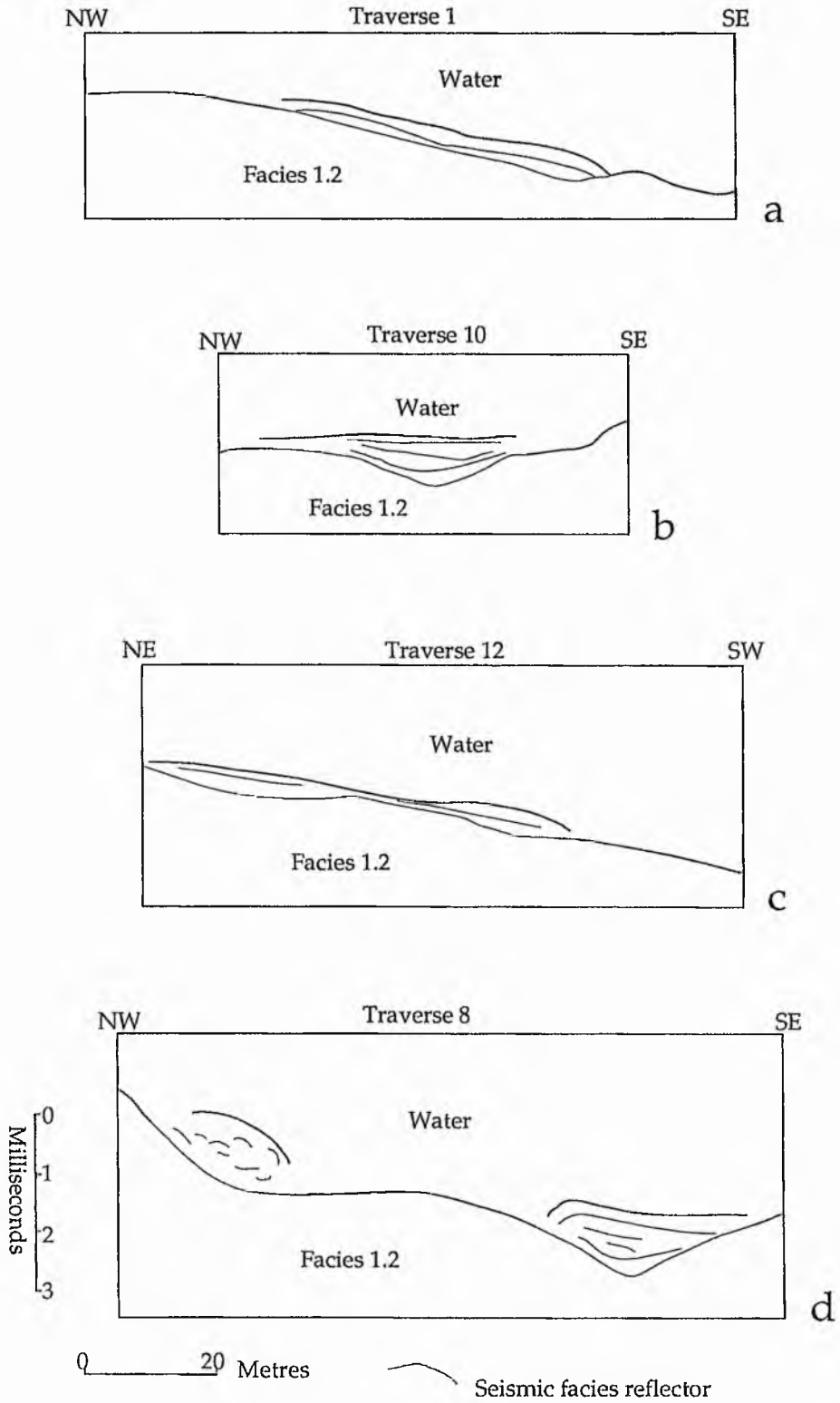


Figure 3.8
124

LOCH LEE

Facies 1.2

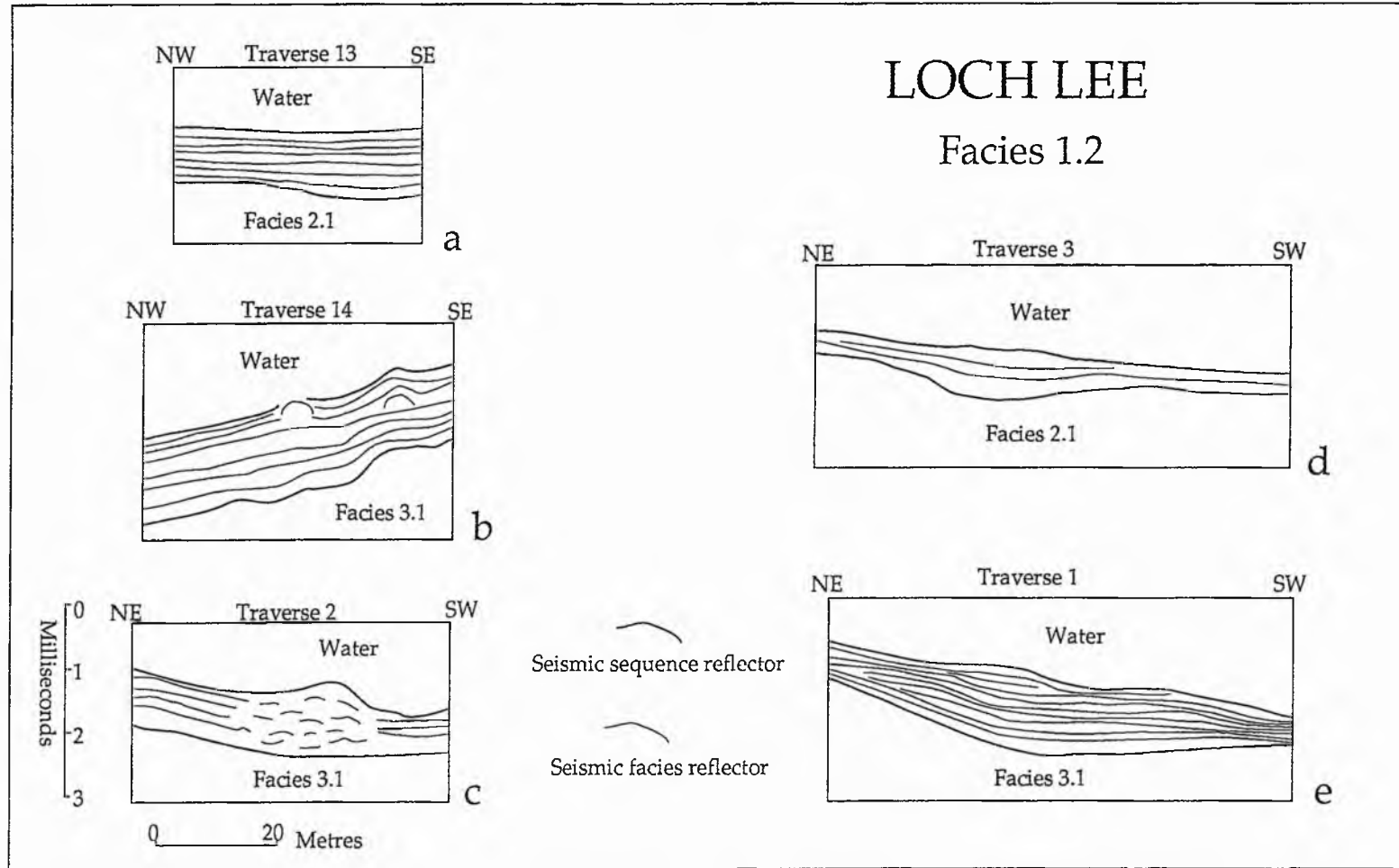


Figure 3.10
126

LOCH LEE

Isopach map

Facies 1.2

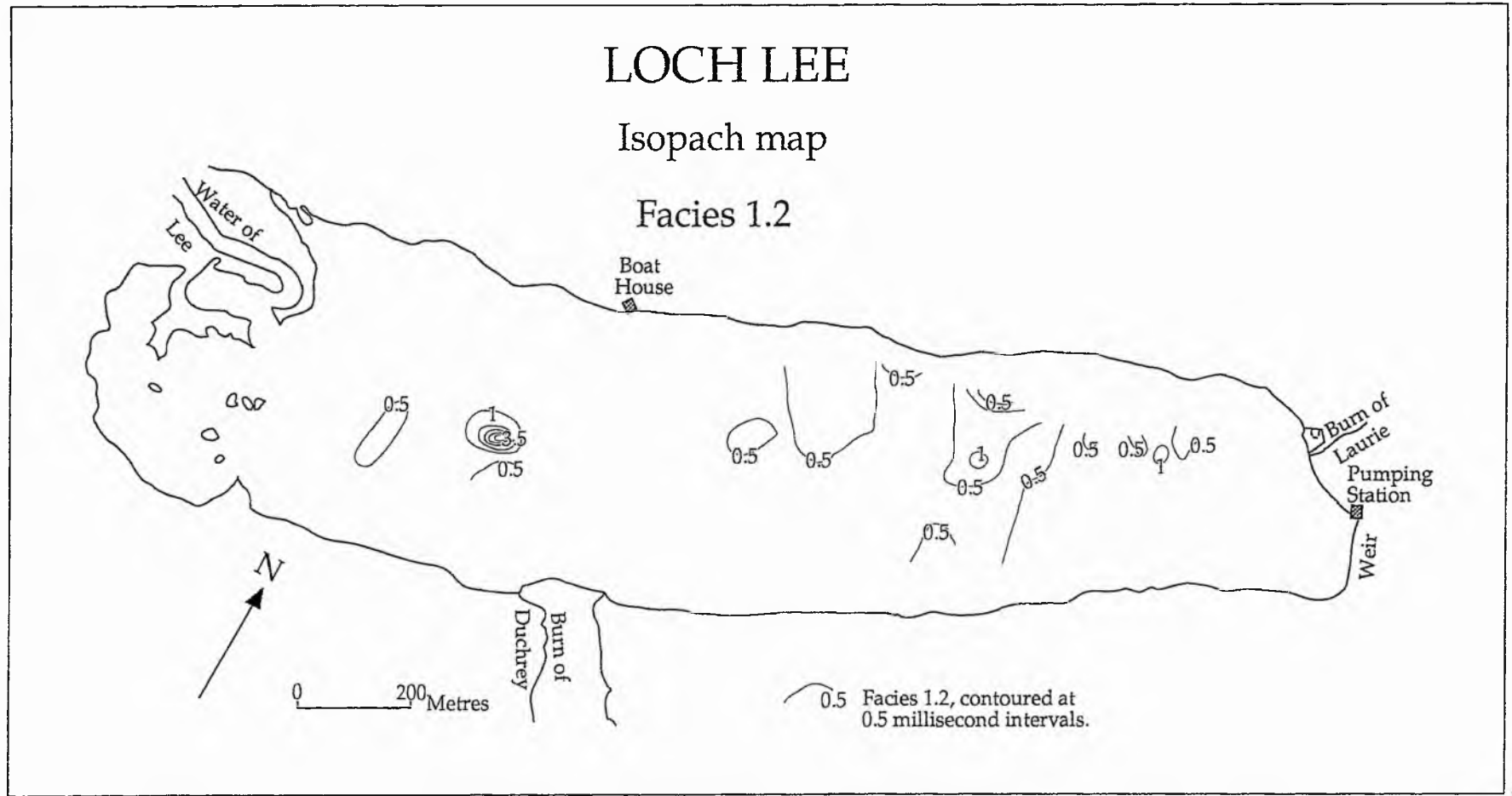
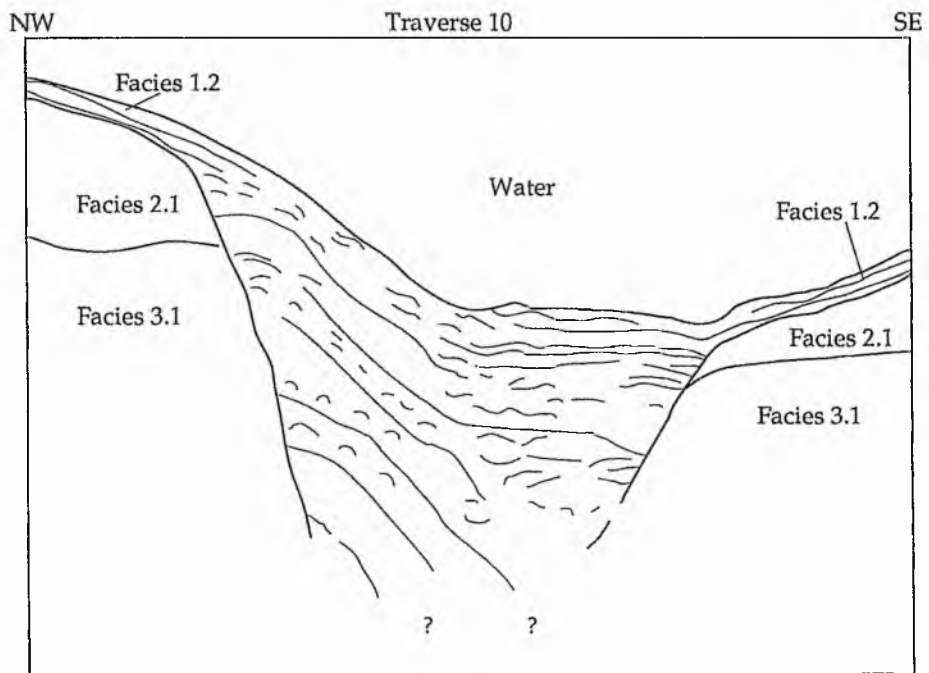
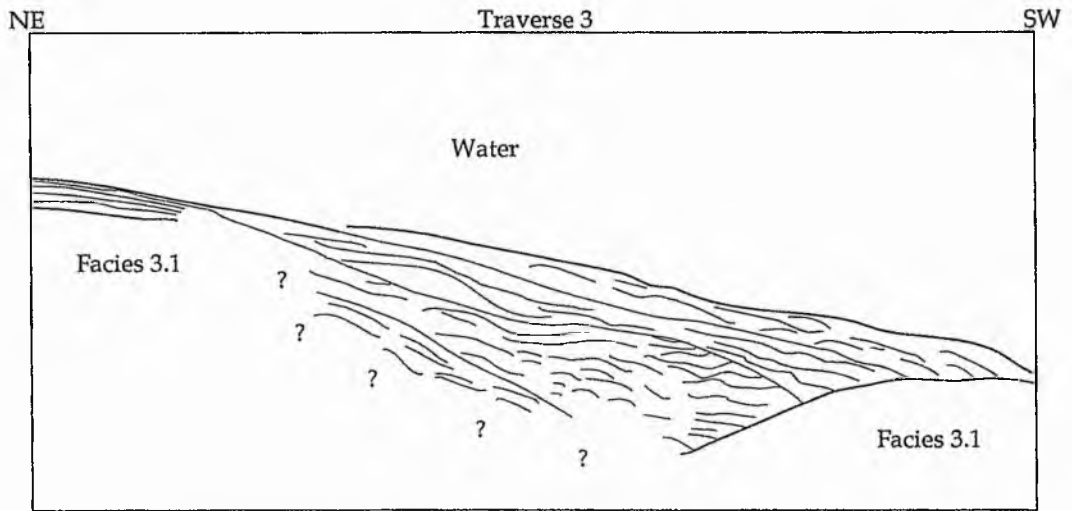


Figure 3.11
127

LOCH LEE

Facies 1.3



0
3
Milliseconds

0 20 Metres

Seismic sequence reflector

Seismic facies reflector

Figure 3.12
128

LOCH LEE

Isopach map
Facies 1.3

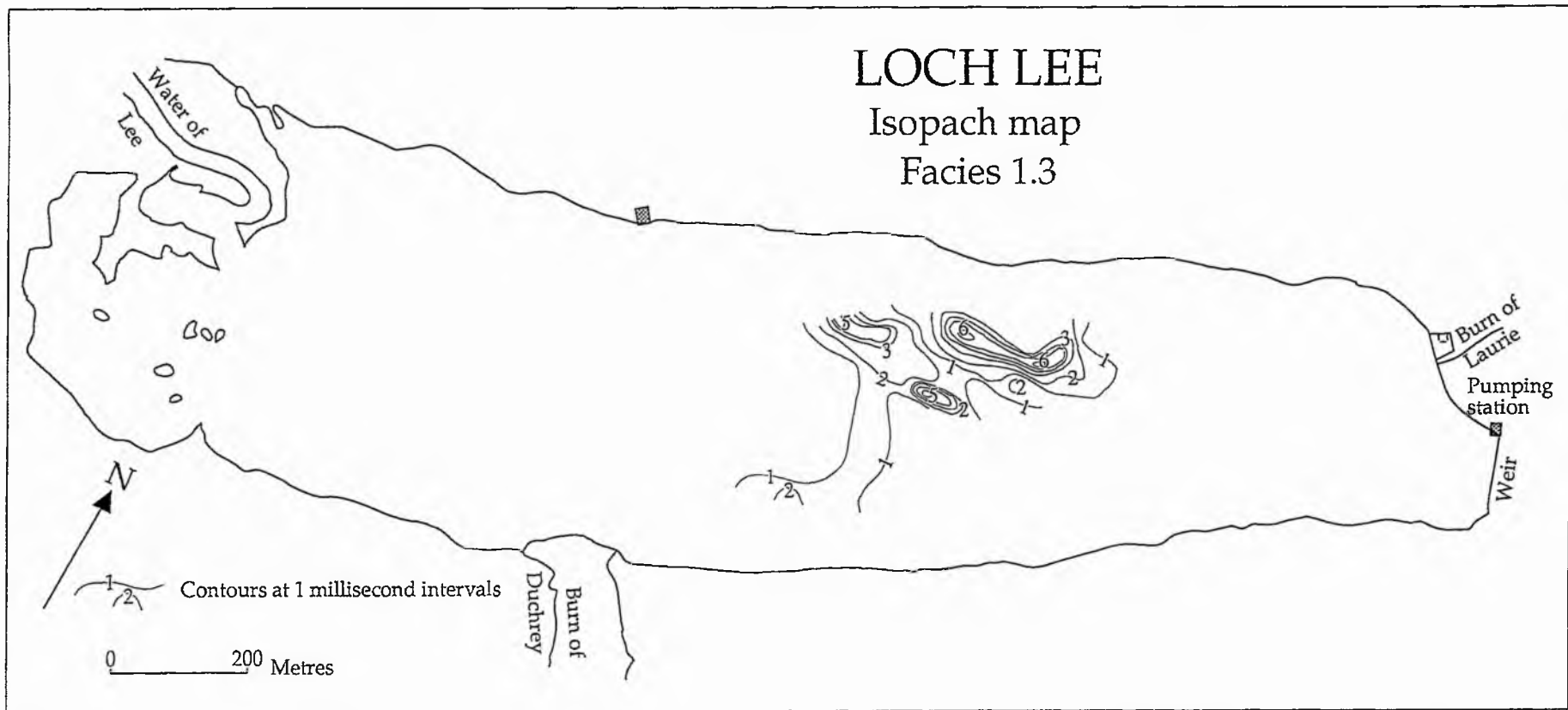


Figure 3.13
129

LOCH LEE

Facies 2.1

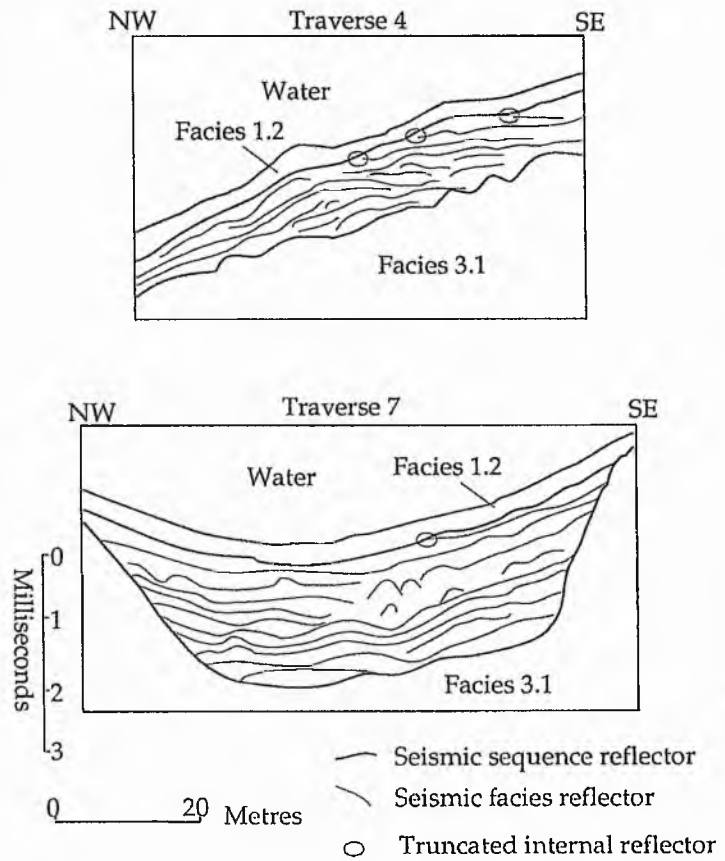


Figure 3.14
130

LOCH LEE

Isopach map

Facies 2.1

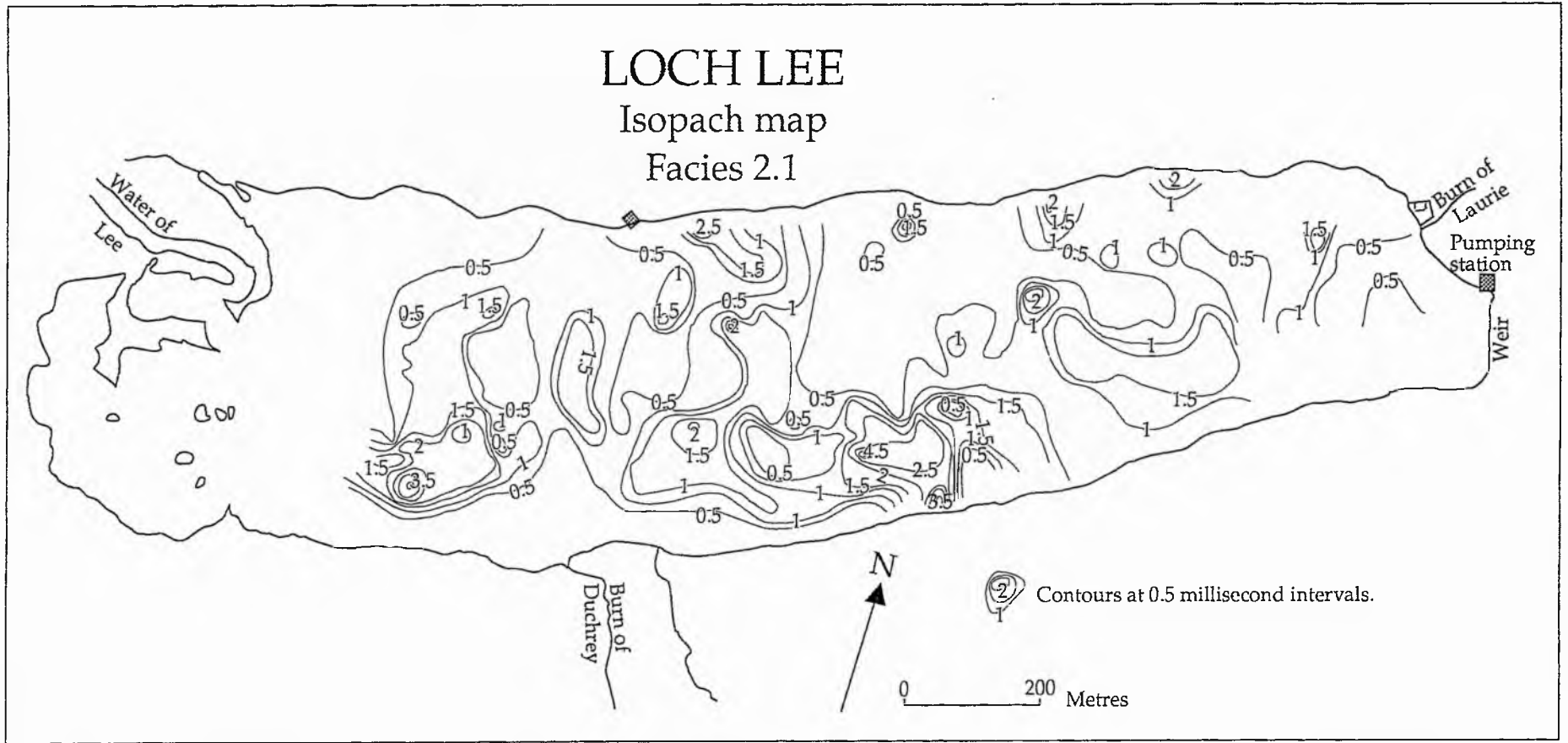


Figure 3.15
131

LOCH LEE

Facies 2.2

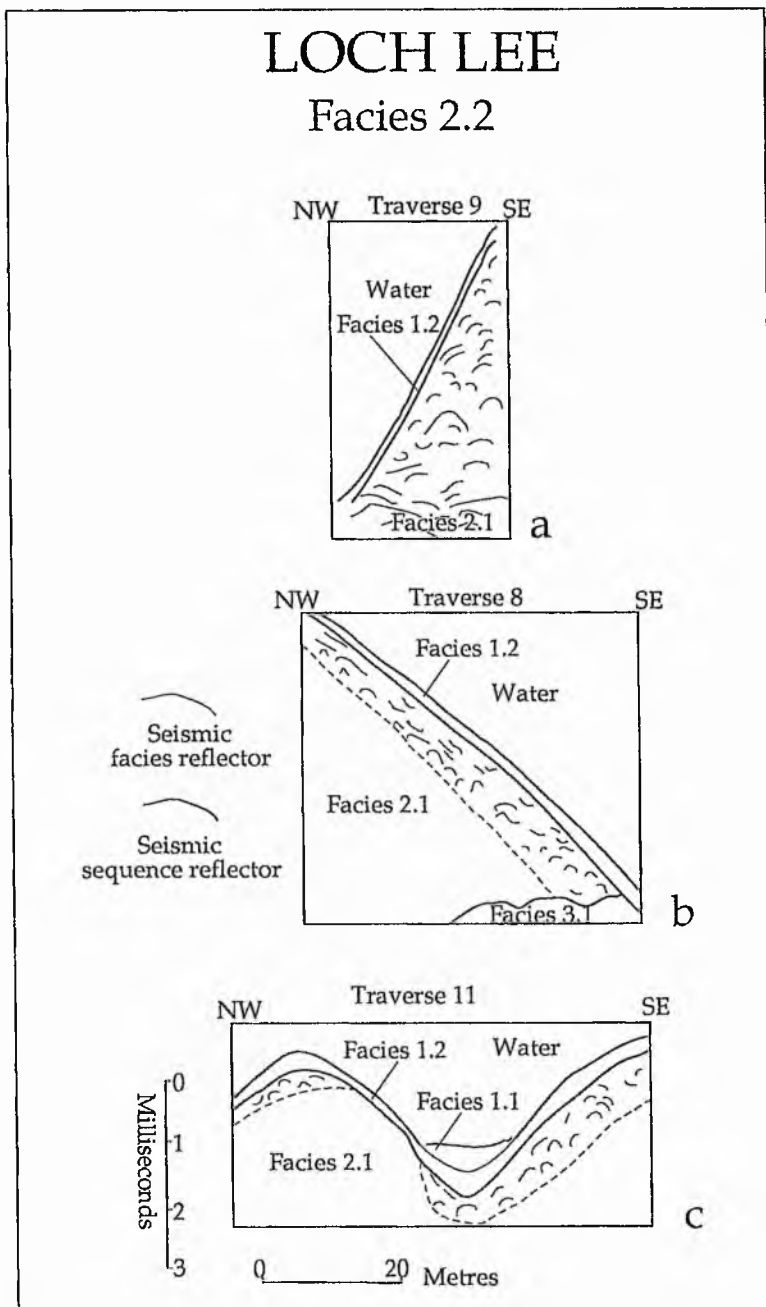


Figure 3.16
132

LOCH LEE

Facies 2.2

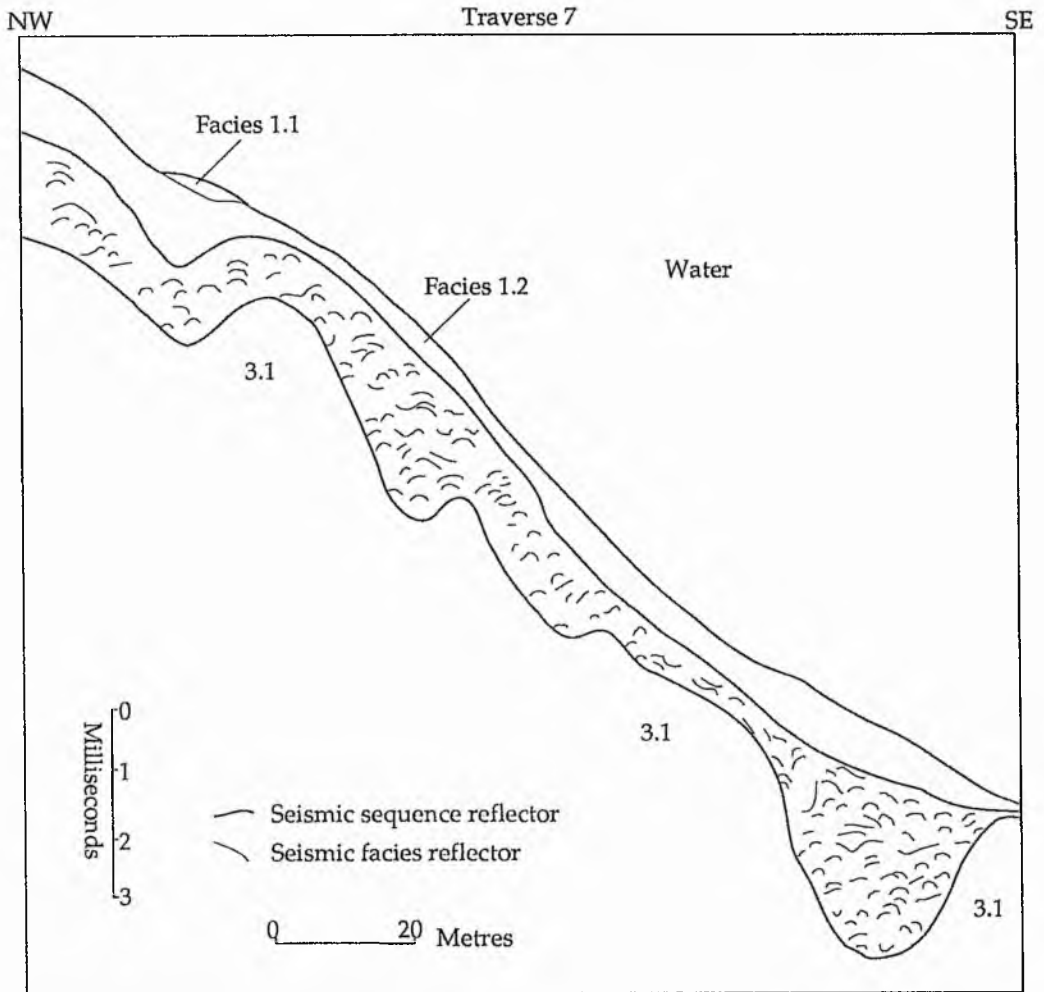


Figure 3.17
133

LOCH LEE

Isopach map

Facies 2.2

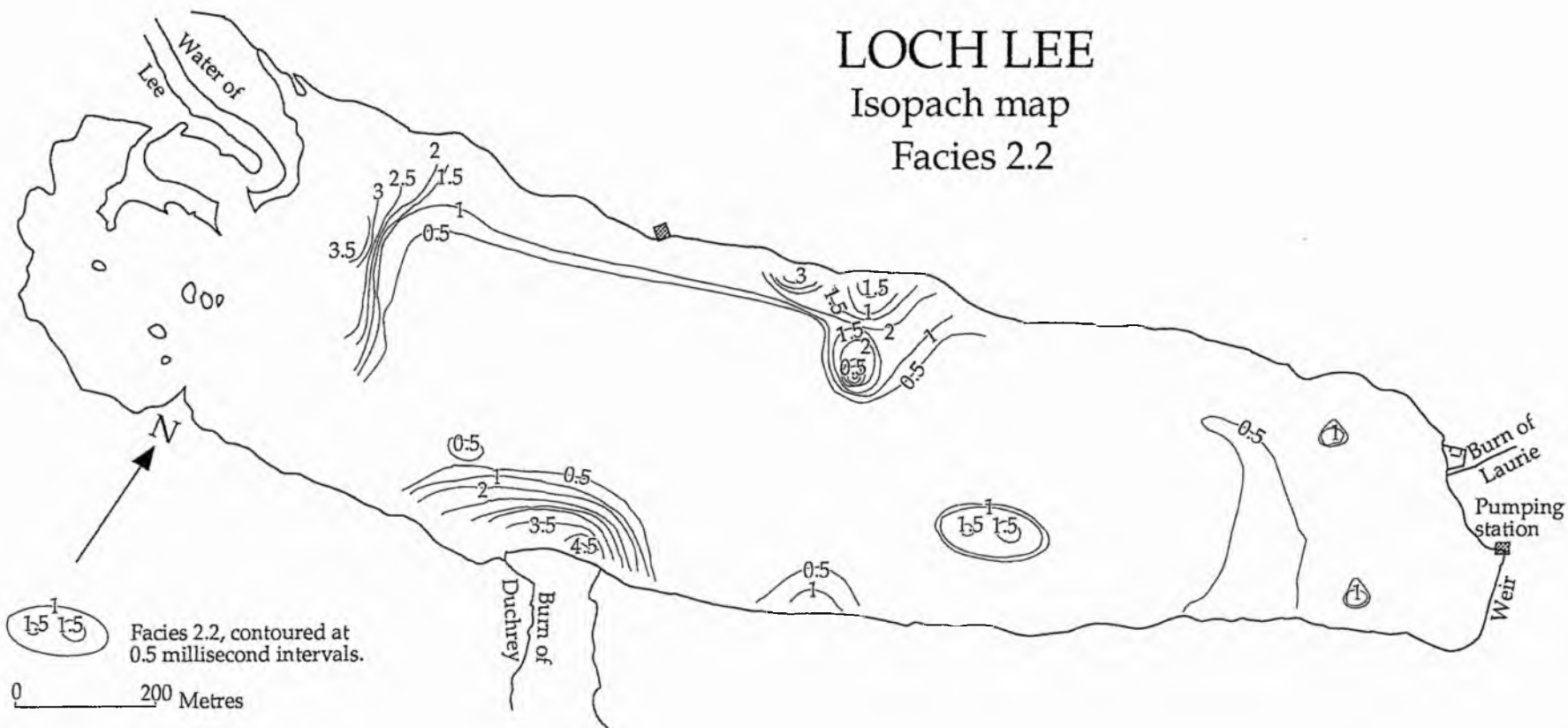


Figure 3.18
134

LOCH LEE

Facies 3.1

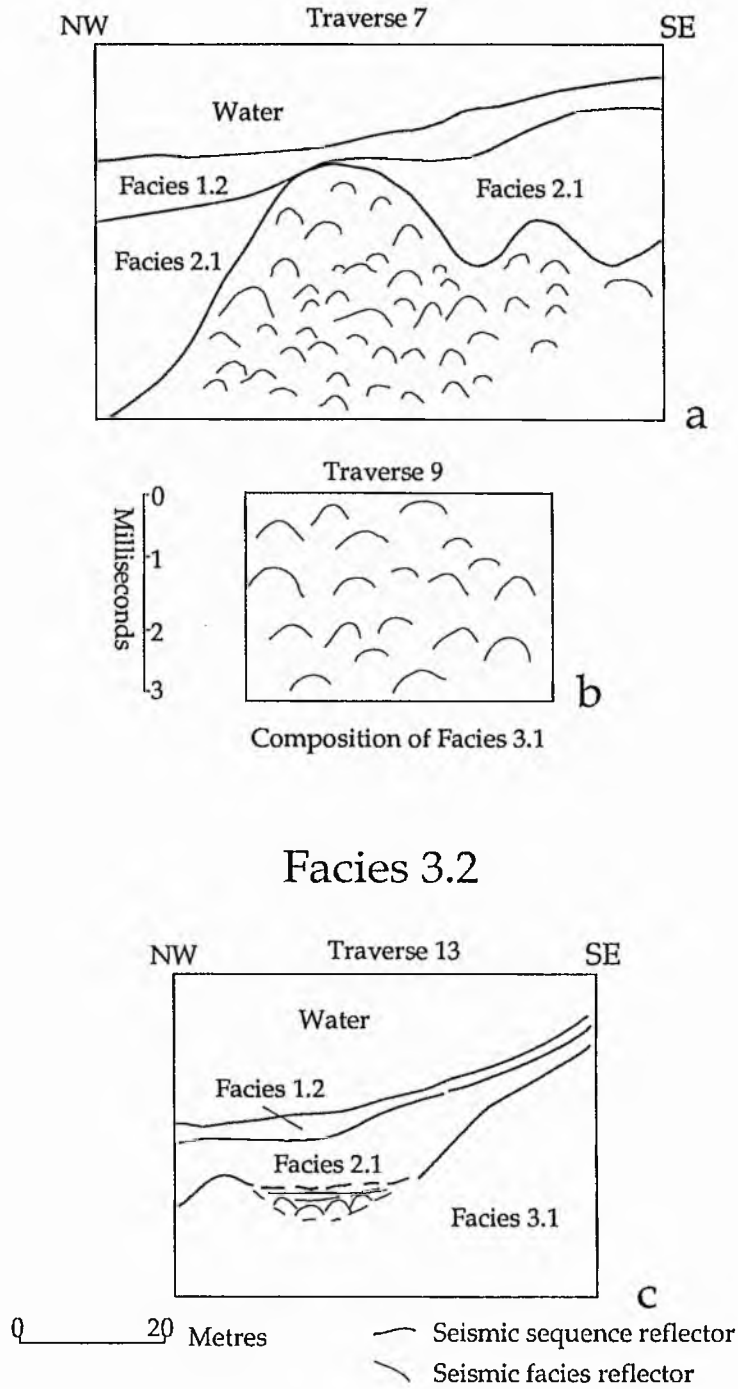


Figure 3.19
135

LOCH CALLATER

Pinger traverse lines

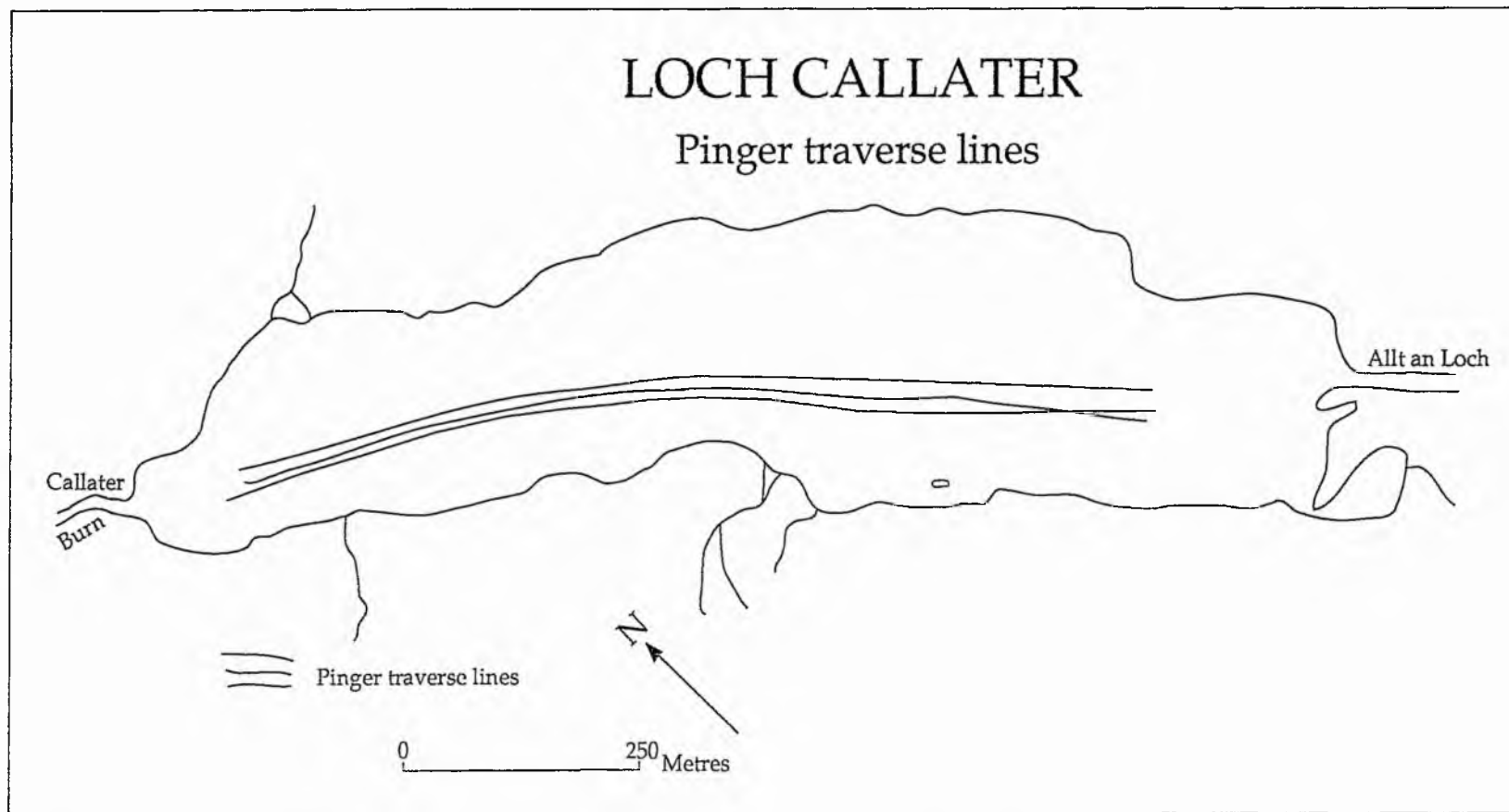


Figure 3.20
136

LOCH CALLATER

Pinger profile Traverse 1

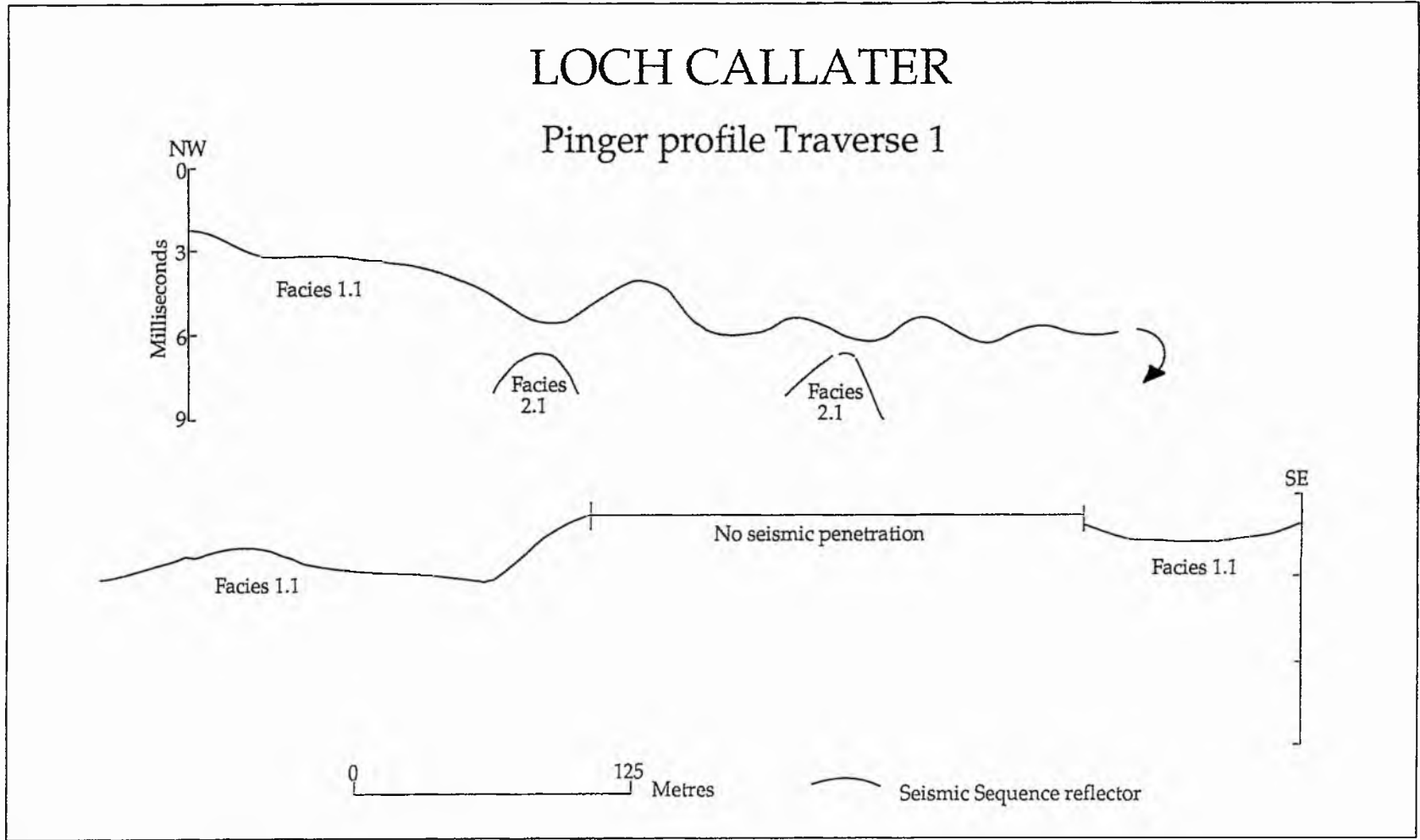
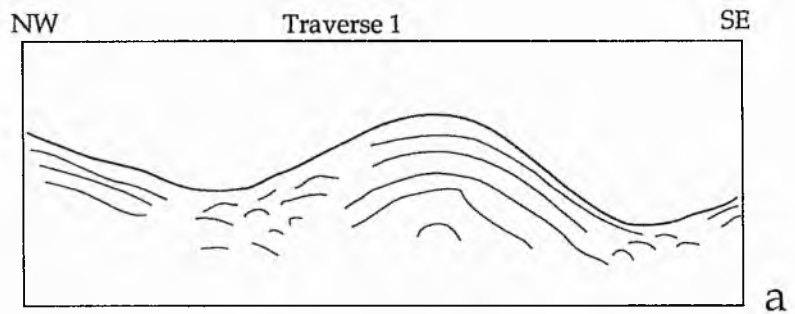


Figure 3.21
137

LOCH CALLATER

Facies 1.1



Facies 2.1

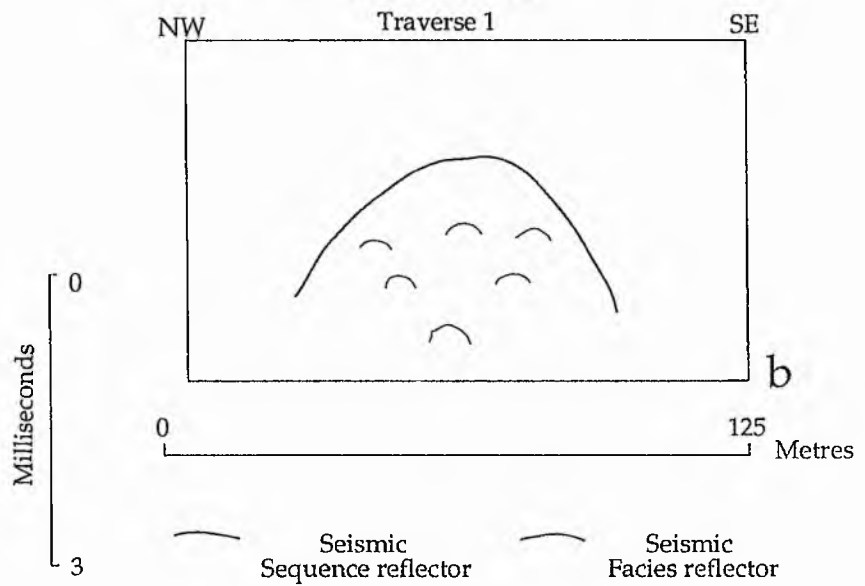
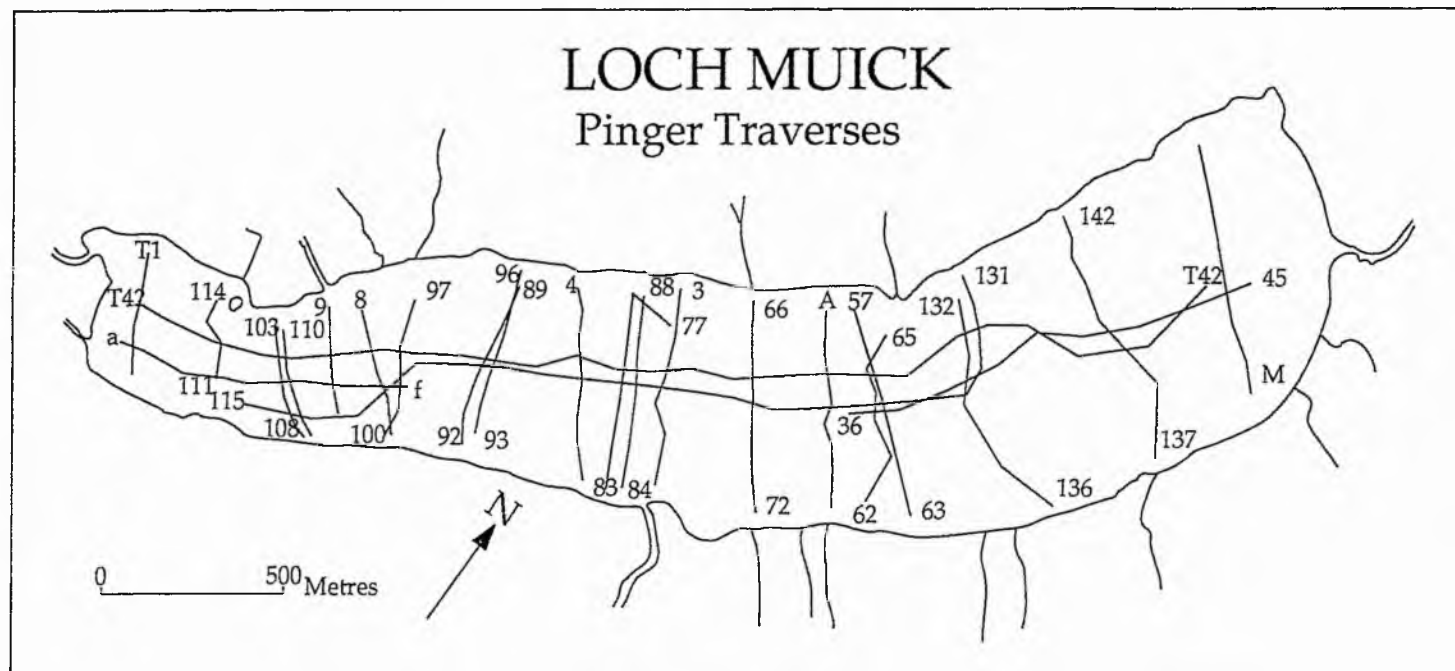


Figure 3.22
138

Figure 3.23
139



LOCH MUICK

Pinger profiles

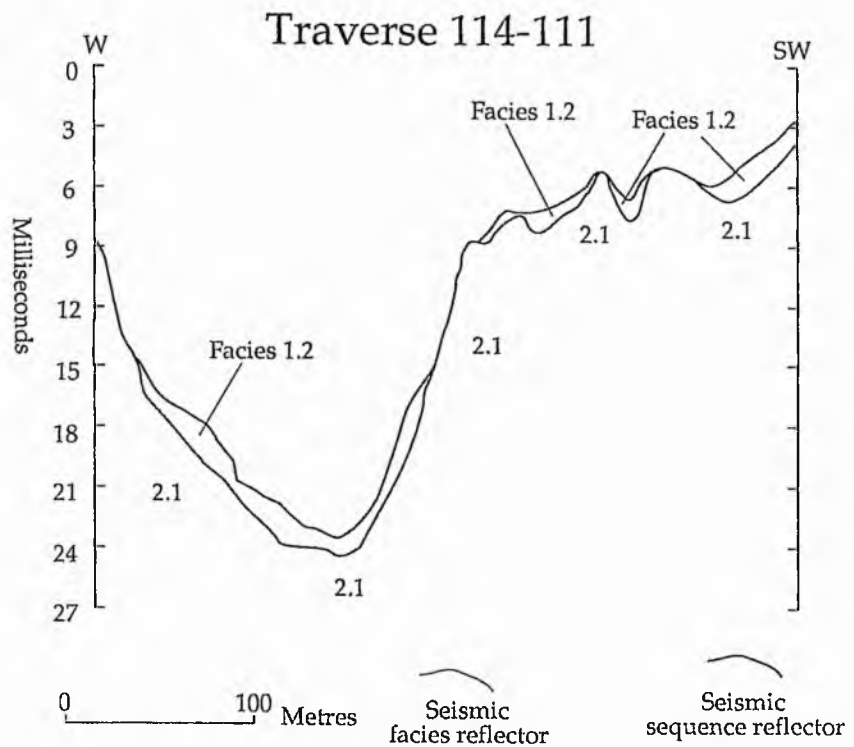
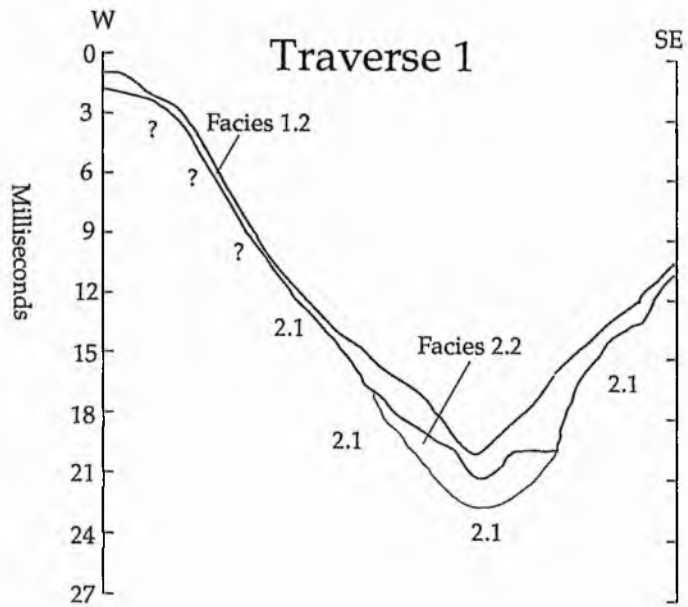


Figure 3.24
140

LOCH MUICK

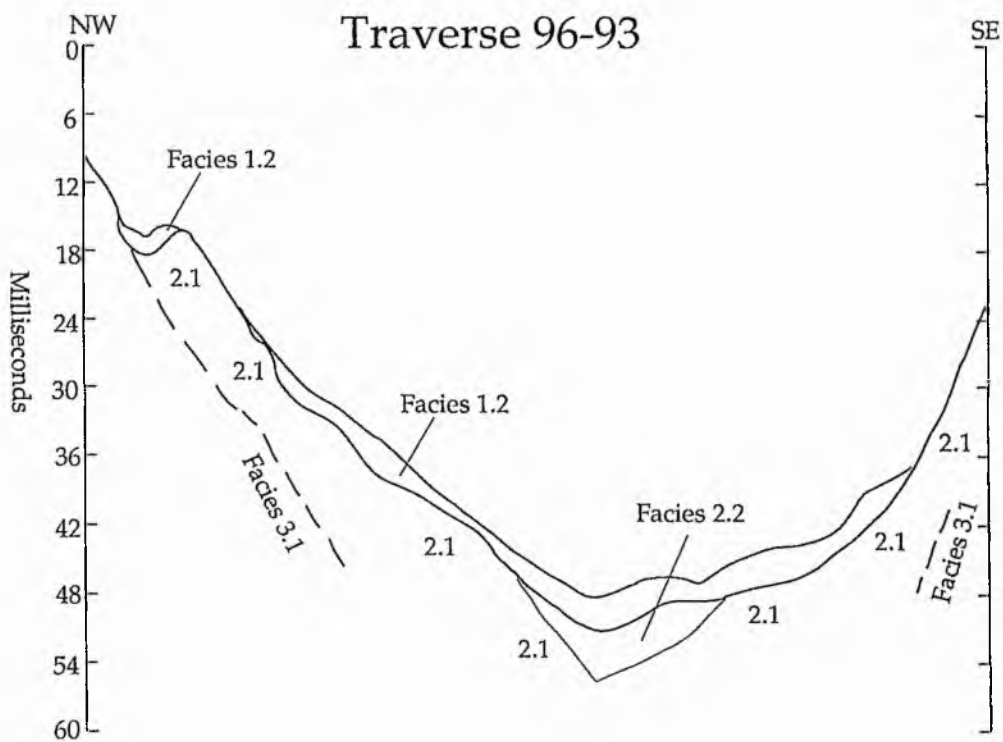
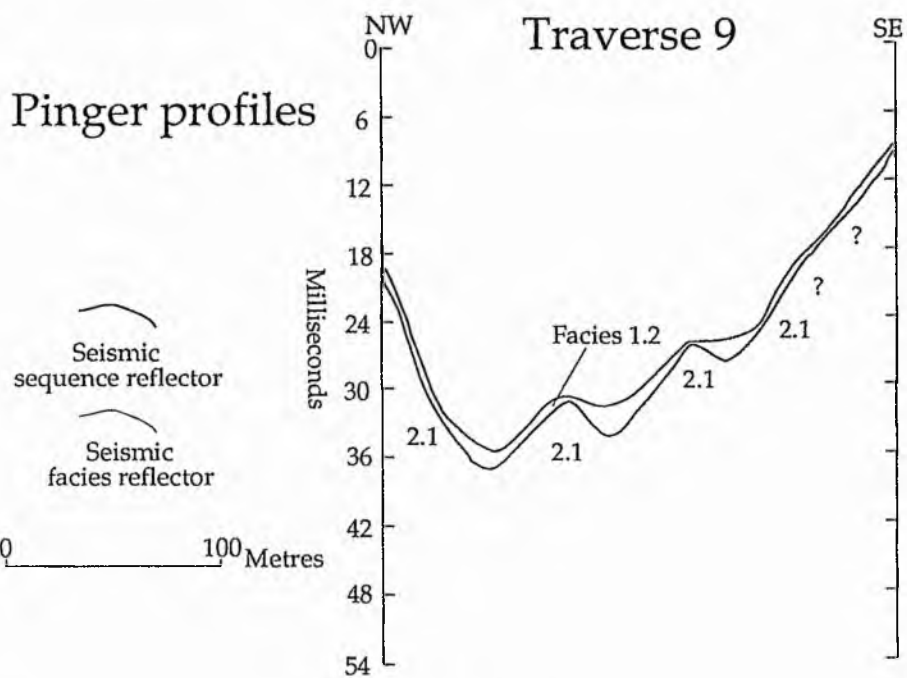


Figure 3.25
141

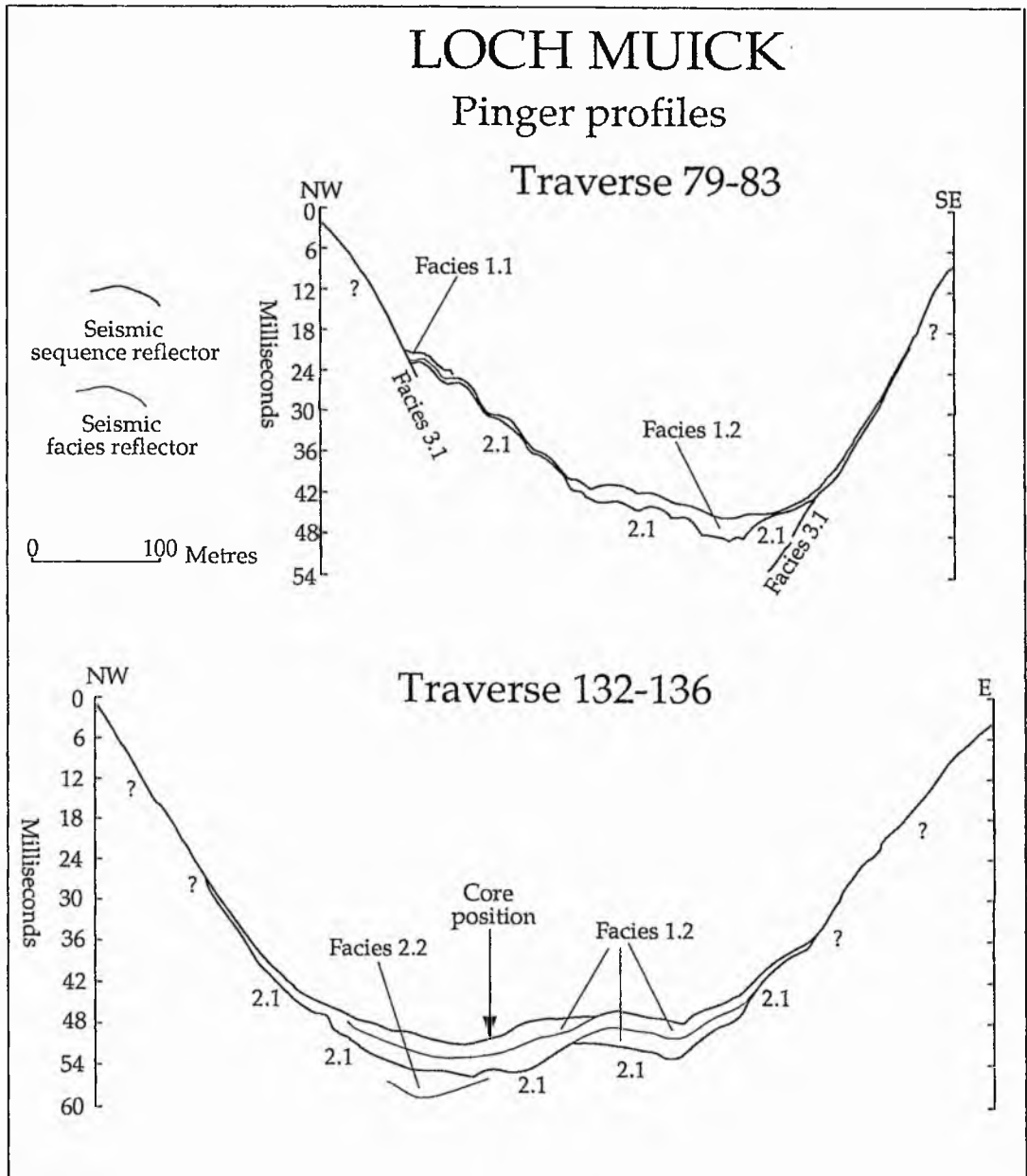


Figure 3.26
142

LOCH MUICK

Pinger profile Traverse 115-131

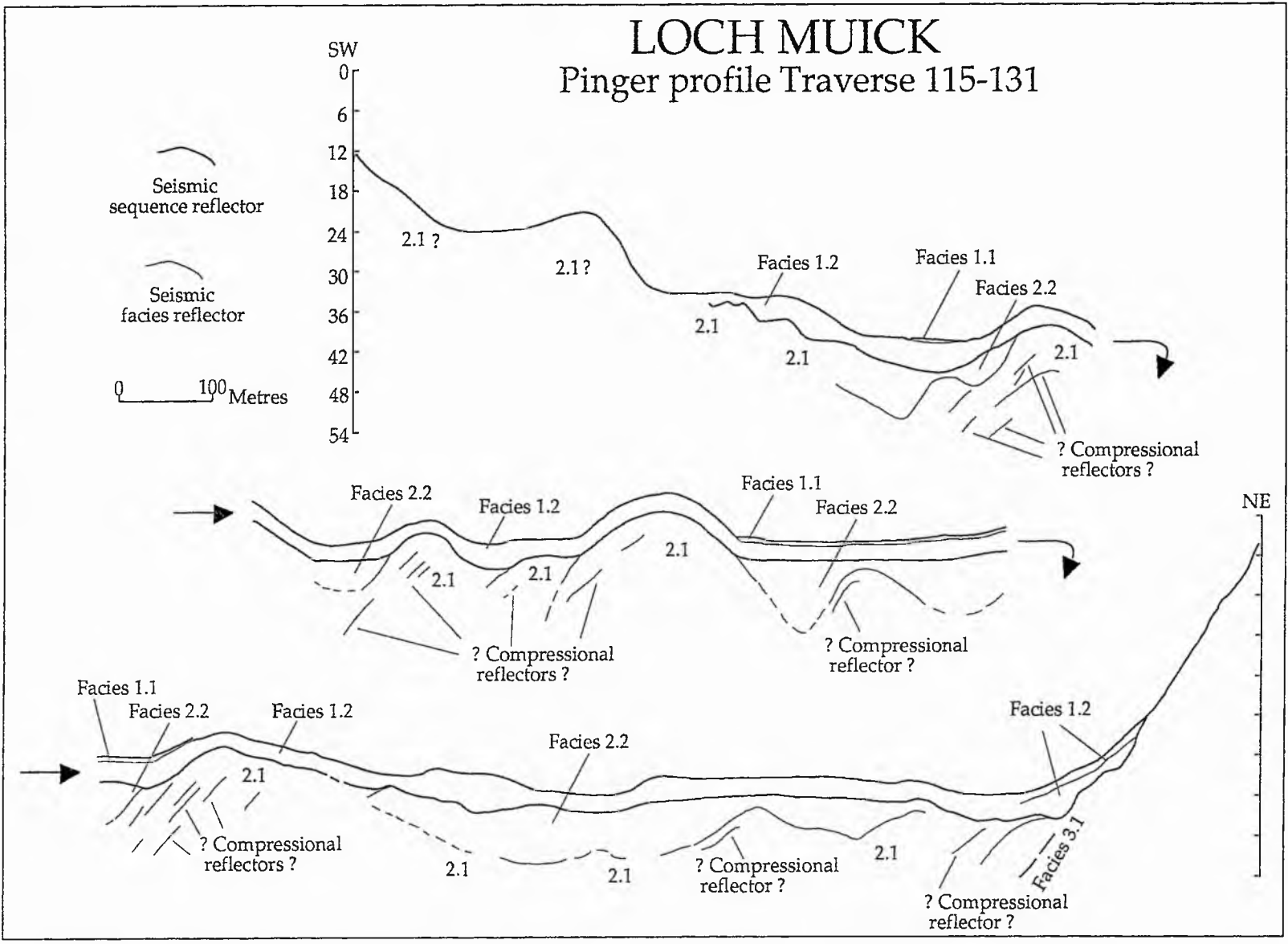


Figure 3.28
144

LOCH MUICK

Facies 1.1

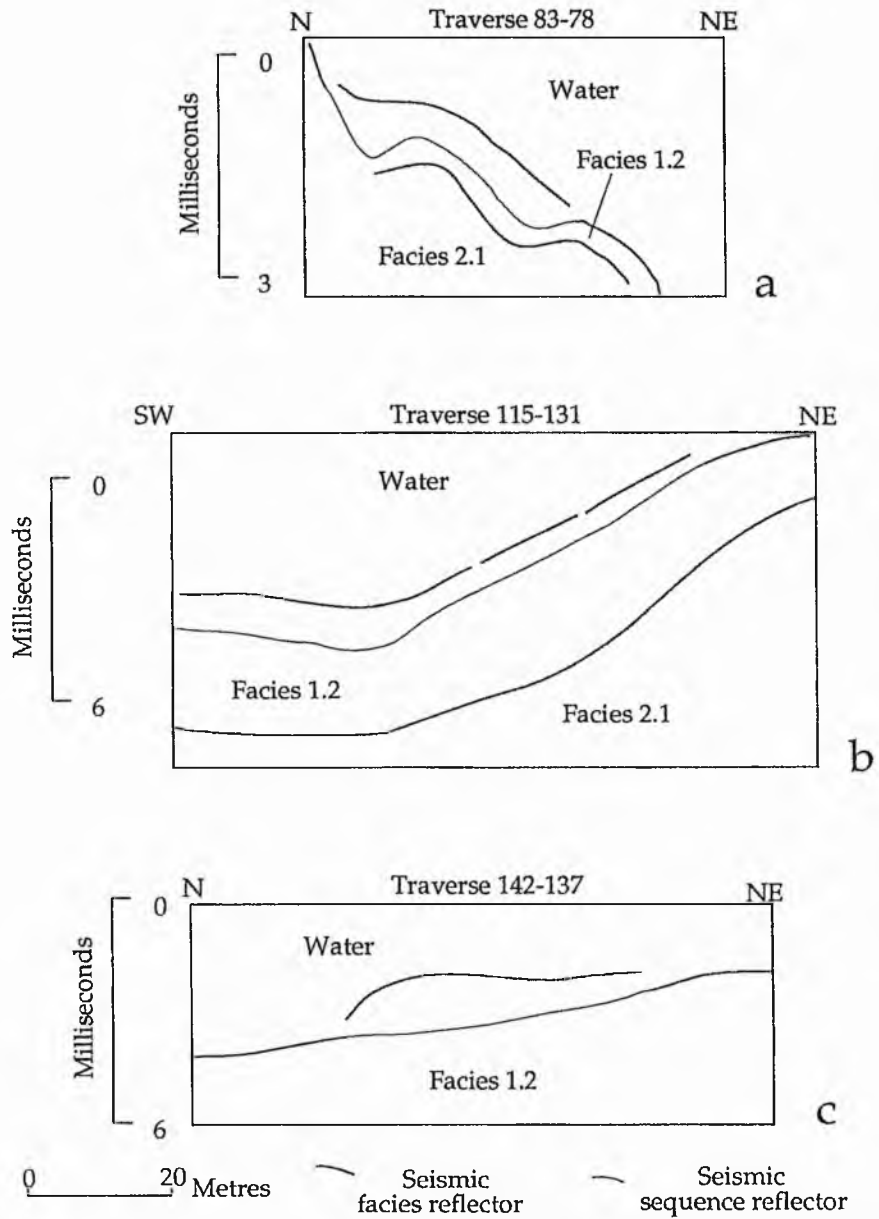
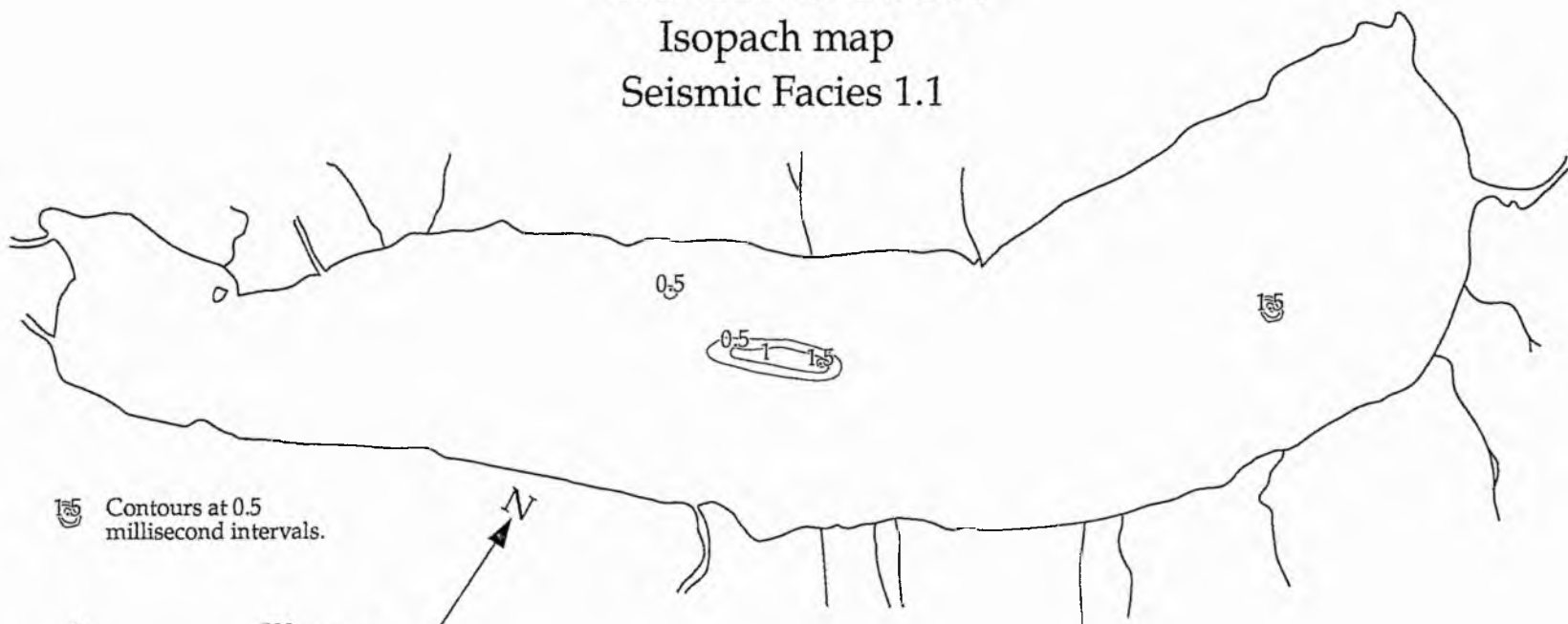


Figure 3.29
145

LOCH MUICK

Isopach map
Seismic Facies 1.1



Contours at 0.5
millisecond intervals.

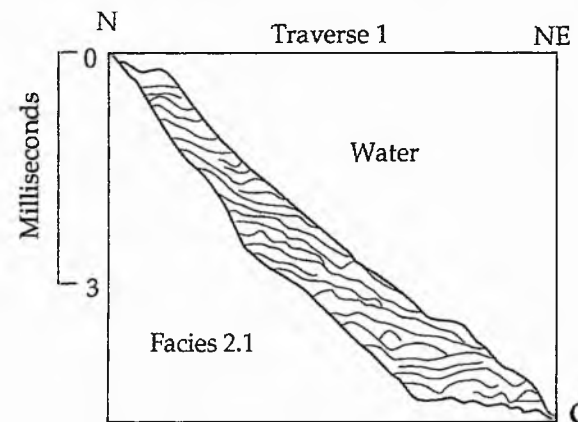
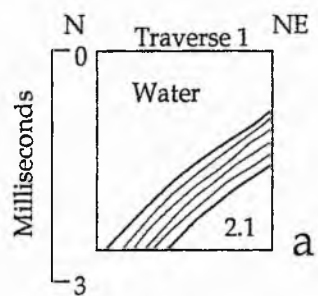
0 500 Metres



Figure 3.30
146

LOCH MUICK

Facies 1.2



— Seismic facies reflector

--- Seismic sequence reflector

0 20 Metres

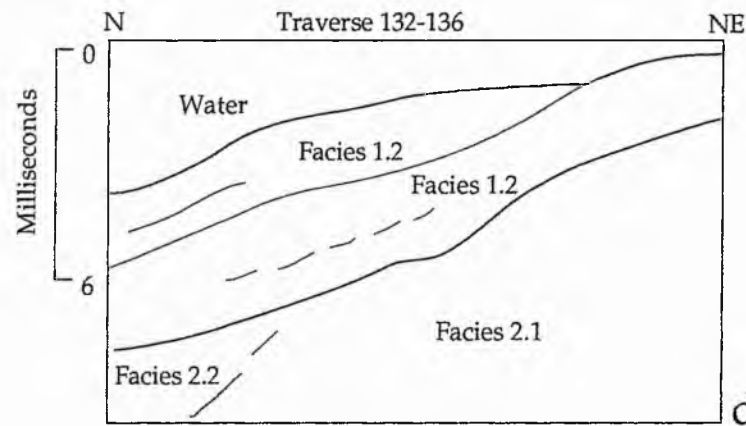
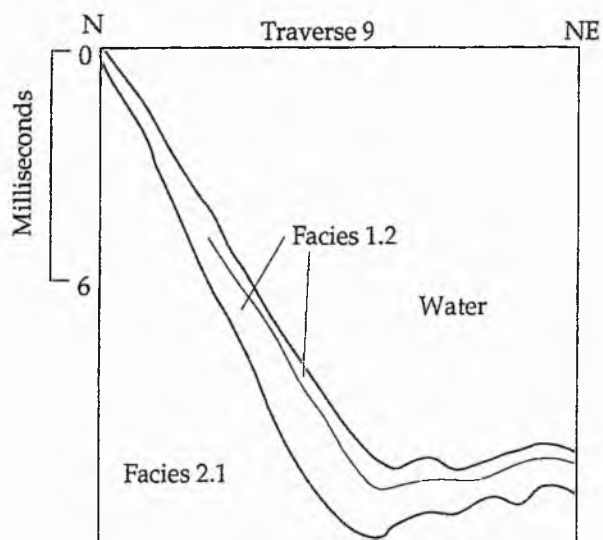
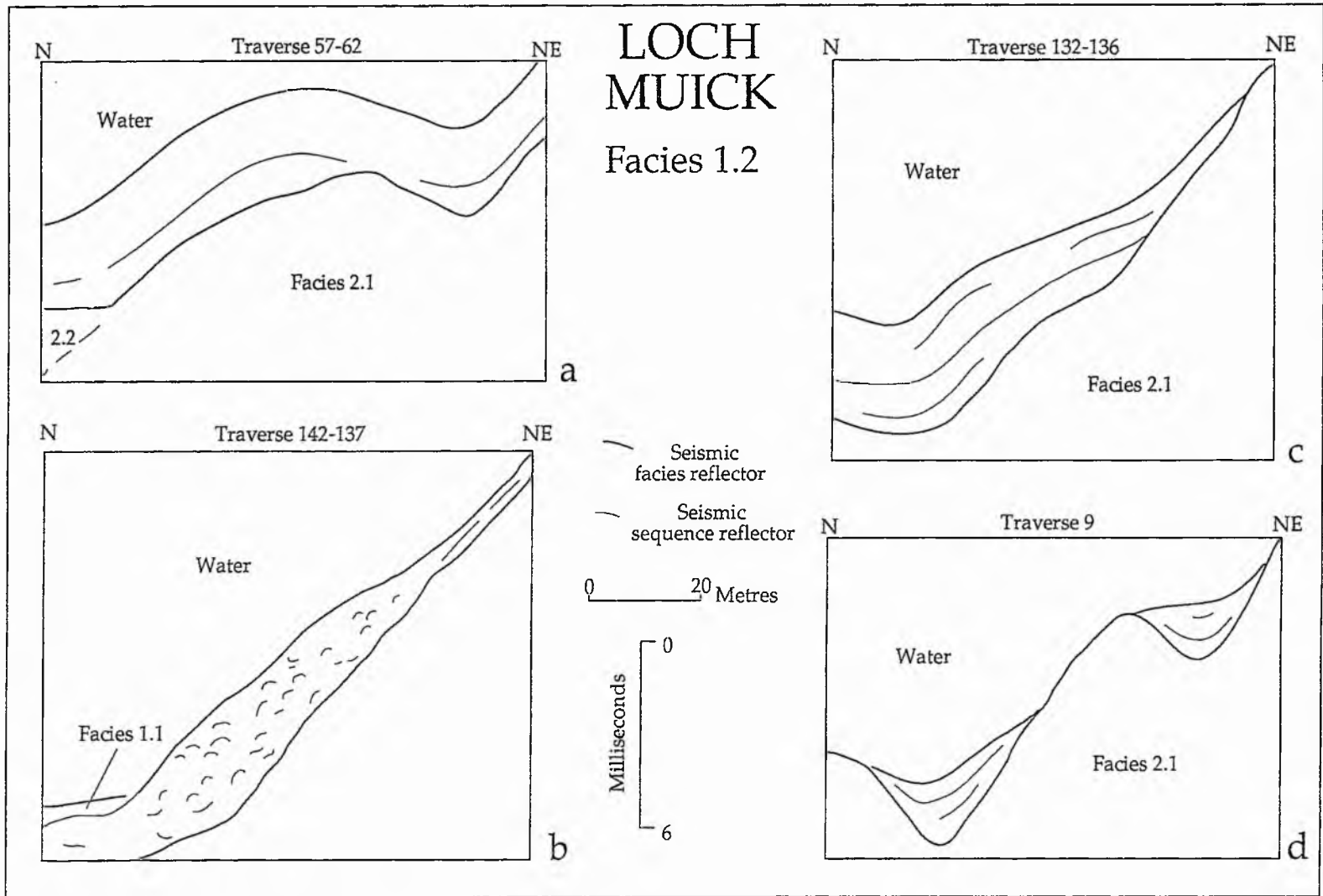


Figure 3.31
147

Figure 3.32
148



LOCH MUICK

Isopach map
Seismic Facies 1.2

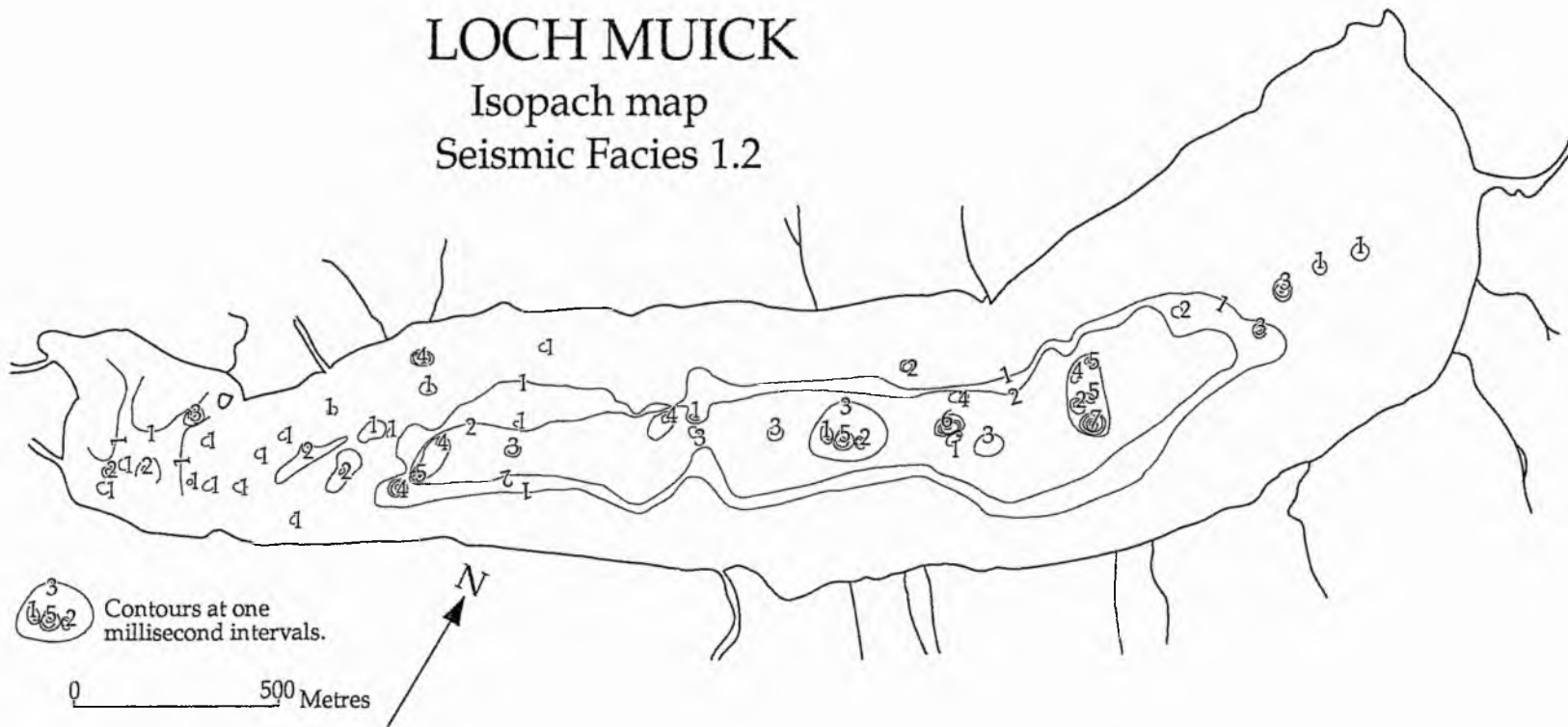


Figure 3.33
149

LOCH MUICK

Facies 2.1

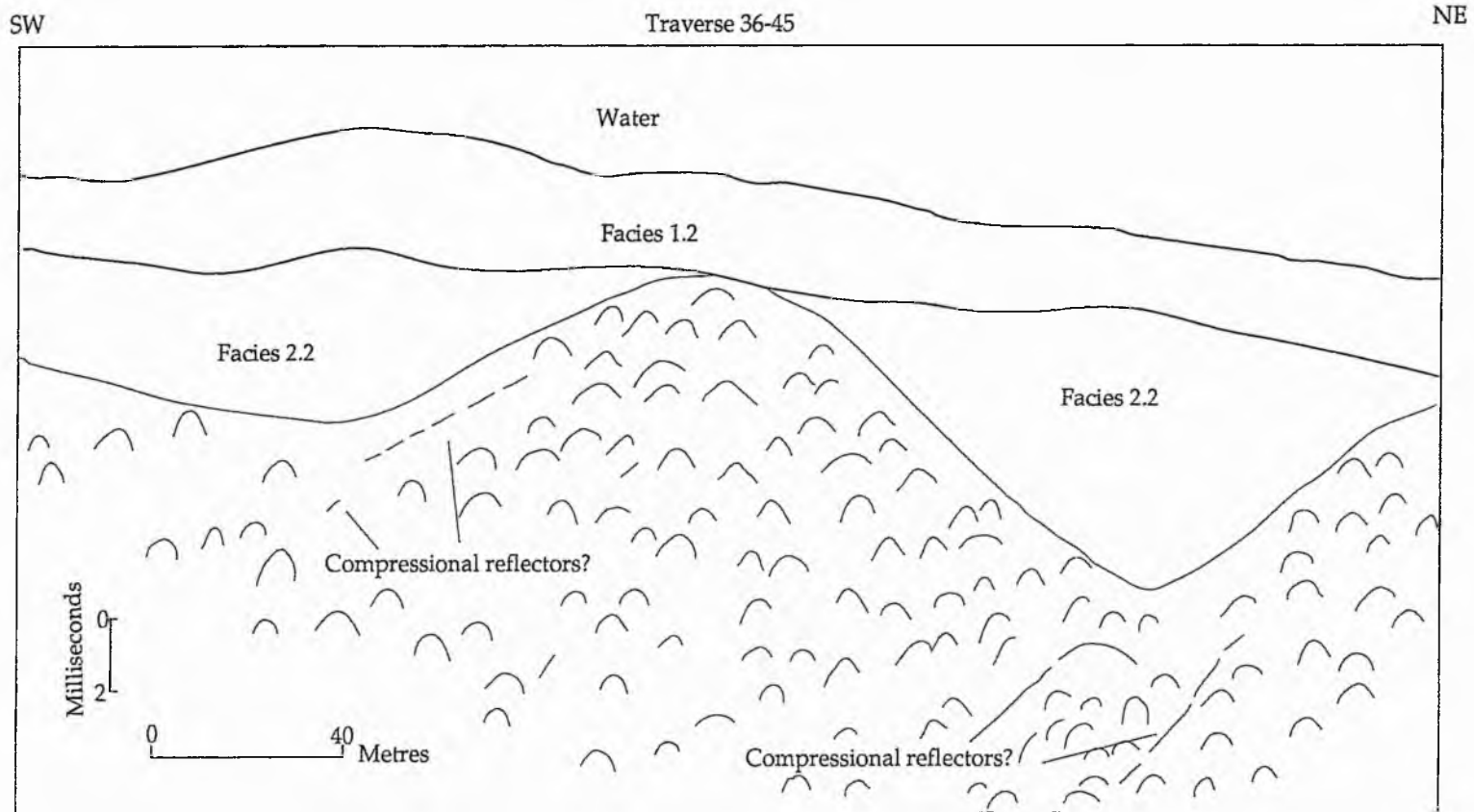
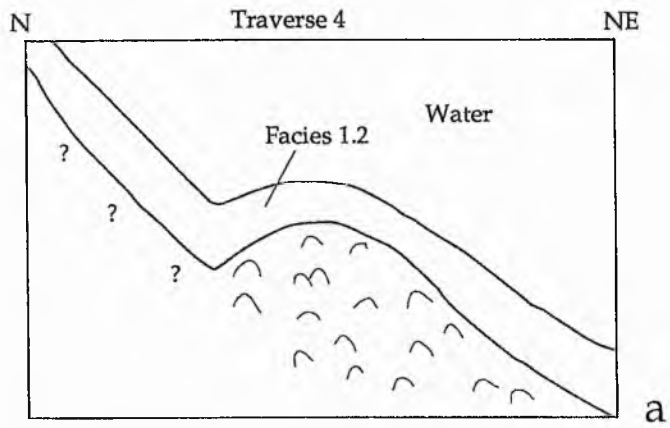


Figure 3.34
150

LOCH MUICK

Facies 2.1



Facies 2.2

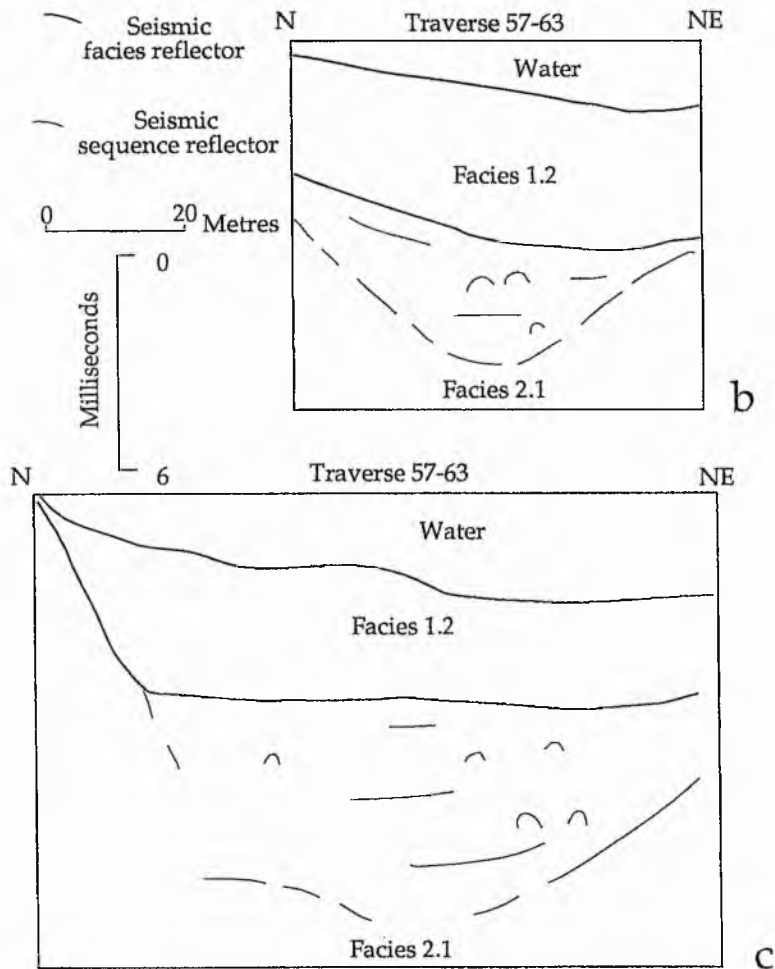


Figure 3.35
151

LOCH MUICK

Isopach map
Seismic Facies 2.2

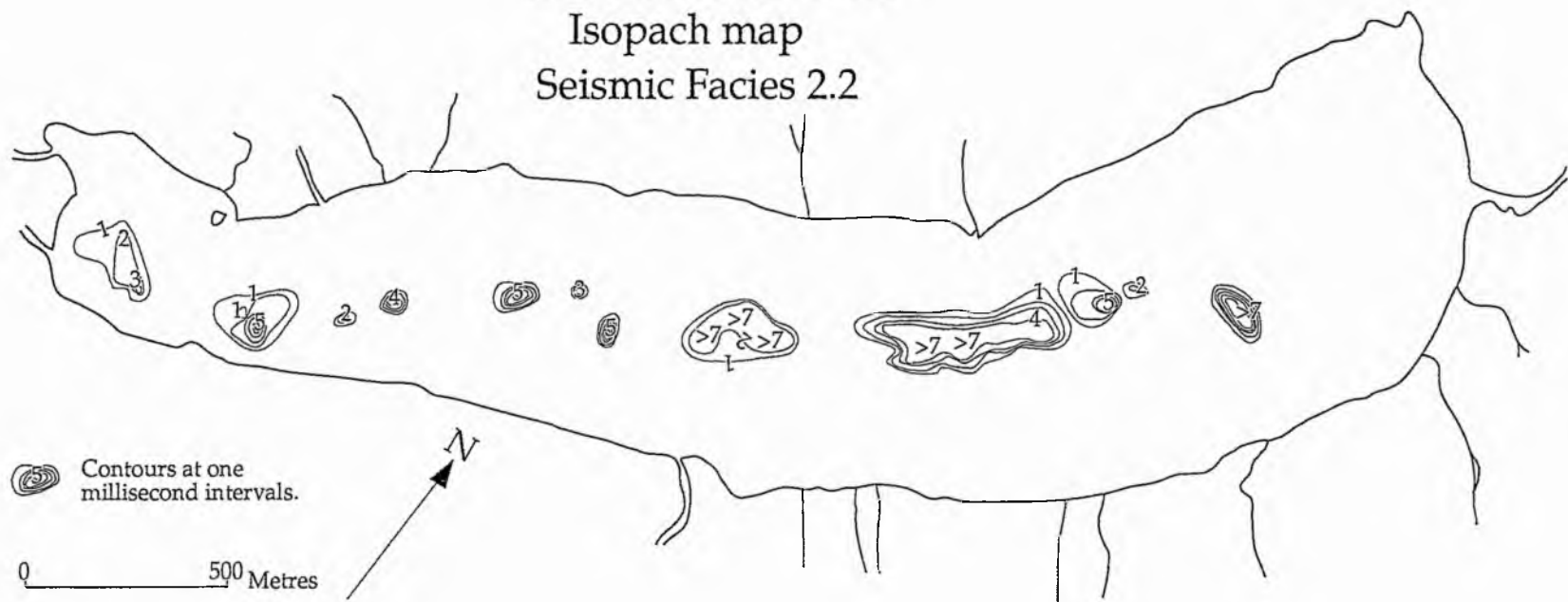


Figure 3.36
152



Plate 3.1 Giffit graphic recorder in use on Loch Callater. Note the number of reflection multiples resulting from operation in shallow water.



Plate 3.2 Waves on Loch Lee, 17 October 1989. View towards the northeast, outlet end.

NW

SE

154

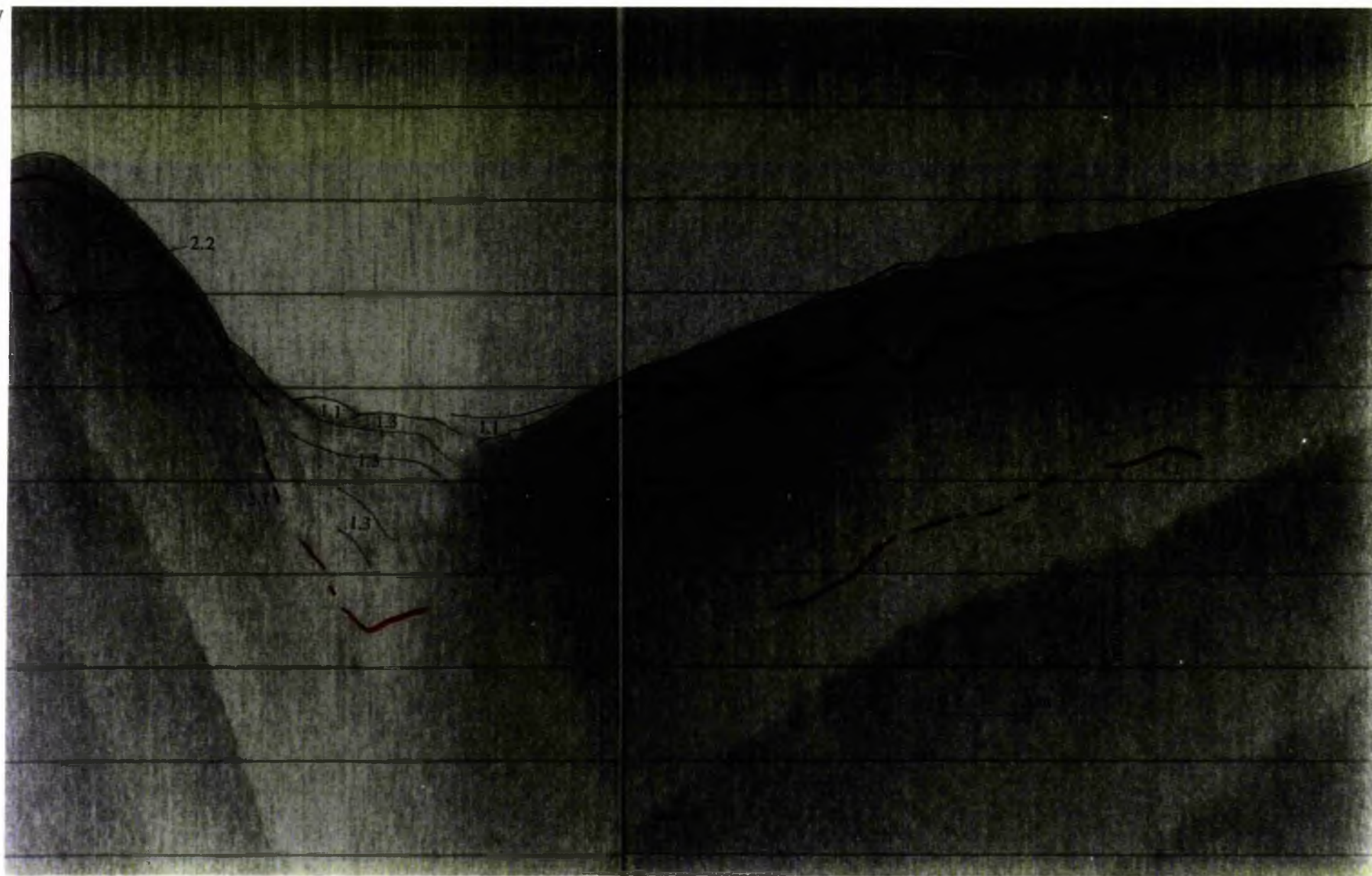
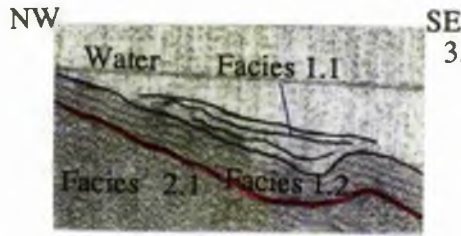
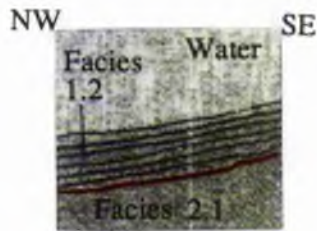


Plate 3.3 Loch Lee: Pinger seismograph, Traverse 8, overdrawn with seismostratigraphic interpretation. Red lines = Sequence boundary Black lines = Facies boundary.

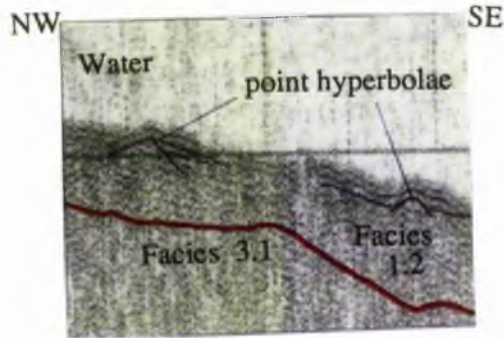
Plate 3.4 Loch Lee: Examples of some seismic facies.



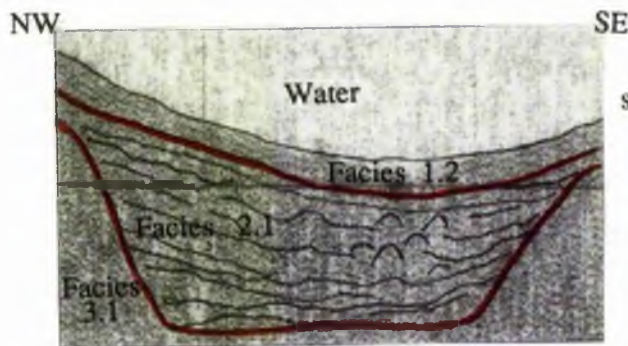
3.4A Facies 1.1, Traverse 10, subparallel lenticular reflectors forming a fill in the underlying topography.



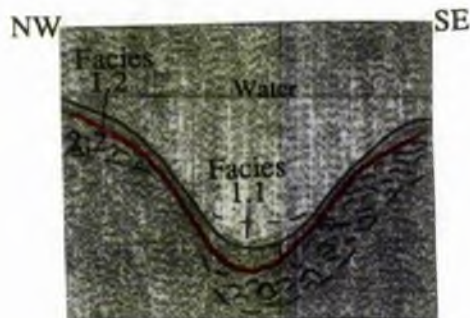
3.4B Facies 1.2, Traverse 13, parallel reflection geometry.



3.4C Facies 1.2, Traverse 14, point hyperbolae truncate parallel wavy reflectors.



3.4D Facies 2.1, Traverse 7, subparallel wavy and hummocky reflectors and concentrations of point hyperbolae.



3.4E Traverse 11, Facies 2.2, chaotic total geometry with scattered point hyperbolae.



Plate 3.5 Pinger array for use on Loch Callater. Float-mounted transducer (left) secured to pole, Giffit graphic recorder on dinghy. External hydrophone not visible.

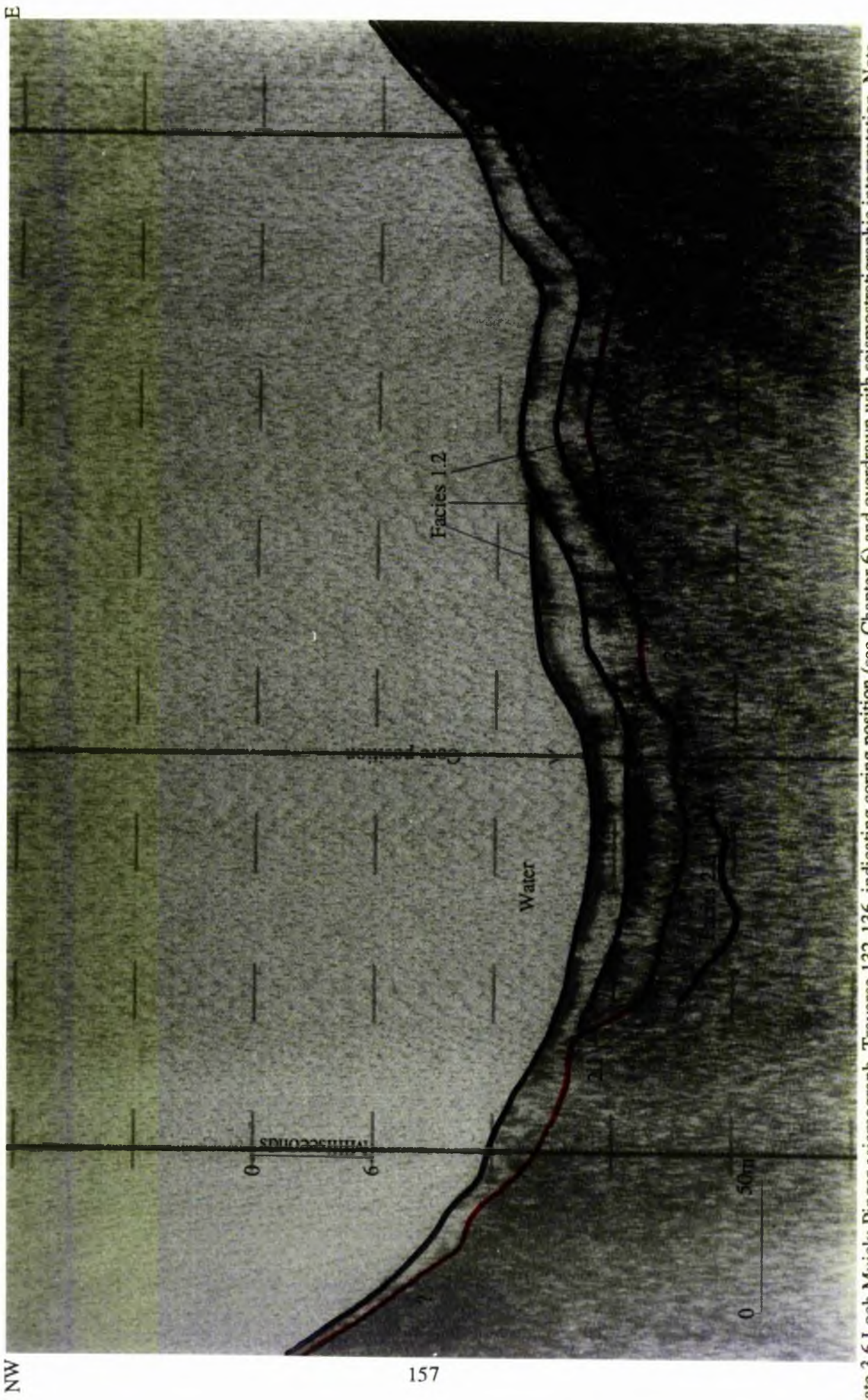


Plate 3.6 Loch Muick: Pinger seismograph, Traverse 132-136, indicating coring position (see Chapter 6) and overdrawn with seismic stratigraphic interpretation. Note double thickness of Facies 1.2. Red lines = Sequence boundary Black lines = Facies boundary.

NW

NE



Plate 3.7 Loch Muick: Pinger seismograph, Traverse 36-45, section between 36-38. Showing the undulating, hummocky surface of Facies 2.1 with internal compressional reflectors and infilling Facies 2.2 overlain by a drape of Facies 1.2. Red lines = Sequence boundary Black lines = Facies boundary.

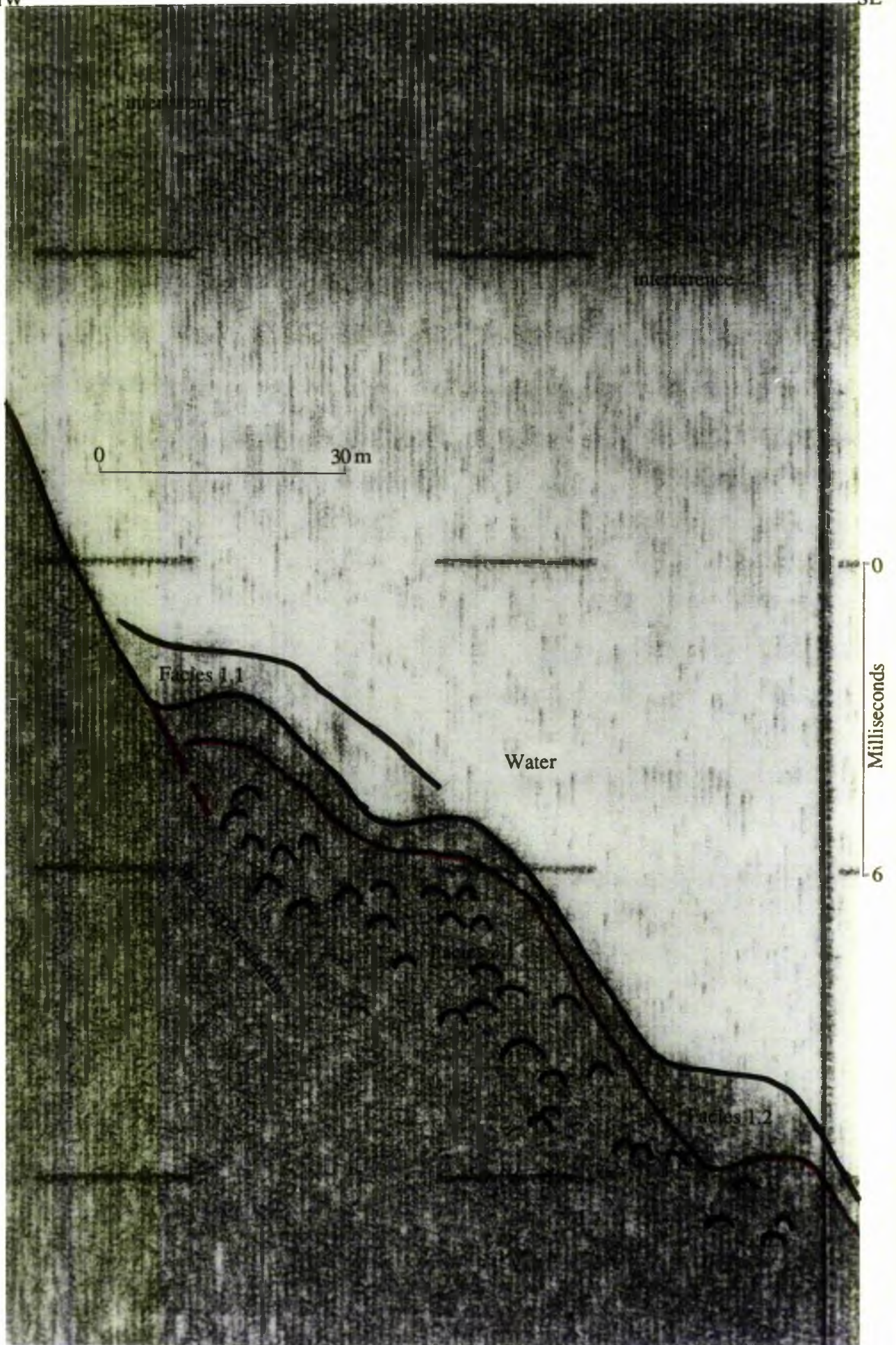


Plate 3.8 Loch Muick: Pinger seismograph, Traverse 77-83, section 79-80. Examples of seismic Facies 1.1 (reflection free internal geometry), Facies 1.2 (poorly defined subparallel reflectors) and Facies 2.1 (containing numerous point hyperbolae).

CHAPTER 4

SIDESCAN SONAR SURVEYS

'Sideways scanning sonar techniques are widely used in marine exploration to seek rock outcrops, to examine the nature of sea bed deposits ... Up to the present time sidescan sonars have rarely been used in inland water bodies ...' (Duck and McManus, 1987a, p. 228).

4.1 INTRODUCTION

In this Chapter are presented data from sidescan sonar surveys carried out on Lochs Lee, Callater and Muick. First, it reviews the development, application, principles and record interpretation of sidescan sonar. Secondly, data obtained using a Klein Hydroscan E401 sidescan sonar system are presented, and non-genetic interpretations are given of the topography and sediment types identified. Genetic interpretations of sidescan sonar data are given in Chapter 7.

4.2 SIDESCAN SONAR

4.2.1 Historical overview

The development of sidescan sonar was a direct result of experimentation with echosounders. It was discovered that by tilting an echosounder transducer from the vertical the reflected acoustic pulses showed the presence of objects within the water column and on the underlying sea floor. The implications of these findings stimulated the rapid development of the 'ASDIC' (Anti (Allied) Submarine Detection Investigation Committee) system during the Second World War, for the detection of enemy submarines. In essence this comprised a single transceiver unit, whose orientation could be controlled by the operator. For geological purposes the transceiver was fixed in position and towed above

the sea bed. Knott and Hersey (1956) introduced the pairing of transducers, to enable features on both sides of the vessel's track to be examined simultaneously, thereby doubling the coverage of the display with no increase in survey time. Formal geological application of the renamed sidescan sonar (SOund NAVigation and Ranging) was not made until 1958, when Chesterman, Clynick and Stride reported a survey of marine sediments. The first sidescan sonar ('Transit sonar') designed for scientific use (Kelvin Hughes) became commercially available in 1962. This apparatus used a single scanning direction and produced a rather crude image (Buller et al., 1975). Since that time advances in technology have greatly improved the images observed by the many systems now available. Recent surveys using dual scanning direction on inland water bodies (e.g. McManus and Duck, 1983) have enabled the recognition of many subaqueous features and allowed suggestions to be made concerning effects of water circulation on subaqueous geomorphic processes. Sidescan sonar surveys of the shelf seas (e.g. Belderson et al., 1970, 1972) have identified gouges attributed to iceberg grounding (e.g. Belderson et al., 1973; Belderson and Wilson, 1973) and sedimentary bedforms including megaripples (e.g. Belderson and Stride 1969; Newton et al., 1973). More recently deep-tow, long range apparatus has been developed. GLORIA (Geological LOng Range Inclined Asdic), which has a maximum range of 22km, has been used to map features on the ocean floor. Surveys have included the Amazon fan (Kenyon, 1989), the Chile Ridge (Westbrook, 1989), around the Aleutian Islands and over much of the eastern North American Shelf (Dobson, 1989). The development of sidescan sonar apparatus such as GLORIA has led Flemming to conclude:-

'Sidescan sonar must be regarded as a major breakthrough - especially for marine geology because, for the first time, it has become possible actually to map the surface features of the sea floor on a broad scale' (Flemming, 1976, p. 67).

4.2.2 Principles of sidescan sonar

Sidescan sonar operates on very similar principles to echosounding (see section 2.2.2 above). Two transducers are contained in a hydrodynamically streamlined towed apparatus, commonly called the 'fish'. The transducers generate pulses of sound with a narrow horizontal beamwidth, typically of $1-2^\circ$, depressed 10° from the horizontal. The narrowness of the horizontal beamwidth is important in determining the transverse resolution (R_t), which is defined as 'The minimum distance between two objects parallel to the line of travel that will be recorded on paper as separate objects.' (Flemming, 1976, p. 68). A wide horizontal beamwidth would result in echoes being received simultaneously from ahead, astern, and aside the survey vessel. The sound pulse length (pulse duration * velocity of propagation) also determines the resolution of the final image. For two closely spaced objects to be separately distinguished, they must be at least one half pulse length apart to prevent the output from masking the return signal.

In common with echosounding and subsurface reflection profiling, the frequency of the acoustic pulse determines the survey range. Due to the rapid attenuation of high frequency sound in water, combined with the spreading of sound away from the source, high frequencies can be used efficiently only in shallow water. D'Olier (1979) reports that over a distance of 100m an acoustic pulse of 300kHz will be totally attenuated, whereas a pulse of 50Hz will suffer a loss of 30% energy and a 5Hz pulse will have been attenuated by only 5%. Thus GLORIA, operating at a frequency of 6.5kHz, has a dual scan range of 22km. As in subbottom profiling, (see section 3.2.2 above) there is a trade-off between the resolution of the record and the scan range obtained. Higher frequencies result in short range, high resolution output, lower frequencies give long range records, but with lower resolution.

During sidescan sonar survey operations, pulses of sound are emitted from the towed transducers, which travel through the water column, and on incidence with the bottom are reflected back to the transducer (see also section 4.2.3 below). The reflected signal is received by the two transducers switched to receiver mode, converted to a pulse of

electrical energy and transmitted to the recording unit through the electromechanical tow cable. The electrical pulse is amplified and graphically presented as a 'sonograph' on a single, continuously recording, drum of electrosensitive paper. The signals from each transducer are presented as a split trace sonograph with a 'centre out display' (Klein Associates, 1985). The electrical current is passed through the paper by two helical electrodes which produce sepia coloured marks of an intensity proportional to the strength of the reflected energy. A composite image is built up by the adjacent plotting of successive electrical pulses. The position of each mark on the paper is determined by the time taken for it to be received by the transducers, on the assumption that :-

$$D = \frac{1}{2} vt$$

where D = distance

v = propagation velocity of water

t = two way travel time

Reflections from the outer parts of the sonar range are amplified by time variable gain to ensure consistent tonal variation.

Isometric records are obtained when vessel speed is matched by sonograph paper output speed. However, this is notoriously difficult to achieve. Photographic methods are frequently used to produce a sonograph mosaic. Sidescan sonar survey accuracy is ultimately dependent on correct vessel handling. Low survey speeds, of 3 to 5 knots (1 knot = 0.52ms^{-1}), are necessary to maximise the time that objects come under the sound beam, and to minimise the effects of pitch, roll and yaw on the 'fish' transducer.

4.2.3 Sidescan sonar record interpretation.

Sonographs obtained from sidescan sonar surveys have been likened to acoustic aerial photographs. The sonographs produced using a dual channel sidescan sonar system, with a split trace graphic output, show the vessel traverse line running down the centre of

the sonograph. Immediately adjacent to this white line, on either side of the vessel track, two dark bands appear representing the transmitted pulse (see Plate 4.1). Further outwards from the centre line lies a white area representing the depth to the bottom when the sonic pulse is travelling through the non-reflective water column. The first return provides a profile of the bottom beneath the fish. Subsequent echoes are received from the floor at successively further distances from the fish. The tonal variations on the sonographs result from the intensity of the reflected signal. This is dependent on two factors:-

- a) the underwater topography
- b) the substrate type.

Topography and underlying substrates can both result in the same reflection intensity and thus, ultimately, in the same graphic output. Experience and skill are therefore crucial for data analysis and interpretation.

4.2.3.1 Underwater topography

An object protruding above the bottom provides a surface from which the outgoing acoustic energy is preferentially reflected, producing a dark mark on the sonograph corresponding to the outline profile of the object. Directly behind the object lies an area of 'acoustic shadow' where the sound pulse does not penetrate. This shadow zone is represented by a lightening of the sonograph behind the object. Areas of depression exhibit a reversal of this dark-light pattern. At the edge of a depression the bottom falls away resulting in the absence of a surface for reflection. This produces a pale tone on the sonograph. The backwall of the depression provides a slope from which reflection towards the transducer occurs, causing a dark return on the sonograph. Slopes facing away from the source cause scattering of energy and are poor reflectors of sound.

On rare occasions protruding objects can appear as lighter areas of the sonograph when they return less reflected energy than the surrounding bottom. This is due to the acoustic properties of the target. Klein Associates (1985) give the example of a wooden

object appearing white against a sandy bottom.

Interpretation of sonographs in Scottish lochs has led to the identification of a suite of subaqueous landforms including shore-parallel steps, rotational slides, blister-like slides, boulder spreads and scour hollows (McManus and Duck, 1983; 1988a).

4.2.3.2 Substrate

Reflection of the acoustic signals from the bottom surrounding distinct targets is termed 'backscatter' or 'bottom reverberation' (Klein Associates, 1985). The underlying substrates can be distinguished by their backscatter characteristics. Porosity of the substrate is an important distinguishing factor. Acoustic impedance has a direct relationship with porosity; low porosity results in low impedance and low backscatter, high porosity results in higher impedance and higher backscatter. The porosity of a sediment is principally dependent on grain size. Taylor Smith and Li (1966) report that clays may have a porosity of 65-82%, silts 45-88% and sands 37-50%. Grain shape, degree of sorting, time elapsed since deposition and sediment compaction are also significant factors in determining backscatter levels. Since sidescan sonar provides data on the surface characteristics of the sediment, removal of surface fines by winnowing can lead to misleading conclusions regarding the nature of the sediment. Thus it is vital that a sediment sampling programme (see Chapter 5) is carried out in conjunction with a sidescan sonar survey to provide the necessary 'ground observations' for calibration of the remotely sensed data.

4.3 METHODOLOGY : AIMS

Sidescan sonar surveys of Lochs Lee, Callater and Muick were undertaken using a Klein Hydroscan E401, high resolution, short range, system operating at 400kHz. This comprises a towed transducer fish, electromechanical tow cable and split trace graphic recorder, producing a sepia coloured sonograph on wet, electrosensitive paper. Survey

speeds were maintained as near constant as possible to 3 knots (1.5ms^{-1}). Due to adverse weather conditions at the time of the Loch Lee and Loch Muick surveys and logistical restrictions on Loch Callater, dead reckoning was the only possible means of position fixing. Event marks were made on the sonographs, and noted on the survey record, when the towed fish passed landmarks on the shores and subaqueous topographical features recognised on the new bathymetrical charts.

The sidescan sonar surveys aimed to:-

- i) Identify topographic and surface sediment type variations within the three water bodies
- ii) Complement echosounder (Chapter 2), subbottom profiling (Chapter 3), coring (Chapter 6) and surface sediment (Chapter 5) data.

4.4 LOCH LEE

4.4.1 Sidescan sonar survey

Loch Lee was surveyed during September 1989. A total of four circuits were made (Figure 4.1), covering a total traverse length of approximately 18km.

4.4.2 Sonograph description and interpretation

To enable easy location of the features recognised, descriptions of the sonographs are presented using the zones identified in Chapter 2 (Figure 2.3). A non-genetic interpretation of the sonographs in each zone is given with the description of the sonographs. A genetic interpretation is given in Chapter 7).

4.4.2.1 Zone 1 Southwestern Shallows

The floor of the southwestern shallows is characterised by low backscatter levels interrupted by large, dark reflectors (Plate 4.2). These reflectors show a distinct linear distribution along the boundary between Zones 1 and 2. The absence of an acoustic

shadow behind the reflectors is thought to be due to the lack of contrast possible with the low backscatter level of the surrounding loch floor. It is believed that this sonograph configuration represents aquatic plants growing in fine sands or silts. During earlier surveys (see Chapter 2, section 2.4.2.1) the existence of weed growth in this area was observed.

4.4.2.2 Zone 2 Central Trough

The nearshore slopes of Zone 2 are characterised by alternate dark and light shore-parallel banding extending a maximum of approximately 45m from the shore (Plate 4.3). This configuration is interpreted as shore-parallel terraces, the dark bands representing the highly reflective back ('riser') of the terrace and the lower intensity areas the flat ('tread'). A maximum of five terraces are identified. High intensity point reflectors (boulders) are recognised lying on the terrace flats, particularly on the most shore proximal terraces. Occasionally acoustic shadow zones occur behind the boulders, suggesting that they protrude a significant distance above the bed. However, this is an unusual occurrence in Loch Lee, therefore it is inferred that most boulders have either a slab-like form, or are partially buried in finer grained sediment. The extremely steep slope angles close to the mouths of the streams on the northern slopes are represented by a very high reflection amplitude (Plate 4.4).

Immediately below the shoreline terraces an area of very low, uniform backscatter occurs (see for example Plate 4.3) at this position throughout Loch Lee. This area frequently runs parallel to the base of the terraces extending up to 20m further into the loch, but on the northern slopes a more irregular distribution occurs (Plate 4.5). Lobes of this low backscatter reflector extend from a promontory into areas of medium backscatter. Very occasionally high intensity boulder reflectors are recognised within this low intensity area confirming that this is not an acoustic shadow zone. It is suggested that this acoustic signature represents fine grained sediment such as silt or mud. This hypothesis is accepted on the basis of evidence from sediment sampling (section 5.3.3).

The remainder of the basin within Zone 2 is composed of a predominantly uniform, medium intensity backscatter reflector. The sediment in this area is fine grained; sediment sampling confirms that the loch floor in this area is covered by mud, sandy mud, silt and sandy silt. An exception to this pattern occurs close to the mouth of the Burn of Duchrey on the northern slopes of Zone 2 (Plate 4.4). Approximately 60m from the loch shore there occurs an area of mottled darker reflectors preceding a lighter area. The dark area is composed of two distinct types of reflection targets. First, those with acoustic shadow zones; this type has a lateral spread of 20m downslope, and secondly irregularly shaped areas of slightly lower reflectivity. The lighter area is approximately 10-15m wide and contains no tonal variations. Thus this dark-light area of sonograph is interpreted as being a slope facing the sonar transducer, composed of boulders with intervening hollows, casting an acoustic shadow onto the slope behind.

Hollows have also been identified in a broad swathe 50-60m wide across the floor of the loch in Zone 2. They are first recognised close to the mouth of the unnamed stream (Figure 4.1) and extend to the northeast over a distance of approximately 600m. High reflectivity boulder signatures occur widely scattered around the base of the shore-parallel terraces. At one location on the southern slopes (Plate 4.6), the high density signature characteristic of a boulder can be recognised below the shore-parallel terrace sequence with a linear, low reflection intensity area running upslope behind it. It is suggested that the low intensity area is a linear topographic low.

4.4.2.3 Zone 3 Northeastern Shallows

Zone 3 is characterised by a much 'rougher' acoustic texture. Shore-parallel terraces extend a maximum of 75m from the shore on both sides of the loch (Plate 4.7). The flats of the terraces are covered by numerous boulders with associated acoustic shadows. The maximum width of the terraces occurs where promontories extend into the loch. The loch floor below the terraces shows a range in backscatter between low and medium levels. Medium backscatter areas, probably composed of fine sand or silt, are located adjoining the

promontories and have a scattering of boulders over the surface. Within the medium backscatter area adjoining the most northwesterly promontory (Plate 4.7), high intensity reflectors face the transducer with a distinct area of acoustic shadow lying behind them. This is interpreted as representing part of the bedrock spur which forms the promontory, exposed through finer grained sediments as a rocky outcrop.

Low backscatter levels occur throughout the remainder of Zone 3, between the promontories and over the central part of the loch floor. This acoustic texture is believed to represent fine silts or muds. Where this texture lies adjacent to the shore-parallel terraces and medium backscatter areas, intermittently distributed boulders occur. On the southern side of the loch the backscatter increases to an intermediate, medium to low level (Plate 4.8) and a distinct mound, marked by a uniform high reflectivity, rises above the loch floor. This mound, also apparent on the bathymetric chart (Figure 2.2), is not composed of individually distinguishable boulders, and does not cast an identifiable acoustic shadow. An interpretation of the genetic processes of this and all other features is given in Chapter 7.

4.5 LOCH CALLATER

4.5.1 Sidescan Sonar Survey

Loch Callater was surveyed during August 1990. The transducer fish was towed at a depth of approximately 1.5m, to reduce the risk of hitting the bottom and damaging the equipment in the very shallow water body. A scan range of 150m was used to shoot four linear traverses along the loch, covering approximately 4km (Figure 4.2). This scan range covered the loch floor from shore to shore. Due to the shallowness of Loch Callater, sidescan sonar surveying could not be carried out at its southeastern extremity.

4.5.2 Sonograph description and interpretation

The description and non-genetic interpretation of the sonographs are given, divided along the longitudinal axis of the loch:- the northeastern and southwestern slopes.

A genetic interpretation is given in Chapter 7.

4.5.2.1 Northeastern slopes

Around the shores of the northeastern side of Loch Callater a series of poorly defined shore-parallel terraces have been recognised on the sonograph from the characteristic dark-light banding associated with changes in the angle of the loch floor. A maximum of three terraces has been identified (Plate 4.9). They are best developed in the embayments along the loch shores, and show evidence of the existence of boulders lying on the flat areas. Below the terraces a wide (approximately 10-20m), dark reflector occurs around the entire perimeter of the loch basin. It has a well defined boundary with the adjoining, low backscatter level reflector downslope. This darker area probably represents a medium to low angle slope, possibly composed of coarser grained sediment, with no boulder sized clasts identifiable lying on the slope surface. The sediment samples obtained from the loch floor (see section 5.4.2) indicate that the surface sediment is predominantly composed of silt, with a gradational boundary through sandy silt to silty sand at the southeastern end of the loch. Thus there is no physical evidence for the existence of a band of distinctly coarser sediment as interpreted from the sonograph. This may be a function of the sediment sampling density or the interpretation of the original sonograph - the tonal intensity resulting from variation in topography as opposed to substrate. Evidence in support of the latter hypothesis is found in the occurrence of boulder sized clasts lying at the boundary between the slope and area of low backscatter. Five concentrations of boulders, of which four can be recognised on Plate 4.9, extend onto the area of low backscatter to a maximum distance of 15-20m. These boulder spreads have distinct acoustic shadows which suggest that they protrude a significant height above the loch floor. The area of low backscatter, indicative of fine grained sediment such as silt, lies broadly parallel with the base of the slope, widening to a maximum of approximately 60m towards the southwestern end of the loch. This low backscatter acoustic signal has a gradational boundary with a medium backscatter reflector that occupies the remainder of the loch floor

within this area. The area of medium backscatter probably represents slight change in slope angle as opposed to substrate composition, since sediment sampling (section 5.4.2) indicates that the loch floor in this area is covered extensively by sediment in the silt grain size fraction.

4.5.2.2 Southwestern slopes

The southwestern slopes are characterised by two distinct groups of sonograph signatures, the first of which can be identified in Plate 4.10. The extremely dark nearshore reflector, indicative of a very steep slope, is followed by an abrupt downslope change to uniform low to medium backscatter reflectors which extend to the outer limits of the surveyed area. No upstanding targets such as boulders have been identified in these areas of fine grained sediment. This group of sonograph signatures is located in the central portion of the southwestern slope extending northwestwards for approximately 150m from the mouths of the two streams (see Figure 4.2).

The second group of sonograph signatures is located along the remainder of the southwestern slopes. It is recognised by the more gradational boundary between the nearshore and lower slopes and the presence of scattered boulders (Plate 4.11). The islet, towards the southeastern end of the loch, is recognised by the acoustic shadow that extends to the loch shore and in effect, acoustically, appears as part of the shore. The sonar record indicates that the shoreline of the islet is composed of numerous boulders and cobbles. This interpretation is confirmed by visual observations made during the survey. Immediately adjacent to the islet to the southeast, high intensity reflectors, with an area of acoustic shadow, indicate the existence of a steep sided ridge extending approximately 60m into the loch from the shore. Boulders are recognised resting on the sides and at the base of the ridge. This second group of reflection signatures also appears at the extreme northwestern end of the loch where a gentle, boulder strewn slope can be traced for approximately 70m from the shore.

Below the nearshore, steeper slopes the loch floor is covered by patches of low to

medium level backscatter reflectors which show an apparently random distribution pattern. It is suggested that this tonal variation is caused by minor variations in topography as analyses of the loch floor surface sediment indicate that it is predominantly composed of sediment in the silt grain size fraction (Chapter 5). Areas of sandy silt and silty sand have been identified only at the northwestern and southeastern extremities of Loch Callater.

4.6 LOCH MUICK

4.6.1 Sidescan sonar survey

Loch Muick was surveyed during April 1989. A total of five traverses covering a distance of approximately 20km were run (Figure 4.3). Equipment to depress the transducer fish, to enable scanning at greater depths, was not available. Due to the extreme depth (maximum 83.2m), width, and angle of slope of the loch, reflected signals were received by only one of the paired transducers. Acoustic pulses projected downslope towards deep water were reflected out into the water body, away from the transducer. Thus, in common with other surveys of deep water bodies (e.g. Loch Earn; McManus and Duck, 1983; Duck and McManus, 1987a), only the upper parts of the loch slopes were examined.

4.6.2 Sonograph description and interpretation

To facilitate the location of features identified on the sonographs, the description and non-genetic interpretation of the sidescan sonar data is divided into two sections along the longitudinal axis of Loch Muick. The northern and southern slope divisions include the western (inlet) shore with the northern slopes and the northeastern (outlet) shore with the southern slopes. A genetic interpretation derived from all the data sources is given in Chapter 7, section 7.2.1.

4.6.2.1 Northern slopes

The slopes adjacent to the mouths of the Allt an Dubh-loch contain two distinct assemblages of acoustic signatures. First, close to the southerly mouth of the Allt an Dubh-loch, an area of low backscatter typical of fine grained sediments such as silts occurs (Plate 4.12). It is scattered with occasional small boulders and cobbles and terminates at a sharp break in slope which appears as a dark band on the sonograph. Confirmation of this interpretation cannot be made as the loch floor surface sediment in this area could not be sampled owing to adverse weather conditions at the time of sampling (see section 5.2.1). Boulders and cobbles can be recognised on the sonograph as a dark acoustic signature, frequently with an acoustic shadow lying directly behind. Below the break in slope an almost uniform area of low backscatter reflection occurs, with no point reflectors. The uniformity is broken by a band of medium reflectivity which is interpreted as a slight increase in slope angle inducing a higher reflectivity than the surrounding, flatter, loch floor. This interpretation is confirmed by reference to the bathymetric chart (Figure 2.15).

The second grouping of acoustic signatures is interpreted as representing shore-parallel terraces. These features appear on the sonograph as alternate dark (steep back slope) and light (flat surface) bands running parallel or subparallel to the loch shore. Two clearly defined shore-parallel terraces have a widespread occurrence in Loch Muick, although occasionally a smaller, poorly developed terrace can be seen at the base of the sequence (Plate 4.12). Boulders can be recognised lying on the nearshore terrace flats (see for example Plate 4.13). Curvilinear, dark signatures on an area of low backscatter with no acoustic shadow (Plate 4.13), close to the boulder spreads are interpreted as representing partially buried sections of tree trunk.

At the base of the sequence of terraces a sharp break in slope occurs, identified by a highly reflective, dark band on the sonograph. Below this level a wide range of acoustic signatures appear. Close to the mouth of Lindsay's Burn (for location see Figure 2.14) a wide area of low backscatter (fine sediment) occurs, with a few small clusters of boulder reflectors which have no acoustic shadow areas, apparently lying partially embedded in the

surface. Also identified on Plate 4.13 is another feature typical of the nearshore northeastern slopes of Loch Muick, namely the boulder spread. This appears as a dense concentration of boulder reflectors extending downslope over an area of low backscatter. Between Lindsay's Burn and the Allt an Dearg the density of these boulder spreads increases to a level whereby only the terminal tongues of each feature can be differentiated where they extend onto areas of low backscatter. The form of these features has been enhanced on a sonograph record (Plate 4.14), which was obtained using a very low sensitivity (tonal variation) setting to enable the distinction of topographic features on the boulder surface. At this low setting several small topographic highs, represented by darkening of the sonograph, with areas of acoustic shadow lying upslope, occur superimposed upon the boulder surface (Plate 4.14). Similar lobate forms have also been distinguished on areas covered by sediment of low to medium reflection backscatter levels.

During the surface sediment sampling programme samples of fine grained material, including mud, sandy mud and sandy silt were obtained throughout the loch, close to the shores, including those areas covered by boulder lobes. This suggests the existence of either a drape of finer grained material over the boulders, areas not covered by boulders, the inability of the grab to hold material of this size (Prior and Bornhold, 1989) or a combination of these factors.

The nearshore slopes around the mouth of the Allt an Dearg show an abrupt change from boulder spreads to areas of high backscatter (coarse grained sediment), with intervening linear areas of medium to low backscatter (finer grained sediment) (Plate 4.15). The island is associated with steep subaqueous slopes, with scattered boulders lying on the surface.

4.6.2.2 Southern slopes

The southern slopes show the same range of sonograph signatures as the northeastern slopes, but variation in distribution of these features occurs.

At the southwestern end of the loch overlapping boulder spreads are distributed

along the shore to the mouth of the Black Burn. Plate 4.16 shows the distinct downslope termination of these features on an area of medium backscatter levels with occasional scattered boulders. Frequently, however, the base of the boulder spreads extends to depths below that covered by the acoustic scan pulse (Plate 4.17). Occasional lighter areas on the sonograph are believed to represent low or medium backscatter levels, probably areas of finer grained sediments remaining uncovered by the boulder spreads. The complex nature of the sonograph in this area makes it impossible to exclude the possibility that at least some of the lighter areas may represent topographic hollows.

The shoreline on this side of the loch is frequently composed of boulders and cobbles (see Plate 4.17) creating a ragged outline. Shore-parallel terraces occur infrequently and are poorly developed having back slopes with a medium reflection intensity (Plates 4.16, 4.17).

In the area surrounding the mouth of the Black Burn, the sonograph shows a gradational change from boulder spreads to an area of low to medium backscatter levels (Plate 4.18). Tonal variation within this area, particularly close to the edges of the Plate, is believed to result from variation in sediment grain size, the palest areas possibly representing mud or very fine silt and the slightly darker areas silt or sand. No boulders have been identified within the central part of this area. The narrow, curvilinear area of very low reflectivity, with a darker band lying directly behind it, close to the shore, has the acoustic signature typical of a topographic low. It is interpreted to be the subaqueous channel associated with the Black Burn, incised into the loch floor sediments.

East of the mouth of the Black Burn the slopes are also covered by extensive boulder spreads. The northeastern shore has a different sonograph signature. Plate 4.19 is interpreted as showing clusters of boulders rising above an area of almost uniform medium to low backscatter levels. Some of the darker areas have fewer point reflectors, which implies that they may be composed of finer grained material such as gravel, the individual clasts being below the resolution of the equipment. The first bottom echo provides a depth profile beneath the fish and shows that there may be a broad visual correlation between the

density of boulder clusters and the depth below surface, boulders occurring on topographic highs. Also recognised on Plate 4.19 is a patchy, irregular, 'smooth' textured, area of dark tonal intensity, with occasional lighter patches. This is interpreted as representing aquatic weed growth in the shallow, nearshore zone.

4.7 CONCLUSIONS AND DISCUSSION

The sidescan sonar surveys of Lochs Lee, Muick and Callater have enabled the recognition of subaqueous landforms and variations in sediment distribution (see sections 4.7.1, 4.7.2, and 4.7.3 below). Many of the subaqueous landforms identified, in particular the shore parallel terraces, subaqueous continuation of promontories and rocky outcrops have been reported from surveys conducted in numerous other Scottish lochs. These include Loch Earn (McManus and Duck, 1983), Loch Lubnaig, Loch Tummel (McManus and Duck 1988b) and Loch Tay (Duck and McManus, 1987a). The extensive boulder spreads and lobate forms recognised in Loch Muick have not previously been reported from any Scottish loch. Variation in sediment composition at stream mouths has also been recognised in Loch Earn where a broad area of 'fan-like sediment accumulations' (McManus and Duck, 1983) is associated with stream inflow. The existence of boulders lying on nearshore terraces and in the nearshore zone has been recorded in all the major lochs referred to above.

Evidence regarding the formational processes of the features identified are discussed in the context of all other data sources (Chapters 2, 3, 5 and 6) in Chapter 7.

4.7.1 Loch Lee

Sidescan sonar records have enabled the identification of subaqueous geomorphic features and variations in the distribution of sediment types. Underwater landforms identified comprise:-

- i) Suites of shore-parallel terraces (a maximum of five) with boulders lying on the nearshore terrace flats.

- ii) Hollows, both in isolation and comprising a broad swathe across the loch floor.
- iii) Mounds composed of boulders and of undetermined composition.
- iv) Steep loch-side slopes.
- v) The subaqueous continuation of subaerial promontories.

Variations in sediment distribution identified include:-

- i) Wide expanses of fine grained material characterised by medium to low backscatter levels, particularly in the southwestern shallows and central trough.
- ii) Very fine grained material located at the base of the shore-parallel terraces.
- iii) Boulders partially buried in finer grained sediments.

Areas of weed growth have also been identified in the shallow water at the southwestern end of the loch.

4.7.2 Loch Callater

Sidescan sonar surveys have enabled the three dimensional recognition of subaqueous geomorphic features and surface sediment distribution. The landforms comprise:-

- i) A maximum of three, poorly defined, shore-parallel terraces within embayments in the loch shore.
- ii) Changes in slope angle, which include very steep nearshore slopes on the southwestern side of the loch.
- iii) A boulder strewn, steep sided ridge extending from the southwestern shore.

Sediment distributions identified from sidescan sonar records include:-

- i) Nearshore boulder spreads.
- ii) Areas of medium to low backscatter covering most of the loch floor, believed to represent fine grained sediment.

4.7.3 Loch Muick

Five types of geomorphic features have been identified on the floor of Loch Muick using sidescan sonar:-

- i) A series of up to three, ill-defined, shore-parallel terraces with boulders lying on the nearshore terrace flats.
- ii) A sharp break in slope at the base of the shore-parallel terraces.
- iii) Lobes of boulders and topographic hollows upon the surface of boulder spreads (see below).
- iv) The extension of the incised channel of the Black Burn into the loch.
- v) Small mounds covered by boulders at the northeastern end of the loch.

Variations in sediment type and distribution have also been recognised:-

- i) Extensive boulder spreads in the nearshore zone on the northeastern and southwestern slopes of the loch.
- ii) Boulder clusters and concentrations of finer grained, highly reflective, material such as gravel, in the shallow water area close to the outlet of the River Muick.
- iii) Large areas of low-medium backscatter levels with occasional scattered boulders close to the base of the terraces which are believed to represent fine grained material such as silt and mud.
- iv) Variation in sediment composition associated with the mouths of influent streams.

In addition, aquatic plant growth in the shallow water area at the extreme northeastern end of the loch has been recognised.

LOCH LEE

Sidescan Sonar traverse lines

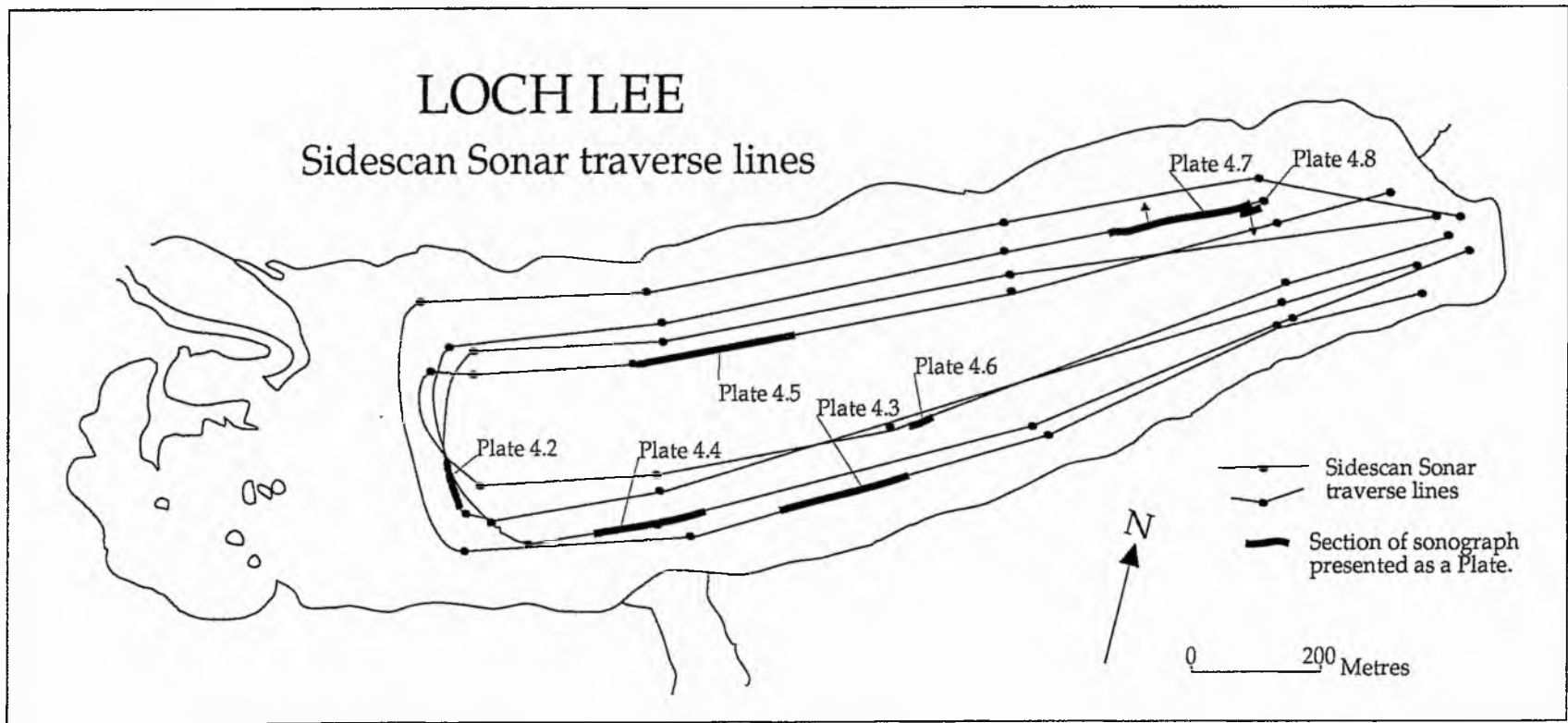


Figure 4.1
179

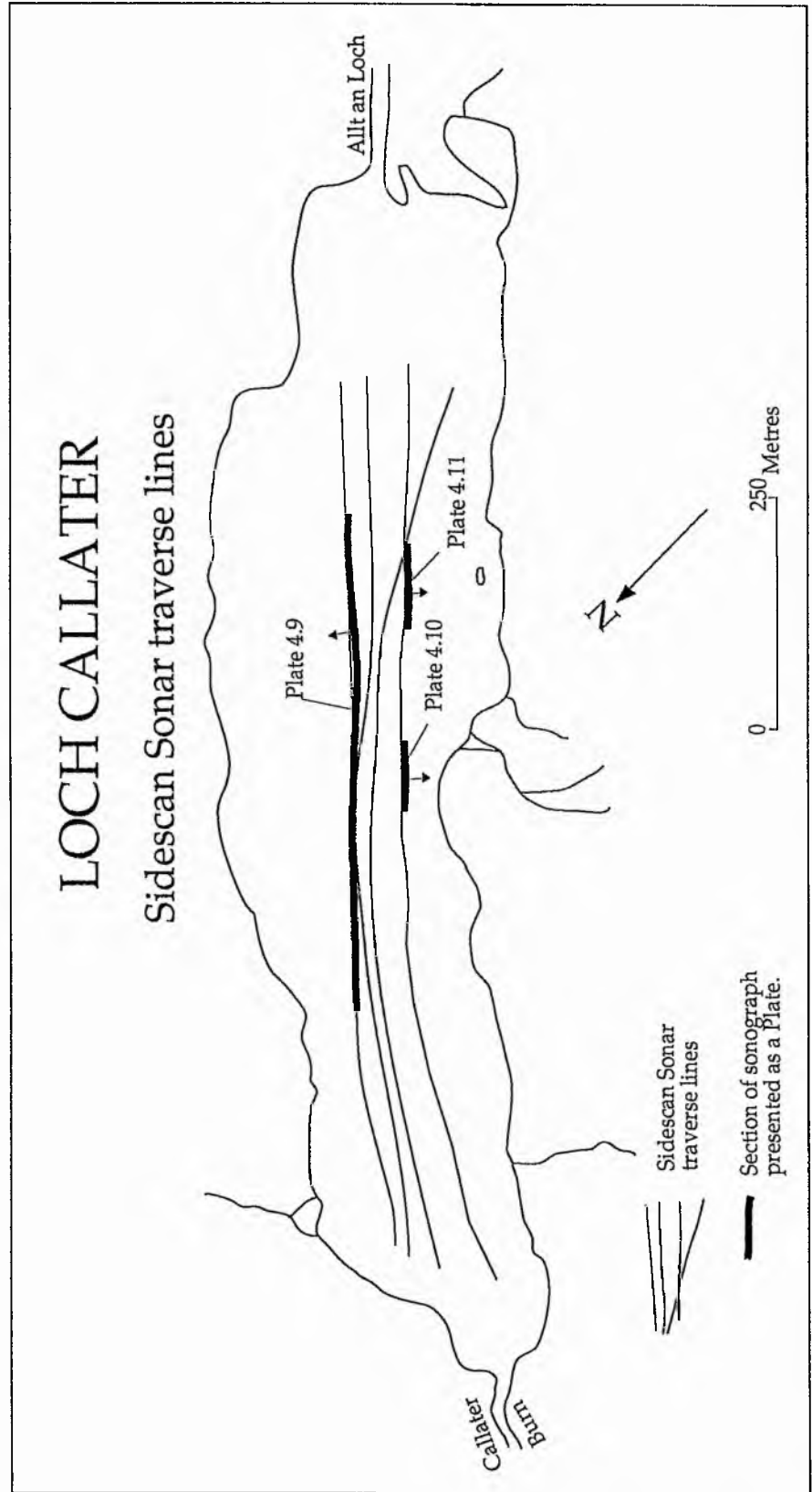


Figure 4.2
180

LOCH MUICK

Sidescan Sonar traverse lines

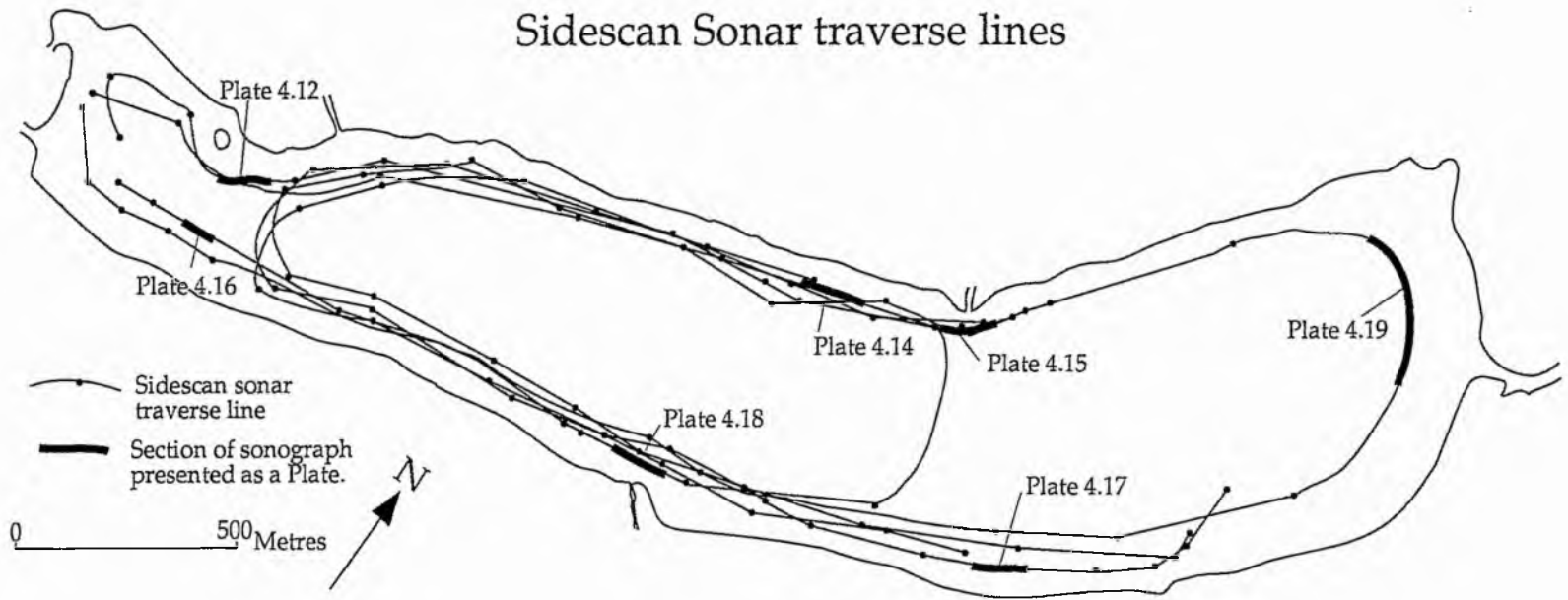


Figure 4.3
181

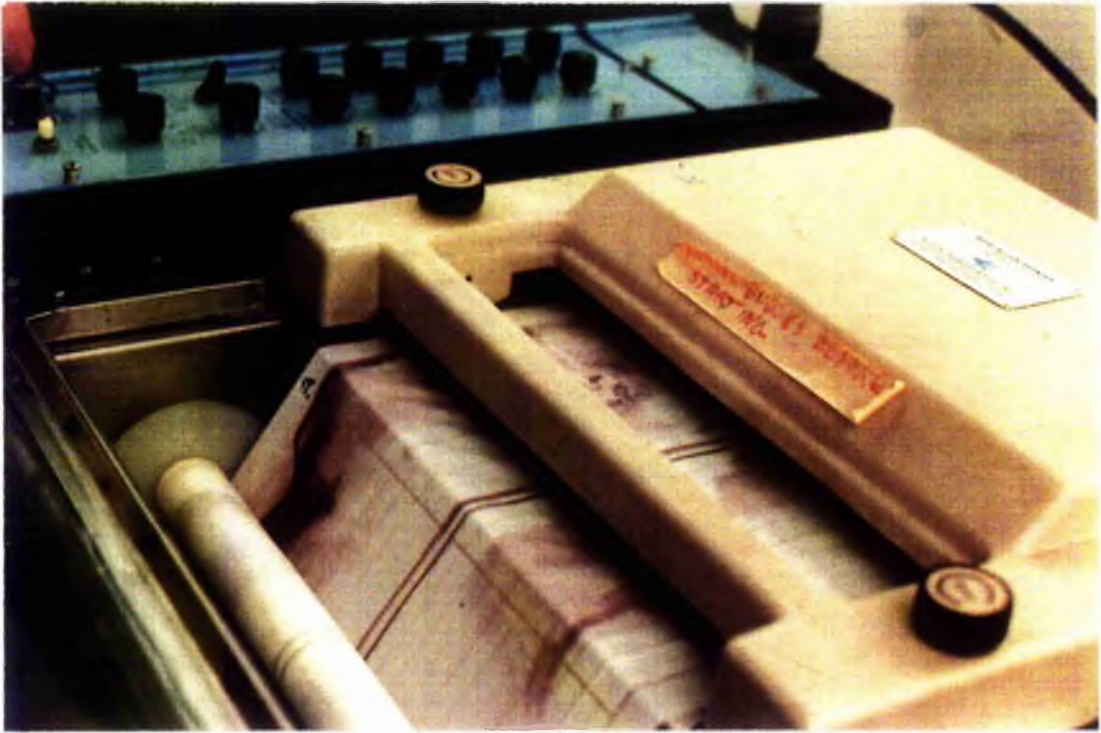


Plate 4.1 Split trace graphic output from the Klein Hydroscan (Model 401) operating on Loch Lee. Note the central trackline of the survey vessel (white), the first return of the sonic pulse (adjacent paired dark lines) and following reflections from the loch floor. In all sonographs presented the vessel track is at the bottom of the Plate. The scan is upslope towards the shore.

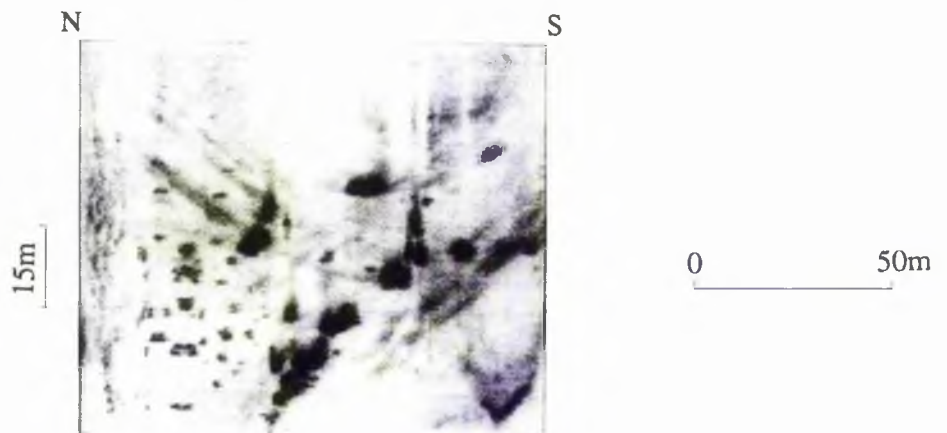


Plate 4.2 Loch Lee: Sonograph, Zone 1. Dark reflectors representing patches of aquatic weed growth distributed over the surrounding low backscatter (fine grained) loch floor.

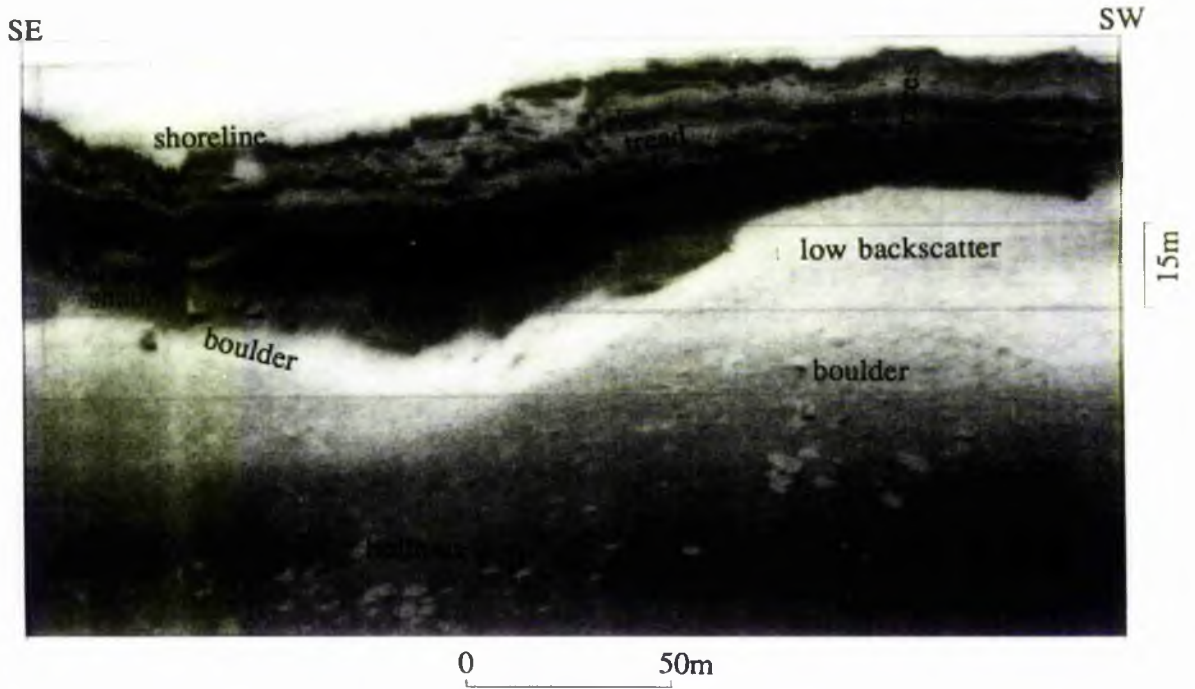


Plate 4.3 Loch Lee: Sonograph. Shore-parallel terraces in Zone 2 showing boulders lying on the most shore-proximal terrace flats. The linear distribution of the low backscatter level below the lowest shore-parallel terrace can be clearly recognised.

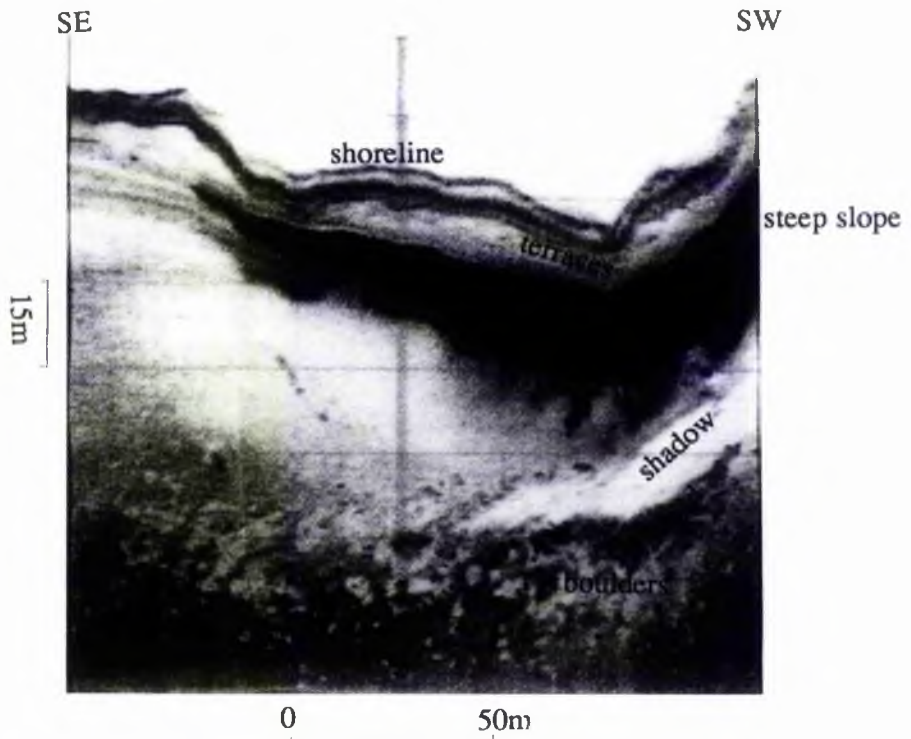


Plate 4.4 Loch Lee: Sonograph, Zone 2. Extremely steep slope angles close to the mouth of the Burn of Duchrey. In the midslope area a mound composed of boulders with a distinct acoustic shadow zone can be recognised.

NW

NE

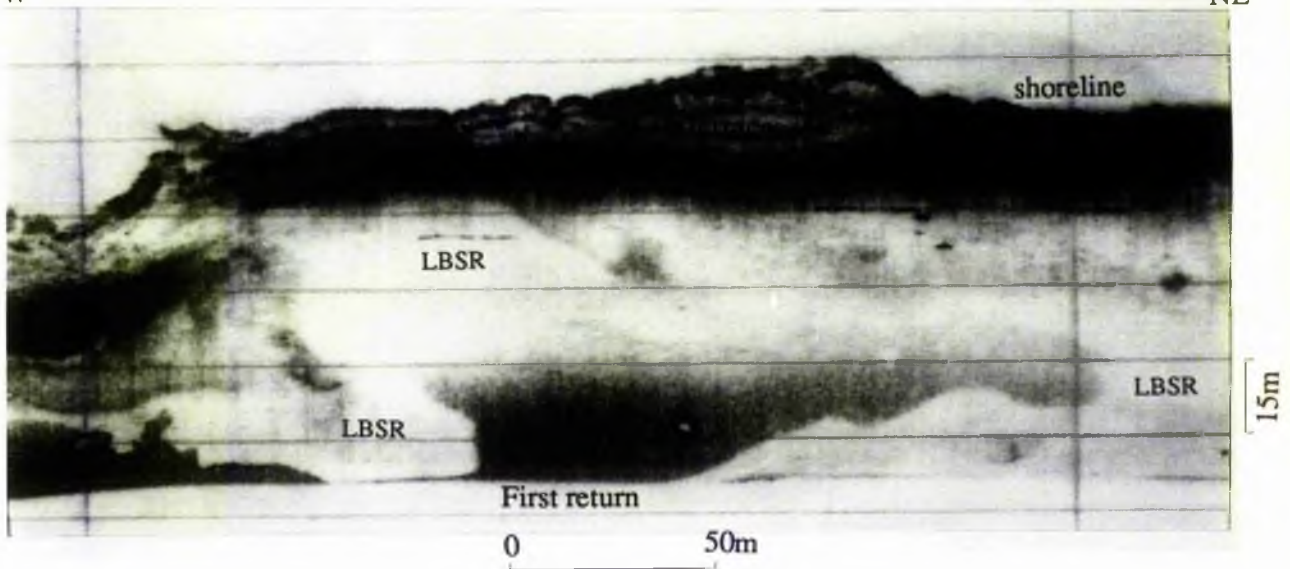


Plate 4.5 Loch Lee: Sonograph, Zone 2. Lobate distribution of the low level backscatter reflector (LBSR) on the northern slopes of Loch Lee.

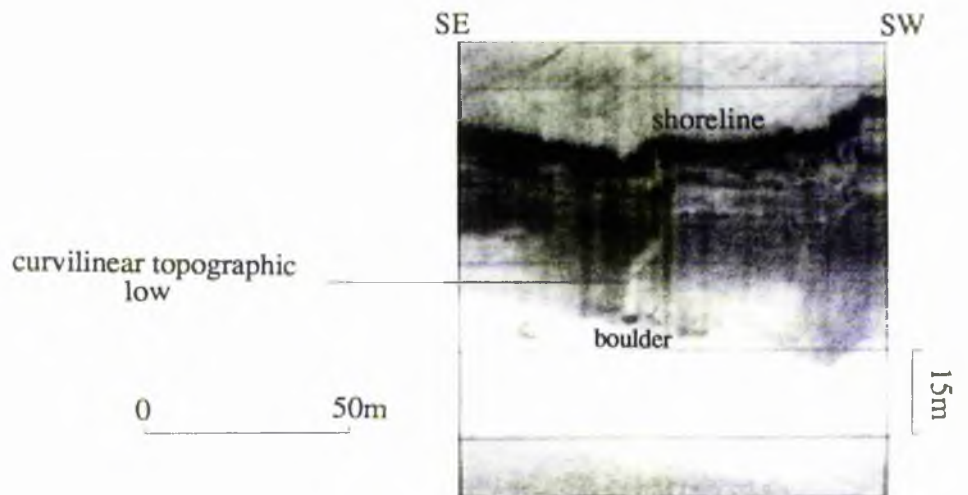


Plate 4.6 Loch Lee: Sonograph, Zone 2. Linear topographic low extending from the base of the shore-parallel terraces and terminating at a boulder.

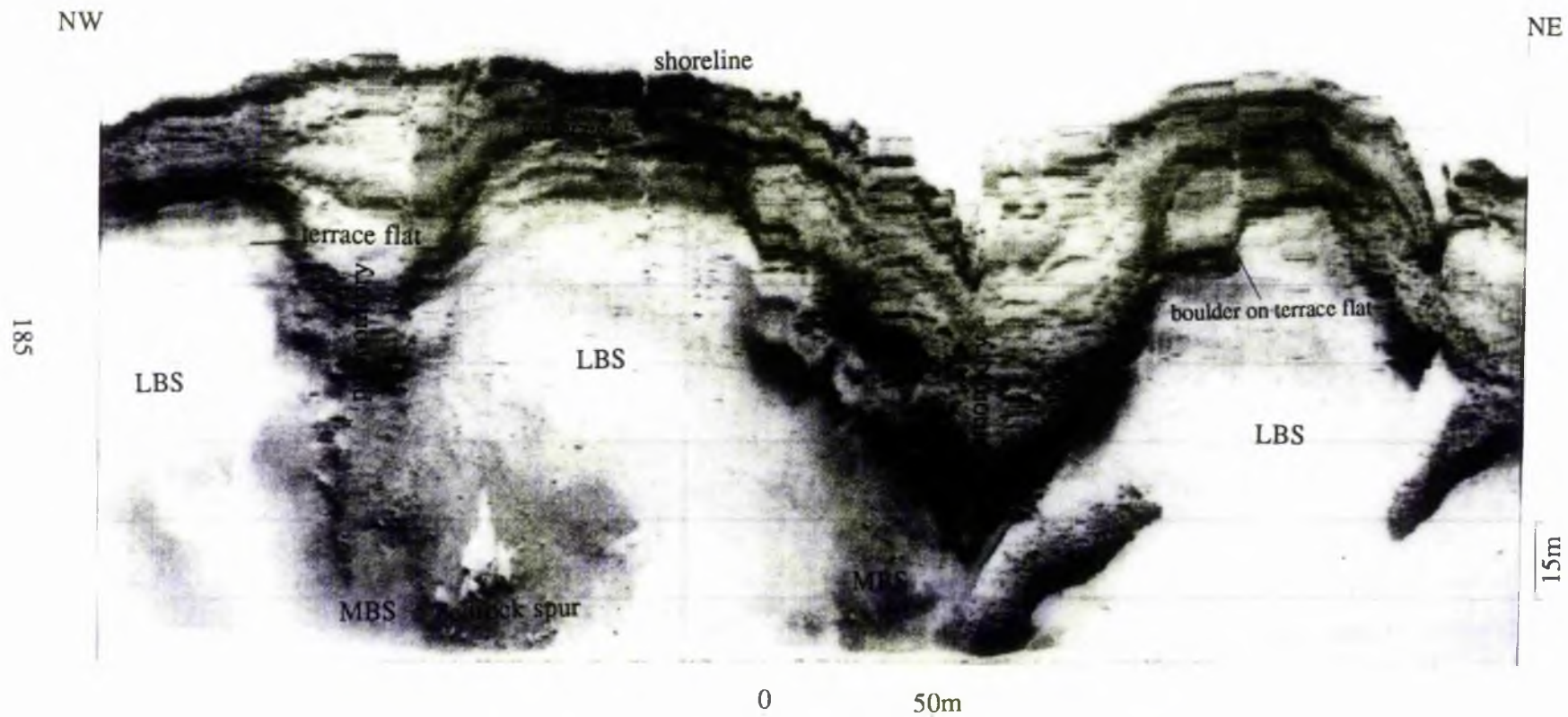


Plate 4.7 Loch Lee: Sonograph, Zone 3. Shore-parallel terraces with a maximum extent of 75m into the loch at the head of promontories. Areas of medium backscatter levels (MBS) with boulders adjoin the promontories and low backscatter levels (LBS) cover the remainder of the loch floor.

Plate 4.8 Loch Lee: Sonograph, Zone 3.
Highly reflective mound rising above the
intermediate backscatter (IBS)
intensity of the surrounding loch floor.

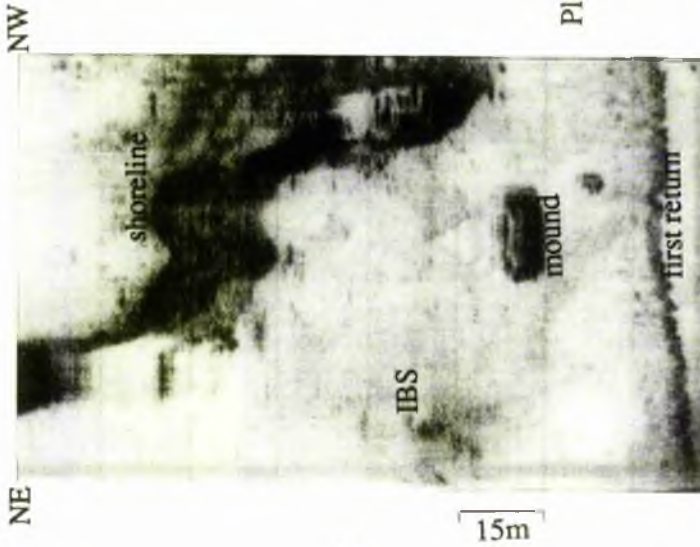
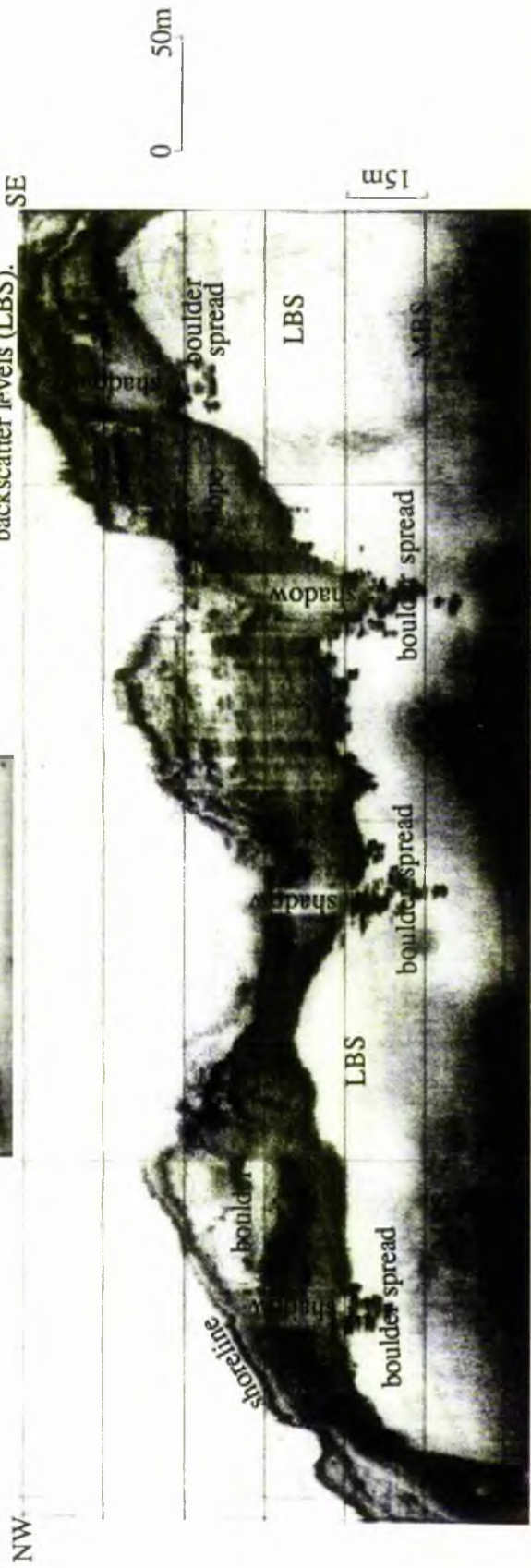


Plate 4.9 Loch Callater: Sonograph, northeastern side.
Shore-parallel terraces, boulder
spreads and relatively featureless loch floor
with areas of medium (MBS) and low
backscatter levels (LBS). SE



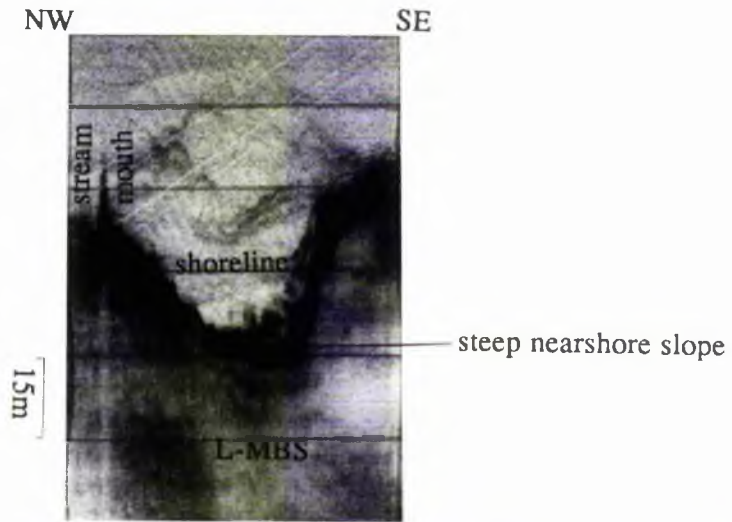


Plate 4.10 Loch Callater: Sonograph, southwestern side. First type of sonograph signatures; steep nearshore slope below which a featureless loch floor composed of low to medium backscatter level (L-MBS) reflectors forms the remainder of the floor.

0 50m

Lateral scale common to both plates

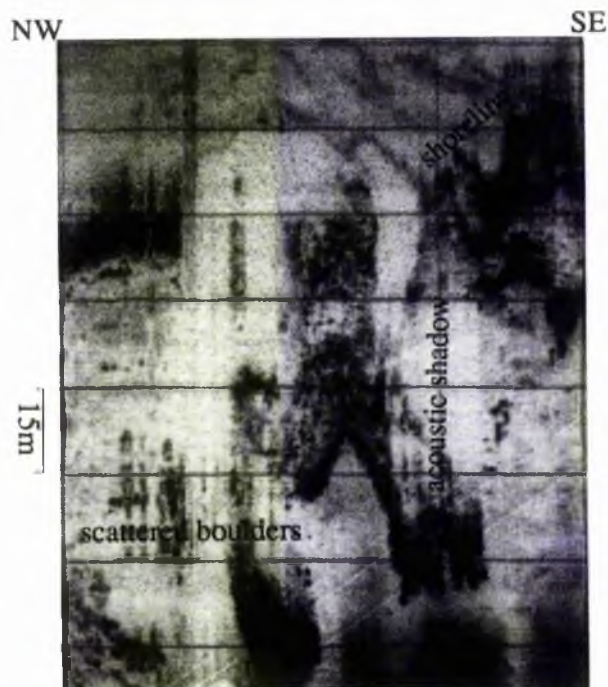


Plate 4.11 Loch Callater: Sonograph, southwestern side. Second type of sonograph signatures; gradational boundary between upper and lower slopes combined with a scattered distribution of boulders. Note the small islet.

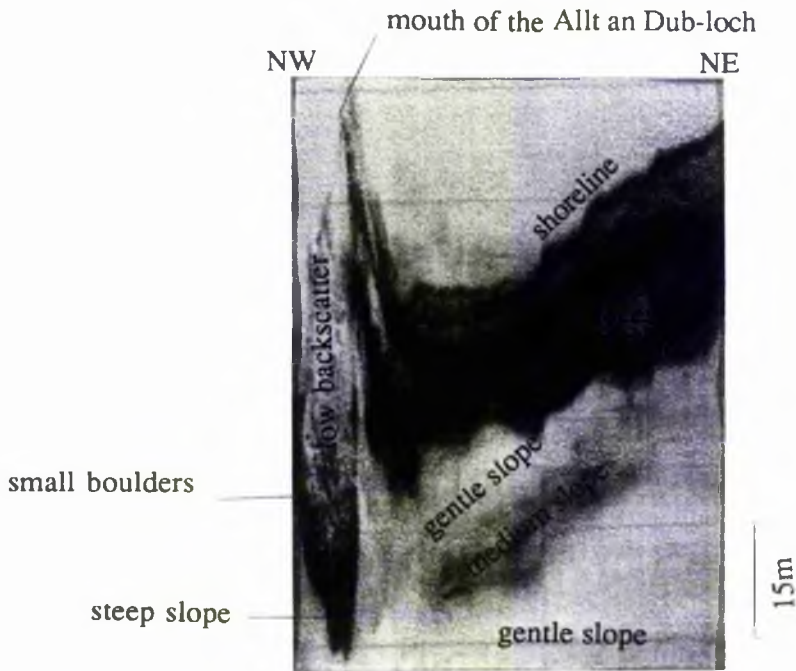


Plate 4.12 Loch Muick: Sonograph, northwestern slopes. The southerly mouth of the Allt an Dubh-loch showing nearshore low backscatter levels with a discontinuous covering of small boulders and cobbles, break in slope and lower angle slopes covered by uniform fine grained sediment. Adjacent shore-parallel terraces can be recognised to the northwest, below which a minor change in slope angle has been identified where darkening occurs on the sonograph.

0 100m

Lateral scale common to both plates

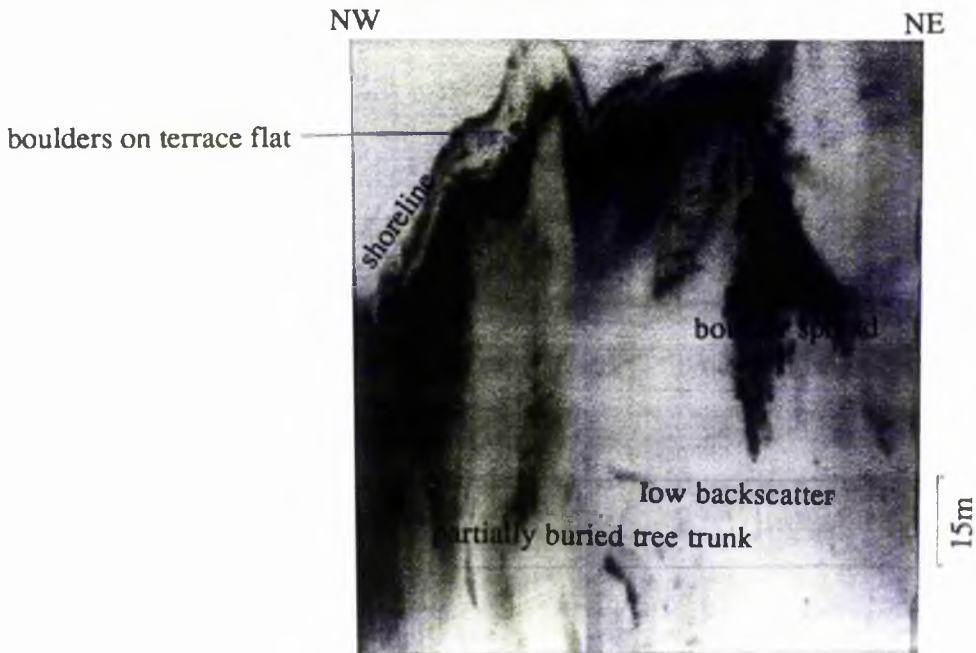


Plate 4.13 Loch Muick: Sonograph, northwestern slopes. Shore-parallel terrace with boulders lying on the terrace flat and a boulder spread on an area of low reflection backscatter close to the mouth of Lindsay's Burn.

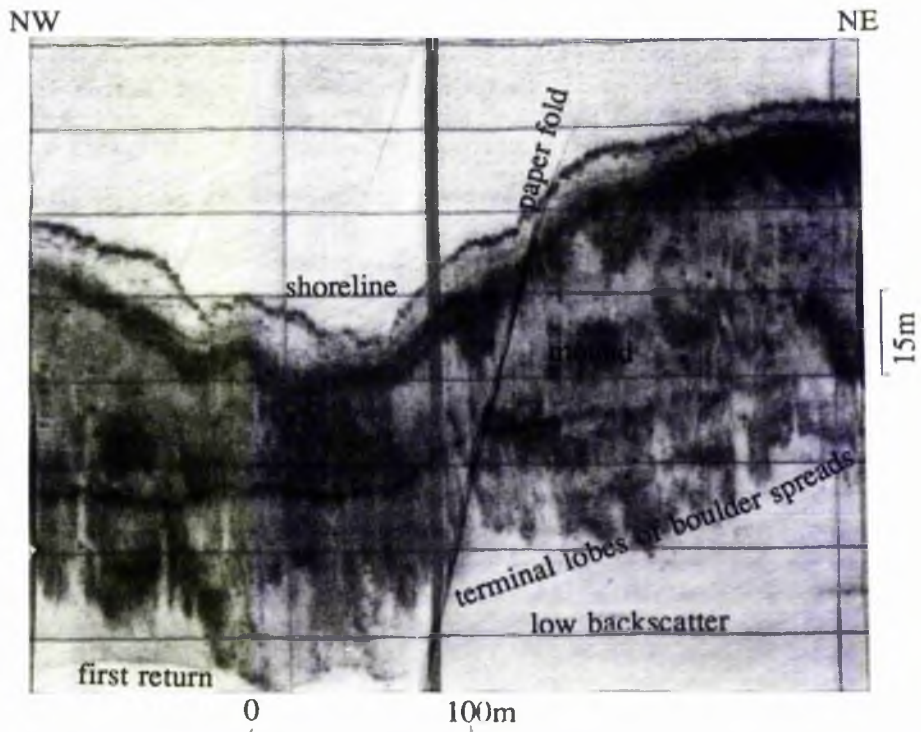


Plate 4.14 Loch Muick: Sonograph, northwestern slopes. Concentration of boulder spreads blanketing the nearshore slopes between Lindsay's Burn and the Allt an Dearg. This sonograph was recorded at a low sensitivity to highlight the topographic variation on the boulder-clad slopes. The darker line which occurs approximately half way down the slope is noise resulting from multiple reflections received by the transducer.

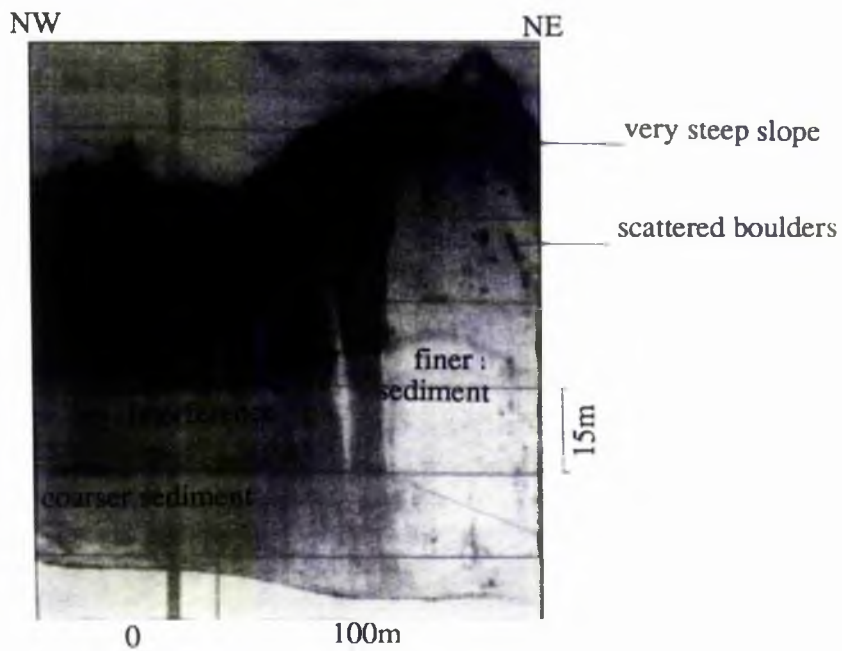


Plate 4.15 Loch Muick: Sonograph, northwestern slopes. Loch slopes close to the mouth of the Allt an Dearg showing high-low backscatter banding representing sediment size variation. The dark areas probably represent fine gravel and the lighter areas fine sand or silt.

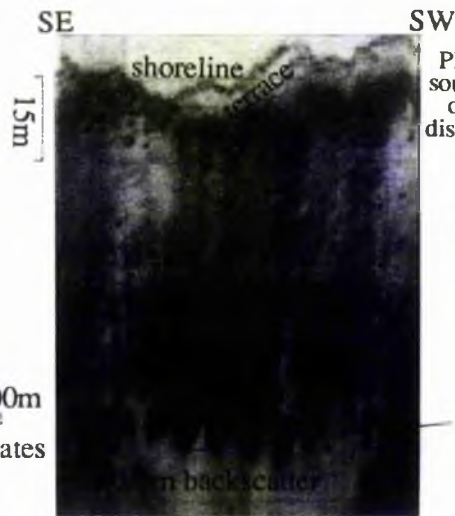


Plate 4.16 Loch Muick: Sonograph, southwestern slopes. Boulder spreads on the nearshore slopes showing distinct lobate downslope termination.

Lateral scale common to all Plates



Plate 4.17 Loch Muick: Sonograph, southwestern slopes. Cobble shoreline, shore-parallel terrace and extensive boulder spreads. White areas on the lower part of the slopes are interpreted as representing finer grained sediments not covered by boulders. The darker line running parallel to the shore is a second reflection received by the transducer.

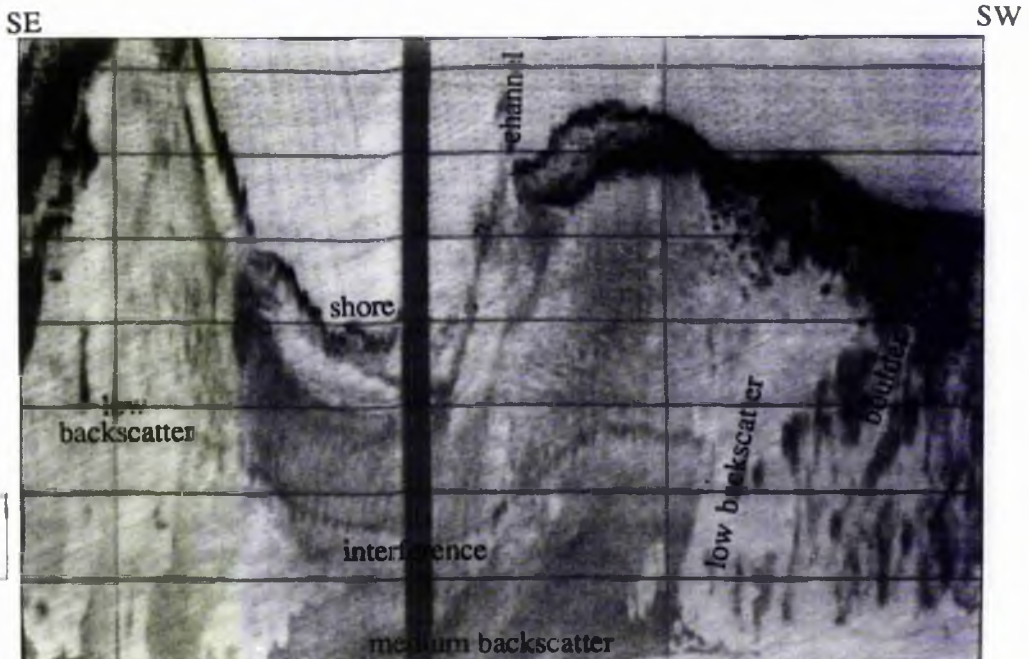


Plate 4.18 Loch Muick: Sonograph, southwestern slopes. The mouth of the Black Burn. Note the short gradational change from boulder spreads to areas of finer grained sediment (low backscatter) at the southwestern and southeastern edges of the Plate. The darker line running parallel to the shore is a second reflection received by the transducer.

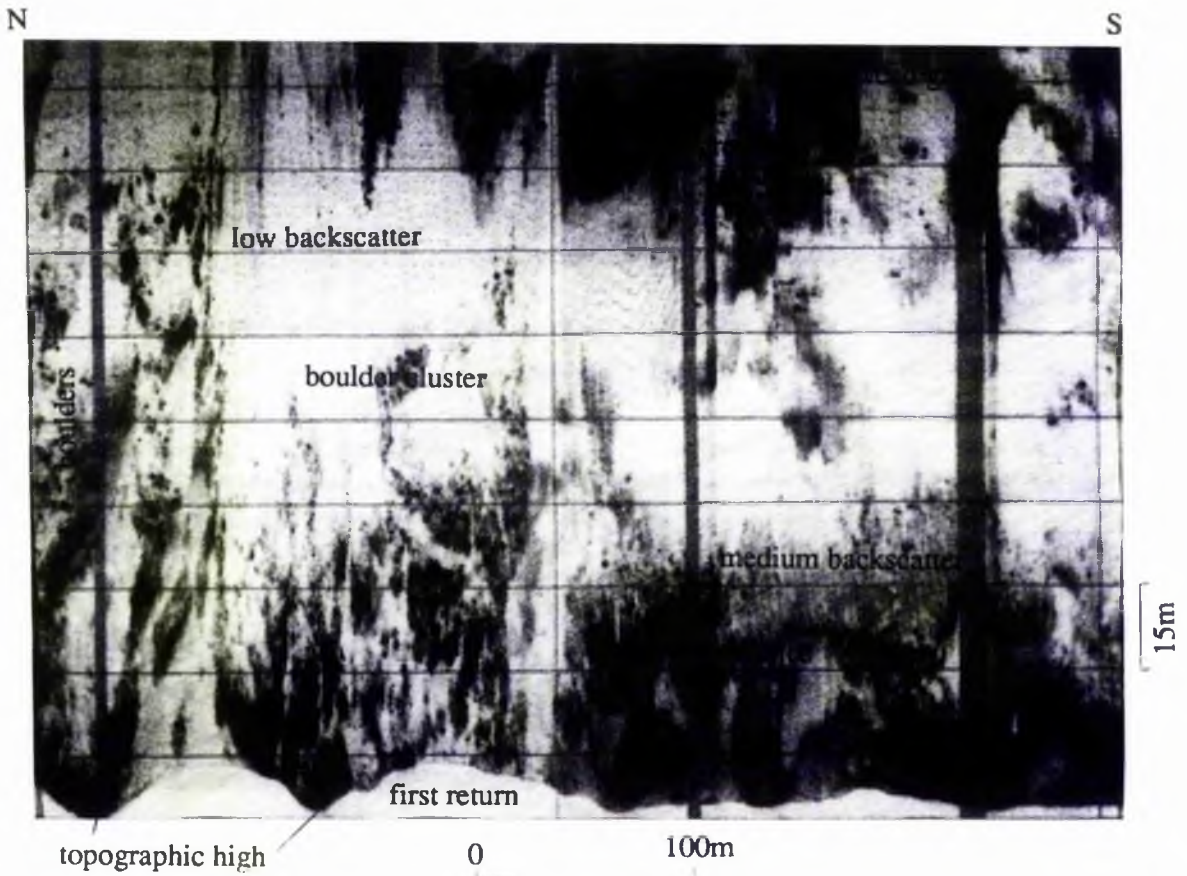


Plate 4.19 Loch Muick: Sonograph, southwestern slopes. The northeastern shore, a shallow water area (see first bottom return) with groups of boulders or rocky outcrops surrounded by areas of low to medium backscatter levels.

CHAPTER 5

SURFACE SEDIMENT ANALYSES

5.1 INTRODUCTION

In this Chapter are presented data from loch floor surface sediment sampling programmes undertaken on Lochs Lee, Callater and Muick. The methodologies of sample collection and analyses are given. The samples were analysed for total organic matter content by loss on ignition and particle size using a SediGraph 5100 analyser. Statistical analyses of the mean, median, standard deviation, and skewness of the samples from all the lochs, and kurtosis on the Loch Callater data only, were carried out. The environments of sediment deposition are determined by QDa-Md analysis. The results and interpretation of these data are reported.

5.2 SURFACE SEDIMENT ANALYSIS

5.2.1 Methodology : Aims

The surface sediment sampling and analysis programme on Lochs Lee, Callater, and Muick aimed to:-

- i) Identify sediment grain size and organic matter content variations within the three water bodies. This provides data to enable genetic interpretations to be made on the formation and distribution of subaqueous landforms identified from a) the bathymetric surveys (Chapter 2) and b) parastratigraphic interpretations of Sequence 1 (Holocene sediment) derived from subbottom reflection profiling.
- ii) Provide essential calibration for the sidescan sonar surveys (Chapter 4).
- iii) Complement echosounder (Chapter 2), subbottom profiling (Chapter 3) and coring (Chapter 6) data. This can provide information on the cause of variation in loch floor signal 'sharpness' identified during echosounder and Pinger surveys.

Surface sediment sampling programmes were carried out on the three lochs using a van Veen grab, modified by the addition of teeth (Lees et al., 1969). Radio position fixing was impossible in all three lochs due to a combination of logistical and meteorological constraints, particularly in the case of Loch Muick. Therefore, dead reckoning was used throughout. The grab was lowered over the side of the survey vessel in the open position (Plate 5.1). When the grab touched bottom, the rope was sharply hauled in, to trigger the jaws. On surfacing the contents of the sample chamber were examined through an inspection hatch at the top of the chamber (Plate 5.2) and then transferred to pre-labelled self-sealing polythene bags. The depth of sampling was obtained by measuring approximately the length of rope paid out during sample collection. The samples were stored at a temperature of 3-4° prior to analysis. A total of 47 samples of approximately 750cc of wet sediment were obtained from Loch Lee (Figure 5.1), 47 from Loch Callater (Figure 5.2) and 43 from Loch Muick (Figure 5.3).

5.2.2 Sample Analyses Methodology

5.2.2.1 Total organic matter content

Total organic matter content was quantified by loss on ignition. Subsamples of approximately 500cc were transferred to large beakers and placed in a drying oven set at 100°C for 24 hours. They were removed, allowed to cool, and gently disaggregated using a pestle and mortar. The samples were brushed through a 2mm mesh sieve and the fraction >2mm was discarded. Subsamples were separated by quartering the whole sieved sample. The subsamples were placed in labelled crucibles of known weight, weighed and heated in a muffle furnace at 550°C for one hour, following the technique of Håkanson and Jansson (1983). After heating, they were removed with tongs, placed in a desiccating chamber to cool, and reweighed. The loss in weight of the sample was calculated and converted into a percentage of the initial dried weight. The weight loss is principally due to combustion of organic substances. However, an undetermined volume of chemically bound water may be lost, from clays in particular, through evaporation at high temperature. The data obtained are presented as distribution maps (Figures 5.4, 5.13, 5.22).

5.2.2.2 Particle size analysis

Particle size analyses were undertaken using a SediGraph 5100 analyser driven by a Zenith computer. Investigations by Welch et al. (1979) have demonstrated that particle size analyses undertaken by SediGraph and the pipette method result in no significant differences, thus permitting comparisons to be made between data sets obtained by the two techniques. All stages of the analysis process, apart from loading into the mixing chamber, were carried out using menu-driven prompts. Details of the procedure are presented in Appendix A.

SediGraph analysis cannot be undertaken on samples containing organic matter. Therefore the organic-free subsamples remaining after combustion were gently brushed through a stack of sieves with 1mm, 500 μ m and 250 μ m mesh sizes. Each fraction was weighed and the weight noted. Approximately 2-3g of the >250 μ m fraction from each sample was weighed into a labelled 50ml beaker and 40ml 1% Calgon dispersing agent (used to prevent particle aggregation) was added. The beaker was then placed in an ultrasonic bath for five minutes.

Sample directories were created on the SediGraph computer to store the analysis data. Information was then inputted for each sample. Where a significant fraction in the sample was >250 μ m, the percentage of the sample submitted for SediGraph analysis was recorded in the sample data. The analysed data were automatically calculated as percentages of the entered amount. A mean density of 2.5gcm³ was used and the 'liquid properties' were set. Calgon (1%) is used in the system both for sediment disaggregation and rinsing between samples. Calibration ('collecting a baseline') of the equipment was undertaken with a sample of Calgon before sediment samples were introduced each day, and on each occasion that the reservoir of Calgon used to rinse the sampling apparatus was replaced.

Each sample was removed from the ultrasonic bath and emptied into the mixing chamber where it was kept constantly agitated by a magnetic stirrer. To ensure that all the sample was available for analysis, the beaker was flushed with Calgon. After checking, the

sample data the sample was loaded into the X-ray chamber and subjected to a high speed scan to determine particle sizes between $250\mu\text{m}$ and $0.50\mu\text{m}$. The distribution of grain sizes was presented as a log probability graph (equivalent spherical diameter/% mass finer) on screen to permit recognition of possible inconsistencies. If a distribution thought to be unusual was obtained, the sample was re-scanned to confirm the distribution. When the data had been collected they were stored on disk and printed out as log probability graphs, and also in the form of a data sheet containing information including the percentage cumulative mass finer from $250\mu\text{m}$, the percentage mass in each size interval, modal and mean diameters (see Appendix B).

Data thus obtained were then used in statistical analyses.

5.2.3 Statistical Analyses

The first statistical analyses carried out in this research were for the sediments of Loch Callater. In this case the sedimentary statistics presented by Folk and Ward (1957) (Appendix C, 1) were used. It was intended that these statistics would be used for all three lochs. However, when analysed, the samples obtained from Lochs Lee and Muick were found to contain a much higher proportion of fine grained material. Thus it was frequently impossible to obtain estimates of the 5th percentile as required by the Folk and Ward parameters. Therefore, following Asaad and McManus (1986), the sedimentary statistics devised by Inman (1952) (Appendix C, 2) were used. These statistics relate to a smaller part of the distribution curve and require particle diameter data from the 16th and 84th percentiles to calculate the mean, standard deviation and skewness of the sediment. Values for these measures were available for the majority of samples. Kurtosis could not be calculated as it requires the input of data from the 5th and 95th percentiles. Where 16th and 84th percentile data could not be obtained for a sample, statistical analysis could not be undertaken, although the median grain diameter could be determined.

QDa-Md analysis to identify the environment and mode of deposition (Buller and McManus, 1972; 1973; 1974) was carried out on all samples in an attempt to discriminate

nearshore and shallow water sediment from that deposited in deep water and to determine whether turbidite deposition has been active in the lochs. This analysis also permits comparison of surface sediment and core samples (Chapter 6).

5.3 LOCH LEE

5.3.1 Total organic matter

The percentage of total organic matter, determined by weight loss on ignition, in the surface sediments of Loch Lee has a range of 1.2% to 86.4% (Appendix D). The distribution of organic matter within the water body is complex (Figure 5.4). Large areas with low (10-20%) organic matter levels occur at the northeastern and southwestern ends of the loch, broadly coincident with the geomorphic zones identified in Chapter 2. However, a small, isolated area, with an organic matter content rising to 45.3%, occurs in Zone 1, aligned with the mouth of the Drain. The central area of the loch is characterised by sediments with more than 50% organic matter, however, the values range between 4.6% on the northern slopes, to two sites where organic matter exceeds 85% of the total sample. The latter occur on the southern slopes close to the mouth of the Burn of Duchrey and near to the centre of the trough at the northeastern end of the Central Trough Zone. At both these sites it was noted at the time of sampling that the sediments were composed of finely comminuted vegetation, principally grasses and sedges. Repeated sampling at these highly organic sites produced no variation in sediment type, therefore the samples were accepted as representative of the surface sediments. The southwestern end of this central zone exhibits a sharp gradient to low values in the shallow part of the loch. More complex distributions showing a broad downslope increase of organic matter content to 50%-60% of the total sample characterise the remainder of this part of Loch Lee (Figure 5.4).

5.3.2 Distribution of surface sediments

Graphs showing the grain size distribution of all surface sediments analysed were plotted using a cumulative probability scale. (e.g. Figures 5.7, 5.15, 5.24)

5.3.3 General sediment texture

Surface sediment textures of <2mm sieved samples from Lochs Lee, Callater and Muick were derived from the ternary diagram given by Folk (1974) (Figure 5.5). Data from Loch Lee are presented in Appendix D, and the distribution of the sand, silt, and clay size fractions is shown in Figure 5.6. It should be emphasized that samples composed predominantly of clastic material >2mm were not analysed. This accounts for the area of no data at the northeastern end of the loch.

A complex distribution of sediment textures is present in Loch Lee. In general, sandy material occurs close to the mouths of streams and around the shores of the loch, excepting two small areas of sandy silt and sandy mud which occur in the centre of the loch. Finer grained mud and silt is distributed throughout the central trough extending from the deepest point to shore-proximal zones on both northern and southern shores. A representative suite of cumulative grain size frequency curves from samples collected along the southwest-northeast axis of Loch Lee and the corresponding weight-diameter frequency graphs is given in Figures 5.7 and 5.8. The latter reveal that many of the sediments show symmetrical distributions, that there is some bimodality in the southwestern deposits, and that strong fine skewness develops towards the centre of the loch.

5.3.4 Mean grain size (M_{ϕ})

The distribution of mean grain size of Loch Lee surface sediments (Figure 5.9) shows a general decrease in grain size away from the shores of the loch and ranges between 2.44ϕ and 10.34ϕ (Appendix E). The central, deep water zone, which comprises the largest area of the loch, is covered by fine grained sediment in the range 6ϕ to 10ϕ . The exception to this trend occurs where one of the samples composed of >80% organic matter

occurs close to the mouth of the Burn of Duchrey. The inorganic content of this sample comprises sandy mud (Folk 1974). The coarsest sediment occurs in the southwestern shallows zone (1), on the slope close to the mouth of the Water of Lee. Sediment adjacent to the latter has a mean diameter of 3ϕ to 5ϕ . Zone 3, the northeastern shallows, is covered by sediment with a mean diameter in the range 4ϕ to 7ϕ .

5.3.5 Standard Deviation/sorting (σ_ϕ)

The spatial variation of surface sediment sorting in Loch Lee is given in Figure 5.10 and descriptions of the degree of sorting follow those given by Folk (1974). Sorting ranges from 0.58ϕ (moderately sorted) in the muds near to the mouth of the unnamed stream on the northern slopes to 6.58ϕ (extremely poorly sorted) in a small area of sandy silts close to the pumping station at the northeastern end of the loch. The data indicate that all the sediment in Loch Lee is relatively poorly sorted when compared to studies of other Scottish lochs (e.g. Duck, 1986; Asaad and McManus, 1986). A lobe of very poorly sorted sediment ($\sigma_\phi = >3\phi$) extends from the northern slopes towards the central trough. The area of least sorted sediment in this lobe coincides with the occurrence of sandy silt and sandy mud. Very poorly sorted sandy mud also occurs close to the mouth of the Burn of Duchrey. The distribution of sediment sorting in Loch Lee is irregular; both the poorest sorted and best sorted sediments occur around the shores of the Loch. However, the central deep water trough, composed of mud and silt, is covered by poorly sorted material with standard deviations ranging between 1ϕ and 2ϕ .

5.3.6 Skewness (α_ϕ)

Skewness quantifies the departure of the mode from the median. The data are presented as a distribution map (Figure 5.11). Skewness values range between $+0.69$ (very positively skewed) and -0.51 (very negatively skewed). The majority of samples (37 from a total of 47 samples, 78%) fall within the nearly symmetrical and positively skewed ranges. The most positively skewed sediments occur in the northeastern shallows close to

the weir. Further small areas in Zone 2 close to the mouth of the Burn of Duchrey and in Zone 1, the southwestern shallows, adjacent to the inflow of the Water of Lee and the Drain. The majority of negatively skewed and very negatively skewed samples are distributed along the long axis of the loch, in Zone 2. A small area of very negatively skewed sediment also occurs on the northern shore in Zone 2.

5.3.7 QDa-Md Analysis

In all cases throughout this thesis, for the purposes of QDa-Md analysis (Buller and McManus (1972), Appendix C), the ϕ based sedimentary statistics of Inman (1952) and Folk and Ward (1957) have been converted to metric (mm) equivalents using the table presented by Page (1955). The QDa-Md data for Loch Lee (Appendix F) were plotted on double logarithmic graph paper. Samples were differentiated according to whether they were obtained close to the shore, river mouths, or in the middle sections of traverses. Selected environmental trend envelopes (quiet water deposition, fluxoturbidites - deposition of fine grained material from suspension - steep gradient turbidites, and fluviatile) identified by Buller and McManus (1972, 1973) were superimposed on the plotted data, which are presented as Figure 5.12. The majority of samples (43 from a total sample of 47, 91%) plot within the quiet water and fluxoturbidite envelopes and where these envelopes overlap with those of steep gradient turbidites and fluviatile deposition. Of the remaining four samples, two fall outside the envelopes and two plot within the steep gradient turbidite and fluviatile envelopes, which have almost coincident positions. Two of the three samples obtained close to the mouths of influent streams plot within the overlapping area of the fluviatile/turbidite/quiet water envelopes. The remaining sample plots within the fluxoturbidite envelope.

5.4 LOCH CALLATER

5.4.1 Total organic matter

The percentage of total organic matter in the surface sediments of Loch Callater ranges between 6.1% and 54.8% (see Appendix G). Over most of the loch floor, however, it exceeds 30%. The highest concentrations (>50%) occur in the areas of deepest water (Figure 5.13). The organic content of the sediment decreases towards the inlet and outlet with the lowest concentrations characterising the shallow water deposits close to the inlet of the Allt an Loch.

5.4.2 General sediment texture

The surface sediment of Loch Callater is predominantly composed of silt (Figure 5.14, Appendix G). A gradational boundary through sandy silt to silty sand occurs in the shallow water at the southeastern end of the loch, where the Allt an Loch is entrant. A small area of sandy silt occurs at the northwestern end. A representative selection of cumulative grain size frequency curves and their corresponding weight/grain diameter frequency graphs from samples obtained along the northwest to southeast axis of Loch Callater are presented in Figures 5.15 and 5.16. The latter indicates that, without exception, the sediments along the axis of the loch are skewed towards coarser grain sizes. The peakedness of the distributions increases towards the southeast.

5.4.3 Mean grain size (M_z)

Mean grain size in Loch Callater ranges between 0.97ϕ and 7.25ϕ (Appendix H). The loch floor is predominantly covered by sediments with a mean grain size in the range 5ϕ to 7ϕ (Figure 5.17). The area covered by sediment with a mean diameter of 5ϕ at the northwestern end of the loch coincides with the ridge separating the two basins identified in Chapter 2, section 2.5.3. The coarsest sediments occur at the southeastern end of the loch, in the shallow water adjoining the mouth of the Allt an Loch, close to the shore. A decrease in grain size from $<1\phi$ to $>5\phi$ over approximately 200m occurs westwards into deeper water from the mouth of the stream.

5.4.4 Standard deviation / sorting (σ)

The sorting of Loch Callater surface sediment (Appendix H) ranges between 0.83ϕ (moderately sorted) and 2.58ϕ (very poorly sorted). The largest part of the loch floor is covered by poorly sorted sediment with a standard deviation of 1ϕ to 1.5ϕ from the mean (Figure 5.18). Small areas of very poorly sorted sediment occur close to the shores at the northwestern and southeastern ends of the loch and in the central trough. The best sorted sediments occur in the nearshore zone.

5.4.5 Skewness (SK_I)

The distribution of this measure in Loch Callater is given in Figure 5.19. The sediment ranges from very positively skewed sediment (+0.73) to very negatively skewed (-0.44). However, 60% of the samples obtained fall within the negative skewed range, none in the positive skewed, and 6% in the very positively skewed range (Appendix H). The marginal nearshore sediments have predominantly nearly symmetrical distributions, with one exception where very positively skewed sediment occurs. The only other occurrence of very positively skewed sediment is in the centre of the loch, on the ridge dividing the two basins. Very negatively skewed sediment occurs in the shallows at the southeastern extremity of the loch and in three small areas on the marginal slopes.

5.4.6 Kurtosis (K_G)

Kurtosis measures the 'peakedness' of a grain size distribution; the ratio between the sorting in the 'tails' of the curve and that in the centre. A platykurtic distribution represents a 'flat' curve where the tails are better sorted than the centre of the curve, and commonly occurs in polymodal deposits (Folk, 1974; Ashley, 1978). A leptokurtic, peaked, distribution results from better sorting in the centre of the curve than in the tails, characteristic of unimodal sediments (Folk, 1974; Ashley, 1978). The surface sediment of Loch Callater has a range of 0.67 (platykurtic) on the northwestern shore to 1.87 (very leptokurtic) close to the inflow of the Allt an Loch (see Figure 5.20). Sediments with a

mesokurtic (normal Gaussian) distribution cover the largest area of the loch floor. However, sediments with a leptokurtic distribution occur around the shores and in association with the very leptokurtic distributions in a broadly linear spread northwest of the mouth of the Allt an Loch. Platykurtic sediment distributions occur in the deep water area, at one point on the southern shore, and in the northwestern basin.

5.4.7 QDa-Md Analysis

The quartile statistics for Loch Callater surface samples (Appendix I) plotted as in section 5.3.7 above are presented in Figure 5.21. The majority of samples (42/47, 89%) fall within the fluxoturbidite (deposition of fine grained material from suspension) envelope, and within the overlapping areas of the quiet water, steep gradient turbidite, and fluvial envelopes. Three samples collected in the central section of traverses plot within the steep gradient turbidite envelope only. One sample, obtained close to the mouth of the Allt an Loch, plots in the fluvial envelope, and three (two close to the shore and one close to the mouth of the main inflow) occur within the area of overlap between the fluvial and steep gradient turbidite depositional environments. Samples obtained from the start and end of traverses predominantly fall within the quiet water and fluxoturbidite envelopes. The majority (75%) of samples obtained close to the inflow of streams fall within the fluvial envelope.

5.5 LOCH MUICK

5.5.1 Total organic matter

The percentage total organic matter of the surface sediments of Loch Muick ranges from 2% to 68.8% (Appendix J). Most of the sediments from the central section of the loch floor contain >50% organic matter. Low concentrations of organic matter occur at the western and northeastern extremities of the loch and close to the island on the northern

shore (Figure 5.22). The highest organic matter content occurs in the central, deepest area of the main basin. The organic content of nearshore sediment is unknown where samples could not be obtained in sections of the loch open to the influence of the wind.

5.5.2 General sediment texture

The floor of Loch Muick is dominated by sediment composed of mud (Figure 5.23). Sandy sediment (sandy mud and sandy silt) is concentrated in the nearshore environment, in the northwestern basin of the loch, and surrounding the outlet of the River Muick. Clay also occurs at one point on the nearshore northern slope. Silt has a limited distribution, restricted to two small areas occurring along the longitudinal axis of the loch. Representative cumulative frequency curves and the corresponding distribution of weight by grain diameter graphs distributed along this axis are given in Figures 5.24 and 5.25. The latter indicate that the majority of sediments are skewed towards coarser grain sizes, although in the deep, easternmost sections, symmetrical distributions are present.

5.5.3 Mean grain size (M_{ϕ})

Mean grain size in Loch Muick ranges between 9.24ϕ and 5.14ϕ (Appendix K). The loch floor is, however, predominantly covered by sediment with a mean grain size of 6ϕ to 8ϕ . Generally, the coarsest sediments are concentrated on the nearshore slopes and finer sediments occur in the deeper areas of the trough (Figure 5.26). Two areas of fine grained ($>9\phi$) material occur at the northwestern end of the main trough, one on the nearshore slope and one near to the middle of the trough.

5.5.4 Standard Deviation/sorting (σ_{ϕ})

The distribution of sorting of Loch Muick surface sediments is given in Figure 5.27. Sorting ranges between 4.82ϕ (extremely poorly sorted) and 0.68ϕ (moderately well sorted) (Appendix K). At most sites, including nearshore and deep water areas, the standard

deviation lies in the range 2σ to 3σ . Both the best and poorest sorted samples were obtained close to the loch shores, excepting one extremely poorly sorted sample collected in the centre of the loch, at the eastern end.

5.5.5 Skewness (α_ϕ)

Most of the loch floor (83%) is covered with sediments that are negatively skewed (-0.1 to -0.3) or nearly symmetrical (-0.1 to 0.1) (Figure 5.28, Appendix K). Skewness values range from -0.58 (very negatively skewed) to +0.28 (positively skewed). Very negatively skewed sediments occur mainly around the shores of the loch, in the small northwestern basin, and one small area occurs in the centre of the main trough. Positively skewed sediment occurs at one locality only, in the main basin, coincident with water depths in excess of 60m.

5.5.6 QDa-Md Analysis

The QDa Md data for the surface sediment of Loch Muick (Appendix L) were plotted and presented using the method given in section 5.3.7 above (Figure 5.29). The majority of samples (90%) fall within the quiet water and fluxoturbidite envelopes, 6% (3 samples) plot in the overlapping area of steep gradient turbidite and fluvial deposition and one sample falls just outside the quiet water envelope.

5.6 DISCUSSION

5.6.1 Loch Lee

The surface sediments of Loch Lee are highly organic, comprising a maximum of 85.4% of the total sample. This value is significantly higher than any reported from any other Scottish water body yet surveyed; e.g. Loch Lomond 23% (Slack, 1954); Loch Tummel 29.8% (Duck, 1986); Loch Earn 25% (Duck, 1987) and nine lowland reservoirs $\leq 25.5\%$ (Duck and McManus, 1987). This phenomenon could result from one or a

combination of factors including incomplete drying of the sample prior to ignition, significant losses of chemically bound water (see section 5.2.2.1 above), a high allogenic and/or authigenic organic input to the loch masking the minerogenic input, or a low minerogenic input. It is believed that experimental error was not the cause and that a combination of the latter three factors is the most probable explanation.

Correlation (Pearson's Product Moment) between the total organic content, water depth and sediment composition of the surface sediments was carried out using the Minitab program for the Apple Macintosh P.C. The data obtained are presented in Table 5.1.

Table 5.1

Loch Lee

Pearson's Product Moment Correlation Coefficient for surface sediment variables.

	Total organic matter (%)	Depth (m)
Depth (m)	0.491	
Clay (%)	0.310	0.430
Silt (%)	0.638	0.344
Sand (%)	-0.778	-0.621

At the 1% confidence level a correlation between any two variables is significant at +/- 0.376 for 47 samples. Thus it may be seen that there is a strong positive correlation between total organic matter, depth and silt content and a very strong (0.2% confidence level) negative correlation between the distribution of organic matter and sand sized particles. These data suggest therefore that sedimentation of organic matter occurs in deep water where silt sized particles are also deposited.

Correlation between particle size and depth shows that there is a positive correlation significant at the 1% confidence level between clay sized particles and depth. Silt sized

particles have a positive correlation with depth significant at the 2% confidence level. Sand sized particles show a very strong (significant at the 0.2% confidence level) negative correlation with depth. These correlations suggest that wave action is responsible for the removal of finer silt and clay sized particles from the nearshore environment to deeper water where deposition of fine particles occurs (see Chapter 7, Discussion for further details).

The surface sediment of Loch Lee is relatively poorly sorted when compared with data obtained from other lochs. Asaad and McManus (1986) report a maximum standard deviation value of 2.6ϕ in Loch Lubnaig, and in Loch Tummel a maximum value of 2ϕ was obtained (Duck, 1986). The floor of Loch Lee is covered by poorly sorted material, much of which falls within the range of extremely poorly sorted sediment within the classification of Folk (1974). The irregular distribution of sorting and the skewness suggest that the anthropogenic input during reservoir construction, impoundment and subsequent maintenance including periods of partial draw-down has significantly affected the characteristics of the surface sediments. Evidence in support of this hypothesis is found in the least sorted (extremely poorly sorted) material which occurs in proximity to the pumping station. Loch Tummel, which has also been dammed to form part of the North of Scotland Hydro-Electric Scheme, exhibits similar, more minor irregularities in the distribution of sorting. However, the sampling density in Loch Tummel (≤ 20 samples/ 1km^2) was considerably lower than that in Loch Lee (47 samples/ 0.9km^2), preventing direct comparison.

The bed of Loch Lee is covered by the least sorted sediment encountered in all three lochs in this study. The distribution of sorting of surface sediments broadly correlates with that of skewness. Areas of least sorted sediment are coincident with very positively skewed sediments; sediments showing greater sorting are negatively to very negatively skewed.

QDa-Md analysis confirms that the majority of samples obtained were deposited in quiet water, by settling through the water column. However, there is a large sample overlap with the steep gradient turbidite and fluvial environmental trend envelopes. In particular,

the extremely poorly sorted sediment close to the pumping station and a sample obtained from the northern slope of the central trough plot within these two envelopes (i.e. sediments deposited from flowing currents). The latter sample does not correspond with any distinct mound form identified on the bathymetric chart (Figure 2.2, section 2.4.2.2) or sonograph (section 4.4.2.2). However, subbottom profiling has identified areas of 'chaotic total' internal reflectors within the surface sediment (Sequence 1, Facies 1.1, section 3.5.2.1.1) which do not exhibit distinct surface forms. The majority of samples obtained close to the mouths of influent streams plot within the fluvial envelope. However, samples collected closest to the shore in all three lochs show no distinct, separate distribution, plotting in the same areas as samples obtained from deeper water. It is suggested that these samples do not plot within the beach environmental trend envelope (not included on Figures 5.12, 5.21 and 5.29 for clarity) as they were obtained from the transitional zone between nearshore and quiet water deposits, in a minimum water depth of approximately 2m, in Loch Lee, 1.5m in Loch Callater and 3m in Loch Muick.

5.6.2 Loch Callater

The surface sediment sampled on the bed of Loch Callater is characterised by the lowest concentration of organic matter of all three lochs investigated in this thesis. However, the maximum (54.8%) and average (>30%) values are still significantly above those obtained in previous surveys (see section 5.6.1 above). It is suggested that the causes of the high organic matter content of the surface sediment are the same as those given in section 5.6.1 above. The majority of the lowland area of the Loch Callater catchment, which is extensively used for recreational purposes, is covered by peat. Localised erosion, particularly adjoining footpaths, has been observed, and is believed to provide the principal source of organic matter which is then subsequently transported to the loch and deposited. Correlation coefficients between surface sediment variables were calculated and the data obtained are presented in Table 5.2.

Table 5.2

Loch Callater

Pearson's Product Moment Correlation Coefficient for surface sediment variables

	Total Organic Matter (%)	Depth (m)
Depth (m)	0.512	
Clay (%)	0.178	0.343
Silt (%)	0.744	0.233
Sand (%)	-0.809	-0.463

For a sample population where $n=47$ a value of ± 0.376 is significant at the 1% confidence level. The percentage of total organic matter has a strong positive correlation, at the 0.2% confidence level, with depth, and an equally significant negative correlation with the percentage sand content in the sediment. The positive correlation, significant at the 0.2% confidence level, between total organic matter and silt sized particles suggests that, in common with Lochs Lee and Muick, the principal depocentres for organic matter and silt sized particles are coincident. This may be due to the settling velocity of the majority of organic matter particles being coincident with that of silt.

The correlation data indicate that depth is a significant factor in determining the distribution of particle size within Loch Callater. Silt and clay sized particles have positive correlations with depth (significant at the 10% and 2% confidence levels respectively). The most significant, negative correlation occurs between the distribution of sand and water depth. These findings are believed to reflect the influence of wave action on the nearshore environment, removing fine sediment to deeper water where deposition occurs. This aspect is dealt with more fully in Chapter 7.

A comparative analysis of skewness values obtained using the Folk and Ward (1957) parameter (used solely in the analysis of Loch Callater sediments), and that of

Inman (1952), which was used in the analysis of data from Lochs Lee and Muick, was carried out in order to determine the comparability of the two types of data set. The analysis showed a maximum difference between values obtained of 0.28, with a mean difference of 5% (Appendix M). Thus it is assumed that these data sets are comparable.

The sediments coating the floor of Loch Callater are typically poorly sorted, but constitute the best sorted of the three lochs in this study. The maximum value obtained (2.58ϕ) is comparable with data obtained from other Scottish lochs (see section 5.6.1 above). The best and least sorted sediment occurs in the nearshore zone. Much of the loch shore is composed of small (approximately 0.5m high) cliffs cut into glacial diamict. The vertical form and lack of vegetation on these cliffs is evidence of contemporary erosion. Thus it is believed that the poor sorting in nearshore sediments is due to recent deposition by bank collapse. Poorly sorted material in the centre of the loch is typical of fine grained lacustrine sedimentation (Thomas et al., 1972; Vernet et al., 1972; Duck, 1986). Skewness and kurtosis data indicate that the majority of the surface sediment has a normal distribution.

5.6.3 Loch Muick

The floor of Loch Muick is covered by sediment with a high (maximum 68.8%) organic matter content. Within this study Loch Muick ranks second after Loch Lee in this measure, but is considerably higher than values obtained from other Scottish lochs (see section 5.6.1 above). In common with Loch Callater, the extensively peat-covered catchment of Loch Muick is used for recreational activity throughout the year, resulting in visible, anthropogenically-induced erosion of the peat, which may then be transported and deposited in the water body.

Correlation between surface sediment variables (Table 5.3) indicates that strong correlations occur between the variables. For a sample population where $n=43$ the 1% confidence level of correlation occurs at ± 0.393 .

Table 5.3

Loch Muick

Pearson's Product Moment Correlation Coefficient for surface sediment variables

	Total organic matter (%)	Depth (m)
Depth (m)	0.680	
Clay (%)	0.574	0.340
Silt (%)	-0.114	0.094
Sand (%)	-0.622	-0.536

Thus there is a strong positive correlation between total organic matter content and depth, significant at the 0.2% confidence level. This degree of confidence is also apparent in the relationship between the distribution of clay sized particles and the percentage of organic matter present. This correlation is unique within the data set of this thesis and data reported from other lochs (e.g. Loch Tummel, Duck, 1986). It is suggested that this correlation may be due to the relative absence of the silt sized fraction in the surface sediments of Loch Muick, the majority of which fall within the mud or sandy mud sediment type defined by Folk (1974). The floors of Loch Callater, and to a lesser extent, Loch Lee are dominated by sediment in the silt size fraction. A strong negative correlation, also significant at the 0.2% confidence level, occurs between the organic matter content and the distribution of sand in the water body.

There is a highly significant (0.2% confidence level) negative correlation between depth and the distribution of sand, although clay sized particles, present also in both mud and silt facies, have a less strong (5% confidence level) positive correlation with depth.

The surface sediments of Loch Muick are not well sorted, the least sorted sediment occurring within the extremely poorly sorted category of Folk (1974). The sediments rank second in the degree of sorting of the three lochs in this study, significantly higher than reported in previous studies (section 5.6.1 above). It is suggested that the best sorted

sediments result from winnowing of fines by wave action and the least sorted from input through erosion and bank collapse. Curray (1960) traced sediment masses offshore through their grain size modal 'signature' which was dissipated only by mixing during transportation. The latter confirms the hypothesis that poor sorting is an 'inherited' characteristic derived from the unsorted glacial tills and solifluction deposits which cover the slopes above the loch.

Loch Muick shows a general sediment distribution typical of Scottish lochs (Loch Tay, Al-Jabbari et al., 1983; Loch Tummel, Duck, 1986; Loch Lubnaig, Asaad and McManus, 1986):- poorly sorted, fine grained sediment in the deeper water, and better sorted, coarser material in shallow water.

Analysis of the skewness of Loch Muick surface sediments indicates that the majority of samples have a normal distribution.

QDa-Md analysis confirms that most surface sediment was deposited in a quiet water lacustrine environment. The vast majority (90%) of samples fall within the range of quiet water deposition or deposition of fine grained material from suspension and only 6% in the steep gradient turbidite and fluvialite, or current dominated, environmental trend envelope.

5.7 CONCLUSIONS

The analyses of the surface sediment samples collected from the floors of Lochs Lee, Callater and Muick by grab sampling has led to the following conclusions:

5.7.1 Loch Lee

The surface sediment of Loch Lee exhibits the following characteristics:-

- i) Extremely high organic matter content compared with data obtained in this study and elsewhere.
- ii) A complex distribution of sediment textures on the loch floor.
- iii) Extremely poorly sorted sediment compared with data obtained in this study and

in previously published research.

iv) A coincidence between poorest sorted sediment and positive skew and *vice versa*.

v) A strong positive correlation between

- a) organic matter content and depth
- b) organic matter and the distribution of silt sized particles
- c) clay sized particles and depth
- d) silt sized particles and depth

vi) A strong negative correlation between

- a) organic matter content and the distribution of sand
- b) sand sized particles and depth

vii) QDa-Md analysis confirms that the majority of samples obtained were deposited in a quiet water environment, with a lesser steep gradient turbidite and fluvialite (current dominant) input.

5.7.2 Loch Callater

i) The organic content of surface sediment is the lowest of the three lochs, but significantly above that of comparable water bodies. It is believed that this is primarily due to anthropogenic destruction of peat deposits.

ii) The loch floor is dominated by sediment in the silt size fraction. Sandy sediment occurs at the main stream inflow and in the nearshore environment.

iii) The surface sediment is typically poorly sorted, within a range encountered in other studies, and is the best sorted of the three lochs in this study.

iv) The distribution of the sediment is dominantly negatively skewed, symmetrical and mesokurtic.

v) A strong positive correlation exists between

- a) depth and organic matter content
- b) organic matter content and particles in the silt fraction

- c) depth and silt sized particles
- d) depth and clay sized particles
- vi) A strong negative correlation exists between
 - a) depth and sand sized particles
 - b) organic matter content and particles in the sand fraction
- vii) QDa-Md analysis indicates that the majority of samples obtained were deposited in quiet water conditions, whereas sediments obtained close to the mouth of the Allt an Loch plotted within the fluvial (current dominant) environmental trend envelope.

5.7.3 Loch Muick

- i) In common with the samples obtained from Lochs Lee and Callater, the surface sediment of Loch Muick has an unusually high organic matter content, intermediate between that determined in Loch Lee and Loch Callater.
- ii) The surface sediment of Loch Muick is dominated by mud. Sandy sediment is restricted to the nearshore zone.
- iii) As in Lochs Lee and Callater, the surface sediment is poorly sorted, having a higher maximum standard deviation than has been previously reported, but is substantially better sorted than the surface sediments sampled in Loch Lee.
- iv) The loch floor is covered by sediment with negatively skewed or symmetrical distributions.
- v) A strong positive correlation exists between
 - a) organic matter and depth
 - b) organic matter and sediment of the clay size fraction
 - c) sediment of the clay size fraction and depth
- vi) A strong negative correlation exists between
 - a) organic matter and sand sized sediment
 - b) depth and sand sized sediment

vii) QDa-Md analysis indicates that the vast majority of surface sediment sampled was deposited in quiet water conditions. Some samples obtained at the nearshore end of traverses plot within the steep gradient turbidite and fluvialite, current dominated, environmental trend envelopes.

LOCH LEE

Surface sediment sample locations.

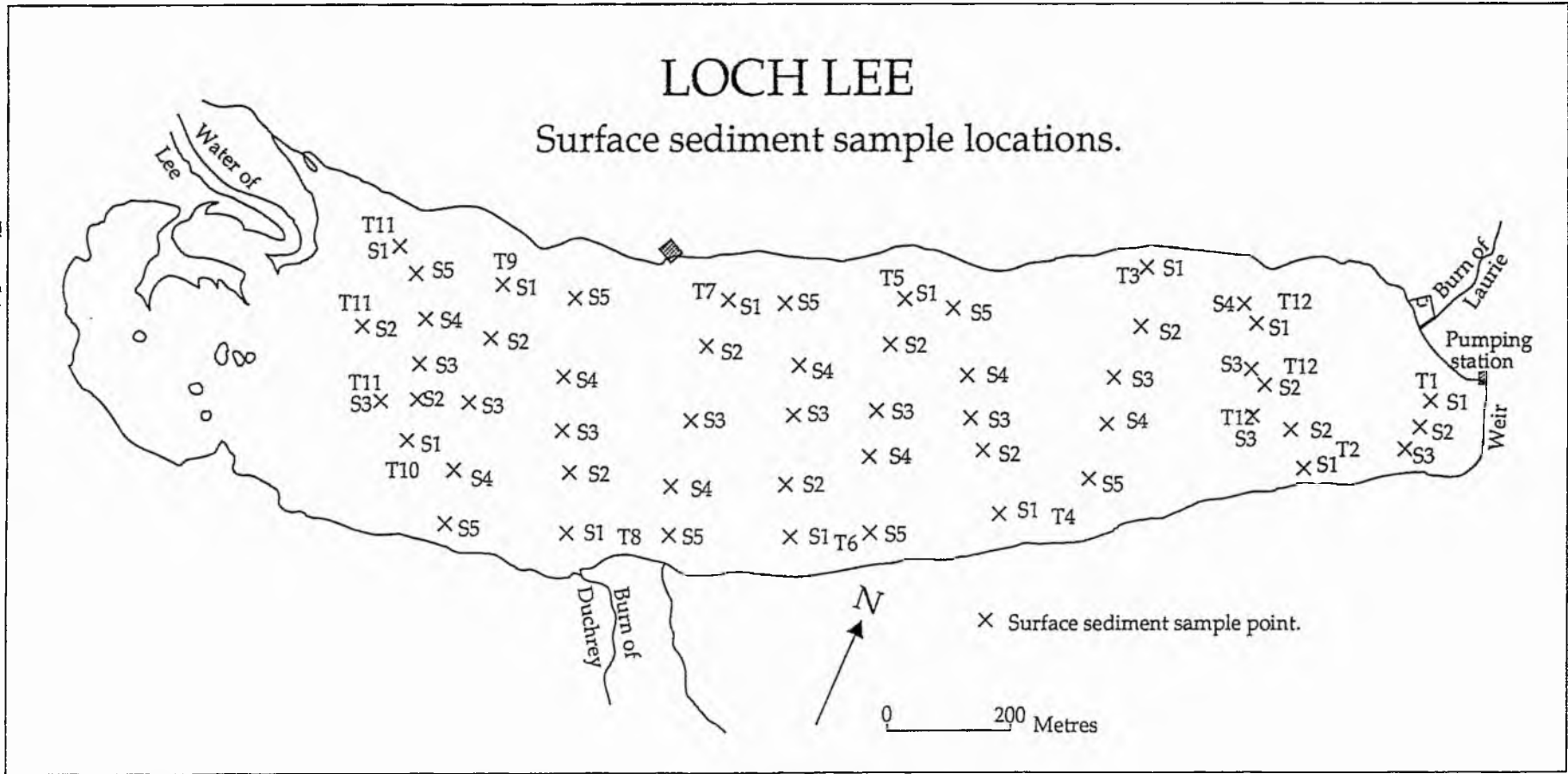


Figure 5.1
215

LOCH CALLATER

Surface sediment sample locations.

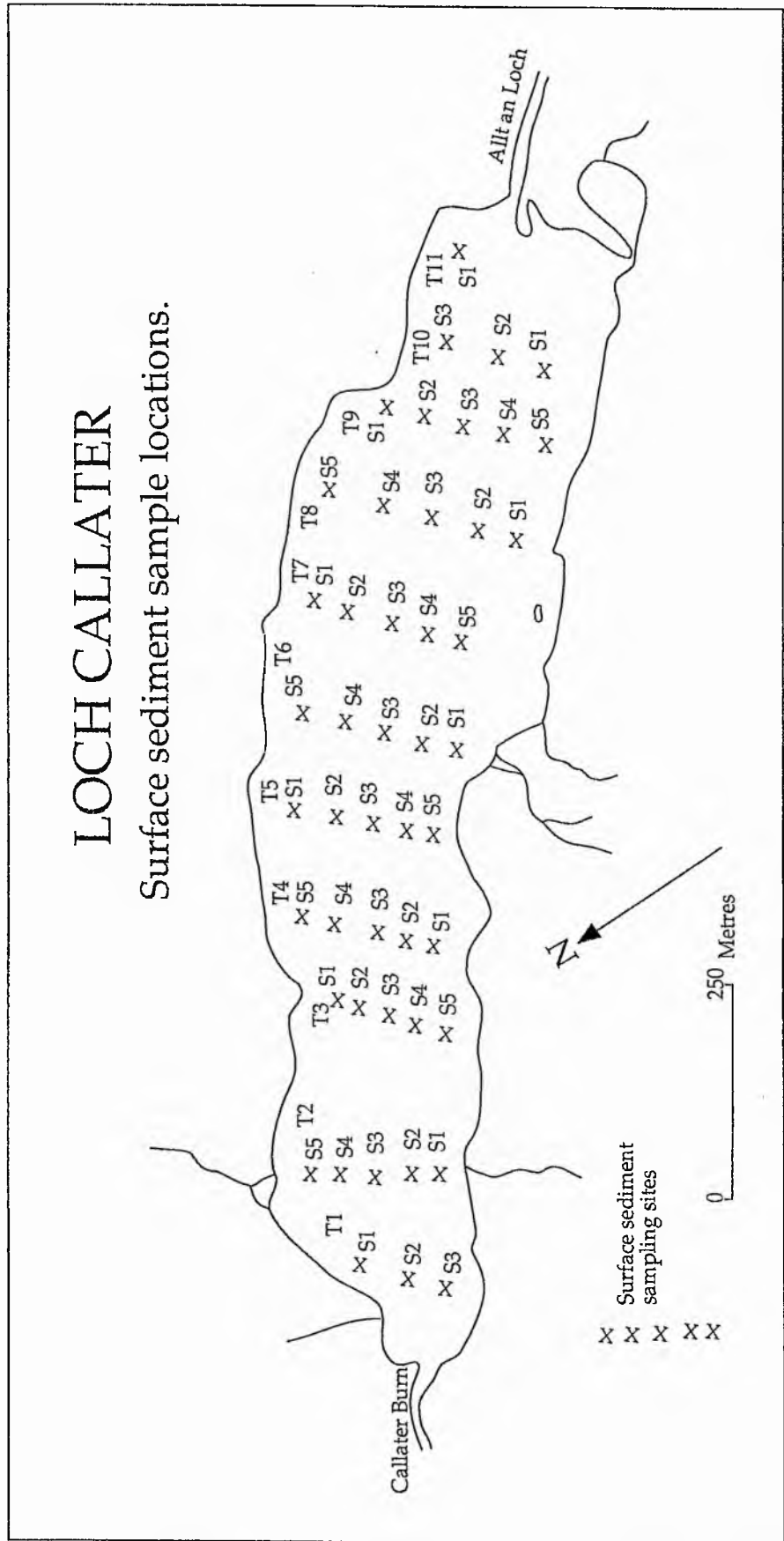


Figure 5.2
216

LOCH MUICK

Surface sediment sample locations.

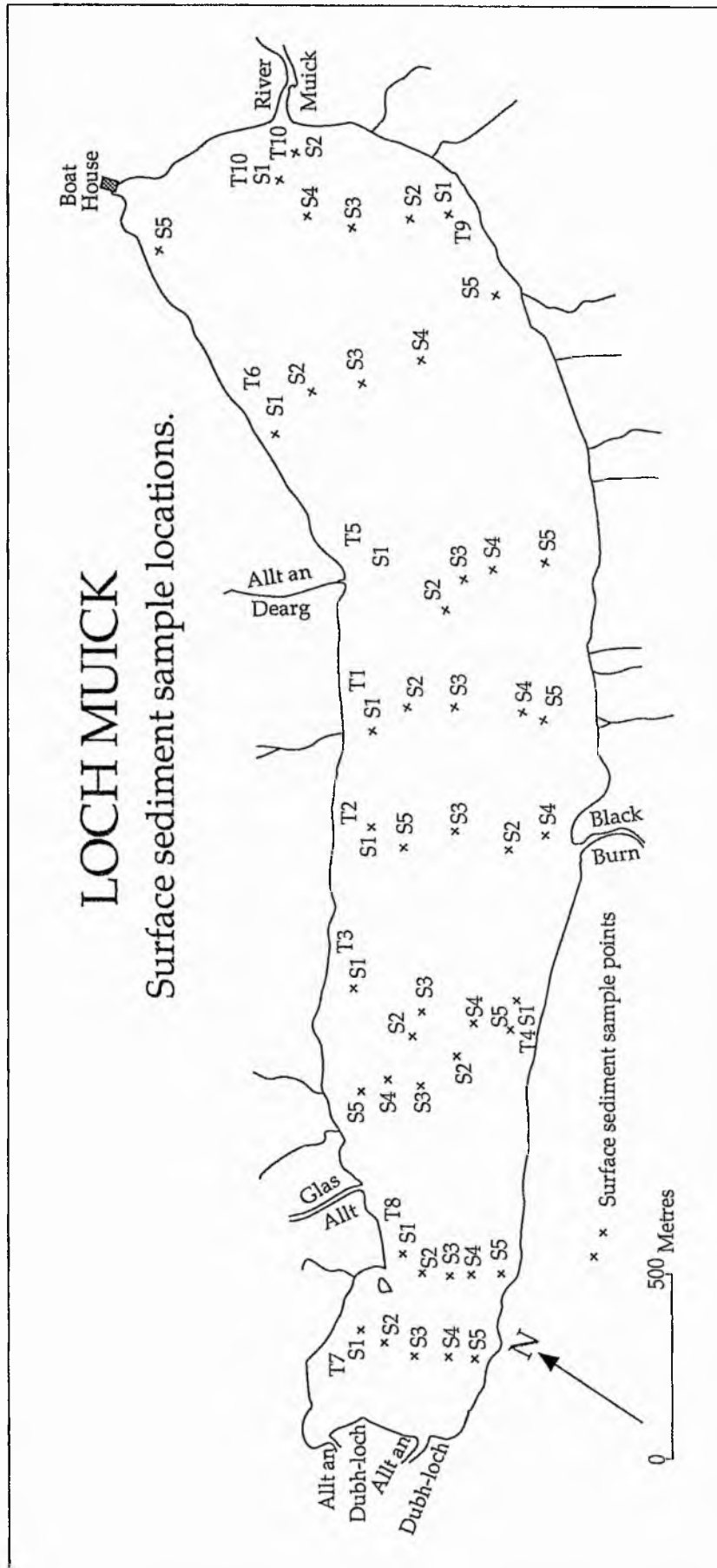


Figure 5.3
217

LOCH LEE

Distribution map of total organic matter
(loss on ignition) of surface sediment.

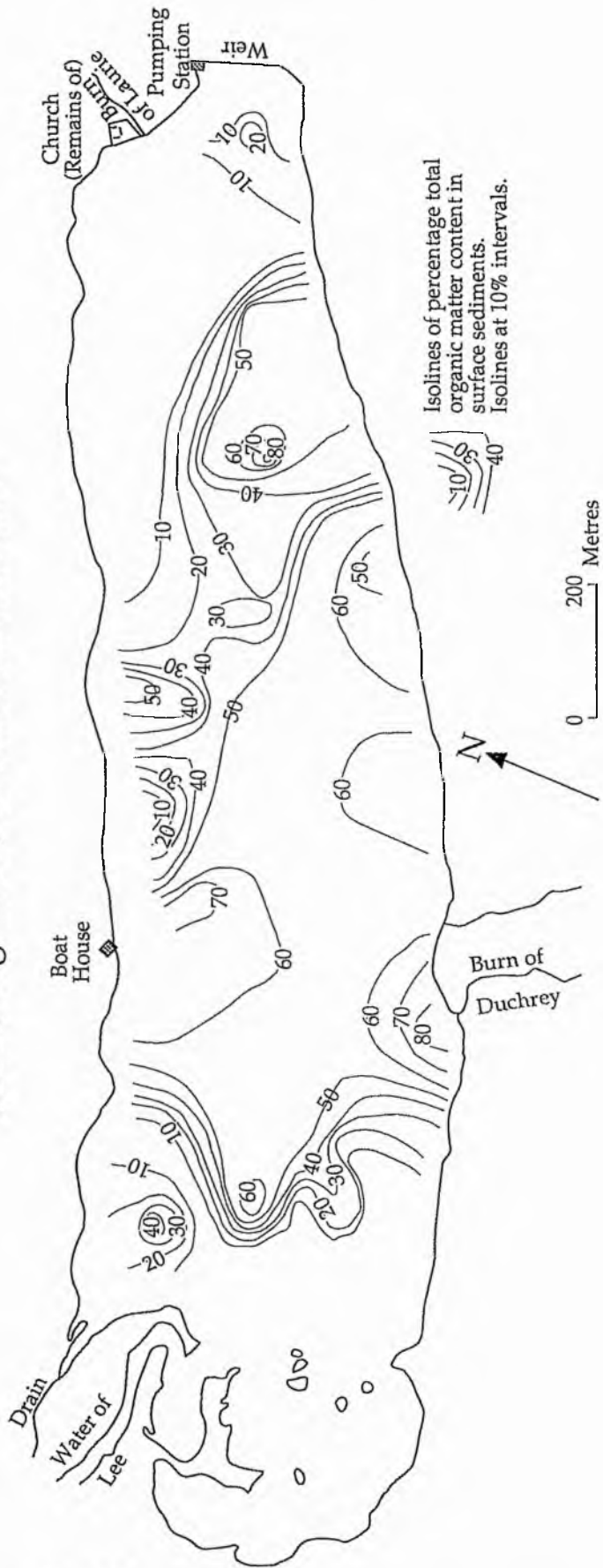
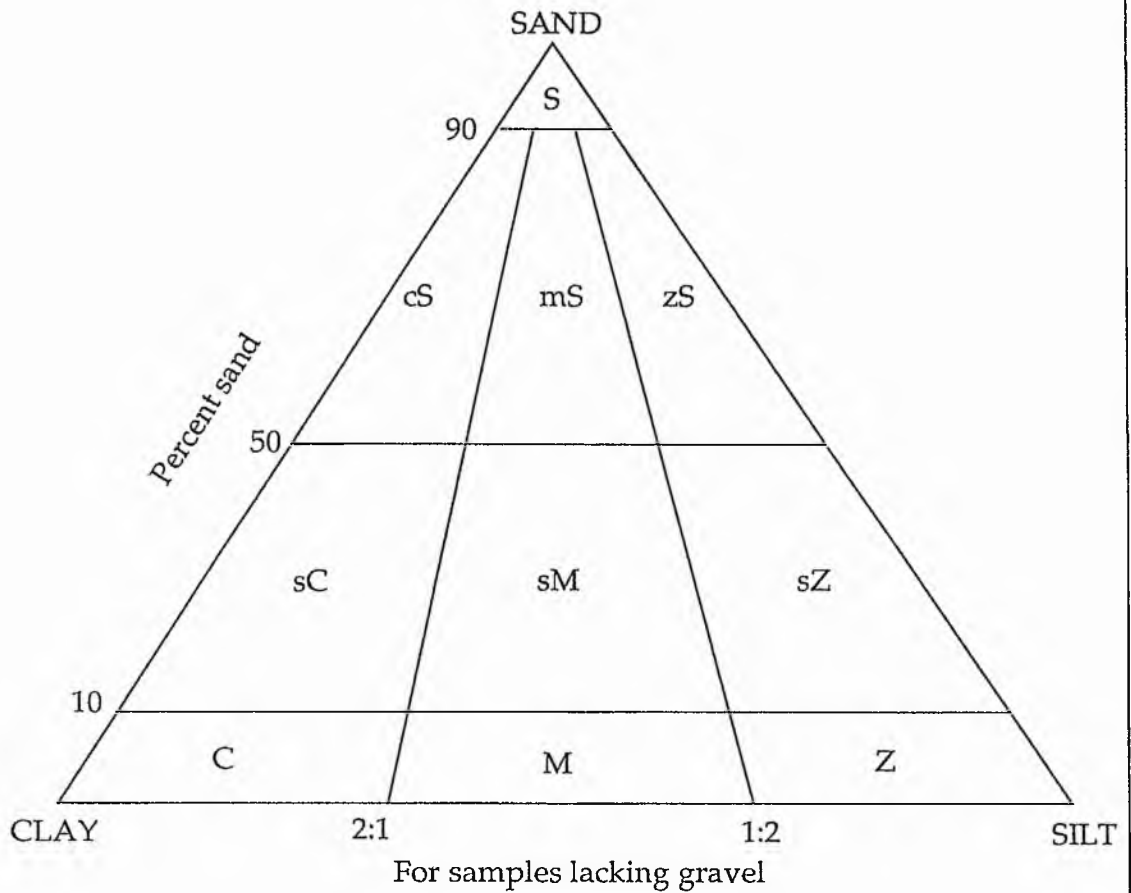


Figure 5.4
218

Ternary diagram for delimiting sediment textures

From Folk (1974)



S, sand; s, sandy
 Z, silt; z, silty
 M, mud; m, muddy
 C, clay; c, clayey

Figure 5.5
 219

LOCH LEE

Distribution map of surface sediment textures derived from the ternary diagram of Folk (1974).

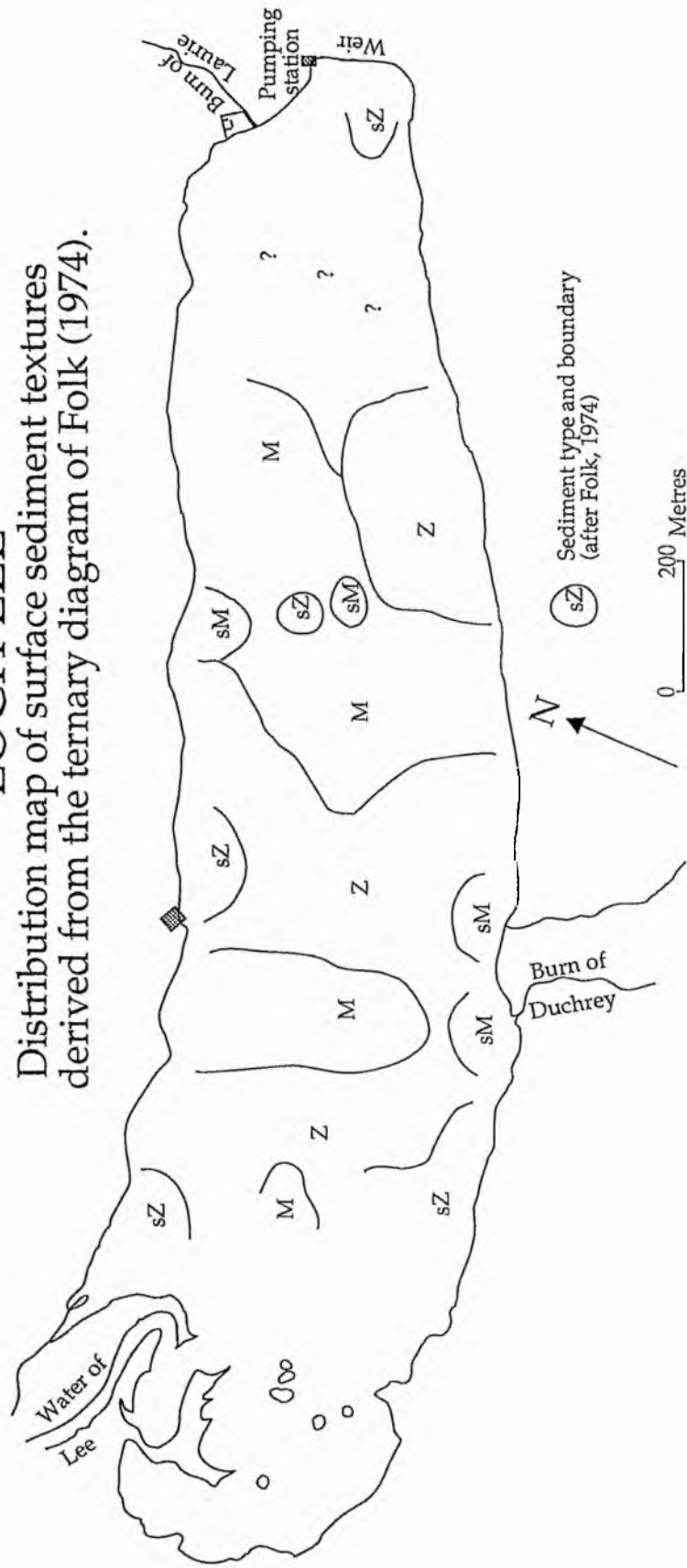


Figure 5.6
220

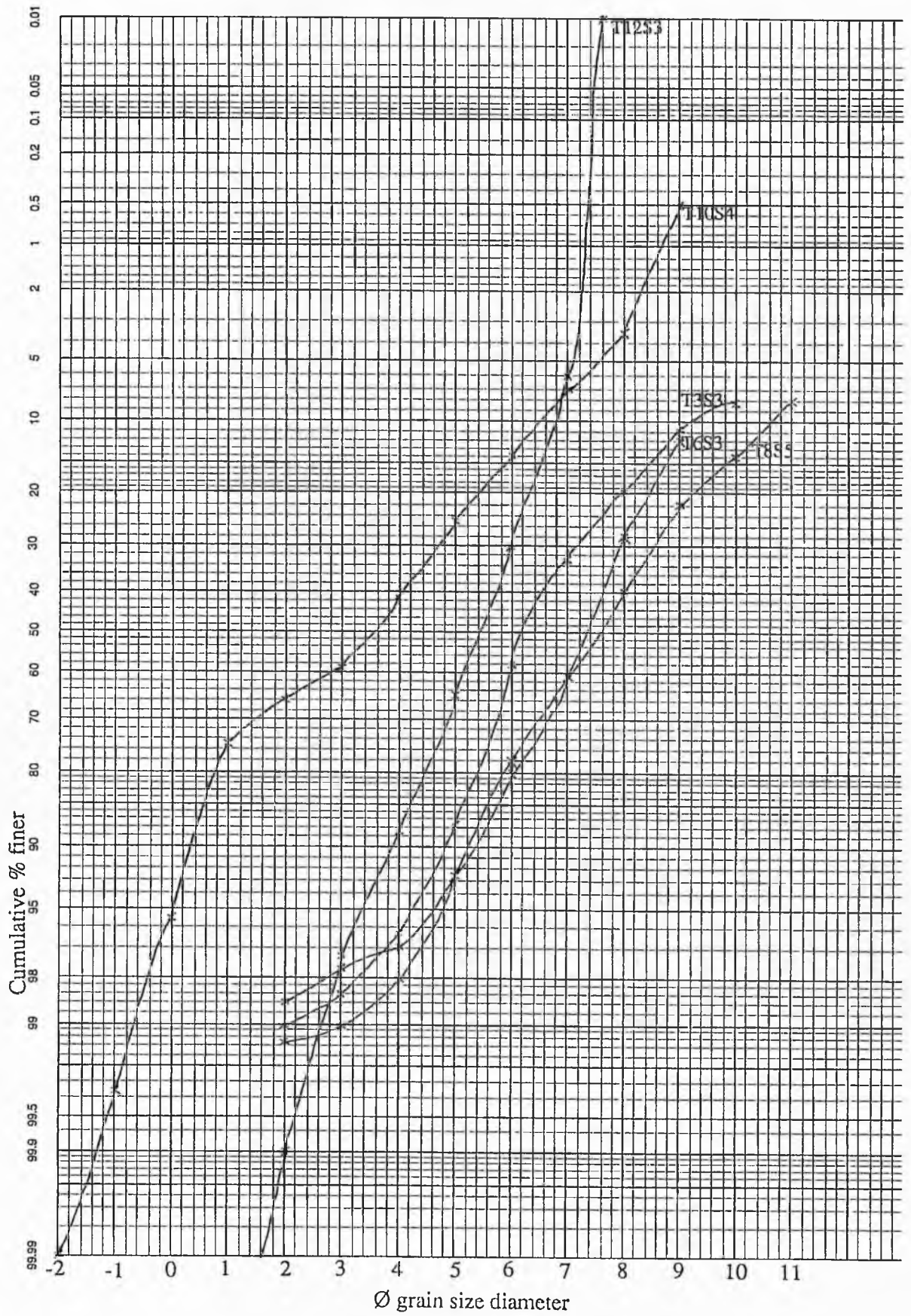


Figure 5.7 Loch Lee: Cumulative percentage frequency curves of surface sediment size.

Frequency graphs of Loch Lee surface sediment

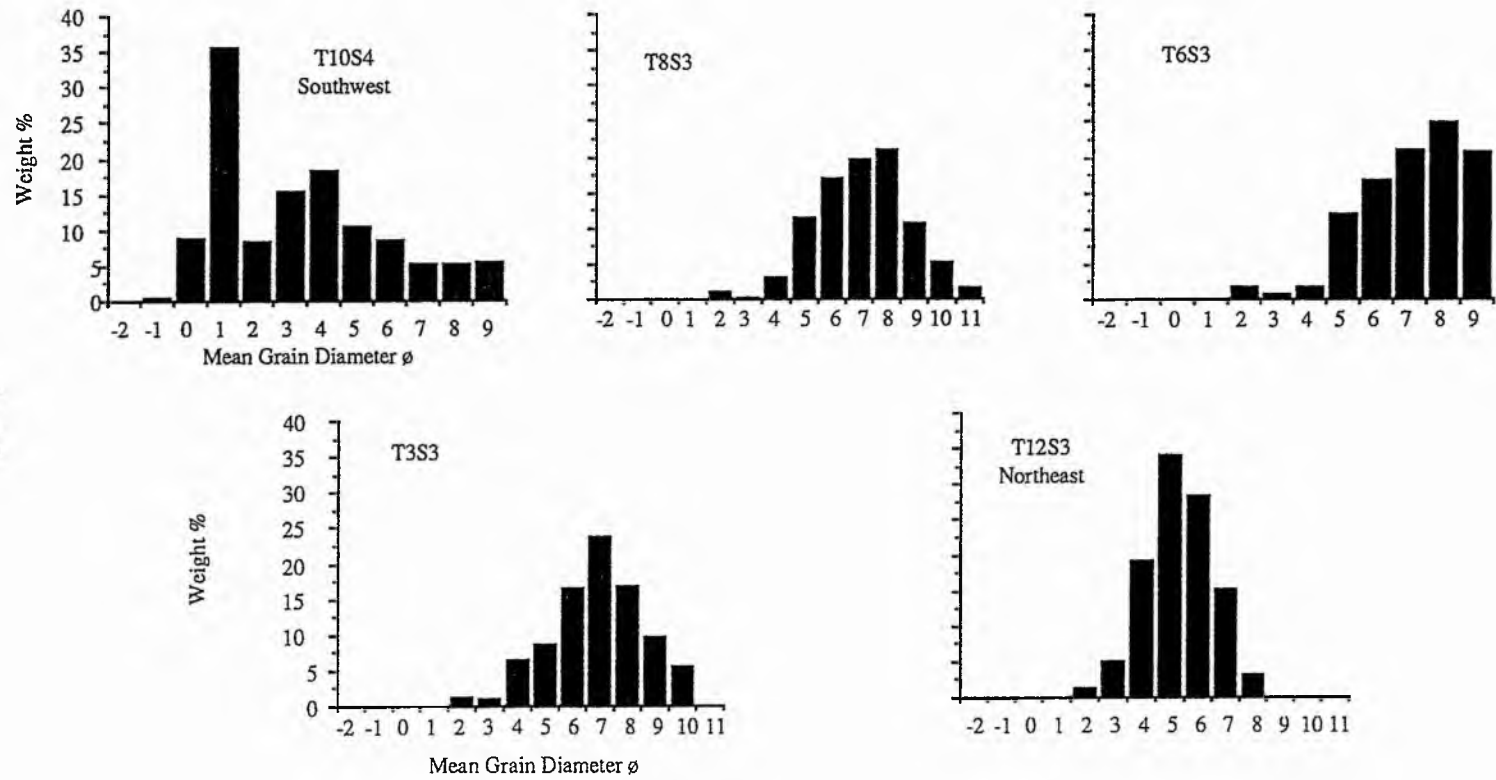


Figure 5.8
222

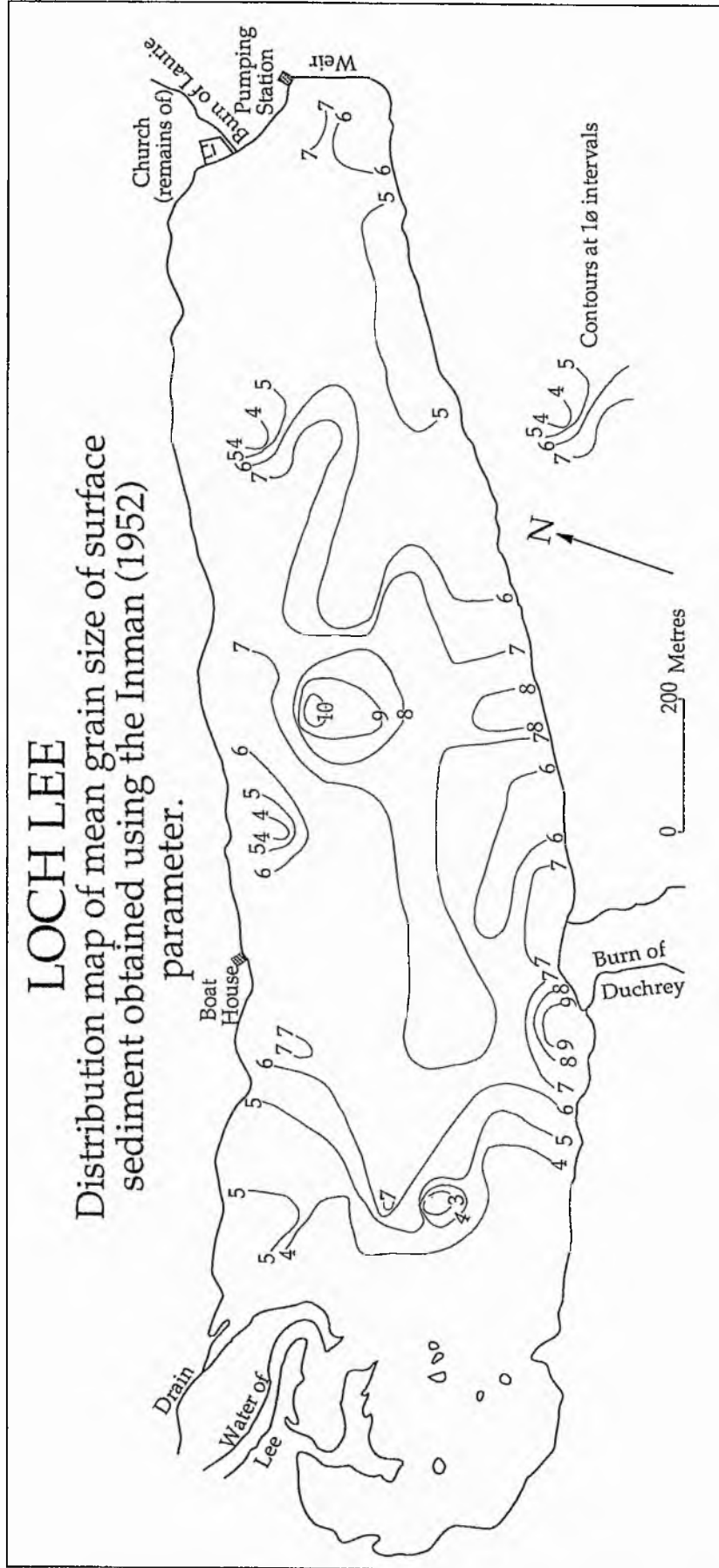
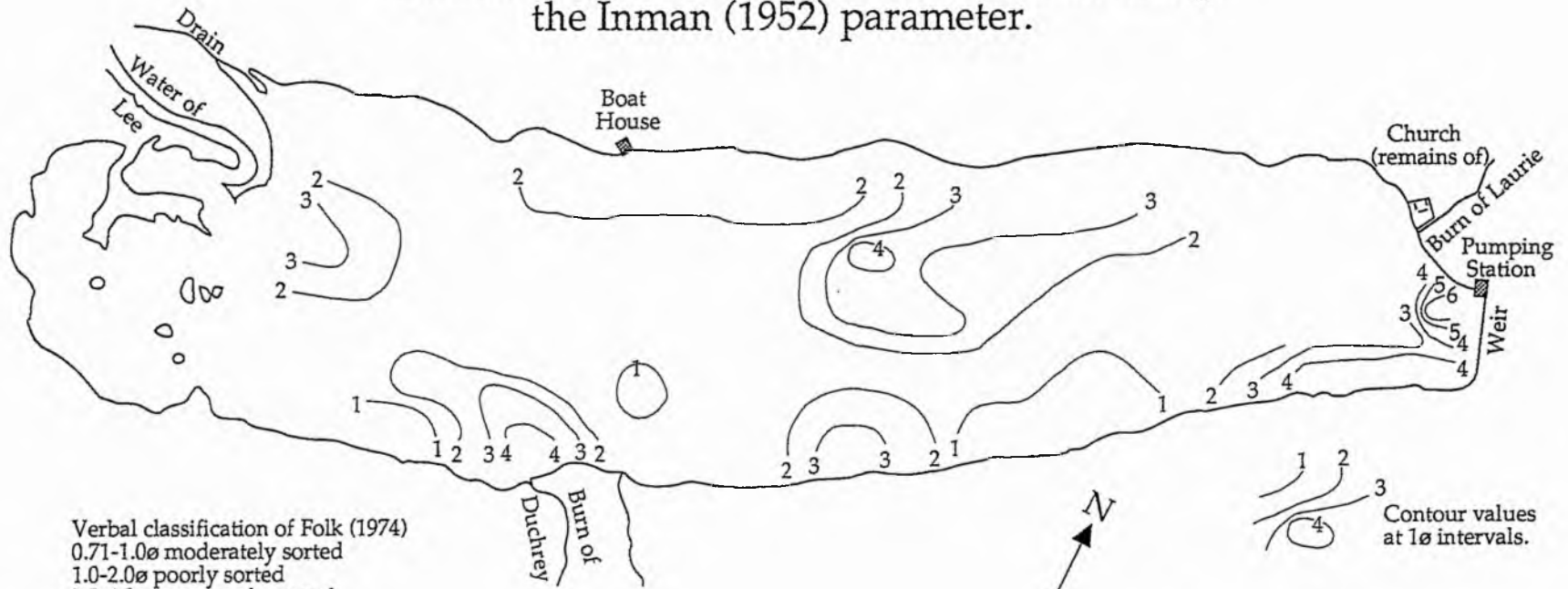


Figure 5.9
223

LOCH LEE

Standard Deviation of surface sediment using
the Inman (1952) parameter.



Verbal classification of Folk (1974)
0.71-1.00 moderately sorted
1.0-2.00 poorly sorted
2.0-4.00 very poorly sorted
>4.00 extremely poorly sorted

Contour values
at 1.0 intervals.

0 200 Metres

Figure 5.10
224

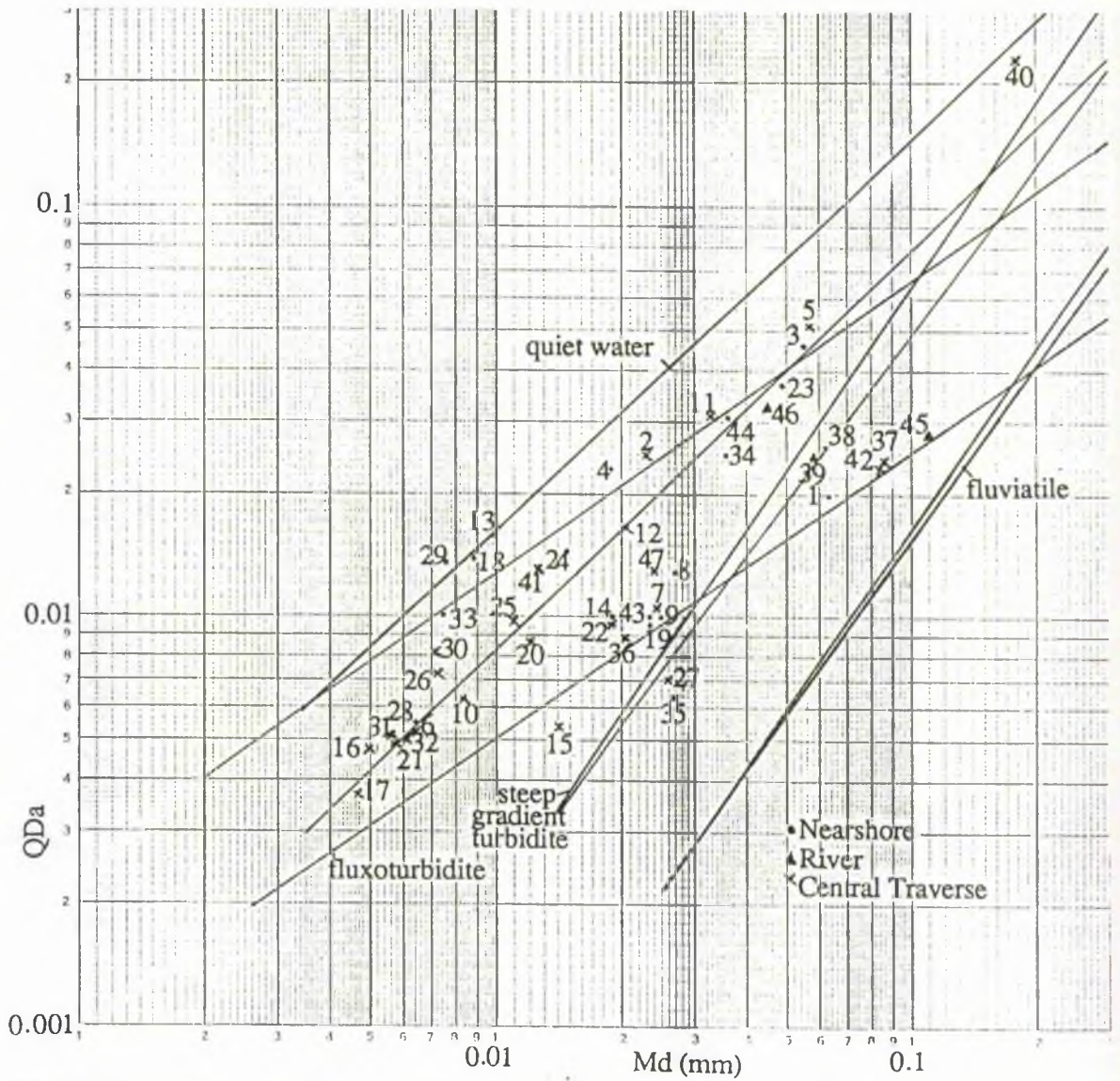


Figure 5.12 Loch Lee: Q_{Da} - M_d plot showing the environmental trend envelopes of Buller and McManus (1972, 1973).

LOCH CALLATER

Distribution map of total organic matter content
(loss on ignition) of surface sediment.

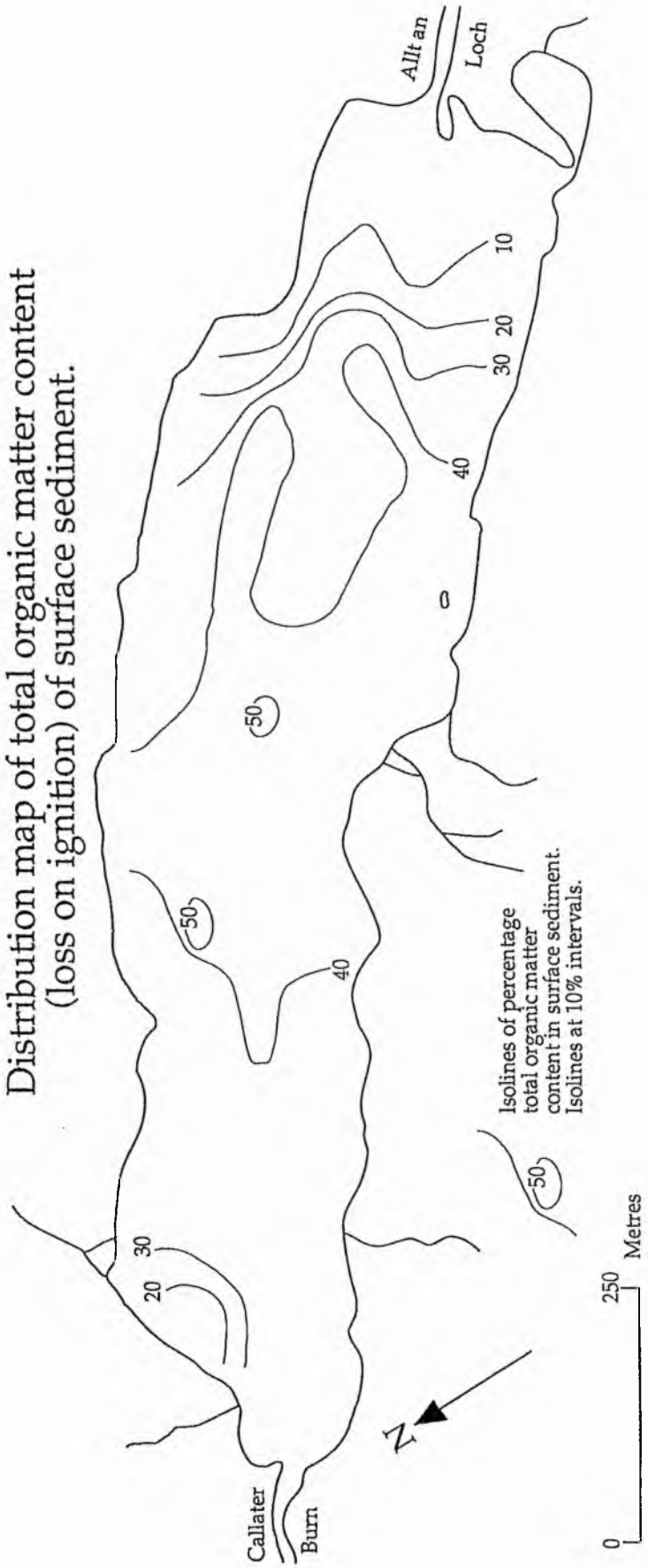


Figure 5.13
227

LOCH CALLATER

Distribution map of surface sediment textures derived from the ternary diagram of Folk (1974).

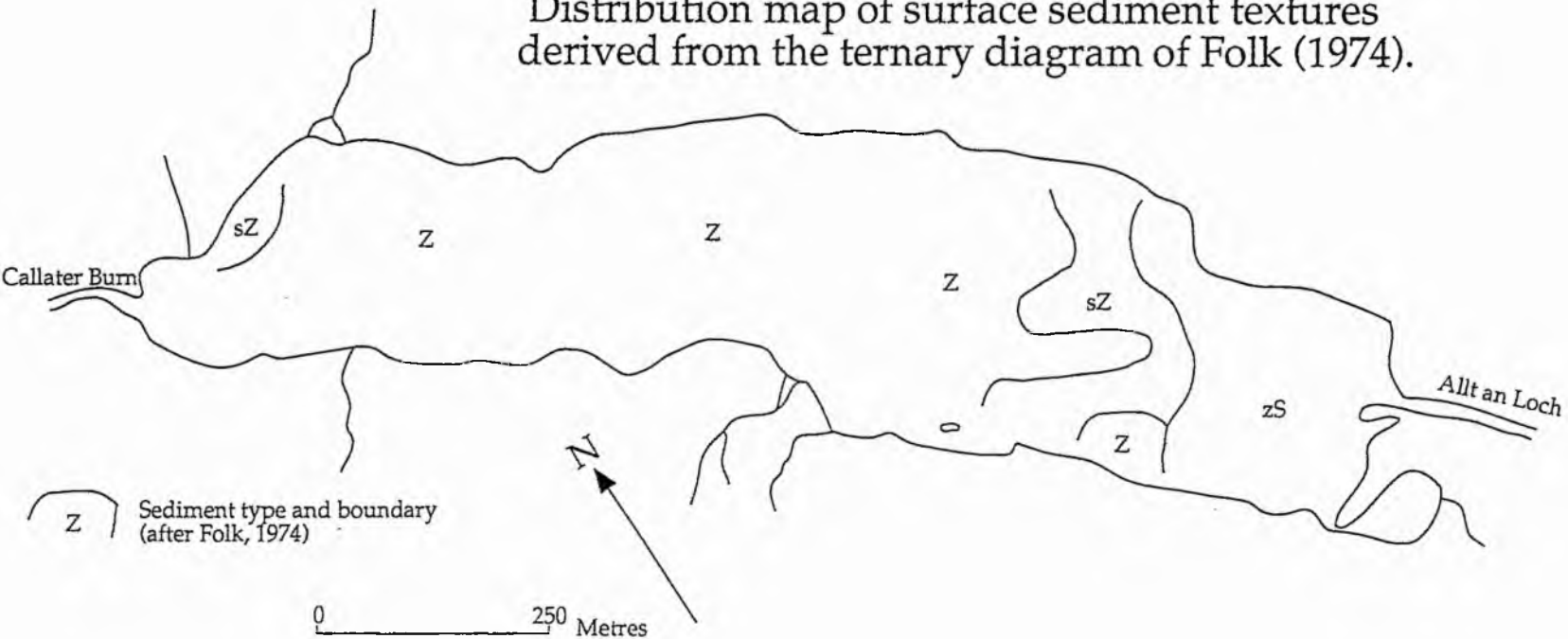


Figure 5.14
228

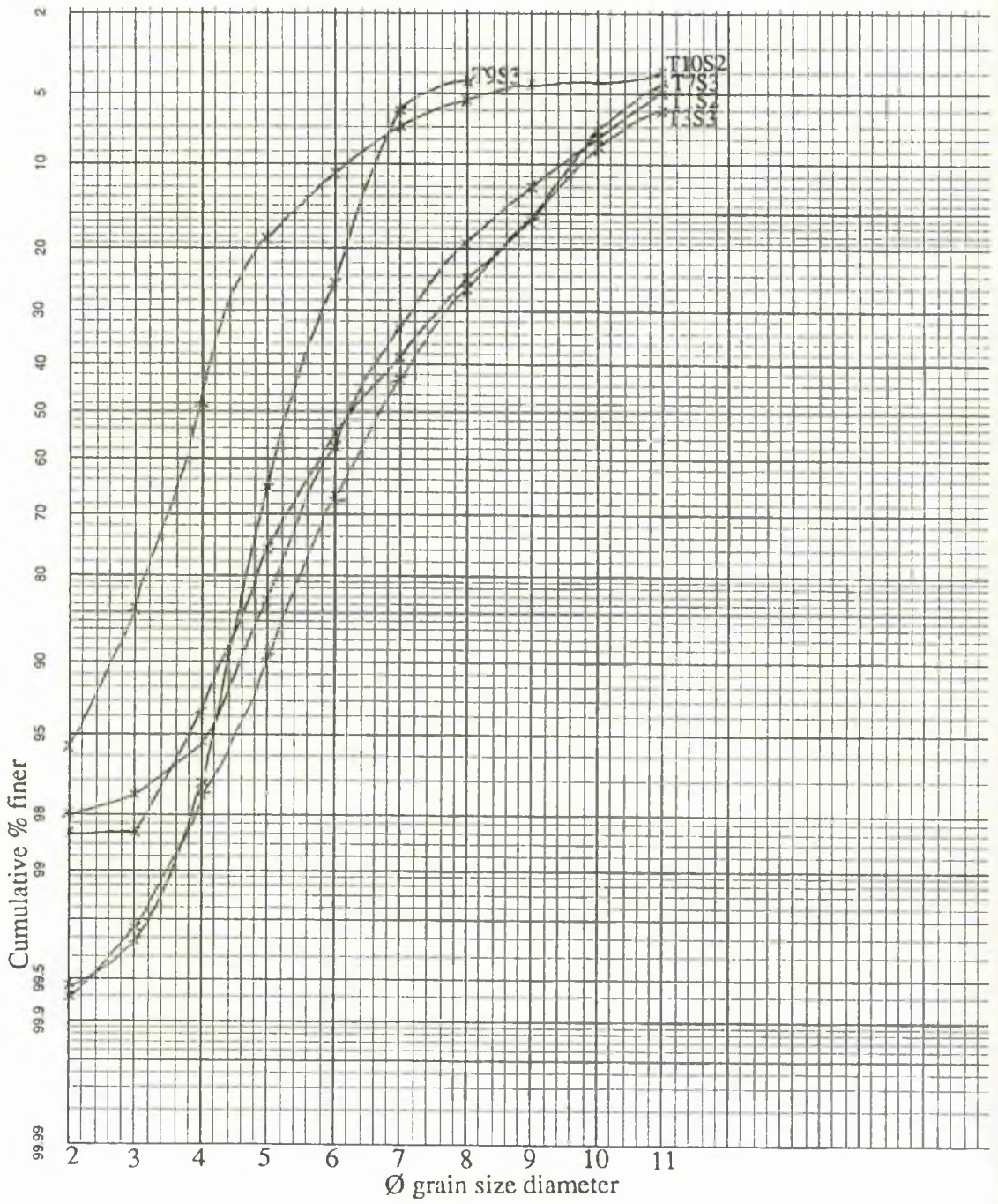


Figure 5.15 Loch Callater: Cumulative percentage frequency curves of surface sediment size.

Frequency graphs of Loch Callater surface sediment

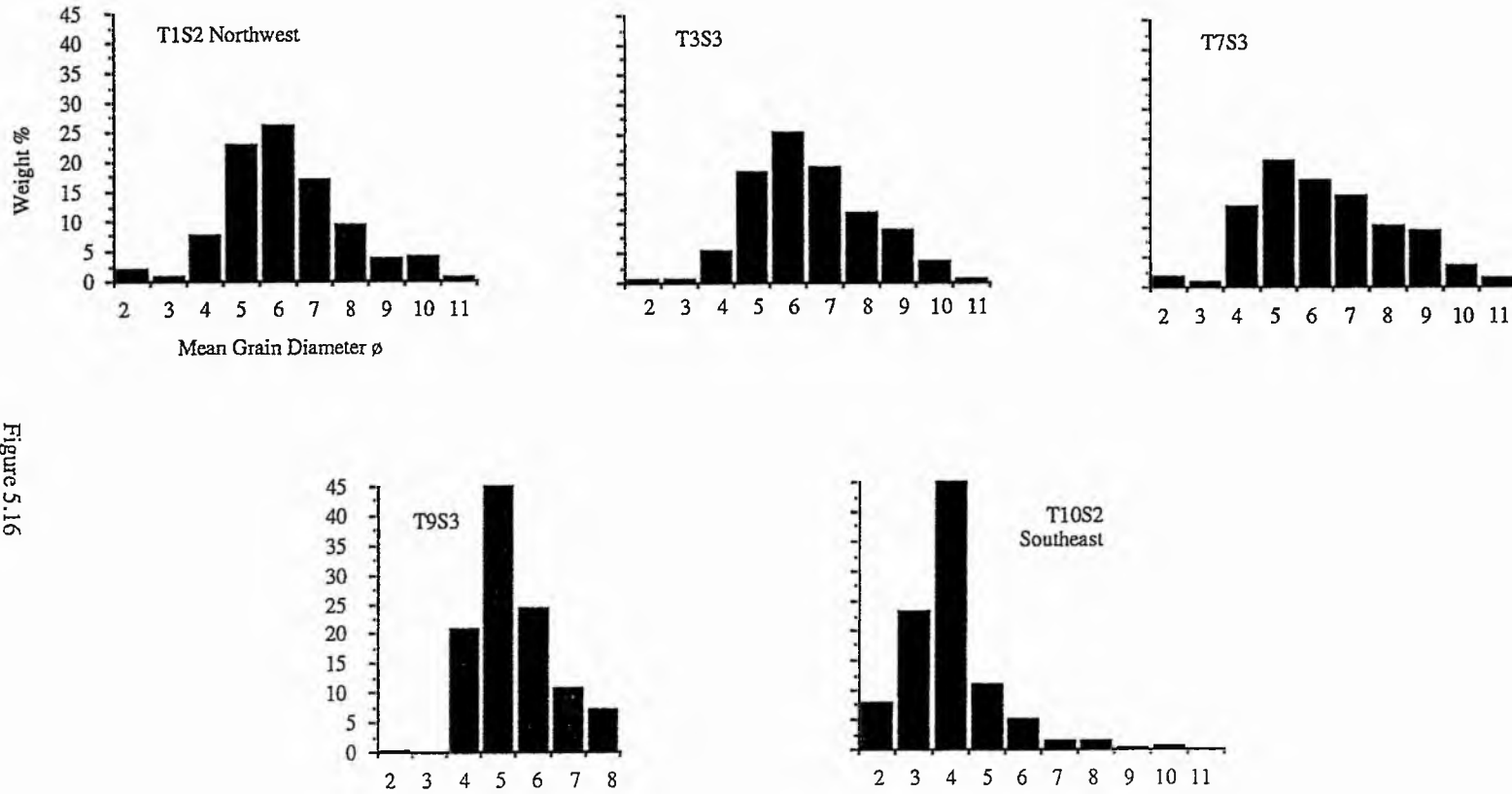


Figure 5.16
230

LOCH CALLATER

Distribution map of mean grain size of surface sediment using the Folk and Ward (1957) parameter.

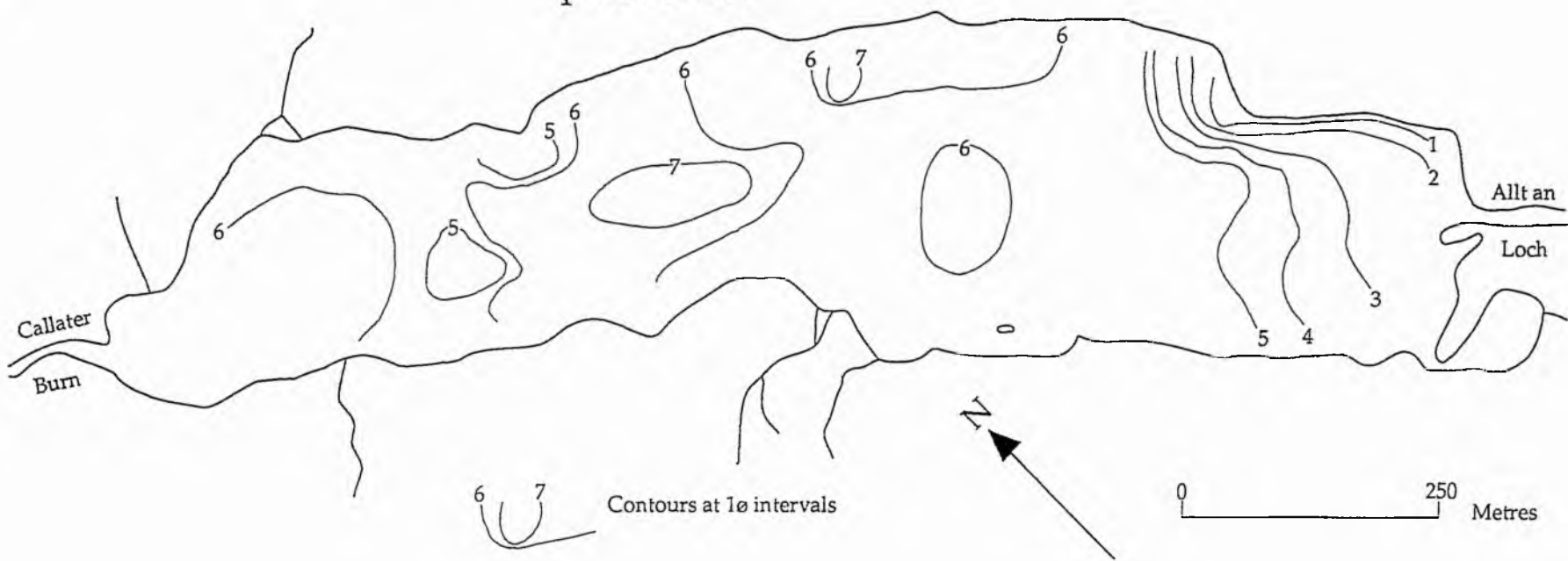


Figure 5.17
231

LOCH CALLATER

Distribution map of Standard Deviation of surface sediment using the Folk and Ward (1957) parameter.

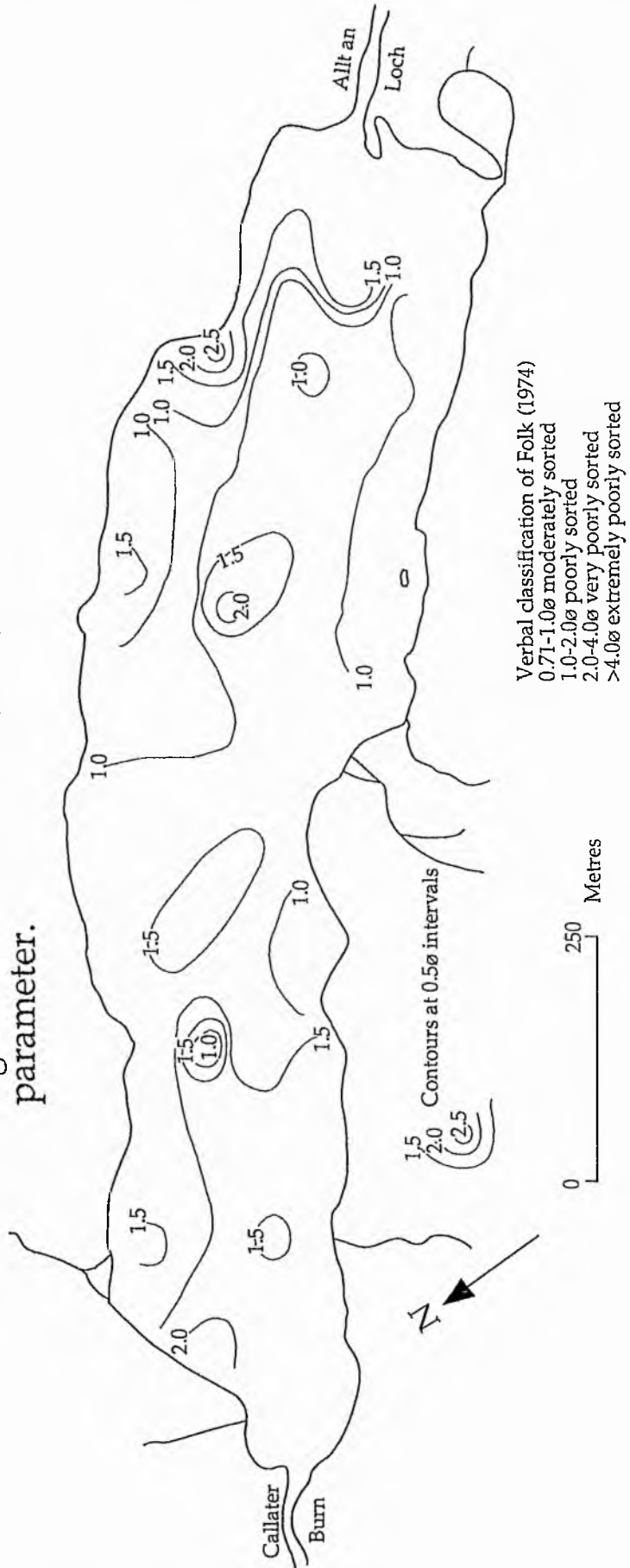
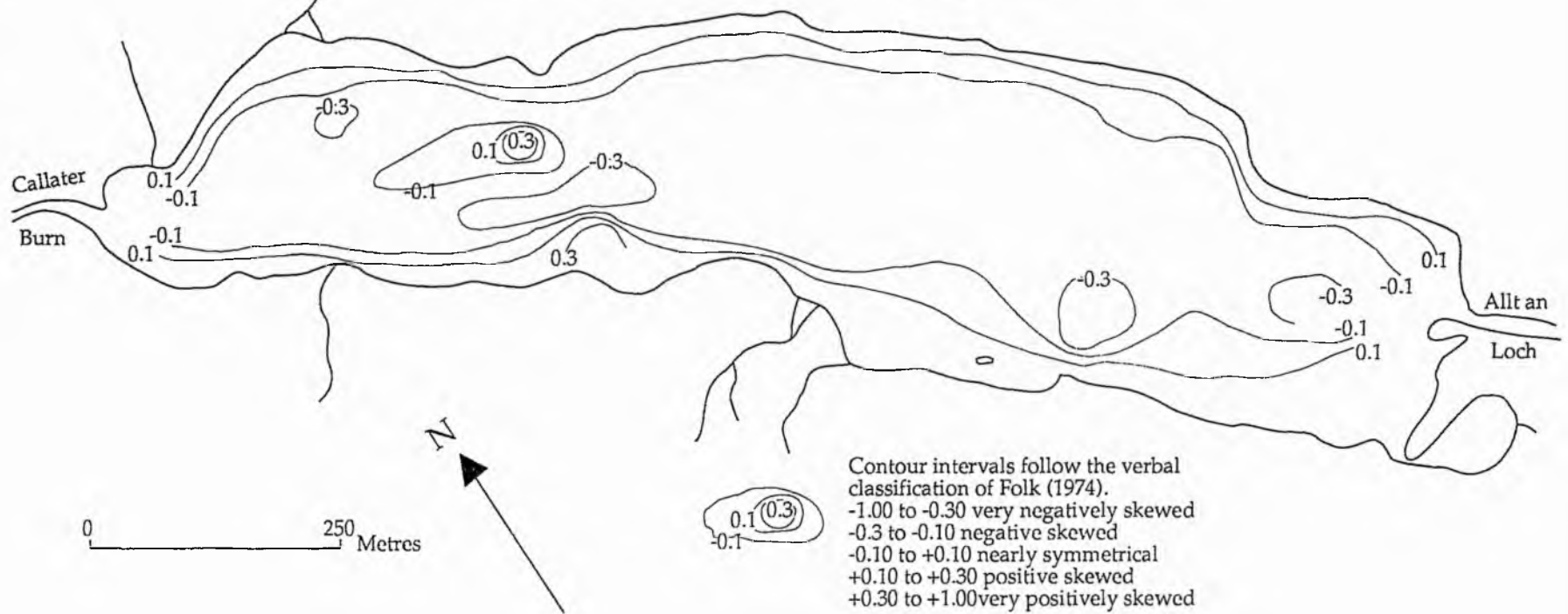


Figure 5.18
232

LOCH CALLATER

Distribution map of Skewness of surface sediment
using the Folk and Ward (1957) parameter.



Contour intervals follow the verbal
classification of Folk (1974).
-1.00 to -0.30 very negatively skewed
-0.3 to -0.10 negative skewed
-0.10 to +0.10 nearly symmetrical
+0.10 to +0.30 positive skewed
+0.30 to +1.00 very positively skewed

Figure 5.19
233

LOCH CALLATER

Distribution map of Kurtosis of surface sediment using the Folk and Ward (1957) parameter.

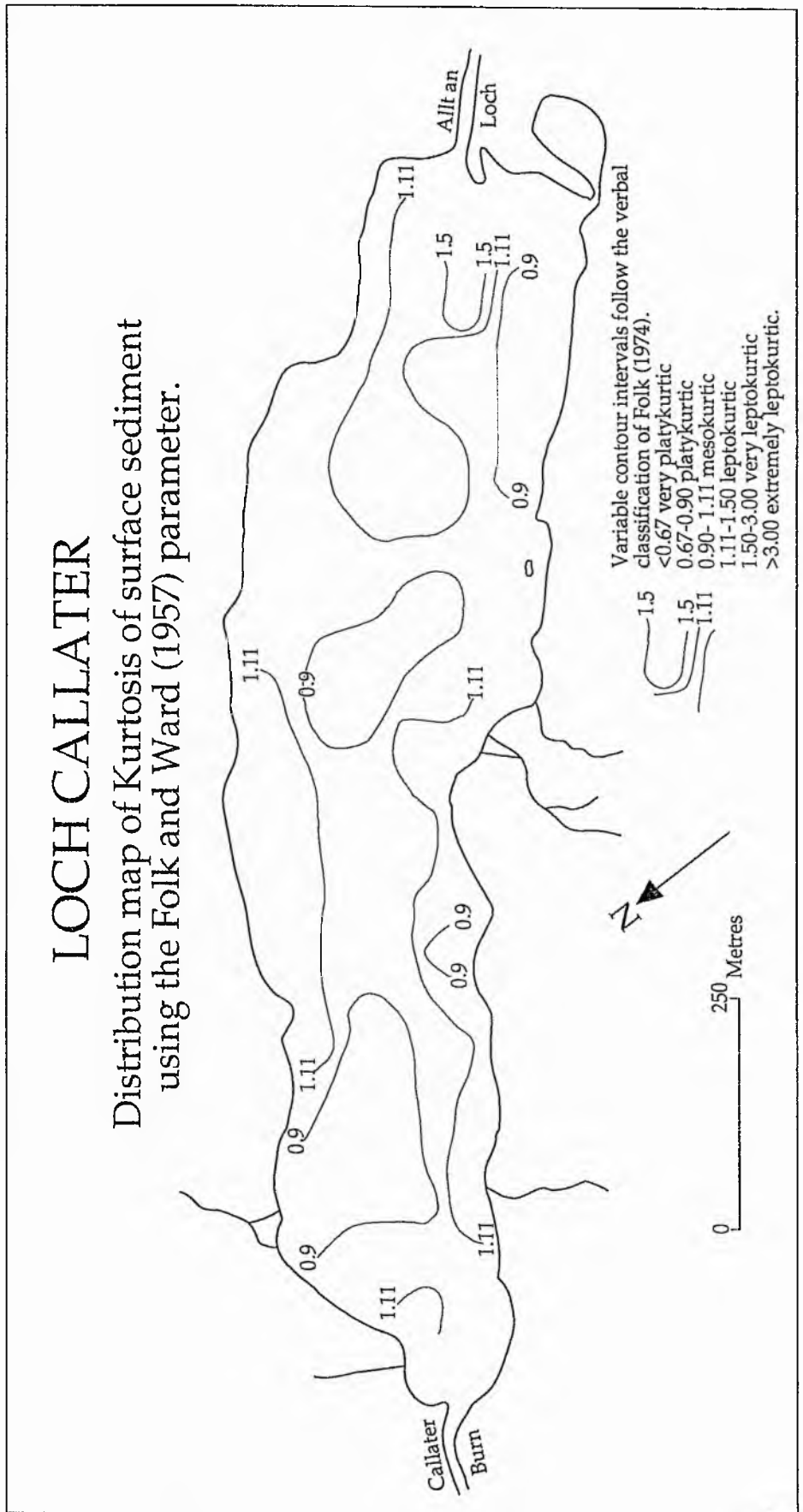


Figure 5.20
234

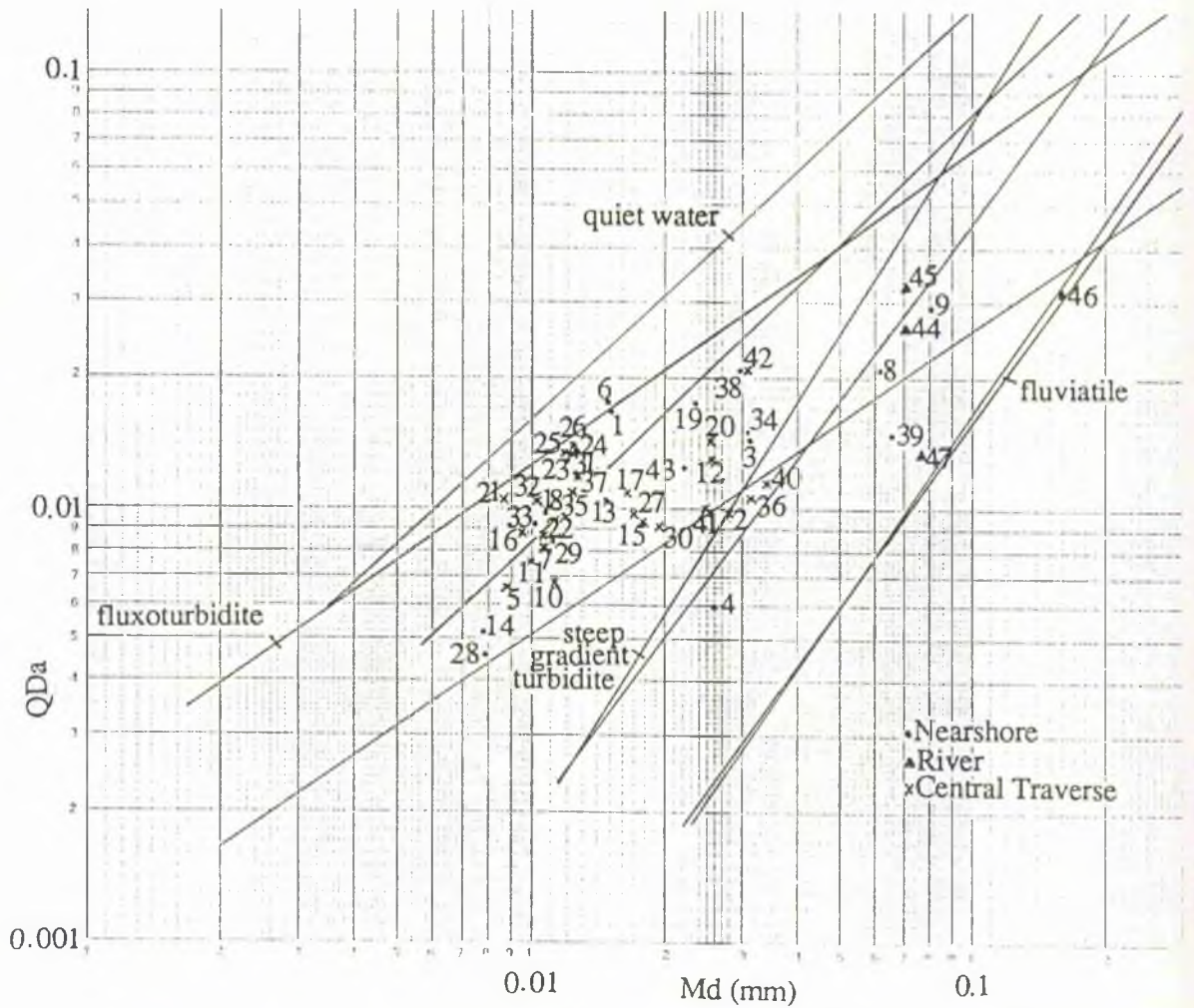


Figure 5.21 Loch Callater: QDa - Md plot showing the environmental trend envelopes of Buller and McManus (1972, 1973).

LOCH MUICK

Distribution map of total organic matter content
(loss on ignition) of surface sediment.

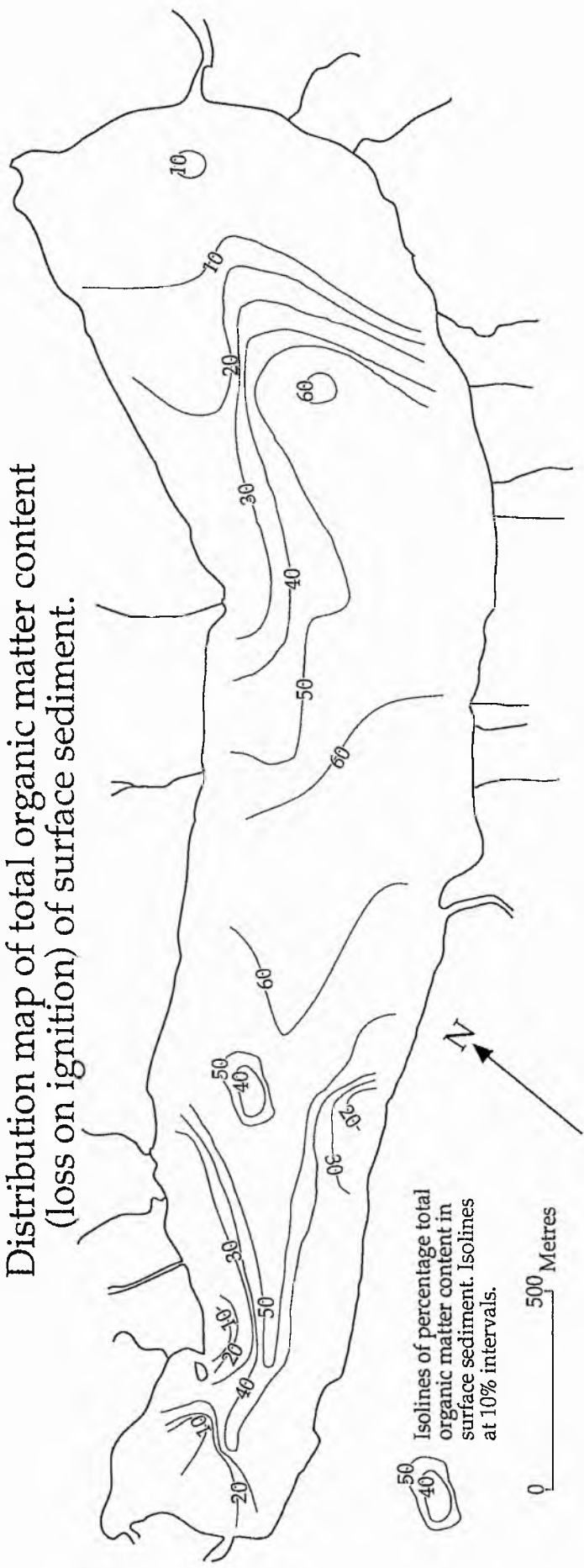


Figure 5.22
236

LOCH MUICK

Distribution map of surface sediment textural facies derived from the ternary diagram of Folk (1974).

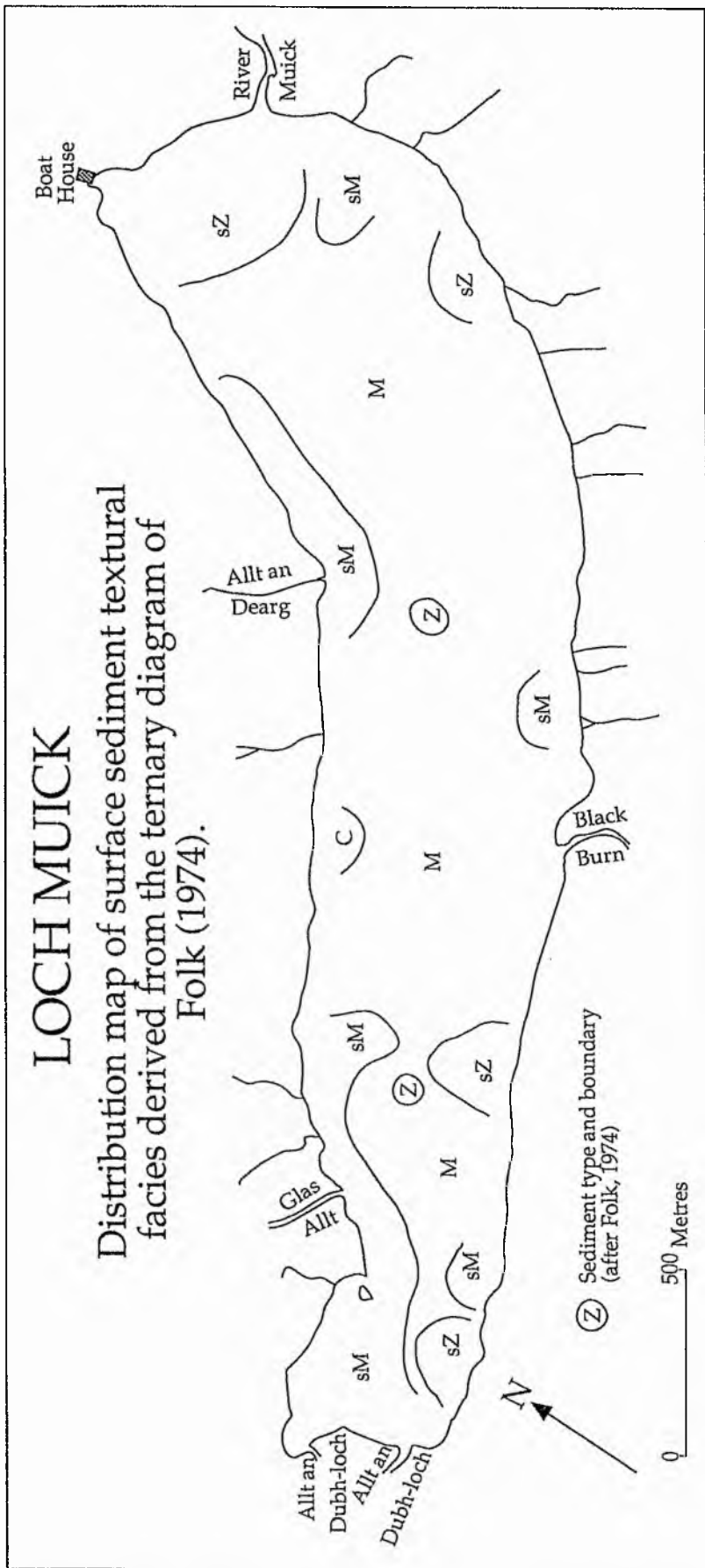


Figure 5.23
237

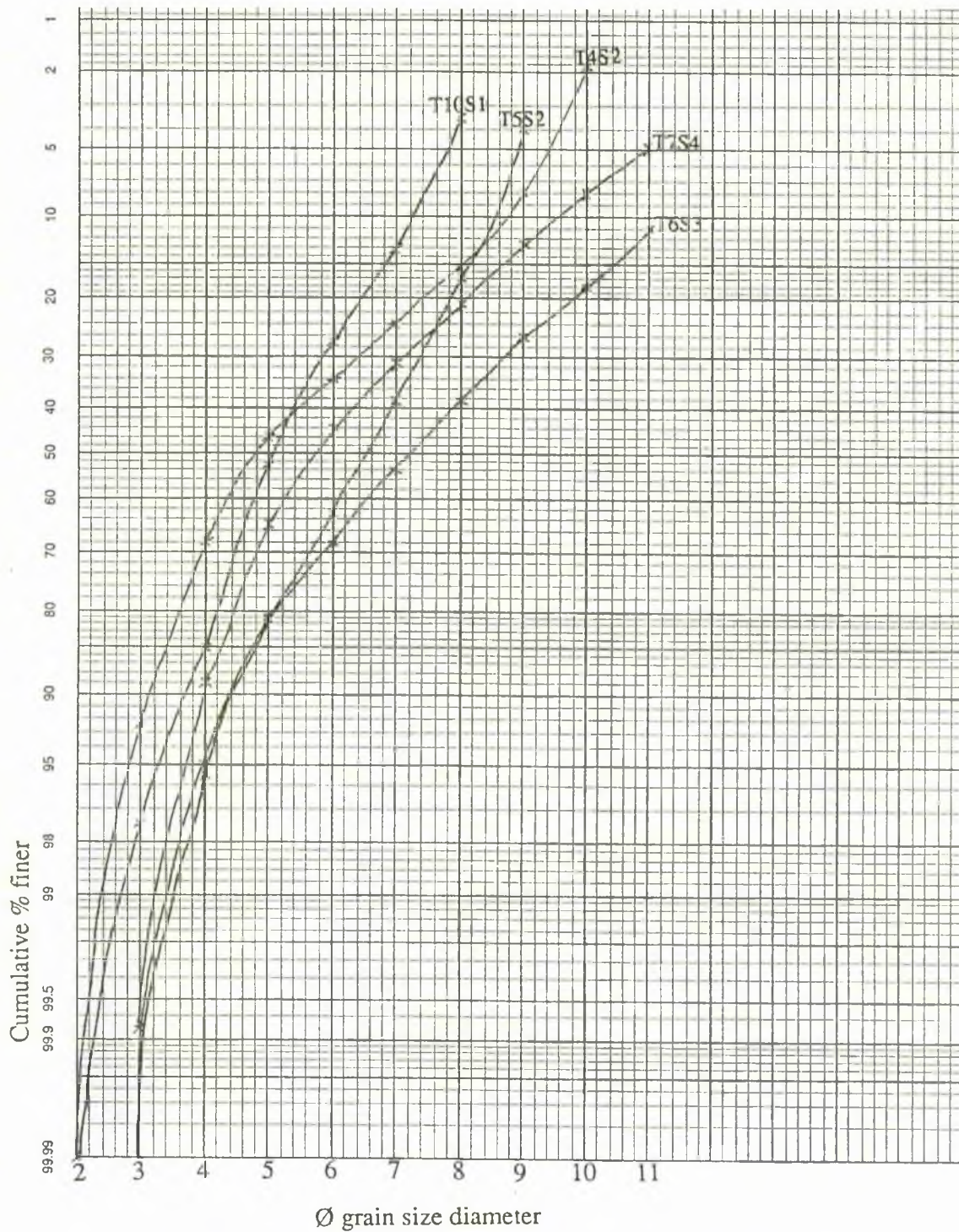


Figure 5.24 Loch Muick: Cumulative percentage frequency curves of surface sediment size.

Frequency graphs of Loch Muick surface sediment

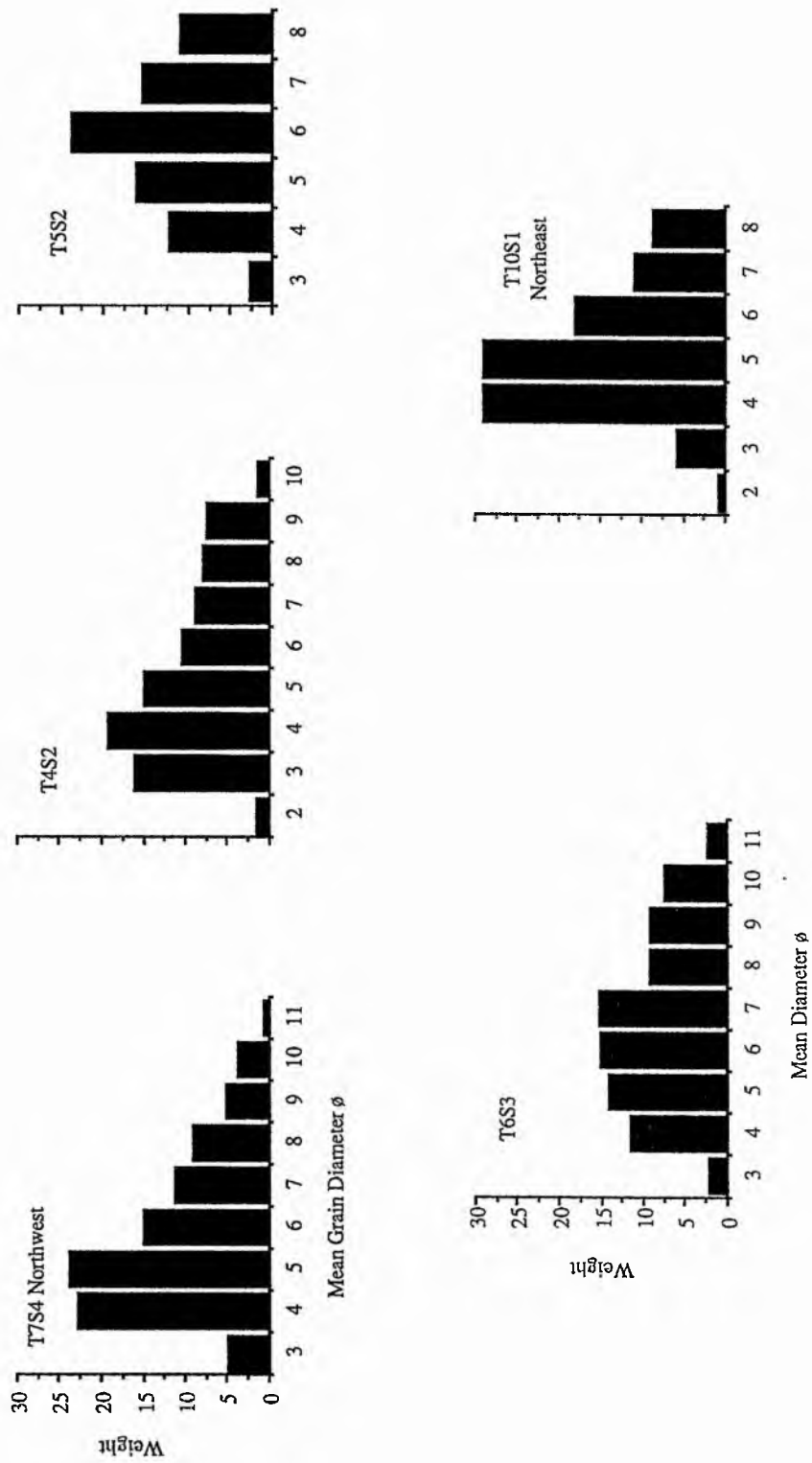


Figure 5.25
239

LOCH MUICK

Distribution map of mean grain size of surface sediment obtained using the Inman (1952) parameter.

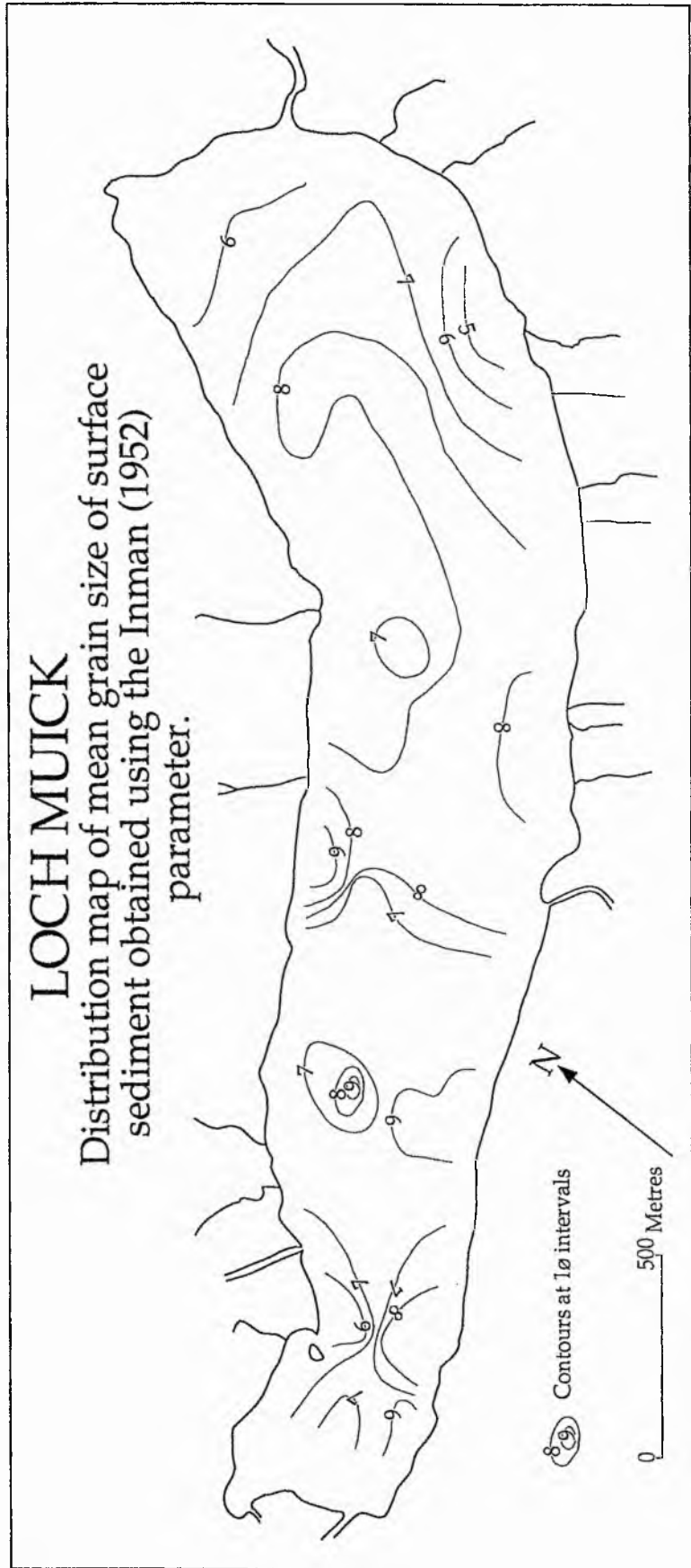


Figure 5.26
240

LOCH MUICK

Distribution map of Standard Deviation of surface sediment using the Inman (1952) parameter.

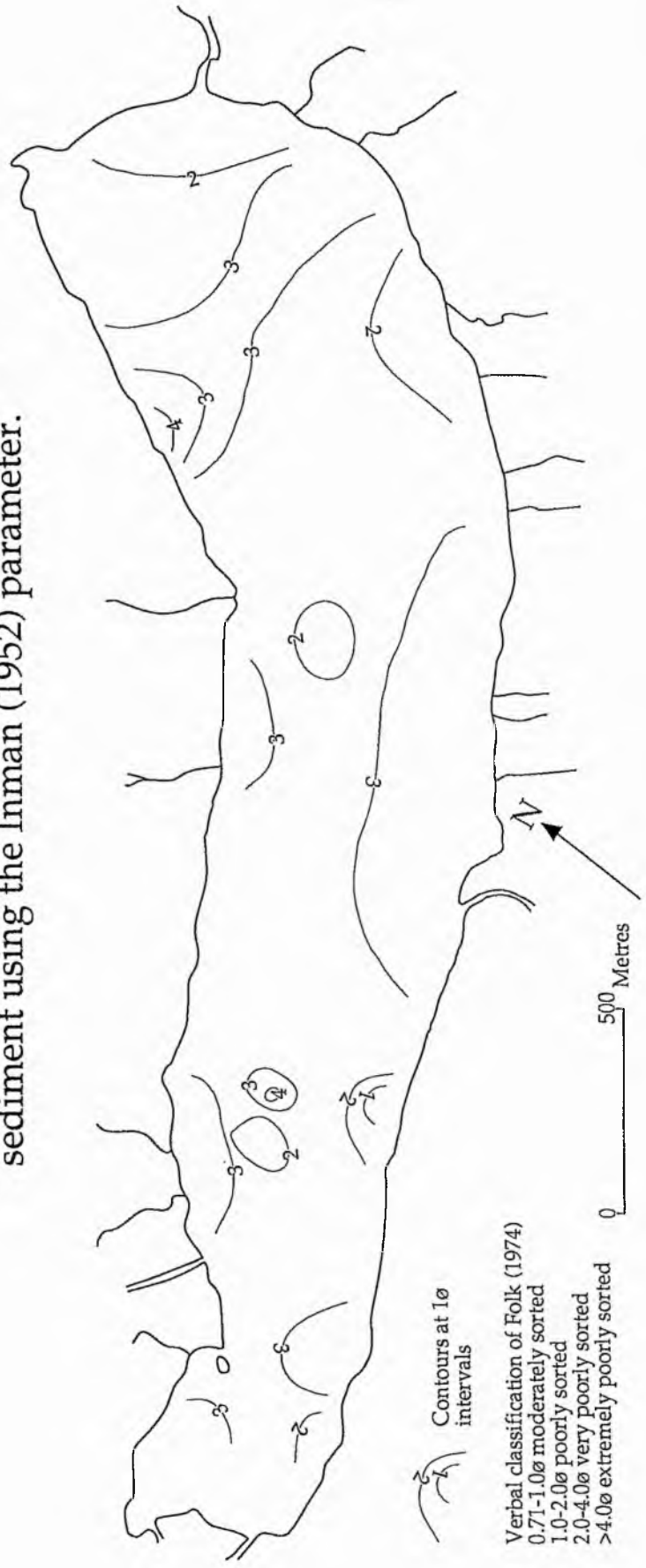


Figure 5.27
241

LOCH MUICK

Distribution map of Second σ Skewness Measure of surface sediment using the Inman (1952) parameter

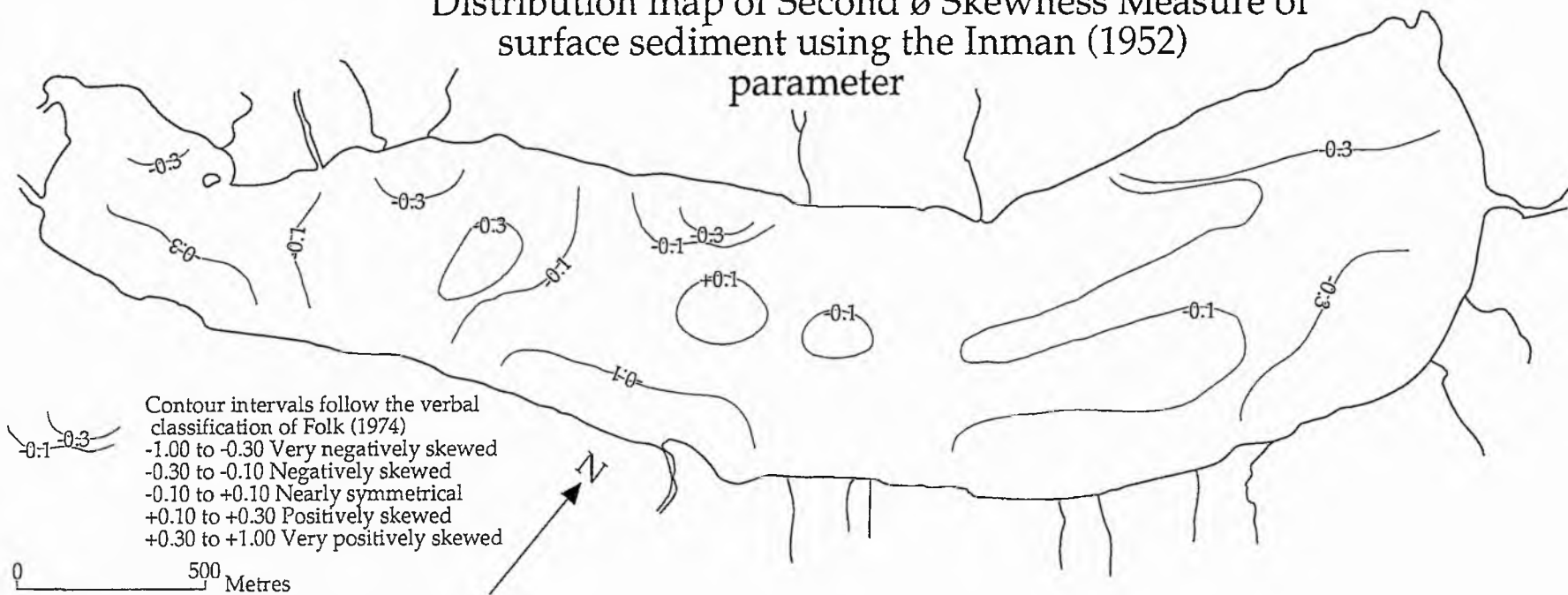


Figure 5.28
242

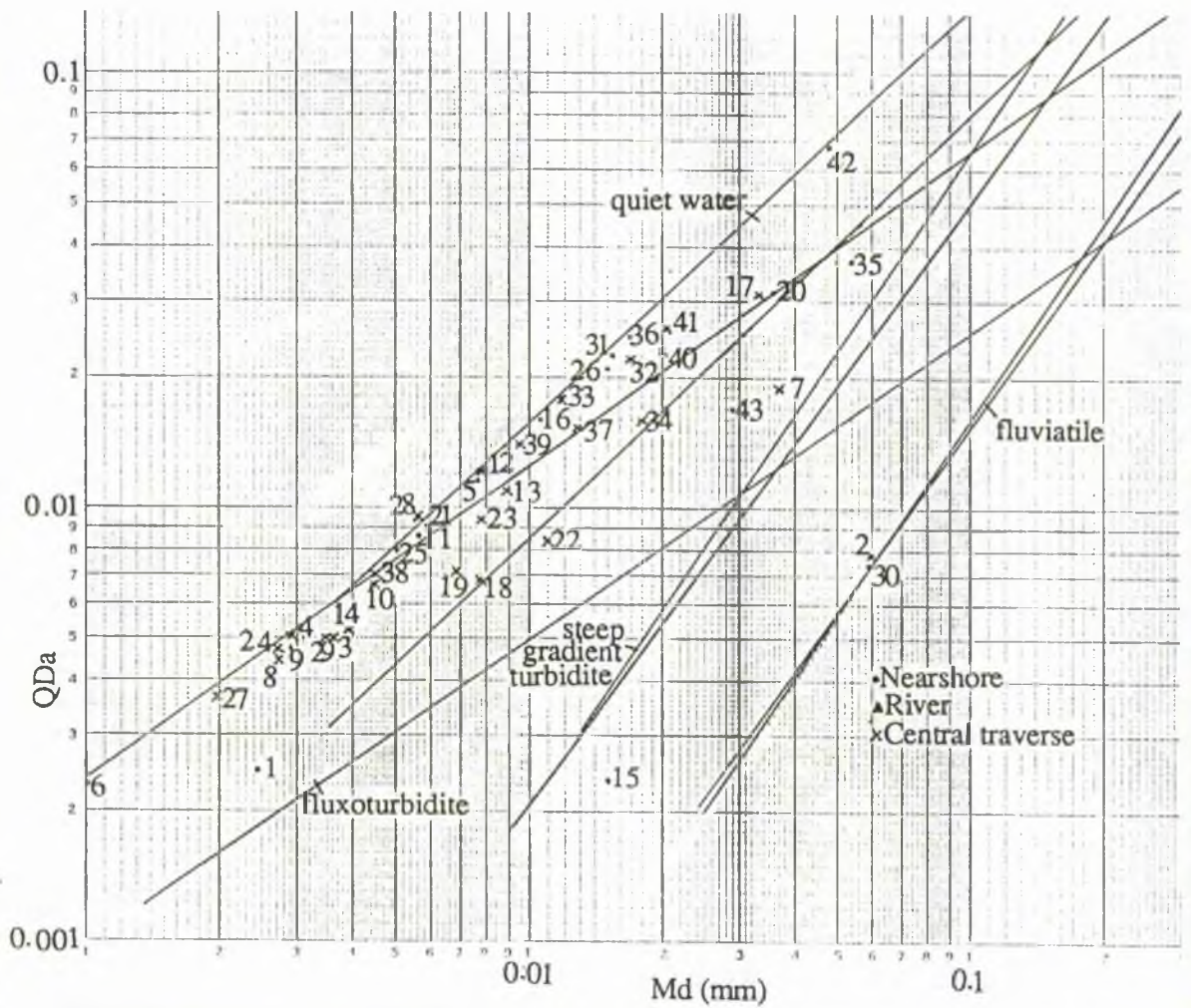


Figure 5.29 Loch Muick: Q_{Da} - M_d plot showing the environmental trend envelopes of Buller and McManus (1972, 1973).



Plate 5.1 Van Veen grab in open position prior to sampling.
Note the teeth at the opening.



Plate 5.2 Van Veen grab in closed position with collected sample visible through viewing hatch.

CHAPTER 6

CORING PROGRAMME AND CORE ANALYSIS

6.1 INTRODUCTION

In this Chapter are presented the data and methodology of analyses undertaken on bottom sediment core material obtained from Lochs Callater and Muick. These analyses comprise visual description, particle size, water content, total organic matter, elemental composition (total extractable Na, K, Ca, Mg, Mn, Fe, Al), mineral composition, X-radiography and pollen content. Descriptions of the coring procedure and analytical data are given. Units of climatic and environmental influence are identified and an environmental reconstruction of each loch catchment is presented.

6.2 METHODOLOGY : AIMS

Sediment cores were obtained from Lochs Callater and Muick. Coring was attempted in Loch Lee, but all attempts failed (see section 6.2.1.1 below). Three different coring devices were used - Russian peat borer, Mackereth corer, and a piston corer. The aim of the coring programme was to :-

- i) Establish down core variations in water content (Loch Muick only), total organic matter, particle size, total extractable elemental composition (total extractable Na, K, Ca, Mg, Mn, Fe, Al), mineral composition, structure and composition (by X-radiography, in Loch Muick only), and pollen content and type (Loch Callater only).
- ii) Complement echosounder (Chapter 2), subbottom profiling (Chapter 3), sidescan sonar (Chapter 4), and surface sediment (Chapter 5) data.
- iii) Enable a palaeoenvironmental reconstruction to be made based upon sedimentary evidence from the cores.

6.2.1 Coring procedure

Three coring techniques were used in investigations of the subbottom sediments of Lochs Lee, Callater and Muick. The simplest is the Russian peat borer which comprises a half cylinder, 50cm long, attached to a series of detachable rods (Figure 6.1). During coring operations the apparatus is pushed into the sediment to sampling depth and the borer rotated through 180° against an anchor plate which protrudes into the sediment, thus remaining stationary. An undisturbed half cylinder of sediment is held against the anchor plate, bisected by a fin. The sample obtained is then transferred to polythene sheeting. Sample rigidity is maintained by a short section of plastic guttering supporting the sample over which the sheeting is rolled, and the sample sealed and labelled. The core is obtained in 50cm sections, the depth of which can be determined by measuring the length of rod used in sampling.

The second technique used was the 1m piston corer. This comprises a coring tube containing a plastic core liner with a hydrodynamically streamlined nose cone which fits within the opening. The apparatus is suspended on a rope, attached to a triggering device, and lowered to approximately 5m above the surface to be cored. The trigger is then released and the corer free-falls to the bottom. On reaching the bottom the nose cone is pushed inside the core liner as the core tube is embedded in the sediment. The corer is then extracted by manual pressure on the rope, and the core liner containing the sediment core removed, sealed and labelled. To continue coring a fresh liner is inserted and the nose cone re-positioned.

The final corer used was the 6m Mackereth corer. This corer is of the stationary piston type (Mackereth, 1958). It is connected to a gas supply (nitrogen) by reinforced plastic tubing and lowered to the loch floor so that the anchor chamber (see Plate 6.1) settles into the surface sediment. Air is then extracted from the anchor chamber until it lies flush with the sediment surface and the coring barrel and outer casing protrude vertically into the water above it. Gas is then introduced into the core barrel casing, driving the core

barrel into the sediment. When the barrel reaches its maximum extent of penetration, gas enters the anchor chamber causing it to rise rapidly from the bottom, removing the extended core barrel and projecting it to the water surface. The corer can then be retrieved.

6.2.1.1 Loch Lee

Attempts at coring in Loch Lee failed due to insurmountable technical problems with the piston corer. Numerous attempts were made to obtain samples. However, all failed, as the triggering mechanism would not operate. Adjustments carried out both in the field and in the workshop did not result in any core material being obtained, nor any evidence that sediment had been lost from the barrel. It is not believed that the problems resulted from a hard loch floor surface as surface samples indicate that mud and silt occur throughout the loch (see Chapter 5, section 5.3.3). Moreover, coring attempts were made over a wide area.

Other coring methods, used on Lochs Callater and Muick, could not be undertaken in Loch Lee. The Russian peat borer used in Loch Callater is operated by a series of rods (see section 6.2.1.2 below), which restricts coring operations to shallow water (approximately 8m). The Mackereth corer used in Loch Muick was unfit for further coring following its retrieval from Loch Muick (see section 6.2.1.3 below).

6.2.1.2 Loch Callater

Two cores (one incomplete) were obtained from Loch Callater during July 1990 using a Russian peat borer operated between two inflatable dinghies anchored to the loch floor. Radio position fixing was impossible for the reasons given in Chapter 2, (section 2.5.2). However, accurate position fixing was possible through a combination of dead reckoning, depth sounding with the borer rods and reference to the bathymetric chart (Figure 2.9). A complete second core was not collected, but a single sample was obtained as a duplicate for analytical purposes. This section was obtained by driving the corer down

until further penetration was impossible and a 'basal' sample was taken.

The identification of coring positions was restricted by the length of rods available. Geomorphological evidence suggests that the entire loch was glaciated, therefore this restriction did not impose significant constraints. On these grounds two sites were selected at the extremities of the loch. Core 1, the complete core, 440cm long, was obtained in the small northwestern basin on an inclined slope angle of 12-15° at a water depth of 7.5m. Core 2 was taken in the northeastern basin in a water depth of 5.2m, on a sub-horizontal slope (0-1°, Figure 6.2).

6.2.1.3 Loch Muick

Coring in Loch Muick was undertaken during October and November 1990 using a 6m Mackereth corer from R.V. Mya and an inflatable dinghy (Plate 6.1). When the corer was deployed it did not rise to the surface on entry of air to the anchor chamber. Bubbles were observed breaking at the water surface. These were due to gas escaping from the anchor chamber through a broken air seal. Therefore the corer had to be lifted by other means. Attempts at dragging it from the bottom by forward propulsion of 'Mya' failed, so the corer was marked with a buoy awaiting further attempts. Finally, in late November, the apparatus was raised through the attachment of the lowering rope to air chambers which were sunk, refilled with air, the rope shortened and retied. This procedure continued until manual tension on the rope could be felt to move the corer. The corer was tied to the stern of 'Mya' and dragged into shallow water for manual recovery. The entire coring procedure took approximately 3 weeks and resulted in the recovery of 500cm of core material. Poor weather, access restrictions and damage to the equipment prevented further use of the Mackereth corer.

The location of the core site (Figure 6.9) was selected from the Pinger seismic reflection profiling records. Two sites, 'inside' and 'outside' the possible Loch Lomond Readvance glacier margin, as identified from echosounder data, were originally proposed for coring. However, as explained above, only at the 'outside' site was cored successfully

6.3 ANALYTICAL TECHNIQUES: DOWN CORE SAMPLES

6.3.1 Sampling procedure

Wet sediment sub-samples were taken at 10cm intervals downwards from the top of the two complete cores (Callater and Muick) using a 5cm³ syringe chamber with the nozzle removed. These sub-samples were placed into labelled crucibles of known weight and were subjected to water content (Loch Muick only), total organic matter content, and particle size analyses. A second set of sub-samples were removed by spatula at approximately the same positions and placed in labelled containers for subsequent chemical analyses.

6.3.2 Determination of water content

The water content of the sub-samples from Loch Muick was determined following the technique given by Eberli (1984). The sub-samples, obtained by filling the chamber of an adapted syringe (see section 6.3.1 above), were extruded into crucibles of known weight which were reweighed and immediately placed in a drying oven set at 105°C for 48 hours. The crucibles were then removed and placed in desiccating chambers for approximately 10 minutes to cool. After cooling the sub-samples and crucibles were reweighed and the weight loss noted. The water content of each sub-sample was calculated from these data.

This analysis was not undertaken for samples taken from the Loch Callater core due to the longer storage time prior to analysis. It is believed that lateral redistribution of water had occurred along the core rendering application of this analysis inappropriate.

6.3.3 Total organic matter content

The materials of known weight remaining after determination of water content were analysed for total organic matter following the technique given in Chapter 5 (section 5.2.2.1).

6.3.4 Particle size analysis

Particle size analysis was undertaken on the materials remaining after determination of total organic matter content. Due to the small amount of material available (approximately 2g), particle size analysis could not be carried out using the SediGraph and was therefore undertaken by a combination of sieving and Coulter Counter (Model TA II). The procedure is listed in Appendix N.

6.3.5 Elemental analysis

Total extractable element analysis of the sub-samples was undertaken using an atomic absorption spectroscope (Model PU900). The elements analysed (Na, K, Ca, Mg, Mn, Fe, Al) were selected on the basis of their value as palaeo-environmental indicators (Engstrom and Wright, 1984; Higgitt et al., 1991) and the availability of suitable hollow cathode lamps for the equipment. The methodology is given in Appendix O.

6.3.6 X-Ray diffraction

Material remaining after subsamples had been removed for elemental analysis was submitted for qualitative analysis of mineral composition by X-Ray diffraction (XRD). The methodology is given in Appendix P.

6.3.7 X-ray analysis of structure and composition

The core from Loch Muick was subjected to X-radiographic analysis which permits rapid, non-destructive analysis of sedimentary material, and can reveal structures not identified through visual inspection (Calvert and Veevers, 1962; Axelsson, 1983). Owing to the nature of the core sections from Loch Callater and the requirement of a relatively confined sample at the X-ray facility to maintain a hygienic environment, it was not possible to analyse the core. The plastic core barrel (total length 6m) was cut into four numbered sections. Each unextruded section was cleaned, identified, and subdivided through the application of lead painted number plates, which are opaque to X-rays, to the

core barrel. Following test exposures carried out to identify the optimum exposure dose and time, the entire core was analysed in sections at 52kV and 100mA for 0.05 seconds.

6.3.8 Pollen analysis

Samples were taken from the lower parts of the two cores from Loch Callater for pollen analysis, by Dr G.W. Whittington. No active participation in either sample preparation or pollen counting was made by the author, since considerable specialist skill and experience is required at both stages. However, resultant data are presented, with permission, from Dr. Whittington (Whittington, 1991).

6.4 LOCH CALLATER

6.4.1 Core description

The 440cm long core from Loch Callater was divided into two units on the basis of colour and visible textural variation.

Plate 6.2 illustrates the basal 30cm (410cm-440cm) of the core. The boundary between the Units 1 and 2 is recognised at a depth of 426cm. At this point there is an abrupt change in colour from brown (Munsell colour 5 Y 3/1) sandy silt to blue-grey (5 GY 5/1) silt. No stratification has been identified within the lower Unit, which experienced disturbance during transit. This colour change is unique within the Loch Callater core.

The upper Unit (2) extends from 426cm to 0cm and is composed of uncontorted, stratified, rich brown, organic sediments, within which terrestrial plant macrofossils of *Calluna vulgaris* and *Betula* are identified. Stratification, recognised by tonal variations in sediment colour, ranging from nearly black to olive green, varies in thickness from 1mm to 2cm.

6.4.2 Total organic matter

The percentage of total organic matter in the complete core obtained from Loch Callater ranges between 1.4% by weight at a depth of 440cm below the top of the core, and

44.1% at a depth of 50cm (see Appendix Q). The organic matter versus depth curve can be divided into three distinct sections according to the concentration of organic matter in each sample. The highest concentrations (30-44%) occur in the upper 90cm of the core (Figure 6.3). Below this depth the organic matter content falls by 14.1%, over a vertical distance of 30cm, to 18.7%. The second section has been defined spanning a vertical distance of 290cm between 120cm and 410cm below the top of the core. The organic matter in this section comprises between 17.3% and 24.7% of the total sample. The final section consists of the lower 30cm of the core where organic content falls significantly at a depth of 420cm from 14.2% of the total sample to 1.4% at 440cm.

6.4.3 Particle size

The data obtained were converted into percentages of sand, silt and clay and sediment textures were derived from the ternary diagram of Folk (1974) (see section 5.3.3; Figure 5.5). The down-core percentages of sand, silt and clay are shown in Figure 6.3, and the sediment textures are presented in Appendix Q. The core is composed entirely of silt and sandy silt. Silt is the dominant sediment type throughout the upper 360cm of the core. Peaks in the percentage of sand at depths of 100cm, 150cm, 210cm, 280cm, 320cm and 340cm form isolated 'spikes' of sandy silt. Between 370cm and 440cm sandy silt is the dominant textural type. Silt occurs within this section of the core at depths of 380cm and 440cm.

6.4.5 QDa-Md Analysis

Particle size data were processed following the procedure given in section 5.3.7 above. The data are given in Appendix R and presented as a graph (Figure 6.4) in which individual samples falling outside the main cluster of points may be located. Of the 45 data points plotted, the majority (42%) plot within the fluxoturbidite environmental trend envelope, and 38% within the steep gradient turbidite envelope. The remaining 20% are distributed as follows: 7% in the overlap between fluxoturbidites and steep gradient

turbidites; 7% in the quiet water envelope; 2% (one sample) in the fluvial environmental trend envelope, and 4% fall just outside the overlap between the fluxoturbidite and steep gradient turbidite envelopes. The single point which occurs in the fluvial environmental trend envelope represents the basal (440cm) sample. It is of note that the subsequent samples taken at 430cm and 420cm plot within the quiet water environmental trend envelope.

6.4.6 Elemental and mineralogical analyses

The data (presented in Appendix S) were plotted as graphs showing down core variation in total extractable elemental and mineral composition (Figures 6.5; 6.6).

6.4.6.1 Sodium

The concentration of sodium in the Loch Callater core ranges from 307.5 mg/kg at a depth of 420cm to 658.7 (180cm) (see Appendix S). The down core distribution of this element is distinctly irregular - composed of a series of peaks and lows in concentration (Figure 6.5). It is suggested that there is a slight trend towards lower concentrations of sodium towards the base of the core. This trend is identified from a depth of approximately 200cm.

6.4.6.2 Potassium

The concentration of potassium ranges between 2770mg/kg (430cm) and 905mg/kg (370cm) (Appendix S). Between 0cm and 360cm the majority of the samples contain concentrations in the range 1400-1700mg/kg (see Figure 6.5). Three significant peaks in excess of 2000mg/kg occur at depths of 80cm, 170cm and 190 cm, and two troughs of less than 1300mg/kg at 40cm and 180cm. Below a depth of 360cm the concentration of potassium falls by 590mg/kg over a distance of 10cm, rising to the maximum of 2770mg/kg over 60cm. Levels of potassium fall to 2462.7mg/kg at the base of the core.

6.4.6.3 Calcium

The variation in down-core concentration of calcium (Figure 6.5) ranges between 8011.4mg/kg (400cm) and 2505mg/kg at a depth of 40cm (see Appendix S). Calcium falls in concentration from a peak of 4481mg/kg at 10cm to 2505mg/kg at 40cm. Between 40cm and 400cm a general increase in concentration is recognised, upon which peaks and troughs are superimposed. Below 400cm a significant fall in the concentration of calcium from the maximum concentration of 8011.4mg/kg to 3788.4mg/kg is continuous over 40cm, to the base of the core.

6.4.6.4 Magnesium

In the upper part of the core the magnesium content averages 4000mg/kg with minor fluctuations. Superimposed upon this pattern, five peaks in concentration in the range 5000mg/kg to 5800mg/kg occur. Between 360cm and 430cm the magnesium content falls to a minimum of 2675mg/kg at 370cm, rising to 6425mg/kg, the second highest value, at a depth of 430cm. The basal sample shows a slight reduction in magnesium concentration to 5382.3mg/kg.

6.4.6.5 Manganese

The down-core profile of manganese can be divided into three distinct sections. First, between 0cm and 100cm (Figure 6.5) the levels of manganese range between 1224.5mg/kg and 1889.3mg/kg (Appendix S). The second section, between 110cm and 280cm, comprises a series of peaks and troughs ranging from 3375.0mg/kg to 10126mg/kg. The final section is composed of significantly lower concentrations of manganese falling almost continuously from 1626mg/kg at 290cm depth to 243.3mg/kg at the base of the core.

6.4.6.6 Iron

The concentration of iron ranges between 20888.7mg/kg (440cm) and

76610.5mg/kg (140cm) (Figure 6.5; Appendix S). The down-core iron profile can be divided into three sections. The upper section extends from 0cm to 110cm in which generally low levels of iron range from 25613.7mg/kg to 47953.1mg/kg occur. The central section is identified from 120cm to 400cm in which concentration falls from >70000mg/kg to 45000mg/kg. Within this section iron concentrations range from 40115mg/kg to 76610.5mg/kg. In the lowest section the iron concentration falls sharply to 20888.7mg/kg in the basal sample.

6.4.6.7 Iron/Manganese ratio

The down-core iron/manganese ratio ranges from 1.5:1 at a depth of 210cm to 85.9:1 at 440cm (Appendix S). The profile (Figure 6.5) has been divided into four sections. The uppermost division is composed of the top 100cm of the core, in which the ratio ranges between 16.8:1 and 30:1 and two minor peaks occur at 40cm and 80cm. The second section is recognised where the Fe:Mn ratio drops to 11.7:1 at 110cm and relatively low ratios in the range 1.5:1 to 16.9:1 are maintained to 280cm below the top of the core. The majority of the samples in this section fall within the 6:1 to 10:1 range. The maxima and minima referred to above form part of a peak and trough sequence between 190cm and 210cm. Section three comprises a 110cm section between 290cm and 390cm in which the ratio increases to between 24.2:1 to 43.5:1. The basal 50cm of the core form the final section in which the Fe:Mn ratio rises from 62.6:1 at the boundary to 85.9:1 at the base of the core.

6.4.6.8 Aluminium

The down-core concentration of aluminium ranges between 11390.2mg/kg at 440cm depth and 24225.4mg/kg at 150cm (see Appendix S, Figure 6.5). The elemental concentration has been divided into three sections. First, the upper 30cm of the core in which the level of aluminium is relatively high, ranging from 19286.5mg/kg at 10cm to 16768.5mg/kg at 30cm. The second section comprises a vertical distance of 50cm, between

40cm and 80cm (inclusive) in which aluminium levels fall to between 13565mg/kg and 14086.8mg/kg. The final section is composed of the remainder of the core, from 90cm to 440cm. The boundary between sections two and three is marked by an increase in aluminium concentration to a maximum of 24225.4mg/kg at 150cm from which point there is a down-core trend towards lower levels of the element, upon which relative peaks and troughs are superimposed, to the lowest concentration at the base of the core, where a level of 11390.2mg/kg is recorded.

6.4.6.9 Mineralogical composition

The X-ray diffraction data were analysed and the presence or absence of quartz, K-feldspar, plagioclase, illite, chlorite and kaolinite noted for each sample. This information is presented as a graph of down-core variation in mineral composition (Figure 6.6). Quartz and plagioclase have widespread down-core distributions and are both absent at two levels; 110cm and 260cm in the case of quartz, and 10cm and 370cm in the case of plagioclase. K-feldspar, illite and kaolinite have a discontinuous, but widespread distribution down-core. Chlorite is identified intermittently to 140cm below the top of the core and at 230cm and 310cm.

6.4.7 Pollen analysis

Pollen diagrams of the basal sections of Cores 1 and 2 are presented in Figures 6.7 and 6.8 (Whittington, 1991).

6.4.7.1 Core 1

In Core 1 Whittington (1991) recognised two local pollen assemblage zones (LPAZ) and a basal layer in which very low pollen concentrations did not permit valid interpretations to be made. The first LPAZ (LC(1)1) is identified from approximately 430cm, where the total organic matter comprises $\geq 10\%$ of the total sample, to 417cm. LC(1)1 is dominated by *Juniperus communis* and badly corroded *Betula* pollen with

significant inputs (10% maximum) of *Salix* and *Pinus* and lesser peaks in Filicales and *Dryopteris* type. The second LPAZ (LC(1)2) is recognised from approximately 415cm depth where a significant decline in the input of *Juniperus* occurs and *Corylus-Betula* gain dominance. Thermophilous taxa including *Pinus*, *Quercus*, *Ulmus* and *Alnus* are also present in this zone.

6.4.7.2 Core 2

This partially complete core (for location see Figure 6.2) reached a maximum penetration of 650cm below the loch floor surface. The basal sediments contain sparse pollen, replaced by polleniferous silt at approximately 637cm which comprise the lowest *Corylus-Betula* LPAZ, (LC(2)1) (Whittington, 1991). Assemblage LC(2)2, dominated by *Corylus* pollen, lies above LC(2)1 at 628cm. This zone also includes low percentages of *Ulmus* and *Quercus* and the decline of *Salix*. The uppermost pollen zone in Core 2 (LC(2)3) is recognised between 609cm and the top of the core where *Pinus* dominates and *Corylus* is in decline.

6.5 LOCH MUICK

6.5.1 Core description

Two units have been recognised in the Loch Muick core on the basis of colour and textural variation.

Unit 1 comprises the basal 25cm of the core (475-500cm) and is composed of unstratified blue-grey silt (Munsell colour 5 GY 5/1). Unit 2 extends from 0cm at the top of the core to 475cm. It is composed of dark brown organic mud within which plant macrofossils of *Calluna* and *Betula* have been recognised. Stratification of the organic mud, ranging in thickness between 1mm and 1cm has been identified from tonal and textural variation. Light-coloured laminae composed of sand and olive green to nearly black

organic-rich layers have been identified within this unit. The boundary between Units 1 and 2 is irregular and unconformable. The uppermost section of the core (approximately 50cm) and basal 50cm was lost during the protracted recovery process.

6.5.2 X-radiography

Plate 6.3 illustrates the X-ray negatives of the entire Loch Muick core. X-ray dosage exhibits lateral variation. The maximum dosage is apparently delivered to the extremities of each section irradiated, resulting in the cyclical lightening of the record at the margins between sections. The 500cm long core has been divided into three lithostratigraphic units on the basis of visual analysis.

6.5.2.1 Unit 1 475cm-500cm

Unit 1 is composed of high density sediment within which no internal structure or coarse clastic content has been recognised from visual examination of the radiographs. The boundary between Units 1 and 2 is unconformable and irregular (Plate 6.3).

6.5.2.2 Unit 2 187cm-475cm

The sediment of Unit 2 is fine grained, stratified, has a medium density and is broken by numerous small fractures which appear as linear, bifurcating or wavy low density (black) lines. It is believed that these were caused by the bending of the core barrel during recovery and transport of the equipment. Within this unit numerous clasts, with long axes of up to 9mm (i.e. pebbles), are distributed apparently randomly. These clasts have been identified as granite, almost certainly of local (Lochnagar complex) origin. High clastic concentrations are recognised between 263cm and 290cm and 328cm and 337cm. Stratified, coarse grained material is also present at 187cm, 197cm and 462cm. The basal 15cm of Unit 2, excluding the coarse grained layer, exhibits laminae and layers of fine grained material. Between 470cm and 475cm sediment density variations enable the

identification of laminations. The upper boundary with Unit 3 is gradational over approximately 5.5cm, but for the purposes of this description is recognised at 187cm, where a coarse grained layer is identified.

6.5.2.3 Unit 3 0cm-187cm

This unit is composed of fine laminae and layers of varying density, ranging in thickness from 1mm to 5mm. Scattered, rounded clasts, with a maximum diameter of 3mm (i.e. granules), occur throughout this unit. Two dipping layers, identified at depths of 65cm and 69.5cm, exhibit concentrations of fine grained clastic material composed of granite (probably Lochnagar complex), with a maximum diameter of 2mm. From 26.5cm to 30.5cm, a stratified, lighter band represents higher density sediment. Similar layers are recognised between 56.5cm and 57cm, 117 and 117.5cm and 163 and 163.5cm. Low density layers, within which no lamination has been identified occur between 144.5cm and 150cm, 159cm and 160cm and 176cm and 176.5cm.

6.5.3 Water content

The down-core variation in water content is presented in Figure 6.10 and Appendix T. The data permit the core to be divided into two sections. The upper section (0cm to 430cm) comprises sediment typically composed of between 70% and 80% water content by weight. At a depth of 200cm the water content drops to 56.7% and at 210cm peaks at 85.8%, the maximum value measured in this core. The lower section is formed of the basal 70cm of the core in which the water content drops from 55.7% at the boundary between sections to 28.9% at 440cm. There is a range in water content in this section of 7.7%, between 30.5% (at 470cm below the top of the core) and 22.8% at a depth of 490cm.

6.5.4 Total organic matter

Total organic matter in the Loch Muick core ranges from 0.04% by weight to 55.5% at a depth of 490cm (Appendix T). The graph of down-core variation in total

organic matter (Figure 6.10) has been divided on the basis of visual examination into two sections. The first section comprises the upper 380cm of the core, in which the organic content of the sediment ranges between 20% and 37% of the total. One peak of 55.5% at a depth of 0cm and three troughs (13.4% at 200cm, 13.4% at 340cm and 17.4% at 350cm) are superimposed upon this section. The lower section extends from 390cm to the base of the core and is composed of sediment with a significantly lower organic matter content. This ranges from 19.6% at the boundary, decreasing to 0.04% at a depth of 490cm.

6.5.5 Particle size

The particle size data were processed as in section 6.4.3 above. The textural data are given in Appendix T, and presented as a down-core frequency graph in Figure 6.10. The sediment comprises combinations of sand and silt; namely silt, sandy silt and silty sand. The upper 110cm of the core is dominated by silt, with a significant, intermittent sandy silt input. From 120cm to 440cm the silt dominance is replaced by sandy silt, which comprises 73% of the samples in this section. Minor, isolated, layers of silty sand and silt occur within the sandy silt. From 450cm, to the base of the core at 500cm, the core is composed entirely of silt.

6.5.6 QDa-Md Analysis

The particle size data were processed as in section 5.3.7 above, and are presented in Appendix U and Figure 6.11. Four environmental trend envelopes are superimposed upon the data points in Figure 6.11. The majority of samples (58%) fall within the fluxoturbidite envelope and a total of 8%, evenly distributed, in the overlap zones between the fluxoturbidite and quiet water and steep gradient turbidite envelopes. Of the remaining 34% of samples, 10% plot within the quiet water envelope, 10% within the overlap zone between the steep gradient turbidite and fluvial envelopes, 6% fall within the steep gradient turbidite envelope and 8% (four samples) plot just outside all the environmental trend envelopes. There is no apparent correlation between the depths from which samples were obtained and the distribution of points between envelopes.

6.5.7 Elemental and mineralogical analyses

The elemental data are presented in Appendix V and as graphs of down-core total extractable elemental concentration in Figure 6.12.

6.5.7.1 Sodium

The down-core concentration of sodium ranges between 253.7mg/kg at a depth of 300cm below the top of the core and 586.1mg/kg at 390cm. The graph (Figure 6.12) shows a distribution composed of peaks and troughs in the sodium levels, having a maximum range between peak and trough of 210.4mg/kg between 220cm and 230cm. The general down-core curve comprises relatively low concentrations, in the range 300mg/kg to 360mg/kg, at the top of the core, rising to the highest value in this section of 542mg/kg at a depth of 250cm. From 250cm to 370cm there is a decline in sodium concentration which includes the minimum value identified in this core. The final section comprises an increase in concentration and subsequent decline, forming a series of peaks and troughs which rise to the maximum value at 390cm and fall to 314mg/kg at the base of the core.

6.5.7.2 Potassium

The down-core variation in concentration of potassium (Figure 6.12) (Appendix V) can be divided into two sections. The upper section, between 0cm and 410cm, is characterised by sediments which have potassium levels dominantly in the range 600mg/kg to 1200mg/kg. Upon this background three major peaks at 100cm (1402.9mg/kg), 270cm to 280cm (1494mg/kg) and 310cm (2155mg/kg) and one major trough (111.6mg/kg at 180cm depth) are superimposed as well as numerous minor features. The lower section, from 420cm to 500cm, is identified as occurring from the peak formed by the maximum concentration (2978.2mg/kg). Within this section the peaked distribution shows a general downward trend as troughs fall from 2056.4mg/kg at 460cm to 1845.2mg/kg at 490cm.

6.5.7.3 Calcium

The down-core calcium concentration shows a gradual increase from values in the range 1100mg/kg to 1200mg/kg at the top of the core, to 1700mg/kg to 1900mg/kg between 320cm to 360cm, and a subsequent decrease to 1200mg/kg to 1600mg/kg at 490cm. Calcium concentrations range between 854mg/kg at a depth of 270cm to 2135mg/kg at 310cm. These values, plus one other peak of 2130mg/kg at the top of the core, represent significant departures from the norm in the down-core concentration of calcium. The basal sample at 500cm shows a slight increase in calcium concentration to 1773.2mg/kg.

6.5.7.4 Magnesium

The down-core magnesium profile has been divided into two sections on the basis of elemental concentration. In the upper section of the core to 400cm there is a steady decrease in magnesium concentration from approximately 1600mg/kg to 850mg/kg although some fluctuations are recognised around 300cm. Below 400cm the magnesium content rises sharply to a maximum of 4566.3mg/kg at 450cm before falling away towards the core base.

6.5.7.5 Manganese

The concentration of manganese in the Loch Muick core ranges from 252.9mg/kg at a depth of 490cm to 5243.7mg/kg at 140cm. The down-core profile, which forms an almost bell-shaped curve, is composed of numerous peaks. There is a trend towards higher manganese levels to a depth of 140cm. Below this point the elemental concentration declines gradually over 280cm through a series of peaks and troughs to 1070mg/kg. The basal 70cm shows a steep decline in manganese levels to <300mg/kg at the base of the core.

6.5.7.6 Iron

The down-core, almost bell-shaped, iron profile exhibits an increase from 27050mg/kg at the top of the core to 77816.5mg/kg at a depth of 60cm. Between 80cm and 180cm the iron concentration stabilises at a plateau of 60000mg/kg to 71000mg/kg, broken by one peak to 81194mg/kg at 140cm. At 210cm the iron level peaks at 104108.2mg/kg, falling irregularly to the lowest concentration of 11413.6mg/kg at 490cm. Within this declining concentration a significant trough to 30839.1mg/kg, represents a variation of 51996.7mg/kg over a vertical distance of 10cm between 260cm and 270cm.

6.5.7.7 Iron/Manganese ratio

The iron/manganese ratio ranges from 8.9:1 at the top of the core to 45.1:1 at a depth of 490cm. The down-core curve comprises two sections. The upper 400cm is composed of relatively low ratios between 8.9:1 and 24.4:1, the majority of which fall within the range 14.5:1 to 20:1. The second section is characterised by higher ratios, the majority falling between 30:1 and 45.1:1.

6.5.7.8 Aluminium

Aluminium concentration exhibits a markedly peaked down-core distribution. The curve (see Figure 6.12) shows an increase in elemental levels from 11525mg/kg at 0cm to the maximum of 18691.5mg/kg at 140cm, followed by a decline, composed of peaks and troughs attaining a minimum of 18691.5mg/kg, to the bottom of the core.

6.5.7.9 Mineralogical composition

The X-ray diffraction data were analysed according to the method described in section 6.4.6.9 above, and are presented in Figure 6.6. Quartz, K-feldspar and plagioclase exhibit widespread occurrence throughout the core. The down-core distribution of illite is divided into three disparate groups occurring between 0cm and 110cm, 230cm to 320cm

and 420cm to 500cm. Illite occurs in 17 of the 51 samples. Chlorite shows a similar distribution to illite, but has a lower frequency, occurring in 10 samples. Kaolinite is present in the basal 70cm of the core, and in two samples at 190cm and 210cm.

6.6 DISCUSSION

6.6.1 Introduction

6.6.1.1 Depth-time profiles in core material

Radiometric dating techniques have not been applied to the core material obtained from Loch Callater or Loch Muick, thus the depth-time profiles are unknown. However, in the case of the entire Loch Callater core, and the upper 475cm of the Loch Muick core, there is no visible evidence of unconformities (see sections 6.4.1, 6.5.1). Therefore, it is assumed throughout that, given the information above, the cores obtained are complete and conformable and that the thickness of sediment accumulated is broadly time dependent.

Non-linear depth-time scales may result from numerous topographic, climatic and anthropogenic inputs. Evidence from the English Lakes (Pennington, 1981) indicates that non-linear depth-time scales occur synchronously with early agricultural practices, at approximately 5kaBP. Pennington (1981) suggests that:-

'The degree of acceleration of the deposition rate appears to have been determined by a combination of variables - intensity of local land use in prehistoric time, availability of soils vulnerable to intensified erosion (particularly peat) and the size of lake.'

Linear scales are reported from remote lochs in northwest Scotland (Pennington et al., 1972) where anthropogenic modification of the loch catchment has been minimal. Taishi et al. (1991) have identified sedimentary anomalies in down-core ^{210}Pb data from Lake Biwa, Japan, due to episodic sedimentation associated with intense rainfall in the lake catchment. Mass movements of unconsolidated lake sediments are widely reported (e.g. Smith, 1959; Mackereth, 1965; Thompson and Kelts, 1974; McManus and Duck, 1983; Hicks et al.,

1990). Slumped material was identified in a core taken from Lake Zug, Switzerland, through the measurement of magnetic susceptibility (Thompson and Kelts, 1974). Significant to this research project in these findings was that differentiation of slumped material by visual examination and mineralogical analysis was not possible.

6.6.1.2 Geochemical stratigraphy

Geochemical analysis provides a method for environmental reconstruction based upon the minerogenic component of core material. Mackereth (1965, 1966) undertook pioneering analyses of sediment taken from cores obtained from the English Lakes. Lake sediments were regarded as 'A sequence of soils derived from the drainage areas of the lakes' (Mackereth, 1965) from which the erosional history of the catchment could be reconstructed. However, difficulties arise in the interpretation of geochemical profiles. Problems in interpretation result from the difficulties in establishing the provenance of mineral matter and post-depositional diagenetic changes (Engstrom and Wright, 1984).

Sodium, potassium, magnesium and calcium are primarily derived by erosion of rocks and soils in the catchment, thus they provide important indicators of weathering, erosion, and soil development (Engstrom and Wright, 1984; Walker and Lowe, 1990; Higgitt et al., 1991). During periods of intensified erosion, the breakdown of soils should result in an increase of these alkali and alkali-earth elements. However, this is complicated by the fact that calcium bonds with organic ligands (e.g. humic and fulvic acids) and has, infrequently, been reported by some researchers as showing a positive relationship with organic matter (e.g. Mackereth, 1966; Walker and Lowe, 1990).

Aluminium is also principally derived by erosion and leaching of bedrock and soils. Solubility of this element is pH dependent, rising significantly when soil pH falls below 5.

The interpretation of down-core iron and manganese concentration variations is notoriously difficult and may deter the undertaking of these analyses. The problems in interpretation are due to quantifying first, the mobility of these elements under certain

conditions, and secondly, post-depositional diagenetic processes. Detailed research on the mobility of these elements extends beyond the broad aims of these analyses within the context of this thesis and is therefore not considered further.

The iron and manganese content of lake sediments is determined by two factors, first, the conditions in the catchment, and secondly, the conditions in the lake. These two elements are derived directly from bedrock erosion or the breakdown of soils (particularly the B horizon, in which concentration may occur). The delivery rate of iron and manganese to the lake basin is dependent on the redox conditions of the soil. During oxidising conditions both elements remain stable and insoluble. On the development of reducing conditions, which can be produced by waterlogging, or the build-up of undecomposed humus on the soil surface, manganese is preferentially removed from the soil. Thus the ratio between iron and manganese is indicative of the redox conditions of soils within the lake catchment (Mackereth, 1966). Studies of sediment from Loch Scionasciag, Sutherland (Pennington et al., 1972) lend support to this hypothesis. The development of blanket peat and waterlogged soils at approximately 5kaBP was found to be synchronous with an increase in the iron and manganese content of the lake sediment.

Deposition of iron and manganese in the lake environment is also dependent on the nature of the bottom waters. Oxygenated bottom waters lead to deposition of the elements onto the surface muds as hydrated oxides and coagulates of humic organic complexes (Engstrom and Wright, 1984). Below the surface typically only the top few centimetres are oxidised below which reducing conditions pertain, caused by microbial activity. Thus iron and manganese may be remobilised and migrate within the sediment column. Exceptions to this occur when rapid sedimentation effectively seals an enriched layer (Engstrom, 1983). The enriched surface layer should therefore be discounted for the purposes of palaeoenvironmental reconstruction. Iron and manganese ratios have also been used in an attempt to define the palaeoredox conditions of lake bottom waters (e.g. Mackereth, 1966; Digerfeldt, 1975). However, this is beyond the scope of this thesis and will not be examined further.

6.6.2 Loch Callater

6.6.2.1 Correlation between variables

Values of Pearson's Product Moment Correlation Coefficient were calculated for the core sediment sample variables following the method given in section 5.6.1 above. The data obtained are presented in Table 6.1. At the 0.2% confidence level a correlation between any two variables is significant at $r=+/-0.444$ for 46 samples; at 1%, $r=+/-0.376$, at 2%, $r=+/-0.342$, at 5%, $r=+/-0.291$, at 10%, $r=+/-0.246$ and at 20%, $r=+/-0.192$.

The strongest positive correlations (at the 0.2% level) are between depth and calcium content, potassium and magnesium and iron and manganese. A weaker positive correlation ($r=0.415$) exists between iron and aluminium and at the 2% level between aluminium and calcium. Strong negative correlations (at the 0.2% level) occur between total organic matter and depth and percentage sand and percentage silt sized particles. Weaker ($\leq 2\%$ level) negative correlations exist between total organic matter and calcium and potassium and calcium.

6.6.2.2 Interpretation of data

The core obtained from Loch Callater presents a complex image of temporal environmental change. Visual, particle size and organic matter analyses of the core material indicate that there have been two major episodes in the history of Loch Callater. Following the report of Pennington, (1977), tentative interpretations are given for iron and manganese concentrations, elements which may have experienced post-depositional diagenetic and migrational change (see section 6.6.1.2).

6.6.2.2.1 Unit 1

This unit, which extends from the base of the core at 440cm to 426cm, is composed of minerogenic blue-grey silt. QDa-Md analysis suggests that silt at the base of the core was deposited under the influence of currents in the water column. Subsequent samples from this unit plot within the quiet water and virtually coincident fluxoturbidite envelopes. Unit 1 can be identified on the majority of chemical profiles (Figure 6.5). During this

Table 6.1
Loch Callater
Pearson's Product Moment Correlation Coefficient for core sediment variables

	Depth (cm)	Sand (%)	Silt (%)	Clay (%)	T.O.M (%)	Na (mg/kg)	K (mg/kg)	Ca (mg/kg)	Mg (mg/kg)	Mn (mg/kg)	Fe (mg/kg)
Sand (%)	0.298										
Silt (%)	-0.047	-0.484									
Clay (%)	0.236	-0.152	0.114								
T.O.M (%)	-0.788	-0.289	0.001	0.062							
Na (mg/kg)	-0.326	-0.099	-0.278	-0.124	0.228						
K (mg/kg)	-0.010	0.007	0.099	-0.137	-0.341	-0.013					
Ca (mg/kg)	0.678	0.119	0.098	0.253	-0.305	-0.090	-0.409				
Mg (mg/kg)	-0.163	-0.105	0.187	-0.101	-0.169	0.128	0.884	-0.339			
Mn (mg/kg)	-0.109	-0.053	0.045	-0.173	-0.131	0.039	-0.003	-0.119	0.060		
Fe (mg/kg)	-0.081	0.018	0.122	-0.206	-0.191	0.185	-0.129	0.118	-0.037	0.467	
Al (mg/kg)	0.018	0.034	0.089	-0.046	-0.097	0.018	-0.298	0.348	-0.137	0.293	0.415

period the input of sodium, calcium, magnesium, manganese, iron and aluminium was relatively low and that of potassium and magnesium was high. The iron/manganese ratio was also high, suggesting either the occurrence of reducing conditions in the lake, resulting in the preferential migration and removal of manganese, or a greater availability of iron for removal by erosion. It is suggested that the latter hypothesis be accepted on the grounds that the low organic content of the sediment would be unlikely to harbour a population of bacteria of a size great enough to produce reducing conditions. The basal 10cm of the core is characterised by very low pollen concentrations. The basal LPAZ LC(1)1 in the complete core (1), between 430cm and 417cm, is dominated by species tolerant of poor soils and cold conditions. This is not typical of early Holocene recolonisation, in which dominant taxa include *Rumex*, *Artemisia*, Cyperaceae and Ericaceae, subsequently replaced by a *Juniperus*-Graminae assemblage. Pollen analyses of minerogenic layers obtained from upland sites in Britain (e.g. Walker, 1975, eastern Grampians; Lowe and Walker, 1977, south and east Grampians; Gray and Lowe, 1977, Scotland; Walker and Lowe, 1990, Skye) have reported low pollen concentrations dominated by sedges and grasses typical of tundra vegetation.

These data suggest that, at the time of deposition of the blue-grey silt, vegetation cover and soil development was minimal and that the source for the silt sized particles was the local bedrock. The last major climatic change in this area was the Loch Lomond Stadial which occurred between approximately 11-10kaBP (see Chapter 1), when Sissons and Grant (1972) proposed that glacial ice extended down Glen Callater, covering the area now occupied by Loch Callater. The occurrence of a single layer, or two layers of minerogenic silt or clay separated by an organic layer, is widely reported from lakes throughout highland Britain (e.g. Sissons et al., 1973, Grampians; Tinsley and Derbyshire, 1976, Peris-Padarn, Wales; Coope and Pennington, 1977, Windermere, English Lakes; Pennington, 1977, northern Scottish lochs; Walker and Lowe, 1990, Skye). The tripartite sequence of clay, organic mud, clay encountered outside the limits of former Loch Lomond Readvance glaciers in infilled basins was first interpreted by Sissons et al., (1973). This

sequence is widely accepted as representing basal Devensian minerogenic deposition upon which organic sediment was deposited during the Lateglacial Interstadial, followed by a final layer of minerogenic sediment laid down during the Loch Lomond Stadial. Where glaciers occupied the site of a basin during the Loch Lomond Stadial, a single minerogenic layer dating from this period is encountered lying upon glacial diamict. Cores extending to glacial diamict are occasionally obtained. However, the tenacity of the minerogenic silt or clay and clast content of glacial diamict make coring and recovery difficult. Contemporary deposition of proglacial lacustrine minerogenic silt and mud transported by proglacial meltwater streams is reported from contemporary glacierised catchments (e.g. Pickrill and Irvine, 1983; Hicks et al., 1990; Mangerud and Svendsen, 1990).

Thus the silt forming the lower unit of the Loch Callater core is interpreted as proglacial lacustrine silt deposited both directly (at a depth of 440cm), and indirectly by settling through the water column, by sediment-charged, proglacial melt water streams. The absence of a coarse grained input is interpreted as indicating that the core site was at a relatively ice-distal position when the silt was deposited. This hypothesis does not require the complete retreat of the glacier from the area now occupied by Loch Callater. Assuming that the ridge which bisects the loch at the northwestern end (see Chapter 2, section 2.5.3.1) existed at the time of silt deposition, the southeastern basin would have acted as an effective sediment trap for coarse grained material, leaving only fine particles available for deposition in the northwestern basin. It is suggested that the variation in environments of deposition (fluvial versus quiet water and fluxoturbidite) may result from the temporary diversion of the meltwater current, possibly by the grounding of remnant icebergs against the ridge that divides the loch.

6.6.2.2.2 Unit 2

The second unit, which extends from 0cm-426cm, is characterised by a major change in the characteristics of the majority of analysed variables. The organic matter content of the sediment increases, the dominance of silt sized particles is replaced by sandy

silt, there are increases in the concentration of sodium, calcium, iron and aluminium, and a decrease in the iron/manganese ratio and the concentration of magnesium and potassium. Mineralogically there is an increase in the input of chlorite in the upper part of the core. QDa-Md analysis reveals that the majority of samples were deposited by two processes; weak currents (sediments in the fluxoturbidite envelope) and by deceleration of turbidity currents on lower slope angles (sediments in the steep gradient turbidite environmental trend envelope) (Buller and McManus, 1973).

These data are interpreted as indicating an amelioration in climate. From 415cm the chionophilous *Juniperus* assemblage is replaced by more thermophilous taxa dominated by *Corylus* and *Betula*, which is an assemblage typical of the early Holocene (e.g Tinsley and Derbyshire, 1976). However, the chemical data do not exhibit an immediate decrease in concentration synchronous with the amelioration in climate indicated from the pollen data. This implies that erosion and weathering of skeletal soils and bedrock in the loch catchment continued into the Holocene, and that a significant proportion of the pollen rain may have been blown into the catchment. The iron/manganese ratio decreases upwards from the base of the unit suggesting that, after the initial development of highly waterlogged soils and preferential manganese removal from the soils in the catchment, there was a progressive, relative improvement in soil drainage through time which caused the reduction in the ratio. The concurrent relative increase in the organic matter content, interpreted as resulting from peat formation and erosion, (see Pennington, 1977) lends further support to this interpretation. Manganese declines very sharply at a depth of 100cm below the top of the core, which is not mirrored in the iron content, causing a slight increase in the iron/manganese ratio which can be interpreted in two ways. First, as a return to oxidising conditions in the catchment reducing manganese mobility. However, the rapid fall in manganese concentration coincides with an increase in organic matter to a maximum of 44.1%. This high organic content is interpreted as indicating the continued existence of peat in the catchment which was subject to intensified erosion (see below, this section). Anaerobic, reducing, conditions are associated with the bacterial decay of organic matter.

Therefore, secondly, it is suggested that the relatively low manganese concentration in the upper part of the core results from remobilisation and removal from the loch system of the element, under reducing conditions.

Within the top 50cm of the core the geochemical profiles show increases in concentration which are interpreted as resulting from increased erosion. The cause of this erosion is believed to be anthropogenic. Studies of sediment input after forest fires have suggested that such events may result in an increase in the delivery of mineral matter to lakes (Wright, 1976; MacDonald et al., 1991). Loch Callater lies within the Invercauld Estate, which is managed for sporting interests, particularly grouse shooting and stalking. Young grouse feed off the spring growth of *Calluna* shoots. Areas of vegetation are selectively burnt to encourage regrowth of *Calluna* to provide fodder for the young birds (Invercauld Estate, pers. comm., 1992; Plate 1.4). It has been observed that frequently in Glen Callater mismanagement of the heather fires has resulted in damage and local loss of soil cover and the total destruction of the flora. Areas of soil susceptible to erosion have therefore been available in the Loch Callater catchment since the start of management practices during the Nineteenth Century. It is believed that this anthropogenically enhanced erosion is responsible for the recent increase in elemental input into Loch Callater, and a probable net increase of sediment input to the loch.

Visual analysis of the organic matter in the core indicates that a significant proportion is of allochthonous origin (see section 6.4.1 above). However, echosounding (see Chapter 2, section 2.5.3.2) and visual observations have identified the existence of an autochthonous source from the aquatic flora of the loch. The slight negative correlation ($r = -0.289$) between sand and organic matter suggests that the allochthonous input is not associated with an input of sand sized sediment at the core site. This is believed to be due to the preferential deposition of sand in the shallow, nearshore environment, close to the stream mouth. Support for this hypothesis is also found in the analysis of the contemporary surface sediment (see Chapter 5, section 5.4.2).

Whittington (1991) reports the absence of typical Lateglacial Stadial (Loch Lomond

Readvance) pollen assemblages from both the Loch Callater cores. Differences are also recognised between the two cores. In the core taken from the northwestern end of the loch, the basal assemblage is co-dominated by *Juniperus* and *Betula*, which are typical of assemblages associated with the later early Holocene. In core 2, taken from the southeastern end of the loch, the *Juniperus-Betula* pollen assemblage is absent, and the basal pollen assemblage is co-dominated by *Corylus-Betula* pollen.

These data are interpreted by Whittington (1991) as indicating the existence of glacier ice cover over the areas in which the cores were taken until the time at which pollen deposition occurred. This implies that the site of core 1 was not deglaciated until relatively late into the early Holocene, when *Juniperus communis* was colonising the landscape. The severely corroded *Betula* input is believed to be derived from the regional pollen rain. If this assumption is correct, the site of core 2, approximately 800m further up Glen Callater, was not deglaciated until the time of deposition of the *Corylus-Betula* pollen assemblage zone. Whittington suggests therefore, that ice could have remained in the Loch Callater basin, covering the site of core 2 during the Postglacial climatic amelioration, into the ninth millenium BP. This has implications regarding the nature and rate of climatic change in the 'continental' climate of the east of Scotland during the Lateglacial stadial (Loch Lomond Stadial) and Postglacial. To test this hypothesis, further palynological analyses and detailed geomorphological mapping would be required.

6.6.3 Loch Muick

6.6.3.1 Correlation between variables

Values of Pearson's Product Moment Correlation Coefficient were calculated for the core sediment sample variables, following the technique outlined in Chapter 5, section 5.6.1 above. The data obtained are given in Table 6.2. For a sample population where $n=51$ a value of ± 0.408 is significant at the 0.2% confidence level, ± 0.345 significant at 1%, ± 0.313 significant at 2%, ± 0.266 significant at 5%, ± 0.224 significant at 10% and 0.175 significant at the 20% confidence level.

Table 6.2
Loch Muick
Pearson's Product Moment Correlation Coefficient for core sediment variables

	Depth (cm)	Sand (%0)	Silt (%)	Clay (%)	T.O.M. (%)	Water (%)	Na (mg/kg)	K (mg/kg)	Ca (mg/kg)	Mg (mg/kg)	Mn (mg/kg)	Fe (mg/kg)
Silt (%)	0.047	-0.986										
Clay (%)	-0.145	-0.394	0.292									
T.O.M (%)	-0.641	0.060	-0.068	-0.023								
Water (%)	-0.579	0.364	-0.415	0.164	0.795							
Na (mg/kg)	-0.157	0.000	-0.025	0.288	-0.109	0.042						
K (mg/kg)	0.451	-0.495	0.528	0.101	-0.569	-0.784	-0.057					
Ca (mg/kg)	0.418	0.021	-0.006	-0.201	-0.037	-0.063	-0.072	0.039				
Mg (mg/kg)	0.453	-0.437	0.475	0.002	-0.638	-0.853	-0.051	0.933	0.142			
Mn (mg/kg)	-0.661	0.364	-0.368	-0.096	0.622	0.729	0.209	-0.769	-0.027	-0.753		
Fe (mg/kg)	-0.546	0.369	-0.362	-0.205	0.524	0.605	0.184	-0.681	-0.068	-0.663	0.931	
Al (mg/kg)	-0.419	0.097	-0.077	-0.231	0.283	0.253	0.030	-0.379	-0.101	-0.337	0.508	0.501

The strongest positive correlations (at the 0.2% level) are between potassium and depth, calcium and depth, magnesium and depth, potassium and silt, magnesium and silt, total organic matter and water content, manganese and total organic matter, iron and organic matter, manganese and water content, iron and water content, potassium and magnesium, manganese and iron, aluminium and manganese, and aluminium and iron. Weaker positive correlations (at the 1% level) exist between sand content and water content, manganese and sand content, and iron and sand content.

Strong negative correlations (at the 0.2% level) occur between depth and total organic matter, water content, manganese, iron, aluminium, sand content and silt content, potassium and sand content, magnesium and sand content, water and silt content, potassium and total organic matter, potassium and water content, magnesium and water content, potassium and manganese, potassium and iron, magnesium and manganese, and magnesium and iron. Weaker (at the 1% level) negative correlations exist between sand content and clay content, silt content and manganese, and silt content and iron.

6.6.3.2 Interpretation of data

The Loch Muick core has been divided into two units primarily on the basis of visual inspection and organic matter content (see sections 6.5.1 and 6.5.4). However, analysis by X-radiography (section 6.5.2) has enabled the identification of an intermediate layer which has a gradational upper boundary, exhibits clear stratification, and has a relatively high clastic content. Thus three textural, radiographically defined, units are recognised in the sub-surface sediments of Loch Muick.

6.6.3.2.1 Unit 1

This unit is recognised between 475cm-500cm and comprises blue-grey silt with a very low organic matter and water content. Sand and clay sized particles form less than 10% of the sediment in this unit. The negative correlation ($r=-0.415$) between silt and water content throughout the entire core is interpreted as indicating a close packing structure

within the silt, leaving few pores available for water retention. It is suggested that the low organic matter levels in Unit 1 are the result of a low allochthonous and autochthonous input resulting from severe climatic conditions associated with the Lateglacial Stadial (see section 6.6.2.2.1 above). Pollen data are not available to test this hypothesis. However, the data presented in this section are indicative of a period of relatively severe, cold, climatic conditions compared to the climate, interpreted from data, in the remainder of the core.

The geochemical data reveal that the inputs of potassium, calcium and magnesium were high, which is interpreted as indicating intensified erosion in the lake catchment (see section 6.6.1.2 above). The fluctuating input of sodium, which is also an index of erosional intensity, is interpreted, in the context of the potassium, magnesium and calcium data, as indicating temporal, and therefore spatial, variation in the availability of this element. Aluminium concentrations are also relatively low in this unit. This is believed to be due to the low organic content of the sediment (see section 6.6.1.2). The principal source of organic matter which is deposited in Loch Muick is believed to be the erosion of the blanket peat which has developed during the Postglacial climatic amelioration following the Loch Lomond Stadial. Peat development is associated with acid soil conditions which could be sufficiently acidic to mobilise aluminium ions. There is a very weak positive correlation ($r=0.283$), significant at the 20% confidence level between aluminium and organic matter in this core. Thus during cold periods, such as the Loch Lomond Stadial and early Postglacial, when peat development was minimal, a decrease in aluminium and organic matter is observed in the sediments of Loch Muick.

The high iron/manganese ratio in Unit 1 could have been caused by highly reducing conditions in the bottom waters resulting in the preferential mobilisation and removal of manganese from the loch, or temporal variation in the availability of manganese, independent of the redox conditions. The latter is considered to be the more acceptable hypothesis for the same reasons given for the Loch Callater core (see section 6.6.2.2.1 above).

QDa-Md analysis suggests that the minerogenic silt of Unit 1 was deposited in a

range of environments. The basal sample falls within the steep gradient turbidite environmental trend envelope, indicative of rapid, pulsatory, current dominated deposition, possibly by slumping or sliding of the sediment mass from the relatively steep slopes surrounding the core site (see Figure 6.2). Samples lying stratigraphically above this sample plot within the fluxoturbidite and quiet water envelopes, suggesting a steady settling of particles from suspension through the water column. A current-dominated input occurs at 460cm and 440cm. It is tentatively proposed that, due to the relatively wide (10cm) sampling interval used throughout the core for all analyses, the sub-samples on which QDa-Md analyses have been undertaken are an unrepresentative sample of possible annual variations in the *mode of deposition* as opposed to the *type* of sediment deposited. Time restrictions prevented further, more detailed QDa-Md analysis of sediment in this unit, which is recommended for future research. Annual variations in the process of deposition (i.e. alternate current dominated and quiet water environments) are normally associated with the development of texturally distinct varves. However, no such textural variation or slumped material has been identified by visual analysis or by X-radiography in the Loch Muick core. This is not a unique finding, since Thompson and Kelts, (1974) reported that differentiation of slumped material by visual examination and mineralogical analysis was not possible. Proglacial lacustrine deposition does not always result in the formation of true varves, particularly in ice-distal positions when significantly coarser grained material (i.e. sand) may have been deposited in a more ice-proximal position (Smith, 1978; Pickrill and Irwin, 1983) or where the sedimentation rate is low (Gilbert and Desloges, 1987). During movement along the loch floor, glacial meltwater underflows would have encountered ridges, mounds and hollows (see Chapter 2, sections 2.6.3.1-2.6.3.3, Chapter 3, sections 3.7.2.2.1 and 3.7.3.2), resulting in a decrease in velocity and consequent loss of entrained material. Hicks et al., (1990) report mass flows of sediment and massive silts in proglacial Ivory Lake, New Zealand.

Unit 1 is interpreted as dating from the Loch Lomond Stadial when it has been proposed that glacial activity reoccurred in the Loch Muick catchment (Sissons and Grant,

1972; Sissons 1972a). It is suggested that the minerogenic silt was deposited in an ice-distal position, directly by glacial meltwater, and indirectly by settling from suspension through the water column. There is QDa-Md analytical evidence that syndepositional subaqueous mass movements occurred. At the time of deposition of Unit 1 the catchment of Loch Muick was poorly vegetated and subject to intense erosional activity.

6.6.3.2.2 Unit 2

The second unit has a distinct, unconformable boundary with Unit 1 recognised by visual analysis and X-radiography. It extends between 187cm-475cm and is characterised by a change in colour from the blue-grey silt to brown, with olive green, black and light brown laminae. The organic content and water content of the sediment increase to 37.5% and 81.9% respectively. The increase in organic matter is interpreted as resulting from the Postglacial climatic amelioration (see section 6.6.2.2.2 above) which led to floral and faunal recolonisation and the development of soils. The unconformity is believed to be the result of mass movement processes, for which there is evidence in Unit 1.

Geochemical indices (potassium, magnesium, sodium) exhibit a decline in concentration, approximately 50cm above the base of Unit 2, which is interpreted as representing a lessening erosion intensity. Within this general decline, peaks in concentration, common to all the alkali and alkali-earth metals, suggest that major erosive events took place in the stabilising environment. This occurred particularly at the onset of climatic amelioration when data indicate that elemental deposition lagged behind sedimentological change. Further evidence for geomorphologically significant events occurring during this time period is found for example at a depth of 200m below the top of the core. At this point there is a major decrease in the water and organic matter content of the sample and an increase in sand. It is suggested that this represents a rapid pulse of sediment associated with a major flood event, when the current of the water influx was sufficiently strong to transport sand sized particles to the centre of the loch. There is historic evidence of major flood events in this, and neighbouring catchments. For example,

in August 1829 the new bridge at Ballater was destroyed by floods (Haldane, 1962, pp174-5). Owing to the absence of radiometric dates in this core it is not possible to correlate any particular event with the sedimentary record.

In Unit 2 the concentration of calcium increases concurrently with the increased total organic matter content. This is believed to represent an example of the bonding of calcium ions with organic ligands identified by Mackereth (1966) (see section 6.6.1.2). This phenomenon does not occur throughout the core, therefore the possibility that there has been a temporal variation in the source availability of calcium cannot be discounted. The increase in aluminium is interpreted as resulting from decreased pH levels caused by the development of peat in the catchment. Correlation between variables suggests that potassium and magnesium are deposited in the silt particle size fraction. Potassium concentration also shows a negative correlation ($r=-0.569$) with organic matter concentration.

Iron and manganese levels are relatively high in Unit 2 and show positive correlations ($r=0.369$ and $r=0.364$, respectively) with sand sized particles and negative correlations with silt sized sediment. The iron/manganese ratio remains relatively low. This is interpreted as indicating that reducing conditions were not severe and therefore that waterlogging of the soils was not extensive, despite the indication from the aluminium levels that acidic conditions were increasingly prevalent.

QDa-Md analysis indicates that the majority of samples were deposited in quiet water or fluxoturbidite conditions. Two samples fall within the steep gradient turbidite/fluvialite environmental trend envelope overlap. It is believed that these samples represent the localised major erosional inputs that are suggested by the geochemical and X-radiography data.

An event or two separate events can be recognised at a depth of 270cm (calcium, iron, aluminium) and 300cm (sodium, potassium, manganese) (see Figure 6.10) in which there is a significant, rapid, apparently temporally restricted, reduction in concentration of the elements listed above. There is no variation in sediment texture, total organic matter or

water content at these depths. It is very tentatively suggested that this decrease in elements within the core may have been caused by a reduction in precipitation intensity. This hypothesis is invoked to explain the cause of the possible reduction of leaching of iron and manganese from the catchment and the reduced erosive capacity of streams entering the loch, resulting in a decline in the input of alkali and alkali-earth metals. However, the possibilities of site-specific processes preventing or modifying elemental deposition or experimental error introduced during sample processing cannot be ruled out.

Unit 2 is interpreted as representing the early- to mid-Postglacial, during which time the ameliorating climate encouraged vegetative regeneration including peat development and reduced the erosional input to the loch. Throughout this period, however, major erosional events maintained an intermittent, but significant, input of minerogenic material to Loch Muick.

6.6.3.2.3 Unit 3

Unit 3 has a gradational boundary with Unit 2, identifiable visually only on the X-radiographs, where the input of clasts >2mm in diameter diminishes. There is no appreciable variation in tone, which remains a range of browns, from almost black to olive-green, or in organic matter content, which is in the range of 20% to 30% across the boundary. Water content fluctuates within the same limits as in Unit 2. There is a decrease in the concentration of calcium, magnesium and potassium, which is believed to represent a decline in erosional intensity. At the top of the core the concentration of these elements increases. As has been outlined in section 6.5.1 above, the upper part of the core containing the most recently deposited sediment was lost during recovery. The return to increased erosion at the top of the core section obtained is believed to represent the initial impact of estate management on the sedimentary input to the loch. This involved the construction of tracks parallel to both loch shores, and a substantial house with outbuildings close to the Glas Allt (for location see Figure 2.14). The validity of this

hypothesis cannot be tested from the data available.

The concentration of sodium fluctuates within Unit 3 as in Unit 2, which is interpreted as indicating an identical reason for this variability. The input of iron, manganese and aluminium decreases, as does the iron/manganese ratio, implying that only mildly reducing conditions occurred within the loch catchment. The decrease in aluminium coincides with an increase in organic matter. This may be due to a relative reduction in the area of peat bogs, and therefore acidic conditions due to anthropogenic impact, or could be totally unrelated to the increased input of organic matter. As has been proposed for variations in concentration of other elements above, it is suggested that there was a decrease in availability of aluminium for redeposition.

QDa-Md analysis indicates that the majority of samples were deposited in a quiet water or fluxoturbidite environment. One sample plots within the fluvial environmental trend envelope and one in the overlap between the fluvial and steep gradient turbidite environments.

Unit 3 is interpreted as representing the middle to late Postglacial, during which time stabilisation of the environment by plants continued and erosion diminished. Occasional, geomorphologically significant events occurred. In the uppermost sediments of this unit, the more recent impact of estate management during the Nineteenth Century may account for a large proportion of the material.

6.7 CONCLUSIONS

Sedimentological, geochemical, statistical and palynological analyses of core material obtained from Loch Callater and Loch Muick have led the following conclusions to be drawn.

6.7.1 Loch Callater

- i) There are two distinct units within the sediments of the Loch Callater core.
- ii) The stratigraphically lower unit is composed of blue-grey, proglacial lacustrine silt. It was deposited both directly and indirectly by meltwater streams, in an ice-distal position. There was minimal vegetation cover or soil development at this time in Glen Callater or surrounding areas. This unit represents sedimentation during the Loch Lomond Stadial (Lateglacial Stadial).
- iii) The upper unit represents Postglacial climatic amelioration. At the base of this unit, colonisation of the catchment by pioneer plant species occurred, and soils started to develop. Erosion of the catchment increased at the base of this unit, but declined as stabilisation of the environment occurred. Finally, the anthropogenic effect of estate management is identified in the increased catchment erosion evident at the top of the core.
- iv) Pollen analysis (Whittington, 1991) suggests that glacial ice remained in the area now occupied by Loch Callater into the ninth millennium BP. A significant time lapse exists between the basal polleniferous sediments of the two cores, which are separated by a lateral distance of approximately 800m. If, through further pollen analysis and geomorphological mapping, this hypothesis be confirmed it has important implications regarding the rate of climatic change in the 'continental interior' of eastern Scotland.

6.7.2 Loch Muick

- i) Three units are present in the sediments of the Loch Muick core.
- ii) The basal unit is composed of blue-grey minerogenic silt deposited in an ice-distal, proglacial lacustrine environment. Sedimentation was disturbed by syndepositional mass movements. Deposition of silt by alternating current and quiet water conditions on an annual basis, but which does not produce visually identifiable varves is tentatively suggested. The catchment of Loch Muick was

poorly vegetated and subject to intense erosional activity. This unit represents sedimentation during the Loch Lomond Stadial.

iii) Unit 2 represents the early to mid Postglacial during which time plant colonisation including peat development occurred and soils were formed. Major erosional events provided an intermittent input of minerogenic and coarse grained material.

iv) Unit 3, the upper part of the core, is indicative of the maintenance of a relatively warm climate. Stabilisation of the landscape by plant colonisation continued and erosion diminished. Very occasional geomorphologically significant events are recorded in the sediment. Anthropogenic impact on the catchment, believed to represent the onset of estate management practices, is identified in the uppermost sediment where geochemical evidence suggests increased erosion.

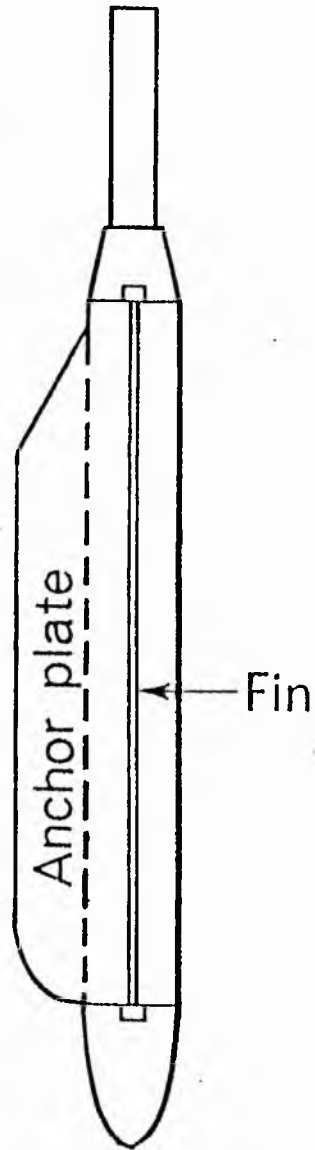


Figure 6.1 The Russian peat borer. After West (1968)

Fin length = 50cm.

LOCH CALLATER

Coring locations

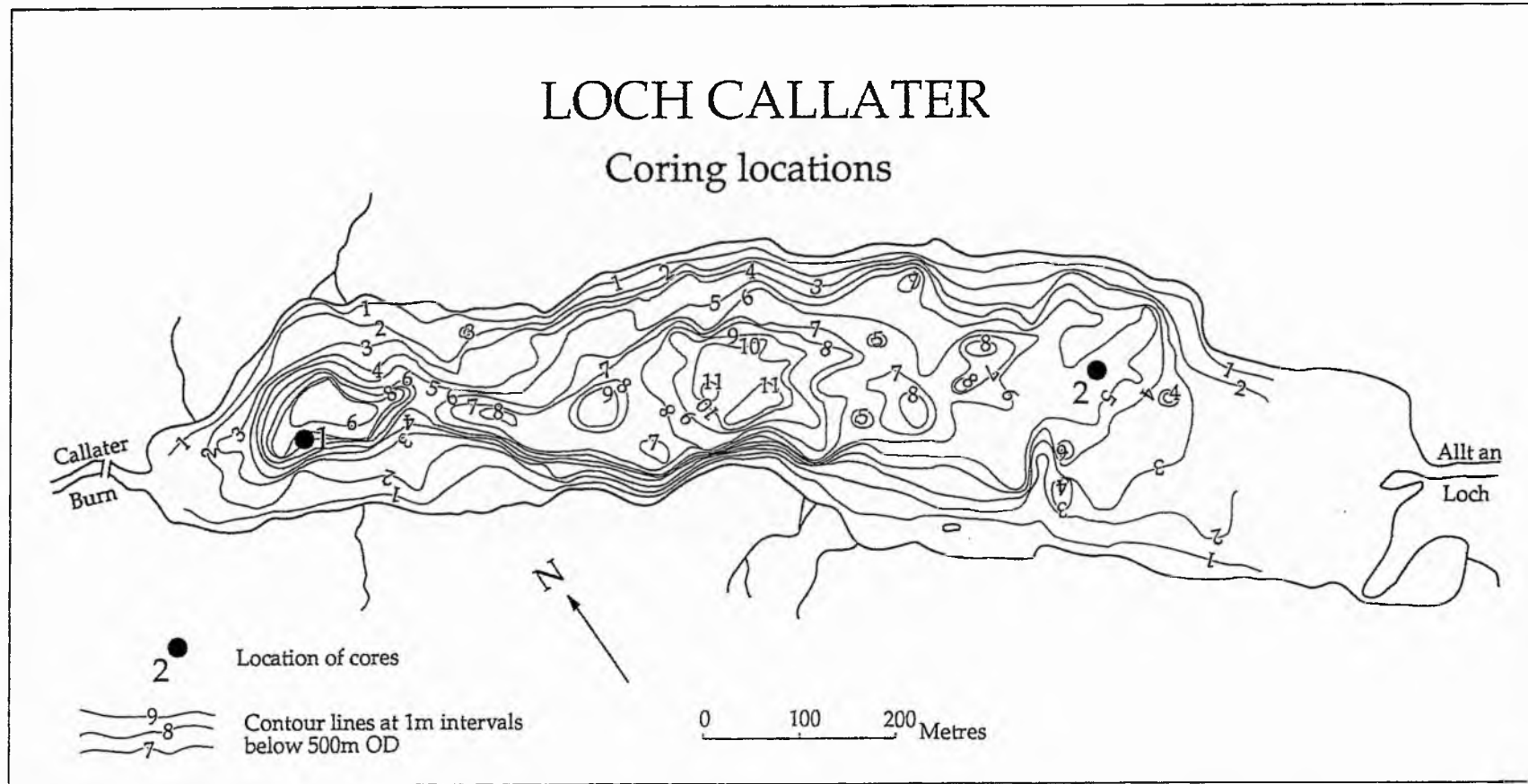


Figure 6.2
285

LOCH CALLATER

Core 1

Down core variation in particle size and total organic matter

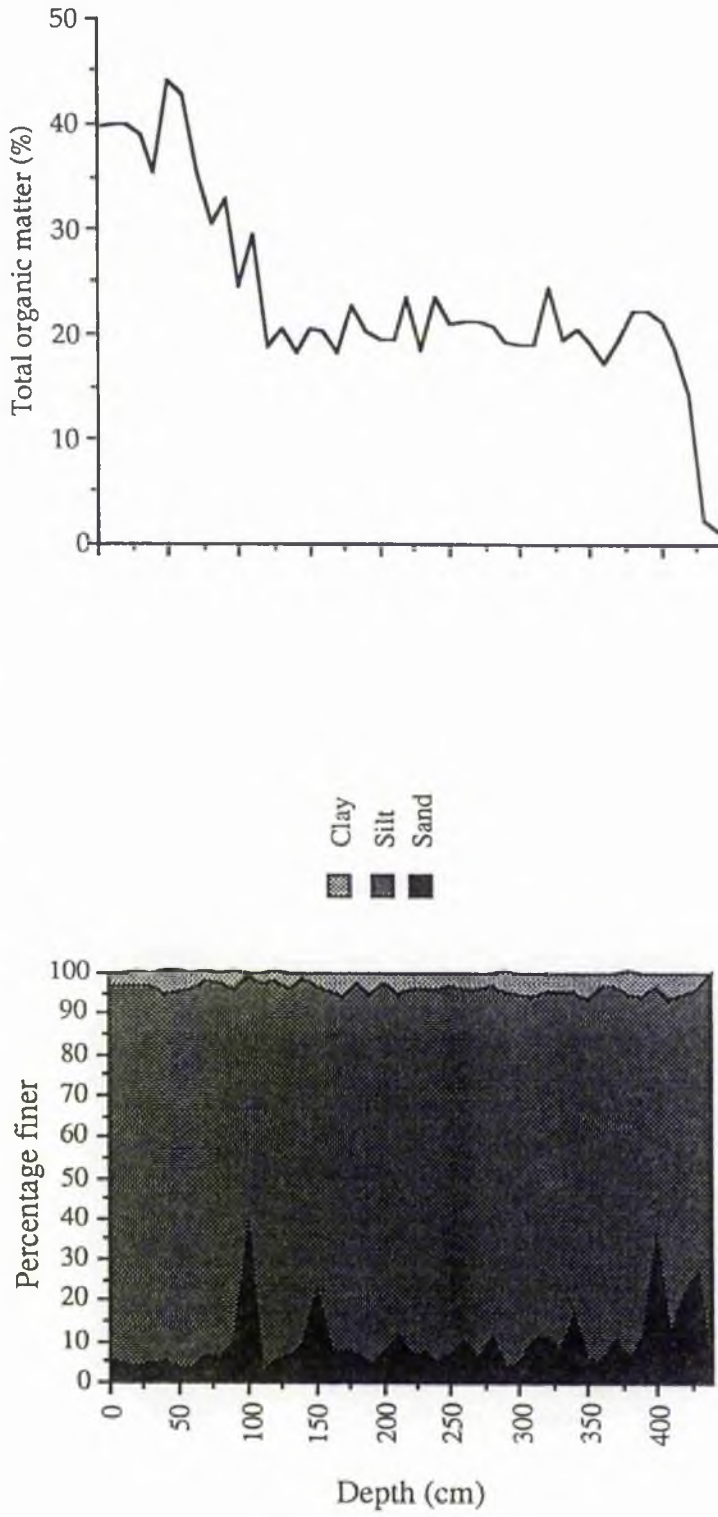


Figure 6.3
286

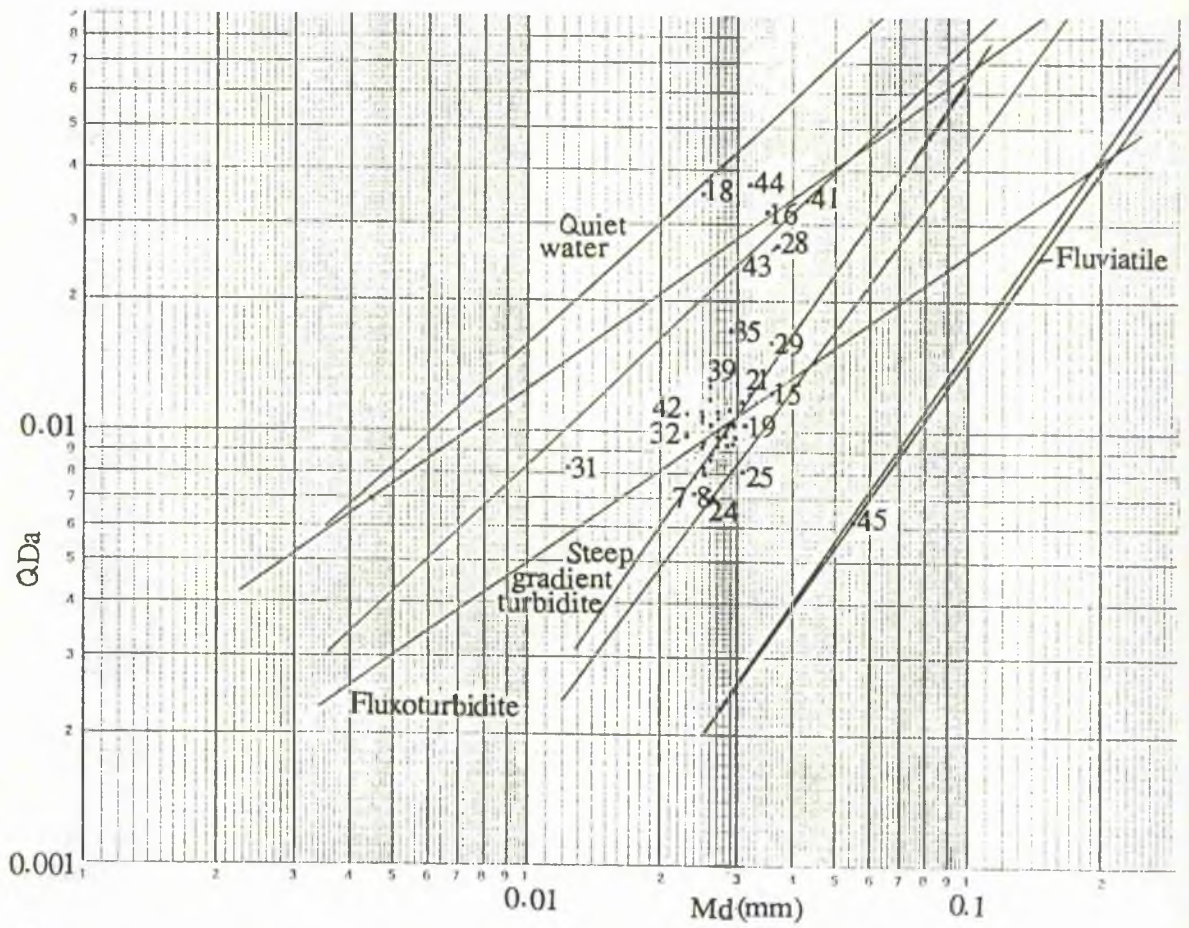


Figure 6.4 Loch Callater: QDa - Md plot showing the environmental trend envelopes of Buller and McManus (1972, 1973).

LOCH CALLATER

Core 1

Down core chemical composition and Fe/Mn ratio

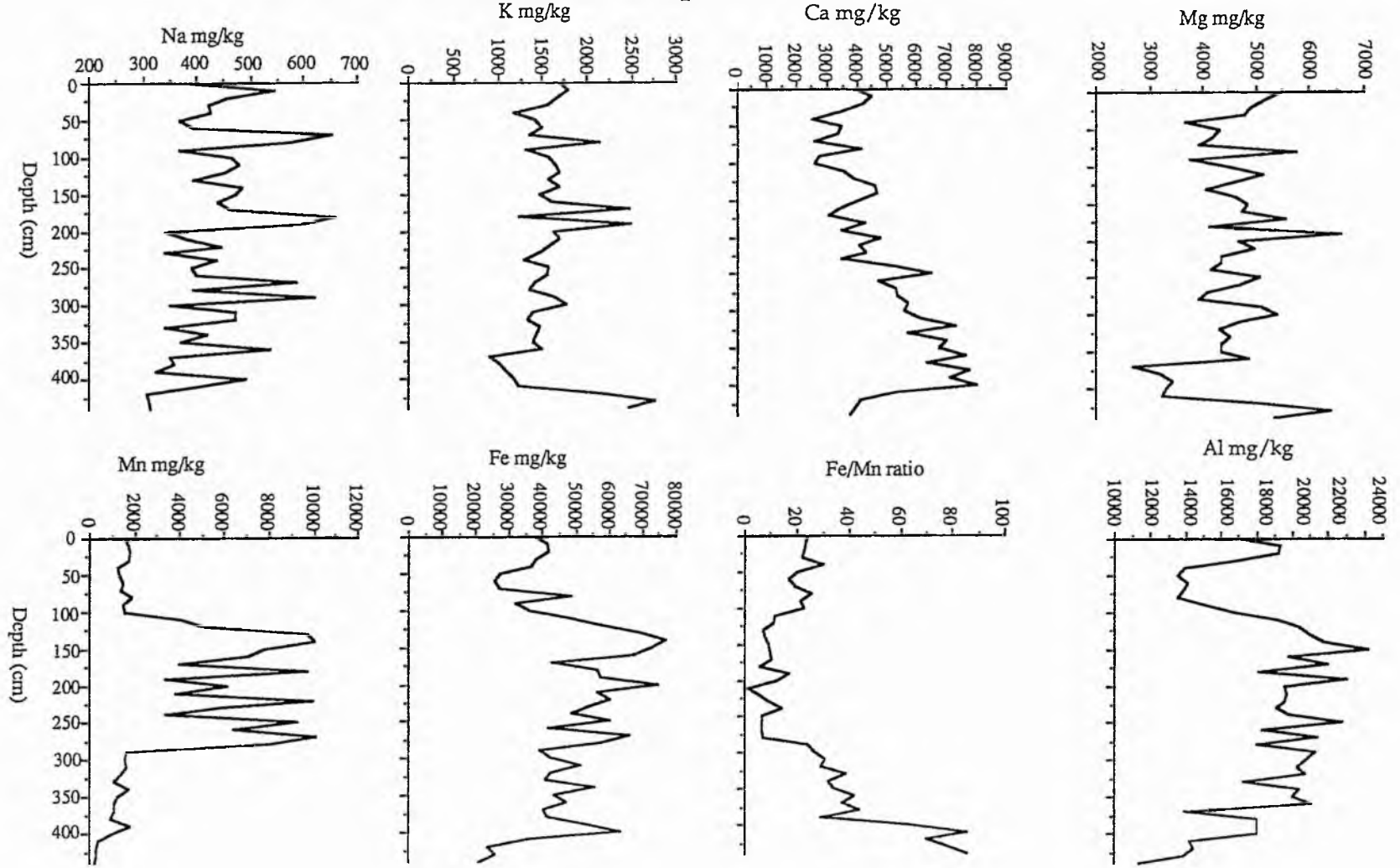


Figure 6.5
288

Down core mineral composition

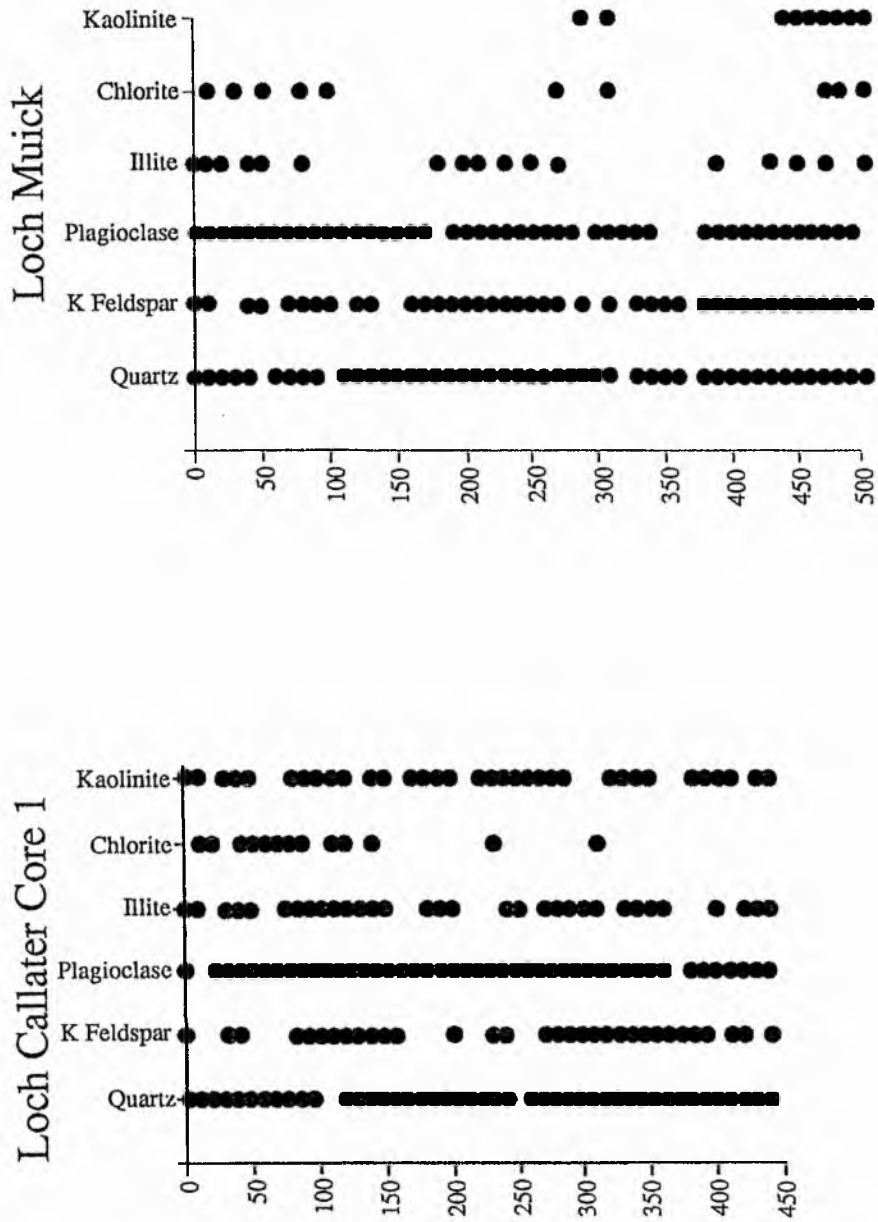


Figure 6.6
289

LOCH CALLATER

Pollen diagram Core 1

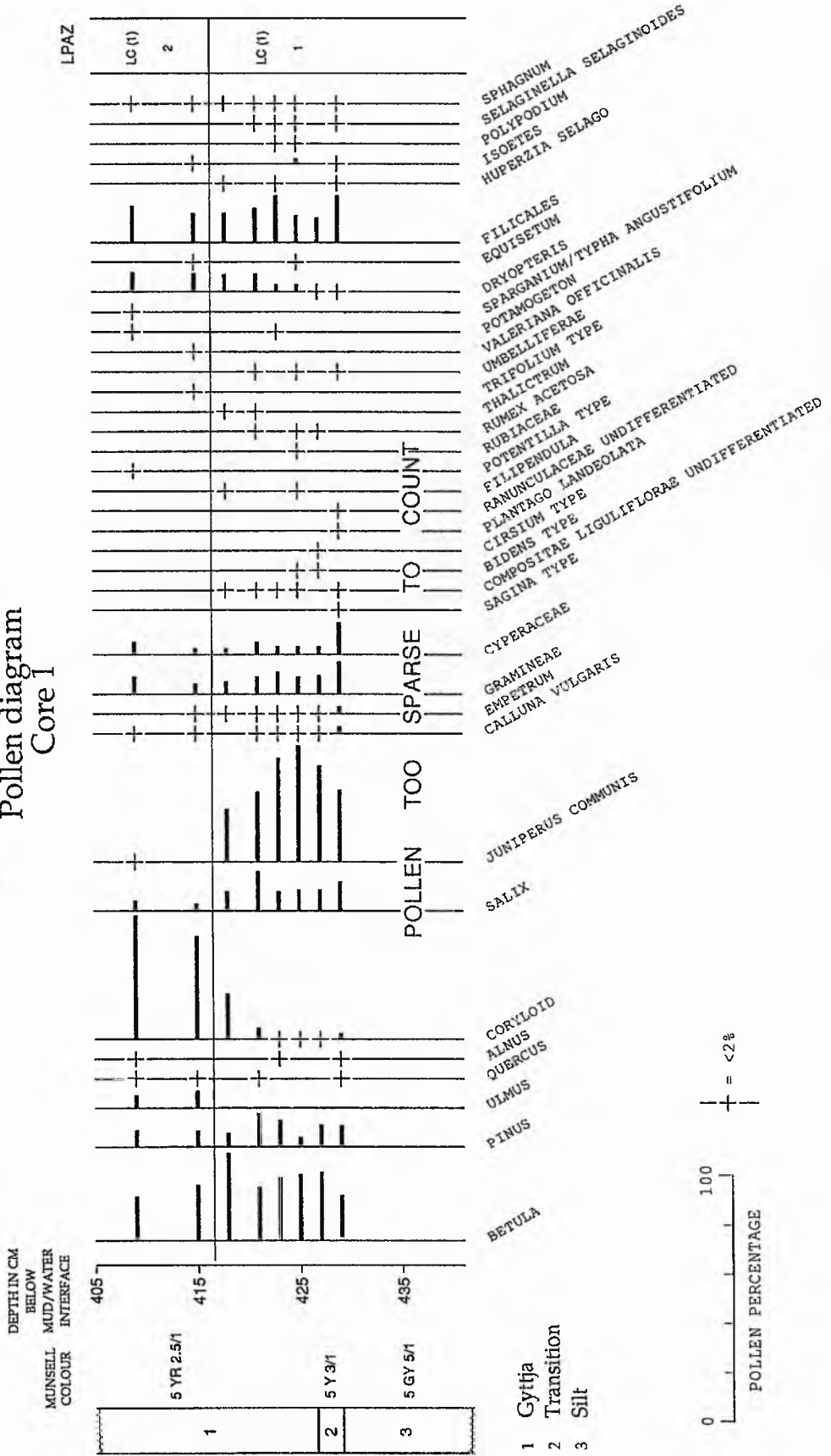


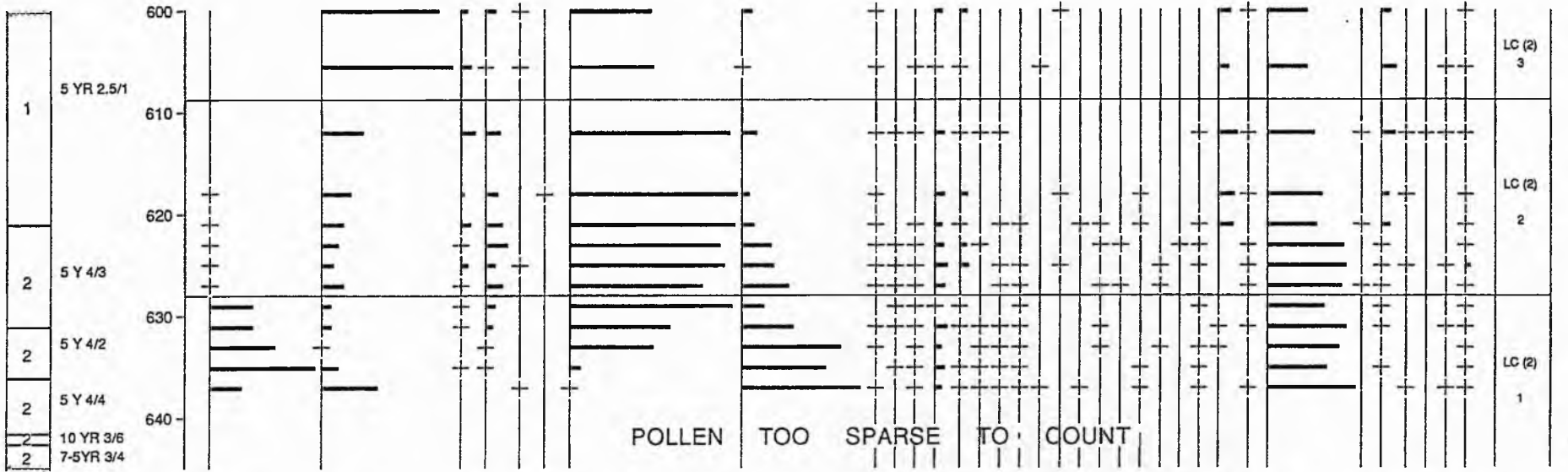
Figure 6.7
290

DEPTH IN CM
BELOW
MUNSELL MUD/WATER
COLOUR INTERFACE

LOCH CALLATER

Pollen diagram Core 2

LPAZ

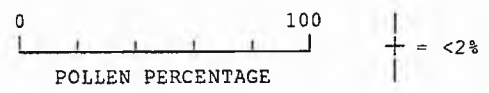


POLLEN TOO SPARSE TO COUNT

Figure 6.8
291

- 1 Gyttja
- 2 Silt

- BETULA
- PINUS
- ULMUS
- QUERCUS
- ALNUS
- FRAXINUS
- CORYLID
- SALIX
- GRAMINEAE
- CYPERACEAE
- CHENOPODIACEAE
- COMPOSITAE
- BIDENS TYPE
- ARTEMISIA
- RANUNCULACEAE
- RUBIACEAE
- RUMEX
- UMBELLIFERAE
- MYRPHILLUM
- POLYGONUM ALTERNIFLORUM
- DRYOPTERIS
- EQUISETUM
- FILICES
- SPERMATOPHYTES
- LYCOPODIUM
- ISOPETES
- HUPERZIA SELAGO
- SPHAGNUM
- SELAGINELLA
- SELAGINOIDES
- ANNOTINUM



LOCH MUICK

Core location

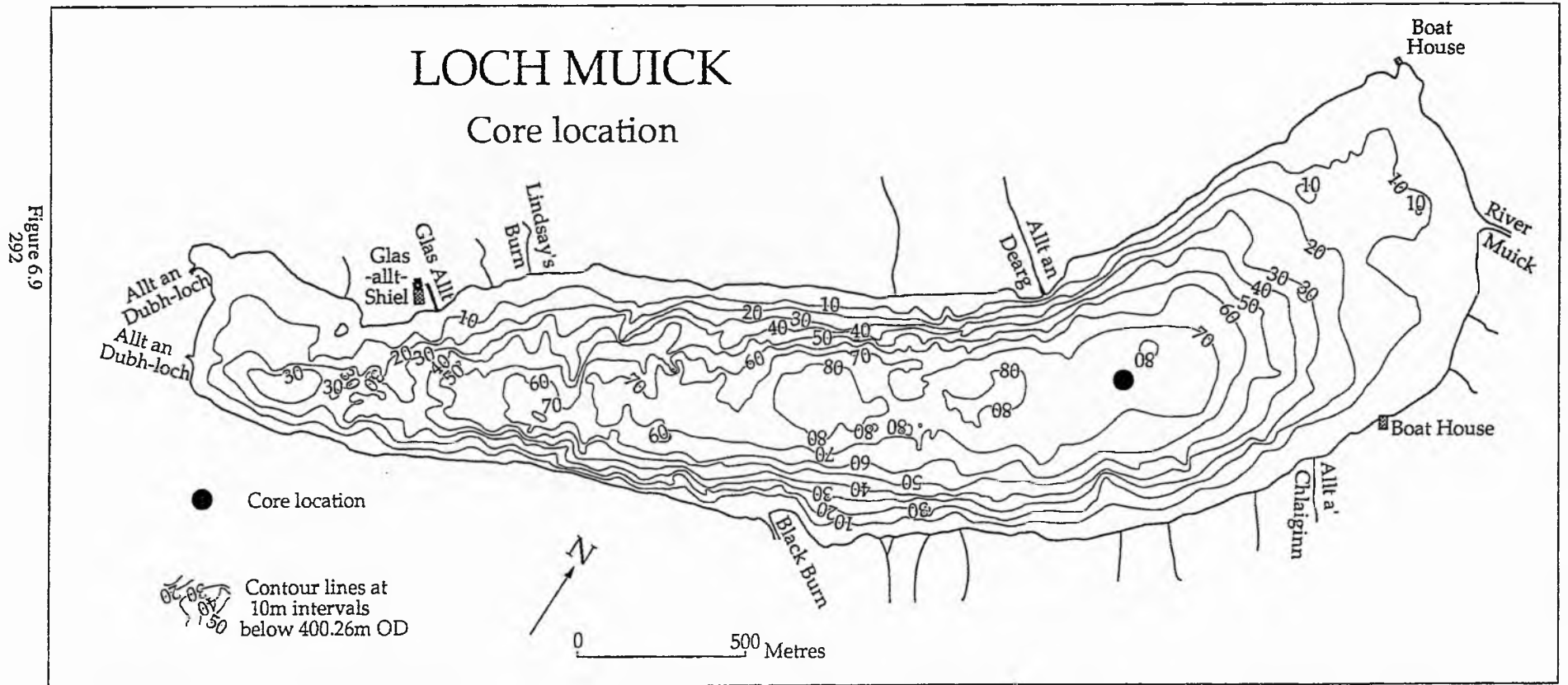


Figure 6.9
292

LOCH MUICK

Down core variation in particle size, total organic matter and water content

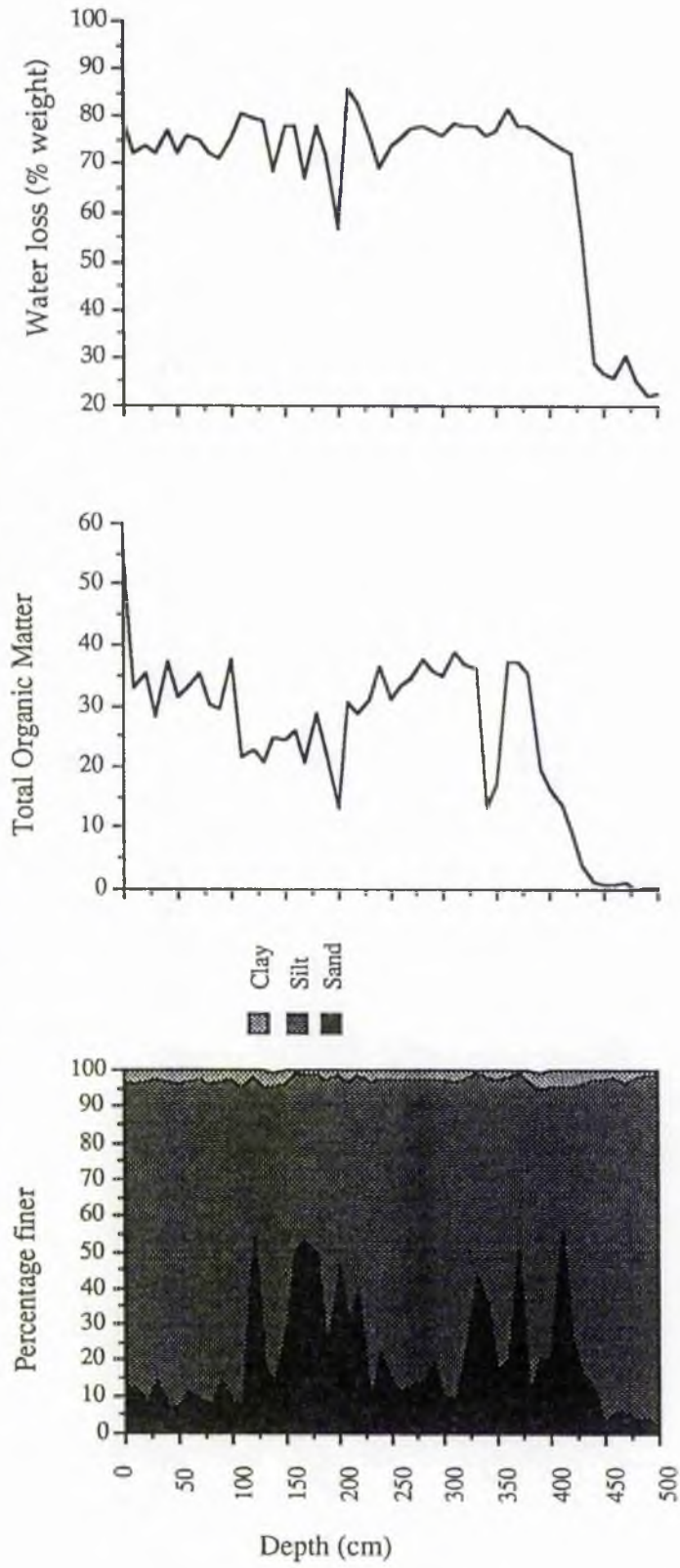


Figure 6.10
293

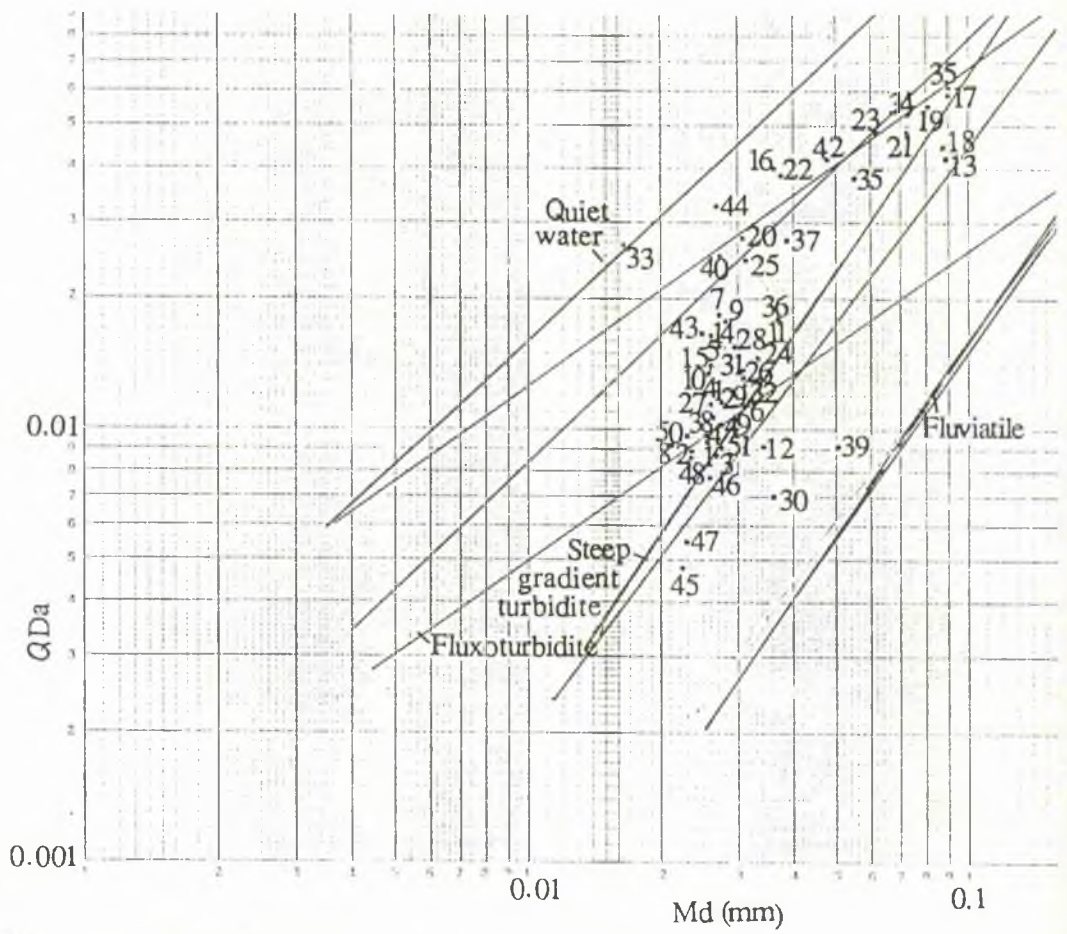


Figure 6.11 Loch Muick: Q_{Da} - M_d plot showing the environmental trend envelopes of Buller and McManus (1972, 1973).

LOCH MUICK

Down core chemical composition and Fe/Mn ratio

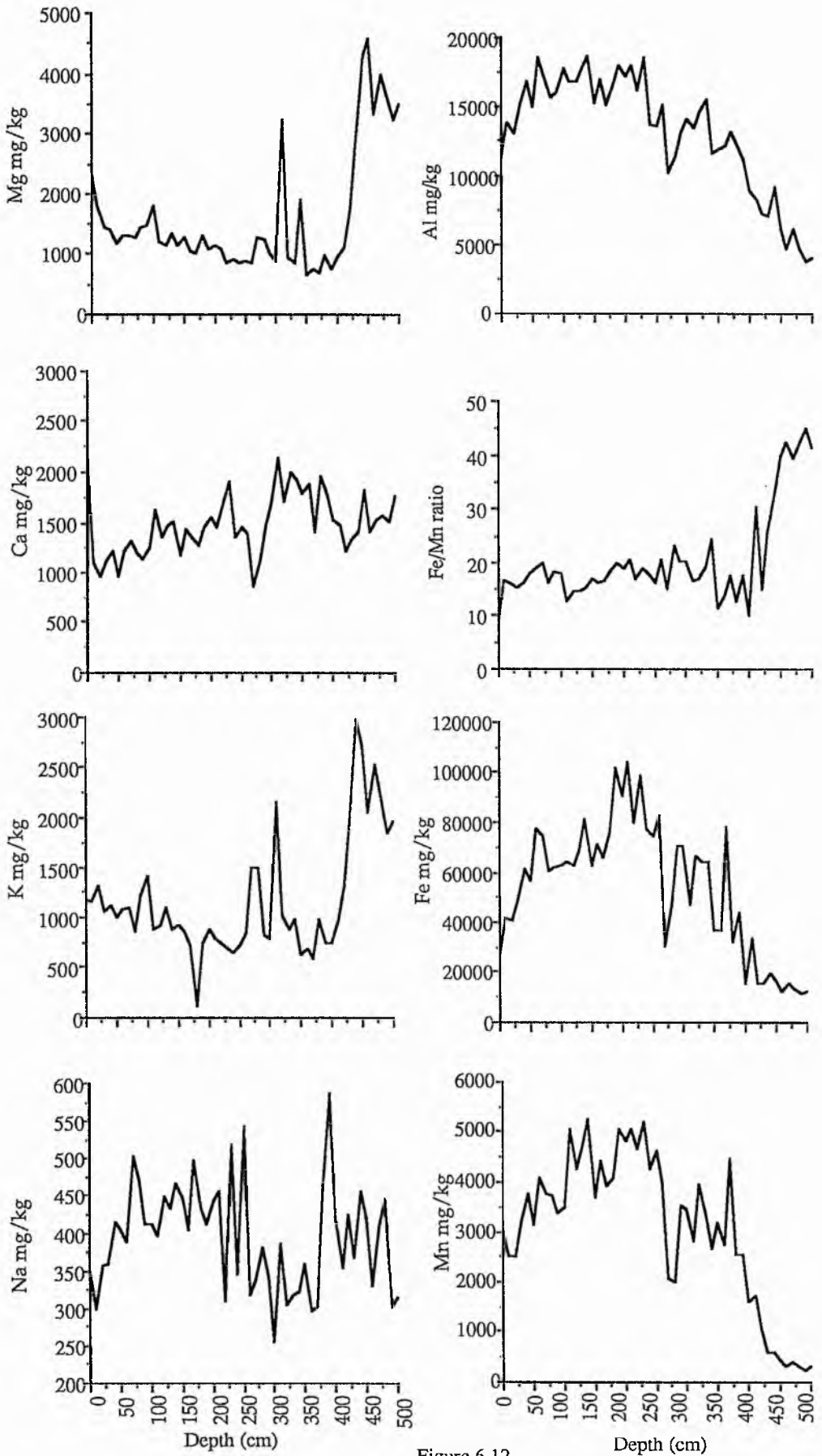


Figure 6.12
295



Plate 6.1 Mackereth corer prior to deployment. The internal piston is contained within the 6m long outer casing, which is attached to the anchor drum (at the left of the photograph). The corer was towed on the inflatable dinghy to the coring site behind R.V. Mya (middleground).



Plate 6.2 Close-up of the tonal and textural transition zone in Core 1 from Loch Callater. The blue-grey silt on the left is Munsell 5GY 5/1 and the brown sandy silt on the right 5Y 3/1.

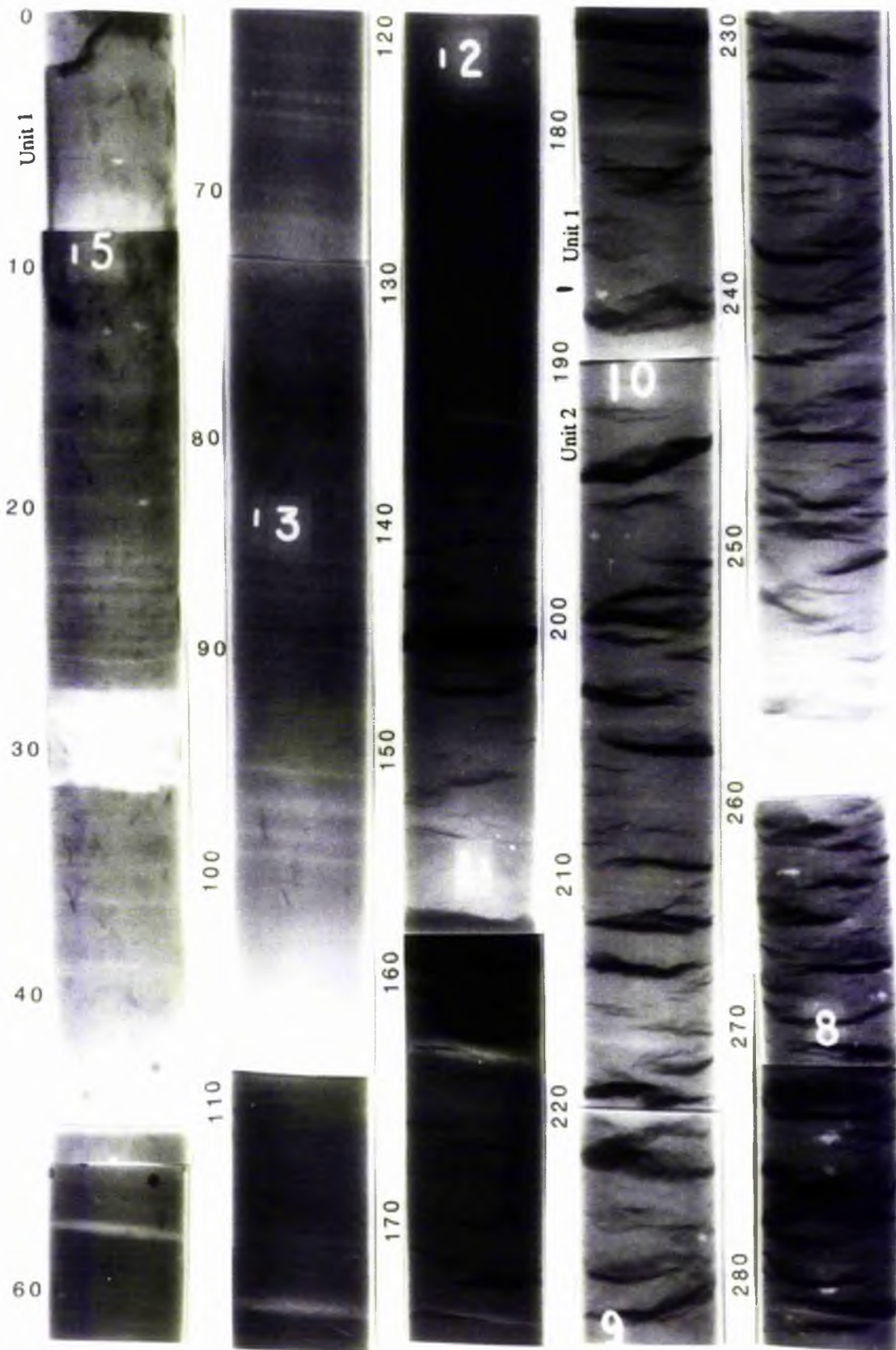


Plate 6.3 Loch Muick: 500cm core X-radiograph negatives. Unit 1, high density sediment extends between 500cm-475cm with an unconformable boundary with Unit 2. Unit 2 extends from 475cm-187cm and comprises fine grained, stratified, medium density sediments broken by small fractures (wavy black lines). Clastic concentrations at 263cm-290cm, 228cm-337cm, 187cm, 197cm and 462cm. The basal 15cm of this unit is composed of laminae of fine grained material. The boundary between Unit 2 and Unit 3 is

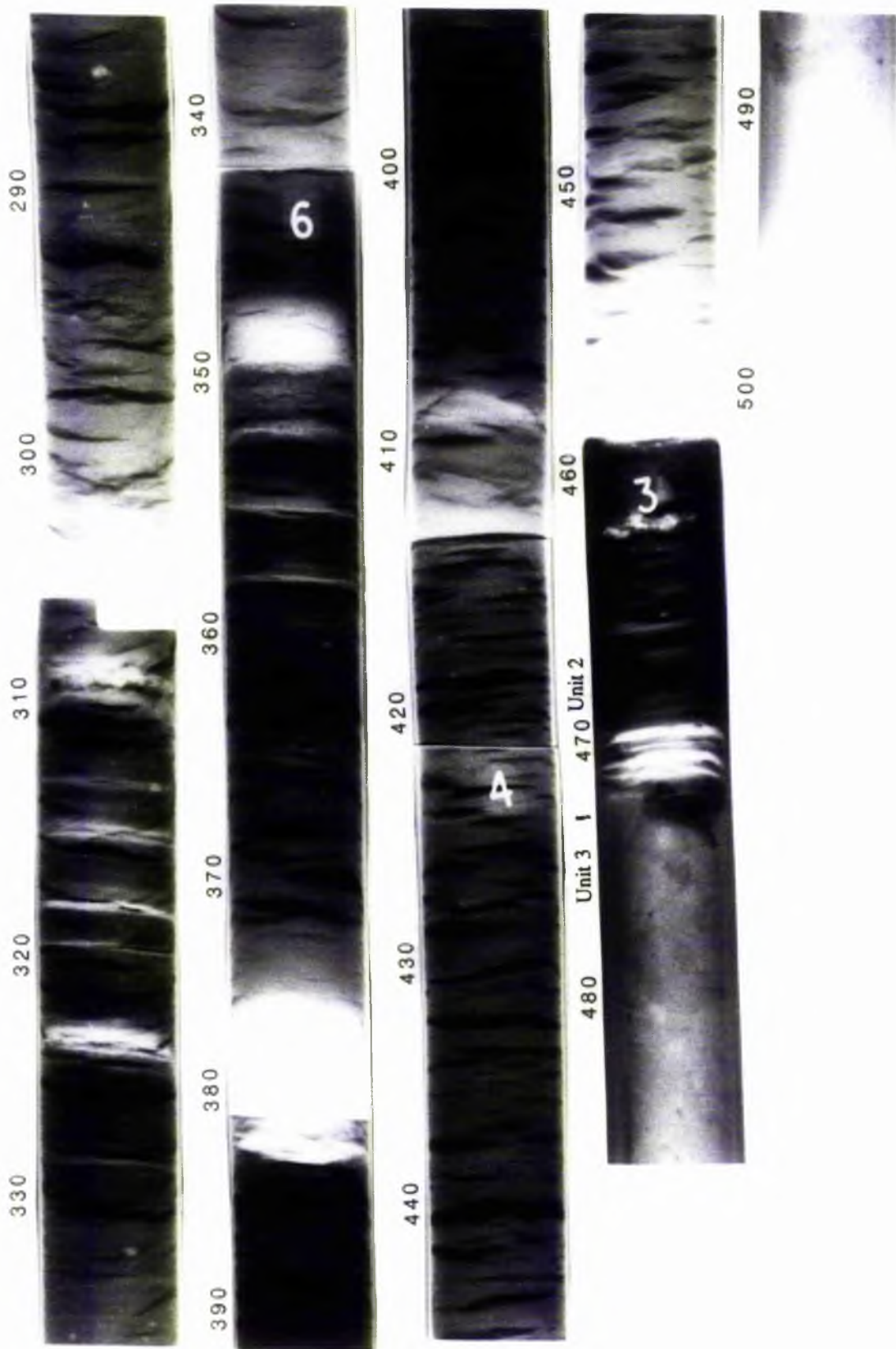


Plate 6.3

gradational over 5.5cm. Unit 3 extends from 187cm-0cm and is composed of fine laminae and strata with occasional, stratified, concentrations of clasts. The core section missing between 46.5cm-55cm was covered by a metal band impervious to X-rays. Lower density spots between 40cm-50cm result from holes drilled in the core barrel.

CHAPTER 7

DISCUSSION

7.1 INTRODUCTION

This Chapter is structured following the seismic sequences identified in Chapter 3. A progressive analysis is made of the data obtained from each loch, examining the former and present processes operational in the water body, which have resulted in variations in the surface texture and form, through to the internal structure of the underlying sediment. The implications of these findings upon the glacial history of the south east Grampians and the valley in question are discussed within the context of each loch. In this Chapter the order in which the lochs are examined is altered to enable the analysis of the water body for which the most complete data set was obtained (Loch Muick) to be made first. The remaining two lochs exhibit many features in common with Loch Muick. Thus to avoid unnecessary repetition, continual cross reference is made to sections where appropriate discussions or analyses have been made.

In conclusion, the interpretations of data obtained from Lochs Muick, Callater and Lee are used to formulate a model for the seismic identification of glaciated and unglaciated water bodies in highland areas during the Loch Lomond Stadial.

Throughout this Chapter, in common with Chapters 1 and 3, to differentiate between descriptions from the subaerial and subaqueous environments, the term 'till' is used to describe subaerial exposures of sediment deposited directly by glacial action and 'glacigenic diamict' is used in reference to that recognised in the sublacustrine environment.

7.2 LOCH MUICK

7.2.1 Sequence 1

7.2.1.1 Surface sediment texture

Information on surface sediment texture is derived primarily from two, complementary survey techniques, sidescan sonar and surface sediment sampling. The broad swathe of remotely sensed data obtained by sidescan sonar is calibrated by point data sources, for which detailed sedimentological analyses have been undertaken. Four major sediment textural associations have been identified in Loch Muick:- boulder covered slopes (boulder spreads), boulder clusters, fluvial input zones, and fine grained sediment. A brief description of the associations, and the probable sediment sources and mode(s) of deposition are given below.

7.2.1.1.1 Boulder covered slopes

The upper sections of the northern and southern slopes of Loch Muick are extensively covered by multiple, overlapping, lobate spreads of boulder sized clasts, recognised only from sidescan sonar records. Pinger seismic subbottom reflection profiling was unable to penetrate this coarse grained deposit (see Figures 3.25, Traverse 96-93; 3.26, Traverse 79-83; 3.26, Traverse 132-136; 3.27; Plate 3.8). The boulder spreads extend along the entire length of the southern slopes, with a short break at the mouth of the Black Burn, and between Lindsay's Burn and the Boathouse on the northern slopes (for locations see Figure 2.15). The upper limit of the features extends to the loch shore. However, the maximum downslope limit cannot be quantified over much of the loch slopes, as it extends to a depth below that covered by the sonar beam. On one section of the northern slopes (Plate 4.14) the lower limit of the boulder spreads can be identified, 75m from the shore, terminating at a depth of approximately 20m. Evidence from the remainder of the loch indicates that the angle of the loch sides is not the sole determining factor

governing the downslope extent of the features. Where the downslope and lateral limits can be recognised on the sidescan sonar record, there is no change in topography apparent on the bathymetric chart (Figure 2.15), despite the 1m contour interval. This implies that the lateral and terminal lobes have an amplitude of less than 1m above the surrounding subaqueous topography.

Surface sediment samples collected from the areas covered by boulder spreads indicate that there are small pockets of finer grained sediment, between individual boulder sized clasts, or a thin veneer of mud, overlying the boulders (section 5.5.2). The van Veen grab used is not designed for the collection of coarse sediment, having a mouth opening of approximately 20cm, and is triggered prematurely on contact with a coarse grained or a hard loch floor, failing to obtain a representative sample. Problems of this nature have been reported elsewhere (e.g. Prior and Bornhold, 1989).

A subaerial sediment source for the boulder spreads is indicated by the upslope continuation of this textural association into the terrestrial environment at the cobble and boulder shoreline. Unlike Lochs Lee and Callater, Loch Muick does not have a significant local sediment source via the erosion of small till cliffs around the loch shore. The coarse grained sediment must therefore be derived from the steep slopes above the loch. Geomorphological mapping of Glen Muick (Figure 1.6) during this research programme demonstrated that there is no distinct, widespread, subaerial continuation of the subaqueous lobate features. An exception to this occurs at the southwestern end of the loch (see section 7.5.4.2.1), where deep, steep-sided gullies run down to the shore, and have been observed to contain unstable clusters of boulders in the base of the channel. It is suggested therefore, that during heavy rainfall (see for example section 6.6.3.2.2), snowmelt, or avalanche activity, subaerial entrainment and mobilisation of this debris occurs, delivering the sediment to the loch via the channel. The distribution of gullies around the shores of Loch Muick is spatially restricted to the relatively thick till on the southwestern slopes, whereas the boulder spreads exhibit a more extensive distribution. This indicates that non-

channelised delivery of coarse grained sediment to the loch must occur. Given the absence of channels on the lochside slopes, entrainment of cobble and boulder sized debris directly as a result of heavy rainfall is unlikely to provide a significant input to the loch. Data reported from comparable catchments suggest that rainfall-induced debris flows, rockfalls and debris entrainment by avalanche activity represent significant sources of sediment supply (Hicks et al., 1990). Debris delivered by channelised flow appears to produce a more uniform subaqueous feature (Plate 4.16) than that entering the loch by other means (Plate 4.14). It is suggested that this may be partially due to the more controlled channelised flow regime, combined with the degree of subaqueous slope uniformity (Figure 2.15). Thus the depth of subaqueous deposition of debris lobes as part of the compound boulder spread form is dependent on the velocity of the debris on entry to the loch and the angle of the loch floor.

It is probable that there is a significant difference in the frequency of input via the two modes of deposition. If the non-channelised entrainment of coarse grained material by overland flow is dominated by avalanche and debris flow/rockfall activity, a distinct seasonality of supply is probable, peaking in intensity during winter and at snowmelt. Where rainfall is concentrated by channelised flow, the capacity for entrainment is increased, enabling transportation of sediment during short duration, high intensity, summer rainfall events and increasing the frequency of sediment delivery to the loch.

The drape and infills of fine grained material over and between the clasts of the boulder spreads is believed to be derived from the finer grained sediment entrained with the larger clasts. QDa-Md data indicate that on entry to the loch the fine grained material becomes suspended in the water column and later settles onto the surface of the features. In the nearshore environment re-entrainment of this sediment, through winnowing by wave activity, occurs (Johnson 1980b) leaving a lag deposit of coarser grained sediment. This partially explains the nearshore distribution of sandy sediment in Figure 5.23 (sections

5.5.2; 5.6.3), mean grain size distribution (Figure 5.26, section 5.5.3), sorting (Figure 5.27, section 5.5.4) and the positive correlation between organic matter and depth (section 5.6.3, Figure 5.22). Further factors influencing these distributions are discussed in section 7.2.1.2.3.2 below.

The distribution of subaqueous boulder spreads is closely linked to the angle of the slopes above the loch. This accounts for the almost total coverage of the southern upper loch slopes, which are flanked by steep subaerial slopes, and the absence of the features at the western and northeastern extremities, and below the gentle slopes adjacent to Glas-allt-Shiel on the northern side of the loch.

It is believed that formation of the boulder spreads in Loch Muick was initiated almost immediately after deglaciation of the trough within the limits of glaciation. Outside the glacier margins formation of these features was probably continuous throughout the Loch Lomond Stadial (for date of the last glaciation in Glen Muick see section 7.2.2.1). Thus it is possible that a proportion of the boulder spreads which currently form the surface layer of sediment in Loch Muick pre-date the Loch Lomond Stadial. Masking of the surface form of the features on the upper slopes has been prevented by removal and redistribution of fine grained sediment by nearshore wave processes.

7.2.1.1.2 Boulder clusters

This sediment association is recognised at the extreme northern end of the loch, on the shallow, gently shelving area of the loch floor adjacent to the River Muick (Figure 2.15). The features comprise concentrations of coarse (maximum boulder sized) sediment lying on the surface of small mounds in the central section of the loch floor (section 4.6.2.2).

There are two possible hypotheses for sediment sources; i) the present subaerial environment, and ii) the environment during the Loch Lomond Stadial. For the former of

the two source areas to have supplied the sediment to this central position in the loch, the only possible mechanism would be by avalanching onto the frozen surface of the loch, during winter. The surface of Loch Muick has been observed to freeze, but relatively infrequently (W. Potts, Pers. Comm. 1989), and not during the period of this research. There is no evidence that the boulders were deposited directly from lake ice, in the centre of the loch, during the spring ice melt. Support for this point is found in the absence of similar deposits on the sonographs in more nearshore positions at comparable depths. Therefore it is suggested that sediments deposited on the lake ice surface were rafted by lake ice down-loch towards the outlet, where deposition of the load occurred.

The second hypothesis, that the boulder clusters are relict features dating from the Loch Lomond Stadial also requires that the sediments reached their present position by ice rafting, given their morphology and position. If the interpretation of Sissons (1972a) and Sissons and Grant (1972) is supported; that glaciers partially occupied the Loch Muick basin; sediment was delivered to the loch outlet area by debris covered icebergs, driven by katabatic winds and currents (cf. McManus and Duck, 1988c), and dumped during melting of the icebergs. Alternatively, if the loch was not glaciated during the Loch Lomond Stadial, the processes inferred for Holocene deposition of the boulder clusters would have been operational, but at an increased frequency. The enhanced sedimentation would be caused by freezing of the loch surface on an annual cycle, as reported from contemporary water bodies in glaciated catchments (e.g. Holdsworth, 1973; Weirich, 1985).

The second hypothesis is thought to be less likely to have resulted in the surface features identified by sidescan sonar, because of the clarity of the boulder clusters on the sonographs and the water depth at which they occur (4m-17m). These depths are significantly beneath the maximum depth at which wave generated currents have been reported to result in entrainment and redeposition of fine grained sediment, even in large water bodies (Alrasoul, 1986; Dearing, 1992). QDa-Md analyses provide further data to indicate that this hypothesis be rejected; the surface sediment samples are typical of quiet

water and fluxoturbidite deposition. Thus there is no evidence of strong current activity. The boulder clusters identified on the floor of Loch Muick are unlikely to be so clearly defined after at least 10,000 years of sediment accumulation. Therefore it is concluded that the first hypothesis be accepted and that the boulder cluster sediment texture association results from recent ice rafting of avalanche debris to the loch outlet during severe winters.

7.2.1.1.3 Fluvial input zones

Fluvial input zones are identified at the mouths of the main influent streams in Loch Muick, the Allt an Dubh-loch, Black Burn, Glas Allt and Allt an Dearg. Sonographs show the areas adjacent to stream inflows to be dominated by a smoother texture, with a low to medium backscatter level (Plate 4.18) and occasional scattered boulders and cobbles (Plate 4.12). Surface sediment sampling confirms that offshore from three of the four major influent streams, sandy sediment occurs on the mud dominated loch floor (Figure 5.23). The exception is the Black Burn, where mud occurs at a depth of 27m, close to the stream mouth. The sediment in this sample is also unusual in having a relatively high (55.6%, Appendix J) organic matter content; sediments offshore from the three other streams have organic matter contents in the range 10%-30%. This variation in sediment texture and organic matter content may result from one, or a number of factors. These include; i) sediment available in the catchment, ii) erosive capacity of the streams and iii) depth and proximity of sampling position from the stream mouth. It is suggested that the first two factors are the significant determinants in loch floor sediment texture. The third factor is not believed to be important, as sampling depths and positions are broadly similar (Appendix J). It is recognised, however, that point sampling techniques, such as grabbing, may yield atypical samples, and necessarily result in generalizations being made.

QDa-Md analysis does not distinguish the samples obtained close to the stream mouths from those of the adjacent loch floor. This may be a result of the selection of

sampling positions (see above), or be indicative of relatively low current velocities at the sample sites. Evidence in support of the former point is found close to the mouth of the Black Burn, where a more distal sample falls within the overlap between the fluvial and steep gradient turbidite environmental trend envelopes. Due to the overlap between envelopes, this sample could represent downslope current activity at a depth of 53m, or turbidite deposition associated with the stream input. In the light of reports from other waterbodies (Gilbert, 1975; Pickrill and Irwin, 1983), where fluvially induced mass movements have been recognised, it is proposed that, in the case of the Black Burn, the sample obtained represents turbidite deposition associated with the stream input.

On the northwestern and southeastern slopes the fine grained sediment deposited at the stream mouths blankets the adjoining margins of the boulder spreads (Plate 4.18) and shows variation in backscatter levels between low and medium backscatter (Plate 4.15). Surface sediment sampling at a sufficiently high density to define these variations sedimentologically was impractical in the time available. It is suggested that they may represent minor variations in grain size or organic matter content.

Two types of topographical features are associated with the fluvial input zones. These comprise the subaqueous channel of the Black Burn, which is cut into fine grained sediment, and deltaic aggradation. Deltaic topography is discussed in section 7.2.1.2.2 below.

7.2.1.1.4 Fine grained sediment

Outside the sediment texture zones given above sonographs show that the loch sides are covered by medium to low backscatter areas and sediment sampling indicates that the loch floor is covered by fine grained sediment (see section 7.2.1.2.4 below). On the northern slopes, between the northern mouth of the Allt an Dubh-loch and the mouth of the Glas Allt, the loch slopes are covered by sandy mud, which appears as a homogenous area of medium backscatter on the sonographs. In deeper water, low backscatter levels occur below the boulder spreads, coincident with the areas of mud, where a downslope textural

variation is recorded (Figure 5.23). The central, deep water area of the loch is dominated by fine grained, highly organic, very poorly sorted sediment, typical of Scottish lochs (e.g. Loch Tay, Al-Jabbari et al., 1983; Loch Tummel, Duck, 1986; Loch Lubnaig, Asaad and McManus, 1986) with a dominant, polymodal, glacial till sediment source. The high percentage of organic matter in the bottom sediments is believed to result from anthropogenically induced erosion of the peat deposits in the catchment (section 5.6.3), and subsequent transportation and deposition in the loch. Evidence from the sonographs indicates that there is also a very coarse grained organic input, in the form of saturated, sunken branches and trunks of trees (Plate 4.13). This is probably directly deposited into the loch from the birch, larch and pine stands growing around the shores (see Plate 1.6). QDa-Md analysis confirms that the majority of samples obtained along the longitudinal axis of the loch were deposited in quiet water or fluxoturbidite conditions, by settling through the water column and minor mass movements. The evidence suggests that the lower slopes and central area of the loch are the accumulation zones for the fine grained sediment entrained by wave action, low density organic matter particles, and the fine grained component of fluvial and avalanche/debris flow inputs (see section 7.2.1.1.1). Post-depositional mass movements, in the form of slumps and slides, are also apparent from the QDa-Md data derived from surface samples, supported by analyses of core material (see section 7.2.2.1 below)

7.2.1.2 Surface sediment topography

Four groups of topographic features are examined in this section:- shore-parallel terraces, deltas, mounds and hollows composed entirely of Sequence 1 sediment, and draped sediment. It is recognised that both shore-parallel terraces and deltas are probably time-transgressive features. In the case of the former, the terraces are probably partially eroded into Sequence 3 Lochnagar Granite Complex bedrock, and the latter possibly has a gradational boundary with Sequence 2 sediment. Neither sidescan sonar nor Pinger seismic subbottom reflection profiling provided sufficient data in these areas to enable

differentiation between sequences in critical areas, therefore they have been included with the other surface sediment topographical features to maintain continuity.

7.2.1.2.1 Shore-parallel terraces

A maximum of three poorly defined shore-parallel terraces, represented by alternate dark-light bands on the sonograph, running parallel or sub-parallel to the shoreline, are recognised in Loch Muick solely on the evidence from sidescan sonar surveys (Plates 4.12, 4.13, 4.14, 4.16, 4.17, 4.18). These features have an extensive distribution, occurring around most of the loch shoreline, excepting the central part of fluvial input zones and where boulder spreads have apparently resulted in infilling and obliteration (see Plate 4.18 for examples). There is also no evidence of shore-parallel terracing on the slopes around the island close to Glas Allt Shiel (Figure 2.15). Echosounder survey (Chapter 2) and subsequent bathymetric charting (Figure 2.15) does not reveal the existence of these features, indicating that the vertical 'riser' must have an amplitude of <1m. The boulder covered horizontal 'treads' have a maximum width of 10m (Plate 4.14), the majority falling in the range 2m-7m. Frequently boulders identified on the flat 'tread' sections do not exhibit areas of acoustic shadow, indicating that they are partially buried in the fine grained sediment of Sequence 1. The composition of the almost vertical, 'riser' sections cannot be determined from the sonographs due to the intense, dark, reflection obtained from these steep slopes. Profiling of the nearshore zone by Pinger did not provide any further information as to the nature of the substrate underlying these features. The substrate may either be Sequence 2, glacial sediment, or Sequence 3, bedrock. These features extend to a maximum depth of approximately 2m.

Shore-parallel terraces have been reported from numerous other Scottish waterbodies (e.g. Loch Earn, McManus and Duck, 1983; Glenfarg Reservoir, Duck and McManus 1985c; Loch Tay, Duck and McManus, 1987a). It has been proved that these features are formed by wave induced erosion of diamict and lacustrine sediment at the

shoreline during periods of lowered water level (Duck and McManus 1985c). The magnitude of the features is partially constrained by the substrate into which they are eroded and partially temporally constrained. Lowered water levels maintained during the summer months restrict erosion to wave dominated processes, effective only over the period of reduced loch volume. Thus shoreline development in Loch Muick is believed to result from short term lowering of the water level during abnormally dry summer seasons when wave erosion by abrasion dominates.

7.2.1.2.2 Deltas

Sediment accumulation at the mouths of the main influent streams is recognised from geomorphological mapping (Figure 1.6), bathymetric surveys (Figure 2.15) and sidescan sonar surveys. In the case of the Allt an Dearg, subaqueous sediment accumulation associated with the stream inflow is identified only on the sidescan sonographs as the topographical expression is <1m. Pinger seismic subbottom reflection profiling did not penetrate any of these sediment accumulations, a phenomenon reported from other waterbodies where the sand content of sediments (confirmed in Loch Muick from the sidescan sonar and sediment sampling programmes) is relatively high (Desloges and Gilbert, 1991). Therefore, the interpretations given below are based on the external topographic expression and surface sediment characteristics and distribution.

Two of the four major influent streams, the Allt an Dubh-loch and the Black Burn, exhibit subaerial deltaic areas (Figure 1.6) indicative of episodic sedimentation events (Ashley, 1988). Particularly extensive deltaic aggradation is recognised adjacent to the inlets of the Allt an Dubh-loch and extending 500m westwards towards the head of the Glen. In common with the features in Glens Callater and Lee (sections 7.3.1.2.2 ; 7.4.5.1, this landform is believed to be time-transgressive, sedimentation starting during the retreat of the Glen Muick glacier from glacial meltwaters (for proposed age see section 7.2.2.1), and continuing at a reduced volume and rate to the present day. In the subaqueous

environment the mouths of these streams are associated with relatively wide areas of shallow water extending approximately 90m into the loch. Sidescan sonar shows that this surface, close to the southerly inlet of the Allt an Dubh-loch has a discontinuous, scattered cover of small boulders and cobbles (Plate 4.12, section 4.6.2.1), lying on a sandy bottom. This sediment association does not occur at the entrance of the Black Burn, which is dominated by finer grained, highly organic mud into which the stream channel is eroded (see section 7.2.1.1.3 above). Below both these relatively flat areas there is a significant increase in slope (Figure 2.15). At the southerly entrance of the Allt an Dubh-loch the steep slope appears as a dark band on the sonograph. Scattered boulders and cobbles can be distinguished on the upper part of this slope (Plate 4.12), but the reflection from the lower, steeper slope prevents distinction of the sediment type or texture. At the base of this slope bathymetric and sidescan sonar evidence indicates that there is a significant break in slope to lower angles. This suite of slope angles - gentle-steep-gentle - in the context of a stream inflow into a water body is interpreted as representing the topset-foreset-bottomset depositional zones of a typical Gilbert type delta (e.g. Thomas, 1984; Carter and Carter, 1991). Delta deposition is widely accredited to episodic deposition resulting from infrequent flood events (Clemmensen and Houmark-Nielsen, 1981; Weirich, 1985) which may account for the entrainment and deposition of relatively large clasts by the small stream. Evidence of the topset-foreset deposition transition is present on the sonograph (Plate 4.12). This comprises the larger clasts, deposited close to the mouth of the stream, resulting from mixing and deceleration of the influent current, and the medium sized cobbles identified at the top of the foreset slope, deposited in this position by current induced rolling over the topset terrace. Bottomset sedimentation at the southerly Allt an Dubh-loch delta is, according to sonograph and surface sediment data, primarily composed of sandy sediment, with a low coarse grained input.

The complete delta slope profile is not distinct at the inflow of the Black Burn. In this locality there is a broad, nearshore shelf, extending to a depth of 5m below water level

at which point a break in slope occurs, falling to 38m. Between depths of 38m and 47m the slope angle declines before descending steeply to the centre of the trough. It is suggested that this profile represents the accretion of deltaic sediments on an extremely steep slope. This results in a laterally extended area of foreset deposition and compressed bottomset zone, possibly prograding over a slope irregularity such as a bedrock knob or morainic accumulation which provided the initial reduction in slope angle.

A more complex area of deltaic aggradation is identified at the mouth of the Glas Allt (Figure 2.15) where the sand dominated (Figure 5.23, section 5.5.2) area of topset deposition is complicated by a steep increase in slope angle between depths of 10m to 15m, followed by a shallow gradient between 15m and 21m below the water surface. Echosounder and sidescan sonar surveys have identified a mound rising to 13m below the loch surface, lying at a depth of 19m-20m. The location and adjacent topography of this mound indicates that it probably represents a slide composed of topset and foreset beds. The source area is believed to be the curved depression located behind the mound. Possible mass movement triggering mechanisms are discussed in section 7.2.1.2.3 below. The mound, resulting from mass movement, appears to have destroyed the foreset form and occupies the area of bottomset deposition. The apparent lack of fluvial modification of the mass movement topography by either erosion or deposition suggests that the subaqueous landform on the Glas Allt delta results from relatively recent mass movement activity.

The inflow of the Allt an Dearg is not associated with a distinct area of deltaic aggradation. Instead a fan of finer sediment, with occasional scattered boulders, covers the steep slope below the mouth of the stream (Plate 4.15). The steepness of this slope is reflected in the relatively high Form Roughness values obtained in the squares adjoining the mouth of the stream (Figure 2.23). It is believed that this landform results from sediment instability on the extremely steep subaqueous loch slopes, possibly combined with a lower sediment input than the other streams considered above. Sediment fans have also been identified by sidescan sonar survey on the steep side slopes of Loch Earn where small streams enter the loch (McManus and Duck, 1983; Duck, 1987).

7.2.1.2.3 Mounds and hollows

This section examines the mounds and hollows composed entirely of Sequence 1 sediments and therefore does not include the spectacular features on the lower slopes and floor of Loch Muick, which Pinger seismic reflection surveys indicate are formed of Sequence 2 glacial sediments, over which Sequence 1 material is draped (see section 3.7.2.1). Two distinct groups of mounds and hollows, other than those discussed in section 7.2.1.1.2 above, are distinguished in Loch Muick:-

- i) Those with an amplitude of $<1\text{m}$, identified only from sidescan sonar survey, and composed of coarse grained boulder spread material.
- ii) Those with an amplitude of $\geq 1\text{m}$, recognised from echosounder and, in the majority of cases, Pinger seismic subbottom reflection profiling surveys.

These subaqueous landforms are named, for the purposes of classification, low amplitude features and high amplitude features, respectively. However, calculation of Håkanson's Form Roughness measure (R_f) (section 2.6.4, Figure 2.23) indicates that neither of these two groups of mounds and hollows is of sufficient amplitude to increase significantly the R_f value obtained.

7.2.1.2.3.1 Low amplitude features

These mounds and hollows are recognised only on the upper parts of the loch slopes. Sidescan sonar enables subaqueous landforms with an amplitude of $\geq 0.2\text{m}$ to be clearly distinguished from the surrounding loch floor (McManus and Duck, 1988a). It is probable that similar features occur downslope, outside the area covered by the survey. Evidence in support of this hypothesis is found in the distribution of sediment sorting (Figure 5.27). It is suggested that the areas of very poorly sorted sediment where there is no topographic expression on the bathymetric chart (Figure 2.15) result from fine grained sediment mass movements associated with the deposition of the boulder spreads. The low amplitude features identified form the terminal sections of the boulder spread deposits

discussed in section 7.2.1.1.1 and illustrated in Plate 4.14. The mounds comprise the terminal lobes of the boulder spreads, whereas the acoustic shadow zones representing the hollows (see section 4.6.2.2) are created by the areas between the lobate deposits.

7.2.1.2.3.2 High amplitude features

High amplitude mounds and hollows in Sequence 1 deposits are differentiated from the glacial features of Sequence 2 by Pinger subbottom seismic reflection profiling, with the exception of the mound close to the Glas Allt inflow, which is recognised as being of Sequence 1 origin primarily on bathymetric data (see section 7.2.1.2.2 above). These features occur on the steep slopes in Zone D, the mid- and lower slopes of Zone C, and at the mouth of the Glas Allt in Zone B (see Figures 2.16 and 2.15). The majority of mounds and hollows consist of pairs of landforms comprising an upslope hollow with a mound downslope. An easily distinguished example of this pairing is located on the southerly slopes on the boundary between Zones C and D. This consists of a hollow 10m deep at a depth of 29m and a mound 2m high a further 25m downslope. The possible reasons for this apparent loss of volume, and the occurrence of hollows with no discernible related mound, are discussed below in this section.

It is proposed that these subaqueous landforms represent a continuum and result from mass movement processes. Carter (1975) lists five possible causes for the failure of a sediment mass due to the reduction of shearing resistance below the applied shear force:-

1. Thixotropic change due to applied shock (e.g. earthquake).
2. Initial metastable sediment accumulation.
3. Oversteepening of the sediment due to undercutting by waves, currents or mass failure.
4. Excess pore water pressure induced by upward flow of fluid through the sediment causing mobilisation.
5. Increase in sedimentary burden from above or increase in the angle of slope on which the sediment rests.

Of these five possible scenarios the first is unlikely to be a significant factor in initiating mass movements as the field area lies outside any of the recorded epicentres of earthquakes in Great Britain (Perry, 1981, p150) and other possible causes of applied shock are unknown. Likewise, the third and fourth factors are probably insignificant in causing mass movements. Evidence from submerged shorelines (section 7.2.1.2.1) suggests that oversteepening of the sediment due to undercutting by waves is restricted to a maximum of 2m below the present water level (currently 400.26m, section 2.6.5). It is probably only significant around the shores of the island where all the survey techniques failed to identify positive topographic evidence of mass movements, but where these processes are inferred as having occurred (see section 7.2.1.2.1 above). The impact of undercutting by currents cannot be quantified, as measurement was considered to be outside the scope of this thesis. Likewise there is probably a small, but unquantified number of mass movements brought about through undercutting by small mass failures. The fourth cause is thought to be insignificant, as it is believed that a concentration of water beneath the sediment pile with a sufficient pressure to cause upward flow only results when major flood events deposit a thick layer of sediment, inhibiting normal subsurface water movement. Evidence of major flood events is inferred from sedimentological data from the core obtained in Loch Muick (see section 6.6.3.2.2). However, Pinger subbottom profiling indicates that recent (i.e. post glacial) sedimentation is focused in the central, deep water, gently sloping trough, whereas the landforms of mass movement occur on the steep upper and mid slopes of the loch basin. It is for this reason that upward water flow is discounted as a major causal component of mass movements in Loch Muick.

Thus there are two remaining causes of mass movements that may account for the subaqueous landforms identified in Loch Muick:- Initial metastable sediment accumulation and increase in sedimentary burden from above. The latter is believed to be the cause of the mass movement that formed the mound and hollow located on the delta at the mouth of the Glas Allt (see section 7.2.1.2.2 above), due to the pulsatory sediment input (Ashley,

1988). Furthermore, Moore (1961) suggests that deltaic deposits have a very low shear strength, and research in Lake Tekapo, New Zealand (Pickrill and Irwin, 1983) indicated that 23% of the lake floor area, particularly the areas of deltaic accumulation, was affected by rotational failures and slumping.

It is suggested that the remaining mounds and hollows resulted from a combination of metastable accumulation of sediment deposited by coarse grained sediment deposition and settling of fines through the water column onto the steep slopes, and the increased sedimentary burden, resulting in an increase in shear stress above the threshold of movement triggering downslope mass movements. Evidence from Pinger seismic subbottom reflection profiling suggests that the mounds are created by slumping, as internal subparallel or parallel reflectors are replaced by chaotic reflectors in the zone of deposition (see section 3.7.2.1.2). Additionally no slide planes have been recognised in association with either the mounds or hollows. This proposed mass movement activity probably contributes to the poor sorting of the surface sediment identified in Chapter 5 (sections 5.5.4, 5.6.3), but this is believed to be primarily an inherited characteristic of the source sediment (till).

In Zone D (Figure 2.16) there are three shallow depressions, ranging between 1m and 3m in depth, in a midslope position, from which gullies extend upslope (Figure 2.15). Pinger data (Figure 3.33) confirm that these features are confined to Sequence 1 sediment. Thus the hollows represent the source depressions of mass movement slumping which resulted in the widespread distribution, as opposed to discrete accumulation, of sediment across the lower slopes, with a probable significant loss of finer sediment to suspension. This type of mass movement could be caused by more loosely packed, unstable sediment than that where mounds are formed. Landforms associated with this deposition zone, but of an insufficient amplitude to be present on the bathymetric chart, may occur downslope. Sidescan sonar surveys were unable to scan to the depth required to confirm or reject this hypothesis. Alternatively, the lower density of survey lines in this area (Figure 2.13) may have resulted in minor omissions.

Pinger subbottom seismic reflection profiling of the areas of mass movement where the smaller mounds and hollows, discussed in this section, occur show that there has been negligible infilling of the features. Thus it is believed that the smaller mounds and hollows result from recent mass movements. Chaotic and subparallel lenticular reflectors identified in Facies 1.2 (section 3.7.2.1.2) probably represent infilled mounds and hollows that no longer exhibit topographic expression.

7.2.1.3 Draped sediment

This section examines the internal structure and composition of Sequence 1 sediment that has no distinct surface morphology, forming a drape over the underlying substrate. Pinger seismic subbottom reflection profiling (Chapter 3), combined with analysis of core material (Chapter 6), provides additional data, complementing the surface sedimentological and morphological information given above. The different approach to data analysis derived from the two techniques produces two classificatory systems for the same sediment, facies and units respectively.

The most recent, poorly consolidated, surface sediment (Facies 1.1) exhibits no seismically definable internal structures. It has a limited distribution within the loch, forming infills in topographic lows of Facies 1.2, and thinning upslope. Surface sediment sampling obtained one sample (T2S3) from the central loch area of Facies 1.1 (Figure 3.30). The sediment texture is mud, with an abnormally low (1.9%) percentage of sand and high total organic matter content (61.1%). However, as indicated in section 3.7.3.1, it is suspected that, despite the high frequency profiling equipment used, the apparently limited distribution of Facies 1.1 results from the low reflection amplitude of the surface reflector as opposed to the actual absence of the facies. This thereby implies that a considerable number of the surface sediment samples, particularly those obtained from depressions on the sides of the loch and the bottom of the basins, are probably composed of Facies 1.1 sediment. Thus the sediment forming Facies 1.1 is dominantly highly organic

mud (T.O.M. 52%-68.8%), with a low sand and high silt content. It is possible that in the small southwestern basin Facies 1.1 is composed of sandy mud, with a lower (38.7%) organic content. It is suggested that Facies 1.1. closely resembles the 'soupy' consistency of Ivory Lake floor described by Hicks et al., (1990).

Lying stratigraphically beneath Facies 1.1, forming the more consolidated draped sediments on the sides and bottom of Loch Muick, is Facies 1.2. This drape is primarily composed of minor subparallel internal reflectors forming a single layer over the underlying sequence. One Pinger traverse (132-136, Figure 3.26, Plate 3.6), from which the core was obtained, indicates the existence of multiple downlapping major reflectors. In the context of the Pinger data alone it was suggested (section 3.7.3.1) that this reflector configuration represents deposition by a rapid, pulsatory sedimentary input. However, coring at this location does not support this formational hypothesis.

Two units were identified within Sequence 1 (sections 6.6.3.2.2, 6.6.3.2.3), with a gradational boundary at 187cm below the top of the core. The lower unit (Unit 2, 187cm-475cm) is interpreted as representing the early- to mid- Postglacial and contains sedimentological and geochemical evidence of major erosional events which decline in intensity towards the boundary with Unit 3. Unit 3 (0cm-187cm) as a whole shows no sedimentological, geochemical or visual evidence of the rapid deposition indicated by Pinger records. The unit exhibits fine laminations and a low clastic content. The available data are interpreted as indicating the decrease in erosion and increase in organic matter content typical of climatic amelioration during the middle to late Postglacial, with an anthropogenic input at the top of the core.

Thompson and Kelts (1974) reported that in one case material deposited by slumping could not be clearly differentiated by visual examination or mineralogical analyses, only by measurement of magnetic susceptibility. This 'invisible slumping' is not thought to have caused the downlapping reflector configuration identified by seismic reflection profiling in Loch Muick. Analysis of the core material indicates that, at the boundary division between Units 2 and 3, there is no sedimentological parameter sufficient

to result in acoustic impedance (see section 3.2.2). There is, however, at 200cm in Unit 2 a significant decrease in the water content of the sediment coincident with a high percentage of sand and low percentage of organic matter. This is believed to be of a sufficient magnitude and in an appropriate stratigraphic position to represent the major internal reflector recorded in Traverse 132-136. Thus the point selected at the gradational boundary between Units 2 and 3 (section 6.5.2.2) is not coincident with the major reflector identified in Facies 1.2.

The internal reflector in Facies 1.2 referred to above is interpreted, in view of core analysis (section 6.6.3.2.2) and previous studies (Taishi et al., 1991), as resulting from rapid deposition associated with a major flood event. QDa-Md analysis (section 6.5.6) indicates that the sample was deposited in relatively quiet water conditions (fluxoturbidite), therefore in a distal position from the point of sediment input. There is no evidence of any previous or subsequent breaks or interruptions in deposition in Units 2 and 3. Thus there is a dichotomy in the interpretation of Facies 1.2/Units 2 and 3.

Sedimentological and geochemical data obtained by analyses of core material suggest that:-

i) At the point where the core was taken, sedimentation has been continuous since at least the end of the Loch Lomond Stadial (section 6.6.3.2.1).

ii) *At this location* the major internal reflector results from significant variations in the water, organic matter and clastic content caused by deposition of sediment during a flood event.

However, seismic reflection profiling indicates that:-

i) The internal reflectors of Facies 1.2 have a downlapping termination configuration typical of rapid, pulsatory deposition.

ii) The internal reflector identified by core analysis can be identified rising to the top of the seismostratigraphic column at the eastern end of the traverse (see Plate 3.6, Figure 3.26).

Given the available, conflicting evidence, it is suggested that the internal reflectors may

result from numerous acoustic impedance variables that, when combined, create an internal reflection configuration comparable to a downlapping termination and therefore that the core data be accepted as representing the depositional history of Loch Muick. It is recognised that this is an imperfect explanation of the available evidence, resting on sedimentological data from one point only, and that further examination of this hypothesis requires additional coring and Pinger profiling of the sediments profiled in Traverse 132-136 and in the remainder of the loch.

7.2.2 Sequence 2

7.2.2.1 Core Unit 1

Coring of the bottom sediment of Loch Muick has identified a sedimentary unit, Unit 1, which has not been differentiated using the Pinger high frequency seismic reflection profiling technique. The possible reasons for the absence of Unit 1 on the seismic record are discussed below. Unit 1 is, however, included within this section covering the glacial sediments of Sequence 2 as sedimentological and mineralogical evidence and reference to published data (e.g. Clague, 1986; Nesje et al., 1991) point to the deposition of the sediment during or immediately after the last glaciation of the catchment (see section 6.6.3.2.1).

Critical in ascertaining the age of this last glaciation in Glens Muick, Callater, and Lee, the subject of which has been the source of considerable contention (see section 1.4.2), are the data obtained from core material collected in Lochs Muick and Callater. Comparison of the analytical data, combined with seismic profiles of the sediment lying below the depth of core penetration, indicate that both lochs have experienced only one period of recent glacial activity. Sedimentary deposition in waterbodies lying outside Loch Lomond Readvance glacier limits is characterised by two minerogenic layers composed of clay, silt and coarser sand and grit sized particles separated by a layer containing a higher level of organic matter. This sequence of sediments is interpreted as representing the Late

Devensian-Lateglacial Interstadial-Loch Lomond Stadial transition (e.g Walker and Lowe, 1990; section 6.6.2.2.1). Thus both subaerial (sections 1.5.4.2.2, 1.5.3.2.2) and sedimentological evidence indicate that the Loch Muick and Loch Callater troughs were occupied by glaciers during the Loch Lomond Readvance. Interpretation of the pollen analyses carried out on the Loch Callater core (sections 6.4.7, 6.6.2.2.1 and section 7.3.3.1 below) further substantiates the proposed age of Unit 1.

The absence of Unit 1 on the seismic records may result from one or a combination of factors. First, the total thickness of the unit may be at or below the limit of resolution of the equipment. Coring has established that the minimum thickness of Unit 1 is 25cm, which also represents the maximum resolution of Pinger 3.5kHz subbottom reflection profiling equipment. Therefore Pinger profiling suggests that, throughout Loch Muick, Unit 1 does not significantly exceed a maximum thickness of 25cm. Secondly, layers of massive silts have been reported as appearing seismically transparent (Mullins et al., 1990). In combination these two factors result in a seismic record that does not permit differentiation of the unit or facies from the adjacent facies (Lineback et al., 1972; Johnson 1980a).

Unit 1 is composed of fine grained silt sized particles that comprise a maximum of 97.9% of the sample after removal of organic matter. The total organic matter and water content of samples obtained from Unit 1 are very low, with a maximum of 0.4% and 25.2% respectively. X-ray radiography indicates that the sediment is massive, but QDa-Md analysis has led to the suggestion that deposition was by alternate current and non-current dominated processes, possibly representing annual variations in the mode of deposition (section 6.6.3.2.1). It is recognised that the interpretations given below are based upon one core only and may, therefore, not form a representative sample of the subbottom sediment. However, given the available data it is considered appropriate to provide interpretations.

Glaciolacustrine silt deposition in a waterbody occurs when a glacier is in direct contact with a lake (Fulton, 1965; Lineback et al., 1974) or immediately after the retreat of the ice tongue(s), by sediment charged glacial meltwater combined with erosion of

subaerial moraine (Davis and Ford, 1982; Clague, 1986). The fine grained and massive nature of Unit 1 silts indicates that deposition occurred in an ice distal position (Smith, 1978). There is no evidence *at this location* of an input from iceberg overturn. This suggests that the sediment of Unit 1 was deposited after the retreat of both the Glen Muick and Black Burn glaciers from the loch basin. Thus the silt was derived from both subaerial erosion and sediment charged glacial meltwater. Analysis of reported data from modern analogues (e.g. Donnelly and Harris, 1989) has led to the conclusion that the fluvial component of the silt (inferred from QDa-Md analysis) was deposited by the distal portion of sediment charged meltwater density underflows. As the glaciers retreated so did the number, velocity and volume of entrained sediment of density underflows. The diminished sediment supply resulted in increased inter- and overflow activity as the density of the influent meltwater decreased (Donnelly and Harris, 1991). The remaining sediment, deposited in quiet water, is typical of the sedimentation of massive silts in the low energy ice-covered lacustrine environment of spring and autumn (Desloges and Gilbert, 1991; Donnelly and Harris, 1991). It is believed that Unit 1 represents the upper part of a continuum of outwash deposits, Facies 2.2 forming the lower, ice proximal, coarser sediment (see section 7.2.2.3 below). Thus it is suggested that the lower boundary is gradational and conformable. The upper boundary is unconformable with Unit 2, laminations within the upper unit terminating against the lower. It is suggested that this unconformity results from syndepositional mass movement of the silt (see section 6.6.3.2.1).

7.2.2.2 Facies 2.1 Topography and sedimentology

The parastratigraphic interpretation of Facies 2.1 (section 3.7.3.2) is that the external form and internal reflector configuration represents glacial diamict resulting from direct glacial deposition. The existence of internal reflectors, believed to have been formed by compaction during glacial overriding of the landforms, further justifies this interpretation. It is therefore proposed that Facies 2.1 is the subaqueous equivalent of the

subaerial till deposits identified through geomorphological mapping (section 1.5.4.2; Figure 1.6).

The subaqueous topography created by the glacial landforms examined in sections 7.2.2.2.1 and 7.2.2.2.2 have a close visual correlation with the Form Roughness (Rf) (section 2.6.4; Figure 2.23). The zone of glacial mounds and hollows (Zone B, section 2.6.3.2) has the highest Form Roughness of the four geomorphological zones followed by the zone in which numerous ridges have been identified (Zone C). The examination of the complete data set, derived from all the techniques used on Loch Muick, indicates that in this water body, where sedimentation has been occurring since the retreat of the ice, the distribution of Rf values, which shows an initial correlation with the former extent of glaciation, cannot be used as a diagnostic indicator.

7.2.2.2.1 Ridges

Bathymetric charting of Loch Muick (Figure 2.15) identified seven prominent ridges or ridge sections located on the mid and lower slopes of the trough. Six ridges occur within one geomorphological zone (Zone C, section 2.6.3.3; Figure 2.16) a 1km section of the loch, and one, more isolated feature, forming the boundary between Zones A and B (section 2.6.3.1), is located approximately 700m up the glen, northwest of Zone C. Pinger subbottom reflection profiles have subsequently shown that these subaqueous landforms are composed of Facies 2.1, glacial diamict. The synthesis of high resolution topographic data obtained from a dense network of high frequency echosounder traverses (section 2.6.2) and Pinger data giving information on the depth of burial by Holocene sedimentation (virtually nil on the steep slopes of the ridges) provides an important information source on the external morphology and internal composition of the ridges.

The ridges which partially cross the Loch Muick trough are unique to the subaqueous environment. There is no evidence that they ever extended to, or above, the present shoreline onto the slopes surrounding the loch; nor have ridges been identified in

the upper parts of Glen Muick by geomorphological mapping (see Figure 1.6). Ridge distribution of this nature has been reported from the marginal valleys of the retreating Barnes Ice Cap, Baffin Island, where extensive areas of proglacial ridge and swale topography have been mapped in the present subaerial environment.

The first recorded description of these features was by Goldthwait (1951) who recognised their environmental origin in naming them 'sub-lacustrine moraines'. Subsequent research carried out by Andrews (1963a, b) and Andrews and Smithson (1966) attempted to quantify and describe the characteristics of the 'cross valley moraines' and suggested possible formational processes. However, it was not until Holdsworth (1973a, b) and Barnett and Holdsworth (1974) undertook an intensive study of 'sublacustrine moraine' formation in proglacial Generator Lake that a consensus of agreement on the processes involved was reached. Observations of the margin of the Barnes Ice Cap in Generator Lake, where sublacustrine moraines were known to be forming (Andrews, 1963a; Barnett et al., 1970), showed that the terminus of the ice was characterised by cliffs formed by rapid mechanical break up in water depths of $\leq 33\text{m}$, and ramps of semi-floating ice where the lake depth exceeded 33m. Sections of ramp were observed to break free and rotate backwards close to the ice margin during the brief summer maximum in lake level. High lake levels were caused by a rapid meltwater influx combined with jamming of the lake outlet by sections of broken lake ice. These data led to the setting up of a model describing the formation of sublacustrine moraines (Barnett and Holdsworth, 1974).

The 'Ramp-Moraine Model' assumes the existence of a retreating ice margin in a deep water ($\geq 30\text{m}$) lake. In this environment, given only minor (1m approx) fluctuations in the lake water level, the unconfined ice front forms semi-floating ramps. Beneath the ramps deposition of subglacial and englacial debris occurs, the external form reflecting the wedge-shaped area beneath the ramp. The size of the proto-sublacustrine moraine is dependent upon the volume of moraine available for deposition and is:-

'Proportional to the time of existence of the ramp or inversely proportional to the maximum summer lake level rise' (Barnett and Holdsworth, 1974, p. 403).

During periods of temporary high lake level, the ramp may become completely submerged, and upward buoyancy force acts upon the ice. This causes the ramp to bend upwards, increasing stress at the point where it departs from the ice margin, which results in calving and rotational displacement of the ramp. Thus the morphology of the sublacustrine moraine is also determined by post depositional ice movements.

The subaqueous landform produced is typically asymmetric in form, having a steep distal (30-40°, Andrews 1963a) slope, often at the angle of rest of boulders and cobbles °, Andrews, 1963a) slope.

They reach a maximum crest height of 35m (attained in the centre of the Rimrock and Isortoq valleys), have an undulating crest, and are composed of short, offset segments. Sublacustrine moraines are frequently arcuate in plan, concave to the ice margin and, where exposed subaerially, terminate below the shoreline of the lake level at which they were formed:-

'They begin as small ridges and gradually emerge from the maze of boulders that are found at higher elevations' (Andrews, 1963a, p. 65).

Studies of the internal composition of the moraines have shown that the proximal slope is more highly compacted than the distal (Barnett and Holdsworth, 1974) and may exhibit shear planes (Andrews, 1963b, p98-99) dipping downwards towards the former direction of glacier movement.

The subaqueous landforms of Loch Muick fit the above description closely. Ridges 1, 2 and 3 are sharply asymmetrical (Figure 2.16), with a gentle slope on the former ice proximal side and a steeper ice distal slope. The remaining ridges, with the exception of that dividing Zones A and B (Traverse 114-111, Figure 3.24), are located on the lower slopes or on the trough bottom and have been subject to more substantial Holocene deposition. Thus the surface expression of these features appears to be more muted. However, Pinger profiling indicates that, beneath the drape of Holocene sedimentation, these ridges are also distinctly asymmetric. All the ridges appear to be composed of separate sections which create a sinuous, disjointed plan outline. Five of the seven

subaqueous landforms exhibit a curved morphology, concave towards the former ice margin. Of the remaining two, Ridge 7 is almost linear and Ridge 3 has a compound form, curving first in an ice concave direction and then ice convex. That Ridge 3 was formed by the same process(es) which created the remaining ridges is undoubted (see below, this section). Pinger data indicate that the ridge is a continuous landform with the apparently isolated mound (section 2.6.3.3) at the base of the southern slope. The broken ridge on the mid/upper southern slope is probably a partially eroded section of Ridge 3. Likewise the remaining ridge sections described in section 2.6.3.3 can be seen to continue across the centre of the trough beneath a drape of Facies 1.2 and infill of Facies 2.2 (Figure 3.28). The maximum height of these buried subaqueous landforms cannot be measured due to the attenuation of the high frequency signal, but is known to exceed 11m.

Pinger subbottom seismic reflection profiling has also enabled the identification of short ridge sections in the centre of the trough, northeast of Ridge 6, which cannot be recognised solely by surface expression (see Plate 3.7). Three buried ridge sections have been identified in Loch Muick extending marginally beyond the mouth of the Allt an Dearg. It is suggested that the spur on the southern slope of the trough, which falls within Geomorphological Zone D (section 2.6.3.4) and is composed of Facies 2.1 sediment, represents the only significant surface morphological expression of the most northeasterly, terminal ridge.

Internally the ridges are composed of numerous boulders in a finer matrix (see section 3.7.3.2). Stratification within Facies 2.1 is restricted to the former ice proximal slopes of the ridges (Plate 3.7; Figure 3.28) and is believed to represent compaction by glacial overriding. In the context of the ramp-moraine model the compressional reflectors of the ridges in Loch Muick are interpreted as representing the shear planes caused by rotational movement of the ramp section after calving.

Thus the subaqueous morphology of Loch Muick is believed to represent an example of sublacustrine moraines (*sensu* Barnett and Holdsworth, 1974) formed during

retreat of the glaciers that occupied Glen Muick during the Loch Lomond Stadial. This finding is a unique record from British waterbodies. A limited number of researchers have identified sublacustrine moraines now exposed subaerially. Peacock and Cornish (1989) report 'cross valley' moraines in lower Glen Roy, deposited by the Spean glacier during the Loch Lomond Readvance, and Benn (1989) has identified and analysed ridges, also formed during the Loch Lomond Readvance, at the site of a former ice dammed lake at Achnasheen, Ross-shire.

The spacing of the Loch Muick sublacustrine moraines, 10 over a distance of approximately 2.1km, is lower than that reported from Baffin Island, where there are ≥ 2000 moraines within a 70km stretch of the Isortoq valley (Andrews and Smithson, 1966). The number of moraines and moraine development is known to be dependent on the stability of the ice front (i.e. time dependent) and the volume of available debris. Subaerial evidence of moraine development (section 1.5.4.2) suggests that the glaciers which debouched into the Loch Muick trough had a debris content typical of valley glaciers which developed during the Loch Lomond Stadial.

The three buried, or partially buried ridges at the extreme northeastern end of the loch are the most poorly developed, exhibiting surface topographic expression at only one point. Due to the location of these ridges within the loch it is believed that the outermost (i.e. most northeasterly) ridge represents the maximum limit of glaciation in Glen Muick, approximately 1.4km further down valley than previously proposed (Sissons, 1972a; Sissons and Grant, 1972). Morainic evidence suggests that this position was attained for a relatively short time, preventing substantial sub-ramp sedimentation. The glacier retreated rapidly from the maximum down valley position. Assuming a continuous debris supply rate, the glacial stillstand at the two completely buried ridges was briefer than at the maximal limit. Barnett and Holdsworth (1974) have shown that in Generator Lake, where debris comprises 8% +/- 2% of the ice volume, a ridge 3m high forms in less than one decade. Thus the buried moraines which have amplitudes of approximately 7m may have developed during periods of 1-2 decades. The absence of sublacustrine moraines on the

steep trough sides associated with the buried moraines could result from:-

- i) Non-development of ice ramps, across the entire ice front and thus sublacustrine moraines.
- ii) Removal of the landforms by post-depositional erosion and mass movement.
- iii) Post-depositional infilling of the topography.

Pinger data indicate that the third hypothesis should be rejected; there is a thin drape of Holocene sediment overlying Sequence 3 (bedrock) on the loch slopes at this location. Available evidence does not permit testing of the first two hypotheses. The coarse grained nature of the glacial sediment would not allow distinction of redeposited sediment from either Facies 2.1 or Facies 2.2 (outwash).

Echosounding has indicated the existence of a broken ridge aligned northeast to east across the shallow water area close to the River Muick (section 2.6.3.4) beyond the maximum Loch Lomond Readvance limit suggested above. This feature is not believed to have been formed by direct glacial action during the Loch Lomond Stadial due to its seismic signature. Pinger profiles of the flat area on which the ridge lies and the slope up to this area (Figure 3.23) indicate that, beneath an occasional thin cover of Facies 1.1, there is a high intensity reflector which could not be penetrated by 3.5kHz sound pulses. It is suggested that this reflector, which can be traced from the slope onto the shallow water area, is not the upper surface of Facies 3.1 due to the irregularity of the surface reflection which is inconsistent with that identified at all other localities. The irregularity is particularly pronounced close to the outlet, and includes the broken ridge. It is tentatively suggested that the reflector represents a lateral, ice distal variation of Facies 2.2, deposited by icebergs (see section 7.2.2.3.2 below).

The morphology of Ridges 6 and 5 suggests that a more significant stillstand of the ice margin occurred at these positions, followed by a rapid retreat during which morainic deposition was flat and featureless, with no compressional reflectors. The next series of stillstands (Ridges 4-1) occur at intervals of approximately 150m apart, parallel to the mouth of the Black Burn. The implications of these ridges on the history of the Black Burn glacier are discussed below (section 7.2.4.2). Ridge 3 is particularly interesting as the

section of Ridge 3 which appears as a large mound at the base of the southern slope (Figure 2.15) is characteristic of a lateral differential in sediment supply at the glacier margin (Barnett and Holdsworth, 1974).

Between Ridge 1 and the Zone A/B dividing ridge, the mid and lower slope subaqueous topography is more muted. A very poorly developed, asymmetrical, partial ridge, composed of Facies 2.1 occurs midslope in Zone B (section 2.6.3.2), but cannot be traced by seismic subbottom profiling in the centre of the loch or on the opposite slope. The remaining subaqueous landforms in this zone are examined more fully in section 7.2.2.2.2 below. The dividing ridge is atypical of sublacustrine moraine form in that it is inferred (section 2.6.3.1) that the landform can be traced into the present subaerial environment. The authors cited above (this section) are adamant that sublacustrine moraines cannot form subaerially and ideally require a water depth $\geq 30\text{m}$. Thus the ridge may have been formed in two ways:-

- i) As a compound subaerial/subaqueous landform.
- ii) As a frontal push moraine.

The push moraine hypothesis does not fit the available data well. It is considered to be unlikely that an actively retreating glacier, which has been shown to have retreated rapidly over a distance of 2km during the brief climatic fluctuation of the Loch Lomond Stadial, should start to advance to an extent whereby the large ridge could be produced. Annual fluctuations in the retreat of glaciers have been shown to result in numerous small (1-2m high) push moraines during minor winter readvances (Boulton, 1986). There is no evidence of such a continuum of landforms in Loch Muick.

Acceptance of the first hypothesis explains the complex plan form of the subaqueous section of the ridge, which curves southwestwards towards the former ice margin. It may also account for the break in slope on the northern half of the ridge at 8m below the surface where it is suggested that the subaerial/subaqueous interface occurs. The proposed subaerial section of the ridge may be a nearshore example of the hummocky drift which occurs around the course of the Glas Allt (Figure 1.6). It is recognised that,

according to the bathymetric chart (Figure 2.15), much of the ridge occurs in water depths currently above 30m. Subbottom profiling (section 3.7.3.1; Traverse 1 Figure 3.24; Figure 3.33), sidescan sonar survey (section 4.6.2.1) and surface sediment sampling (sections 5.5.1, 5.5.2, 5.5.3) has however, indicated that substantial infilling (4.2m maximum) of the small basin enclosed by the ridge has occurred, through distal deltaic deposition and settling through the water column. Therefore, at the time of deposition of the ridge, there would have been a sufficient water depth to permit sublacustrine moraine formation.

The identification of sublacustrine moraines in the Loch Muick trough has important implications regarding both the glacial history of Glen Muick and in the wider context of the accurate identification of former glacier termini in the lacustrine environment where only subaerial evidence is available. This subject is fully examined in section 7.2.4 below.

7.2.2.2.2 Mounds and hollows

Zone B (section 2.6.3.2) is characterised by an area of mounds and hollows concentrated in the centre of the trough. Interpretation of Pinger subbottom profiles suggests that these subaqueous landforms are composed of glacial diamict, partially infilled with Sequence 1 Holocene sediments, which differs from that forming the ridges in exhibiting no internal structure (i.e. compressional reflectors). Thus these mounds and hollows differ from the large mound at the base of the southern slope (section 7.2.2.2.1) in that they do not comprise the partially buried topographic maxima and minima of sublacustrine moraines. Andrews and Smithson (1966) report conical kames associated with the Baffin Island exposed sublacustrine moraines, which on topographical grounds alone resemble the mounds on the floor of Loch Muick, but given the sedimentological information from Pinger surveys this clearly cannot be the case in Loch Muick.

The absence of stratification indicates that current dominated processes were not involved in the formation of the mounds and hollows. Eyles et al. (1987) and Mooers (1990) report examples of relief inversion caused by former sublacustrine *in situ* melting of

stagnant glacier ice during and after deglaciation, with the same processes operating as during the formation of subaerial kettle holes (Maizels, 1977). Sublacustrine hollows are also created by the escape of buried ice. Reid and Callender (1965) observed the emergence of a debris covered iceberg 30m wide and 350m long, with an estimated weight of between 170 and 200 tons from the bottom of proglacial 'Miller Lake', Alaska. Subsequent profiling of the area of emergence identified a hole on the lake floor 20m deep, 360m long and 60m wide. Smaller, debris covered icebergs have been reported to emerge from an ice cored subaqueous ridge in Briksdal Lake, Norway (McManus and Duck, 1988c).

Thus the mounds and hollows on the floor of Loch Muick are believed to have been formed by one of three processes:-

- i) Subbottom in situ melt out of buried ice blocks.
- ii) Escape of buried ice.
- iii) A combination of the two processes above.

The data available do not permit the distinction of the processes involved to be made. It is proposed that burial of the ice occurred just prior to or whilst the Glen Muick glacier terminated at the locations of the mounds and hollows, permitting the rapid burial of dense, basal, debris-rich ice.

7.2.2.3 Facies 2.2 Topography and sedimentology

The parastratigraphic interpretation of Facies 2.2 (section 3.7.3.2) is that the external form - topographic infill, horizontal stratification of coarse grained sediment, and dominance of finer grained material is indicative of glacial outwash, termed subaqueous outwash by Rust and Romanelli (1975). This facies has a partially gradational lateral and basal boundary with Facies 2.1 (Figure 3.28) which indicates approximately synchronous deposition. Coring has shown that, at the upper sequence boundary of Facies 2.2 with Facies 1.2, Pinger profiling does not permit differentiation of the fine grained outwash sediment which comprises Unit 1 (section 7.2.2.1). The Unit 1 material, which contains no component coarser than sand, is interpreted as representing outwash deposition after the

retreat of glaciers from the Loch Muick trough, and thus provides the upper part of the outwash continuum of which Facies 2.2 forms the lower and basal parts. The upper boundary between Facies 2.2 in the form of Unit 1 and Facies 1.2 is unconformable due to syndepositional mass movement (see section 7.2.2.1).

7.2.2.3.1 Central trough drape and infill

The subaqueous outwash in Loch Muick is unusual in that no distinct external topography, excepting that of an infill or drape, has been identified. Reports from numerous other proglacial water bodies have proved the existence of proglacial deltas or fans created by the inflow of sediment-charged meltwater at distinct points along the glacier front (e.g. Andrews and Smithson, 1966; Pennington, 1981; Gravenor et al., 1984; Ashley, 1988). This implies that outwash sedimentation by meltwater inflows in Loch Muick was either widespread across the ice front or was dominated by intraglacial or supraglacial flow. The lateral extent of the sublacustrine moraines indicates that ramp formation extended across the loch where water depths were $\geq 30\text{m}$ in the majority of cases. Pinger evidence suggests that during ramp formation meltwater escape from the central part of the ice front was extremely restricted. Thus meltwaters must have debouched into the loch along the nearshore, cliffed ice margin in water depths $\leq 30\text{m}$, and through intra- and supraglacial channels. The absence of a subglacial meltwater input across the major part of the glacier front is believed to explain the low boulder content and high proportion of fine grained material in the subaqueous outwash relative to that of the sublacustrine moraines; the coarsest component of the glacially entrained debris was incorporated directly into the sublacustrine moraines.

Seismic subbottom profiling indicates that the coarser fraction of the finer grained sediment entering the loch by the processes discussed above was deposited in an ice proximal position, creating a partial gradational boundary in the topographic irregularities of Facies 2.1. The finer component was deposited in more ice distal locations forming a drape with a non-gradational boundary over the topography of Facies 2.1 and a gradational

transition with the coarser ice proximal subaqueous outwash (Figure 3.28, Plate 3.7) and the fine grained sediment of Unit 1 (section 7.2.2.1). Boulder point hyperbolae within the finer grained matrix (Figure 3.35b, c) are interpreted as representing dropstone deposition by icebergs (Thomas and Connell, 1985) which is examined further in section 7.2.2.3.2 below.

7.2.2.3.2 Northeastern shallows

The area of loch floor close to the outlet of the River Muick forms a broad platform of shallow water. Water of less than 10m depth extends an average of 10m into the loch at its northernmost extremity (section 2.6.3.4). Seismic penetration of this area is limited, showing a very thin, discontinuous distribution of Facies 1.2 lying stratigraphically above an irregular, seismically impenetrable layer. This is composed of numerous boulder clusters which are interpreted as being of Holocene age (section 7.2.1.1.2 above), deposited by ice rafting of avalanche debris. The nature of the underlying sediment cannot be determined using the high frequency Pinger source. However, the size of the shallow water area suggests that, if it is a sedimentary feature, it is not composed entirely of sediment deposited during the Holocene. The morphology and location of this feature adjacent to the only available outlet zone of Loch Muick suggests an alternative hypothesis, that of iceberg enhanced sedimentation (e.g. Dowdeswell and Dowdeswell, 1989).

Identification of the processes involved in the formation of the subaqueous landforms of Loch Muick provides two distinct processes by which icebergs are ultimately driven by katabatic winds and currents towards the outlet (McManus and Duck, 1988c). First, there is direct calving from the ice front, from either ramp or cliffed areas. The latter is likely to contain a higher proportion of entrained debris available for ultimate deposition than the former as a significant volume of the debris from basal ramp ice would have been deposited during the formation of sublacustrine moraines. The second process of iceberg formation is via the escape of buried ice as proposed in section 7.2.2.2.2. Both Reid and Callender (1965) and McManus and Duck (1988c) draw attention to the volume of debris

and 'dirty' appearance of formerly buried ice blocks. Thus, if a large number of the hollows on the floor of Loch Muick were formed by buried ice escape, the volume of debris delivered to the shallows adjacent to the outlet could be considerable. Tracking of icebergs in Briksdal Lake, Norway (McManus and Duck, 1988c) has shown that during melting the diminishing bergs migrate shorewards and may ultimately become stranded on the outlet dam. In the case of Loch Muick, the partial ridge identified in Zone D, outside the Loch Lomond Readvance glacier limit proposed in this thesis (sections 7.2.2.2.1, 7.2.4.1), may be formed almost entirely of iceberg drop and dump material of Loch Lomond Stadial age. Alternatively this feature could be a morainic ridge of Devensian age which acted as a trap for icebergs, thereby inducing substantially higher sedimentation rates. The morainic barrier across the northeastern shore is also believed to date from the Devensian glaciation (see section 7.2.4 for discussion) which implies that a proto- Loch Muick has existed from that time. This further implies that iceberg deposition occurred against this barrier during the Devensian deglaciation, and thus the northeastern shallow water zone is a time transgressive feature. This long period of accretion is believed to account for the substantial beach of granitic clasts which range from coarse sand through intermediate grades to boulders. Occasional massive boulders, $\geq 3\text{m}$ in all dimensions, occur partially buried in the beach and in water depths of 2-3m. The age or mode of deposition of these massive clasts could not be ascertained by the methods employed in this research.

Examination of the morainic retaining ridge at the northeastern end of Loch Muick suggests that the effluent River Muick has maintained its outlet in broadly the same position since the deposition of the ridge. Exposures of the ridge sediment at the river cutting show fluvially deposited gravels in a sandy matrix indicative of the former existence of a wider channel. However, eroded areas on the ridge expose till typical of that found elsewhere in Glen Muick.

7.2.3 Sequence 3

Sequence 3 (Facies 3.1) is interpreted as representing the underlying Lochnagar Granite Complex bedrock (section 3.7.3.3). The smooth outline of the upper surface of this facies is believed to result from glacial erosion probably compounded over multiple glacial episodes.

7.2.4 Implications regarding the glacial history of Loch Muick

7.2.4.1 The extent of the Loch Lomond Readvance glaciation in Loch Muick

Research undertaken for this thesis has shown that the previously defined subaerial glacier limits proposed by Sissons (1972a) and Sissons and Grant (1972) (Figure 1.2) and upheld by geomorphological mapping carried out during this project (section 1.5.4.2; Figure 1.6) are not supported by data obtained from the subaqueous environment. On bathymetric grounds alone it can be seen that there is a continuity of subaqueous landforms across the former subaerial limit of the Glen Muick glacier which is located approximately parallel to the course of Lindsay's Burn (see Figure 2.15). There are, however, complexities associated with the Loch Lomond Readvance glacier limit proposed in this thesis, which indicates that glacial ice extended a further 1.4km down valley. These complexities are examined below.

7.2.4.1.1 The absence of subaerial evidence of glacial deposition

The new geomorphological map (Figure 1.6; section 1.5.4.2) indicates that there is a clear down valley limit of hummocky till on the northern slopes above Loch Muick (Plate 1.6) where Sissons et al., (1973, p.75) noted that:-

'The hummocky moraine terminates in Loch Muick.'

Bathymetric charting has proved that this assertion is incorrect, but that ridges do occur in the vicinity of the proposed subaerial limit. On the southern slopes the former glacier limit is less clear. It is suggested that it is marked by a thinning in the depth of till on the lower

slopes opposite the limit on the northern slopes. However, this limit is considerably more equivocal than that on the northern slopes, and is not marked as a former glacier limit on Figure 1.6 for this reason. Till occurs on the lower southern slopes between the probable Glen Muick glacier limit and that of the Black Burn glacier, and intermittently at the base of the slopes on both sides of the loch northeast of the mouth of the Black Burn. In the context of the subaerial evidence alone it was suggested all the till deposits outside the 'distinct' limits represent outliers of Devensian origin (section 1.5.4.2.2). Given the new subaqueous evidence, presented in this thesis, a reinterpretation of the subaerial data in Glen Muick is urgently required. This also suggests that these findings have important wider implications for the interpretation of subaerial glacial geomorphology adjacent to deep ($\geq 30\text{m}$) water bodies. Further research into this topic is essential to demonstrate the significance of these findings.

The ridges beneath the surface of Loch Muick have been shown to conform closely to those identified on Baffin Island which are accepted to have been formed by the processes given in the ramp moraine model (Barnett and Holdsworth, 1974). Thus the Loch Muick ridges are believed to be the first recorded example of these landforms in the subaqueous environment in Britain (see section 7.2.2.2.1). Ridge formation occurs in a pro/subglacial ice marginal position where the semi-floating ramp snout of the glacier extends down the water body beyond the grounded margin (see section 7.2.2.2.1). Therefore, at the maximum extent of glaciation sublacustrine moraines can form significant distances ahead of the grounded ice margin (600m at Austerdalsisen, Norway, Theakstone, 1989; Booth, 1986) where subaerial deposition is occurring. In the case of Loch Muick this ice-front morphology may explain the existence of till southwest of and at the mouth of the Allt an Dearg on the northern slopes, whereas the terminal buried sublacustrine moraine ridge has been identified approximately 100m northeast of this position. On the southern slopes the evidence is not as clear cut; till occurs at the base of the slopes beyond the maximum glacier limit proposed on the basis of subaqueous data sources. Pinger seismic profiling has not enabled identification of the subsurface,

subaqueous extension of the subaerial 'proglacial' deposit in Loch Muick whereas those deposits within and at the proposed glacier maximum can be traced subaqueously as Facies 2.1 deposits. This occurrence of the 'proglacial' till, which is not unique in the literature (Kurtz and Anderson, 1979), can be explained in two ways:-

i) The deposit results from proglacial subaerial debris flow activity during the Loch Lomond Readvance which is sedimentologically indistinguishable from direct glacigenic sedimentation (Kurtz and Anderson, 1979).

ii) The deposit dates from the Devensian glaciation.

The absence of an identifiable subaqueous continuation of this till as either Facies 2.1 or 2.2 which would be expected if it were formed by proglacial debris flow activity indicates that the evidence does not support the former hypothesis. These data further imply that if the assumption that the deposit is glacigenic or was formed in a glacier proximal position is correct, and a comparable subaqueous deposit does exist, it would lie stratigraphically beneath Facies 2.1 or 2.2. Thus it has either been eroded by subsequent processes, is too thin to be identified by Pinger profiling, or occurs beneath Sequences 1 and 2 below the depth of seismic penetration. It is for these reasons that the second hypothesis, that the deposit dates from the earlier Devensian glaciation, is accepted. However, it is recognised that this interpretation is based upon negative evidence and that further seismic subbottom profiling combined with coring is required to examine these hypotheses satisfactorily.

Over a substantial area of the lower slopes, between the previously defined Loch Lomond Readvance ice limits and those proposed in this thesis, there is no identifiable subaerial evidence of the lateral ice limit. Given the available subaqueous evidence, the former existence of glacial ice at these intervening positions along the present loch shoreline, which has not altered altitudinally since the Loch Lomond Stadial (see section 7.2.4.1.2) is incontrovertible. Ice cliffs would have developed along the loch shoreline to water depths of $\leq 30\text{m}$ and assuming that ice debris content was dispersed across the glacier margin, subaerial glacigenic sedimentation would have occurred. It follows therefore that nearshore glacigenic sediments were either:-

i) Removed by lacustrine processes.

ii) Modified by subaerial processes.

or were removed by a combination of both process types.

The first hypothesis, of removal by lacustrine processes, conforms with the processes and models invoked to explain the subaqueous landforms of Loch Muick. Both processes, of sublacustrine moraine and hollow formation by buried ice escape, require the sudden release of a substantial volume of ice into the loch, and ice cliff retreat results in relatively minor calving of icebergs. All these processes initiate wave motion of the loch waters. Reid and Callender (1965) report the occurrence of a major wave, associated with the release of a buried iceberg, which swept the across the lake eroding shoreline sediment. Gustavson (1975) and Duck and McManus (1981) record instances where icebergs calving from cliffs set up waves causing erosion of lake shorelines.

In the case of Loch Muick the sublacustrine moraines indicate that there were in excess of 10 major calving events, of sufficient magnitude to form ridges and deform underlying sediment, during the Loch Lomond Stadial. The proportion of hollows in Zone B formed by escape of buried ice cannot be quantified (section 7.2.2.2.2). Waves created by these mechanisms would result in undercutting of recently deposited, unvegetated glacial shorelines, causing collapse into the loch and removal of the finer components to deeper water. Over a period of time repeated wave action could lower the profile of nearshore sediment accumulations. Contributing factors to this process include the fetch, the angle of slope of the area upon which till deposition occurred, the size of the area covered by till, the thickness of the deposit, and the composition of the till. It is suggested that relatively thick, coarse grained deposits on large, flat-lying areas with a short fetch distance would be more resistant to wave attack. The position of the deposit relative to the former ice front also contributes to the survival of the sediment; that deposited at the northeastern end of the loch would have been subject to a greater period of wave erosion with a greater fetch than till at the southwestern end. Subsequent wave erosion during the Holocene is enhanced at the northeasterly end of the loch where the wave fetch is greatest from the dominant down valley wind.

The second hypothesis, of modification by subaerial processes, is also supported by subaerial and subaqueous data collected during this project. Sidescan sonar surveys of the upper loch slopes have shown that they are extensively covered by boulder spreads (section 7.2.1.1.1). These features are believed to have a subaerial origin, from avalanche and debris flow/slide activity on the slopes above the loch, which has been occurring since the retreat of the ice inside the limits proposed here and since the Devensian glaciation beyond the Loch Lomond Readvance limits in Glen Muick. Thus a substantial volume of sediment from the slopes above Loch Muick has been deposited into the loch, which almost certainly includes till from the lower slopes. Winnowing by waves in the nearshore environment has removed the fine grained matrix of the till leaving the large clasts on the surface of the loch floor.

The distribution of the till around the shores of Loch Muick is therefore indicative of a combination of subaerial and subaqueous processes - supporting both hypotheses. The large areas of till at the southwestern end of the loch have been and still are subject to relatively low erosion potential by wave action due to the restricted fetch and the dominant wind direction towards the northeast. The well developed and preserved landforms on the northern slope, particularly in the vicinity of the subaerial limit proposed by Sissons (1972a) and Sissons and Grant (1972) are believed to result from a combination of low slope angle, broad area of deposition and sheltered position behind the promontory upon which Glas-allt-Shiel is built (Figure 2.15). The southern slopes are more uniform in profile at the southwestern end of the loch and do not exhibit a distinctive external topography, consisting of a thick till deposit into which gullies have been eroded. This channeling of erosive activity at specific points is believed to explain the continued widespread distribution of the till in a less favourable position. It is suggested that the remaining till deposits, close to the new proposed maximum limit of Loch Lomond Readvance glaciation in the glen, represent the fortuitous survival of lateral deposits between debris flow/avalanche paths and upon the flat land at the mouth of the Allt an Dearg.

7.2.4.1.2 Former loch water level

The ramp moraine model requires:-

- i) That the glacier debouches into a water body with a depth $\geq 30\text{m}$ over a large part of the basin.
- ii) The temporary raising of the lake water level to initiate bending and ultimately calving of the ramp.

Thus the vertical extent of the ridges below the current water level, combined with information on the altitude of the available spillway and subaerial/subaqueous geomorphology, can provide a means of estimating the former water level during the Loch Lomond Readvance in Loch Muick.

The spillway of Loch Muick is formed by a low morainic ridge which is believed to be of Devensian origin and therefore is not 'The latest moraine thrown down by the glacier that once crept down the glen' (Collet and Johnston, 1906 p108). The ridge has a rounded profile and a maximum amplitude of approximately 2m above the surrounding topography and 3m above the present water level, bordered on the loch side by beach deposits and landward by extensive peat accumulation. It is the only altitudinally significant landform on the broad plain at the northeastern end of Loch Muick which could act as a barrier to the loch waters. There is no evidence on the lochward slopes of the ridge of former high loch levels. The maximum loch water level that could have been attained before significant breaching of the barrier occurred would have been approximately 3m above the present loch level. If this had occurred positive feedback would almost certainly have destroyed a significant part of the ridge. Further evidence of the former loch water level is found in the existence of well defined glacial landforms in sheltered positions on the shores of the loch, at the current water level. In common with the remainder of the loch shoreline, these features exhibit no evidence of lake shorelines associated with higher water levels. It follows therefore, that the water level of Loch Muick was never maintained at +3m above its present level, if at all, for more than brief periods.

Sidescan sonar surveys have proved the existence of former lower loch levels during which erosional shore-parallel terraces were formed (section 7.2.1.2.1). The age of these shorelines, which extend to approximately 2m below the present water surface, is unquantified, but they are believed to be of recent, Holocene, origin.

The sublacustrine moraines terminate upslope at depths ranging between 75m and 20m, although the latter are poorly developed. Barnett and Holdsworth (1974) suggest that sublacustrine moraines can be formed in water marginally shallower than 30m, but that, as is the case in Loch Muick, vertical development is restricted. The fact that some sublacustrine moraines terminate at depths considerably below 30m depth does not require the water level to have dropped by 30m-40m; ramps do not usually develop across the entire ice front. Therefore sublacustrine moraine data, combined with the other sources given above, are interpreted as indicating that the water level in Loch Muick has not altered significantly (>1m) since the retreat of glaciers from the Loch Muick trough.

This implies that the ramp calving mechanism, reliant upon a rapid spring rise in water level until the outflow becomes ice free, was temporally restricted, with the result that there is no subaerial evidence of its existence. It may also be contributory in determining the relative magnitude of the ridges, in particular partially buried Ridge 3 (Figure 2.16), which may have been formed by deposition over several seasons during which there was an insufficient rise in lake level to cause ramp calving.

7.2.4.2 Deglaciation of the Black Burn valley

The subaqueous and subaerial evidence discussed above has important implications regarding the timing of deglaciation in the Black Burn valley as well as Glen Muick as a whole. The newly proposed limit suggests that if the Black Burn glacier, for which there is substantial subaerial evidence, existed during the Loch Lomond Stadial contemporaneously with the main Glen Muick glacier, the two glaciers were confluent. The subaerial

geomorphology associated with the entrance of the Black Burn glacier into Glen Muick and Loch Muick, comprising two lateral moraines on the eastern side of the Black Burn, is significant in determining both the age and timing of deglaciation in this valley.

If the interpretation of the age of the new glacier limit identified in Loch Muick is correct, then it is believed that the main Glen Muick glacier, during advance down the glen, would have destroyed landforms associated with the Black Burn glacier at the possible zone of confluence at the loch shoreline. However, well-preserved lateral moraines have been recorded extending down to the present shoreline (Figure 1.6). This landform configuration indicates that:-

i) The Black Burn glacier dates from the last period of glaciation when glacier recrudescence occurred in the valley, which was broadly coincident with the main Glen Muick glacier, which has been shown to be of Loch Lomond Readvance age.

ii) The lateral moraines were formed after the retreat of the Glen Muick glacier.

From the available data it cannot be ascertained absolutely whether confluence of the two glaciers occurred. A possible indicator that this was the case is found in the form of the upper part of the terminal ridge on the southern slope. This ridge has no topographical or seismic expression on the northern slopes. Therefore it is suggested that the subglacial debris input from the Black Burn glacier contributed to the formation of the upper part of this ridge providing a significant debris source which was unavailable on the northern slopes. The lateral moraines are believed to have formed after the retreat of the Glen Muick glacier, the Black Burn glacier possibly maintaining this position for a considerable length of time. This would explain the freshness of the features which were protected from wave attack by the continued presence of the glacier. There is no evidence in the subaqueous environment of sublacustrine terminal features associated with the Black Burn glacier in Loch Muick. Deltaic accumulation blanketing the loch floor at the mouth the Black Burn (section 7.2.1.2.2) prevented seismic penetration in this area.

7.3 LOCH CALLATER

7.3.1 Sequence 1

7.3.1.1 Surface sediment texture

As in section 7.2.1.1, data on the surface sediment texture are derived primarily from two survey techniques, sidescan sonar and surface sediment sampling. Three major sediment textural associations have been recognised in Loch Callater:- boulder spreads, fluvial input zones and fine grained sediment. The characteristics of each association are described briefly and a genetic interpretation made.

7.3.1.1.1 Boulder spreads

Five discrete boulder spreads have been recognised on the nearshore, northeastern slopes of Loch Callater as concentrations of upstanding point reflectors with acoustic shadows lying to the shoreward side (Plate 4.9). On the nearshore, southwestern side the distribution of the boulders is more scattered, distributed over the gentler slopes at the eastern end of the loch. The first type of boulder spread, which has a clear point input, could be formed by three processes, separately, or in combination:-

- i) Avalanche entrainment of slope debris.
- ii) Mass movement of slope materials.
- iii) Wave erosion of the shoreline sediment.

The first and second hypotheses are closely linked, both being at least partially dependent upon the angle of slope to determine the efficiency of the process. The slopes above the northeastern shore of Loch Callater, unlike Glen Muick, do not exhibit evidence of recent avalanche or debris flow/slide activity that would have a direct impact on loch sedimentation. The hummocky till blanketing the lower slopes of Glen Callater around the shores of the loch (Figure 1.5, especially above the northeastern shore; Plates 1.3, 1.4) acts as an effective trap for debris moving downslope. Further evidence opposing the first hypothesis is found in the nearshore distribution of boulder spreads on the northeastern

slopes. The surface of Loch Callater is known, and has been observed, to freeze during the winter, to ice thickness depths $>7\text{cm}$. Avalanches reaching the loch shores and descending onto lake ice would result in a more dispersed distribution by sliding across the ice, thereby extending greater distances from the shore. Likewise, redistribution of sediments deposited on the ice could be expected to occur during spring melt and break up. This process is invoked to partially explain the dispersed boulder spreads observed on the southwestern slopes, where steep hummocky till abuts the loch shore, but probably provides a lower sediment input on the northeastern side. Also significant in producing a dispersed spread of clastic material would be the entrainment and lifting of shoreline clasts by lake ice in winter, which are subsequently deposited in deeper water during the spring melt.

The third hypothesis, of wave induced erosion of shoreline sediments, explains the available data more efficiently. Unlike Loch Muick, where steep slopes extend to the loch shore unbroken over the majority of the shoreline length, the gentler slopes adjacent to Loch Callater are frequently broken at the shoreline by a small, unvegetated, almost vertical cliff cut into the hummocky till, which varies in height between approximately 0.5m and 1m. Analyses of surface sediment samples have shown that at the eastern end of the loch very poorly sorted (Figure 5.18) coarse grained (Figure 5.17) sediment occurs in a location where recent bank collapse is believed to have occurred as a result of wave action (section 5.6.2). Due to the shallow water depth in this area (1m-2m) sidescan sonar survey could not be carried out, preventing an examination of the surface expression of this phenomenon. However, it is suggested that the nearshore boulder spreads, all of which occur in areas of cliffed shoreline, represent examples of earlier wave erosion activity from which relatively finer grained sediment has been subsequently winnowed and redispersed to central loch depocentres. Grab sampling thus obtained only finer, interstitial, silt sized particles (section 5.4.2; Figure 5.14) trapped between the larger clasts for the same reasons discussed in Loch Muick (section 7.2.1.1.1). The relatively low density of discrete boulder spreads is interpreted as indicating a low frequency of meteorological events of sufficient magnitude, duration and direction to create wave conditions suitable for major erosional events. It is believed therefore that the majority of shoreline erosion inferred from surface

sediment and geomorphological data occurs as a result of minor bank collapse during lower wave energy conditions.

7.3.1.1.2 Fluvial input zones

Loch Callater is fed by a total of seven streams, of which only two, the Allt an Loch and the unnamed, forked stream on the southwestern shore, exhibit any evidence of subaerial deposition (Figure 1.5; see section 7.3.1.2.2). The remainder constitute ephemeral channels which have been observed virtually to disappear during dry periods in the summer months. Information regarding the nature of the fluvial input zones is available from surface sediment sampling and subaerial geomorphological surveys. Sidescan sonar survey of the sediment texture of both 'major' stream mouths was unsuccessful:- the forked stream enters the loch at a steep subaqueous slope (Figure 2.9), the intense reflections from which dominate the sonograph (Plate 4.10), and the Allt an Loch enters Loch Callater at a broad, shallow area where sidescan sonar, and to an extent, echosounder survey was impossible.

The loch floor sediment at the mouth of the Allt an Loch contains the highest percentages of sand encountered in the loch (84.7% maximum, see Appendix G) which is classified as having a sandy silt texture (Folk, 1974). This forms a gradational boundary through silty sand to silt which covers the majority of the remainder of the loch floor (Figure 5.17). The inflow is not associated with significantly poorer sorted sediment overall, (Figure 5.18) however, the sediment is very leptokurtic (Figure 5.20). The dominance of sand sized particles and relative absence of organic matter (Figure 5.13) indicates that current reworking of the influent sediment is occurring, leading to a lag deposit dominated by sand, and redeposition of finer grained and less dense organic matter over the remainder of the loch floor. This interpretation is confirmed by QDa-Md analysis (Figure 5.21). Data from samples obtained closest to the mouth of the Allt an Loch fall within the fluvial environmental trend envelope.

The forked stream does not appear to have any significant impact upon the

sedimentology of the loch floor. QDa-Md analysis of the grab sample obtained closest to the mouth of the stream places it within the overlap between the quiet water and fluxoturbidite environmental trend envelopes. This indicates that weak current activity, if any at all, occurs at this point, and that the mode of deposition does not differ from that of the majority of samples obtained from the surface of the loch floor. The QDa-Md data are upheld by analysis of the sediment texture which, in common with organic matter, grain size, sorting, skewness, and kurtosis data, shows no variation attributable to the inflow of the stream.

7.3.1.1.3 Fine grained sediment

Surface sediment sampling has shown that, away from the fluvial input zone of the Allt an Loch, the majority of the loch floor is covered by silt (sediment texture classification of Folk, 1974; section 5.4.2; Figure 5.14) (see also section 7.3.1.2.4 below). The only exception to this occurs at the northern end of the loch where one sample of silty sand was obtained. It is believed that this sample represents sediment from a recent cliff collapse, where there has been incomplete post-collapse removal of coarse grained material by wave action. This interpretation is supported by the occurrence of very poorly sorted sediment at this location (Appendix H, Figure 5.18). Correlation between variables has shown that a strong negative relationship exists between sand and water depth (section 5.6.2) which is almost certainly due to sorting by wave action. Sidescan sonar survey of the loch floor indicates that the central part of the loch is covered by areas of uniform, topographically and sedimentologically featureless low to medium backscatter (Plate 4.9; Plate 4.10). Analysis of sonograph data in conjunction with surface sediment textures and the bathymetric chart (Figure 2.9) indicates that the tonal variation in backscatter levels is due to minor changes in the angle of loch floor slope.

The loch floor is dominated by highly organic, poorly sorted, sediment with a dominantly negatively skewed, symmetrical or mesokurtic distribution (section 5.7.2). The most poorly sorted sediment occurs at nearshore locations due to bank collapse, and in the central area of the loch, where the levels of organic matter are high, in common with Loch

Muick and other Scottish lochs (see section 7.2.1.1.4). Although the lowest of the three lochs examined in this thesis, the organic content of the sediment is higher than that reported from comparable water bodies. This is believed to be due to anthropogenically induced erosion in the catchment (section 5.6.2; section 6.6.2.2.2) since the commencement of estate management in the Nineteenth Century. QDa-Md analysis indicates that the majority of samples were deposited in quiet water or fluxoturbidite conditions, only three fall within the steep gradient turbidite envelope which signifies turbulent current activity (see section 7.3.1.2.3 below).

7.3.1.2 Surface sediment topography

Sidescan sonar, echosounder and Pinger seismic reflection profiling surveys have enabled the identification of four groups of topographic features on the floor and sides of Loch Callater. These comprise shore-parallel terraces, deltas, mounds and hollows, and draped sediment. Each group of features is described and a genetic origin suggested.

7.3.1.2.1 Shore-parallel terraces

A suite of three shore-parallel terraces have been identified on sonographs obtained from Loch Callater (Plate 4.9). There is no evidence to suggest that they were formed by different processes than those which created the shore-parallel terraces in Loch Muick - by wave erosion during periods of lowered water level (section 7.2.1.2.1 above). Geomorphological and pollen evidence (section 7.3.3.1) indicates that the area now occupied by Loch Callater was completely glaciated during the Loch Lomond Stadial and therefore that the shore-parallel terraces must post-date the retreat of the Glen Callater glacier from this position. The absence of these features from the bathymetric chart (Figure 2.9) suggests that they have a vertical amplitude of <1m, and measurements taken from the sonograph indicate that they have a maximum width of 17m, although widths in the range of 3m-5m are more usual. These subaqueous landforms are recognised only on the

northeastern slopes of the loch (section 4.5.2.1) where it is believed that they are eroded into Sequence 2 (diamict) sediment which forms hummocky till landforms along the shore of the loch. As there is no discernible variation in sediment type or vegetative cover, it is suggested that the apparent lack of shore-parallel terraces on the southwestern slopes may be due to one, or a combination of factors given below:-

- i) The angle of subaqueous slope along the southwestern shore.
- ii) The sidescan sonar response to the subaqueous topography.

The first point refers to the two extremes of slope angles encountered on the southwestern slopes (section 4.5.2.2):- very steep slopes and very shallow, boulder covered slopes. Both these types of slope angle would result in rapid destruction of shorelines eroded during lowered loch levels. Steep angle slopes formed in the glacial diamict which surrounds the loch could be destabilised by wave undercutting, leading to upslope collapse and destruction of the shoreline. In very broad, shallow water areas, like those at the southern end of Loch Callater, lowered water levels of up to 3m, would still leave a shallow water area close to the shoreline over which dissipation of wave energy would occur, reducing the erosive capacity of the waves. Thus shorelines eroded in low slope angle locations would be poorly developed, with a low vertical amplitude. Furthermore, in this location, sidescan sonographs have shown that scattered boulder spreads are distributed across the loch bottom (section 7.3.1.1.1) which are interpreted as resulting from deposition by avalanche activity. The age of these deposits is unknown. However, if this proposed depositional process occurred after the formation of minor shore-parallel terraces, it would result in partial blanketing and destruction of the landforms.

The second point, that of the response of sidescan sonar to the topography, is relevant to the very steep slope angles. If small remnants of shore-parallel terraces survive on this steep slope, in common with Loch Muick (section 7.2.1.1.1), the strong return signals from the highly reflective slope would mask the weaker signals returning from the flat 'treads' of the terraces. Due to the nature of the survey and the amplitude of the landforms involved, the significance of this factor, and that examined above, in determining the distribution of shore-parallel terraces cannot be quantified.

Comparison of the bathymetric chart of Collet and Johnston, (1906) with that completed during this research has led to the suggestion that differences in the water level at the times of survey, combined with the choice of different datum levels, resulted in some of the variations recognised (section 2.5.4). The relative importance of each of these factors in determining the -2.3m difference in depth between the 1905 and 1989 surveys cannot be determined. However, this information appears to indicate that reduced water levels have occurred in Loch Callater which could result in the formation of shore-parallel terraces during a temporally restricted period. This hypothesis is supported by the findings of Duck and McManus (1985c) who reported the rapid development of such features in lacustrine and glacial sediments during the draw-down of Glenfarg Reservoir.

7.3.1.2.2 Deltas

Two deltas are recognised from geomorphological mapping in Glen Callater (Figure 1.5), bathymetric surveys and sidescan sonar surveys in the loch. Pinger seismic reflection profiling of the subaqueous portion of the deltas was prevented by a combination of extremely shallow water, which restricted both the survey process and penetration, and a high sand content (in the case of the Allt an Loch) which prevented acoustic pulse penetration (see section 7.2.1.2.2 above). The deltas are located at the mouths of the main influent, the Allt an Loch, and the unnamed forked stream entering Loch Callater from the southwestern shore.

Subaerially, the Allt an Loch is bordered for much of its course by a broad, alluvial plain (Figure 1.5) which has been demonstrated to have increased in area by approximately 0.4ha between the 1905 and 1989 bathymetric surveys (section 2.5.4). This represents an average decrease in loch surface area of 50m² per annum. It is not possible to estimate accurately the time elapsed since the former, larger, Loch Callater started to infill, due to the absence of data on the temporal variation of the rate of sedimentation and the underlying subsurface topography of the alluvial plain. The latter could have provided a further important data source, had time been available to complete a survey, and therefore this sub-project is considered meritorious for further research. Given the proposed date of the last

glaciation in Glen Callater (see section 7.3.3.1 below), it is suggested that deposition of the alluvial plain started during the retreat of the Glen Callater glacier during the Loch Lomond Stadial, at approximately the time when the head of the alluvial plain identified on Figure 1.5 was deglaciated. It is believed that this position marks the former maximum extent of Loch Callater. To the east of this point hummocky till extends almost entirely across the floor of the glen. It is possible that at the time of ice retreat the alluvial plain formed a typical sandur plain, fed by extreme flood events associated with spring and summer melt, and that a substantial part of the annual deposition occurred at this time (for references see section 7.2.1.2.2 above). However, the information given above shows that this landform is a time transgressive feature which is continuing to accumulate.

Subaqueously the Allt an Loch delta forms a broad area of shallow (<3m) water, 200m long, across the southeastern end of the loch, descending by a gentle gradient towards the central, deeper water zone. It is suggested that the break between topset and foreset deposition occurs at approximately 4m and the foreset-bottomset transition at approximately 5m (see Figure 2.9). This interpretation is supported by the surface sediment texture (Figure 5.14) which shows a progression from sandy silt on the proposed topset depositional zone, through silty sand (foreset) to silt at the bottomset zone. The pattern is broken at only one point, close to the ridge (offshore from 'A', Figure 2.9) where silt apparently infills a topographic low.

The forked stream entering Loch Callater on the southwestern shore flows across a gently sloping delta built out into the loch and abutting the hummocky till surface. The present location of the influent stream is at the extreme southeastern edge of the delta surface. At the time of geomorphological mapping (see section 1.5.3.2) the delta surface was entirely vegetated, exhibiting no evidence of recent sediment deposition. In the subaqueous environment the delta is marked by very steep slopes on both sonograph and echogram records. No surface sediment textural variation has been recognised close to the mouth of the stream (section 7.3.1.1.2). It is suggested therefore that the delta at the mouth of the stream is a relict landform that is currently no longer rapidly actively accumulating like that associated with the Allt an Loch. Possible periods of episodic deltaic accumulation

can be inferred from the down core analysis of particle size in Facies 1.1 (Unit 2, section 6.4.3). This shows that infrequent peaks in sand deposition have occurred at the core location (1, Figure 6.2) which are believed to have been entrained and deposited by the three minor streams which enter the northwestern basin, during major flood events. During such events in the loch catchment, flow in the forked stream would also be enhanced leading to deltaic accumulation in both the subaerial and subaqueous environments. However, the infrequency of these events in the sedimentary record, the apparent misfit size, and location of the stream on the delta surface leads to the suggestion that the majority of accumulation occurred immediately after the deglaciation of this part of the loch catchment, and during the early Holocene. During this period the valley was sparsely vegetated (section 6.4.7) and periglacial processes, in association with meltwater runoff in spring and summer would provide a substantial sediment load to the proto- drainage system, enabling rapid build up of deltaic deposits over a relatively short time (Ashley, 1988). From the available data, it is believed that subsequent major flood events have had only minor modifying effects upon the deltaic form. It is recognised that no chronological data exist to support this hypothesis, but examples of rapid delta and fan accumulation during the Loch Lomond Stadial have been widely reported elsewhere (e.g. Peacock and Cornish, 1989).

7.3.1.2.3 Mounds and hollows

This section examines the minor, surficial topographic features which Pinger surveys have shown to be composed entirely of Sequence 1 sediment. A total of five hollows on the upper parts of the loch slope and two mounds on the loch floor are recognised on the bathymetric chart (Figure 2.9). These areas are associated with the chaotic stratal seismic facies reflectors (section 3.6.2.1) identified on Pinger seismic profiles. QDa-Md analysis suggests that some of these mound and hollow features (for example, the hollow closest to the mouth of the Allt an Loch) are associated with rapid, localised, turbidity flows (steep gradient turbidite environmental trend envelope) whereas

samples obtained in the same area as other subaqueous landforms with the same external morphology are indicative of slow sedimentation through the water column or restricted current activity. The reasons for this disparity are believed to be due to two factors:-

- i) Sampling strategy.
- ii) Post-formational sedimentation.

Due to the nature of point sampling, complete coverage of the loch floor at the survey density of echosounder or sidescan sonar surveys was impossible. The sampling framework was based upon the available sidescan sonar data which was used to indicate potential areas of sediment variation where surface sampling would aid sonograph interpretation. This did not include all the areas where mounds and hollows have been shown to be located. Secondly, samples were obtained from areas where mounds and hollows occur, but QDa-Md analysis indicates a quiet water environment of deposition. It is suggested that partial post-formational infilling of the features has occurred, indicating that they are relatively older than those which retain a steep gradient turbidite QDa-Md signature. Quantitative evidence of this phenomenon is unavailable due to the constraints on Pinger profiling in the shallow waters of Loch Callater (Figure 3.20).

As in Loch Muick, it is proposed that the majority of the mounds and hollows of Loch Callater represent a continuum of landforms created by mass movement processes. Of the five causes given in section 7.2.1.2.3.2 (Carter, 1975), the first (applied shock) is discounted for the same reasons as those given for Loch Muick. Likewise, the impact of excess pore water pressure is unquantified. Core data suggest that major flood events, of a magnitude great enough to impound water at a sufficient pressure to cause upward flow and mass movement appear infrequently in the sedimentary history of the loch and therefore have had a minor impact on the surface morphology. It is possible that the hollow on the upper northeastern slope at a depth of approximately 1.5m results from undercutting by waves during the low lake levels indicated by submerged shorelines (section 7.3.1.2.1). Alternatively, this hollow, like those in the remainder of the loch northwest of point A (Figure 2.9), may result from initial metastable accumulation of sediment. This process, or increased sedimentation from above in the foreset deltaic deposition zone, are suggested to

be the causal processes which formed the hollow close to the northeastern shore.

The series of hollows adjacent to the ridge offshore from point A are not believed to have formed as the result of mass movement processes. The location of these features, proximate to a ridge and the delta at the mouth of the Allt an Loch lead to the interpretation that they are formed by differential fluvial deposition against the ridge.

In common with Loch Muick, not all the mounds and hollows formed by mass movement comprise linked pairs of upslope hollows and downslope mounds. The reasons for the apparent absence of these features are believed to be the same for the two lochs; a widespread downslope distribution of sediment/infilling of the upslope hollow, a result of echosounder survey line density, or a combination of both factors.

7.3.1.2.4 Draped sediment

This sediment comprises the remainder of Sequence 1 sediment not examined above, that has no distinct external form other than a drape over the underlying topography. Information on the internal structure of Sequence 1 draped sediment is obtained from Pinger survey and core analysis.

Pinger seismic subbottom reflection profiling indicates that the sediment comprises parallel or subparallel draped reflectors, typical of lacustrine sedimentation (section 3.6.3.1). Scattered boulder reflectors, occurring within Facies 1.1 only at the extreme northwestern end of Loch Callater, are interpreted as resulting from anthropogenic action during winter, when cobbles are thrown onto the loch ice, subsequently falling through the least consolidated sediment at ice melt. No major internal reflectors indicative of sedimentologically significant events are recognised within Facies 1.1. Traverse 1 (Figure 3.21) appears to show that there is an inverse relationship between underlying subsurface topography and loch floor topography. In practice this is believed to result from the reduced penetration of the Pinger signals in the shallower water above the crests of these features, which are believed to be cored with glacial sediment. Temporal constraints prevented testing of this hypothesis by coring.

Facies 1.1 is equivalent to Unit 2 in Core 1 (Figure 6.2), which has a maximum measured thickness of 6.4m (Core 2) and has been shown seismically to exceed 6.75m over much of the loch floor. Sedimentologically Unit 2 is composed of sediment of the same texture as that on the surface - silt, with occasional samples of sandy silt interpreted as resulting from deposition during flood events, which increase in frequency towards the base of the unit. It is this homogeneity of sediment texture which results in minimal variation in acoustic impedance and thus no major internal reflectors. Geochemical, sedimentological and organic matter analyses (see Chapter 6) are all indicative of a steadily ameliorating climate and, in the upper portion of Unit 2, the increasing anthropogenic impact on the loch catchment. QDa-Md analysis indicates that the majority of sediments sampled were deposited by weak currents or decelerating turbidity flows. The latter are coincident with peaks in sand input and thus enable a further refinement of the interpretation to be made: the coarser grained material was deposited during a flood by turbulent undercurrents, almost definitely originating from the mouth of the minor unnamed stream closest to the core site (Figure 6.2). A detailed discussion and interpretation of all the variables, including pollen analysis, critical in providing the relative age of this unit (see section 7.3.3.1 below) has been given in section 6.6.2.2.2 above.

7.3.2 Sequence 2

7.3.2.1 Core Unit 1

In common with Loch Muick, coring has identified the existence of a minerogenic sandy silt/silt unit which does not appear on Pinger seismic profiles. The reasons for this omission are believed to be the same as those given in section 7.2.2.1, particularly the factor relating to thickness of the deposit and resolution of the equipment, as the maximum penetration into Unit 1 achieved by coring indicates that it has a maximum possible thickness in excess of only 14cm.

Data discussed in section 7.3.3.1, supported by geochemical analytical data (section

6.6.2.2.1) indicate that this unit dates from the end of the Loch Lomond Stadial, during deglaciation, or the immediate Postglacial during early climatic amelioration. Support for deposition during the latter period in the upper part of Unit 1 is found in the 71% increase in organic matter (Appendix Q). QDa-Md analysis indicates a decline in current activity at this location, from fluvial sedimentation to settling through the water column in quiet water conditions at the top of the unit. There is no evidence of a coarse sediment input (>sand sized particles), which leads to the suggestion that this sediment was deposited in an ice distal, low energy, position where iceberg drop and dump input was unimportant sedimentologically. This implies that the part of Unit 1 sampled in this research was deposited after the retreat of the Glen Callater glacier from the Loch Callater basin. Thus the sediment would be derived from suspended sediment charged glacial meltwater underflows and localised erosion of subaerial morainic deposits (see section 7.2.2.1 for references). Sedimentation of finer particles during winter is another probable source for Unit 1. However, the absence of varves observed during coring suggests that this was not the dominant mode of sedimentation.

It is suggested that this unit marks the upper part of a continuum of outwash deposits, which have not been identified seismically (for possible reasons see section 7.3.2.2 below).

7.3.2.2 Facies 2.1

In contrast to Loch Muick, only one glacial seismic facies has been identified in Loch Callater. Due to the shallowness of the water body and the depth of overlying sediment seismic penetration was restricted, resulting in the identification of Facies 2.1 in only two locations, where water depth was greatest (Figure 3.21). This facies, on the basis of external form and internal seismic reflectors (Figure 3.22), is interpreted as representing glacial diamict (section 3.6.3.2). The precise form of the buried landforms identified by Pinger cannot be ascertained due to the unsuitability of the loch for cross traverses. Where these features have no surface expression it is impossible to differentiate hummocks from

ridges in cross section. It is suggested that the absence of subaqueous outwash on Pinger profiles is also due to shallow water and restricted penetration. This is compounded by the fact that reports elsewhere (Liverman, 1991) and experience has shown in Loch Muick, where outwash does not completely obscure the topography, the deposit is restricted to topographic lows where it forms an infill. Thus in Loch Callater, where only the upper parts of the diamict surface are recognised seismically, the probability of identifying a low-level infill are significantly reduced. The minerogenic sediment of Unit 1 (section 7.3.2.1) is interpreted as representing the upper part of an outwash continuum comprising basal, coarse, ice-proximal sediment containing iceberg dropstones, through finer grained sediment with dropstones as the glacier retreated, to the fine grained, dropstone free sediment of Unit 1 deposited after the retreat of the glacier from the loch trough.

It is proposed that the diamict identified seismically represents the subaqueous continuation of the subaerial landforms described in section 1.5.3.2 and on the geomorphological map (Figure 1.5). Owing to the low level of seismic profile data of this sequence it is necessary to use bathymetric data (Figure 2.9) combined with observations from Sequence 1, where a drape can be identified covering the underlying topography. The ridge which divides the loch into two basins (section 2.5.3.1) is believed to be composed of glacial diamict, representing a stillstand of the glacier snout during retreat. The composition, internal structure and formational processes which created this proposed moraine cannot be further investigated as it does not extend upslope subaerially. Another ridge extends part way across the loch from the southwestern shore close to point 'A' (Figure 2.9). Evidence for a glacial origin of this ridge is stronger than that for the other ridge, as the small promontory at point 'A' is formed by the subaerial continuation of the subaqueous ridge, which merges over a short distance into the surrounding hummocky till surface. It is suggested that the central section of the ridge, between the subaerial and subaqueous sections, was removed by wave erosion and infilled by fluvially transported sediment (section 7.3.1.2.2). Examination of the truncated promontory exposure revealed apparently structureless diamict comprising fine grained, matrix supported, subangular clasts. There is no evidence of slump structures associated with a former ice core (Duck

and McManus, 1985a) or compressional faults resulting from seasonal push moraine formation (Boulton, 1986). The water depth of Loch Callater is prohibitively shallow to permit sublacustrine moraine formation, which requires a minimum depth of 30m (section 7.2.2.2.1) for ramp formation. Therefore, during retreat of the Glen Callater glacier in Loch Callater, the glacier snout was cliffed, or indeterminate where stagnating ice occurred (see section 7.3.3.1).

7.3.3 Implications regarding the glacial history of Loch Callater.

7.3.3.1 The last glacial period in Glen Callater

Four data sets obtained from surveys undertaken in Loch Callater enable the first accurate relative dating of the last glaciation in Glen Callater, and thus the adjoining glens, to be made. The four complementary data sets comprise Pinger seismic subbottom reflection profiles, and sedimentological, geochemical and pollen analyses of core material.

Pollen analyses undertaken on the basal section of Unit 2, Core 1 and on Core 2 reveal the existence of polleniferous sediment overlying the pollen free minerogenic sandy silt (Unit) which is interpreted as representing ice distal subaqueous outwash (section 7.3.2.1). The non-gradational boundary between Units 1 and 2, Core 1, is clearly defined at 426cm (Plate 6.2) and there is no evidence of syndepositional or post-depositional disturbance at the boundary. The boundary between minerogenic and organic sediment in Core 2 is equally well defined, at a depth of 638cm. The pollen assemblages identified in the basal organic sediments of both cores are unusual in that the pollen assemblages of pioneer species, reported elsewhere from sites occupied by glaciers dating from the Loch Lomond Readvance, are absent at both locations (section 6.6.2.2.1). This can be explained in two ways:-

- i) That the last glacial period in Glen Callater was not the Loch Lomond Readvance.
- ii) That sedimentation was prevented at the two core locations during deglaciation when plant colonisation started.

The first hypothesis is rejected on the basis of the Pinger data (see section 7.3.2.2). This

data show that lying directly beneath Facies 1.1 is glaciogenic sediment, deposited during the same period as the glaciogenic landforms identified in the subaerial environment (section 7.3.2.2; Figure 1.5). Sugden (1977) suggested that the glacial landforms mapped by Sissons and others in the corries in this area could date from the Little Ice Age which occurred during the 17th-19th Centuries. Research by Rapson (1985) has shown that Sugden's hypothesis could not be supported by pollen analysis from high level corries in the Cairngorms and Lochnagar. This thereby precludes the relatively low level valley glaciers, identified by geomorphological mapping in Glens Callater and Muick, from forming during this period.

Thus the remaining period of extreme climatic conditions and glacier recrudescence since the retreat of Devensian ice is the Loch Lomond Readvance. Areas outside the direct influence of Loch Lomond Readvance glacial activity have been shown to exhibit a tripartite sedimentary division (see section 6.6.2.2.1). In Loch Callater, sedimentological and geochemical evidence from Core 1, combined with visual examination (section 6.4.1), indicate that the Loch Lomond Readvance is not represented by a tripartite sedimentary division, and that the variation between Units 1 and 2 is unique within the core. Thus the absence of minerogenic sediment at other positions within the core is an accurate representation of sedimentological variation as opposed to a sampling omission. Pinger profiles show that glaciogenic sediment underlies Facies 1.1 and almost definitely underlies Unit 1 (compare with Loch Muick, section 7.2.2.1). Therefore the ameliorating climate inferred from the pollen analyses must date from the last full glacial period in Glen Callater when glaciogenic sediment was deposited. Given the absence of the tripartite Loch Lomond Stadial sequence or any other evidence of deteriorating climate within Unit 2, and the almost definite presence of an outwash-glaciogenic sequence, this glacial period must be the Loch Lomond Readvance.

This interpretation supports that of Sissons (1972b, p42) who indicated that the key to dating the last glaciation in Glen Callater was through pollen analysis. The interpretation given here opposes that of Clapperton (1986) and Sugden and Clapperton (1975) who, in

the light of Rapson's (1985) report on the absence of glaciers in high corries during the Little Ice Age, asserted that the former valley glaciers in Glens Callater and Muick could have formed through 'Catastrophic stagnation of ice fields and glaciers' (Clapperton, 1986) during the Devensian deglaciation (section 1.4.2). The additional temporal constraint presented in this thesis demonstrates the value of seismic subbottom reflection profiling in age determination, when combined with geochemical and pollen analyses of core material.

Given that the last glacial activity in Glen Callater dates from the Loch Lomond Readvance, an explanation must be found for the absence of the earliest Postglacial pollen assemblages. Examination of the stratification at the boundary between the polleniferous and minerogenic sediment did not reveal evidence of syn- or post-depositional mass movements or erosion. QDa-Md analysis supports these observations. The basal sample falls within the fluvial environmental trend envelope, and samples taken above and below the boundary (430cm and 420cm) fall within the quiet water and fluxoturbidite envelopes respectively. This indicates that turbidite deposition associated with major sedimentary events and possible mass movement or erosion of underlying sediments has not occurred at this location. Thus sedimentary anomalies are not believed to be the cause of the absence of early pollen assemblages.

The alternative scenario is that an inactive, stagnant mass of glacier ice became detached from the main Glen Callater glacier, effectively preventing deposition at the two core sites (section 6.6.2.2.2). Pinger profiles are unable to provide data regarding the nature of the underlying topography, therefore it cannot be ascertained whether or not stagnation topography exists beneath the drape of recent sediment. However, pollen analyses suggest that core site 1 became ice free first, during the deposition of the chionophilous *Juniperus* pollen assemblage, which is typical of the later part of the early Holocene. At site 2 (Figure 6.2), approximately 800m further up valley at the southeastern end of the loch, the *Juniperus* pollen assemblage is absent and the basal pollen assemblage is co-dominated by *Corylus-Betula* pollen, indicative of ameliorating climatic conditions. The absolute dates of the time period involved are not known as radiometric dating has not

been carried out. Moreover, the accuracy of radiocarbon dates obtained from this period is now under question (Amman and Lotter, 1989; section 1.4.1). This interpretation of the data, that glacial ice existed at the Loch Callater site possibly into the ninth millenium BP, has important implications regarding the nature and rate of climatic change in the east of Scotland during the Loch Lomond Stadial and Postglacial. Examination of these implications is beyond the scope of this thesis and requires further palynological analyses and geomorphological mapping at a large scale.

7.3.3.2 The age of the Loch Callater trough

That Loch Callater is a moraine-dammed loch has not been questioned since the survey of Collet and Johnston (1906, p. 110), who described the loch as:-

'A true barrier basin, dammed up by a frontal moraine.'

No evidence from this project has indicated that this view is incorrect (see Plate 1.4). However, the data discussed above (section 7.3.3.1) provide the first evidence of the length of existence of the water body. These data demonstrate that the subaerial and subaqueous glacial deposits in upper and middle Glen Callater, including the morainic barrier, almost definitely date from the Loch Lomond Readvance glaciation. The proto-Loch Callater is believed to have existed since the retreat of the glacier from the morainic barrier. The period of lacustrine sedimentation cannot be precisely determined, but from pollen analysis is known to have been occurring since at least the later part of the early Holocene. Subaerial geomorphological mapping, combined with data from the 1905 survey has shown that the loch surface area has been reduced by fluvial deposition of a broad alluvial plain by 0.4ha in 84 years. The alluvial plain extends a further kilometre towards the head of the valley (Figure 1.5) and is interpreted as defining the former maximum extent of Loch Callater. A large volume of debris entrained in the glacier, evidenced by the extensive subaerial till deposits, was available for deposition by meltwater streams. Thus the maximum loch length was almost certainly maintained for a brief period only, due to

rapid fluvial accumulation. The lateral extent of ice stagnation in the loch trough and the possible effects this situation may have had on outwash sedimentation cannot be quantified. However, it is suggested that the topographic irregularities associated with the upper limit of stagnating ice may have caused meltwater current deceleration and the preferential deposition of entrained coarse sediment. As discussed in section 7.3.1.2.2 above, further surveys including electrical resistivity and ground impulse radar would potentially be of value in the examination of the nature of the sediment underlying the alluvial plain.

7.4 LOCH LEE

7.4.1 Sequence 1

7.4.1.1 Surface sediment texture

Data regarding the surface sediment texture are derived from two sources, sidescan sonar and surface sediment samples. In contrast with Lochs Muick and Callater, the coarse grained surface sediment component does not dominate the nearshore slopes or comprise discrete textural associations such as boulder spreads or clusters. Boulders and cobbles occur relatively infrequently on the loch slopes and are scattered widely. Thus three sediment textural associations are recognised in the Loch Lee basin:- fluvial input zones, coarse grained sediment, and fine grained sediment.

7.4.1.1.1 Fluvial input zones

Five streams flow into Loch Lee, of which the main influent is the Water of Lee. Owing to the shallowness of the loch, and vegetative growth close to the mouth of this stream and the nearby drain (Figure 2.2), surveys could not be undertaken in this area. One sonograph (Plate 4.2) was obtained from the southwestern shallows. This revealed patches of aquatic weed growing on a low backscatter loch floor. In the absence of calibration from surface sediment analyses in this area, comparison was made with the remainder of the loch, resulting in an interpretation of this seismic response as fine grained sediment,

possibly silt. The most proximal sediment sample to the mouth of the Water of Lee is very poorly sorted (Figure 5.10) and has a mud texture, atypical of fluvially deposited sediment, but in common with large areas of the loch floor (Figure 5.6). Sandy silts near to the northern and southern shores may indicate that the influent current enters the loch against the southern shore, and that the drain provides an important contribution to the loch floor sediment. The sediment close to the southern shore also has a greater mean diameter (2.44 ϕ maximum) which it is suggested results from deceleration of the current on entry to the waterbody. This further implies that a channel, possibly that occupied by the stream prior to reservoir impoundment (section 1.5.2.1) exists across part of the loch floor, like that of the Black Burn (section 7.2.1.1.3), permitting continued entrainment of relatively coarse grained sediment across 250m of loch floor before deposition at a depth of 3.2m (Appendix E). QDa-Md analysis of sediment from this area falls within the overlap between the steep gradient turbidite and quiet water environmental trend envelopes. Analysis of the sediment sorting (Figure 5.10; Appendix E) aids differentiation between these two depositional processes as it indicates that the sediment in the area in question is moderately sorted, a relatively high degree of sorting in the context of this loch. Research has shown that fine sediment deposited by settling through the water column is typically poorly sorted (Thomas et al., 1972; Duck, 1986; section 5.6.2) thus indicating that currents, and therefore turbidites as opposed to quiet water sedimentation were the most probable mode of deposition. These turbidity currents can be demonstrated to be small scale, as samples 300m eastwards were deposited under quiet water conditions. Thus it is suggested that the turbidity currents result from localised rapid, unstable deposition and subsequent mass movement during flood events.

The mouth of the Burn of Duchrey and the neighbouring unnamed stream do not exhibit sedimentological variation identifiable on sidescan sonographs (Plate 4.4) due to the high offshore slope angle (Figure 2.2) which dominates sonographic records. The most notable feature of the loch floor sediment at the mouth of the Burn of Duchrey is the extremely high (85.4%; Appendix D) organic matter content. Repeated sampling at this

location identified no variation in loch floor sediment, therefore the sample was accepted as representative. The clastic component of the sediment in the sample is extremely fine grained, resulting in an unusual decrease in mean grain size, extremely poor sorting, and a pronounced positive skewness close to the stream mouth (Figure 5.9), phenomena that do not occur in any of the other lochs studied. The sediment at the mouth of the unnamed stream is also relatively high in organic matter, but the effect on the sorting (1.67ϕ , poorly sorted), mean grain size (7.34ϕ), and skewness (0.05, nearly symmetrical) is less pronounced than at the mouth of the Burn of Duchrey. The nature of the organic matter, finely comminuted vegetation comprising stems of grasses and sedges, suggests that it was deposited by stream flow clearing drainage channels of organic matter built up in summer, during autumnal rainfall preceding the survey.

No sedimentary variation associated with the inflow of the minor Burn of Laurie has been recognised from sidescan sonographs or surface sediment samples.

7.4.1.1.2 Coarse grained sediment

As noted in section 7.4.1.1 above, coarse grained sediment of boulder or cobble size occurs relatively infrequently in Loch Lee. The highest concentration of boulders on the sediment surface is illustrated in Plate 4.4 where the occurrence is linked to a mound on the high angle slope beneath the mouth of the Burn of Duchrey (see section 7.4.1.2.2). Scattered boulders occur partially buried within finer sediment represented by low backscatter. In Plates 4.3 and 4.7 the surrounding sediment is silt and mud respectively. Partially buried clastic material is also located on the 'treads' of shore-parallel terraces (Plate 4.7) and in one case there is evidence of a boulder which has slid from a shore-parallel terrace onto finer grained sediment through which a curvilinear topographic low has been cut (Plate 4.6). The clarity of this subaqueous landform indicates that it is of recent origin and has not been subject to substantial post erosional infilling.

The relative absence of coarse grained sediment in the surface sediment must be

explained by restricted supply as opposed to rapid sedimentation covering the deposits. Pinger subbottom profiling indicates that boulders are equally infrequent within Sequence 1 sediment. The cause of this restricted supply is believed to be twofold:-

- i) Slope morphology.
- ii) Restricted area of bare rock surfaces.

Plate 1.1 illustrates the effects of slope form. Where suitable source areas of clastic material are located the boulders and cobbles eroded from the bedrock form lobate landforms with distinct downslope limits at a break in slope approximately 10m-20m above the loch shore on both sides of the loch. Thus boulder movement downslope by mass movement or erosional processes is severely restricted. These landforms occur beneath the majority of bedrock outcrops above the loch (Figure 1.4). The other cause, that of restricted supply, is partially covered above. Only three outcrops occur above the loch that, slope morphology permitting, could provide debris subsequently deposited in Loch Lee. It is possible that avalanche could transport clastic material to the loch. However, the data available, both subaerial and subaqueous, do not support this hypothesis. Unlike Loch Muick there is not a substantial debris supply available from gully erosion of glacial sediment (section 7.2.1.1.1), nor are there cliffs actively eroding into till surfaces as have been recognised as contributing coarse grained sediment to Loch Callater (section 7.3.1.1.1).

7.4.1.1.3 Fine grained sediment

This section examines the fine grained loch floor surface sediment outside the zones of fluvial input. The differentiation of the sediment types identified by particle size analysis on sidescan sonographs is complex due to the input from the varied underwater topography, and is therefore dismissed as a diagnostic sediment indicator in this context. Mud and silt texture sediments cover the majority of the floor area of Loch Lee. Sandy mud and sandy silt occurs nearshore and has a very strong (significant at the 0.2% confidence level) negative correlation with depth. Sandy sediment also occurs at two points in the centre of the loch. QDa-Md analysis indicates that these samples were deposited in the fluxoturbidite or quiet water environments, which is unusual for relatively coarse sediment

in a mid loch location. Examination of the bathymetric chart reveals that mass movement of the surface sediment has occurred in this area (see section 7.4.1.2.2) and it is therefore suggested that these sedimentary anomalies are an indirect, relatively distal, product of these movements; hence the QDa-Md data. Sidescan sonar data suggest that the nearshore surface sediment is relatively consolidated. This is illustrated in Plate 4.6, where a boulder lies only partially buried by silty surface sediment, and the slide scar behind it is clearly outlined, indicating that the sediment through which it has been cut has not slumped and infilled the feature.

The surface sediment of Loch Lee has an extremely high organic matter content, above that recorded from the other lochs in this study and elsewhere (see section 5.6.1 for references). This is believed to be partly due to anthropogenic pressure on the catchment by estate management, other recreational usage including ramblers, the high level of grazing by sheep and Red Deer resulting in the erosion of peat deposits, and the time of year at which the samples were obtained when the maximum amount of organic matter is available to be transported to the loch. This inferred recent deposition is believed to explain the high organic content recorded close to the loch shores, which would be temporally restricted. Despite this distribution, the underlying distribution is of increased organic matter content with depth, due to the low density, and thus high redistributive capacity by wave action, of organic matter. It is suggested that had sufficient time been available, a comparative study of organic matter distribution in autumn and spring would have provided information on the effects of surface sediment redistribution and sediment focusing in Loch Lee.

The degree of sorting in the surface deposits of Loch Lee is also below that of Lochs Muick and Callater. The largest part of the loch floor is dominantly covered by poorly sorted material, which is probably an inherited characteristic from the predominantly extremely poorly sorted till deposits from which the sediment is eroded (Curry, 1960). However, it is proposed that this characteristic is also partly due to the anthropogenic impact of reservoir impoundment, dam construction and subsequent maintenance at the eastern end of the loch and partly due to the impact of the highly organic material at the mouth of the

Burn of Duchrey. The low mean grain size (9.25ϕ) of the minerogenic content of this material is similar to that found in central loch locations elsewhere (see section 5.6.2) from which poorly sorted sediment has been reported.

7.4.1.2 Surface sediment topography

7.4.1.2.1 Shore-parallel terraces

In common with Lochs Muick and Callater, the nearshore slopes of Loch Lee are broken by a series of shore-parallel terraces. A maximum of five terraces extending 75m from the loch shore (e.g. Plates 4.5, 4.6, 4.7), with an amplitude of <1m, have been formed by the processes discussed in section 7.2.1.2.1 above. The situation in Loch Lee differs from the other two lochs in this study in that the water level has been artificially raised by approximately 1m (section 1.5.2.1). Thus a former shoreline, which was occupied for a considerable period, and below which former low water level shorelines almost definitely developed, should be identifiable on sonographic records. Unfortunately determination of the pre-impoundment shoreline is not simplified by the post-impoundment fluctuations in water level associated with increased extraction during periods of low rainfall in the district. During 1990 the water level dropped by approximately 3m due to the enhanced supply demands during a dry summer. Examination of the bathymetric chart (Figure 2.2) indicates that two wide terrace flats exist at a depth of approximately 1m. These features can be clearly identified on the northwestern promontory (Plate 4.7). It is suggested, on the grounds of lateral development and continuity, that the lower terrace flat (marked on the Plate) may represent the former shoreline of Loch Lee prior to impoundment.

7.4.1.2.2 Mounds and hollows

Pinger and bathymetric evidence indicate that the subaqueous landforms of Loch Lee, of a sufficient magnitude to be identified on the bathymetric chart in the central zone (Zone 2) of the loch (for boundaries see Figure 2.3), were formed by mass movements following initial metastable sediment accumulation and increased sedimentary burden from

above. The other three causal factors proposed by Carter (1975) are discounted for the reasons given in section 7.2.1.2.3.2 which apply equally to Loch Lee. The mouths of the Burn of Duchrey and the other unnamed stream are not associated with subaerial deltaic aggradation (Figure 1.4) nor is there Pinger or bathymetric evidence of subaqueous delta formation. However, the same mode of mass movement initiation as that proposed for deltas in Lochs Muick and Callater, that of increased sedimentary burden from above on the extremely steep subaqueous slope angle, is believed to have initiated the mass movement which resulted in the suite of mounds and hollows at the break in slope (Plate 4.4). It is proposed that the large number of boulders lying on the surface of the mound and scattered over the adjacent loch floor result from entrainment from the underlying sediment (Sequence 2 or 3) during mass movements. The size of the clasts involved (>1m) is believed to exceed the entrainment capacity of either stream and there is no evidence of a subaerial source by mass movement or erosion.

The mounds and hollows within Zone 3, the northeastern shallows, are interpreted as having been derived from a combination of processes. The majority are composed of Sequence 1 sediment which Pinger profiles show to be composed of chaotic internal reflectors. Two, however, are composed of sediment from Sequences 2 and 3 and are therefore examined in sections 7.4.2.2 and 7.4.3.

Hollows of an insufficient amplitude to permit identification on echograms, and which therefore do not appear on the bathymetric chart, occur in a broad swathe across the loch floor on the southern side of Loch Lee (Plate 4.3). Pinger profiles in this area show that scattered boulders occur in the surface sediment. In the light of the interpretation given in section 7.4.1.1.2 above, it is considered unlikely that these boulders have been deposited by natural processes. It is proposed that the boulders represent anchor weights lost or discarded during moored boat based fishing activity which has been observed on the loch, and that the minor hollows in which boulders do not occur are formed on anchor weight recovery.

7.4.1.3 Internal composition

This section examines the internal sedimentary structures, composition and formational processes of Sequence 1 facies based solely upon Pinger profile data, due to the lack of core data (section 6.2.1.1).

7.4.1.3.1 Facies 1.1

Facies 1.1, which has a reflection amplitude marginally above that of background noise, forms a low density infill in the underlying topography and lobate features on gentle slopes at the top of the seismostratigraphic column. Grab samples obtained from areas where Facies 1.1 is known to occur suggest that it has a mud texture, with a range in organic matter levels between <10% to >40%. It is possible, however, that these samples do not reflect the composition of Facies 1.1, but the underlying sediment (Facies 1.2; Figure 3.8; Facies 1.3; Figure 3.13) due to the low density of Facies 1.1, which may not be sufficient to trigger the jaws of the grab. Facies 1.1 in Loch Lee is comparable with the same Facies identified in Loch Muick (section 7.2.1.3), which is interpreted as having a 'soupy' consistency (Hicks et al., 1990). This sediment is interpreted as representing the most recently deposited, fine grained, Holocene lacustrine deposit (section 3.5.3.1).

7.4.1.3.2 Facies 1.2

This sediment can be traced extensively across the floor of Loch Lee, ranging in thickness from <0.5m to 5.25m. It is from this facies that the majority of surface sediment samples have been obtained, and analysis of these samples, combined with the detailed data of internal reflectors available from Pinger profiles, indicates that the sediment of which Facies 1.2 is composed is typical of lacustrine sedimentation in quiet water conditions. QDa-Md analysis, internal reflectors and surface topography prove that small scale mass movements currently occur within the surface layers (section 7.4.1.2.2) and have been taking place since sedimentation of this facies was initiated. Anthropogenic impact is

marked in three ways. First, by the enhanced organic input from high grazing densities and recreational pursuits, secondly by disturbance of the upper strata of Facies 1.2 by anchor pits and weight drops during moored fishing activity, and thirdly by activities associated with reservoir maintenance and water extraction.

Truncated internal reflectors of the underlying Facies 2.1 (Figure 3.14), at the unconformable boundary between Sequences 1 and 2, suggest that the cessation of sedimentation of Sequence 2 sediment was a relatively sudden event. There is no seismic evidence of a return to Sequence 2 sedimentation during Sequence 1. Rapid deposition at the start of Sequence 1 (Facies 1.2) sedimentation is inferred from the truncated seismic configuration typical of erosion. The absence of a coarse grained seismic signature containing boulder reflectors throughout the loch suggests that the erosive event associated with the start of Sequence 1 deposition was not avalanche induced. It is proposed that the unconformity was created by a sudden flood event depositing sediment distinct from that of Sequence 2 and, in the light of the suggested age of the Sequence 2 deposits (see section 7.4.5.1), containing a significantly higher organic content. Coring and analysis of the loch floor sediment is required to substantiate sedimentologically the interpretations given above.

7.4.1.3.3 Facies 1.3

This facies occupies a topographic hollow in the loch floor approximately 9m deep into which prograding clinoforms extend from shallow water into deeper water. The internal reflectors are typical of those resulting from episodic sedimentation events. It has been suggested that this facies is formed by the entrainment of fine grained materials from the nearshore environment and subsequent deposition in deep water, below the depth of surface water wave base (section 3.5.3.1). Further downslope redistribution occurs by mass movement. The relatively low seismic reflectivity of this facies compared with that of Facies 1.2 indicates that it has a lower density and is more poorly consolidated. Håkanson (1978) and Johnson (1980b) stress the importance of the potential maximum effective

fetch, water depth, shape of the water body, frequency and duration of high winds, and sedimentation rate of fine grained sediment in determining the frequency and magnitude of sediment redistribution events.

Wind speed, direction and duration data are not available for Glen Lee and thus the critical conditions and frequency of sediment redistribution events could not be evaluated. However, observations made during surveys curtailed by high winds indicate that Force 8 and Force 9 winds from the west, which resulted in wave heights of 0.5-0.7m and visible nearshore entrainment of fine sediment, have a frequency of at least 2-3 events per year, and probably occur significantly in excess of this figure. Sedimentation rates of fine grained sediment in the nearshore and shallow water zones of Loch Lee in the intervening periods between significant wind events, especially in autumn, inferred on the basis of the distribution of organic matter (section 7.4.1.1.3), are believed to be sufficient to prevent erosion of consolidated sediment from the loch floor or shores. However, during the periods of the year when the delivery rate of organic and minerogenic matter to the loch is lower, it is suggested that erosion of consolidated sediment occurs. This is believed to explain the relatively well developed shore-parallel terraces on the gentle slope at the northeastern end of the loch, and the appearance of bedrock outcrops on the loch floor (Plate 4.7) (Johnson, 1980b).

7.4.2 Sequence 2

In the absence of complementary data from sediment cores this section and sections 7.4.3 and 7.4.4 reiterate the highlights of the findings reported in Chapter 3 and suggest interpretations of the data to provide a complete overview of the seismic- and lithostratigraphy of Loch Lee.

7.4.2.1 Facies 2.1

This facies is composed of subparallel wavy and hummocky reflectors and contains scattered boulder reflectors close to the loch shores. The lower, unconformable boundary follows the underlying topography, and the facies forms a blanket infill over much of the

upper surface of Sequence 3 (Figure 3.15). Where the lower boundary of Facies 2.1 is in contact with Facies 3.2 the sequence boundary appears conformable. The seismic response of this facies has a lower intensity than that of the analytically proven, highly organic, mud and silt of unconformable overlying Facies 1.2. Facies 2.1 is parastratigraphically interpreted as representing two distinct sediment populations, boulders and fine grained sediment drape, derived from the subaerial and lacustrine environments respectively. It is suggested that the boulder input was derived from rockfall activity and that the fine grained sediment from fluvial and slope wash inputs. The proposed age of these deposits is given in section 7.4.5.1 below.

7.4.2.2 Facies 2.2

Facies 2.2 has a gradational lateral boundary with Facies 2.1 and is characterised by a much higher concentration of boulder hyperbolae in a matrix of chaotic internal reflectors. These seismic characteristics, combined with the limited distribution of the facies, which is primarily restricted to the nearshore zone (Figure 3.18), have led to the interpretation that the sediment is derived from the slopes surrounding Loch Lee. The exact mode of delivery (debris flow/rockfall/avalanche) is suggested in the light of the interpretation of the modes of deposition of Facies 2.1 and is therefore believed to be dominated by avalanche activity (see section 7.4.5.1).

At the northeastern end of the loch, nearest the southern slope, the deposit of Facies 2.2, which is almost circular in plan, forms the core of the flat topped mound identified on Figures 2.2 and 2.5 and Plate 4.8. This mound is covered by a thin veneer of Sequence 1 sediment which. Data reported by Johnson (1980b) suggest that wave motions, and possibly associated currents, restrict substantial deposition of low density organic material onto this surface. However, it is also evident from the existence of this depositional veneer, that wave erosion at the current water level was not the formational process behind the distinctive flat top of the mound. The water depth above the feature prior to impoundment

is also believed to have been too great, even at the lowered water levels evidenced from shore-parallel terraces (section 7.4.1.2.1), to have enabled substantial wave induced erosion to occur. Thus two hypotheses for the formation of this mound are proposed:-

i) The mound was truncated by wave erosion during a reduced lake level for which there is no sonographic or Pinger evidence.

ii) The mound was artificially modified during reservoir construction.

Due to the nature of the available evidence and the non-availability of data regarding reservoir construction from Tayside Region, verification or rejection of either of these hypotheses is not possible.

7.4.3 Sequence 3

7.4.3.1 Facies 3.1

Facies 3.1 occurs throughout Loch Lee and is composed almost entirely of boulder hyperbolae, to an extent where stratification within the matrix, if present, cannot be differentiated. The upper surface of Facies 3.1 has a hummocky external form which is unconformable with overlying Sequence 2 sediment. Internal reflectors of Facies 2.1 terminate against the sides of topographic lows of the facies (Figure 3.14) by onlap updip and downlap downdip. This unconformity marks a sharp break in the mode and style of sedimentation from lacustrine/subaerial (Sequence 2) to a seismic signature typical of glacial sedimentation (see section 3.5.3.3 for references).

Where infilling by subsequent sedimentation has not completely blanketed the surface topography of Facies 3.1 it forms mounds rising above the surface of the surrounding loch floor. An example of this occurs at the northeastern end of the loch, in a position equidistant from the northern and southern shores.

7.4.3.2 Facies 3.2

This facies is characterised by internal stratification, which is entirely absent from Facies 3.1. The basal boundary of Facies 3.2 is gradational with Facies 3.1 rendering distinction of the boundary difficult. This facies occupies topographic lows of Facies 3.1 and exhibits graded bedding from extremely coarse grained material at the base of the facies to stratified, fine grained sediment at the top. The apparently conformable upper boundary, coincident with the sequence boundary, is marked by a higher intensity (coarser grained sediment) reflector which can be traced to the unconformity between Facies 3.1 and Facies 2.1. This facies is interpreted as representing glacial outwash ranging from ice proximal sediment deposited almost immediately after the retreat of the glacier, resulting in a gradational boundary, to fine grained sediment deposited when Loch Lee was in a relatively ice distal position.

7.4.4 Sequence 4

Sequence 4 (Facies 4.1) is represented by a high amplitude reflector at the base of the seismostratigraphic column identified in Loch Lee. The smooth external form and relatively high reflectivity of this reflector are interpreted as representing the underlying, ice moulded, gneiss or schist bedrock. Plate 4.7 illustrates a sonograph where bedrock is interpreted to outcrop on the surface of the loch floor at the base of a promontory. The promontories are also believed to be cored by bedrock, but subsequent sedimentation has obscured the majority of low angle surfaces, preventing more detailed analysis of bedrock surfaces.

7.4.5 Implications regarding the glacial history of Loch Lee

7.4.5.1 The age of the last glacier to occupy the Loch Lee trough

Determination of the age of the last glacier to occupy the Loch Lee trough is based solely upon the subaqueous sedimentary record highlighted above, and the subaerial geomorphological map of Glen Lee (section 1.5.2.2). Absolute or relative dating

techniques (e.g. pollen analysis) were not carried out due to the non-availability of core material. Critical in assessing the relative age of the deposits are Sequences 1 and 3, and the geomorphological data, which indicate that the last glaciation in Glen Lee did not reach Loch Lee, and which enable the period of deposition of Sequence 2 to be inferred.

Analysis of the present surface sediment (Sequence 1) has shown that rockfall input to the loch at present and during recent sedimentary history has been severely restricted (section 7.4.1.1.2). This is believed to be primarily due to the current relatively equable climate which has reduced the importance of freeze-thaw processes of rock breakdown and has enabled stabilisation of the slopes above Loch Lee by growth of vegetation. Thus it follows that Sequence 2, which is composed of facies containing significant proportions of boulder sized clasts, must have been deposited during a period of climatic deterioration when freeze-thaw processes were active and vegetation cover reduced, assisting downslope transportation of debris to the loch.

Within recent sedimentary history two periods of reduced temperatures are recorded, the Little Ice Age and the Loch Lomond Stadial. In the absence of core material it is necessary to compare data from the two other lochs in the study. Examination and analysis of core material combined with subbottom Pinger profile data from Lochs Muick and Callater have indicated that there are records for one cold period only when simultaneous organic carbon, sedimentological and geochemical change occurred. Pollen analysis of the sediment lying directly stratigraphically above this minerogenic layer proves that a chionophilous pollen association, typical of early Holocene plant recolonisation after the Loch Lomond Stadial occurs at this position. This thereby implies that the minerogenic sediment dates from the Loch Lomond Stadial and the period immediately after deglaciation (see section 7.3.3.1). Thus the last period of climatic deterioration to affect substantially Lochs Muick and Callater, the closest of which lies approximately 12.5km distant from Loch Lee (Figure 1.1), was the Loch Lomond Stadial. The absence of an identifiable sedimentary change during the Little Ice Age is not unique to the lochs studied in this thesis. Research by Rapson (1985) has indicated that, at an altitude in excess of 750m, in

the lochan occupying the Northeast Corrie of Lochnagar, accumulation of peat was continuous and apparently not subject to inputs of coarse grained material. Therefore it is apparent that the impact of the climatic cooling during the Little Ice Age would be considerably less important in Glen Lee and Loch Lee where the loch lies at an altitude of 272m.

The last period during which significant rockfall and development of boulder lobes occurred was the Loch Lomond Stadial (Sissons and Grant, 1972). It is recognised that the period of deposition of the complete population of boulder lobes is disputed, and that evidence exists to show that accretion of these landforms was not entirely restricted to the Loch Lomond Stadial (White and Mottershead, 1972; Sugden, 1973; Sissons 1973b, 1980b). Indeed, this is supported by the findings from Sequence 1 sediments which indicate the continued deposition of large clastic material to the present day, but at a considerably reduced rate and volume (section 7.4.1.1.2). Given the high concentration of boulders identified within Sequence 2 sediment, particularly in Facies 2.2, this facies is interpreted as representing the lacustrine equivalent of subaerial boulder lobes identified outside the proposed Loch Lomond Readvance glacier limits elsewhere (Sissons and Grant, 1972; Figure 1.4). Thus it is proposed that Sequence 2 dates from the Loch Lomond Stadial.

In the context of this interpretation, it is suggested that the spatially restricted Facies 2.2 represents deposition dominated by debris laden avalanches during seasonal snowmelt (Weirich, 1985) with a probable input from debris slides/rockfalls. The transition between Facies 2.2. and 2.1 is gradational through coarse grained material to fine grained stratified sediment, representing outlying, scattered boulders from the avalanche deposits.

Facies 2.1 by definition must also date from the Loch Lomond Stadial, containing interfingering, nearshore, coarse grained subaerially derived deposits and stratified, fine grained sediment deposited in the lacustrine environment. Geomorphological mapping has confirmed the former existence of two glaciers in Glen Lee which are believed to have formed during the Loch Lomond Stadial (Sissons, 1973b; Figure 1.4; section 1.5.2.2.2).

Assuming that the inference of the age of Sequence 2 deposits given above is correct, two sediment sources of fine grained material are envisaged. First, the fine grained component of avalanche and debris flows, and secondly the fluvial input from proglacial outwash streams. The second mode of sediment delivery almost certainly entrained and transported coarse grained clastic material. However, Pinger profiles indicate that this component does not occur within Facies 2.1. This can be explained by reference to the subaerial geomorphology (Figure 1.4). Terraces composed of coarse grained outwash material occur at the head of Glen Lee, adjacent to and just inside the former maximum limit of the Glen Lee valley glacier. It is suggested that the coarse grained sediment component was deposited at this former ice proximal position. North west of Loch Lee a broad alluvial plain fills the valley floor, through which the Water of Lee flows, over a distance of 2.5km. It is proposed that, in common with Loch Callater, this landform was largely formed through deposition of medium and fine grained sediment by proglacial outwash streams from both the Glen Lee and Carlochty glaciers onto the valley floor or into a larger Loch Lee during the Loch Lomond Stadial. Deposition has continued, almost certainly at a reduced rate, during the Holocene. Thus the area of valley floor occupied by Loch Lee was in an ice distal position during the Loch Lomond Stadial and received sediment dominated by the fine grained fraction of glacial outwash. It is suggested that investigation of the subsurface sedimentology, which was not possible in the time available, could provide a valuable insight into ice distal deposition in Glen Lee and permit verification or rejection of the hypothesis above.

A modern analogue of this situation is reported by Smith et al. (1982) from Peyto Lake, Western Alberta. At this location fine grained sediment is transported 3km from the Peyto glacier snout to be deposited via underflow currents on the lake floor. Due to this mode of deposition, accumulation areas are strongly influenced by the underlying topography (Liverman, 1991). It is thus inferred from the evidence of the external draped, topographic infill form, that a similar situation, plus additional settling of suspended sediment beneath lake ice in winter, occurred in Loch Lee.

The seismic distinction between Sequences 1 and 2, both of which are dominated by fine grained material, is believed to result from the presumed absence of organic matter from Sequence 2 sediment (see sections 7.2.2.1 and 7.3.2.1). The reflected seismic signal varies according to numerous sedimentological factors including water content (section 3.2.2), which has been shown to have a strong positive correlation with organic matter, significant at the 0.2% level in Loch Muick (Table 6.2; section 6.6.3.1). Analyses of Loch Muick and Loch Callater core sediment also suggest that deposition of organic matter was severely curtailed during the Loch Lomond Stadial (sections 6.6.2.2.1; 6.6.3.2.1; 7.2.2.1; 7.3.2.1).

The interpretation, based upon subaerial, sublacustrine, modern analogue and reports from Loch Lomond stadial sites, that Sequence 2 dates from the Loch Lomond Stadial has further important implications on the age of underlying Sequence 3. This sequence, composed of glacial outwash sediment and glacial diamict typical of that reported elsewhere (for references see section 3.5.3.3) and identified in Lochs Muick and Callater, is the only direct glacial sediment recognised in Loch Lee. The question arises therefore as to when this sediment was deposited.

Subaerial evidence from the Glen Lee and Carlochty glaciers is conclusive that the nearest glacial terminus was situated a minimum of 1.5km from the present loch shores. However, an undifferentiated till surface has been identified at the mouth of the Inchgrundle valley approximately 50m from the western shore of Loch Lee (Figure 1.4). On the basis of subaerial evidence (section 1.5.2.2.2) this has been interpreted as dating from the Devensian glaciation, but it is important that this interpretation is verified from the loch profile data set. Pinger profiles of the area in question demonstrate the existence of a substantial accumulation of Facies 2.1 (Figure 3.15). If this subaerial till deposit dated from the Loch Lomond Stadial, seismic evidence of a fluvio-glacial outwash input within Facies 2.1, containing a significant proportion of large clastic material due to the ice proximal position of the loch, could be expected (Mullins et al., 1991). There is no evidence of sediment of this nature and therefore the conclusion of the interpretation based

upon the subaerial geomorphology is supported. Thus the sediment of Sequence 3 must pre-date the Loch Lomond Stadial and consequently must have been deposited during the Devensian glaciation.

The two facies identified in Sequence 3 illustrate the retreat of the Devensian ice through initial glacial diamict deposition and contemporaneous deposition of horizontally stratified, coarse grained outwash material, to fine grained sedimentation when Loch Lee was in a relatively ice distal position. The fine grained sediment of the upper part of Facies 3.2 closely resembles that of Facies 2.1 which was deposited in a comparable position and environment. It is believed to be for this reason that, where these two facies are in contact the sequence boundary appears to be conformable, although elsewhere it is shown to be unconformable.

Within the newly proposed Holocene-Loch Lomond Stadial-Devensian stratigraphy for Loch Lee there is one chronostratigraphic period for which there is no seismic evidence, namely the Lateglacial Interstadial. This period occurred between the Devensian glaciation and Loch Lomond Stadial. In areas outside the direct influence of glaciers during the Loch Lomond Stadial the Lateglacial Interstadial is marked by organic material deposited above Devensian sediments (Sissons et al., 1973; section 6.6.2.2.1). The apparent chronostratigraphic hiatus may be explained by one of the two hypotheses below:-

- i) The Lateglacial Interstadial deposit was eroded during the Loch Lomond Stadial.
- ii) The Lateglacial Interstadial sediment stratum is of an insufficient thickness to meet the resolution requirements of the Pinger equipment.

The first hypothesis requires that, during the fluvial deposition of fine grained sediment, all evidence of the previous interstadial was removed from the underlying, complex topography. Data examined above (this section) suggest that deposition of Facies 2.1 was via underflow currents and settling through the water column, and thus did not involve high energy conditions where substantial erosion of underlying sediment could occur. If subaqueous fluvial erosion by underflow currents did occur during the Loch Lomond Stadial it is suggested that erosion would be concentrated on topographic highs, with

subsequent enhanced deposition into the adjacent enclosed hollows. However, as noted above, there is no seismic evidence of enhanced deposition in the hollows of Sequence 3. The 'conformable' boundary in the hollows is marked by a stronger seismic reflector interpreted as representing coarser grained deposition followed by finer grained inorganic stratified sedimentation.

The second hypothesis requires that the sediment deposited during the Lateglacial Interstadial does not exceed a 25cm thickness, which is the approximate resolution of the 3.5kHz Pinger equipment used in profiling. As Tipping (1988) has noted, the depth of sediment dating from this period varies widely between and within basins. Walker et al., (1988) report a thickness of Interglacial Stadial sediment in excess of 40cm from Loch Ashik (surface area approximately 0.02km²), Skye. However, seismic evidence suggests that in Loch Lee a thickness in excess of 25cm is nowhere attained and therefore, in common with distal outwash sediment in Lochs Muick and Callater (sections 7.2.2.1; 7.3.2.1), the Lateglacial Stadial sediment is not recorded on seismic profiles.

It is acknowledged that all the interpretations in this section have been made without reference to core material which has provided important subsidiary and substantiating information in Lochs Muick and Callater. It is recognised that a coring programme combined with radiometric dating of Loch Lee sediment is essential to confirm or reject the hypotheses given above.

Thus, from the data available, it is proposed that sedimentation in Loch Lee was indirectly affected by the Loch Lomond Readvance in Glen Lee, and that the last period during which the loch trough was occupied by glacier ice was during the Devensian glaciation. This interpretation supports that based solely upon subaerial geomorphological mapping (section 1.5.2.2.2).

7.5 MODELLING THE LOCH LOMOND STADIAL IN THE LACUSTRINE ENVIRONMENT

7.5.1 Introduction

In this section the characteristic seismic signatures recognised in Lochs Muick, Callater and Lee, and core data where available, are assimilated in the formulation of a model. This model aims to provide the first comparative database for the seismic identification of former Loch Lomond Readvance ice margins in the highland lacustrine environment. Data are primarily derived from the central loch sections of the profiles where the complete stratigraphy can be recognised, seismic penetration permitting. Elements from core data and interpretation which do not appear on seismic profiles are included in the model as their absence from the profiles is believed to be a function of local effects on sedimentation or equipment irregularities which may not have a wider application.

The Loch Lomond Stadial climatic cooling event represents an ideal subject for the formulation of a model enabling the seismic identification of extra glacial and glaciated water bodies in highland areas as the critical sedimentological evidence lies well within the depth of penetration of high resolution seismic reflection profiling. Thus extremely detailed seismic data, which can be correlated between loch basins, can be obtained.

7.5.2 A model for the seismic identification of glaciated and extra glacial water bodies during the Loch Lomond Stadial

This model, which is illustrated graphically in Figure 7.1, is divided into two parts, extra glacial and glaciated waterbodies.

In extra glacial water bodies the top of the stratigraphic column is marked by parallel and subparallel reflectors with a range of boundary reflection intensity levels from very low, representing the most recently deposited, unconsolidated sediment, to high intensity, where well consolidated sediment occurs. Areas of low intensity reflectors have a gradational boundary with higher intensity reflectors. Major parallel or subparallel

reflectors within this sequence are most frequently caused by coarser grained sediment deposited during flood events. Laterally restricted chaotic reflectors represent post depositional mass movements. Sampling has shown the sediment of this sequence to be fine grained, highly organic with a mud or silt texture. Nearshore profiles may show scattered, or occasionally concentrated, boulders eroded from shoreline materials or deposited by mass movement from the subaerial environment. The basal boundary between sediments deposited in the Holocene and Loch Lomond Stadial sequences is delineated by an erosional unconformity.

The sequence composed of Loch Lomond Stadial sediment is marked by a high reflection amplitude boundary beneath which subparallel wavy or hummocky reflectors with a uniform medium internal backscatter level occur. Scattered point hyperbolae increase in concentration towards the shores, dominating the seismic response, forming a distinct facies, and interfingering at a gradational boundary with the subparallel reflectors. This sequence drapes the underlying topography. It represents deposition from two environments; fluviially derived fine grained minerogenic glacial outwash sediment deposited by settling through the water column in an ice distal position, and coarse grained clastic material delivered by subaerial avalanche activity. Glacier proximity is recognised by the seismic response to grain size variation. Stratified point hyperbolae represent an ice proximal position: subparallel or parallel internal reflectors containing rare point hyperbolae in the centre of the lake delineates ice distal sedimentation.

An unconformable lower boundary will be encountered where sedimentation of the underlying Lateglacial Stadial Sequence is spatially restricted, has a pronounced topography, or is totally absent. Limited erosion and redeposition of the underlying sequence may also result in an unconformity.

Evidence for the Lateglacial Interstadial is likely to be found in topographic hollows of the underlying substrate where the vertical thickness of the unit exceeds that of the resolution of the seismic profiling equipment. It is suggested that, where it occurs, Lateglacial Stadial sediment will exhibit a similar seismic signature to Holocene sediment,

but containing more numerous major internal reflectors derived from sedimentation by enhanced fluvial and slope input. Due to the temporal constraint of this warm period, sediment deposited during the Lateglacial Stadial is likely to be relatively thin and spatially restricted. Therefore it is proposed that the sequence boundary between the Lateglacial Interstadial and underlying Devensian material will be unconformable in the vast majority of cases, the reflectors terminating upslope by onlap.

The Devensian glaciation is marked by a sequence composed of two distinct facies. That representing glacial diamict is characterised by a highly reflective, distinctive hummocky or undulating external form. Internal reflections are dominated by point hyperbolae within a matrix of medium to high backscatter levels. This facies is frequently unstratified. However, where deposition has taken place in a water body exceeding 30m depth, reflectors dipping up-glacier may be recognised on the glacier proximal slope beneath ridge topography. A gradational boundary occurs between the glacial diamict facies and horizontally stratified point hyperbolae representing glacier proximal outwash deposition. This facies exhibits a vertical decrease in point hyperbolae and increase in subparallel reflectors characterising the reduction in sediment size associated with glacial retreat.

The Holocene sequence in formerly glaciated water bodies does not differ from that which occurs in extra glacial water bodies described above. The lower sequence boundary is unconformable, reflectors terminating by lapout, due to non deposition over irregular underlying topography. Occasionally the unconformity is erosive due to mass movements or erosion by currents.

The second sequence (Loch Lomond Readvance/Stadial) is composed of two facies. The upper facies lies beneath a boundary with a high reflection amplitude. It comprises subparallel and parallel reflectors at the top of the facies grading downwards to discontinuous subparallel reflectors and high concentrations of stratified point hyperbolae (Figure 7.1) in a finer grained matrix with a medium to high internal backscatter level. This facies infills the underlying topography of the other facies in this sequence, forming the

sequence boundary in most locations. At the base of the facies the boundary, composed of point hyperbolae, is partially gradational with the basal sedimentary facies identifiable by high frequency seismic reflection profiling, indicating contemporaneous deposition. This facies represents glacial outwash grading upwards from coarse proglacial material to fine ice distal sediment.

The basal facies which has a characteristically hummocky and ridged external form lies beneath a high reflection amplitude boundary, which may dissipate laterally and become gradational in topographic lows. It is composed of numerous point hyperbolae contained within a matrix of high internal backscatter. Where this facies occurs in water depths in excess of 30m internal reflectors dipping towards the former glacier may occur beneath ridges that run parallel to the former ice front. In some cases these ridges may be of a sufficient height to rise above the infilling outwash to form an unconformable sequence boundary with Holocene sediment. This facies represents glacial diamict dating from the Loch Lomond Readvance glaciation, infilled by glacial outwash deposited during the Loch Lomond Stadial and early Holocene.

7.5.3 Discussion

Within the framework of this model precise locations of former Loch Lomond Readvance glaciers in the lacustrine environment can be identified from seismic surveys. The process is simplified where subbottom or subaqueous topography marks a clearly defined glacial terminus. In locations where the topography is muted it is proposed that the model will enable the determination of glaciated and unglaciated sublacustrine areas and permit identification of a spatially restricted terminal zone.

The model is designed to be applicable to lakes situated in valley bottoms in highland areas where the lake acts as a trap for sediment eroded from the upper parts of the valley. It represents the complete stratigraphic succession, confirmed by coring within the lochs included in this study and elsewhere. However, as demonstrated in Lochs Muick, Callater and Lee, variation in the thickness and distribution of seismic sequences and facies

occurs within and between water bodies. This can cause complications where the vertical thickness of a particular facies or sequence falls below that of the vertical resolution of the seismic profiling equipment and is therefore not identifiable upon the seismic profiles. Thus it is recommended that a thorough, detailed, seismic survey be undertaken of the entire waterbody where a Loch Lomond Readvance ice margin is believed to occur, not restricted to the proposed terminal area identified by subaerial evidence. Findings of this research show clearly that subaerial evidence cannot be accurately extrapolated into the subaqueous environment.

It is recognised that this model, in common with all models, is a simplification of reality derived from the analysis of data from a limited sample of water bodies. Consequently further testing of this model is required to ascertain its applicability and to extend and develop its diagnostic capabilities.

A MODEL FOR THE SEISMIC IDENTIFICATION OF GLACIATED AND EXTRA GLACIAL WATER BODIES DURING THE LOCH LOMOND STADIAL

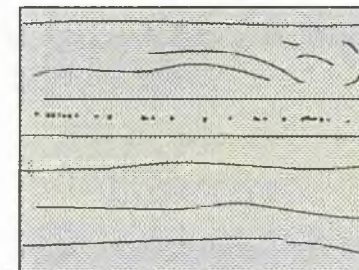
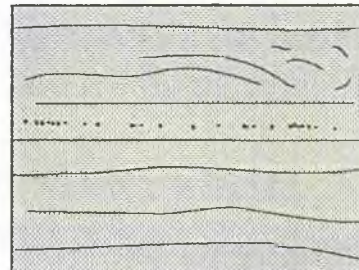
Proposed
chronology

Extra glacial

Glaciated

Holocene

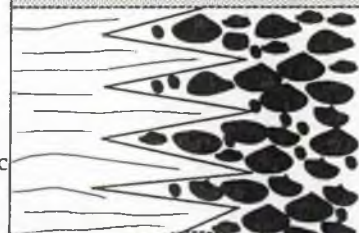
Fine grained highly organic stratified lacustrine sediment with evidence of post depositional mass movement and coarse grained fluvial input



Fine grained highly organic stratified lacustrine sediment with evidence of post depositional mass movement and coarse grained fluvial input

Loch Lomond
Stadial

Nearshore coarse grained avalanche debris interfingering with poorly stratified fine grained minerogenic glacial outwash in the centre of the water body



Glacial outwash exhibiting graded bedding from extremely coarse ice proximal sediment to stratified silt deposited in an ice distal position. Clusters of boulders deposited by icebergs occur in the lower half of this unit

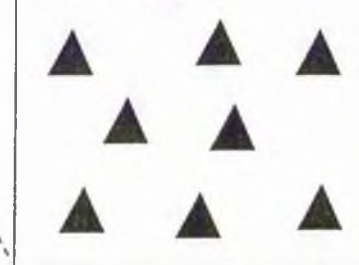
Lateglacial
Interstadial

Stratified organic sediment
Crudely sorted graded outwash



Devensian

Glacigenic
diamict



Glacigenic diamict containing compressional reflectors dipping up-glacier in sublacustrine moraine ridges formed in water depths greater than 30m

- Gradational boundary
- Unconformable boundary
- Conformable boundary

CHAPTER 8

CONCLUSION

8.1 INTRODUCTION

This final Chapter has two aims, first to present a summary of the findings from the research as a whole, and secondly to suggest a number of questions which further research into sublacustrine glacier termini needs to address.

8.2 GLACIER TERMINI AND THE SUBAQUEOUS ENVIRONMENT

The recognition of the former existence of glaciers in the subaerial environment has a history as long as the science of Quaternary Studies. Playfair (1802), and Agassiz (1840) in his evangelistic tour of Britain, noted subaerial evidence in support of the 'Ice Age', which established a basis upon which a substantial volume of data has accumulated, particularly within the last two decades (Chapter 1, *passim*). However, investigation of glacial geomorphology and sedimentology in the subaqueous environment, especially in the multitude of Scottish freshwater lochs, has been an area largely neglected by academic research. There are frequent instances in the literature of the arbitrary drawing of 'probable' or 'interpolated' glacier termini across a water body without examination of the subaqueous evidence (e.g. Sissons and Grant, 1972, Loch Muick, Aberdeenshire; Sissons, 1977b, Gorm Loch Mor, Sutherland, Loch a'Bhealaich and Loch na h-Oidhche, Wester Ross; Sissons, 1979a, Loch Awe, Argyll; Sissons, 1980b, Loch Ericht, Inverness-shire). The key issue raised by these interpretations and interpolations is that researchers undertaking geomorphological mapping have hitherto assumed that subaerial and subaqueous glacier activity and dynamics do not differ significantly, despite evidence from modern glaciated environments to the contrary (section 7.2.4.1.1). Although coring and pollen analyses of small lochans and infilled basins 'inside' and 'outside' former glacier limits have been used to determine subaerial glacier termini, neither database nor model existed to enable the identification of the limits of glaciation *within* the lacustrine environment.

This thesis provides the first investigation and model of the complete glacial sedimentary signal from large water bodies (e.g. Loch Callater, Loch Muick). The deployment of seismic survey equipment, normally restricted to marine waters, has enabled the identification and description of glacial sediment within the original environment of deposition. Continuously recording seismic survey techniques provide substantially more data than can be derived from point sampling by coring. Moreover, penetration of coring-resistant sediment, including glacial diamict, supplies additional internal and external structural and textural information. The highlights of findings during this research project are presented below.

8.3 THE CASE STUDIES

Three lochs were selected for study on the grounds of their spatial proximity and subaerial evidence indicating that the troughs experienced widely differing conditions during the last glacial period (Sissons, 1972a; Sissons and Grant, 1972; section 1.5.4.2), now known to be the Loch Lomond Stadial (Chapter 6, section 6.6.2.2.2; Chapter 7, *passim*).

Subaerial evidence suggested that two glaciers terminated in Loch Muick (Figure 1.2, section 1.5.4.2). Data from initial echosounder surveys were used to construct a bathymetric chart, contoured at 1m intervals (figure 2.15). The chart reveals that the loch floor and sides are highly irregular and can be visually divided into four zones on the basis of geomorphological variation (section 2.6.3). The visual demarcation of these zones is confirmed through the application of Håkanson's Form Roughness parameter (section 2.6.4; Figure 2.23). Significantly, the zone composed of subaqueous ridges and troughs, is continuous across both proposed subaerial glacier limits (Figure 2.16), which are marked as 'probable' on the geomorphological map of Sissons and Grant (1972).

Pinger high frequency (3.5kHz) seismic reflection profiling equipment, which has a

resolution of approximately 25cm was employed to determine the sedimentary texture and structure of the subbottom sediment (Chapter 3). Seismic sequences and facies were identified from the seismic profiles, enabling parastratigraphic interpretation of the data to be made. Within Loch Muick two sequences are recognised. The upper sequence represents fine grained, draped, Holocene lacustrine sediment containing strata of coarse grained material deposited during flood events within which small scale mass movements have been shown to occur (section 7.2.1.2.3.2). The lower sequence is composed of two facies. One, which forms the ridges referred to above and also mounds and hollows, is glacial diamict and the other comprises graded glacial outwash sediment with occasional coarse grained inputs from iceberg drop and dump.

Thus the ridges identified on the bathymetric chart are cored by glacial diamict. Evidence from Loch Callater has shown that this material dates from the Loch Lomond Stadial. However, profiles showed that the sublacustrine glacier limit determined by the outermost ridge apparent on the bathymetric chart is in fact succeeded down valley by three cross valley ridges completely buried by outwash and Holocene sediment. The outermost ridge, beyond which there is no evidence of subbottom glacial diamict, is therefore proposed to be the terminal position of Loch Lomond Readvance glaciation in Glen Muick, approximately 1.4km further down valley than previously suggested.

Internal structures identified within the glacial diamict suggest that the ridges (sublacustrine moraines) were formed by the ramp moraine mechanism (Barnett and Holdsworth, 1974; section 7.2.2.2.1) which requires a water depth >30m. It follows that, as the subaerial geomorphology suggests, the water level of Loch Muick was not higher during the Loch Lomond Stadial, and has not altered substantially since. The sublacustrine moraines identified in Loch Muick are the first examples to have been reported from the present lacustrine environment in Britain. The mounds and hollows composed of glacial diamict are believed to have formed by the escape and in situ melting of buried ice (section 7.2.2.2.2).

The absence of subaerial evidence for this newly proposed glacier limit, which implies that the Black Burn and Glen Muick glaciers were confluent, is partially explained by reference to the sidescan sonographs (Chapter 4). These records indicate that there has been substantial mass movement and erosional activity on the slopes surrounding Loch Muick which have resulted in the deposition of coarse grained sediment in dense boulder spreads across the nearshore slopes (section 7.2.1.1.1). A further contributory factor is also invoked; erosion by waves induced by the calving of icebergs and release of proglacial ice ramps (section 7.2.4.1.1).

Coring has provided calibration for the upper part of the seismic stratigraphy (Chapter 6) and enabled identification of a stratum which has a thickness below that of the resolution of the Pinger profiling equipment. Geochemical and sedimentological analyses of core material indicate that the Little Ice Age (section 1.4.2) did not significantly affect erosion or deposition in the Loch Muick catchment. These analyses permit identification of the boundary between Loch Lomond Stadial minerogenic fine grained outwash deposition and Holocene sediment. Analyses of the latter exhibit evidence of ameliorating climatic conditions and, in the upper parts, the anthropogenic impact upon deposition in the loch (section 6.6.3.2).

Analytical data derived from point sampling of surface sediments (Chapter 5) have been used in conjunction with records from sidescan sonar surveys (Chapter 4) to determine the nature and form of contemporary lacustrine sedimentation. Application of these techniques has enabled the recognition of subaqueous landforms including deltas, shore-parallel terraces, boulder clusters, boulder spreads and mounds and hollows in shallow water or sandy sediment, where penetration by Pinger profiling was not achieved (Chapter 7).

The sublacustrine glacier limit identified in this project must bring into question the validity of drawing 'interpolated' limits across waterbodies, even in areas where the subaerial evidence appears unequivocal. It has further implications regarding climatic modelling. A further 1.4km of glacial ice in this location represents a substantial increase in

the volume of ice in the south east Grampians, an area where rainfall levels have been low for at least the past 12kaBP. This must therefore undermine the predictions derived from climatic models based upon subaerial data with interpolated subaqueous margins (section 1.1), particularly former glaciers in the lacustrine environment. Taking a wider viewpoint, the repercussions of these findings upon the data inputs to predictive models of climatic change have substantial implications for locational planners of strategic installations including nuclear power stations and dumping areas, at a time when climatic change is at the forefront of global and national government and public concern. The unpredicted behaviour of a glacier in a water body close to a nuclear installation could have, at best, a significant financial and political impact and, at worst, cause a major environmental disaster.

Geomorphological mapping suggests that Loch Callater was entirely covered by glacial ice (Chapter 1) during the Loch Lomond Stadial. Analyses of Pinger profiles and two cores obtained from Loch Callater (Chapter 6) have confirmed that the previously disputed age of the last glaciation (section 1.4.2) in this and adjacent glens is the Loch Lomond Readvance. In common with Loch Muick, the impact of the Little Ice Age is not apparent in core material. Pollen analyses indicate that glacial retreat was not continuous. It is proposed that a stagnant mass of ice occupied the eastern part of the loch basin into the ninth millenium BP preventing deposition of pollen typical of the early Holocene in this area. This finding has important implications regarding the nature and rate of climatic change in the 'continental' climate of the east of Scotland during the Loch Lomond Stadial and Postglacial.

Seismic profiles of the loch floor have confirmed the assertion of Collet and Johnston (1906) that Loch Callater was formed by the damming of the Allt an Loch by moraines, deposited during the Loch Lomond Readvance. Two glacigenic ridges have been identified within the loch which are interpreted as representing temporary halts during the retreat of the Glen Callater glacier (section 7.3.2.2). Glacial outwash material forms infills in the subbottom glacial topography and is believed to have formed a significant part of the alluvial plain associated with the Allt an Loch (section 7.3.1.2.2). Comparison of the

bathymetry between the 1905 and 1989 surveys shows that there has been a substantial increase in area of the alluvial plain at the head of the loch, amounting to 0.4ha over 84 years (section 2.5.4).

Loch Lee was not directly affected by glacier ice during the Loch Lomond Stadial. Geomorphological mapping (section 1.5.2.2) has shown that the glacier most proximal to Loch Lee during this period occupied a corrie 1.5km from the loch shore.

The bathymetric chart of Loch Lee (Figure 2.2), which represents the first recorded charting of the loch, indicates that it has a significantly lower topographic diversity than that recorded from Lochs Muick and Callater. Seismic surveys, both surface and subbottom profiles, indicate the reasons for this variation. Underlying the surface strata of highly organic, poorly sorted, fine grained material (Chapter 4, *passim*; Chapter 5, *passim*) lies a seismic sequence composed of two facies. One facies is composed of fine grained, stratified sediment draped over the underlying sequence of hummocky glacial diamict and outwash. This facies interfingers with a second, nearshore, highly clastic facies which is interpreted as resulting from deposition of slope materials by avalanche and debris flow activity. Sidescan sonographs (Chapter 4) indicate that sedimentation of this nature does not occur at present. Previously published data (see section 7.4.5.1) indicate that the last period of enhanced avalanche and rockfall activity occurred during the Loch Lomond Stadial. Thus this sequence is proposed to date from the Loch Lomond Stadial, when the loch was in an ice distal location and received substantial fine grained sediment input from glacial outwash streams.

It is suggested therefore that the underlying sequence of glacial diamict and outwash, in the context of sublacustrine and subaerial data, dates from the Devensian glaciation.

This research project has illustrated the importance of the use of multiple seismic techniques in the identification of glacier termini and the value of 'control' coring and surface sediment sampling surveys. Bathymetric charts constructed from echosounder

surveys provide an important benchmark upon which to base subsequent surveys but, as has been shown in the case of Loch Muick, post depositional sedimentation can blanket the glacier terminal zone. Thus if the position of a glacier terminus is based upon echosounder survey alone an incorrect conclusion may be drawn. Sidescan sonar surveys have restricted direct diagnostic value in the location of former glacier termini in water bodies where substantial sedimentation has occurred after glacial retreat, masking the underlying topography. They do, however, provide important information on current lacustrine processes and sediment type and distribution which, when used in conjunction with Pinger subbottom reflection profiles can be used to infer changes in processes operating within the water body. Dix (1992, pers. comm.) has successfully used sidescan sonar to locate Loch Lomond Readvance glacier termini in the marine environment where currents have prevented sedimentation onto morainic ridges. Pinger seismic subbottom reflection profiling provides the most important source of information in the lacustrine environment due to its penetrative capacity, degree of internal detail recorded from within seismic sequences and facies and relative ease of collection of a substantial, continuous data set. As has been shown above, coring of the loch floor, on a considerably reduced scale than would otherwise be necessary, is beneficial to identify strata of thicknesses which fall below the vertical resolution of the profiling equipment.

Seismic surveys of the three lochs have shown that each has a characteristic seismic response representative of the sedimentary history of the water body. Assimilation of these data has enabled the formulation of a model for the seismic identification of glaciated and extra glacial water bodies during the Loch Lomond Stadial.

8.4 THE IMPLICATIONS OF THE MODEL

The model presented in section 7.5.2, and illustrated in Figure 7.1, is composed of two seismostratigraphic columns representing the typical seismic response from highland waterbodies which were; i) glaciated and ii) occupied an extra glacial position during the Loch Lomond Stadial. It describes the subbottom topography and seismic signal associated with precisely definable glacier termini (i.e a glacigenic diamict ridge). The model also permits the demarcation of a spatially restricted terminal zone where the subbottom topography is muted or has been subject to post depositional erosion.

The formulation of this model finalizes the testing of the hypothesis:-

'It is possible to identify the presence of former Loch Lomond Readvance glaciers in lakes, infer the related processes, and define the limits of glaciation through the geophysical analysis and seismostratigraphic interpretation of lake sediments' (section 1.2, p.2).

As has been illustrated in section 8.3 above, the former existence or non existence of glaciers within the three water bodies, and the glacier termini where relevant have been identified. The environments and processes of deposition have been inferred. In combination these factors permit the formulation of a diagnostic model for the seismic identification of Loch Lomond Readvance glacier termini in the lacustrine environment. Thus the hypothesis is accepted.

The simplification of reality presented in the model is designed to be used in highland, valley bottom water bodies where deposition of a complete succession of sediments is possible. It is recognised that the morphology and internal structure of terminal glacigenic ridges varies according to glacier regime (section 7.2.2.2.1; section 7.3.2.2). Nevertheless the model is believed to represent accurately the seismic response from sediment either side of the terminal zone. Depth variation of the seismic sequences will occur within and between water bodies, and thus a control for seismic profiles, in the form of coring, is essential.

Further research must be undertaken to investigate the wider applicability of this model, both spatially and temporally. Studies which have passively assumed the limits of

glaciers in the lacustrine environment must be further examined in the light of the findings in this thesis. Models of climatic change which have been developed in the past, based upon the available subaerial evidence, must be critically examined to ascertain their validity.

In the context of this research four related issues connected with the seismic investigation of former glacier termini in Lochs Muick, Callater and Lee must be investigated:-

i) Additional relative or, if possible within the constraints of the method (section 1.4.1), radiometric dating of the subbottom sediments in Lochs Muick and Lee, is needed to further substantiate the ages assigned to the seismic sequences.

ii) It is necessary to carry out further coring and analyses of core material from Loch Muick, Loch Callater and Glen Callater, in the latter case to enable testing of the hypothesis that stagnant ice existed in the glen into the ninth millenium and to examine the further implications of these findings.

iii) It is recommended that an examination of the subsurface topography and sedimentology of the alluvial plains associated with the main influent streams by resistivity and coring be made. Thus the hypotheses regarding proglacial outwash sedimentation in Lochs Lee and Callater could be tested.

iv) Deployment of lower frequency seismic profiling equipment with a greater penetrative capacity is needed to enable the determination of the depth of sediment fill within the loch troughs and to examine the erosive efficiency of the Loch Lomond and Devensian glaciers.

It is important, given the information presented in this thesis, that the limits of glaciation in the lacustrine environment be examined as extensively as those in the subaerial environment, to provide an accurate database against which models of climatic change can be tested.

APPENDIX A

OPERATION OF THE SEDIGRAPH 5100

Setting up the SediGraph

At startup the Zenith computer which drives the SediGraph 5100 displayed the Main Function Menu. From this sub-menus were chosen using the function keys. The procedure given below was followed for each sample.

To create a sample directory

First the Utilities Menu was selected from the Main Function menu, then the Sample Directory Menu from the Utilities Menu and 'Add sample directory' was chosen from the Sample Directory Menu. A directory name (e.g.LMuick) was entered.

To input sample information

From the Main Function menu the Sample Information Menu was selected. The 'Add sample information' option was selected from this menu and screen prompts requiring the entering of sample information (identity, specific density if known) were followed. When the prompt 'Type of run' appeared a screen toggle was operated to select 'High Speed'.

To input liquid information

Following the input of sample information the program prompted for information on the properties of the solution in which the sample is suspended. Calgon is routinely used in the Physical Laboratory. The data required (liquid type, concentration) were entered.

To select report options

The SediGraph enables data obtained to be presented in graphic and / or tabular form. Following the input of liquid information a screen prompt which required choice of printed report type appeared and a log probability graph and data table were selected.

Sample preparation

Samples were prepared for analysis as described in Chapter 5, section 5.2.2.2.

APPENDIX A CONTINUED
OPERATION OF THE SEDIGRAPH 5100

Sample analysis

The X-Ray facility of the SediGraph was activated. From the Main Function Menu the Automatic Analysis / Status sub-menu was chosen. Following the screen prompts the sample directory name was entered and the sample information within it checked. On returning to the Main Function Menu, the 'Rinse' option was chosen and the system was rinsed automatically with 1% Calgon from a reservoir designed for this purpose.

After rinsing, the 'Collect a baseline' option was selected from the Main Function Menu to calibrate the SediGraph to the 1% Calgon used for sample suspension and rinsing between samples. This procedure was undertaken at the start of each working day and when the Calgon in the reservoir was replaced.

Following calibration the system was drained from the 'Drain system' option on the Main Function Menu. Once the mixing chamber, where samples are introduced, was emptied a screen prompt required the prepared sample to be loaded into the mixing chamber. In the mixing chamber samples are constantly agitated by a magnetic stirrer. When the loading procedure was completed the screen display reverted automatically to the Analysis Status Menu. The sample details were displayed and checked again. On confirming the sample information, the analysis procedure automatically started. When the analysis was completed the data appeared on the computer screen. Re-analysis of the sample at this stage was possible. If the data were accepted as representative and consistent, the data were automatically printed.

The system was rinsed and the next sample introduced. On completion of the analyses the system was rinsed (from the Main Function Menu) and the X-Ray and power supply were terminated.

APPENDIX B

EXAMPLE OF A SEDIGRAPH DATA SHEET

LOCH LEE

SediGraph 5100 V2.02
 SAMPLE DIRECTORY / NUMBER: LL22
 SAMPLE 1D : T3S2
 SUBMITTER: P.A.LOWE
 OPERATOR : P.A.LOWE
 SAMPLE TYPE: L.LEE SURFACE
 LIQUID TYPE : 1% CALGON
 ANALYSIS TEMP : 30.1 deg C
 RUN TYPE : High Speed

UNIT NUMBER : 1
 START 10:22:04 08/23/90
 REPRT 10:29:26 08/23/90
 TOT RUN TIME 0:04:52
 SAM DENS : 2.5000 g/cc
 LIQ DENS : 0.9951 g/cc
 LIQ VISC : 0.7707 cp
 REYNOLDS NUMBER : 21.45
 FULL SCALE MASS % : 100

STARTING DIAMETER: 250.00µm
 ENDING DIAMETER : 0.50µm

MASS DISTRIBUTION

MEDIAN DIAMETER : 7.46µm MODAL DIAMETER : 12.90 µm

DIAMETER (µm)	CUMULAT. MASS FINER (%)	MASS IN INTERVAL (%)
250.00	100.0	0.5
180.00	99.3	0.2
125.00	99.0	0.3
90.00	98.1	0.8
64.00	96.0	2.2
50.80	93.5	2.4
40.30	90.3	3.2
32.00	86.2	4.1
25.40	81.2	5.0
20.16	75.5	5.7
16.00	69.6	5.9
12.70	63.5	6.1
10.08	57.5	6.0
8.00	51.7	5.8
6.35	46.1	5.6
5.04	40.3	5.7
4.00	34.7	5.7
3.17	29.8	4.9
2.52	25.4	4.4
2.00	20.2	5.3
1.58	15.0	5.2
1.26	11.5	3.5
1.00	9.0	2.5
0.79	7.2	1.9
0.63	5.7	1.5
0.50	3.9	1.8

APPENDIX C
SEDIMENTARY STATISTICS

1. FOLK AND WARD (1957)

Mean $M_z = \frac{\phi_{16} + \phi_{50} + \phi_{84}}{3}$

Inclusive Graphic Standard Deviation $\sigma_I = \frac{\phi_{84} - \phi_{16}}{4} + \frac{\phi_{95} - \phi_5}{6.6}$

Inclusive Graphic Skewness $Sk_I = \frac{\phi_{16} + \phi_{84} - 2\phi_{50}}{2(\phi_{95} - \phi_{16})} + \frac{\phi_5 + \phi_{95} - 2\phi_{50}}{2(\phi_{95} - \phi_5)}$

Graphic Skewness $K_G = \frac{\phi_{95} - \phi_5}{2.44(\phi_{75} - \phi_{25})}$

2. INMAN (1952)

Mean $M\phi = \frac{1}{2}(\phi_{16} + \phi_{84})$

Measure of Sorting (Standard Deviation) $\sigma\phi = \frac{1}{2}(\phi_{84} - \phi_{16})$

Second Phi Skewness Measure $\alpha_2\phi = \frac{\frac{1}{2}(\phi_5 - \phi_{95}) - \phi_{50}}{\sigma\phi}$

3. QDa-Md (Buller and McManus, 1972)

$$QDa = \frac{P_{25} - P_{75}}{2}$$

$$Md = P_{75}$$

where P_{25} = 25th percentile
 P_{50} = 50th percentile
 P_{75} = 75th percentile

APPENDIX D

Organic matter, sand, silt and clay percentages of Loch Lee surface sediment with sampling depths and textural classification after Folk (1974) for samples lacking gravel.

Sample	Depth m	Organic content %	Sand %	Silt %	Clay %	Sediment type
T1S1	3	1.5	28.8	17.7	31.5	-
T1S2	5	25.3	20.5	53.2	26.3	sZ
T1S3	3	1.7	37.8	32.4	22.4	-
T2S1	3	1.2	23.4	13.7	17.2	-
T3S2	10	7.4	27	49	4.8	-
T3S3	16	52.1	3.8	63.4	32.8	M
T3S4	14	86.4	6.1	90.5	3.4	Z
T3S5	10.5	44.9	5.9	94.1	0	Z
T4S1	10.5	73.9	4.3	95.7	0	Z
T4S2	14	57	2.3	73.7	24.5	Z
T4S3	19.5	29.7	26.8	46.9	26.3	sM
T4S4	20	26.8	15.7	66.7	17.6	sZ
T4S5	8	11	13.6	54.7	31.7	sM
T5S1	11	53.8	2.2	77	20.8	Z
T5S2	28.5	42.9	3.7	44.9	51.4	M
T5S3	24	53.3	2.2	54.6	43.2	M
T5S4	15.5	54.6	1.6	56.2	42.2	M
T5S5	14.5	53.2	7	51.9	41.1	M
T6S1	14.5	63.7	2.7	89	8.3	Z
T6S2	18.5	64.4	2.3	77.1	20.6	Z
T6S3	28	55.7	3.1	58.6	38.3	M
T6S4	26	51	1.4	83.4	15.2	Z
T6S5	7	4.6	20.9	58.8	3.9	-
T7S1	12	43.7	11.3	66.8	21.9	sZ
T7S2	21	74.7	6.4	75.1	18.5	Z
T7S3	28	56.6	3.1	65.2	31.7	Z
T7S4	22	53.7	3.8	96.2	0	Z
T7S5	7	53.5	3.1	63.2	33.7	M
T8S1	5	85.4	10	50.7	39.3	sM
T8S2	16	58.4	4	61.3	34.7	M
T8S3	25.5	58.1	2.1	58.6	39.3	M
T8S4	26	58.5	1.8	63.9	34.3	M
T8S5	12	59.9	4.5	57.5	38.0	M
T9S1	9.5	7.3	28.5	62.2	9.3	-
T9S2	18	49.1	1.3	86.4	12.3	Z
T9S3	15	52.6	1.4	83.7	14.9	Z
T9S4	7	6.8	24.5	37.7	3.5	-
T9S5	3	19.8	48.9	51.1	0	sZ
T10S1	3	29.1	42.3	52.2	5.5	sZ
T10S2	7	7.2	39.3	26.7	0	-
T10S3	7.5	69.1	3	49.3	27.7	M
T10S4	4	7	28.3	35.1	6	-
T10S5	2.5	45.3	2.9	91	9.1	Z
T11S1	2	26.6	31.9	62.9	5.2	sZ
T11S2	2	2.98	20.8	26.0	12.7	-
T11S3	2	8.3	23.8	54.9	8.5	-
T12S3	7.5	53.4	11.5	88.5	0	sZ

APPENDIX E

Phi-based sedimentary statistics (after Inman, 1952) of Loch Lee surface sediment.

Sample	Median diameter (ϕ)	ϕ Arithmetic Mean	Standard Deviation	Skewness
T1S1	3.95	7.15	6.58	0.49
T1S2	5.40	6.85	3.10	0.47
T1S3	4.17	6.96	4.04	0.69
T2S1	2.45	4.65	4.35	0.51
T3S2	4.11	3.11	2.94	-0.34
T3S3	7.29	7.47	1.94	0.09
T3S4	5.37	5.65	1.11	0.25
T3S5	5.16	5.2	0.77	0.05
T4S1	5.30	5.45	0.91	0.16
T4S2	6.91	7.30	1.86	0.21
T4S3	4.89	6.52	3.79	0.43
T4S4	5.63	6.07	2.11	0.21
T4S5	6.65	7.17	2.95	0.18
T5S1	5.69	6.81	1.81	0.62
T5S2	8.16	10.34	4.76	0.46
T5S3	7.64	9.35	3.35	-0.51
T5S4	7.75	7.28	1.37	-0.34
T5S5	6.81	8.38	3.8	0.41
T6S1	5.43	5.93	1.13	0.44
T6S2	6.34	6.82	1.66	0.29
T6S3	7.46	7.21	1.49	-0.16
T6S4	5.71	6.47	1.44	0.53
T6S5	4.34	3.35	2.52	-0.39
T7S1	6.14	6.47	2.15	0.15
T7S2	6.44	6.48	1.66	0.02
T7S3	7.12	7.11	1.82	0
T7S4	5.25	5.24	0.58	0.02
T7S5	7.26	7.34	1.67	0.05
T8S1	7.05	9.25	4.75	0.46
T8S2	7.11	7.25	2.09	0.07
T8S3	7.48	7.78	1.9	0.16
T8S4	7.36	6.85	1.16	-0.44
T8S5	7.07	7.08	2.09	0
T9S1	4.83	4.95	1.53	0.08
T9S2	5.46	6.05	1.15	0.51
T9S3	5.59	6.42	1.36	0.61
T9S4	3.50	3.21	2.60	-0.11
T9S5	4.00	4.05	0.89	0.06
T10S1	4.10	4.49	1.21	0.32
T10S2	3.20	2.44	1.91	-0.40
T10S3	6.30	7.42	2.88	0.39
T10S4	6.50	3.16	2.59	-0.13
T10S5	5.40	5.90	1.15	0.43
T11S1	4.77	5.09	1.79	0.18
T11S2	3.17	3.8	3.2	0.20
T11S3	4.47	4.7	1.9	0.12
T12S3	5.38	5.35	1.16	-0.03

APPENDIX F

Metric (mm) sedimentary statistics (after Krumbein, 1936) of Loch Lee surface sediment.

Sample	QDa	Md
T1S1 1	0.01995	0.0647
T1S2 2	0.02500	0.0237
T1S3 3	0.04640	0.0556
T2S1 4	0.02375	0.0183
T3S2 5	0.05120	0.0579
T3S3 6	0.00520	0.0064
T3S4 7	0.01040	0.0242
T3S5 8	0.01300	0.0280
T4S1 9	0.01015	0.0254
T4S2 10	0.00625	0.0083
T4S3 11	0.03185	0.0337
T4S4 12	0.01650	0.0202
T4S5 13	0.01685	0.0100
T5S1 14	0.01060	0.0194
T5S2 15	0.00545	0.0140
T5S3 16	0.00470	0.0050
T5S4 17	0.00370	0.0047
T5S5 18	0.01415	0.0089
T6S1 19	0.00955	0.0232
T6S2 20	0.00875	0.0123
T6S3 21	0.00495	0.0057
T6S4 22	0.00985	0.0191
T6S5 23	0.03705	0.0494
T7S1 24	0.01450	0.0142
T7S2 25	0.00990	0.0115
T7S3 26	0.00725	0.0072
T7S4 27	0.00705	0.0263
T7S5 28	0.00555	0.0065
T8S1 29	0.01355	0.0076
T8S2 30	0.00810	0.0072
T8S3 31	0.00510	0.0056
T8S4 32	0.00500	0.0061
T8S5 33	0.01025	0.0074
T9S1 34	0.02565	0.0352
T9S2 35	0.00665	0.0227
T9S3 36	0.00900	0.0208
T9S4 37	0.02435	0.0884
T9S5 38	0.02665	0.0625
T10S1 39	0.02565	0.0583
T10S2 40	0.02300	0.1088
T10S3 41	0.01355	0.0127
T10S4 42	0.23360	0.0884
T10S5 43	0.01040	0.0237
T11S1 44	0.03195	0.0367
T11S2 45	0.02895	0.1111
T11S3 46	0.03385	0.0451
T12S3 47	0.01350	0.0240

APPENDIX G

Loch Callater sand, silt, clay and organic matter percentages of surface sediment with sampling depths and textural classification after Folk (1974).

Sample	Depth m	Organic matter %	Sand %	Silt %	Clay %	Sediment type
T1S1	1.5	17.8	15.8	63.8	20.4	sZ
T1S2	2.0	35.2	4.9	76.2	18.9	Z
T1S3	2.0	35.5	6.9	74.4	18.7	Z
T2S1	2.0	36.0	42.7	76.6	16.7	Z
T2S2	2.5	38.2	4.0	66.7	29.3	Z
T2S3	8.5	35.3	2.8	70.4	26.8	Z
T2S4	9.0	33.9	2.5	97.5	0	Z
T2S5	2.5	32.1	7.6	92.4	0	Z
T3S1	3.0	36.0	8.6	79.4	12.0	Z
T3S2	4.0	33.4	2.6	97.4	0	Z
T3S3	5.5	41.8	2.6	71.4	26.0	Z
T3S4	5.0	38.4	7.1	84.8	8.1	Z
T3S5	2.0	39.9	6.5	81.6	11.9	Z
T4S1	3.0	40.2	2.3	97.7	0	Z
T4S2	6.0	42.8	1.6	86.2	12.2	Z
T4S3	8.0	40.6	3.1	66.9	30.0	Z
T4S4	8.0	54.8	2.9	85.6	11.5	Z
T4S5	3.5	39.0	3.7	71.4	24.9	Z
T5S1	2.0	42.0	8.5	84.1	7.4	Z
T5S2	4.5	43.3	9.9	82.8	7.3	Z
T5S3	9.0	46.2	1.7	66.8	31.5	Z
T5S4	11.0	40.5	1.9	78.5	19.6	Z
T5S5	5.0	43.4	8.6	85.4	6.0	Z
T6S1	3.0	43.0	9.1	84.1	6.8	Z
T6S2	7.0	44.2	7.4	85.8	6.8	Z
T6S3	7.0	53.1	8.4	91.6	0	Z
T6S4	6.5	45.9	2.9	95.5	1.6	Z
T6S5	3.0	35.6	3.8	83.1	13.1	Z
T7S1	6.0	36.4	2.6	75.0	22.4	Z
T7S2	6.5	42.7	5.1	94.9	0	Z
T7S3	6.5	37.7	6.1	68.8	25.1	Z
T7S4	6.0	39.0	3.7	66.8	29.5	Z
T7S5	4.0	41.7	4.2	87.7	8.1	Z
T8S1	1.5	41.3	12.0	88.0	0	sZ
T8S2	4.0	37.2	5.6	82.7	11.7	Z
T8S3	5.5	39.4	13.2	81.6	5.2	sZ
T8S4	5.0	42.2	3.9	93.3	2.8	Z
T8S5	3.0	28.4	13.9	86.1	0	sZ
T9S1	1.5	6.1	82.6	17.4	0	zS
T9S2	2.5	37.3	17.0	83.0	0	Sz
T9S3	2.5	46.2	2.7	97.3	0	Z
T9S4	2.5	28.8	16.1	83.9	0	sZ
T9S5	1.5	32.5	9.0	91.0	0.5	Z
T10S1	1.5	14.2	58.7	41.3	0	zS
T10S2	2.0	9.2	52.5	42.2	5.3	zS
T10S3	1.5	10.6	62.7	37.3	1.6	zS
T11S1	1.5	3.4	84.7	15.3	1.4	zS

APPENDIX H

Phi-based sedimentary statistics (after Folk and Ward, 1957) of Loch Callater surface sediment.

Sample	Median (ϕ)	$M_z \phi$	$\sigma_1 \phi$	SK _I	KG
T1S1	6.05	6.31	2.38	-0.17	1.03
T1S2	6.29	6.51	1.70	-0.14	1.26
T1S3	6.25	6.37	1.76	-0.11	0.99
T2S1	6.31	6.57	1.59	-0.25	1.30
T2S2	6.81	6.84	1.29	-0.11	0.78
T2S3	6.65	6.87	1.81	-0.17	0.88
T2S4	6.60	6.37	1.04	+0.34	0.88
T2S5	5.95	5.87	1.87	-0.08	0.67
T3S1	5.75	5.88	1.50	-0.15	1.15
T3S2	6.48	6.23	0.92	+0.44	0.75
T3S3	6.65	6.97	1.62	-0.44	0.81
T3S4	5.29	5.55	1.30	-0.33	1.04
T3S5	6.00	6.03	1.53	-0.10	1.15
T4S1	7.00	6.57	0.90	+0.73	0.87
T4S2	5.80	6.06	1.39	-0.35	1.21
T4S3	6.72	7.13	-	-	-
T4S4	5.93	6.06	1.87	-0.20	1.12
T4S5	6.53	6.81	-	-	-
T5S1	5.42	5.56	1.33	-0.24	0.95
T5S2	5.30	5.5	1.37	-0.26	1.11
T5S3	6.83	7.25	-	-	-
T5S4	6.40	6.61	1.73	-0.24	1.19
T5S5	5.40	5.56	1.27	-0.18	1.16
T6S1	5.20	5.40	1.26	-0.29	1.11
T6S2	5.34	5.50	1.29	-0.27	1.16
T6S3	5.34	5.34	0.99	-0.01	0.87
T6S4	5.88	5.89	0.94	+0.09	0.83
T6S5	6.96	7.01	0.83	+0.09	1.12
T7S1	6.48	6.67	1.59	-0.19	0.98
T7S2	5.70	5.66	0.96	+0.09	0.95
T7S3	6.31	6.59	2.12	-0.24	0.95
T7S4	6.60	6.95	-	-	-
T7S5	6.51	6.37	1.29	+0.09	0.78
T8S1	5.00	5.13	0.99	-0.33	0.91
T8S2	5.62	5.89	1.47	-0.30	1.21
T8S3	4.93	5.11	1.28	-0.27	1.39
T8S4	5.26	5.35	0.85	-0.20	1.14
T8S5	5.06	5.10	1.05	-0.05	1.04
T9S1	0.58	0.97	2.58	-0.30	0.80
T9S2	4.80	4.92	1.04	-0.12	1.15
T9S3	5.28	5.41	0.88	-0.22	0.96
T9S4	4.97	5.02	1.01	-0.09	0.94
T9S5	5.50	5.51	1.11	-0.02	0.89
T10S1	3.83	3.88	0.76	-0.07	0.88
T10S2	3.81	3.98	1.52	-0.33	1.87
T10S3	3.70	3.72	1.02	-0.15	1.25
T11S1	2.60	2.60	1.61	-0.08	1.15

APPENDIX I

Metric (mm) sedimentary statistics (after Krumbein, 1936) of Loch Callater surface sediment.

Sample	QDa	Md
T1S1 1	0.01735	0.0151
T1S2 2	0.00985	0.0128
T1S3 3	0.01155	0.0131
T2S1 4	0.00660	0.0126
T2S2 5	0.00665	0.0089
T2S3 6	0.01810	0.0100
T2S4 7	0.00815	0.0103
T2S5 8	0.01220	0.0162
T3S1 9	0.01280	0.0186
T3S2 10	0.00680	0.0112
T3S3 11	0.00760	0.0100
T3S4 12	0.01395	0.0256
T3S5 13	0.01105	0.0156
T4S1 14	0.00520	0.0078
T4S2 15	0.00960	0.0179
T4S3 16	0.00880	0.0095
T4S4 17	0.01015	0.0164
T4S5 18	0.00980	0.0108
T5S1 19	0.01755	0.0234
T5S2 20	0.01470	0.0254
T5S3 21	0.01180	0.0088
T5S4 22	0.00865	0.0118
T5S5 23	0.01305	0.0237
T6S1 24	0.01375	0.0272
T6S2 25	0.01325	0.0247
T6S3 26	0.01350	0.0247
T6S4 27	0.00985	0.0170
T6S5 28	0.00275	0.0080
T7S1 29	0.00850	0.0112
T7S2 30	0.00915	0.0192
T7S3 31	0.01315	0.0126
T7S4 32	0.01080	0.0103
T7S5 33	0.00925	0.0110
T8S1 34	0.01490	0.0313
T8S2 35	0.01135	0.0203
T8S3 36	0.01565	0.0328
T8S4 37	0.01195	0.0261
T8S5 38	0.02165	0.0300
T9S1 39	0.01561	0.0669
T9S2 40	0.01535	0.0342
T9S3 41	0.01025	0.0257
T9S4 42	0.02170	0.0319
T9S5 43	0.01260	0.0221
T10S1 44	0.02635	0.0703
T10S2 45	0.33450	0.0713
T10S3 46	0.03200	0.1649
T11S1 47	0.01365	0.0769

APPENDIX J

Loch Muick sand, silt, clay and organic matter percentages of surface sediment with sampling depths. Textural classification follows Folk (1974) for samples lacking gravel.

Sample	Depth m	Organic matter %	Sand %	Silt %	Clay %	Seiment type
T1S1	20	51.7	3.2	39.3	57.5	M
T1S2	50	46.0	3.8	63.9	38.8	M
T1S3	78	57.5	2.2	45.5	52.3	M
T1S4	60	66.4	4.3	39.8	55.9	M
T1S5	45	64.4	13.2	45.6	41.2	sM
T2S1	21	61.6	3.4	22.5	74.1	C
T2S2	53	68.8	6.4	42.4	51.2	M
T2S3	80	61.1	1.9	40	58.1	M
T2S4	27	55.6	3	41.7	55.3	M
T2S5	32	61.9	2.4	48	49.6	M
T3S1	19	53.9	3.1	55.3	41.6	M
T3S2	39	47.9	11.9	43.2	44.9	sM
T3S3	42	52.9	1.3	63.8	34.9	M
T3S4	61	58.7	2.7	47.3	50	M
T3S5	43	11.7	10.1	89.9	0	sZ
T4S1	41	41.7	11.3	57.4	31.3	M
T4S2	66	57.2	31.6	52.6	15.8	sZ
T4S3	54	56.8	3	67.1	29.9	Z
T4S4	20	58.1	3.8	62.4	34.8	M
T4S5	12	29.4	27	41.9	31.5	sM
T5S1	17	22.6	11	44.9	43.1	sM
T5S2	78	55.8	4.9	77.7	17.4	Z
T5S3	79	50.9	3.4	60.3	36.3	M
T5S4	80	57.8	2.4	40.8	56.8	M
T5S5	48	51.0	7	47.9	45.1	M
T6S1	11	28.8	21.3	43.8	34.9	sM
T6S2	36	13.2	3	36.1	61.9	M
T6S3	59	54.6	4.7	57.1	38.2	M
T6S4	50	60.4	2.5	45.6	51.9	M
T6S5	6	7.3	49.3	41.5	9.2	sZ
T7S1	5	22.6	15	51.8	33.2	sM
T7S2	11	4.3	33.2	34.9	31.9	sM
T7S3	21	40.6	10.8	56.1	33.1	sM
T7S4	27	37.1	10.9	68.7	20.4	sZ
T7S5	15	37.5	44.8	47.2	8	sZ
T8S1	8	6.0	23.9	47.6	28.5	sM
T8S2	13	27.2	13.4	63.3	25.3	sZ
T8S3	33	57.4	7.9	44.3	47.8	M
T8S4	36	38.7	12.7	48.4	38.9	sM
T9S3	7	4.2	24.9	48.3	26.8	sM
T9S4	11	7.1	11.8	56.8	21.4	sZ
T9S5	3	5.2	40.6	41.6	17.8	sZ
T10S1	3	14.6	14.8	81.9	3.3	sZ

APPENDIX K

Phi-based sedimentary statistics (after Inman, 1952) of Loch Muick surface sediment.

Sample	Median (ϕ)	ϕ Arithmetic Mean	Standard Deviation (ϕ)	Skewness
T1S1	8.66	8.66	3.14	0
T1S2	7.37	7.54	2.23	-0.08
T1S3	8.11	8.42	2.64	-0.12
T1S4	8.41	8.63	3.18	-0.07
T1S5	7.05	7.12	3.0	-0.02
T2S1	10.19	9.24	2.56	-0.37
T2S2	8.09	8.18	3.43	-0.03
T2S3	8.54	8.13	2.34	-0.18
T2S4	8.43	8.73	3.09	-0.10
T2S5	8.00	7.84	2.33	-0.07
T3S1	7.49	7.71	2.30	-0.10
T3S2	7.00	9.08	4.82	-0.43
T3S3	6.81	7.56	2.34	-0.32
T3S4	8.00	7.93	2.18	-0.03
T3S5	6.04	5.49	0.68	+0.28
T4S1	6.58	6.9	2.61	-0.12
T4S2	4.90	5.73	2.25	-0.37
T4S3	7.05	7.14	1.78	-0.05
T4S4	7.20	7.2	1.92	-0.04
T4S5	5.32	7.44	3.85	-0.55
T5S1	7.41	7.25	2.8	+0.06
T5S2	6.48	6.44	1.57	+0.03
T5S3	6.99	7.40	2.32	-0.18
T5S4	8.52	8.78	2.92	-0.09
T5S5	7.65	8.05	3.34	-0.12
T6S1	6.07	7.75	4.06	-0.41
T6S2	8.97	8.91	3.11	+0.02
T6S3	7.23	7.61	2.68	-0.14
T6S4	8.10	8.15	2.46	-0.02
T6S5	4.08	4.91	1.82	-0.46
T7S1	6.01	7.14	3.14	-0.36
T7S2	5.89	6.49	3.11	-0.19
T7S3	6.40	7.10	2.73	-0.26
T7S4	5.79	6.42	2.17	-0.30
T7S5	4.20	5.14	1.93	-0.49
T8S1	5.95	6.55	2.85	-0.21
T8S2	6.28	6.56	2.25	-0.12
T8S3	7.79	8.5	3.85	-0.18
T8S4	6.72	8.13	3.97	-0.36
T9S3	5.21	7.34	3.68	-0.58
T9S4	5.61	6.34	2.66	-0.27
T9S5	4.30	5.66	2.58	-0.50
T10S1	5.09	5.43	1.39	-0.24

APPENDIX L
Metric (mm) sedimentary statistics (after Krumbein, 1936) of Loch Muick surface sediment.

Sample	QDa	Md
T1S1 1	0.00250	0.0025
T1S2 2	0.00780	0.0610
T1S3 3	0.00500	0.0036
T1S4 4	0.00500	0.0029
T1S5 5	0.01150	0.0076
T2S1 6	0.00260	0.0010
T2S2 7	0.01930	0.0370
T2S3 8	0.00450	0.0027
T2S4 9	0.00470	0.0029
T2S5 10	0.00670	0.0039
T3S1 11	0.00860	0.0056
T3S2 12	0.01200	0.0078
T3S3 13	0.01100	0.0089
T3S4 14	0.00515	0.0039
T3S5 15	0.00235	0.0152
T4S1 16	0.01605	0.0105
T4S2 17	0.03170	0.0335
T4S3 18	0.00685	0.0076
T4S4 19	0.00710	0.0068
T4S5 20	0.00900	0.0250
T5S1 21	0.01290	0.0059
T5S2 22	0.00845	0.0112
T5S3 23	0.00940	0.0079
T5S4 24	0.00470	0.0027
T5S5 25	0.00810	0.0050
T6S1 26	0.02100	0.0149
T6S2 27	0.00370	0.0020
T6S3 28	0.00945	0.0067
T6S4 29	0.00500	0.0036
T6S5 30	0.00735	0.0591
T7S1 31	0.02250	0.0155
T7S2 32	0.02220	0.0169
T7S3 33	0.01680	0.0118
T7S4 34	0.01630	0.0183
T7S5 35	0.03750	0.0544
T8S1 36	0.02560	0.0162
T8S2 37	0.01540	0.0129
T8S3 38	0.00700	0.0045
T8S4 39	0.01475	0.0095
T9S3 40	0.02300	0.0270
T9S4 41	0.02665	0.0205
T9S5 42	0.06800	0.0480
T10S1 43	0.01740	0.0294

APPENDIX M

Comparison between values for Skewness obtained from surface sediment data from Loch Callater using the sedimentary statistics given by Folk and Ward (1957) and Inman (1952).

Sample	Folk and Ward (1957)	Inman (1952)	Absolute difference
T1S1	-0.17	-0.12	0.05
T1S2	-0.14	-0.2	0.06
T1S3	-0.11	-0.10	0.01
T2S1	-0.25	-0.24	0.01
T2S2	-0.11	-0.03	0.08
T2S3	-0.17	-0.17	0
T2S4	+0.34	+0.31	0.03
T2S5	-0.08	+0.10	0.18
T3S1	-0.15	-0.12	0.03
T3S2	+0.44	+0.37	0.07
T3S3	-0.44	-0.26	0.18
T3S4	-0.33	-0.30	0.03
T3S5	-0.1	-0.03	0.07
T4S1	+0.73	+0.68	0.05
T4S2	-0.35	-0.30	0.05
T4S3	-	-	-
T4S4	-0.20	-0.14	0.06
T4S5	-	-	-
T5S1	-0.24	-0.17	0.07
T5S2	-0.26	-0.23	0.03
T5S3	-	-	-
T5S4	-0.24	-0.20	0.04
T5S5	-0.18	-0.20	0.02
T6S1	-0.29	-0.24	0.05
T6S2	-0.27	-0.20	0.07
T6S3	-0.01	-0.02	0.01
T6S4	+0.09	+0.06	0.03
T6S5	+0.09	+0.06	0.03
T7S1	-0.19	-0.18	0.01
T7S2	+0.09	+0.15	0.06
T7S3	-0.24	+0.19	0.05
T7S4	-	-	-
T7S5	+0.09	+0.15	0.06
T8S1	-0.33	-0.18	0.15
T8S2	-0.30	-0.30	0
T8S3	-0.27	-0.24	0.03
T8S4	-0.20	-0.17	0.03
T8S5	-0.05	-0.05	0
T9S1	-0.30	-0.02	0.28
T9S2	-0.12	-0.07	0.05
T9S3	-0.22	-0.22	0
T9S4	-0.09	-0.07	0.02
T9S5	-0.02	-0.01	0.01
T10S1	-0.07	-0.14	0.07
T10S2	-0.33	-0.23	0.10

APPENDIX N

Sample preparation and analysis by Coulter Counter

1. Sieve sediment. Discard fraction $>2\text{mm}$.
2. Sieve $<2\text{mm}$ fraction through 1mm , $500\mu\text{m}$, $250\mu\text{m}$, $125\mu\text{m}$ and $63\mu\text{m}$ mesh. Weigh and record weight of each fraction.
3. Transfer approximately 1mg of $<63\mu\text{m}$ fraction to a watchglass.
4. Add 3-5 drops detergent to sub-sample and stir.
5. Transfer small amount of dispersed sub-sample to 250ml beaker.
6. Add 5ml Isoton electrolyte, stir, fill to 250ml .
7. Place beaker in ultrasonic bath for 5 minutes.
8. Place beaker under orifice tube and electrode of Coulter Counter.
9. Await 'counting complete' light illumination and note percentage of total sample weight from digital display.

APPENDIX O

Total extractable element preparation and analysis.

1. Oven dry sub-samples at 100°C for 24 hours.
2. Gently disaggregate and brush through 2mm sieve.
3. Discard fraction >2mm.
4. Weigh approximately 1g of material <2mm into labelled conical beaker and note exact weight.
5. Add 1ml deionised water. Mix by swirling.
6. Add 20ml concentrated HNO₃.
7. Place beaker on heated sand bath at 100°C for 1 hour.
8. Allow to cool.
9. Add 6ml 30% H₂O₂, return to sand bath for 30 minutes.
10. Allow to cool.
11. Filter into 100ml volumetric flasks.
12. Fill flasks to 100ml with deionised water.
13. Remove 1ml of the sub-sample into sampling test tube and add 3ml deionised water.
14. Insert element hollow cathode lamp and calibrate AAS with standard solution of element to be analysed.
15. Aspirate samples in turn.

APPENDIX P

Sample preparation and analysis by X-Ray Diffraction.

1. Crush sub-samples <2mm.
2. 'Backpack' into analysis plates.
3. Place in diffractometer.
4. Irradiate from cobalt anode, excitation conditions set at 40kV 25Ma.
5. Scan between 5° and 50° , 2θ , at 0.02° , $2\theta/\text{second}$.
6. Data outputs as $\text{\AA}/\text{scan angle}$.

APPENDIX Q

Sand, silt, clay and organic matter percentages of Loch Callater core sediment with sample depth and textural classification after Folk (1974) for samples lacking gravel

Sample	Depth (cm)	Sand (%)	Silt (%)	Clay (%)	Sediment type	Total organic matter (%)
1	0	5.0	92.0	3.0	Z	39.7
2	10	4.7	91.9	3.7	Z	40.0
3	20	3.9	92.8	3.9	Z	40.0
4	30	4.4	92.1	3.4	Z	39.1
5	40	5.4	89.6	5.5	Z	35.4
6	50	3.4	92.1	5.0	Z	44.1
7	60	3.3	92.7	3.8	Z	42.7
8	70	6.5	91.3	2.8	Z	35.3
9	80	6.1	91.4	2.5	Z	30.4
10	90	10.3	85.5	4.7	Z	32.8
11	100	36.7	62.5	1.1	sZ	24.6
12	110	2.2	94.9	3.2	Z	29.5
13	120	5.3	92.6	2.5	Z	18.7
14	130	6.5	89.6	3.8	Z	20.4
15	140	9.9	88.5	1.6	Z	18.2
16	150	22.0	74.9	2.9	sZ	20.5
17	160	7.7	87.7	4.6	Z	20.3
18	170	7.8	86.6	5.6	Z	18.3
19	180	6.6	90.7	2.8	Z	22.9
20	190	4.0	90.8	5.4	Z	20.3
21	200	6.9	90.2	3.0	Z	19.5
22	210	11.4	83.6	4.9	sZ	19.4
23	220	6.7	89.6	3.9	Z	23.6
24	230	7.2	88.6	4.3	Z	18.4
25	240	5.4	90.6	4.2	Z	23.6
26	250	6.8	90.0	3.5	Z	21.0
27	260	9.8	86.6	3.8	Z	21.2
28	270	6.1	90.3	3.6	Z	21.2
29	280	10.9	86.0	2.9	sZ	20.7
30	290	4.1	91.0	5.0	Z	19.3
31	300	4.6	90.1	5.5	Z	19.0
32	310	10.3	83.6	5.8	Z	18.9
33	320	11.1	84.0	4.9	sZ	24.7
34	330	7.8	87.6	4.8	Z	19.6
35	340	16.3	79.3	4.3	sZ	20.5
36	350	5.9	87.7	6.5	Z	19.2
37	360	5.5	91.0	3.5	Z	17.3
38	370	10.6	86.4	2.9	sZ	19.4
39	380	5.6	89.0	5.5	Z	22.4
40	390	10.9	83.4	5.6	sZ	22.3
41	400	34.6	62.4	3.0	sZ	21.3
42	410	11.6	81.6	7.0	sZ	18.7
43	420	21.3	73.5	5.2	sZ	14.2
44	430	26.7	69.1	4.0	sZ	2.4
45	440	0.4	99.6	0.0	Z	1.4

APPENDIX R

Metric (mm) statistics (after Krumbein, 1936) of Loch Callater core sediment.

Sample	Depth (cm)	Md	QDa
1	0	0.0270	0.00920
2	10	0.0263	0.00885
3	20	0.0284	0.00980
4	30	0.0282	0.00925
5	40	0.0240	0.00785
6	50	0.0249	0.00805
7	60	0.0245	0.00720
8	70	0.0259	0.00730
9	80	0.0290	0.00945
10	90	0.0313	0.01180
11	100	N/A	N/A
12	110	0.0294	0.00965
13	120	0.0249	0.01085
14	130	0.0278	0.00975
15	140	0.0364	0.01225
16	150	0.0349	0.03230
17	160	0.0282	0.00935
18	170	0.0259	0.00035
19	180	0.0313	0.01020
20	190	0.0250	0.00935
21	200	0.0324	0.01265
22	210	0.0274	0.01075
23	220	0.0296	0.01025
24	230	0.0268	0.00710
25	240	0.0313	0.00805
26	250	0.0292	0.01110
27	260	0.0256	0.00920
28	270	0.0372	0.02660
29	280	0.0361	0.01595
30	290	0.0263	0.01050
31	300	0.0123	0.00820
32	310	0.0263	0.01185
33	320	0.0263	0.01195
34	330	0.0272	0.01115
35	340	0.0290	0.01705
36	350	0.0252	0.00825
37	360	0.0268	0.08950
38	370	0.0261	0.01275
39	380	0.0232	0.00970
40	390	0.0261	0.01255
41	400	0.0430	0.03412
42	410	0.0238	0.01105
43	420	0.0300	0.02425
44	430	0.0321	0.03770
45	440	0.0540	0.00605

APPENDIX S
Elemental composition of Loch Callater core sediment and Fe/Mn ratio

Sample	Depth (cm)	Na mg/kg	K mg/kg	Ca mg/kg
1	0	375.7	1693.3	3907.8
2	10	543.9	1786.4	4481.0
3	20	453.6	1665.0	4147.5
4	30	420.8	1558.1	3466.9
5	40	426.8	1173.7	2505.0
6	50	367.4	1405.1	3470.7
7	60	394.2	1482.0	3358.2
8	70	652.3	1354.5	2569.7
9	80	573.2	2128.6	4122.6
10	90	365.3	1311.3	2782.7
11	100	464.5	1573.4	2582.4
12	110	478.0	1653.3	3555.7
13	120	450.5	1678.2	3881.1
14	130	393.0	1577.1	4582.0
15	140	485.6	1684.8	4618.4
16	150	471.7	1464.7	4001.9
17	160	440.0	1615.0	3425.0
18	170	462.3	2477.3	3030.1
19	180	658.7	1232.5	4251.5
20	190	597.0	2492.5	3447.7
21	200	339.6	1618.3	4770.2
22	210	383.0	1686.5	4034.8
23	220	443.6	1570.2	4282.1
24	230	340.9	1472.3	3498.0
25	240	435.0	1295.0	5225.0
26	250	389.2	1566.8	6442.1
27	260	400.0	1540.0	4700.0
28	270	584.6	1406.2	5282.2
29	280	391.5	1345.3	5376.5
30	290	618.7	1621.7	5723.5
31	300	350.0	1770.0	5590.0
32	310	470.0	1385.0	6125.0
33	320	470.4	1331.3	7302.3
34	330	341.7	1467.3	5693.4
35	340	418.7	1430.7	7003.9
36	350	369.2	1397.2	6736.5
37	360	535.0	1495.0	7625.0
38	370	350.0	905.0	6335.0
39	380	355.3	1026.0	7752.7
40	390	325.6	1107.2	7139.2
41	400	489.6	1182.0	8011.4
42	410	398.0	1243.7	5308.4
43	420	307.5	2132.9	4131.9
44	430	310.0	2770.0	3940.0
45	440	312.8	2462.7	3788.4

APPENDIX S continued
Elemental composition of Loch Callater core sediment and Fe/Mn ratio

Sample	Mg mg/kg	Mn mg/kg	Fe mg/kg	Fe/Mn ratio	Al mg/kg
1	5460.9	1553.1	37670.3	24.3	17019.0
2	5184.6	1741.5	41202.5	23.7	19286.4
3	4915.2	1799.6	41595.2	23.1	19177.4
4	4774.5	1698.4	38091.1	22.4	16768.5
5	3668.7	1224.5	36747.9	30.0	13912.6
6	4329.6	1340.6	27288.9	20.4	13565.0
7	4176.6	1521.9	25613.7	16.8	14086.8
8	3914.3	1394.4	27445.2	19.7	13799.8
9	5767.7	1889.3	48708.8	25.8	13544.3
10	3758.7	1451.4	31641.6	21.8	15090.0
11	4505.4	1553.4	36028.9	23.2	16743.2
12	5129.4	4083.6	47953.1	11.7	19198.2
13	4613.8	5094.0	57920.7	11.4	20440.5
14	4049.7	9741.2	68955.2	7.1	20985.0
15	4618.4	10014.8	76610.5	7.6	21749.2
16	4856.0	7750.7	72790.4	9.4	24225.4
17	4760.0	7050.0	67050.0	9.5	19785.0
18	5547.7	4025.1	42743.7	10.6	22005.0
19	4131.7	9690.6	56586.8	5.8	18088.8
20	6582.0	3393.0	57263.6	16.9	23000.0
21	4685.3	6123.8	74975.0	12.2	19635.3
22	4985.0	3832.9	56467.6	1.5	19721.3
23	4361.9	9925.2	59920.2	6.0	19626.1
24	4362.6	5953.5	54298.4	9.1	19150.2
25	4160.0	3375.0	48790.0	14.5	19825.0
26	5064.8	9276.4	59930.1	6.5	22784.4
27	4715.0	6405.0	41875.0	6.5	18340.0
28	4092.7	10126.0	65877.0	6.5	21355.8
29	3940.7	8012.0	56777.1	7.1	18087.3
30	5104.7	1626.7	39346.3	24.2	21247.5
31	5405.0	1570.0	42315.0	27.0	20780.0
32	4685.0	1685.0	51350.0	30.5	20280.0
33	4319.3	1441.4	42222.2	29.3	20645.6
34	4502.5	1060.3	40718.5	38.4	17261.3
35	4341.9	1714.8	55334.0	32.3	20368.8
36	4366.2	1287.4	43637.7	33.9	19955.0
37	4880.0	1120.0	46875.0	41.9	21050.0
38	2675.0	1080.0	40115.0	37.1	13940.0
39	3213.2	950.9	41376.3	43.5	18018.0
40	3451.9	1803.6	52855.7	29.3	18031.0
41	3308.6	1008.9	63155.2	62.6	18006.9
42	3228.8	412.9	35402.9	85.7	14213.9
43	5114.0	337.3	23650.7	70.1	14439.4
44	6425.0	325.0	25440.0	78.3	13855.0
45	5382.3	243.3	20888.7	85.9	11390.2

APPENDIX T

Sand, silt, clay, organic matter and water content percentages of Loch Muick core sediment with sample depth and textural classification after Folk (1974) for samples lacking gravel.

Sample	Depth (cm)	Sand (%)	Silt (%)	Clay (%)	Sediment type	Total organic matter (%)	Water content (%)
1	0	11.7	85.3	2.8	sZ	55.5	79.2
2	10	12.4	83.5	4.0	sZ	32.8	72.3
3	20	7.8	88.9	3.1	Z	35.5	74.0
4	30	13.9	83.3	2.8	sZ	28.1	72.4
5	40	6.9	89.7	3.1	Z	37.2	77.2
6	50	7.5	88.9	3.4	Z	31.3	72.5
7	60	11.3	85.2	3.3	sZ	32.8	76.0
8	70	9.3	87.8	3.1	Z	35.9	75.1
9	80	7.9	88.1	4.0	Z	30.4	72.5
10	90	13.4	83.3	3.3	sZ	29.2	71.4
11	100	8.3	89.2	2.5	Z	37.6	75.7
12	110	8.2	87.0	4.8	Z	21.7	80.6
13	120	54.1	43.9	2.0	zS	22.8	79.7
14	130	18.6	77.1	4.4	sZ	20.9	78.9
15	140	12.4	83.3	3.9	sZ	24.8	68.7
16	150	28.4	67.9	3.8	sZ	24.3	77.9
17	160	51.0	48.5	0.8	zS	25.8	77.9
18	170	52.8	45.7	1.5	zS	20.6	67.3
19	180	49.0	49.7	1.3	sZ	28.7	78.2
20	190	22.5	74.8	2.7	sZ	22.0	71.9
21	200	45.4	53.2	1.6	sZ	13.4	56.7
22	210	29.8	67.0	2.9	sZ	30.6	85.8
23	220	39.0	59.7	1.2	sZ	28.5	82.5
24	230	8.8	87.9	3.2	Z	30.9	75.8
25	240	21.4	76.2	2.4	sZ	36.3	69.2
26	250	13.5	83.7	2.9	sZ	30.9	73.8
27	260	11.3	85.9	2.8	sZ	33.5	75.5
28	270	12.8	84.3	2.9	sZ	34.5	77.3
29	280	13.7	83.8	2.6	sZ	37.5	77.8
30	290	18.9	78.2	3.0	sZ	35.8	76.8
31	300	9.9	87.6	2.6	Z	35.1	76.2
32	310	8.9	87.6	3.5	Z	38.7	78.5
33	320	21.4	76.1	2.4	sZ	36.9	78.3
34	330	43.1	56.0	1.0	sZ	36.2	77.8
35	340	35.9	62.2	1.9	sZ	13.4	75.7
36	350	16.9	80.3	2.8	sZ	17.4	77.2
37	360	20.7	77.2	2.2	sZ	37.1	81.9
38	370	50.8	48.3	0.8	zS	37.1	77.9
39	380	10.6	86.0	3.4	Z	35.3	77.8
40	390	21.0	73.5	5.0	sZ	19.6	76.7
41	400	19.7	75.9	4.5	sZ	16.3	75.1
42	410	56.0	39.2	4.8	zS	13.7	73.2
43	420	24.4	71.3	4.4	sZ	9.0	72.1
44	430	16.5	79.9	3.6	sZ	3.9	55.7
45	440	11.6	85.9	2.4	sZ	1.1	28.9
46	450	2.1	95.3	2.6	Z	0.9	26.9
47	460	6.1	91.8	1.9	Z	0.8	25.8
48	470	5.2	90.7	4.0	Z	1.1	30.5
49	480	4.1	94.0	1.7	Z	0.1	25.2
50	490	4.0	94.8	1.0	Z	0.4	22.2
51	500	1.0	97.9	1.4	Z	0.4	22.8

APPENDIX U

Metric (mm) statistics (after Krumbein, 1936) of Loch Muick core sediment.

Sample	Depth (cm)	Md (mm)	QDa (mm)
1	0	0.0527	0.00950
2	10	0.0237	0.00885
3	20	0.0272	0.00870
4	30	0.0268	0.01080
5	40	0.0274	0.01550
6	50	0.0313	0.01160
7	60	0.0276	0.12100
8	70	0.0278	0.01080
9	80	0.0282	0.01240
10	90	0.0263	0.01360
11	100	0.0254	0.00970
12	110	0.0344	0.00915
13	120	0.0896	0.04190
14	130	0.0263	0.01670
15	140	0.0268	0.01380
16	150	0.0364	0.04030
17	160	0.0902	0.05900
18	170	0.0878	0.04555
19	180	0.0813	0.05545
20	190	0.0313	0.02770
21	200	0.0723	0.04850
22	210	0.0377	0.03935
23	220	0.0625	0.04825
24	230	0.0337	0.01465
25	240	0.0313	0.02460
26	250	0.0313	0.01305
27	260	0.0250	0.01190
28	270	0.0296	0.01550
29	280	0.0272	0.01170
30	290	0.0359	0.00700
31	300	0.0313	0.01360
32	310	0.0306	0.01295
33	320	0.0162	0.02685
34	330	0.0738	0.05360
35	340	0.0548	0.03820
36	350	0.0374	0.01810
37	360	0.0390	0.02755
38	370	0.0902	0.06170
39	380	0.0511	0.00915
40	390	0.0276	0.02490
41	400	0.0261	0.01125
42	410	0.0477	0.04220
43	420	0.0250	0.01685
44	430	0.0270	0.03280
45	440	0.0226	0.00480
46	450	0.0261	0.00770
47	460	0.0229	0.00550
48	470	0.0234	0.00975
49	480	0.0274	0.01065
50	490	0.0298	0.00960
51	500	0.0276	0.00890

APPENDIX V
Elemental composition of Loch Muick core sediment and Fe/Mn ratio.

Sample	Depth (cm)	Na mg/kg	K mg/kg	Ca mg/kg
1	0	350.0	1180.0	2130.0
2	10	299.7	1163.8	1093.9
3	20	357.8	1322.0	964.2
4	30	360.0	1055.0	1120.0
5	40	413.7	1121.6	1221.3
6	50	404.6	999.0	955.0
7	60	388.8	1076.7	1211.3
8	70	504.4	1107.8	1305.6
9	80	469.5	864.1	1193.8
10	90	412.5	1207.7	1143.1
11	100	412.9	1402.9	1253.7
12	110	395.4	880.8	1626.6
13	120	448.6	912.2	1355.9
14	130	432.4	1088.4	1461.2
15	140	467.6	890.5	1512.4
16	150	446.4	912.7	1175.6
17	160	403.7	862.4	1430.7
18	170	499.0	723.5	1352.3
19	180	433.7	111.6	1276.1
20	190	412.9	751.2	1447.7
21	200	442.7	885.5	1552.2
22	210	455.9	776.5	1447.9
23	220	309.6	754.2	1658.3
24	230	520.0	680.0	1910.0
25	240	346.0	641.9	1359.0
26	250	542.8	727.0	1449.2
27	260	318.4	850.7	1393.0
28	270	337.6	1494.5	854.0
29	280	381.1	1494.4	1108.3
30	290	345.0	830.0	1470.0
31	300	253.7	776.1	1691.5
32	310	385.0	2155.0	2135.0
33	320	304.3	1027.9	1706.5
34	330	317.1	877.1	2001.9
35	340	322.7	988.0	1926.5
36	350	358.9	618.1	1784.6
37	360	297.9	680.2	1876.8
38	370	301.2	582.3	1420.6
39	380	456.8	978.1	1951.3
40	390	586.1	746.4	1773.5
41	400	419.1	753.4	1536.9
42	410	354.6	989.0	1468.5
43	420	425.0	1320.0	1220.0
44	430	367.4	1961.2	1330.6
45	440	455.9	2978.2	1412.2
46	450	418.4	2701.8	1824.5
47	460	332.1	2056.4	1412.2
48	470	409.9	2527.4	1538.4
49	480	445.5	2237.2	1571.5
50	490	302.5	1845.2	1517.8
51	500	314.6	1968.0	1773.2

APPENDIX V continued
Elemental composition of Loch Muick core sediment and Fe/Mn ratio.

Sample	Mg mg/kg	Mn mg/kg	Fe mg/kg	Fe/Mn ratio	Al mg/kg
1	2330.0	3035.0	27050.0	8.9	11525.0
2	1803.2	2522.4	41903.1	16.6	13851.0
3	1446.3	2524.8	40499.2	16.0	13091.4
4	1410.0	3225.0	49585.0	15.4	15145.0
5	1166.5	3748.7	61016.9	16.3	16854.4
6	1308.6	3141.8	56143.8	17.9	15014.9
7	1311.0	4062.8	77816.5	19.1	18554.3
8	1275.9	3778.4	74678.5	19.8	16864.4
9	1428.5	3721.2	60489.5	16.3	15739.2
10	1456.2	3384.6	62276.3	18.4	16133.2
11	1781.0	3492.5	62537.3	17.9	17840.8
12	1216.2	5075.0	64264.2	12.7	16866.8
13	1141.5	4282.1	62761.7	14.7	16919.2
14	1351.8	4731.6	68886.6	14.6	17743.5
15	1144.2	5243.7	81194.0	15.5	18691.5
16	1284.7	3680.5	63045.6	17.1	15312.5
17	1031.9	4416.7	71385.8	16.2	17048.8
18	1012.9	3922.2	65668.6	16.7	15214.5
19	1301.1	4062.8	76171.5	18.7	16610.1
20	1069.6	5069.6	101641.7	20.0	18029.8
21	1134.3	4810.9	90696.5	18.9	17248.7
22	1092.1	5050.1	104108.2	20.6	18061.1
23	849.1	4670.3	79620.3	17.0	16183.8
24	930.0	5205.0	98500.0	18.9	18595.0
25	852.5	4287.8	77281.8	18.0	13671.0
26	886.4	4616.5	74900.4	16.2	13625.5
27	865.6	4004.9	82835.8	20.7	15149.2
28	1276.0	2075.4	30839.1	14.9	10243.3
29	1233.7	1985.9	46073.2	23.2	11339.0
30	1000.0	3515.0	70700.0	20.1	13140.0
31	870.6	3447.7	70298.5	20.4	14069.6
32	3240.0	2825.0	46800.0	16.6	13455.0
33	948.1	3942.1	67015.9	17.0	14640.7
34	852.3	3320.1	64122.8	19.3	15525.2
35	1881.8	2651.4	64597.8	24.4	11663.3
36	658.0	3185.4	36595.2	11.5	11844.4
37	764.6	2740.8	37234.3	13.6	12120.1
38	697.7	4452.8	78564.2	17.6	13142.5
39	988.0	2532.2	32492.5	12.8	12269.1
40	741.4	2535.0	44268.5	17.5	11107.2
41	943.1	1601.8	16067.8	10.0	8932.1
42	1113.8	1733.2	33736.2	30.3	8291.7
43	1730.0	1070.0	16070.0	15.0	7185.0
44	2830.1	595.8	15362.4	25.8	7115.1
45	4276.5	594.6	19603.5	33.0	9088.2
46	4566.3	418.7	16684.9	39.8	6191.4
47	3320.1	297.3	12621.4	42.5	4737.3
48	3981.0	389.6	15479.5	39.7	6078.9
49	3648.6	310.3	13123.1	42.3	4769.7
50	3244.0	252.9	11413.6	45.1	3789.6
51	3481.5	294.7	12232.7	41.5	4001.0

BIBLIOGRAPHY

- Aarseth, I., Ø. Lonne and O. Giskeodegaard (1989) Submarine slides in glaciomarine sediments in some western Norwegian fjords. *Mar. Geol.* **88** 1-21.
- Agassiz, L. (1840) On the evidence of the former existence of glaciers in Scotland, Ireland and England. *Proc. Geol. Soc. Lond.* **3** 327-332.
- Al-Ansari, N.A. (1976) *Sediments and sediment discharge in the River Earn, Scotland*. Unpublished PhD Thesis Univ. Dundee.
- Al-Ansari, N.A. and McManus, J (1980) A re-investigation of the bathymetry of Loch Earn. *Scot. Geog. Mag.* **96** 105-113.
- Al-Bayati, K.M. and J. McManus (1984) The bathymetry and sedimentology of Loch Benachally, Perthshire. *Scot. J. Geol.* **20** 65-71.
- Al-Jabbari, M.H., N.A. Al-Ansari and J. McManus (1983) The bathymetry and sedimentology of Loch Tay, Scotland. *J. Wat. Resour.* **2** 70-89.
- Alrasoul, A.H.A. (1986) *Wave-shoreline sediment interactions in Loch Earn, Scotland*. Unpublished PhD Thesis Univ. Dundee.
- Amman, B. and A.F. Lotter (1989) Late-Glacial radiocarbon- and palynostratigraphy on the Swiss Plateau. *Boreas* **18** 109-126.
- Andrews, J.T. (1963a) The cross-valley moraines of North-Central Baffin Island, N.W.T.: a descriptive analysis. *Geog. Bull.* **19** 49-77.
- Andrews, J.T. (1963b) The cross-valley moraines of North-Central Baffin Island: A quantitative analysis. *Geog. Bull.* **20** 82-129.
- Andrews, J.T. and B.B. Smithson (1966) Till fabrics of the cross-valley moraines of North-Central Baffin Island, Northwest Territories, Canada. *Bull. Geol. Soc. Am.* **77** 271-290.
- Asaad, N.M. and J. McManus (1986) The bathymetry, sediment and sedimentation of Loch Lubnaig, Scotland. *J. Wat. Resour.* **5** 187-205.
- Ashley, G.M. (1978) Interpretation of polymodal sediments. *J. Geol.* **86** 411-420.
- Ashley, G.M. (1988) Classification of glaciolacustrine sediments. In: *Genetic Classification of Glacigenic Deposits*. Ed. R.P. Goldthwait and C.L. Matsch Balkema Rotterdam 243-260.
- Axelsson, V. (1983) The use of X-ray radiographic methods in studying sedimentary properties and rates of sediment accumulation. *Hydrobiol.* **103** 65-69.
- Ballantyne, C.K. (1989) The Loch Lomond Readvance on the Isle of Skye, Scotland: glacier reconstruction and palaeoclimatic implications. *J. Quat. Sci.* **4** 95-108.
- Bally, A.W. (1987) Foreward. In: *Atlas of seismic stratigraphy*. Ed. A.W. Bally A.A.P.G. Studies in Geology 27. Tulsa Vol 1.
- Barnett, D.M. (1967) Development, landforms and chronology of Generator Lake, Baffin Island. *Geog. Bull.* **9** 169-188.

- Barnett, D.M. and Holdsworth, G. (1974) Origin, morphology and chronology of sublacustrine moraines, Generator Lake, Baffin Island, Northwest Territories, Canada. *Can. J. Earth Sci.* **11** 380-408.
- Barnett, D.M., D. Forbes and K. Whytock (1970) Generator Lake, Baffin Island and Tasiujaq Cove, Ekalugad Fiord, Baffin Island, N.W.T. 1968. *Can. Oceanog. Cen. 1970 Data Record Series 1*.
- Barrow, G., L.W. Hinxman and E.H. Cunningham-Craig (1904) *Balmoral* Scotland Sheet 65 Solid and Drift Edition 1" Series Mem. Geol. Surv. Scotland
- Barrow, G., E.H. Cunningham-Craig and L.W. Hinxman (1912) Glacial and Recent deposits. In: *The Geology of the Districts of Braemar, Ballater and Glen Clova (Explanation of Sheet 65)* Mem. Geol. Surv. Scotland Edinburgh 125-127.
- Belderson, R.H. and A.H. Stride (1969) Tidal currents and sand wave profiles in the north-eastern Irish Sea. *Nature* **222** 74-75.
- Belderson, R.H. and J.B. Wilson (1973) Iceberg plough marks in the vicinity of the Norwegian Trough. *Norsk Geol. Tidsskr.* **53** 323-328.
- Belderson, R.H., N.H. Kenyon and A.H. Stride (1970) Holocene sediments on the continental shelf west of the British Isles. *Inst. Geol. Sci. Report* **70/14** 159-170.
- Belderson, R.H., N.H. Kenyon, A.H. Stride and A.R. Stubbs (1972) *Sonographs of the sea floor. A picture atlas*. Elsevier Amsterdam.
- Belderson, R.H., N.H. Kenyon and J.B. Wilson (1973) Iceberg plough marks in the north-east Atlantic. *Palaeogeog. Palaeoclim. Palaeoecol.* **13** 215-224.
- Bellaiche, G., V. Coutellier and L. Droz (1986) Seismic evidence of widespread mass transport deposits in the Rhone deep sea fan: their role in fan construction. *Mar. Geol.* **71** 327-340.
- Ben-Avraham, Z., G. Shaliv and A. Nur (1986) Acoustic reflectivity and shallow sedimentary structure in the Sea of Galilee, Jordan Valley. *Mar. Geol.* **70** 175-189.
- Benn, D.I. (1989) Controls on sedimentation in a Late Devensian ice-dammed lake, Achnasheen, Scotland. *Boreas* **18** 31-42.
- Bennett, M.R. and N.F. Glasser (1991) The glacial landforms of Glen Geusachan, Cairngorms: a reinterpretation. *Scot. Geog. Mag.* **107** 116-123.
- Booth, D.B. (1986) The formation of ice-marginal embankments into ice-dammed lakes in the Eastern Puget Lowland, Washington, U.S.A., during the Late Pleistocene. *Boreas* **15** 247-263.
- Boulton, G.S. (1986) Push-moraines and glacier-contact fans in marine and terrestrial environments. *Sedimentol.* **33** 677-698.
- Boulton, G.S., P.N. Chroston and J. Jarvis (1981) A marine seismic study of late Quaternary sedimentation and inferred glacier fluctuations along western Inverness-shire, Scotland. *Boreas* **10** 39-51.

- Boulton, G.S., P.W.V. Harris and J. Jarvis (1982) Stratigraphy and structure of a coastal sediment wedge of glacial origin inferred from Sparker measurements in glacial Lake Jokulsarlon in southeastern Iceland. *Jokull* **32** 37-47.
- Bouye, C. (1983) *Etude des correlations entre la reponse sismique haute resolution de quelques de depots meubles et leurs caracteristiques sedimentologiques*. Ph.D Thesis Sp. Oceanologie Univ. Perpignan (Fr).
- Broecker, W.S. and G.H. Denton (1989) The role of ocean-atmosphere reorganizations in glacial cycles. *Geochim. et Cosmochim. Acta* **53** 2465-2501.
- Broecker, W.S., D. Peteet, and D. Rind (1985) Does the ocean-atmosphere have more than one stable mode of operation? *Nature* **315** 21-26.
- Broecker, W.S., M. Andree, W. Wolfli, H. Oeschger, G. Bonani, J. Kennett and D. Peteet (1988) The chronology of the last deglaciation: implications to the cause of the Younger Dryas event. *Paleoceanog.* **3** 1-19.
- Browne, M.A.E. and D.K. Graham (1981) Glaciomarine deposits of the Loch Lomond Stade glacier in the Vale of Leven between Dumbarton and Balloch, west-central Scotland. *Quat. Newsltr.* **34** 1-7.
- Buller, A.T. and J. McManus (1972) Simple metric sedimentary statistics used to recognise different environments. *Sedimentol.* **18** 1-21.
- Buller, A.T. and J. McManus (1973) Modes of turbidite deposition deduced from grain size analyses. *Geol. Mag.* **109** 491-500.
- Buller, A.T. and J. McManus (1974) The application of quartile deviation-median diameter curves to the interpretation of sedimentary rocks. *J. Geol. Soc.* **130** 79-83.
- Buller, A.T., C.D. Green and J. McManus (1975) Dynamics and sedimentation: The Tay in comparison with other estuaries. In *Nearshore sedimentation*. Ed. J. Hails and A.Carr Wiley London 201-250.
- Calvert, S.E and J.J. Veevers (1962) Minor structures of unconsolidated marine sediments revealed by X-radiography. *Sedimentol.* **1** 287-295.
- Canals, M., E. Catafau and J. Serra (1988) Sedimentary structure and seismic facies of the inner continental shelf north of the Ebro delta (northwestern Mediterranean Sea). *Cont. Shelf Res.* **8** 961-977.
- Carter, R.M. (1975) A discussion and classification of subaqueous mass-transport with particular application to grain-flow, slurry-flow and fluxoturbidites. *Earth Sci. Rev.* **11** 145-177.
- Carter, L. and R.M. Carter (1990) Lacustrine sediment traps and their effect on Continental Shelf sedimentation - South Island New Zealand. *Geo-Marine Ltrs.* **10** 93-100.
- Chambers, R (1855) Further observations on glacial phenomena in Scotland and the North of England. *Edin. New Phil. J.* **1** 97-103.
- Charlesworth, J.K. (1955) Lateglacial history of the Highlands and Islands of Scotland. *Trans. R. Soc. Edin.* **62** 769-928.

- Chesterman, W.D., P.R. Clynick and A.H. Stride (1958) An acoustic aid to sea bed survey. *Acustica* 8 285.
- Clague, J.J. (1986) The Quaternary stratigraphic record of British Columbia - evidence for episodic sedimentation and erosion controlled by glaciation. *Can. J. Earth. Sci.* 23 885-894.
- Clapperton, C.M. (1986) Glacial geomorphology of northeast Lochnagar. In: *Essays for Professor R.E.H. Mellor*. Ed. W. Ritchie, J.C. Stone and A.S. Mather University of Aberdeen Aberdeen 390-396.
- Clapperton, C.M., A.R. Gunson and D.E. Sugden (1975) Loch Lomond Readvance in the eastern Cairngorms. *Nature* 253 710-712.
- Clemmensen, L.B. and M. Houmark-Nielsen (1981) Sedimentary features of a Weichselian glaciolacustrine delta. *Boreas* 10 229-245.
- Colhoun, E.A. and Synge, F.M. (1980) The cirque moraines at Lough Nahanagan, County Wicklow, Ireland. *Proc. R. Irish. Acad.* 80B 25-45.
- Colladon J.D. and F.K. Sturm (1827) The compression of liquids (In French) *Ann. Chim. Phys. Series 2* 36 Part IV Speed of sound in liquids. 236-257.
- Collet, L.W. and Johnston, T.N. (1906) On the formation of certain lakes in the Highlands. *Proc. R. Soc. Edin.* 26 107-112.
- Coppock, J.T. (1976) *An Agricultural Atlas of Scotland*. John Donald Edinburgh.
- Coope, G.R. (1975) Climatic fluctuations in Northwest Europe since the last interglacial, indicated by fossil assemblages of Coleoptera. In: *Ice Ages: Ancient and Modern*. Ed. Wright A.E. and F. Moseley Seel House Press Liverpool 153-168.
- Coope, G.R. and W. Pennington (1977) The Windermere Interstadial of the Late Devensian. *Phil. Trans. R. Soc. Lond. B* 280 337-339.
- Cornish, R. (1981) Glaciers of the Loch Lomond Stadial in the Western Southern Uplands of Scotland. *Proc. Geol. Assn.* 92 105-114.
- Cronan, D.S. (1972) Skewness and kurtosis in polymodal sediments from the Irish Sea. *J. Sed. Pet.* 42 102-106.
- Cronin, S.P., H.F. Lamb and R.J. Whittington (in press) Sedimentation in an upland lake in Mid Wales. In: Proc. B.G.R.G. Spring Field Mtg: *Geomorphology and sedimentology of lakes and reservoirs*.
- Curray, J.R. (1960) Tracing sediment masses by grain size modes. 21st Int. Geol. Cong. Rept. *Int. Assn. Sedimentol.* Pt. 23 119-130.
- D'Olier, B. (1979) Side-scan sonar and seismic reflection profiling. In: *Estuarine hydrography and sedimentation*. Ed. K.R. Dyer. Estuarine and brackish-water sciences association handbooks. C.U.P. Cambridge 57-86.
- Damuth, J.E. (1975) Echo character of the Western Equatorial Atlantic floor and its relationship to the dispersal and distribution of terrigenous sediments. *Mar. Geol.* 18 17-45.

- Dancer, M.J.B., J.A. Dowdeswell and R.J. Whittington (1992) Late Quaternary stratigraphy and sedimentology of Lake Bala, Wales. In: Proc. B.G.R.G. Spring Field Mtg: *Geomorphology and sedimentology of lakes and reservoirs*. Ed. J. McManus and R.W. Duck Wiley *In Press*.
- Dansgaard, W., H. Clausen, N. Gundestrup, C. Hammer, S. Johnsen, P. Kristins-dottir and N. Reeh (1982) A new Greenland ice core. *Science* **218** 1273-1277.
- Dansgaard, W., J.W.C. White and S.J. Johnsen (1989) The abrupt termination of the Younger Dryas climate event. *Nature* **339** 532-533.
- Dardis, G.F. (1985) Genesis of Late Pleistocene moraine ridges, South-Central Ulster, Northern Ireland. *Earth Surf. Proc. and Landf.* **10** 483-495.
- Davis, M.B. and M.S. Ford (1982) Sediment focusing in Mirror Lake, New Hampshire. *Limnol. Oceanogr.* **27** 137-150.
- Deacon, M. (1971) *Scientists and the Sea 1650-1900 a study of marine science*. Academic Press London.
- Dearing, J.A. (1992) Sediment yields and sources in a Welsh upland lake-catchment during the past 800 years. *Earth Surf. Proc. and Landf.* **17** 1-22.
- Denton, G and T. Hughes (eds) (1981) *The Last Great Ice Sheets* Wiley New York.
- Desloges, J.R. and R. Gilbert (1991) Sedimentary record of Harrison Lake: implications for deglaciation in southwestern British Columbia. *Can. J. Earth Sci.* **28** 800-815.
- Digerfeldt, G. (1975) The post-glacial development of Ranviken Bay in Lake Immeln. III. Palaeolimnology. *Geol. For. Stockh. Forh.* **97** 13-28.
- Dobson, M.R. (1989) In: GLORIA: The second decade. T.J.G. Francis. *J. Geol. Soc. Lond.* **146** 1031-1032.
- Donnelly, R. and C. Harris (1989) Sedimentology and origin of deposits from a small ice-dammed lake, Leirbreen, Norway. *Sedimentol.* **36** 581-600.
- Dowdeswell, J.A. and E.K. Dowdeswell (1989) Debris in icebergs and rates of glaci-marine sedimentation: observatios from Spitsbergen and a simple model. *J. Geol.* **97** 221-231.
- Duck, R.W. (1982) *Physical sedimentology of some lake systems*. Unpublished PhD Thesis Univ. Dundee.
- Duck, R.W. (1986) Bottom sediments of Loch Tummel, Scotland. *Sed. Geol.* **47** 293-395.
- Duck, R.W. (1987) Aspects of physical processes of sedimentation in Loch Earn, Scotland. In *International Geomorphology 1986* Part 1 Ed. V. Gardiner Wiley 801-821.
- Duck, R.W. and J. McManus (1981) Ice-collapse induced waves and graded gravel ridges on a lake beach. *Earth. Surf. Proc. and Landf.* **6** 203-206.
- Duck, R.W. and J. McManus (1985a) Short-term bathymetric changes in an ice-contact proglacial lake. *Nor. Geol. Tidsskr.* **39** 39-45.

- Duck, R.W. and J. McManus (1985b) Bathymetric charts of ten Scottish lochs. *Tay Estuary Research Centre Report No.9*. Univ. Dundee.
- Duck, R.W. and J. McManus (1985c) A sidescan sonar survey of a previously drawn-down reservoir: a control experiment. *Int. J. Rem. Sensing* **6** 601-609.
- Duck, R.W. and J. McManus (1987a) Sidescan sonar applications in limnoarchaeology. *Geoarch: An Int. J.* **2** 223-230.
- Duck, R.W. and J. McManus (1987b) Sediment yields in lowland Scotland derived from reservoir surveys. *Trans. R. Soc. Edin.* **78** 369-377.
- Duck, R.W. and J. McManus (1990) Relationships between catchment characteristics, and use and sediment yield in the Midland Valley of Scotland. In: *Soil Erosion on Agricultural Land*. Ed. J. Boardman, I.D.L. Foster and J. Dearing Wiley 285-299.
- Eberli, G.P. (1984) Water content and bulk density of Zugo sediments. *Contr. Sedimentol.* **13** 115-124.
- Engstrom, D.R. (1983) *Chemical stratigraphy of lake sediments as a record of environmental change*. Unpubl. PhD Thesis Univ. Minnesota.
- Engstrom, D.R. and H.E. Wright (1984) Chemical stratigraphy of lake sediments as a record of environmental change. In *Lake sediments and environmental history*. Ed. E.Y. Haworth and J.W.G. Lund Leicester Univ. Press Leicester 11-68.
- Eyles, N., B.M. Clark and J.J. Clague (1987) Coarse-grained sediment gravity flow facies in a large supraglacial lake. *Sedimentol.* **34** 193-216.
- Finckh, P. and K. Kelts (1976) Geophysical investigations into the nature of pre-Holocene sediments of Lake Zurich. *Eclogae Geol. Helv.* **69** 139-148.
- Finckh, P., K. Kelts, A. Lambert (1984) Seismic stratigraphy and bedrock forms in perialpine lakes. *Bull. Geol. Soc. Am.* **95** 1118-1128.
- Flemming, B.W. (1976) Side-scan sonar: a practical guide. *Int. Hydrog. Rev.* **53** 65-91.
- Folk, R.L. (1954) The distinction between grain size and mineral composition in sedimentary rock nomenclature. *J. Geol.* **62** 344-359.
- Folk, R.L. (1974) *Petrology of Sedimentary Rocks*. Hemphil Austin Texas.
- Folk, R.L. and W.C. Ward (1957) Brazos River bar: A study in the significance of grain size parameters. *J. Sed. Pet.* **27** 3-26.
- Fulton, R.J. (1965) Silt deposition in Late-glacial lakes of southern British Columbia. *Am. J. Sci.* **263** 553-570.
- Gammelsaeter, H. and K. Haugland (1970) Continuous seismic profiling in Storfjorden N.W. Norway. *Nor. Geol. Tidsskr.* **50** 231-239.
- Gilbert, R and J.R. Desloges (1987) Sediments of ice-dammed, self-draining Ape Lake, British Columbia. *Can. J. Earth Sci.* **24** 1735-1747.

- Goldthwait, R.P. (1951) Deglaciation of north central Baffin Island. (Abstract) *Bull. Geol. Soc. Am.* **62** 1443-1444.
- Grant, J.A. and R. Schreiber (1990) Modern swathe sounding and sub-bottom profiling technology for research applications: The Atlas Hydrosweep and Parasound systems. *Mar. Geophys. Res.* **12** 9-19.
- Gravenor, C.P., V. Von Brunn and A. Dreimanis (1984) Nature and classification of waterlain glaciogenic sediments, exemplified by Pleistocene, Late Paleozoic and Late Precambrian deposits. *Earth Sci. Rev.* **20** 105-166.
- Gray, J.M. and J.J. Lowe (1977) The Scottish Lateglacial environment : A synthesis. In: *Studies in the Scottish Lateglacial Environment*. Ed. J.M. Gray and J.J. Lowe 163-181 Pergamon Oxford.
- Grosswald, M.G. (1980) Late Weichselian ice sheet of Northern Eurasia. *Quat. Res.* **13** 1-32.
- Gustavson, T.C. (1975) Sedimentation and physical limnology in proglacial Malaspina Lake, Alaska. In: *Glaciofluvial and Glaciolacustrine Sedimentation*. Ed. A.V. Jopling and B.C. McDonald S.E.P.M. Sp. Publ. **23** 249-273.
- Håkanson, L. (1974) A mathematical model for establishing numerical values for topographical roughness for lake bottoms. *Geogr. Annlr.* **56A** 183-200.
- Håkanson, L. (1977) On lake form, lake volume and lake hypsographic survey. *Geogr. Annlr.* **59A** 1-29.
- Håkanson, L. (1978) The influence of wind, fetch, and water depth on the distribution of sediments in Lake Vanern, Sweden. *Can. J. Earth. Sci.* **14** 397-412.
- Håkanson, L. (1981) *A manual of lake morphometry*. Springer Verlag Berlin.
- Håkanson, L. and M. Jansson (1983) *Principles of lake sedimentology*. Springer Verlag Berlin.
- Haldane, A.R.B. (1962) *New Ways Through the Glens*. Nelson London.
- Hequette, A. and P.R.Hill (1989) Late Quaternary seismic stratigraphy of the inner shelf seaward of the Tuktoyatuk Peninsula, Canadian Beaufort Sea. *Can. J. Earth Sci.* **26** 1990-2002.
- Hersey, J.B. (1963) Continuous reflection profiling. *The Sea* **3** 47-72.
- Hicks, D. M., M.J. McSaveney and T.J.H. Chin (1990) Sedimentation in proglacial Ivory Lake, Southern Alps, New Zealand. *Arc. and Alp. Res.* **22** 26-42.
- Higgitt, S.R., F. Oldfield and P.G. Appleby (1991) The record of land use change and soil erosion in the late Holocene sediments of the Petit Lac d'Annecy, eastern France. *The Holocene* **1** 14-28.
- Holdsworth, G. (1973a) Ice deformation and moraine formation at the margin of an ice cap adjacent to a proglacial lake. In: *Research in Polar and Alpine Geomorphology* Ed. B.D. Fahey and R.D. Thompson 187-99 Geo Abstracts Norwich.

- Holdsworth, G. (1973b) Ice calving into the proglacial Generator Lake, Baffin Island, N.W.T., Canada. *J. Glaciol.* **12** 235-250.
- Hoppe, G. (1959) Glacial geomorphology and inland ice recession in northern Sweden. *Geogr. Annlr.* **41A** 193-212.
- Howell, F.T. (1971) A continuous seismic profile survey of Windermere. *Geol. J.* **7** 329-334.
- Hutchinson, D.R., W.M. Ferrebee, H.J. Knebel and R.J. Wold (1981) The sedimentary framework of the southern basin of Lake George, New York. *Quat. Res.* **15** 44-61.
- Hyne, N.J., P. Chelminski, J.E. Court, D.S. Gorsline and C.R. Goldman (1972) Quaternary history of Lake Tahoe, California-Nevada. *Bull. Geol. Soc. Am.* **83** 1435-1448.
- Inman, D.L. (1952) Measures for describing the size distribution of sediments *J. Sed. Pet.* **22** 125-145.
- Jansen, J.H.F. (1976) Late Pleistocene and Holocene history of the northern North Sea, based on acoustic reflection records. *Neth. J. Sea Res.* **10** 1-43.
- Johnson, R.G. and B.T. McClure (1976) A model for Northern Hemisphere continental ice sheet variation. *Quat. Res.* **6** 325-353.
- Johnson, T.C. (1980a) Late glacial and Postglacial sedimentation in Lake Superior based on seismic reflection profiling. *Quat. Res.* **13** 380-391.
- Johnson, T.C. (1980b) Sediment redistribution by waves in lakes, reservoirs and embayments. In: *Proceedings of the Symposium of Surface Water Impoundments*. Ed. H. Stephan Am. Soc. Civil Eng. New York 1307-1317
- Johnson, T.C. and T.W. Davis (1989) High resolution seismic profiles from Lake Malawi, Africa. *J. African Earth Sci.* **8** 383-392.
- Jones, G.B., G.D. Floodgate and J.D. Bennell (1986) Chemical and microbiological aspects of acoustically turbid sediments: Preliminary investigations. *Mar. Geotech.* **6** 315-333.
- Kaye, G.W.C. and T.H.Laby (1966) *Tables of physical and chemical constants*. 13 Ed. Longman London.
- Kenyon, N.H. (1989) In: GLORIA: The second decade. T.J.G. Francis. *J. Geol. Soc. Lond.* **146** 1031-1032.
- Kirby, R.P. (1971) The bathymetrical re-survey of Loch Leven, Kinross. *Geog. J.* **137** 372-8.
- Klein Associates (1985) Sonograph interpretation manual. Klein U.S.A.
- Knott, S.T. and J.B. Hersey (1956) Interpretation of high resolution echo-sound techniques and their use in bathymetry, marine geophysics and biology. *Deep-Sea Res.* **4** 36-44.
- Krumbein, W.C. (1936) The use of quartile measures in describing and comparing sediments. *Am. J. Sci.* **37** 98-111.

- Krumbein, W.C. and L.L. Sloss (1963) *Stratigraphy and Sedimentation*. Freeman San Francisco.
- Kurtz, D.D. and J.B. Anderson (1979) Recognition and sedimentologic description of recent debris flow deposits from the Ross and Weddell Seas, Antarctica. *J. Sed. Pet.* **49** 1159-1170.
- Lamb, H.F., C. Duigan, J.H.R. Gee, R.W. Maxted, R.J. Whittington, K. Kelts, G. Lister, F. Neissen, A. Merzouk, M. Badraoui and H. Chellai (1992) Project Salaam: Studies of High Atlas lakes- preliminary results. In: Proc. B.G.R.G. Spring Field Mtg: *Geomorphology and sedimentology of lakes and reservoirs*. Ed. J. McManus and R.W. Duck Wiley *In Press*.
- Landmesser, C.W., T.C. Johnson and R.J. Wold (1982) Seismic reflection study of recessional moraines beneath Lake Superior and their relationship to regional deglaciation. *Quat. Res.* **17** 173-190.
- Lawson, T.J. (1986) Loch Lomond Advance glaciers in Assynt, Sutherland and their palaeoclimatic implications. *Scot. J. Geol.* **22** 289-298.
- Leenhardt, O. (1969) Analysis of continuous seismic profiles. *Int. Hydrog. Rev.* **46** 51-80.
- Lees, A., A.T. Buller and J. Scott (1969) Marine carbonate sedimentation processes, Connemara, Ireland. An interim report. *Reading Univ. Geol. Rep.* **2**.
- Lewis, K.B. (1971) Slumping on a continental slope inclined at 1°-4°. *Sedimentol.* **16** 97-110.
- Lineback, J.A., D.L. Gross, R.P. Meyer and W.L. Unger (1971) High resolution seismic profiles and gravity cores of sediments in southern Lake Michigan. Studies of Lake Michigan bottom sediments 8 *Environmental Geology Notes* **47**.
- Lineback, J.A., D.L. Gross and R.P. Meyer (1972) Geologic cross sections derived from seismic profiles and sediment cores from southern Lake Michigan. Studies of Lake Michigan Bottom Sediments 9 *Environmental Geology Notes* **54**.
- Lineback, J.A., D.L. Gross and R.P. Meyer (1974) Glacial tills under Lake Michigan. Studies of Lake Michigan Bottom Sediments 11 *Environmental Geology Notes* **69**.
- Liverman, D.G.E. (1991) Sedimentology and history of a Late Wisconsinan glacial lake, Grande Prairie, Alberta, Canada. *Boreas* **20** 241-257.
- Lowe, J.J. (1991) Stratigraphic resolution and radiocarbon dating of Devensian Lateglacial sediments. In: *Radiocarbon dating: Recent applications and future potential* Ed. Lowe, J.J. Quaternary Proceedings 1 QRA Cambridge 19-25.
- Lowe, J.J. and M.J.C. Walker (1977) The reconstruction of the Lateglacial environment in the Southern and Eastern Grampian Highlands. In: *Studies in the Scottish Lateglacial Environment*. Ed. J.M. Gray and J.J. Lowe 101-118 Pergamon Oxford.
- Lowe, J.J., J.M. Gray and J.E. Robinson (Eds) *Studies in the Late-Glacial of North-West Europe*. Pergamon Oxford.

- Lowe, P.A., R.W. Duck and J. McManus (1991a) A bathymetric reappraisal of Loch Muick, Aberdeenshire. *Scot. Geog. Mag.* **107** 110-115.
- Lowe, P.A., R.W. Duck and J. McManus (1991b) Bathymetric Charts of three South East Grampian Lochs. *Tay Estuary Research Centre Report No.10*, Univ. Dundee, Univ. St. Andrews.
- Lowe P.A. (1992) Underwater geomorphology of Loch Lomond Readvance ice limits in Loch Muick, Aberdeenshire, U.K. In: Proc. B.G.R.G. Spring Field Mtg: *Geomorphology and sedimentology of lakes and reservoirs*. Ed. J. McManus and R.W. Duck Wiley In Press.
- MacDonald, G.M., C.P.S. Larsen, J.M. Szeicz and K.A. Moser (1991) The reconstruction of boreal forest fir history from lake sediments: A comparison of charcoal, pollen, sedimentological, and geochemical indices. *Quat. Sci. Rev.* **10** 53-71.
- Mackereth, F.J.H. (1958) A portable core sampler for lake deposits. *Limnol. and Oceanog.* **3** 181-191.
- Mackereth, F.J.H. (1965) Chemical investigations of lake sediments and their interpretation. *Proc. R. Soc. B* **161** 295-309.
- Mackereth, F.J.H. (1966) Some chemical observations on Post-Glacial lake sediments. *Proc. R. Soc. Edin. Sect. B.* **250** 166-213.
- Maclaren, C. (1855) Notice of ancient moraines in the parishes of Strachur and Kilmun, Argyleshire. *Edin. New Phil. J.* **1** 189-203.
- Maizels, J.K. (1977) Experiments on the origin of kettle-holes. *J. Glaciol.* **18** 291-303.
- Mangerud, J. and J.I. Svendsen (1990) Deglaciation chronology inferred from marine sediments in a proglacial lake basin, western Spitsbergen, Svalbard. *Boreas* **19** 249-272.
- Manley, P.L. and R.D. Flood (1989) Anomalous sound velocities in near-surface, organic-rich, gassy sediments in the central Argentine Basin. *Deep-Sea Res.* **36** 611-623.
- Matthews, J.A., A.G. Dawson and R.A. Shakesby (1986) Lake shoreline development, frost weathering and rock platform erosion in an alpine periglacial environment, Jotunheimen, southern Norway. *Boreas* **15** 33-50.
- Mawdsley, J.B. (1936) The washboard moraines of the Opawica-Chibougamou area, Quebec. *Proc. and Trans. R. Soc. Can.* **30** 9-12.
- Mayer, L. (1979) The origin of fine scale acoustic stratigraphy in deep-sea carbonates. *J. Geophys. Res.* **84** 6177-6184.
- McManus, J. and R.W. Duck (1983) Sidescan sonar recognition of subaqueous landforms in Loch Earn, Scotland. *Nature* **303** 161-162.
- McManus, J. and R.W. Duck (1988a) Internal seiches and subaqueous landforms in lacustrine cohesive sediments *Nature* **334** 511-513.
- McManus, J. and R.W. Duck (1988b) Scottish freshwater lochs and reservoirs: a physical perspective. *Scot. Geog. Mag.* **104** 97-107.

- McManus, J. and R.W. Duck (1988c) Localised sedimentation from icebergs in a proglacial lake in Briksdal, Norway. *Geogr. Annlr.* **70A** 215-223.
- McQuillin, R. and D.A. Ardu (1977) *Exploring the geology of shelf seas*. Graham and Trotman London.
- Meckel, L.D. and A.K. Nath (1977) Geologic considerations for stratigraphic modelling and interpretation. In: *Seismic stratigraphy - applications to hydrocarbon exploration*. Ed. C.E. Payton A.A.P.G. Mem. 26 Tulsa 417-438.
- Mercer, J.H. (1969) The Allerod oscillation: a European climatic anomaly? *Arct. and Alp. Res.* **1** 227-234.
- Mitchum, R.M. and P.R. Vail (1977) Seismic stratigraphy and global changes in sea level, Part 7; Seismic stratigraphic interpretation procedure. In: *Seismic stratigraphy - applications to hydrocarbon exploration*. Ed. C.E. Payton A.A.P.G. Mem. 26 Tulsa 135-144.
- Mitchum, R.M., P.R. Vail, J.B. Sangree (1977a) Seismic stratigraphy and global changes in sea level, Part 6; Stratigraphic interpretation of seismic reflection patterns in depositional sequences. In: *Seismic stratigraphy - applications to hydrocarbon exploration*. Ed. C.E. Payton A.A.P.G. Mem. 26 Tulsa. 117-133.
- Mitchum, R.M., P.R. Vail, S.Thompson (1977b) Seismic stratigraphy and global changes of sea level, Part 2; The depositional sequence as a basic unit for stratigraphic analysis. In: *Seismic stratigraphy - applications to hydrocarbon exploration*. Ed. C.E. Payton A.A.P.G. Mem. Tulsa. 26 53-62.
- Mooers, H.D. (1990) Ice-marginal thrusting of drift and bedrock: thermal regime, subglacial aquifers, and glacial surges. *Can. J. Earth Sci.* **27** 849-862.
- Moore, D.G. (1961) Submarine slumps *J. Sed. Pet.* **31** 343-357.
- Mortimer, C.H. and E.B. Worthington (1940) A new application of echo-sounding *Nature* **143** 212-214.
- Muller, H.E. (1976) Observations of interactions between water and sediment with a 30kHz sediment echosounder. *Mar. Geol.* **19** 448-452.
- Mullins, H.T. and E.J. Hinchey (1989) Erosion and infill of New York Finger Lakes: Implications for Laurentide ice sheet deglaciation. *Geol.* **17** 622-625.
- Mullins, H.T., N. Eyles and E.J. Hinchey (1990) Seismic reflection investigation of Kalamalka Lake: a "fiord lake" on the interior plateau of southern British Columbia. *Can. J. Earth. Sci.* **27** 1225-1235.
- Mullins, H.T., N. Eyles and E.J. Hinchey (1991) High-resolution seismic stratigraphy of Lake Macdonald, Glacier National Park, Montana, U.S.A. *Arc. and Alp. Res.* **23** 311-319.
- Murray, J. and L. Pullar (1910) *Bathymetrical Survey of the Freshwater Lochs of Scotland*. Edinburgh Challenger Office 5 Vols.
- Nesje, A., M. Kvamme, N. Rye and R. Løvlie (1991) Holocene glacial and climatic history of the Jostedalsgreen region, western Norway; evidence from lake sediments and terrestrial deposits. *Quat. Sci. Rev.* **10** 87-114.

- Newton, R.S., E.Siebold and F. Werner (1973) Facies distribution patterns in the Spanish Sahara Continental Shelf mapped with side scan sonar. *Meteor. Forsch., Ergebnisse, C.* **15** 55-57.
- Ohle, W. (1978) Ebullition of gases from sediment, conditions, and relationship to primary production of lakes. *Vehr. Int. Ver. Limnol.* **20** 957-962.
- Oldershaw, W. (1974) The Lochnagar Granitic Ring Complex, Aberdeenshire. *Scot. J. Geol.* **10** 297-309.
- Page, H.G. (1955) Phi-millimeter conversion table. *J. Sed. Pet.* **25** 285-292.
- Palmer, H.D. (1967) An introduction to marine seismic reflection surveys. *Dames and Moore Engineering Bulletin* **33**.
- Payne, A and D.E. Sugden (1990) Topography and ice sheet growth. *Earth Surf. Proc. and Landf.* **15** 625-639.
- Payton, C.E. (1977) Ed. *Seismic stratigraphy - applications to hydrocarbon exploration*. A.A.P.G. Mem. 26 Tulsa.
- Peacock, J.D. and R. Cornish (1989) *Glen Roy area - Field Guide*. Quat. Res. Assn. Cambridge.
- Peacock, J.D., D.D. Harkness, R.A. Houseley, J.A. Little and M.A. Paul (1989) Radiocarbon ages for a glaciomarine bed associated with the maximum of the Loch Lomond Readvance in West Benderloch, Argyll. *Scot. J. Geol.* **25** 69-79.
- Pennington, W. (1977) Lake sediments and the Lateglacial environment in northern Scotland. In: *Studies in the Scottish Lateglacial Environment*. Ed. J.M. Gray and J.J. Lowe 119-142 Pergamon Oxford.
- Pennington, W. (1981) Records of a lake's life in time: the sediments. *Hydrobiol.* **79** 197-219.
- Pennington W., E.Y. Haworth, A.P. Bonny and J.P. Lishman (1972) Lake sediments in northern Scotland. *Phil. Trans. R. Soc. B* **264** 191-294.
- Perry, A.H. (1981) *Environmental Hazards in the British Isles*. George Allen and Unwin London.
- Peteet, D., J.S. Vogel, D.E. Nelson, J.R. Southon, R.J. Nickman and L.E. Heusser (1990) Younger Dryas climatic reversal in Northeastern USA? AMS ages for an old problem. *Quat. Res.* **33** 219-230.
- Pethick, J. (1984) *An introduction to coastal geomorphology*. Arnold London.
- Pickrill, R.A. and J. Irwin (1983) Sedimentation in a deep glacier-fed lake - Lake Tekapo, New Zealand. *Sedimentol.* **30** 63-75.
- Playfair, J. (1802) *Illustrations of the Huttonian theory of the earth*. Edinburgh.
- Price, R.J. (1983) *Scotland's environment during the last 30,000 years*. Scottish Academic Press Edinburgh.

- Prior, D.B. and B.D. Bornhold (1989) Submarine sedimentation on a developing Holocene fan delta. *Sedimentol.* **36** 1053-1076.
- Ramsbottom, A.E. (1976) Depth charts of the Cumbrian lakes. *Freshwater Biological Association Scientific Publication No.33* F.B.A.
- Rapson, S.C. (1985) Minimum age of corrie moraine ridges in the Cairngorm Mountains, Scotland. *Boreas* **14** 155-159.
- Ravenne, C. (1978) Etude bibliographique des publications d'Exxon concernant l'interpretation stratigraphique des sections sismiques. *Rev. I.F.P.* **26**.
- Reid, J.R. and Callender, E. (1965) Origin of debris-covered icebergs and mode of flow of ice into 'Miller Lake', Martin River Glacier, Alaska. *J. Glaciol.* **5** 497-504.
- Reynolds, J.M. (1990) High resolution seismic reflection surveying of shallow marine and estuarine environments. *Mar. Geophys. Res.* **12** 41-48.
- Rind, D., D. Peteet, W.S. Broecker, A. McIntyre and W.F. Ruddiman (1986) The impact of cold North Atlantic sea surface temperatures on climate: implications for the Younger Dryas cooling (11-10k). *Clim. Dynam.* **1** 3-33.
- Robinson, M. and Ballantyne, C.K. (1979) Evidence for a glacial readvance pre-dating the Loch Lomond Advance in Wester Ross. *Scot. J. Geol.* **15** 271-277.
- Rokoengen, K., T. Bugge and M. Lofaldli (1979) Quaternary geology and deglaciation of the continental shelf off Troms, north Norway. *Boreas* **8** 217-227.
- Rose, J., J.J. Lowe and R. Switsur (1988) Plant debris from beneath till from the type area of the Loch Lomond Readvance. *Scot. J. Geol.* **24** 113-124.
- Ruddiman, W.F. and A. McIntyre (1981) The North Atlantic during the last deglaciation. *Palaeogeogr., Palaeoclimatol., Palaeoecol.* **35** 145-214.
- Rust, B.R. and R. Romanelli (1975) Late Quaternary subaqueous outwash deposits near Ottawa, Canada. In: *Glaciofluvial and glaciolacustrine sedimentation*. Ed. A.V. Jopling and B.C. McDonald S.E.P.M. Sp. Publ. **23** Tulsa 177-192.
- Rust, V.H. (1935) Mehrfach-Reflexionen beim Echoloten auf weichem Grund. *Die Naturwiss.* **23** 387-389.
- Schubel, J.R. and E.W. Schiemer (1973) The cause of the acoustically impenetrable or turbid, character of Chesapeake Bay sediments. *Mar. Geophys. Res.* **2** 61-71.
- Seymour, H.J. (1939) Bathymetric survey of three lakes in Co. Wicklow. *Proc. R. Irish Acad.* **45B** 297-299.
- Simpson, J.B. (1933) The lateglacial readvance moraines of the Highland border west of the River Tay. *Trans. R. Soc. Edinb.* **57** 633-45.
- Sissons, J.B. (1967a) *The Evolution of Scotland's Scenery*. Oliver and Boyd Edinburgh.
- Sissons, J.B. (1967b) Glacial stages and radiocarbon dates in Scotland. *Scot. J. Geol.* **3** 375-381.

- Sissons, J.B. (1972a) The last glaciers in part of the S.E. Grampians. *Scot. Geog. Mag.* **88** 168-181.
- Sissons J.B. (1972b) Glacial Readvances in Scotland. In: *Problems of the deglaciation of Scotland*. Ed. C.J. Caseldine and W.A. Mitchell StAG Special Publication 1 Univ. St. Andrews 5-16.
- Sissons, J.B. (1973a) Hypothesis of deglaciation in the eastern Grampians, Scotland. *Scot. J. Geol.* **9** 96.
- Sissons, J.B. (1973b) Delimiting the Loch Lomond Readvance in the eastern Grampians. *Scot. Geog. Mag.* **89** 138-139.
- Sissons, J.B. (1974) A Lateglacial icecap in the central Grampians, Scotland. *Trans. Inst. Br. Geog.* **62** 95-114.
- Sissons, J.B. (1975) The Loch Lomond Readvance in the south-east Grampians. In: *Quaternary studies in north-east Scotland*. Ed. A.M.D. Gemmell Aberdeen 23-29.
- Sissons, J.B. (1977a) The Loch Lomond Readvance in southern Skye and some palaeoclimatic implications. *Scot. J. Geol.* **13** 23-36.
- Sissons, J.B. (1977b) The Loch Lomond Readvance in the northern mainland of Scotland. In: *Studies in the Lateglacial environment of Scotland*. Ed. J.M.Gray, and J.J. Lowe Pergamon Oxford 25-60.
- Sissons, J.B. (1977c) Former ice-dammed lakes in Glen Morriston, Inverness-shire, and their significance in upland Britain. *Trans. Inst. Br. Geog.* **2** 224-242.
- Sissons, J.B. (1978) The parallel roads of Glen Roy and adjacent glens, Scotland. *Boreas* **7** 229-244.
- Sissons, J.B. (1979a) The Loch Lomond Stadial in the British Isles. *Nature* **280** 199-203.
- Sissons, J.B. (1979b) The Loch Lomond Advance in the Cairngorm Mountains. *Scot. Geog. Mag.* **95** 66-82.
- Sissons, J.B. (1979c) The limit of the Loch Lomond Advance in Glen Roy and vicinity. *Scot. J. Geol.* **15** 31-42.
- Sissons, J.B. (1980a) The Loch Lomond Advance in the Lake District, northern England. *Trans. R. Soc. Edin.* **71** 13-28.
- Sissons, J.B. (1980b) Palaeoclimatic inferences from Loch Lomond Advance glaciers. In: *Studies in the Lateglacial of north-west Europe*. Ed. J.J. Lowe, J.M. Gray and J.E. Robinson Pergamon Oxford 31-43.
- Sissons, J.B. and Grant, A.J.H. (1972) The last glaciers in the Lochnagar area, Aberdeenshire. *Scot. J. Geol.* **8** 85-93.
- Sissons, J.B. (1983) Quaternary. In: *Geology of Scotland*. Ed. G.Y. Craig Scottish Academic Press Edinburgh 399-424.
- Sissons, J.B. and D.G. Sutherland (1976) Climatic inferences from former glaciers in the south-east Grampian Highlands, Scotland. *J. Glaciol.* **17** 325-346.

- Sissons, J.B. and M.J.C. Walker (1974) Late glacial site in the central Grampian Highlands. *Nature* **249** 822-824.
- Sissons, J.B., J.J. Lowe, K.S. R. Thompson and M.J.C. Walker (1973) Loch Lomond Readvance in the Grampian Highlands of Scotland. *Nature Phys. Sci.* **244** 75-77.
- Slack, H.D. (1954) The bottom deposits of Loch Lomond. *Proc. R. Soc. Edin. B* **65** 213-238.
- Sloss, L.L. (1963) Sequences in the cratonic interior of North America. *Bull. Geol. Soc. Am.* **74** 93-113.
- Smith, A.J. (1959) Structures in the stratified Late-glacial clays of Windermere, England. *J. Sed. Pet.* **29** 447-453.
- Smith, N.D. (1978) Sedimentation processes and patterns in a glacier-fed lake with low sediment input. *Can J. Earth Sci.* **15** 741-756.
- Smith, N.D., M.A. Venol and S.K. Kennedy (1982) Comparison of sedimentation regimes in four glacier-fed lakes of western Alberta. In: *Research in glacial, glacio-fluvial, and glaciolacustrine systems*. Ed. R. Davidson-Arnott, W. Nickling and B.D. Fahey Geo Books Norwich 203-238.
- Stocks, V.T. (1935) Erkundungen uber Art und Schichtung des Meeresbodens unt Hilfe von Hochfrequenz-Echoloten. *Die Naturwiss.* **23** 383-387.
- Sugden, D.E. (1970) Landforms of deglaciation in the Cairngorm Mountains, Scotland. *Trans. Inst. Br. Geog.* **51** 102-219.
- Sugden, D.E. (1972) Deglaciation of the Cairngorms and its wider implications. In: *Problems of the deglaciation of Scotland*. Ed. C.J. Caseldine and W.A. Mitchell StAG Special Publication 1 Univ. St. Andrews 17-28.
- Sugden, D.E. (1973) Delimiting Zone III glaciers in the Eastern Grampians. *Scot. Geog. Mag.* **89** 63-64.
- Sugden, D.E. (1977) Did glaciers form in the Cairngorms in the 17th-19th centuries? *Cairn. Club. J.* **18** 189-201.
- Sugden, D.E. (1980) The Loch Lomond Advance in the Cairngorms (a reply to J.B. Sissons). *Scot. Geog. Mag.* **96** 18-19.
- Sugden, D.E and C.M. Clapperton (1975) The deglaciation of Upper Deeside and the Cairngorm mountains. In: *Quaternary Studies in North East Scotland*. Ed. A.M.D. Gemmell QRA 30-37.
- Synge, F.M. (1956) The glaciation of North East Scotland. *Scot. Geog. Mag.* **72** 131-143.
- Taishi, H., S. Okuda, T. Shiki and K. Kashiwaya (1991) A sedimentary anomaly and the related sedimentation process in Lake Biwa, Japan. *Z. Geomorph. Suppl. Bd.* **83** 241-249.
- Talbot, H.F. (1833) Proposed method of ascertaining the greatest depth of the ocean. *Phil. Mag. 3rd Series* **3** 92.

- Taylor Smith, D. and W.N. Li (1966) Echo-sounding and sea-floor sediments. *Mar. Geol.* **4** 353-364.
- Theakstone, W.H. (1989) Further catastrophic break-up of a calving glacier: observations at Austerdalsisen, Svartisen, Norway 1983-87. *Geogr. Annlr.* **71A** 245-253.
- Thomas, G.S.P. (1984) A Late Devensian glaciolacustrine fan-delta at Rhosesmor, Clwyd, North Wales. *Geol. J.* **19** 125-141.
- Thomas, G.S.P. and R.J. Connell (1985) Iceberg drop, dump and grounding structures from Pleistocene glacio-lacustrine sediments, Scotland. *J. Sed. Pet.* **55** 243-249.
- Thomas, R.L., A.L.W. Kemp, C.F.M. Lewis (1972) Distribution, composition and characteristics of the surficial sediments of Lake Ontario. *J. Sed. Pet.* **42** 66-84.
- Thompson, R. and K. Kelts (1974) Holocene sediments and magnetic stratigraphy from Lakes Zug and Zurich, Switzerland. *Sedimentol.* **21** 577-596.
- Thompson, R. and D.J. Morton (1979) Magnetic susceptibility and particle-size distribution in recent sediments of the Loch Lomond drainage basin, Scotland. *J. Sed. Pet.* **49** 801-812.
- Tinghuan, L. and J. Bo (1989) Seismic facies analysis of the seafloor instabilities in the Pearl River Mouth Region. *Mar. Geotech.* **8** 19-31.
- Tinsley, H.M and E. Derbyshire (1976) Late-glacial and postglacial sedimentation in the Peris-Padarn rock basin, North Wales. *Nature* **260** 234-238.
- Tipping, R.M. (1988) The recognition of glacial retreat from palynological data: a review of recent work in the British Isles. *J. Quat. Sci.* **3** 171-182.
- Upton, P.S., T. Harrison, C.G. Smith and C.W. Thomas (1989) *Braemar* Sheet 65W Solid Edition 1:50000 Series B.G.S N.E.R.C.
- Vail, P.R. (1977) Seismic stratigraphy and global changes in sea level. In: *Seismic stratigraphy-applications to hydrocarbon exploration*. Ed. C.E. Payton A.A.P.G. Mem 26 Tulsa 49-212.
- Vail, P.R. and R.M. Mitchum (1977) Seismic stratigraphy and global changes in sea level, Part 1; Overview. In: *Seismic stratigraphy - applications to hydrocarbon exploration*. Ed. C.E. Payton A.A.P.G. Mem. 26 Tulsa 51-52.
- Vail, P.R. (1987) Seismic stratigraphy interpretation procedure. In: *Atlas of seismic stratigraphy* Ed. A.W. Bally A.A.P.G. Studies in Geology 27 Vol 1 Tulsa 1-10.
- Van Overeem, A.J.A. (1978) Shallow penetration, high-resolution subbottom profiling. *Mar. Geotech.* **3** 61-85.

- Van Wagoner, J.C., H.W. Posamentier, R.M. Mitchum, P.R. Vail, J.F. Sarg, T.S. Loutit and J. Hardenbol (1988) An overview of the fundamentals of sequence stratigraphy and key definitions. In: *Sea-level changes: an integrated approach*. Ed. C.K. Wilgus, B.S. Hastings, C.G. St.C. Kendall, H.W. Posamentier, C.A. Ross, J.C. Van Wagoner S.E.P.M. Sp. Pub. 42 Tulsa 39-46.
- Vernet, J-P, R.L. Thomas, J-M Jacquet, R. Friedli (1972) Texture of the sediments of the Petit Lac (Western Lake Geneva). *Eclogae Geol. Helv.* **65** 591-610.
- Walker, M.J.C. (1975) Two Lateglacial pollen diagrams from the eastern Grampian Highlands of Scotland *Pollen et Spores* **17** 67-92.
- Walker, M.J.C., C.K. Ballantyne, J.J. Lowe and D.G. Sutherland (1988) A reinterpretation of the Lateglacial history of the Isle of Skye, Inner Hebrides, Scotland. *J. Quat. Sci.* **3** 135-146.
- Walker, M.J.C. and J.J. Lowe (1990) Reconstructing the environmental history of the last glacial-interglacial transition: Evidence from the Isle of Skye, Inner Hebrides, Scotland. *Quat. Sci. Rev.* **9** 15-49.
- Watts, W.A. (1980) Regional variation in the response of vegetation of Late-Glacial climatic events in Europe. In: *Studies in the Scottish Lateglacial Environment*. Ed. J.M. Gray and J.J. Lowe 1-22 Pergamon Oxford.
- Weirich, F.H. (1985) Sediment budget for a high energy glacial lake. *Geogr. Annlr.* **67A** 83-99.
- Welch, N.H., P.B. Allen, D.J. Galindo (1979) Particle-size analysis by Pipette and SediGraph. *J. Environ. Qual.* **8** 543-546.
- West, R.G. (1968) *Pleistocene geology and biology*. Second Ed. 1977 Longman London.
- Westbrook, W. (1989) In: GLORIA: The second decade. T.J.G. Francis. *J. Geol. Soc. Lond.* **146** 1031-1032.
- White, E.J. and R.I. Smith (1982) *Climatological maps of Great Britain*. Institute of Terrestrial Ecology N.E.R.C. Cambridge.
- White, I.D. and D.N. Mottershead (1972) Past and present vegetation in relation to solifluction on Ben Arkle, Sutherland. *Trans. Proc. Bot. Soc. Edinb.* **41** 475-489.
- Whittington, G.W. (1991) *Palynological investigations into the basal sediments of Loch Callater: a preliminary report*. Dept of Geog. and Geol. Internal Report Univ. St. Andrews.
- Widess, M.B. (1973) How thin is a thin bed? *Geophys.* **38** 1176-1180.
- Williams, S.J. (1982) *Use of high resolution seismic reflection and sidescan sonar equipment for offshore surveys*. Coastal Engineering Technical Aid 82-5 Fort Belvoir.
- Wingfield, R. (1990a) The origins of major incisions within the Pleistocene deposits of the North Sea. *Mar. Geol.* **91** 31-52.

- Wingfield, R. (1990b) Glacial incisions indicating Middle and Upper Pleistocene ice limits off Britain. *Terra Nova* **1** 538-548.
- Wood, A.B., F.D. Smith and J.A. McGeachy (1935) A magnetostrictive echodepth recorder. *Trans. Inst. Elec. Eng.* **76** 550-563.
- Worzel, J.L. (1959) Extensive deep sea subbottom reflections identified in white ash. *Proc. Nat. Acad. Sci. U.S.* **45** 349-359.
- Wright, R.F. (1976) The impact of forest fire on the nutrient influxes to small lakes in northeastern Minnesota. *Ecology* **57** 657-659.